TECHNICAL REPORT HSM-R30-69

JULY 31, 1969

EXHIBIT A

Contract No. NAS8-21425

FINAL REPORT
COMPARATIVE ANALYSIS OF ACOUSTIC TESTING TECHNIQUES

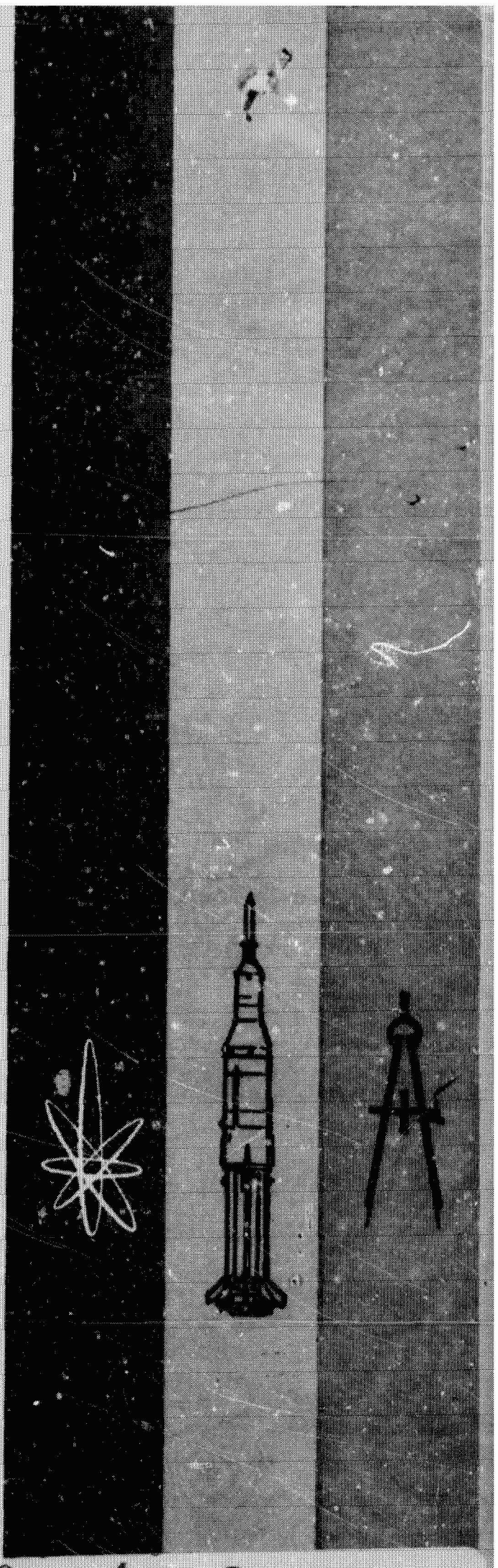

SPACE DIVISION CHRYSLER CORPORATION

HUNTSVILLE OPERATIONS

TECHNICAL REPORT HSM-R30-69

FINAL REPORT

COMPARATIVE ANALYSIS OF ACOUSTIC TESTING TECHNIQUES

CONTRACT NAS8-21425

EXHIBIT A

Prepared for

GEORGE C. MARSHALL SPACE FLIGHT CENTER
MARSHALL SPACE FLIGHT CENTER, ALABAMA 35812

By

W. J. Gruner

Vibration and Acoustics Group

July 1969

SPACE DIVISION CHRYSLER CORPORATION
HUNTSVILLE OPERATIONS

1312 North Meridian Street
Huntsville, Alabama 35807

FOREWORD

The research work reported herein was conducted by the Vibration and Acoustics Group of Chrysler Huntsville Operations for the Marshall Space Flight Center as Exhibit A of Contract NAS8-21425. The work was initiated under the cognizance of the Advanced Methods and Research Section of the Vibration and Acoustics Branch, Structures Division, Propulsion and Vehicle Engineering Laboratory, and completed under the technical surveillance of the Dynamics Technology Section, Advanced Technology Branch, Analytical Mechanics Division of the Astronautics Laboratory.

This research was conducted from July 1968 to July 1969 and is a portion of the continuing effort to improve methods for qualifying spacecraft structures and components to vibration and acoustic levels commensurate with mission requirements.

Acknowledgement is made of the mutually enlightening technical discussions with the Contracting Officer's Representative, Lester D. Saint. The assistance of Dr. T. N. Lee and other members of the Vibration and Acoustics Group, Chrysler Corporation, is recognized. Participation of personnel of the Test and Evaluation Section of Chrysler Michoud Operations, especially R. E. Jezek in acquisition of the empirical data and R. A. Klecka of the Manufacturing Department, Chrysler Huntsville Operations for fabrication of an acoustic waveguide must be noted. Grateful acknowledgement is also given to the patience and skill exercised by Mrs. L. I. Pittman in typing the manuscript.

ABSTRACT

This report is the result of an analytical and empirical research program directed toward improving laboratory simulation of space vehicle system acoustic fields. State-of-the-art methods for calculation of vibratory response of spacecraft structural members to acoustic fields are presented in terms of modal analyses, statistical energy techniques and coincidence effects. Empirically derived vibro-acoustic transfer functions for four panel configurations are compared to predicted results.

Results of the analyses are utilized to derive recommended methods and procedures for simulating the vibratory response of structures and components to acoustic fields in various types of labroatory facilities. Results of radiation damping, mass loading and exposed surface area analyses and experiments are also detailed. Logical recommendations for future efforts are presented.

TABLE OF CONTENTS

TABLE OF CONTENTS

LIST OF ILLUSTRATIONS

LIST OF ILLUSTRATIONS (Continued)

LIST OF ILLUSTRATIONS (Continued)

LIST OF ILLUSTRATIONS (Continued)

LIST OF ILLUSTRATIONS (Continued)

LIST OF ILLUSTRATIONS (Continued)

LIST OF ILLUSTRATIONS (Concluded)

LIST OF TABLES

NOMENCLATURE

Notation	Description
a	Differential static pressure (oscil . .ng shock wave)
a	Panel dimension (radiation damping analysis)
a	Radius of panel
a_1	Spacing of width-direction stiffeners
A_1	Correlation decay constant in x direction
A_2	Correlation decay constant in y direction
A_p	Panel Area
A_t	Correlation area
AL	Acceleration level, dB re 1 g
b	Width of panel
b'	Width of panel subject to excitation
b_1	Spacing of length-direction stiffeners
c	Ambient speed of sound, 1090 ft/sec
c_B	Panel bending wave velocity
c_c	Critical damping
c_f	Local coefficient of skin friction (boundary layer noise)
c_ℓ	Panel longitudinal wave velocity
c_r	Radiation damping
D	Engine exit diameter (rocket engine noise)
D	Vehicle diameter (oscillating shock wave)
$D(\Omega)$	Average directivity function of incident acoustic energy (statistical response analysis)
D_{eff}	Effective diameter, $\sqrt{N}$ D, (rocket engine noise)
DC	Rocket engine noise liftoff directivity correction

NOMENCLATURE (Continued)

Notation	Description
e	Natural logarithm base
E	Young's modulus of panel skin
E'	Young's modulus of panel stiffeners
f	Frequency, Hz
f_{jk}, f_{mn}	Natural frequency, Hz
f_e	Critical frequency
Δf	Frequency bandwidth
F_f	Frequency modification factor
F_m	Amplitude modification factor
F_{jk}, F_{mn}	Normal modes
g	Acceleration of gravity, 32.176 ft/sec^2
G_∞	Mechanical point input conductance of plate
$G^2(kR)$	Near field function (rocket engine noise)
h	Thickness of panel skin
h	Smeared out thickness of stiffeners
h_1	Height constant, $h + h_2$
h_2	Height of stiffeners at $\vec{r}$
H	Vehicle altitude (rocket engine noise at liftoff)
H_{jk}	Complex magnification factor
HC	Hydrodynamically coincident
HF	Hydrodynamically fast
HS	Hydrodynamically slow
I_1	Moment of inertia of one length-direction stiffener with respect to neutral axis of cross-section of panel

Notation	Description
I_2	Moment of inertia of one width-direction stiffener with respect to neutral axis of cross-section of panel
$\tilde{I}_{jkmn}$	Cross spectral density of generalized force
I_{jkmn}	Normalized cross spectral density of generalized force
J_{jkmn}	Joint acceptance
j,k,m,n	Mode indices
k,K	Wave number, $2\pi f/c$, $2\pi f/U_c$, $2\pi f/c_\ell$
k_p	Plate free bending wave number, ω/c_B
K	Panel radiation damping coefficient
ℓ	Length of panel
ℓ'	Length of panel subjected to excitation
ℓ_x,ℓ_y,ℓ_z	Chamber dimensions
L	Horizontal distance from vehicle centerline to the acoustic monopole source (rocket engine noise)
L_1	Flow-wise boundary layer correlation length
L_2	Transverse boundary layer correlation length
m_e	Equipment mass
m_s	Unloaded panel mass
M_{jk}	Generalized mass
M_s	Panel mass
M_∞	Free stream Mach number
n_s	Panel modal density
n_x,n_y,n_z	Acoustic modal indices
N	Number of engines (rocket engine noise)
OA	Overall
p^2	Mean square acoustic pressure

NOMENCLATURE (Continued)

Notation	Description
p_1^2	Mean square acoustic pressure (rocket engine noise, equivalent single engine model)
p_2^2	Mean square acoustic pressure (rocket engine noise, equivalent single engine model)
P_r	Panel perimeter
r	Radial distance from vehicle centerline to receiver location (rocket engine noise)
$\vec{r}$	Position vector
R	Distance from a particular source to receiver (rocket engine noise)
Re_x	Reynolds number based on distance x, $U_\infty x/\nu$
s	Vertical distance from engine exhaust plane to mean impingement point on exhaust deflector. (Rocket engine noise, ground plane environments)
S	Strouhal number
s'	Area of panel exposed to excitation, $b'\ell'$
S_r	Cross-section area of progressive wave facility
S_s	Oscillating shock wave pressure spectral density
$s_{ww}(\vec{r},f)$	Displacement spectral density
$s_{ww}^{\cdot\cdot}(\vec{r},f)$	Velocity spectral density
$s_{ww}^{\cdot\cdot\cdot\cdot}(\vec{r},f)$	Acceleration spectral density
$S_{3rd}(f)$	One-third octave band sound pressure level in dB
SF	Dimensionless empirical power function (rocket engine noise)
t	Time
$\bar{t}_c$	Mean time at lower static pressure (oscillating shock wave)
$\bar{t}_k$	Mean time at higher static pressure (oscillating shock wave)

Notation	Description
T	Thrust per engine (rocket engine noise)
T_t	Total stage thrust, NT, (rocket engine noise)
TBL	Turbulent boundary layer
TFL	Transfer function level, dB
U_c	Eddy convection speed (boundary layer noise)
U_e	Exhaust speed at the engine exit plane (rocket engine noise)
U_∞	Vehicle freestream velocity
W_f	Fixed position pressure spectral density normalized by mean square pressure (boundary layer noise)
W'	Moving axis turbulence pressure spectral density normalized by mean square pressure (boundary layer noise)
x	Coordinate
x,y	Coordinates of $\vec{r}$
x_1	Flow-wise coordinate (boundary layer noise)
x_2	Transverse coordinate (boundary layer noise)
$X_j(x)$	Function of x
X_o	Location of acoustic source from engine exit plane, measured along exhaust path (rocket engine noise)
$Y_k(y)$	Function of y
α	Acoustic propagation loss coefficient
α_1	Length parameter, $A_1 K\ell$
α_2	Width parameter, $A_2 Kb$
δ^*	Boundary layer displacement thickness
ζ	Radiation damping ratio, c_r/c_c

NOMENCLATURE (Continued)

Notation	Description
ζ_{jk}, ζ_{mn}	Damping ratio's
η	Separation distance in y-direction, $\lvert y_1 - y_2 \rvert$, (modal response analysis)
η	Damping factor
θ	Angle between deflected exhaust and the radius to the receiver location in the horizontal plane (rocket engine noise)
θ	Mean eddy lifetime (boundary layer noise)
θ	Fairing angle (oscillating shock wave)
κ	Radius of gyration
λ	Wavelength
λ_1	Frequency parameter, $K\ell$, (modal response analysis)
λ_2	Frequency parameter, Kb, (modal response analysis)
ν	Kinematic viscosity (boundary layer noise)
ν	Poisson's ratio (modal response analysis)
ξ	Normalized cross-correlation coefficient (boundary layer noise)
ξ	Separation distance in x-direction, $\lvert x_1 - x_2 \rvert$, (modal response analysis)
Ξ	Wave-number frequency spectrum (boundary layer noise)
$\Pi(f)$	Input power to panel
ρ	Panel skin mass density
ρ'	Mass density of panel stiffeners
ρ_s	Panel surface mass density
ρ_o	Ambient density of air
$\rho_o c_o$	Characteristic acoustic impedance of air, 2.61 lb-sec-ft^{-3}

NOMENCLATURE (Concluded)

Notation	Description
σ	Poisson's ratio for panel
σ_{rad}	Radiation efficiency
τ_o	Wall shear stress (boundary layer noise)
$\Phi_{pp}(\vec{r}_1,\vec{r}_2,\omega)$	Cross-spectral density function
Φ	Directivity factor (rocket engine noise)
$\Phi_{pp}(\omega)$	Homogeneous excitation spectral density
$\Phi_{ww}(\vec{r},\omega)$	Displacement response spectral density
$\Phi_{\dot{w}\dot{w}}(\vec{r},\omega)$	Velocity response spectral density
$\Phi_{\ddot{w}\ddot{w}}(\vec{r},\omega)$	Acceleration response spectral density
ω	Frequency, rad/sec
ω_{jk},ω_{mn}	Natural frequencies, rad/sec
$\dot{\omega}$	Weight flow per engine (rocket engine noise)
$\dot{\omega}_t$	Total stage weight flow, $N\dot{\omega}$, (rocket engine noise)

SECTION I. INTRODUCTION

More comprehensive methods of acoustically simulating flight dynamic environments are required to optimize performance reliability relative to weight, volume, packaging, etc. Simulation of the acoustic pressure spectral density can usually be performed satisfactorily. However, current testing methods (reverberant and progressive wave testing) do not completely reflect the wide variance in the spatial distribution of pressure amplitudes, do not reflect pressure field coherency, and do not generally provide the equivalent damage potential as the flight vibration environment. This program of research was designed to alleviate the above stated problems by improving the utilization of existing acoustic test facilities for the environmental testing of advanced space vehicle payloads and associated equipment.

This program has employed state-of-the-art analytical techniques to derive acoustic-vibration energy transforms. Acoustic field characteristics of service and simulation environments are discussed in detail in Section II. Section III presents techniques of estimating vibratory response of structural elements to acoustic loading utilizing normal-mode and statistical energy analyses. Expected effects of varying the radiation damping, area exposed to the acoustic field and equipment loading are also discussed in Section III.

A discussion of the empirical program is presented in Section IV including characteristics of the test facility and test specimens. The vibratory response of simple panels, a stiffened panel and a mass loaded test specimen was monitored when subjected to progressive acoustic waves at normal and parallel incidence, reverberant acoustic waves and localized exposure to intense progressive acoustic waves at parallel incidence. Test procedures, test configuration and accumulated test data are included herein to make this final report self-contained.

Section V presents comparison of analytical expectations and empirical results including transfer function levels, effects of radiation damping, mass loading and exposed area.

Section VI presents recommended methods for simulation of service acoustic fields within existing simulation laboratories and Section VII presents logical recommendations for the most fortuitous expenditure of future efforts.

SECTION II. ACOUSTIC FIELD CHARACTERISTICS

Prior to the calculation of structural vibratory response, it is necessary to be knowledgeable of the pertinent characteristics of the acoustic fields to which a specimen might be exposed. The primary facets are the acoustic pressure spectral density, variation in the pressure spectral density over the specimen surface and the acoustic field spatial correlation. Mathematical models are developed and presented herein for various service and simulation environments.

A. Service Acoustic Environments

The acoustic fields to which advanced space vehicle payloads will be exposed may be categorized as noise due to rocket engines or motors, turbulent boundary layer pressure perturbations, unsteady pressures due to oscillation of shock waves and wake impingement pressures. The acoustic environment of operational equipment located within the payload compartment is a function of the external surface acoustic pressures but is further complicated by acoustic energy absorption coefficients of the internal surfaces, payload compartment dimensions normalized by the acoustic wavelength, shielding, internal acoustic sources and sound radiated by nearby vibrating surfaces. Primary emphasis in the subsequent paragraphs is devoted toward modeling the acoustic environments encountered at the external surface of a payload module.

1. Rocket Engine Noise

The noise generated by space vehicle booster rocket engines during static firing, launch and subsonic flight can be well predicted utilizing a Chrysler modification (references 1, 2) of the methods proposed by references 3 and 4.

Acoustic environments produced by the intense turbulent shear layer in rocket engine exhaust have been characterized by many investigators. Lighthill (references 5, 6) treated the source as fluctuating lateral quadrapoles; however, empirical results exhibit characteristics of modified monopoles. It seems that no simple source chain of monopoles, dipoles, or quadrapoles can completely describe empirical results. The significance of Lighthill's theory is the identification of a dependency of the generated acoustic power on jet velocity, although the $U_e^8 D^2$ relationship is not directly applicable to current high thrust rocket motors with highly supersonic exit velocities. It has been demonstrated (references 4, 7) that for large spatial acoustic source distributions (i.e., for large diameter engines with exhaust speeds at the nozzle exit plane greater than Mach 3) source directivity can be ascribed to sound refraction resulting from thermal and velocity gradients in the turbulent exhaust.

It is possible to describe the effective acoustic source location, power and directivity, considering a source chain of monopoles, utilizing the following assumptions:

(1) The principle acoustic power generation mechanism is the flow regime of maximum turbulence.

(2) The acoustic intensity is dependent on the magnitude of the turbulent exhaust gas fluctuations.

(3) The source frequency is a function of the characteristic size of the fluctuating eddies which in turn is a function of longitudinal position.

A model from which the engine-generated acoustic environment may be defined is shown in figure 1 depicting a series of postulated monopole acoustic sources lying along the mean exhaust path. The monopole chain hypothesis places the higher frequency sources in the proximity of the exhaust plane with the source distance inversely dependent upon frequency. An empirical determination of source distance from the exit plane is presented in figure 2.

The source acoustic power as defined empirically by Dyer in conjunction with the aforementioned source distance is shown in figure 3. This power spectrum is excellent for the prediction of acoustic levels generated by rocket engines of the general type from which it was derived (small rocket engines with exhaust velocities on the order of Mach 2) but for the current and future classes of propulsive systems, sound pressure levels obtained utilizing this power spectrum function are too low and shifted toward higher frequencies. The proposed modification attempting to accommodate the flow mixing by the multiple engines of a booster stage is presented in reference 3. The current treatment utilizes a model consisting of (1) a large nozzle with the same flow volume, but with a diameter corresponding to an exit area equal to the total exit area of all engines; and (2) multiple acoustic source chains, one for each operating engine. Numerical addition of the mean square pressures predicted for the single equivalent engine and those predicted for a sum of separate engines agrees very well with available empirical data of the Saturn IB and Saturn V systems. This prediction technique yields a broader spectrum than that from reference 3 and may exhibit double peaks, one frequency peak corresponding to an effective engine diameter $D_{eff} = D(N)^{1/2}$ and one corresponding to a single engine diameter. The decay of sound pressure levels with distance for lower frequencies is also less than that of reference 3 but is in good agreement with Saturn V measured data.

Empirical liftoff indices must be introduced to modify the sound field distribution subsequent to holddown release and prior to free flight. A relationship to determine the amplitude of this effect as a function of height above the launch pad, frequency and vehicle velocity (figure 4) has been calculated from existing Saturn flight data, reference 8. Other directivities (angular field distributions) resulting from the deflector configuration and location with respect to exhaust may be considered. However, since orientation of the booster with respect to its exhaust is not necessarily the same during checkout firings and launch, only the sound pressure levels on the side of the vehicle toward the exhaust are predicted.

A "near-field" factor (figure 5) is also defined to modify values in the reactive portion of the acoustic field near the source where corrections must be incorporated.

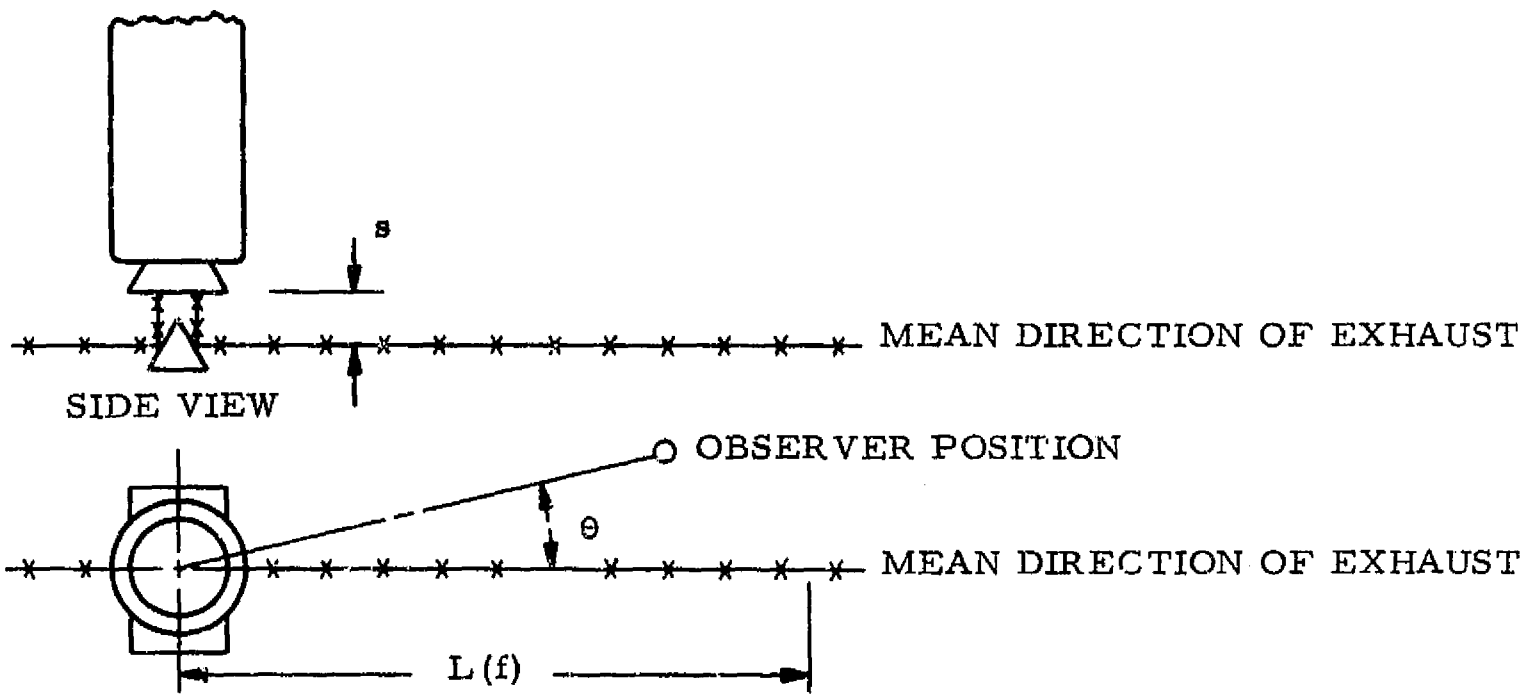

FIGURE 1. ACOUSTIC SOURCE PREDICTION GEOMETRY

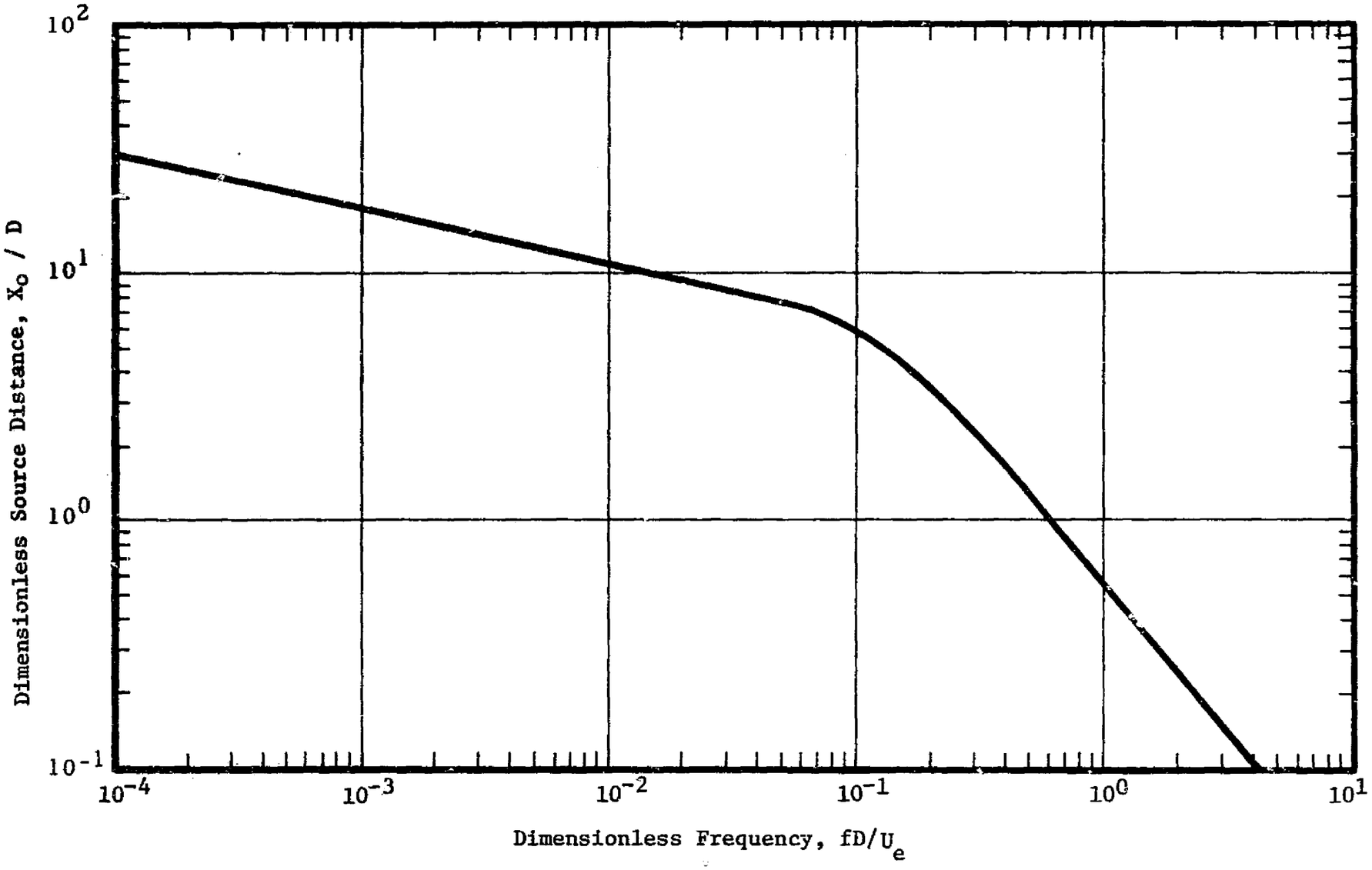

FIGURE 2. APPARENT ACOUSTIC SOURCE DISTANCE

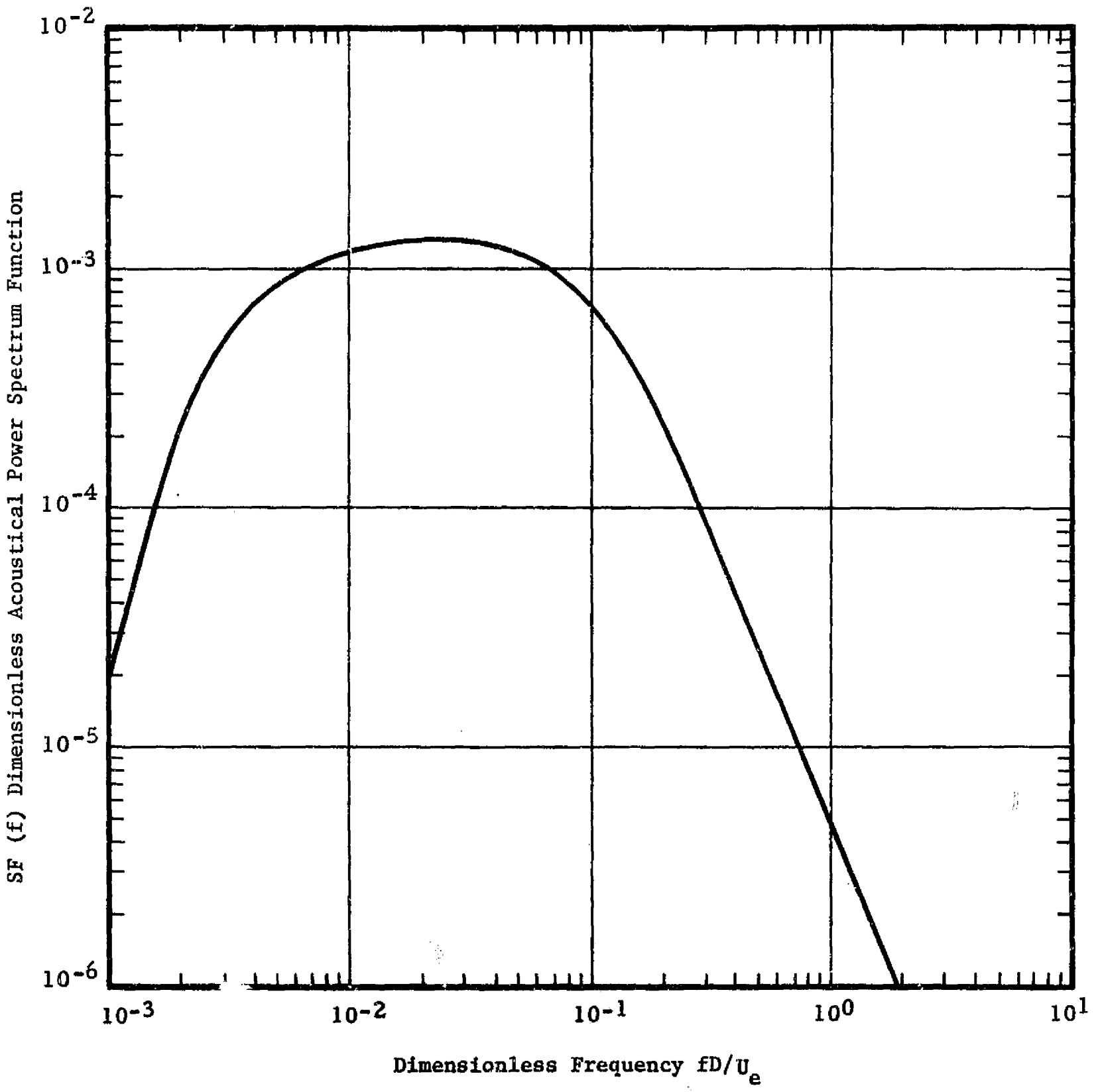

FIGURE 3. APPARENT ACOUSTIC POWER SPECTRUM FUNCTION

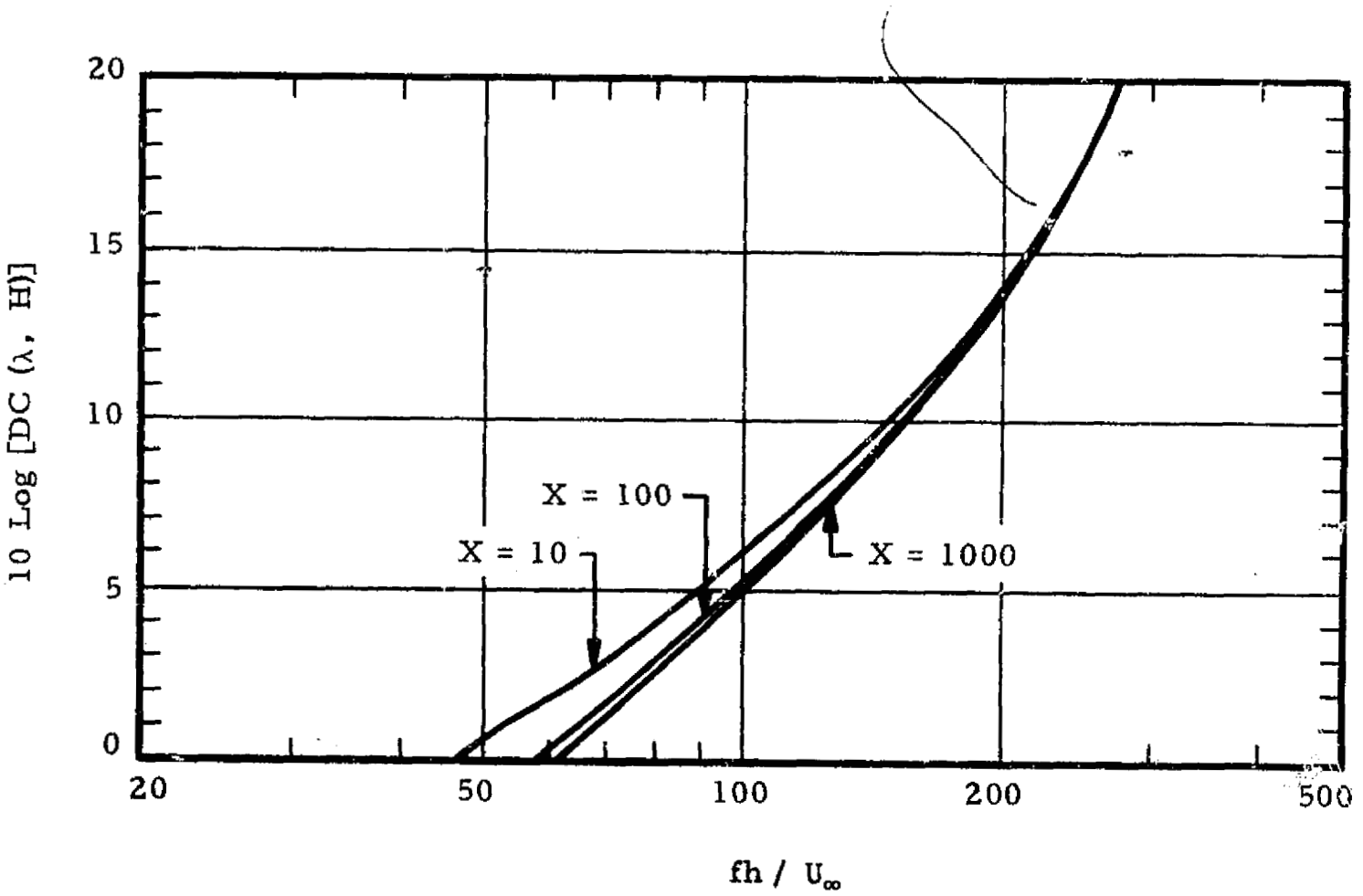

FIGURE 4. DIRECTIVITY CORRECTION SUBSEQUENT TO HOLDDOWN RELEASE

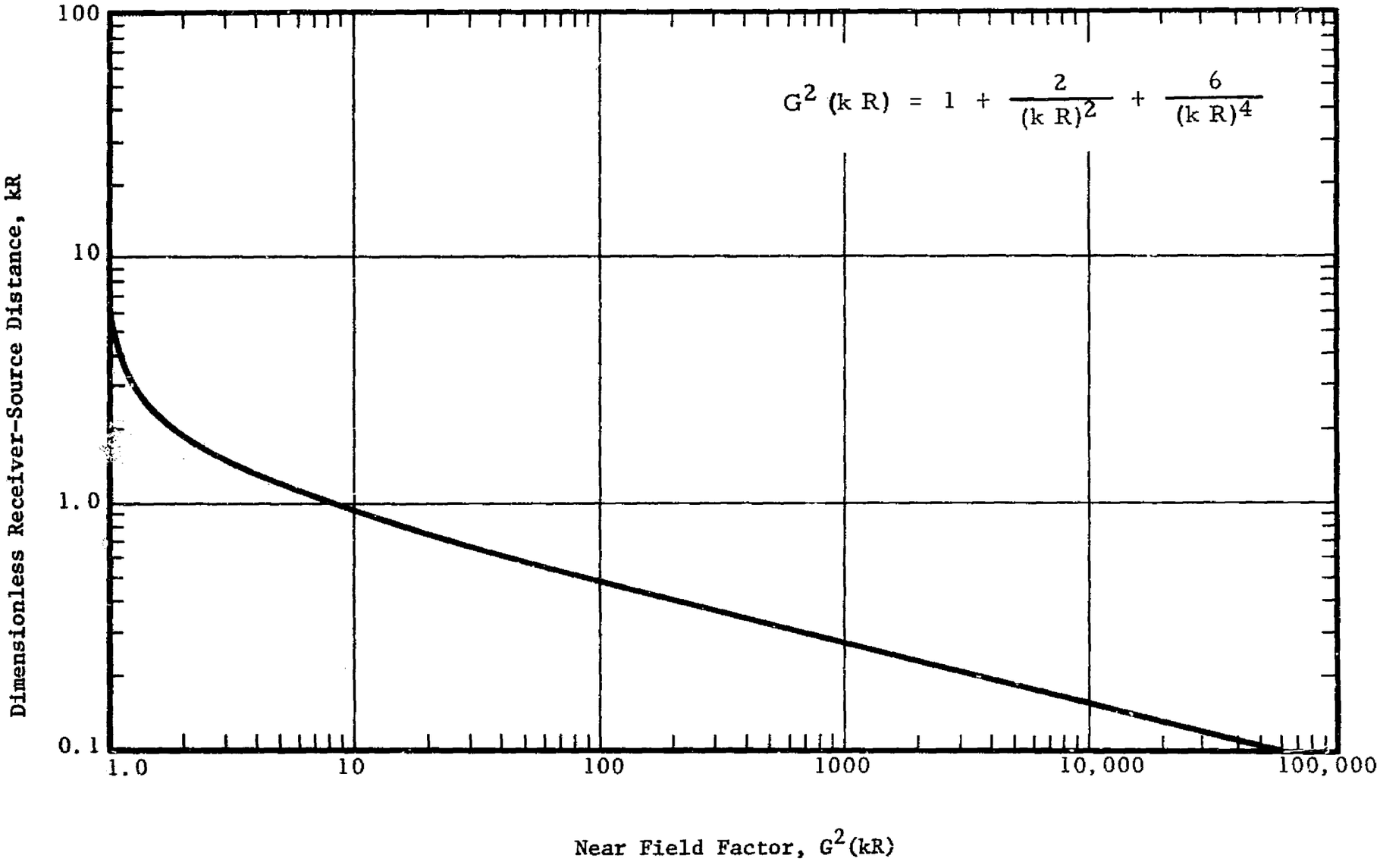

FIGURE 5. ROCKET ENGINE ACOUSTICAL NEAR FIELD FACTOR

The mean square sound pressure $(lb/ft^2)^2$ over a frequency bandwidth Δf at a particular location is given by:

$$p^2(f_i,\Delta f) = p_1^2 + p_2^2 \tag{1}$$

$$p_1^2(f_i,\Delta f) = \frac{SF(f)\ DT^2\ N\ \rho_o c_o\ g\ G^2(kR)\ \Delta f\ \Phi(r,\Theta,f)}{2U_e\ \dot{\omega}\ R^2(r,\Theta,f)}\ e^{-\alpha(f)R} \tag{2}$$

$$p_2^2(f_i,\Delta f) = \frac{SF(f)\ D_{eff}\ T_t^2\ \rho_o c_o\ g\ G^2(kR)\ \Delta f\ \ \Phi(r,\Theta,f)}{2U_e\ \dot{\omega}_t\ R^2(r,\Theta,f)}\ e^{-\alpha(f)R} \tag{3}$$

where

$$R = (r^2 + L^2(f) - 2\ rL\ \cos\ \theta)^{1/2},\ R \geq 1$$

$$L(f) = X_o(f) - s$$

Substituting appropriate values for ρ_o, c_o, and g, the acoustical power spectral densities become

$$p_1^2(f) = 42\ \frac{SF(f)\ D\ T^2\ N\ G^2(kR)}{U_e\ \dot{\omega}\ R^2} \tag{4}$$

$$p_2^2(f) = 42\ \frac{SF(f)\ D_{eff}\ T_t^2\ G^2\ (kR)}{U_e\ \dot{\omega}_t\ R^2} \tag{5}$$

NOTE: SF(f) and R are not identical for (4) and (5). The numerical values in (4) are derived from single engine data; a single hypothetically equivalent system is utilized to derive the numerical values of (5). The absorption is set equal to one for simplicity, and the uniform directivity (after liftoff) around the vehicle surface is utilized.

The longitudinal correlation of acoustic surface pressures may be estimated by cos $k(x-x_o)$. The lateral correlation is estimated to be substantially greater than the longitudinal coefficient as equal wave fronts may be visualized propagating along the vehicle surface from the acoustic source. Figures 6 and 7 present empirically verified octave band longitudinal and lateral correlations of rocket engine noise. The eventual loss of correlation as the circumferential distance is increased is caused by (a) the shielding effect of the vehicle and (b) the lack of coherency for various regions of a sound source of large spatial extent.

In addition to the liftoff modification previously discussed (figure 4), engine-generated sound pressure levels during flight are decreased due to:

(a) An effective increase in the apparent source distance which occurs as the vehicle freestream velocity increases with respect to the speed of sound. The resultant decrease in the acoustic environment is produced by multiplying the numerator of equations (4) and (5) by $(1 - U_\infty/c)^2$ where U_∞ is the vehicle freestream velocity.

(b) A decrease in the shear velocity which occurs as the vehicle speed increases. This decrease is on the order of $(1 - U_\infty/U_e)^4$ where the exponent 4 applies in the vicinity of the vehicle surface. This decrease, however, is small compared to that discussed in the previous paragraph and it is usually ignored since engine generated acoustic pressures will not be propagated to the vehicle when $U_\infty/c > 1.0$.

2. Boundary Layer Noise

Estimation of unsteady flight pressures at the surface of a space vehicle is facilitated by the categorization of aerodynamic sources - attached turbulent boundary layer, separated flow, wakes, and shock wave oscillation. Shock wave oscillation and wake environmental characterization are treated in subsequent paragraphs. Attached turbulent boundary layer noise and unsteady pressures due to separated flow conditions are basically similar and are discussed below.

Consider the instantaneous acoustic pressure $p(x_1, x_2, t)$ at a position x_1, x_2 on a flat rigid surface with an attached turbulent boundary layer, homogeneous in both time and space. The normalized cross-correlation coefficient is:

$$\xi(x_1, x_2, t) = \frac{1}{\overline{p^2}} \left\langle p(x_1, x_2, t)\, p(x_1 + \Delta x_1, x_2 + \Delta x_2, t + \Delta t) \right\rangle \qquad (6)$$

from which a wave number-frequency spectrum is obtained by Fourier transform

$$\Xi(k_1, k_2, \omega) = \frac{1}{(2\pi)^3} \int_{-\infty}^{\infty} \int_{-\infty}^{\infty} \int_{-\infty}^{\infty} \xi(x_1, x_2, t) \exp\left[-i(k_1 x_1 + k_2 x_2 - \omega t)\right] dx_1 dx_2 dt \qquad (7)$$

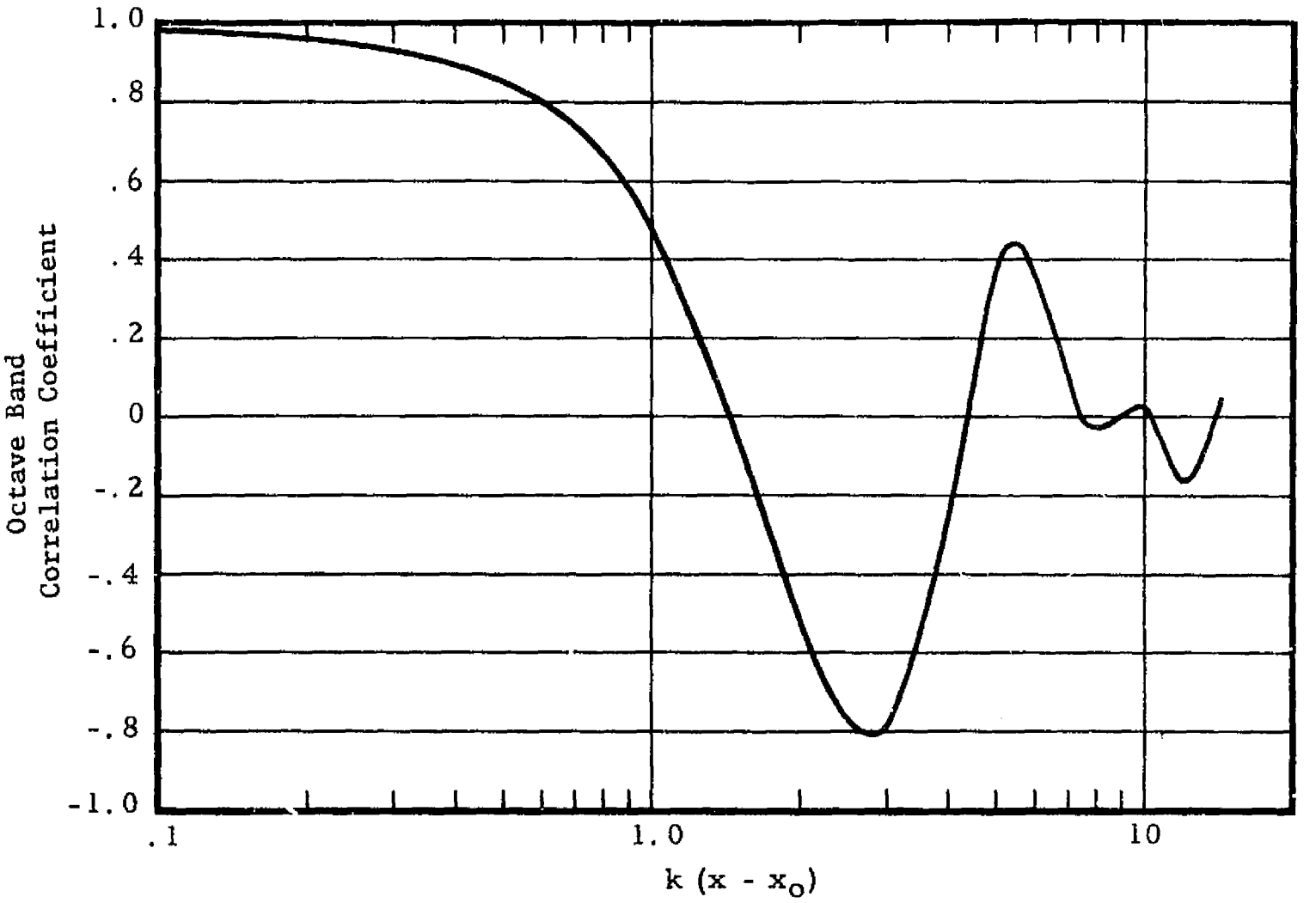

FIGURE 6. EMPIRICALLY VERIFIED LONGITUDINAL CORRELATION OF ROCKET ENGINE NOISE

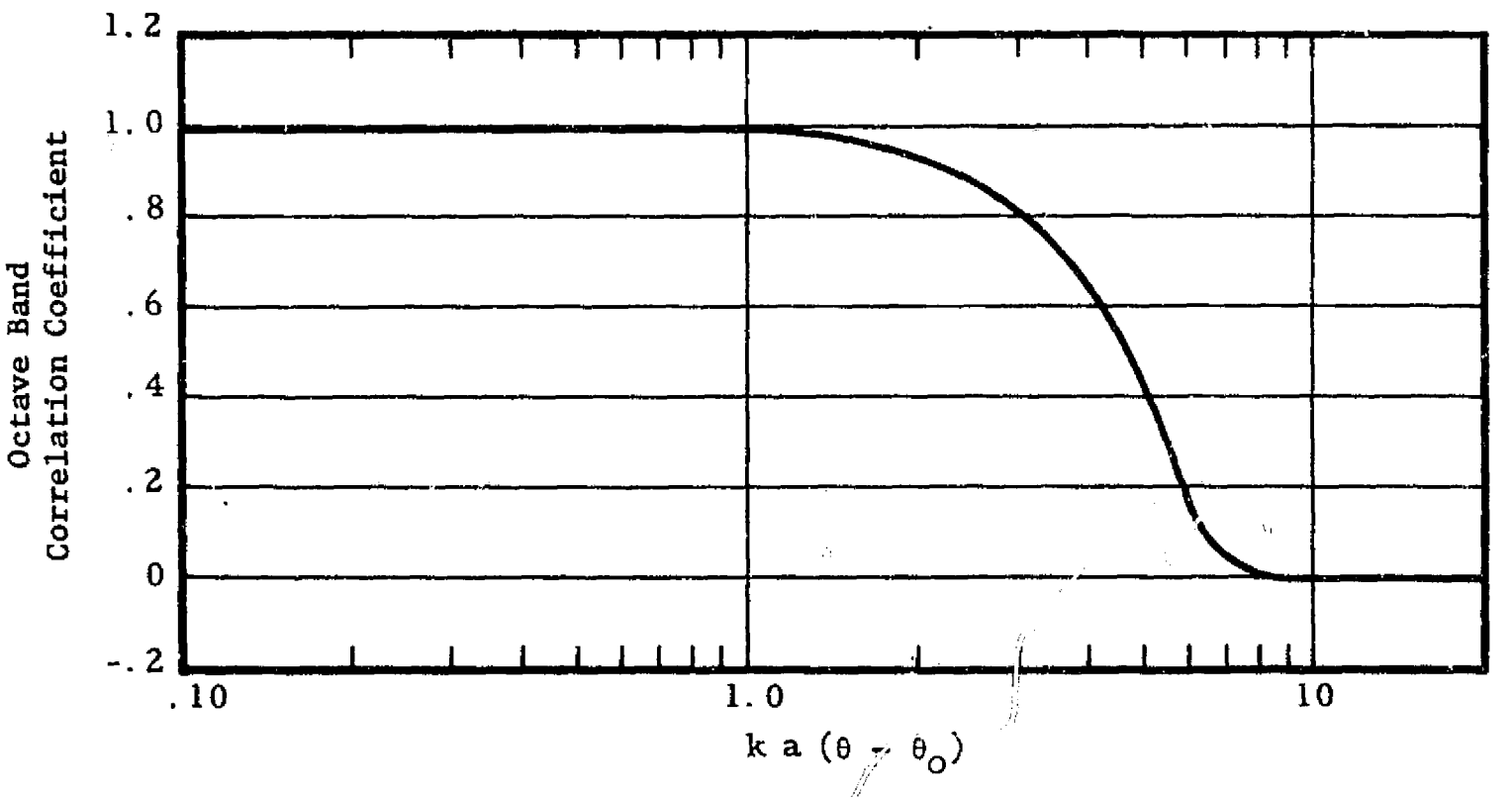

FIGURE 7. EMPIRICAL LATERAL CORRELATION OF ROCKET ENGINE NOISE

Several specialized forms of correlation coefficient and associated spectra are more recognizable:

(a) Flow-wise spatial correlation and cross-power spectral density

$$\Xi_1(k_1) = \frac{1}{2\pi}\int_{-\infty}^{\infty} \xi_1(x_1)\ \exp\ [-ik_1x_1]dx_1 \tag{8}$$

where

$$\xi_1(x_1) = \xi\ (x_1,0,0)$$

(b) Transverse spatial correlation and cross-power spectral density

$$\Xi_2(k_2) = \frac{1}{2\pi}\int_{-\infty}^{\infty} \xi_2(x_2)\ \exp\ [-ik_2x_2]dx_2 \tag{9}$$

where

$$\xi_2(x_2) = \xi(0,x_2,0)$$

(c) Surface correlation and cross-power spectral density

$$\Xi_{12}(k_1,k_2) = \frac{1}{(2\pi)^2}\int_{-\infty}^{\infty}\int_{-\infty}^{\infty} \xi_{12}(x_1,x_2)\ \exp\ [-i(k_1x_1 + k_2x_2)]dx_1dx_2 \tag{10}$$

where

$$\xi_{12}(x_1x_2) = \xi(x_1,x_2,0)$$

(d) Autocorrelation and power spectral density

$$\Xi_f(\omega) = \frac{1}{2\pi}\int_{-\infty}^{\infty} \xi_f(t)\ \exp\ [i\omega t]dt \tag{11}$$

$$\xi_f(t) = \xi(0,0,t)$$

(e) Analogous functions may be defined to describe the true temporal fluctuations of the convected wall pressure, which are the chief source of sound radiation and power transfer to structural elements at high frequencies.

$$\Xi'(\omega) = \frac{1}{2\pi}\int_{-\infty}^{\infty} \xi'(t)\, \exp\,[i\omega t]dt \tag{12}$$

where

$$\xi'(t) = \xi(x_1 = U_{c_1}t,\ x_2 = U_{c_2}t, t)$$

The convection velocity of eddies has been shown empirically to be dependent upon eddy size (frequency):

$$U_c(k_1)/U_\infty = 0.6 + 700(k_1\delta^* + 10)^{-3.5} \tag{13}$$

however, by choice of axes

$$U_{c_1} = U_c,\ U_{c_2} = 0 \tag{14}$$

which is supported empirically by references 9 and 11.

From equation (14)

$$\xi'(t) = \xi(U_c t, 0, t)$$

If a separable correlation model is assumed

$$\xi(x_1,x_2,t) = \xi_1(x_1 - U_c t)\ \xi_2(x_2)\ \xi'(t) \tag{15}$$

and

$$\Xi(k_1,k_2,\omega) = \Xi_1(k_1)\ \ \Xi_2(k_2)\ \ \Xi'(\omega - k_1\ U_c) \tag{16}$$

Equation (15) is not valid if eddy convection velocity is a function of frequency but a solution in the form of equation (16) is still possible.

Experimentation yields correlation functions of a type which are mathematically determinable:

$$\xi_1(x_1) = (1 - |x_1|/L_1)\ \exp\,[-\ |x_1|/L_1] \tag{17}$$

$$\xi_2(x_2) = \exp\left[-|x_2|/L_2\right] \tag{18}$$

$$\xi'(t) = \exp\left[-|t|/\theta\right] \tag{19}$$

Where L is the correlation length and θ is the mean eddy lifetime.

Corresponding wave number and frequency spectra are obtained from equations (17), (18), and (19)

$$\Xi_1(k_1) = 2\, k_1^2\, L_1^3 / \left(k_1^2\, L_1^2 + 1\right)^2 \tag{20}$$

$$\Xi_2(k_2) = (\pi L_2)^{-1} \left(k_2^2 + L_2^{-2}\right)^{-1} \tag{21}$$

$$\Xi'(\omega) = \theta/\pi\, (\omega^2\theta^2 + 1) \tag{22}$$

These spectra have been evaluated utilizing empirical values (references 9, 10, 11, 12) with $\theta = 9\ \delta^*/U_\infty$ and $L_1 = L_2 = 2\delta^*$, and are shown in figures 8, 9, and 10.

The unsteady pressure spectrum at a fixed point on the vehicle is

$$\Xi_f(\omega) = \int_{-\infty}^{\infty}\int_{-\infty}^{\infty} \Xi(k_1,k_2,\omega)dk_1\, dk_2 = \int_{-\infty}^{\infty} \Xi_1(k_1)\, \Xi'(\omega - k_1U_c)dk_1 \tag{23}$$

Upon substitution and integration

$$\Xi_f(\omega) = \frac{1}{\pi}\left(\frac{20}{11}\,\sigma\,\omega^2 + \frac{2}{11}\,\sigma^3\right)\left(\sigma^2 + \omega^2\right)^{-2} \tag{24}$$

where

$$\sigma = 11\ U_c/18\ \delta^*$$

This function is presented graphically by figure 11.

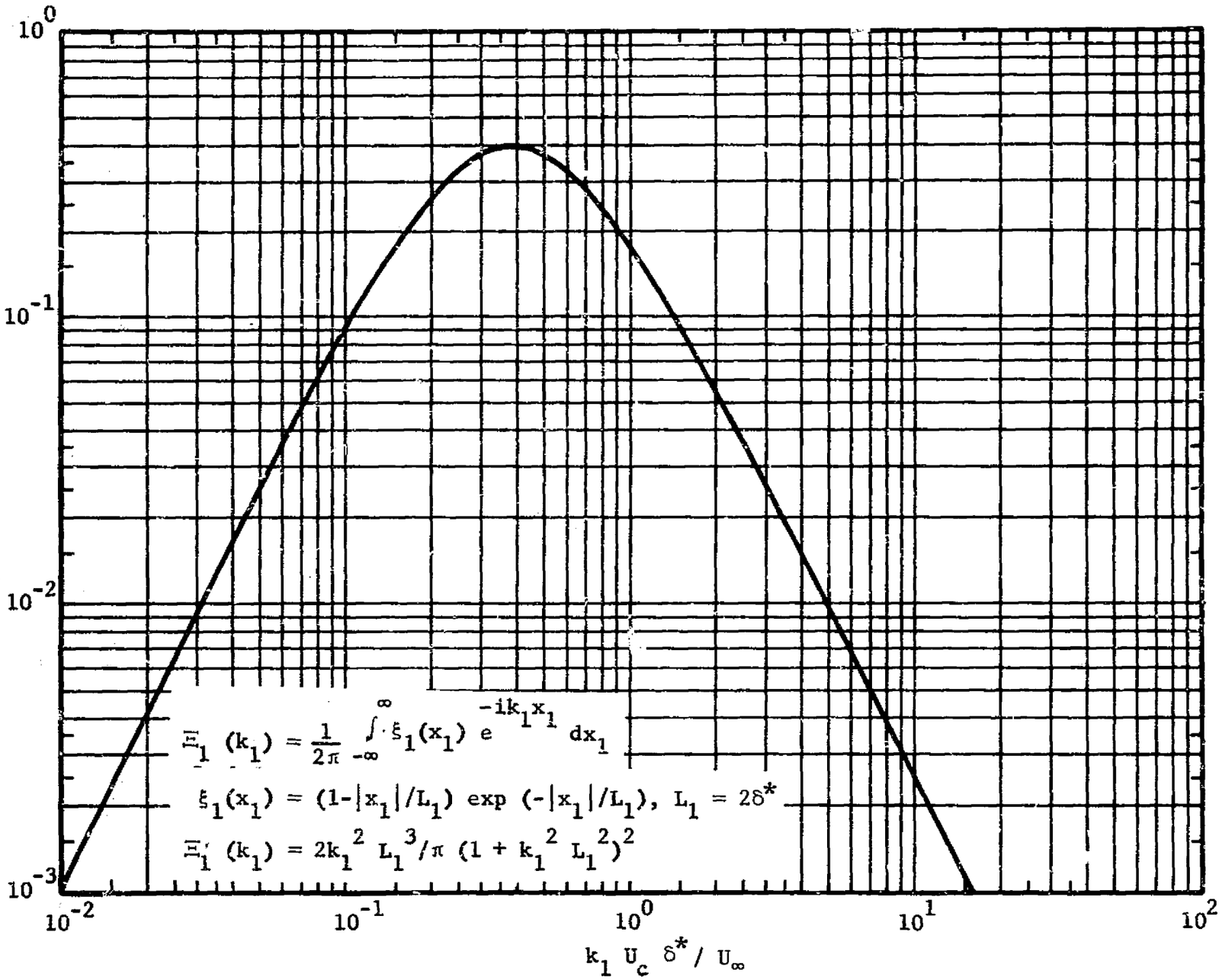

FIGURE 8. LONGITUDINAL BOUNDARY LAYER NOISE WAVE NUMBER SPECTRUM

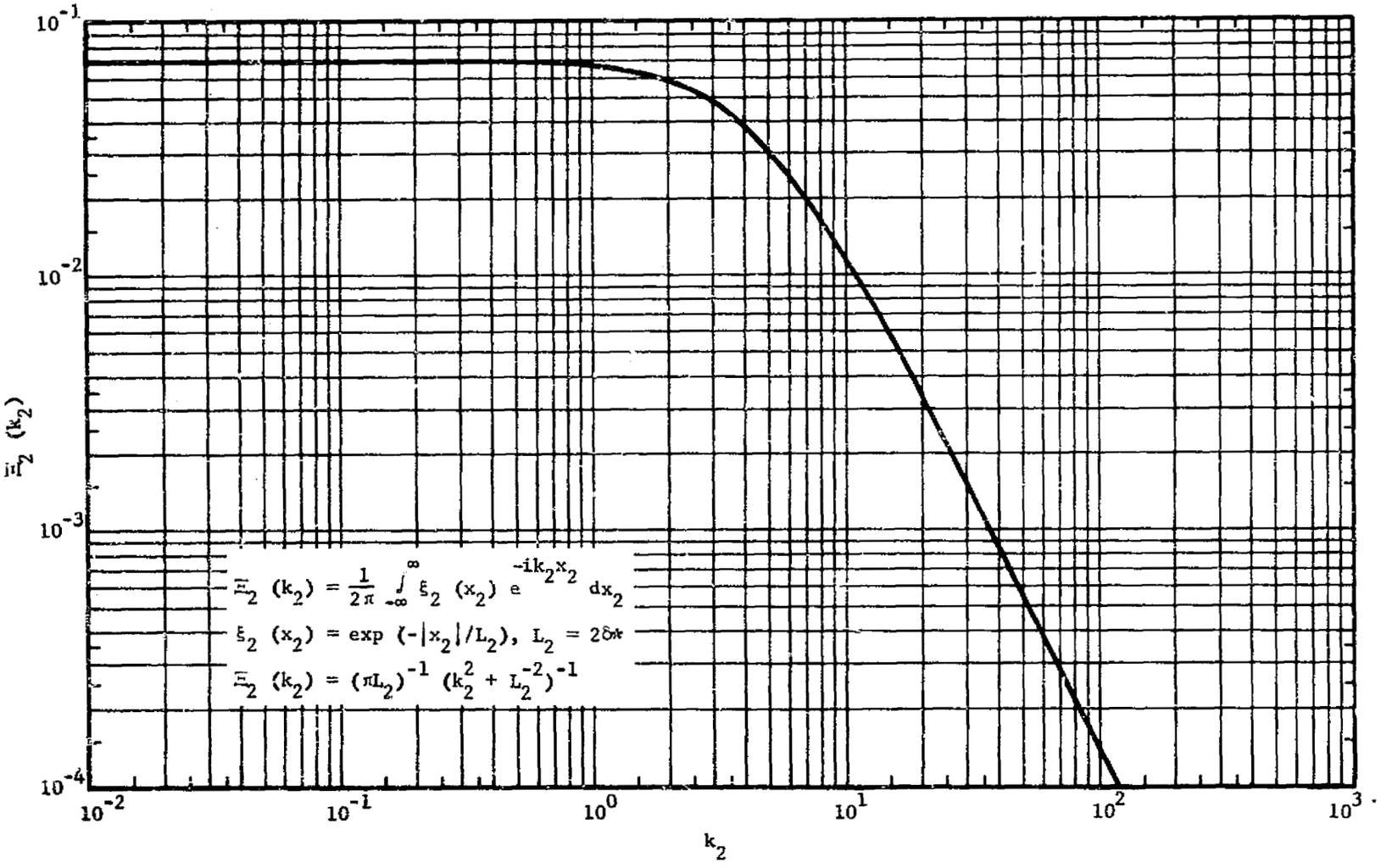

FIGURE 9. TRANSVERSE BOUNDARY LAYER NOISE WAVE NUMBER SPECTRUM

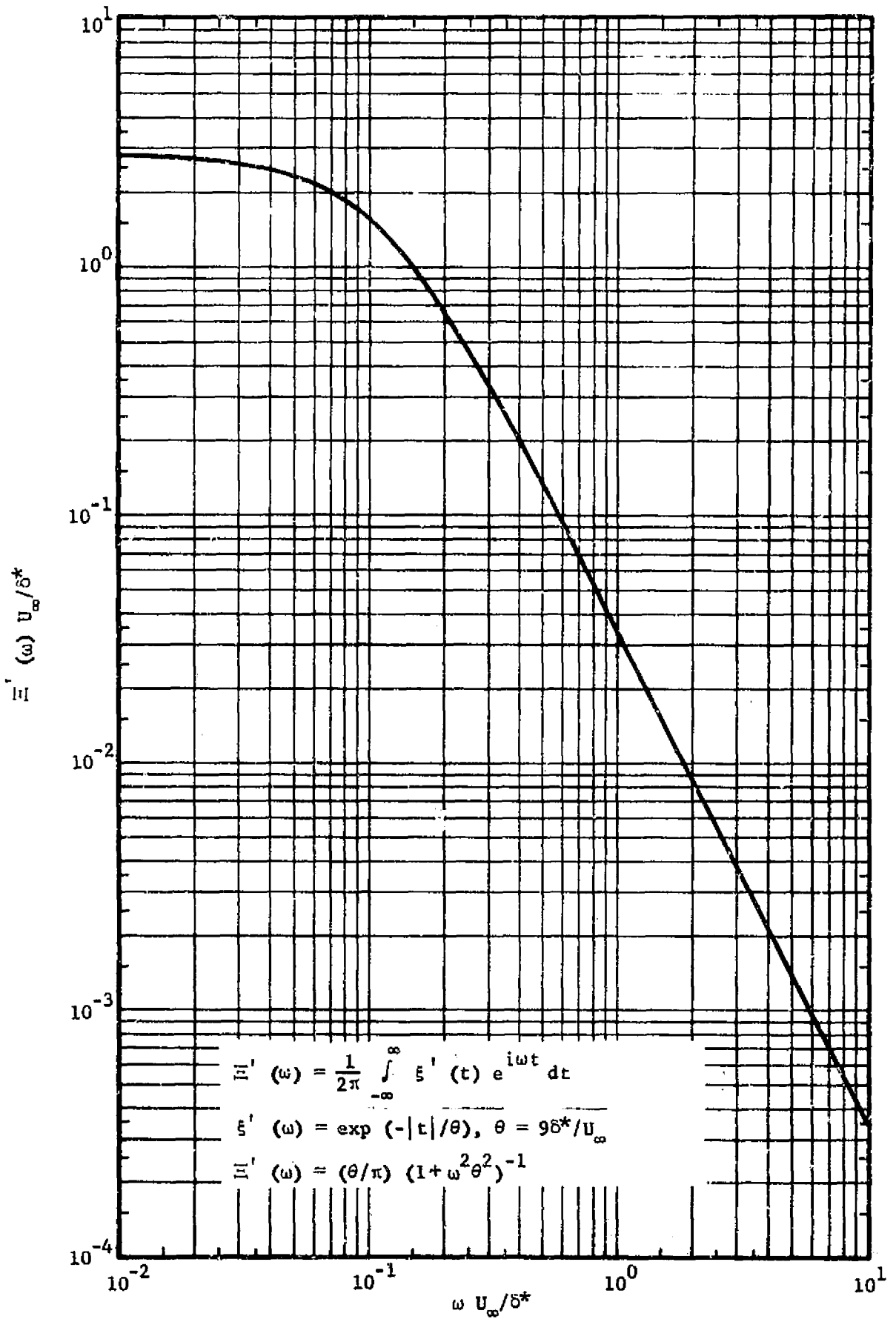

FIGURE 10. MOVING AXIS TURBULENCE SPECTRUM

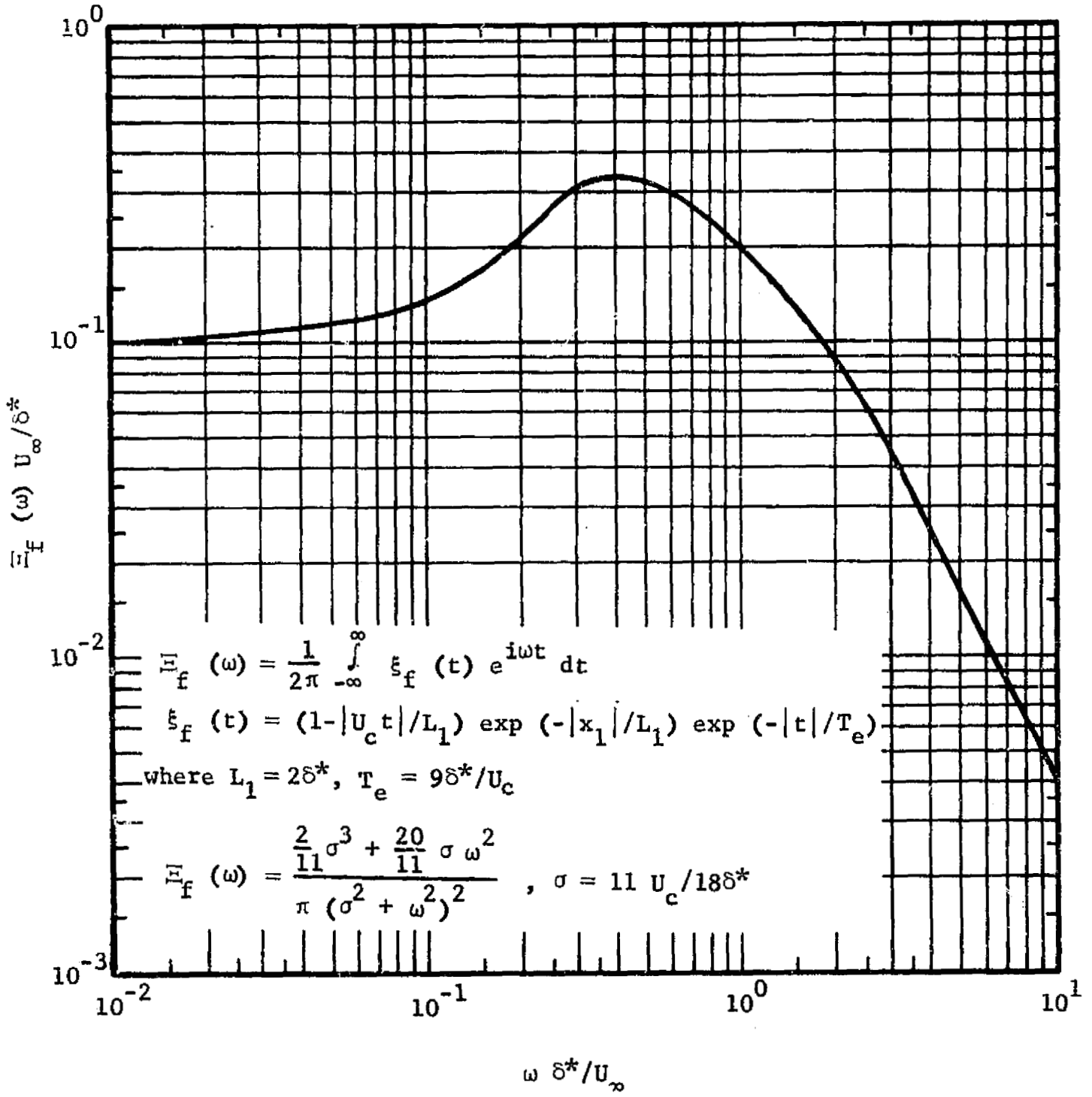

FIGURE 11. FIXED POSITION POWER SPECTRAL DENSITY

Direct measurement of $\Xi_f(\omega)$ necessitates correction due to the finite surface area of the transducer. Figure 12 shows corrected nondimensional measured power spectral density, $W(f) = p^2(f)/p^2_{OA}\ \Delta f$, in terms of the nondimensional f δ^*/U_c. For comparison purposes

$$\Xi_f(\omega) = W_f(f)/4\pi \tag{25}$$

which includes a factor of 2 since $\Xi_f(\omega)$ includes both positive and negative frequencies and a factor of 2π to convert from radians per unit time to Hertz. Figure 13 shows $\Xi'(\omega)$ and $\Xi_f(\omega)$ converted to the dimensions of the measured quantities.

$$W'(f) = 4\pi[\Xi'(\omega)] = 4\theta\ (1 + \omega^2\theta^2)^{-1} \tag{26}$$

$$W_f(f) = 4\pi[\Xi_f(\omega)] = 8\sigma\ (10\omega^2 + \sigma^2)/11(\sigma^2 + \omega^2)^2$$

The good agreement of $W_f(f)$ with the measured boundary layer noise spectra ($f\ \delta^*/U_\infty > .02$) implies that $W'(f)$ is a good approximation to the moving axis spectrum.

Given the normalized boundary layer spectrum above a rigid surface, the total mean square acoustic pressure must be related to flow parameters in order to compute the pressure spectral density. Figure 14 shows the overall rms pressure normalized to the wall shear stress, $\tau_o = 0.5\ \rho\ U_\infty^2\ c_f$, as a function of Mach number, where c_f is the local coefficient of skin friction. The following formulae for boundary layer displacement thickness and local coefficient of friction enable the computation of boundary layer noise for a flight vehicle with attached or separated turbulent boundary layer flow:

Smooth Flat Plate (reference 13)

$$\begin{aligned} \delta^* &= 0.4625\ x\ (U_\infty x/\nu)^{-0.2} \\ c_f &= 0.02296\ (U_\infty x/\nu)^{-0.139} \end{aligned} \tag{27}$$

Attached Turbulent Boundary Layer (reference 2)

$$\begin{aligned} \delta^* &\sim 0.0525\ x\ (U_\infty x/\nu)^{-0.2} \\ c_f &\sim 0.036\ (U_\infty x/\nu)^{-0.139} \end{aligned} \tag{28}$$

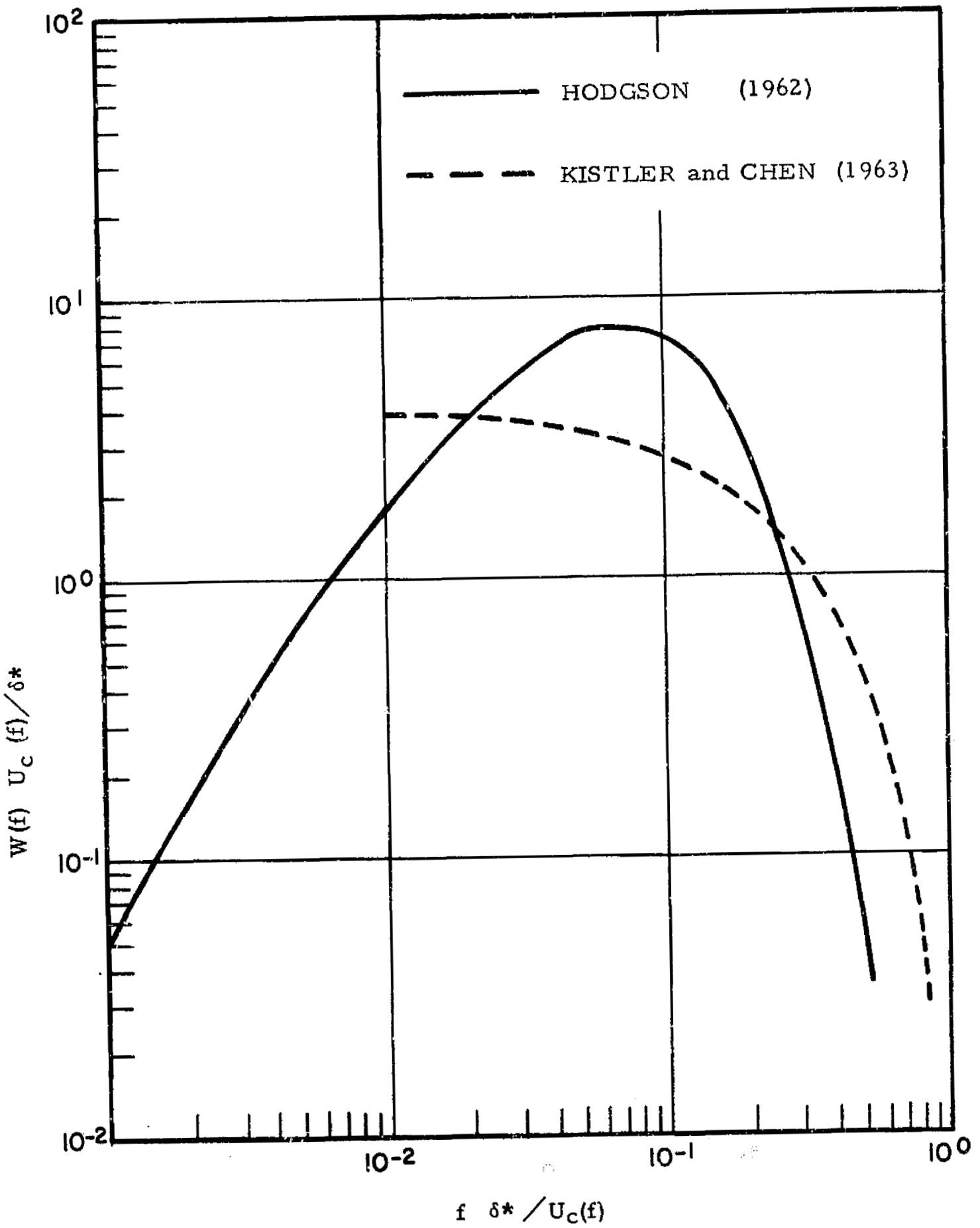

FIGURE 12. NONDIMENSIONAL MEASURED ACOUSTIC SPECTRA

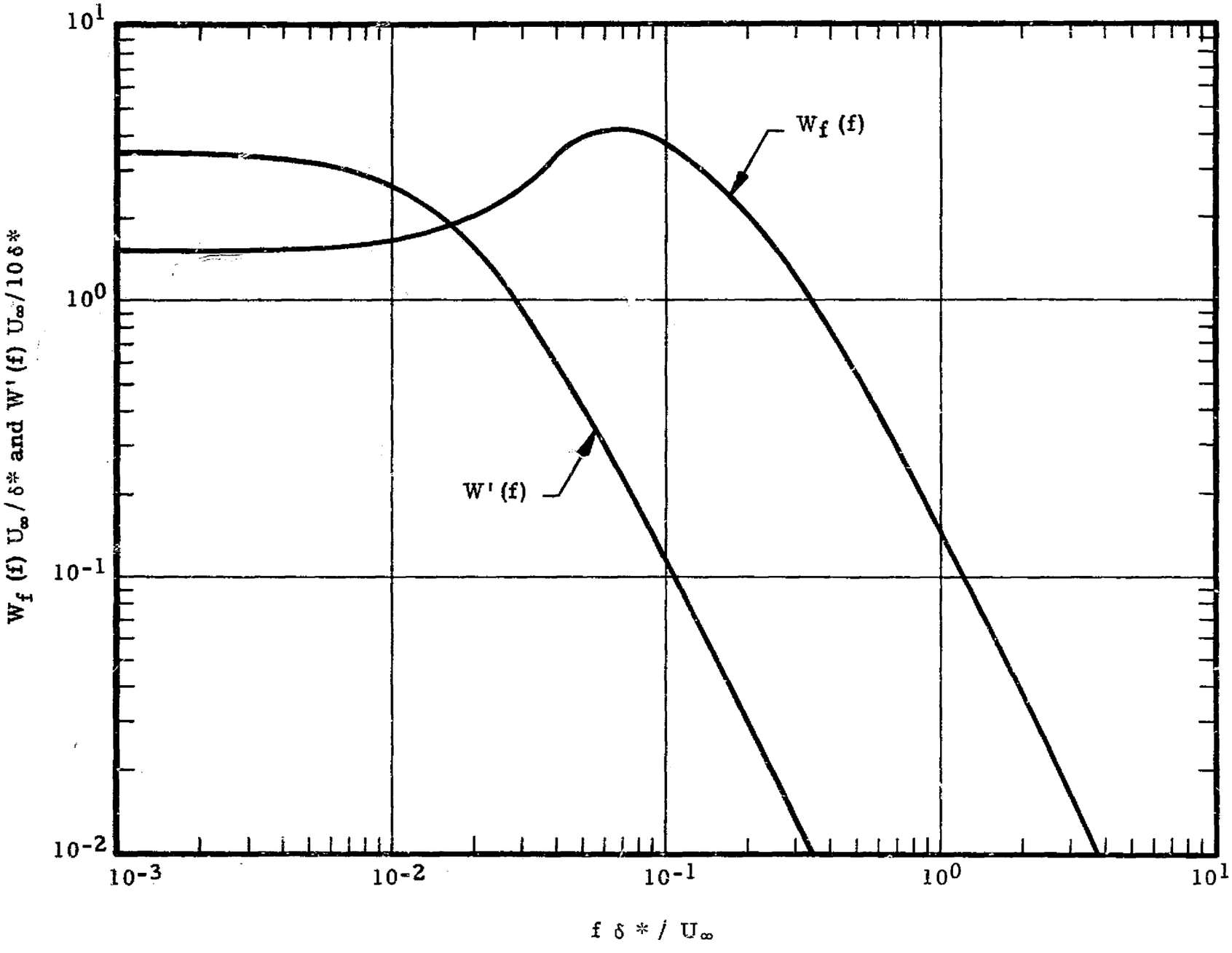

FIGURE 13. THEORETICAL SPECTRA IN MEASURED DIMENSIONS

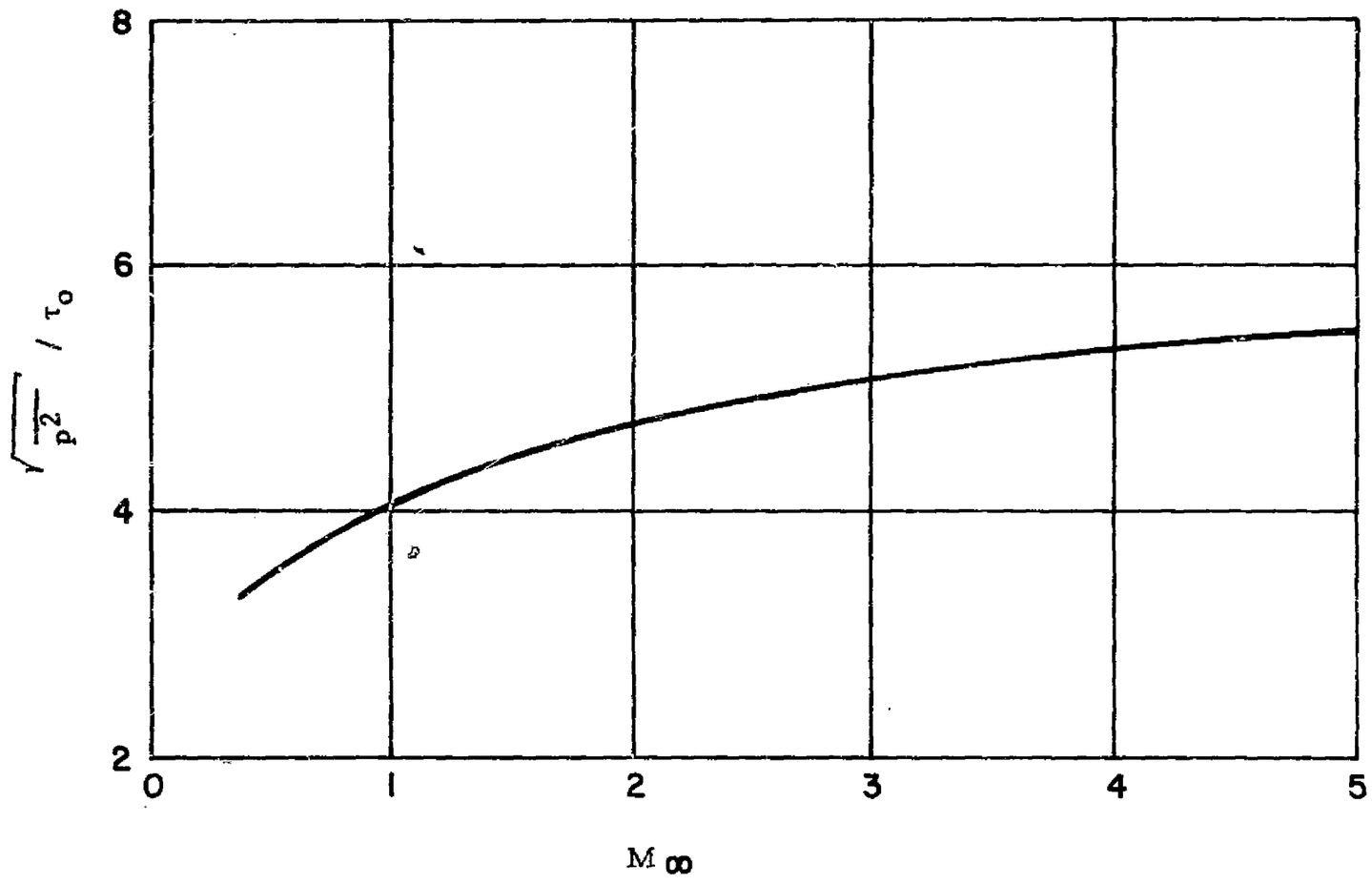

FIGURE 14. MACH NUMBER VARIATION OF NORMALIZED COMPOSITE ROOT-MEAN-SQUARE WALL PRESSURE FLUCTUATIONS

Separated flow (reference 2)

$$\delta^* \sim 0.139 \times (U_\infty x/\nu)^{-0.2}$$
$$c_f \sim 0.072 \ (U_\infty x/\nu)^{-0.139} \qquad (29)$$

3. Oscillating Shock Waves

Fluctuating pressures of unsteady shock waves have been studied empirically by reference 14. The mean shock wave position (figure 15) and composite pressure coefficient (figure 16) were defined. However, the position of the shock can be defined analytically:

$$x_i/D = 10^{[6M_\infty + 3.15 \log (\theta/15) - 5.7]} \qquad (30)$$

for

$$0.65 \leq M_\infty \leq 1.0$$

and

$$5^o \leq \theta \leq 30^o$$

The data of figure 16 can be fitted satisfactorily by combining the relationship of the pressure at $x_i/D = 0$ (p_{OA_o}) relative to q,

(31)

$$20 \log p_{OA_o}/q = -30.5 + 0.7 \ \theta \ dB$$

and the variation of overall sound pressure level relative to that at $x_i/D = 0$ which is given by

$$20 \log p_{OA}/p_{OA_o} = -30 \log [1 + 3.04 \ (x_i/D)] \qquad (32)$$

yielding

$$p_{OA}^2 = q_\infty^2 \ 10^{.07\theta - 3.05} / (1.0 + 3.04 \ x_i/D)^3 \qquad (33)$$

for

$$-0.1 \leq x_i/D \leq 1.2$$

and

$$5^o \leq \theta \leq 30^o$$

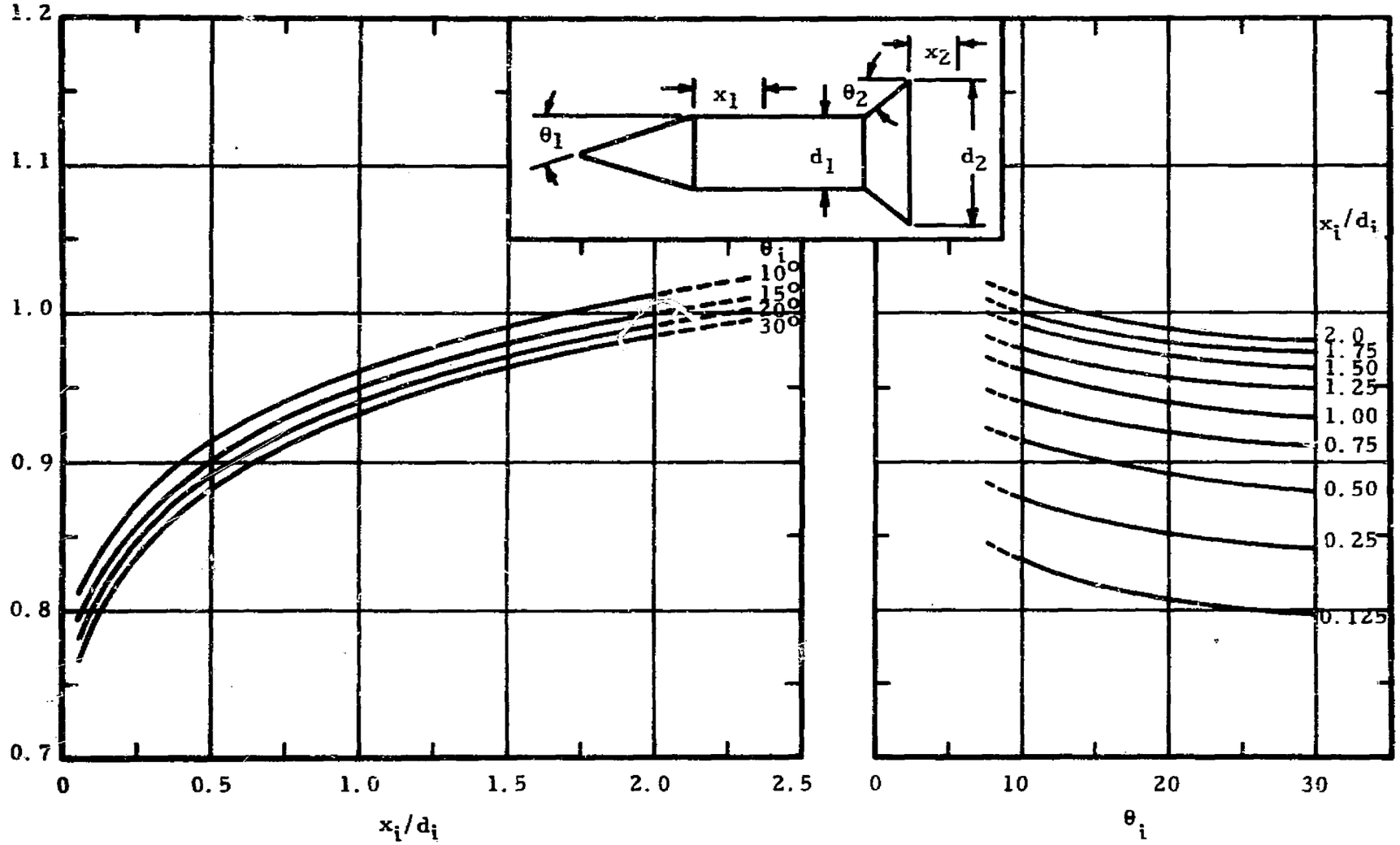

FIGURE 15. MACH NUMBER FOR MAXIMUM SHOCK-INDUCED SOUND PRESSURE LEVEL, GIVEN TRANSITION ANGLE, AND NONDIMENSIONAL DISTANCE AFT OF SHOULDER

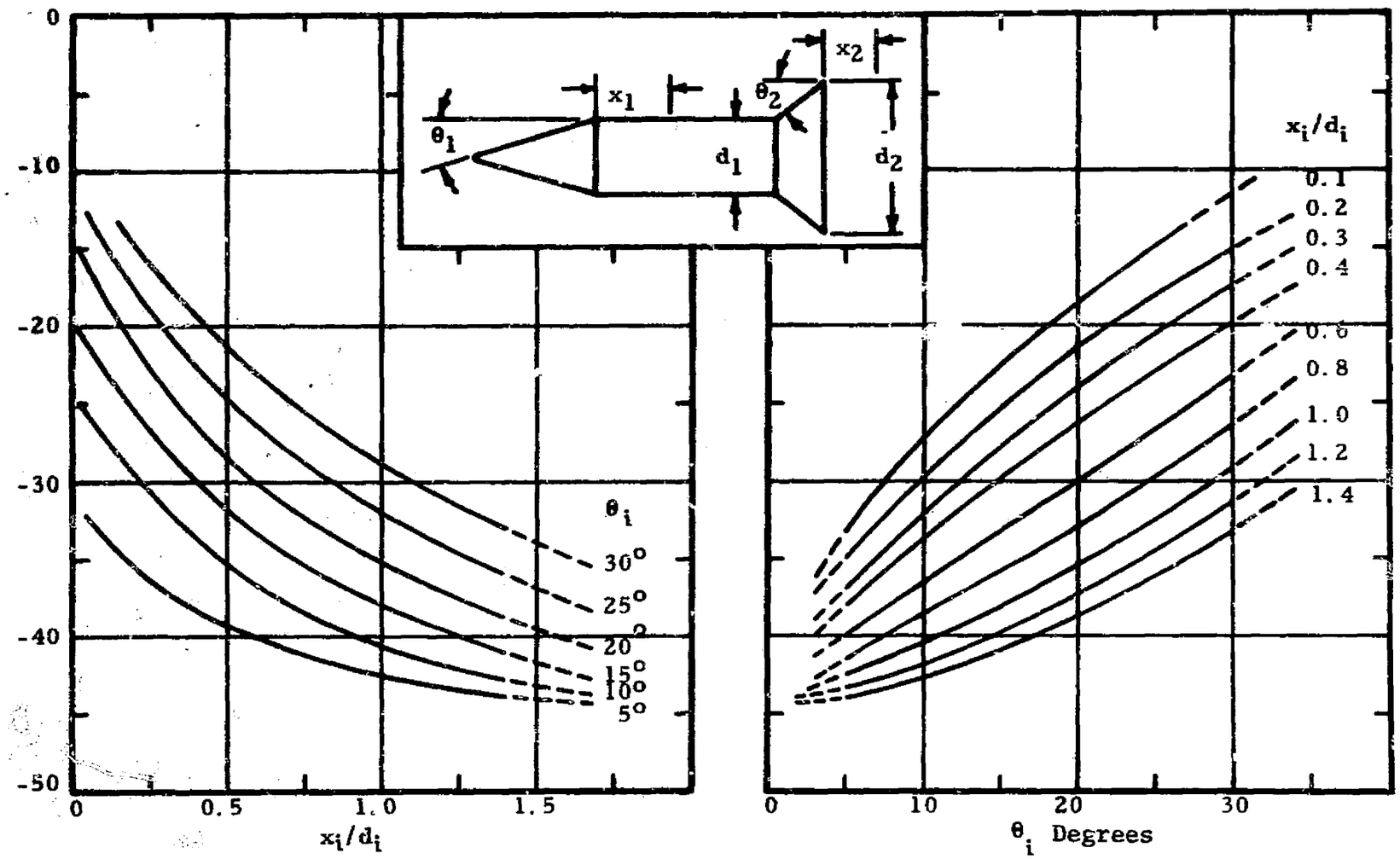

FIGURE 16. DEPENDENCY OF MAXIMUM SHOCK-INDUCED PRESSURE COEFFICIENT ON TRANSITION ANGLE AND NON-DIMENSIONAL DISTANCE AFT OF SHOULDER

The normalized spectral density is given by

$$W_s(f) = p^2(f)/p_{OA}^2 = 4\beta/(\omega^2 + \beta^2) \tag{34}$$

where

$$\beta = 0.617\ x_i U_\infty/D$$

x_i and D are in ft, U_∞ in ft/sec, f in Hz,

q_∞ in lb/ft^2 and θ in degrees

The fluctuating shock pressure spectrum level is

$$10 \log S_s(f) + 127.582 \tag{35}$$

where

$$S_s(f) = p_{OA}^2\ W_s(f)$$

and for x_i/D between the shoulder and the mean shock location, $S_s(f)$ should be evaluated at the location of the shock wave.

For x_i/D aft of the shock wave the actual value of x_i/D should be inserted into the following equations:

Combining (32) and (35) yields

$$S_s(f) = \left\{q_\infty^2\ 10^{(0.07\theta - 3.05)}/(1.0 + 3.04\ x_i/D)^3\right\}\left\{4\beta/(\omega^2 + \beta^2)\right\} \tag{36}$$

and simplifying

$$S_s(f) = \frac{10^{0.07\theta}\ \gamma\ q_\infty^2}{(16180\ f^2 + 156\ \gamma^2)(1 + 3.04\ \gamma/U_\infty)^3} \tag{37}$$

where

$$\gamma = x_i U_\infty/D$$

One-third octave band sound pressure levels may be obtained from

$$10 \log [fS_s(f)] + 121.22$$

and the overall sound pressure level may be calculated

$$\text{OA SPL} = 10 \log \int_0^\infty S_s(f)\, df + 127.582$$

or equivalently

$$10 \log \left[\sum_i f_i\, S_{si}\, (f)\right] + 121.22$$

The above analysis seems more satisfying than utilization of a group of charts and is directly related to observable physical phenomena. These equations agree well with measured wind tunnel model data (references 14, 15, and 16) and empirical data from full scale space vehicle measuring programs (references 6 and 17). Coherency of the fluctuating pressure associated with an oscillating shock wave has not been adequately defined at present; hence a conservative estimate of unity within the shock wave oscillation may be utilized. The rms travel σ of the shock wave has been estimated $\sigma = 0.125\ x_i$, (reference 17).

4. Wake Impingement

The fluctuating pressure environment of a wake has been investigated (references 19 and 20). Results suggest that Reynolds and Strouhal numbers based on wake momentum thickness characterize wakes from a wide class of symmetric bodies. At very low Reynolds numbers, $R < 100$, the large eddy structure dominates the wake. Experiments show that the Strouhal number of the peak frequency (constant percentage bandwidth spectra) continues to increase with Reynolds number and then stablizes at a value of 0.2 for $R \geq 8 \times 10^3$. Since the Reynolds number for space vehicle systems greatly exceeds the sensitive range, a Strouhal number $S = fd/U_\infty = 0.2$ based on the tower diameter can be utilized. Figure 17 presents a non-dimensional spectrum for wake impingement. The rms pressure coefficient (i.e. rms fluctuating pressure divided by freestream dynamic pressure) for wake impingement is approximately 0.1. Correlation coefficients similar to jet engine noise may be anticipated.

5. Compartment Noise

The acoustic fields to which components within a compartment are exposed are composed of a combination of hydrodynamic pressure fields, standing wave fields and reverberant acoustic fields. Internal acoustic fields are functions of the external pressure fields averaged over all external area, the mean transmission loss of the exterior wall structures, the energy absorption characteristics of the interior surfaces and the characteristic acoustic impedance of the medium internal to the compartment. The acoustic field, for frequencies less than the fundamental acoustic resonance (i.e, where the acoustic wave length is equal to or larger than twice the maximum unrestricted compartment dimension), can be classified as a hydrodynamic pressure field. Since the compartment is not large enough to support acoustic wave motion, the oscillating pressure field which exists will be of nearly equal phase throughout the enclosed volume and no increases due to reflection will occur at compartment boundaries.

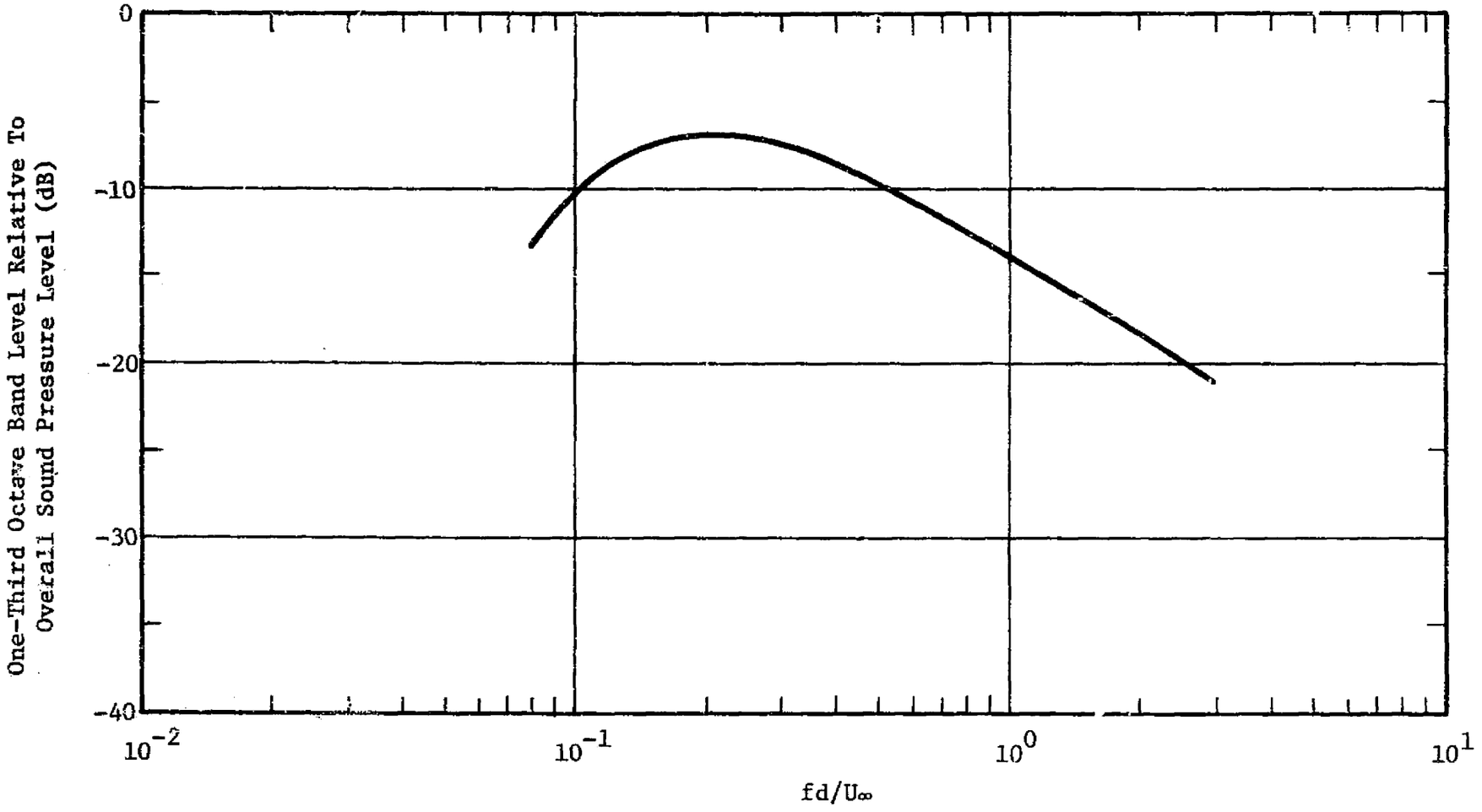

FIGURE 17. NONDIMENSIONAL SPECTRUM FOR WAKE IMPINGEMENT

At the compartment fundamental acoustic frequency the sound pressure level at the boundaries may be up to six dB higher than the transmitted level. Correlation coefficients can be approximated in this range by cos kx.

At higher frequencies a diffuse field will exist and the resultant mean square acoustic pressure will be proportional to the acoustic energy transmitted through the exterior walls and inversely proportional to the total surface and volume acoustic energy absorption. Correlation coefficients in a diffuse field can be expressed analytically as (sin kr)/kr.

B. Simulation Acoustic Fields

The exact characteristics of simulation acoustic fields in the laboratory or at a static firing test stand must be determined empirically. Both the acoustic pressure spectral level and the correlation coefficient should be measured at the surface of structural elements. The subsequent paragraphs portray the significant traits of particular fields.

Boundary-layer induced vibratory response of structural elements is primarily due to the turbulent energy at wave lengths near the free bending wave length of the panel. Acoustic simulation of unsteady aerodynamic loads near the panel free bending wave number is not feasible due to the discussed wave length relationships in the previous paragraph. Generally, acoustic simulation of vibratory response even in a narrow band of wave numbers about the panel bending wave number, cannot be accomplished because in the normal stationary medium (air), acoustic frequencies corresponding to such wave lengths will generally be greater than the panel response frequencies. The situation may be improved if exact simulation of the acoustic loading environment is not required, that is, if only the vibratory response simulation is desired. It can be shown that in the reverberant frequency response region of a specimen the reverberant energy may dominate the input energy in any small segment. In such cases, the response of the system will be determined by the reverberant field which is dependent primarily upon structural damping.

1. Progressive Wave

An acoustic progressive wave facility is a convenient apparatus for obtaining a relatively high level one-dimensional acoustic pressure field. If minor perturbations are ignored, the acoustic properties in such a facility with an anechoic termination will be virtually a function of only axial location. A wave front should lie along a cross section and the relative phase in the axial direction should depend upon wave number and relative distance. The correlation in the vertical and transverse direction should be unity and in the axial direction it should be cos kx. Test variables include angle of incidence i.e., testing may be performed at grazing, normal or at a prescribed angle of incidence. Thus the correlation coefficient along any particular test specimen may be varied between 1 and cos kx.

2. Reverberant

A reverberant test facility most nearly simulates the environment encountered by the equipment within a compartment of the space vehicle at higher frequencies. Such a facility produces a diffuse field i.e., the acoustic energy density approaches uniformity for all directions at central locations within the test chamber. The acoustic spectrum can be shaped, dependent upon the available power and the energy absorption characteristics of the facility. The correlation coefficient for diffuse field conditions becomes (sin kr)/kr.

3. Air Jets

The use of air jets as an acoustic source will not greatly influence response unless the test specimen is placed very near the source. That is, the use of an air jet source in a reverberation chamber will not affect the correlation coefficient in the reverberant field, etc. If the specimen is placed in the flow, the acoustic field will be due to a combination of jet noise and boundary layer noise. The direct field of an air jet is due to aerodynamic sources and can be treated similarly to the previous discussed rocket engine and boundary layer noise. Exact pressure and correlation characteristics in such an acoustic test field should be measured.

4. Wind Tunnels

Utilization of a wind tunnel facility as a technique for estimating vehicle structural response is not generally recommended. A wind tunnel facility may be utilized, however, if defined test conditions are stringently maintained and intimate judicious interpretation is applied to the resultant data.

The primary difficulty in much wind tunnel structural response simulation is the isolation of the turbulent boundary layer acoustic sources from background noise sources inherent in the operation of the facility. This difficulty is present because major transonic wind tunnel systems have not been designed to meet acoustic criteria. Figures 18 and 19 portray typical sources of unsteady pressure in continuous and blowdown wind tunnel systems.

The tunnel background noise (reference 21) is a combination of the following sources which are convected or radiated to the test specimen.

a. Component Resonance

Component resonances which are excited will perturb local flow, producing variation at the resonant frequencies.

b. Vortex Shedding

Screen, heat exchanger tubes, turning vanes, cavities and chambers may shed vortices at various tunnel operating conditions.

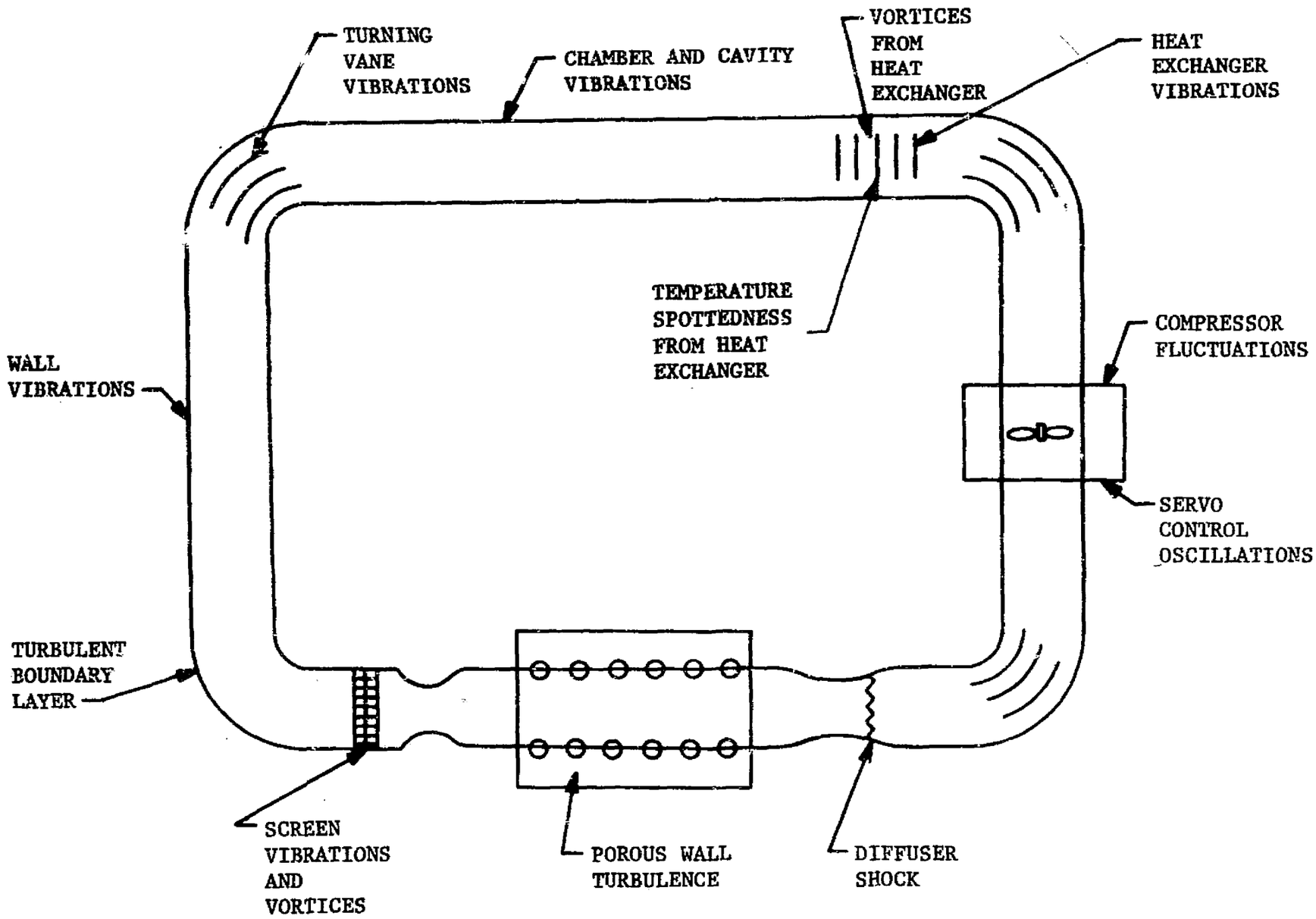

FIGURE 18. UNSTEADY PRESSURE SOURCES IN CONTINUOUS FLOW WIND TUNNELS

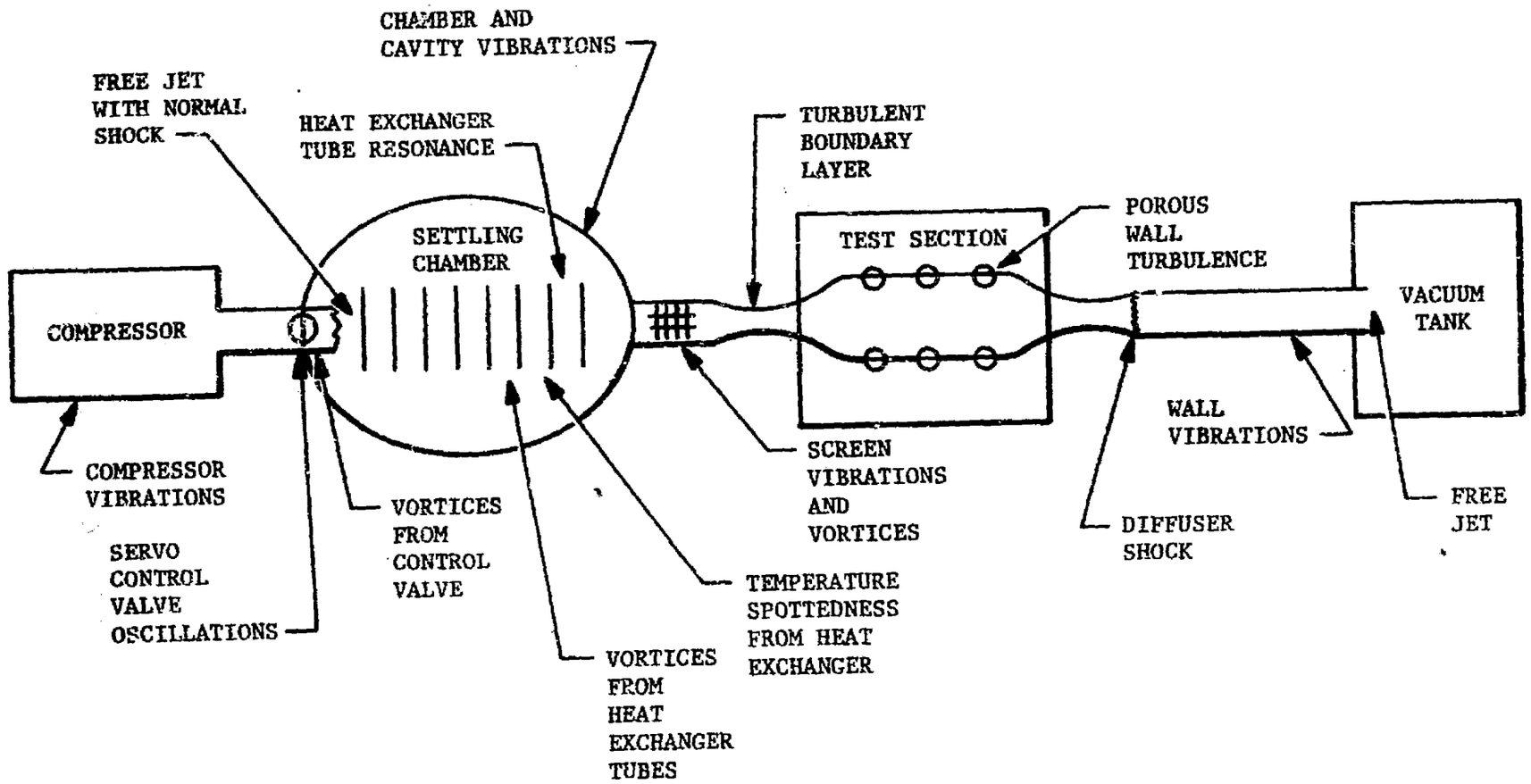

FIGURE 19. UNSTEADY PRESSURE SOURCES IN BLOWDOWN WIND TUNNELS

c. Wind Tunnel Wall

A turbulent boundary layer will be developed along the wall of the wind tunnel facility and produce pressure fluctuations throughout the wind tunnel system.

d. Porous Walls

Porous or slotted walls are utilized in the test sections of transonic wind tunnel facilities to eliminate the effects of reflected shock waves on static pressure measurements. These wall configurations do not totally eliminate shock reflections as can be visualized by shadowgraph or Schlieren photography. It is believed that the shock reflection will still contribute significantly to local unsteady pressure amplitudes. Further, hole or slot patterns produce acoustic resonances which are dependent on the flow Mach number.

e. Compressors

Pressure fluctuations are induced by thrust and torque components and vortex wakes from each rotor stage, interacting with subsequent rotary elements. Compressor blade vibration and motor speed variation will also produce unsteady pressures. The major components of the compressor noise will be at harmonics of the blade passage frequency.

f. Servo Control

Instabilities in the servo-system will be transmitted to the flow stream. In a blowdown facility the control valve is sometimes followed by a free supersonic jet possessing regular jet noise sources. The supersonic stream can be terminated by strong shock waves which will interact with the jet noise.

g. Diffuser

Normal shock waves at the diffuser throat will interact with the boundary layer and for subsonic flow disturbances may be transmitted upstream to the test section. In a closed loop system disturbances may propagate to the test section for all flow conditions if the perturbations are not damped out.

h. Heat Exchanger

Uneven heating in the heat exchanger causing some hot spots may result in pressure fluctuation at the test specimen.

i. Exhaust System

Acoustic resonances of an open pipe as well as external noise which may be transmitted to the test specimen by structural vibration will be present in the blowdown exhaust system.

The resultant pressure at a point, i, of the test specimen, p_r, is related to the background noise, p_b, and the flow induced noise at the test specimen, p_m, (see figure 20) as follows:

$$p_r^2 (x_i, y_i, z_i, t) = p_m^2 (x_i, y_i, z_i, t) + p_b^2 (x_i, y_i, z_i, t) \quad (38)$$

and the pressure cross correlation between locations i and j will be

$$R_{pr} (i, j, \tau) = R_{pm} (i, j, \tau) + R_{pb} (i, j, \tau) \quad (39)$$

if the background and the flow-induced pressures at the test specimen are statistically independent. The cross power spectral densities are related as follows:

$$S_{pr} (i, j, \omega) = S_{pm} (i, j, \omega) + S_{pb} (i, j, \omega) \quad (40)$$

Thus the response of the test specimen will be due to the flow component S_{pm} and the background component S_{pb} (S_{pb} can be obtained by Fourier transform of R_{pb}). In order to determine the structural response to S_{pm} alone, the response to S_{pb} must be known and subtracted from the total structural response or $S_{pb} << S_{pm}$.

If the response of a structural element only to the flow field of a wind tunnel system is determined, the relevancy of the unsteady flow field must still be determined.

The cross correlation of flow-noise is dependent upon boundary layer displacement thickness (references 11, 12 and 22) which is in turn a function of Reynolds number. The flight vehicle Reynolds number is usually several orders of magnitude larger than that of a practical wind tunnel facility. Hence, the exact dependency of the structural response on the cross correlation coefficient must be known in advance or the wind tunnel boundary layer must be thickened. The former requires an a priori knowledge of the structural response while the latter mechanism is not practical for most structural elements. Also the tunnel size precludes the use of large test specimens, otherwise flow blockage will occur.

C. Component Influence on Local Acoustic Field

The imposition of any structural element must necessarily modify the characteristics inherent to the acoustic field existing prior to insertion. Such perturbations are due to scattering of the acoustic field and the vibratory response of the structural element which must inherently radiate a secondary acoustic field. This effect is not further analyzed, since only minor effects are anticipated as long as component volume is less than 10% of a reverberation chamber for diffuse field testing and the component area is less than 10% of the cross-sectional area of a progressive wave test facility when components are to be immersed in a progressive wave field.

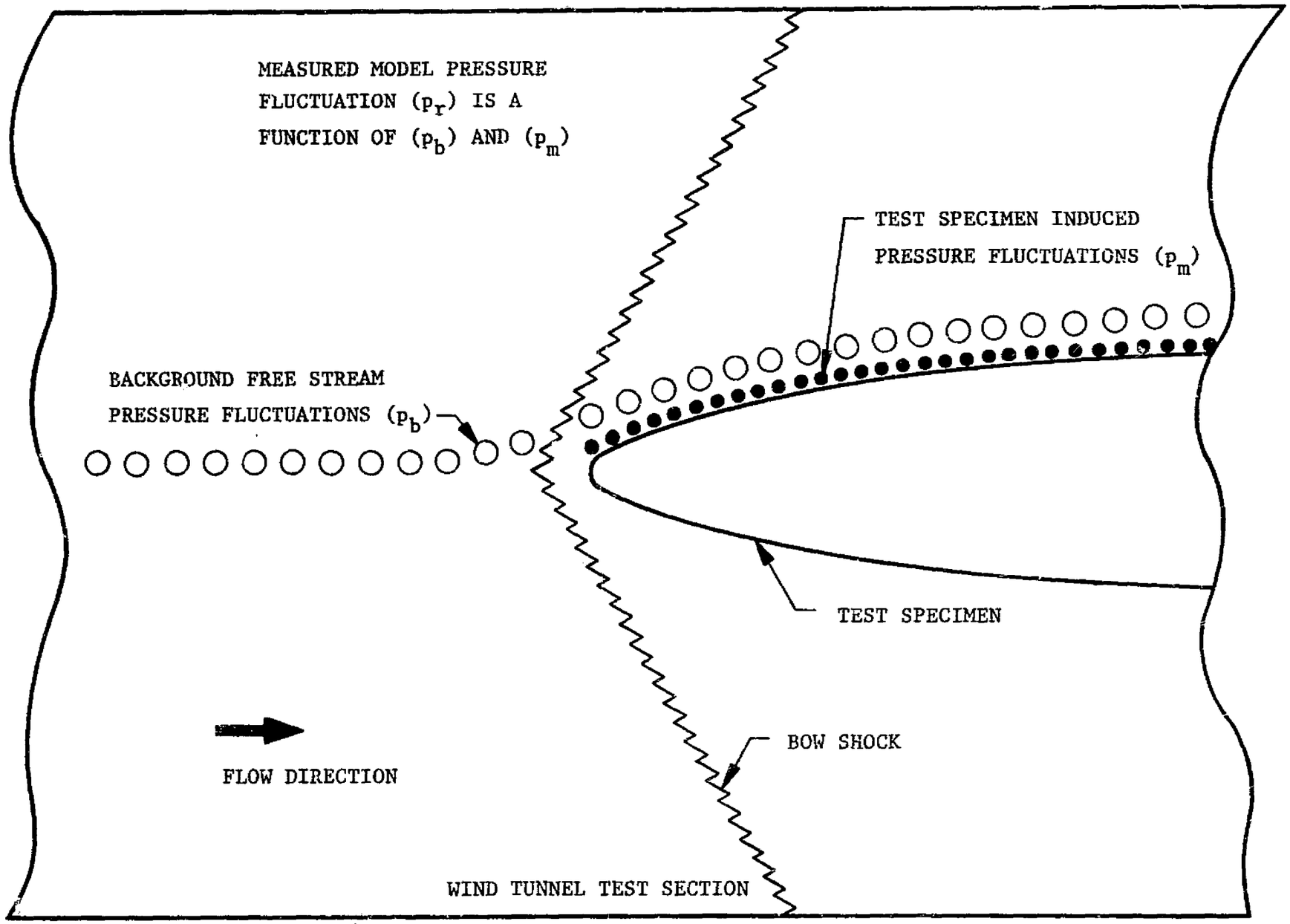

FIGURE 20. COMPONENTS OF UNSTEADY PRESSURE AT TEST SPECIMEN SURFACE

SECTION III. ELEMENTS OF STRUCTURAL RESPONSE TO SONIC EXCITATION

Two methods of estimating vibratory response of panel-type structure is presented herein. The modal analysis technique is the typical classical analysis as adapted and developed by Dr. T. N. Lee of Chrysler, Huntsville Operations. The statistical energy analysis is developed from the concept forwarded by Dr. R. H. Lyon of Bolt Beranek and Newman Inc. Transfer function levels are prepared for the specimen to be utilized in the empirical portion of the program of work. Effects of radiation damping, equipment loading and exposed area are also discussed in this section.

Previous investigations of the response of aerospace structures to acoustic stimuli such as jet or rocket engine noise, boundary layer noise or oscillating shock excitation have been largely of an empirical nature. Mahaffey-Smith, Franken, Eldred et al, and Barrett (references 23 - 28) generally determined as a function of acoustic pressure, the acceleration normalized by bulk descriptors such as gross vehicle weight, vehicle diameter or vehicle thrust. These experimenters generally lacked sufficient reliable data and consequently could not adequately define the effects of many significant parameters on the damage potential of structural vibration. Measured flight vibration and acoustic data were quite sparce and often unreliable. Purely theoretical treatments often have become unwieldy, overly complicated and impractical due to the degree of structural definition required.

A. Modal Analysis

The displacement spectral density at point r(x,y) of a two dimensional structure is given by the following equation (see reference 29).

$$\Phi_{ww}(\vec{r},\omega) = \sum_{j,k,m,n} F_{jk}(\vec{r})\, F_{mn}(\vec{r})\, H_{jk}(\omega)\, H^{*}_{mn}(\omega)\, I_{jkmn} \qquad (41)$$

where

$\Phi_{ww}(\vec{r},\omega)$ = displacement spectral density as a function $\vec{r}$ and ω

$\vec{r}$ = position vector of the point concerned

ω = frequency in radians per second

$F_{jk}(\vec{r})$ = normal mode of structure

$$H_{jk} = \frac{1}{M_{jk}[\omega^2_{jk} - \omega^2 + 2\, i\, \zeta_{jk}\omega_{jk}\omega]} \qquad (42)$$

H^{*}_{jk} = is the complex conjugate of H_{jk}

$$M_{jk} = \int M F_{jk}(\vec{r})\, dr = \text{generalized mass} \qquad (43)$$

$M = M(\vec{r})$ = mass distribution of the structure

ζ_{jk} = damping ratio corresponding to j, k mode

$i = \sqrt{-1}$

ω_{jk} = natural frequency of the structure

The natural frequencies of a simply supported rectangular panel reinforced by stiffeners are given by (reference 30)

$$\omega_{mn} = \sqrt{\frac{1}{\rho h}}\left[D_x\left(\frac{m\pi}{\ell}\right)^4 + 2H\left(\frac{m\pi}{\ell}\right)^2\left(\frac{n\pi}{b}\right)^2 + D_y\left(\frac{n\pi}{b}\right)^4 \right]^{1/2} \qquad (44)$$

where

m,n = mode indices

$$D_x = \frac{Eh^3}{12(1-\nu^2)} + \frac{E'I_1}{b_1}$$

$$D_y = \frac{Eh^3}{12(1-\nu^2)} + \frac{E'I_2}{a_1}$$

$$H = \frac{Eh^3}{12(1-\nu^2)}$$

ρ = mass density of panel

E = Young's modulus of panel

E' = Young's modulus of stiffeners

ν = Poisson's ratio of panel

h = thickness of panel

a_1 = spacing of width-direction stiffeners

b_1 = spacing of length-direction stiffeners

ℓ = length of panel (x = 0 to x = ℓ)

b = width of panel (y = 0 to y = b)

I_1 = moment of inertia of one length-direction stiffeners with respect to middle axis of cross-section of panel

I_2 = moment of inertia of one-width-direction stiffeners with respect to middle axis of cross-section of panel

The cross spectral density of the generalized force of the excitation is also defined (reference 29).

$$I_{jkmn}(\omega) = \int\int \Phi_{pp}(\vec{r}_1,\vec{r}_2,\omega)\, F_{jk}(\vec{r}_1)\, F_{mn}(\vec{r}_2)\, d\vec{r}_1\, d\vec{r}_2 \qquad (45)$$

where

$\Phi_{pp}(\vec{r}_1,\vec{r}_2,\omega)$ = the cross spectral density function of the excitation

Many types of acoustic fields may be adequately represented by

$$\Phi_{pp}(\vec{r}_1,\vec{r}_2,\omega) = \Phi_{pp}(\omega)\, e^{-\frac{A_1\omega}{c}|x_1-x_2|} - \frac{A_2\omega}{c}|y_1-y_2| \qquad (46)$$

where

Φ_{pp} = the homogeneous spectral density of the pressure field over the structure

$(x_1,y_1),(x_2,y_2)$ = the coordinates of locations $\vec{r}_1$ and $\vec{r}_2$

ω = frequency

c = speed of sound

A_1,A_2 = spatial correlation coefficients in the x and y directions

Equation 46 may be directly utilized as follows

For boundary layer noise

$$A_1 = (2k_1\delta^*)^{-1} \quad , k_1 = \frac{\omega}{U_{c_1}}$$

$$A_2 = (2k_2\delta^*)^{-1} \quad , k_2 = \frac{\omega}{U_{c_2}} \tag{47}$$

For a plane progressive wave at parallel incidence

$$\Phi_{pp}(\vec{r}_1,\vec{r}_2,\omega) = \Phi_{pp}(\omega) \cos k|x_1-x_2| \tag{48}$$

which can be approximated by simulation of the first zero-crossing

$$A_1 = 3$$

$$A_2 = 0$$

For a plane progressive wave at normal incidence

$$\Phi_{pp}(\vec{r}_1,\vec{r}_2,\omega) = \Phi_{pp}(\omega) \tag{49}$$

and

$$A_1 = 0$$

$$A_2 = 0$$

For a reverberant acoustic field

$$\Phi_{pp}(\vec{r}_1,\vec{r}_2,\omega) = \Phi_{pp}(\omega) \ (\sin kr)/kr \tag{50}$$

which can be approximated by

$$\Phi_{pp}(\vec{r}_1,\vec{r}_2,\omega) = \Phi_{pp}(\omega)[\sin k|x_1-x_2|/k|x_1-x_2|][\sin k|y_1-y_2|/k|y_1-y_2|] \tag{51}$$

The envelope of which is simulated by

$$A_1 = 1.6$$

$$A_2 = 1.6$$

The displacement response spectral density at any point $\vec{r}$ (x,y) is given by reference 30.

$$\Phi_{ww}(\vec{r},\omega) = S'^2\Phi_{pp}(\omega) \sum_{\substack{j,k,m,n \\ = 1,2,\ldots}} \frac{F_{jk}F_{mn}A_{jkmn}l_{jkmn}}{M_{jk}M_{mn}\omega^2{}_{jk}\omega^2{}_{mn}C^2{}_{jkmn}} \qquad (52)$$

$$= \sum_{j,k,m,n} w^2_{jkmn}$$

where

w^2_{jkmn} = general term of the series

$\Phi_{ww}(\vec{r},\omega)$ = displacement spectral density in $(\text{inch})^2$/rad. per sec.

$\Phi_{pp}(\omega)$ = spectral density of the excitation in $(\text{PSI})^2$/rad. per sec.

S' = $b'\ell'$ = area of panel subjected to excitation in $(\text{inch})^2$ (53)

b' = width of panel subjected to excitation

ℓ' = length of panel subjected to excitation

The mode shapes are approximated by those of panels of uniform thickness

$$F_{jk} = F_{jk}(\vec{r}) = \sin \frac{j\pi x}{\ell} \sin \frac{k\pi y}{b}$$

$$F_{mn} = F_{mn}(\vec{r}) = \sin \frac{m\pi x}{\ell} \sin \frac{n\pi y}{b}$$

where

b = width of panel (54)

ℓ = length of panel

The modal masses are approximated by those of uniform thickness panel

$$M_{jk} = M_{mn} = \frac{Mb\ell}{4} \tag{55}$$

M = ρh = mass per unit area

ρ = mass density of panel

h = thickness of panel

$\vec{r}$ = position vector of point concerned

x,y = coordinates of $\vec{r}$

ω = $2\pi f$ = frequency in rad./sec.

f = frequency in Hertz

ω_{jk}, ω_{mn} = natural frequencies given by equation (44)

$$A_{jkmn} = A_{jkmn}(\omega)$$

$$= \left[1- \left(\frac{\omega}{\omega_{jk}}\right)^2\right]\left[1- \left(\frac{\omega}{\omega_{mn}}\right)^2\right] + 4\,\zeta_{jk}\zeta_{mn}\,\frac{\omega^2}{\omega_{jk}\omega_{mn}}$$

$$C^2_{jkmn} = C^2_{jkmn}(\omega) = A^2_{jkmn}(\omega) + B^2_{jkmn}(\omega)$$

$$B_{jkmn}(\omega) = 2\left\{\frac{\zeta_{mn}\omega}{\omega_{mn}}\left[1- \left(\frac{\omega}{\omega_{jk}}\right)^2\right] - \frac{\zeta_{jk}\omega}{\omega_{jk}}\left[1- \left(\frac{\omega}{\omega_{mn}}\right)^2\right]\right\} \tag{56}$$

The normalized cross spectral density of the generalized force of the excitation for different mode combinations is given by

$$\begin{aligned}
\tilde{I}_{jkmn} &= I_{jm}I_{kn} && \text{for } j = m,\ k = n \\
\tilde{I}_{jkmn} &= I_{jm}I'_{kn} && \text{for } j = m,\ k \neq n \\
\tilde{I}_{jkmn} &= I'_{jm}I_{kn} && \text{for } j \neq m,\ k = n \\
\tilde{I}_{jkmn} &= I'_{jm}I'_{kn} && \text{for } j \neq m,\ k \neq n
\end{aligned} \tag{57}$$

$$I_{jm} = I_{jm}(\omega) \frac{2A_2 b\omega}{c} \left[\frac{1}{\left(\frac{A_1 \ell\omega}{c}\right)^2 + (j\pi)^2} + \frac{1}{\left(\frac{A_1 \ell\omega}{c}\right)^2 + (m\pi)^2} \right]$$

$$+ (k\pi)(n\pi) \frac{2 + e^{\frac{-A_1 \ell\omega}{c}} \left[(-1)^{j+1} + (-1)^{m+1} \right]}{\left[\left(\frac{A_1 \ell\omega}{c}\right)^2 + (j\pi)^2 \right] \left[\left(\frac{A_1 \ell\omega}{c}\right)^2 + (m\pi)^2 \right]} \qquad (58)$$

for $j = m$

$$I_{kn} = I_{kn}(\omega) = \frac{2A_2 b\omega}{c} \left[\frac{1}{\left(\frac{A_2 b\omega}{c}\right)^2 + (k\pi)^2} + \frac{1}{\left(\frac{A_2 b\omega}{c}\right)^2 + (n\pi)^2} \right]$$

$$+ (k\pi)(n\pi) \frac{2 + e^{\frac{-A_2 b\omega}{c}} \left[(-1)^{k+1} + (-1)^{n+1} \right]}{\left[\left(\frac{A_2 b\omega}{c}\right)^2 + (k\pi)^2 \right] \left[\left(\frac{A_2 b\omega}{c}\right)^2 + (n\pi)^2 \right]} \qquad (59)$$

for $k = n$

$$I'_{jm} = I'_{jm}(\omega) = (j\pi)(m\pi) \frac{2 + e^{\frac{-A_1 \ell\omega}{c}} \left[(-1)^{j+1} + (-1)^{m+1} \right]}{\left[\left(\frac{A_1 \ell\omega}{c}\right)^2 + (j\pi)^2 \right] \left[\left(\frac{A_1 \ell\omega}{c}\right)^2 + (m\pi)^2 \right]}$$

$$+ \frac{m}{\left(\frac{A_1 \ell\omega}{c}\right)^2 + (m\pi)^2} \left[\frac{(-1)^{i-m} - 1}{2(j-m)} + \frac{(-1)^{j+m} - 1}{2(j+m)} \right]$$

$$+ \quad \frac{j}{\left(\frac{A_1 \ell \omega}{c}\right)^2 + (j\pi)^2} \left[\frac{(-1)^{m-j} - 1}{2(m-j)} + \frac{(-1)^{m+j} - 1}{2(m+1)} \right] \qquad (60)$$

for $j \neq m$

$$I'_{kn} = I'_{kn}(\omega) = (k\pi)(n\pi) \frac{2 + e^{\frac{-A_2 b\omega}{c}} \left[(-1)^{k+1} + (-1)^{n+1} \right]}{\left[\left(\frac{A_2 b\omega}{c}\right)^2 + (k\pi)^2 \right] \left[\left(\frac{A_2 b\omega}{c}\right)^2 + (n\pi)^2 \right]}$$

$$+ \quad \frac{n}{\left(\frac{A_2 b\omega}{c}\right)^2 + (n\pi)^2} \left[\frac{(-1)^{k-n} - 1}{2(k-n)} + \frac{(-1)^{k+n} - 1}{2(k+n)} \right]$$

$$+ \quad \frac{k}{\left(\frac{A_2 b\omega}{c}\right)^2 + (k\pi)^2} \left[\frac{(-1)^{n-k} - 1}{2(n-k)} + \frac{(-1)^{n+k} - 1}{2(n+k)} \right] \qquad (61)$$

for $k \neq n$

where

A_1 = correlation decay constant in length-direction

A_2 = correlation decay constant in width-direction

c = speed of sound in air

The displacement response spectral density at $\vec{r}$ (x,y) in $(\text{inch})^2/\text{Hertz}$ is given by

$$S_{ww}(\vec{r},f) = 2\pi \, \Phi_{ww}(\vec{r},\omega) \qquad (62)$$

The acceleration response spectral density at $\vec{r}(x,y)$ in $\left(\frac{\text{inch}}{\text{sec}^2}\right)^2$/rad. per sec. is given by

$$\Phi^{\cdots\cdots}_{ww}(\vec{r},\omega) = \omega^4 \Phi_{ww}(\vec{r},\omega) \tag{63}$$

The acceleration response spectral density in g^2/Hertz is given by

$$S^{\cdots\cdots}_{ww}(\vec{r},f) = 4.215093 \times 10^{-5}\ \Phi^{\cdots\cdots}_{ww}(\vec{r},\omega) \tag{64}$$

The mean-square acceleration is g^2 is given by

$$G^2(\vec{r}) = \int S^{\cdots\cdots}_{ww}(\vec{r},f)df \tag{65}$$

The root-mean-square acceleration in "g" is given by

$$G(\vec{r}) = [G^2(\vec{r})]^{1/2} \tag{66}$$

The excitation spectral density in $(PSI)^2$/rad. per sec. is given by

$$\Phi_{pp}(\omega) = \frac{1}{2\pi}\ (10)^{\left[\frac{S_{pp}(f)\ -\ 170.576}{10}\right]} \tag{67}$$

The excitation spectral density in decibels/Hertz is given by

$$S_{pp}(f) = S_{3rd}(f) - 10\ \log_{10}\ (0.23157f) \tag{68}$$

where

$S_{3rd}(f)$ = the one-third octave excitation pressure level in decibels (input)

B. Transfer Function Level From Modal Analyses

An analytical transfer function was obtained from Program RSRCP1, Response of Simply-Supported Rectangular Panels Cross-Reinforced with Stiffeners, developed by Dr. T. N. Lee under research Contract NAS8-21403. The input acoustic spectral density was nominally equal to 100 dB (see figure 21, table 1). Vibratory responses were calculated for test specimens I, II and III (see section IV for full test specimen details) at coordinates (15, 20), (2` 5, 30) and (26.25, 35) for each

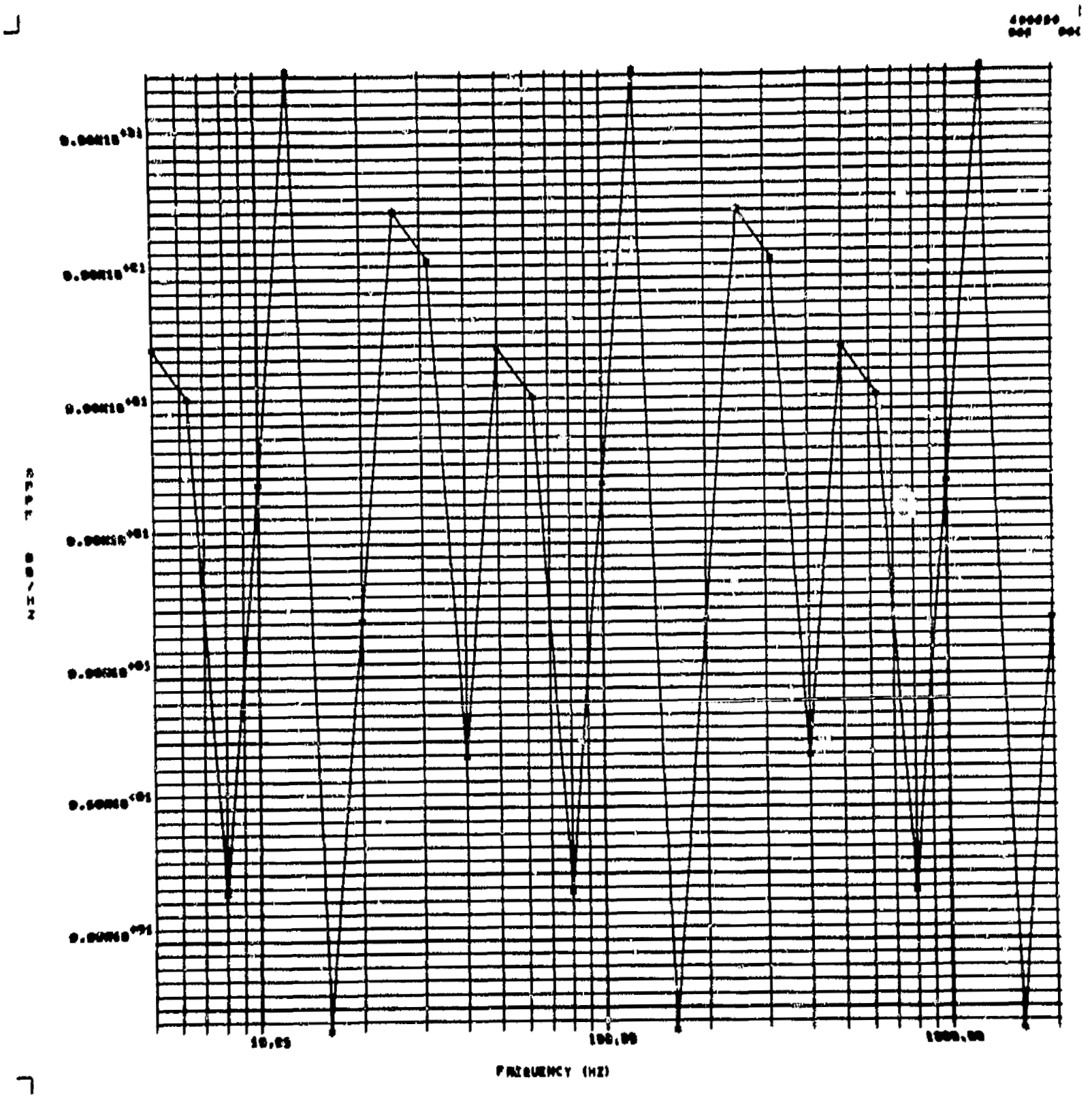

FIGURE 21. SPECTRAL DENSITY OF ACOUSTIC INPUT TO COMPUTER PROGRAM RSRCP1

TABLE 1. ACOUSTIC EXCITATION INPUT TO COMPUTER PROGRAM

INPUT EXCITATION			
ONE-3RD OCTAVE MEAN FREQUENCY F3RD	ONE-3RD OCTAVE LEVEL IN DECIBELS S3RD	SPECTRAL DENSITY IN DECIBELS/HERTZ SPPF	SPECTRAL DENSITY IN PSI SQ/RAD/SEC FIPW
5.000	100.600	99.965	0.13826E-07
6.300	101.600	99.961	0.13814E-07
8.000	102.600	99.924	0.13696E-07
10.000	103.600	99.954	0.13793E-07
12.500	104.600	99.985	0.13892E-07
16.000	105.600	99.913	0.13663E-07
20.000	106.600	99.944	0.13761E-07
25.000	107.600	99.975	0.13859E-07
31.500	108.600	99.971	0.13847E-07
40.000	109.600	99.934	0.13728E-07
50.000	110.600	99.965	0.13826E-07
63.000	111.600	99.961	0.13814E-07
80.000	112.600	99.924	0.13696E-07
100.000	113.600	99.954	0.13793E-07
125.000	114.600	99.985	0.13892E-07
160.000	115.600	99.913	0.13663E-07
200.000	116.600	99.944	0.13761E-07
250.000	117.600	99.975	0.13859E-07
315.000	118.600	99.971	0.13847E-07
400.000	119.600	99.934	0.13728E-07
500.000	120.600	99.965	0.13826E-07
630.000	121.600	99.961	0.13814E-07
800.000	122.600	99.924	0.13696E-07
1000.000	123.600	99.954	0.13793E-07
1250.000	124.600	99.985	0.13892E-07
1600.000	125.600	99.913	0.13663E-07
2000.000	126.600	99.944	0.13761E-07

panel for normal and grazing incidence progressive wave and reverberant acoustic excitation. Predicted modal frequencies from equation (44) for specimens I, II and III are shown in Tables 2, 3 and 4. Table 5 shows a sample computer input for test specimen III at coordinate (26.25, 35) excited by an acoustic progressive wave at parallel incidence.

A vibro-acoustic transfer function is defined as the acceleration level in dB re 1 g minus the acoustic level in dB re 2×10^{-5} N/M^2. The computed accleration spectral density from Program RSRPC1 was converted to db re 1 g and the constant 100 dB acoustic spectral density excitation was subtracted from the vibration level to obtain the transfer function shown on the ordinate of Figures 22 through 48. Table 6 presents an index of the presented analytical transfer functions.

C. Statistical Energy Theory

The theory of the statistical treatment of vibratory response of structural elements to acoustic excitation is found in the literature. (See for example references 31-35.) This theory is generally adequate when typical panel dimensions are larger than the wave length of panel bending modes. The fundamental relationships necessary to proceed in the statistical analysis are the following

$$S_{ww}^{\cdot\cdot\cdot\cdot}(f) = \omega^2 S_{ww}^{\cdot\cdot}(f) = \omega^4 S_{ww}(f) \tag{69}$$

and

$$\Pi(f) = S_{ww}^{\cdot\cdot\cdot\cdot}(f)\ \eta\rho_s/\omega \tag{70}$$

where

$S_{ww}^{\cdot\cdot\cdot\cdot}(f)$ is the response acceleration spectral density

$S_{ww}^{\cdot\cdot}(f)$ is the response velocity spectral density

$S_{ww}(f)$ is the response displacement spectral density

$\omega = 2\pi f$ is the circular frequency

η is the structural loss factor

ρ_s is the surface mass density

$\Pi(f)$ is the excitation power input per unit surface area

The vibratory response of the simply-supported thin panel to convected turbulence is categorized by modal behavior, depending on the relationship of trace wave speed and the convection speed. If the projection of the trace wave speed along the direction of convection is:

TABLE 2. PREDICTED MODAL FREQUENCIES FOR TEST SPECIMEN I

m	n	Hertz	radian/sec.	m	n	Hertz	radian/sec.
1	1	6.58884	41.39893	5	5	164.72109	1034.97314
1	2	19.23942	120.88486	5	6	211.10655	1326.42159
1	3	40.32372	253.36143	5	7	265.92572	1670.86064
1	4	69.84174	438.82861	5	8	329.17862	2068.29031
1	5	107.79348	677.28642	5	9	400.86523	2518.71060
1	6	154.17894	968.73487	6	1	89.60827	563.02538
1	7	208.99812	1313.17392	6	2	102.25885	642.51131
1	8	272.25101	1710.60359	6	3	123.34315	774.98788
1	9	343.93763	2161.02390	6	4	152.86117	960.45507
2	1	13.70479	86.10977	6	5	190.81291	1198.91289
2	2	26.35537	165.59570	6	6	237.19837	1490.36133
2	3	47.43967	298.07227	6	7	292.01754	1834.80037
2	4	76.95769	483.53945	6	8	355.27044	2232.23007
2	5	114.90943	721.99726	6	9	426.95705	2682.65036
2	6	161.29489	1013.44570	7	1	120.44406	756.77235
2	7	216.11407	1357.88477	7	2	133.09464	836.25829
2	8	279.36696	1755.31444	7	3	154.17894	968.73486
2	9	351.05358	2205.73474	7	4	183.69696	1154.20204
3	1	25.56471	160.62783	7	5	221.64870	1392.65987
3	2	38.21529	240.11377	7	6	268.03415	1684.10829
3	3	59.29959	372.59033	7	7	322.85333	2028.54735
3	4	88.81761	558.05752	7	8	386.10622	2425.97702
3	5	126.76935	796.51533	7	9	457.79284	2876.39734
3	6	173.15481	1087.96376	8	1	156.02382	980.32656
3	7	227.97398	1432.40282	8	2	168.67439	1059.81250
3	8	291.22688	1829.83249	8	3	189.75869	1192.28906
3	9	362.91350	2280.25281	8	4	219.27671	1377.75624
4	1	42.16860	264.95313	8	5	257.22845	1616.21405
4	2	54.81918	344.43906	8	6	303.61391	1907.66248
4	3	75.90348	476.91562	8	7	358.43308	2252.10153
4	4	105.42150	662.38280	8	8	421.68598	2649.53122
4	5	143.37323	900.84062	8	9	493.37260	3099.95154
4	6	189.75869	1192.28906	9	1	196.34754	1233.68799
4	7	244.57787	1536.72812	9	2	208.99812	1313.17392
4	8	307.83077	1934.15781	9	3	230.08241	1445.65048
4	9	379.51739	2384.57813	9	4	259.60043	1631.11768
5	1	63.51645	399.08565	9	5	297.55217	1869.57547
5	2	76.16703	478.57158	9	6	343.93763	2161.02393
5	3	97.25133	611.04814	9	7	398.75681	2505.46298
5	4	126.76935	796.51533	9	8	462.00970	2902.89264
				9	9	533.69632	3353.31296

TABLE 3. PREDICTED MODAL FREQUENCIES FOR TEST SPECIMEN II

m	n	Hertz	radian/sec.
1	1	32.94422	206.99463
1	2	96.19711	604.42431
1	3	201.61861	1266.80711
1	4	349.20870	2194.14304
1	5	538.96739	3386.43210
1	6	770.89468	4843.67419
1	7	1044.99057	6565.86957
1	8	1361.25505	8553.01794
1	9	1719.68813	10805.11938
2	1	68.52397	430.54882
2	2	131.77687	827.97851
2	3	237.19836	1490.36131
2	4	384.78846	2417.69724
2	5	574.54716	3609.98633
2	6	806.47444	5067.22845
2	7	1080.57033	6789.42377
2	8	1396.83481	8776.57214
2	9	1755.26788	11028.67358
3	1	127.82356	803.13914
3	2	191.07646	1200.56883
3	3	296.49796	1862.95164
3	4	444.08805	2790.28757
3	5	633.84674	3982.57663
3	6	865.77402	5439.81873
3	7	1139.86992	7162.31410
3	8	1456.13440	9149.16248
3	9	1814.56747	11401.26392
4	1	210.84299	1324.76561
4	2	274.09589	1722.19528
4	3	379.51738	2384.67809
4	4	527.10748	3311.91403
4	5	716.86617	4504.20313
4	6	948.79346	5961.44525
4	7	1222.88934	7683.64050
4	8	1539.15382	9670.78894
4	9	1897.58691	11922.89050
5	1	317.58226	1995.42822
5	2	380.83515	2392.85788
5	3	486.25665	3055.24072
5	4	633.84674	3982.57663
5	5	823.60544	5174.86572
5	6	1055.53271	6632.10745
5	7	1329.62860	8354.30310
5	8	1645.89310	10341.45154
5	9	2004.32616	12593.55298
6	1	448.04134	2815.12686
6	2	511.29424	3212.55655
6	3	616.71574	3874.93939
6	4	764.30584	4802.27533
6	5	954.06454	5994.56439
6	6	1185.99182	7451.80658
6	7	1460.08771	9174.00183
6	8	1776.35219	11161.15027
6	9	2134.78525	13413.25171
7	1	602.22029	3783.86176
7	2	665.47318	4181.29136
7	3	770.89468	4843.67419
7	4	918.48477	5771.01013
7	5	1108.24348	6963.29932
7	6	1340.17075	8420.54138
7	7	1614.26665	10142.73669
7	8	1928.53111	12129.88501
7	9	2288.96420	14381.78669
8	1	780.11906	4901.63275
8	2	843.37196	5299.06244
8	3	948.79346	5961.41525
8	4	1096.38354	6885.73113
8	5	1286.14224	8081.07025
8	6	1518.06983	9538.31238
8	7	1792.15541	11260.50757
8	8	2108.42990	13247.65613
8	9	2466.86298	15499.75757
9	1	981.73768	6168.43985
9	2	1044.99057	6565.86957
9	3	1150.41208	7228.25244
9	4	1298.00217	8155.58838
9	5	1487.76065	9347.37732
9	6	1719.68814	10805.11951
9	7	1993.78403	12527.81492
9	8	2310.04852	14514.70326
9	9	2668.48160	16765.79471

TABLE 4. PREDICTED MODAL FREQUENCIES FOR TEST SPECIMEN III

m	n	Hertz	radian/sec.	m	n	Hertz	radian/sec.
1	1	100.45216	631.15955	5	6	3326.01028	20897.73945
1	2	341.12423	2143.34683	5	7	4346.55054	27310.18311
1	3	759.47159	4771.90082	5	8	5558.95789	34927.96338
1	4	1347.71802	8467.96228	5	9	6954.54919	43696.72217
1	5	2104.74442	13224.49951	6	1	1972.46063	12393.33594
1	6	3030.27048	19039.75146	6	2	1999.52788	12563.40442
1	7	4124.19989	25913.11279	6	3	2112.01379	13270.17444
1	8	5386.49231	33844.33008	6	4	2388.10217	15004.88892
1	9	6817.12836	42833.28174	6	5	2884.50064	18123.85254
2	1	234.66820	1474.46384	6	6	3616.27774	22721.74365
2	2	401.80864	2524.63818	6	7	4572.66931	28730.92920
2	3	788.70657	4955.58960	6	8	5737.66132	36050.79004
2	4	1364.49693	8573.38733	6	9	7098.35889	44600.30518
2	5	2115.60272	13292.72424	7	1	2683.57437	16861.39551
2	6	3037.88635	19087.60327	7	2	2703.61633	16987.32275
2	7	4129.85449	25948.64160	7	3	2787.97357	17517.35498
2	8	5390.87207	33871.84912	7	4	3002.71500	18866.61523
2	9	6820.63361	42855.30566				
3	1	499.88197	3140.85110	7	5	3411.00952	21432.00537
3	2	597.02554	3751.22223	7	6	4048.92450	25440.14355
3	3	904.06944	5680.43591	7	7	4922.15576	30926.81763
3	4	1434.41533	9012.69751	7	8	6020.08020	37825.28027
3	5	2161.48093	13580.98547	7	9	7328.70441	46047.60889
3	6	3070.11813	19290.12158	8	1	3504.33057	22018.35889
3	7	4153.71338	26098.55151	8	2	3519.77722	22115.41309
3	8	5409.25330	33987.34180	8	3	3585.10391	22525.87280
3	9	6835.24420	42947.10693	8	4	3754.69125	23591.42139
4	1	879.94431	5528.85327	8	5	4088.76309	25690.45679
4	2	938.67281	5897.85535	8	6	4634.51495	29119.51685
4	3	1158.62874	7279.87921	8	7	5414.31909	34019.17090
4	4	1607.23454	10098.55273	8	8	6428.93817	40394.21094
4	5	2279.99930	14325.65845	8	9	7668.29779	48131.33691
4	6	3154.82626	19822.35840	9	1	4434.65939	27863.78687
4	7	4216.83636	26495.16479	9	2	4446.94305	27940.96777
4	8	5457.98773	34293.54932	9	3	4498.93774	28267.66040
4	9	6873.97791	43190.47803	9	4	4635.36163	29124.83667
5	1	1371.13506	8615.09583	9	5	4910.05659	30850.79614
5	2	1409.65729	8857.13818	9	6	5373.22998	33761.00049
5	3	1564.92081	9832.68762	9	7	6058.90460	38069.22119
5	4	1921.06763	12070.42419	9	8	6980.66760	43857.32911
5	5	2511.30399	15778.98877	9	9	8136.62438	51123.92236

TABLE 5. TYPICAL STRUCTURAL INPUT PARAMETERS FOR COMPUTER PROGRAM RSRCP1

INPUT PARAMETERS

PL = PANEL LENGTH = 0.40000E 02
B = PANEL WIDTH = 0.30000E 02
RHO = MASS DENSITY OF PANEL = 0.25100E-03
HS = PANEL THICKNESS = 0.40000E-01
CI = DAMPING RATIO = 0.70000E-01
X = COORDINATE OF VECTOR R = 0.35000E 02
Y = COORDINATE OF VECTOR R = 0.26250E 02
FINN = CONSTANT TO DETERMINE OCTAVE BAND CENTER FREQUENCIES = 0.18000E 02
A1 = DECAYING CONSTANT - LENGTH = 0.30000E 01
C = SPEED OF SOUND = 0.13500E 05
PLP = LENGTH OF PANEL SUBJECTED TO EXCITATION = 0.40000E 02
BP = WIDTH OF PANEL SUBJECTED TO EXCITATION = 0.30000E 02
A2 = DECAYING CONSTANT - WIDTH = 0.00000E-38
E = YOUNGS MODULUS OF PANEL = 0.10000E 08
EP = YOUNGS MODULUS OF STIFFENERS = 0.10000E 08
VIP = POISSONS RATIO = 0.30000E 00
AL1 = SPACING OF Y - DIRECTION STIFFENERS = 0.13375E 02
BL1 = SPACING OF X - DIRECTION STIFFENERS = 0.10000E 02
AI1 = MOMENT OF INERTIA OF ONE Y - DIRECTION STIFFENER = 0.53000E-01
AI2 = MOMENT OF INERTIA OF ONE X - DIRECTION STIFFENER = 0.53000E-01
H2 = LARGEST HEIGHT OF STIFFENERS AT VECTOR R = 0.00000E-38
HP = SMEARED-OUT THICKNESS OF STIFFENERS = 0.28000E-01
RAD = RADIUS OF SHELL = 0.10000E 32
RHOP = MASS DENSITY OF STIFFENERS = 0.25100E-03

TABLE 6. INDEX OF VIBRO-ACOUSTIC TRANSFER FUNCTIONS

Case	Panel	Location	Excitation
I.A.1.	30"x40"x.040 A1, Unstiffened	15,20	Progressive Wave, Normal
I.A.2.		15,20	Progressive Wave, Parallel
I.A.3.		15,20	Reverberant
I.B.1.		22.5,30	Progressive Wave, Normal
I.B.2.		22.5,30	Progressive Wave, Parallel
I.B.3.		22.5,30	Reverberant
I.C.1.		26.25,35	Progressive Wave, Normal
I.C.2.		26.25,35	Progressive Wave, Parallel
I.C.3.		26.25,35	Reverberant
II.A.1.	30"x40"x 0.20 A1, Unstiffened	15,20	Progressive Wave, Normal
II.A.2.		15,20	Progressive Wave, Parallel
II.A.3.		15,20	Reverberant
II.B.1.		22.5,30	Progressive Wave, Normal
II.B.2.		22.5,30	Progressive Wave, Parallel
II.B.3.		22.5,30	Reverberant
II.C.1.		26.25,35	Progressive Wave, Normal
II.C.2.		26.25,35	Progressive Wave, Parallel
II.C.3.		26.25,35	Reverberant
III.A.1.	30"x40"x.040 A1, Stiffened	15,20	Progressive Wave, Normal
III.A.2.		15,20	Progressive Wave, Parallel
III.A.3.		15,20	Reverberant
III.B.1		22.5,30	Progressive Wave, Normal
III.B.2.		22.5,30	Progressive Wave, Parallel
III.B.3.		22.5,30	Reverberant
III.C.1		26.25,35	Progressive Wave, Normal
III.C.2.		26.25.35	Progressive Wave, Parallel
III.C.3.		26.25,35	Reverberant

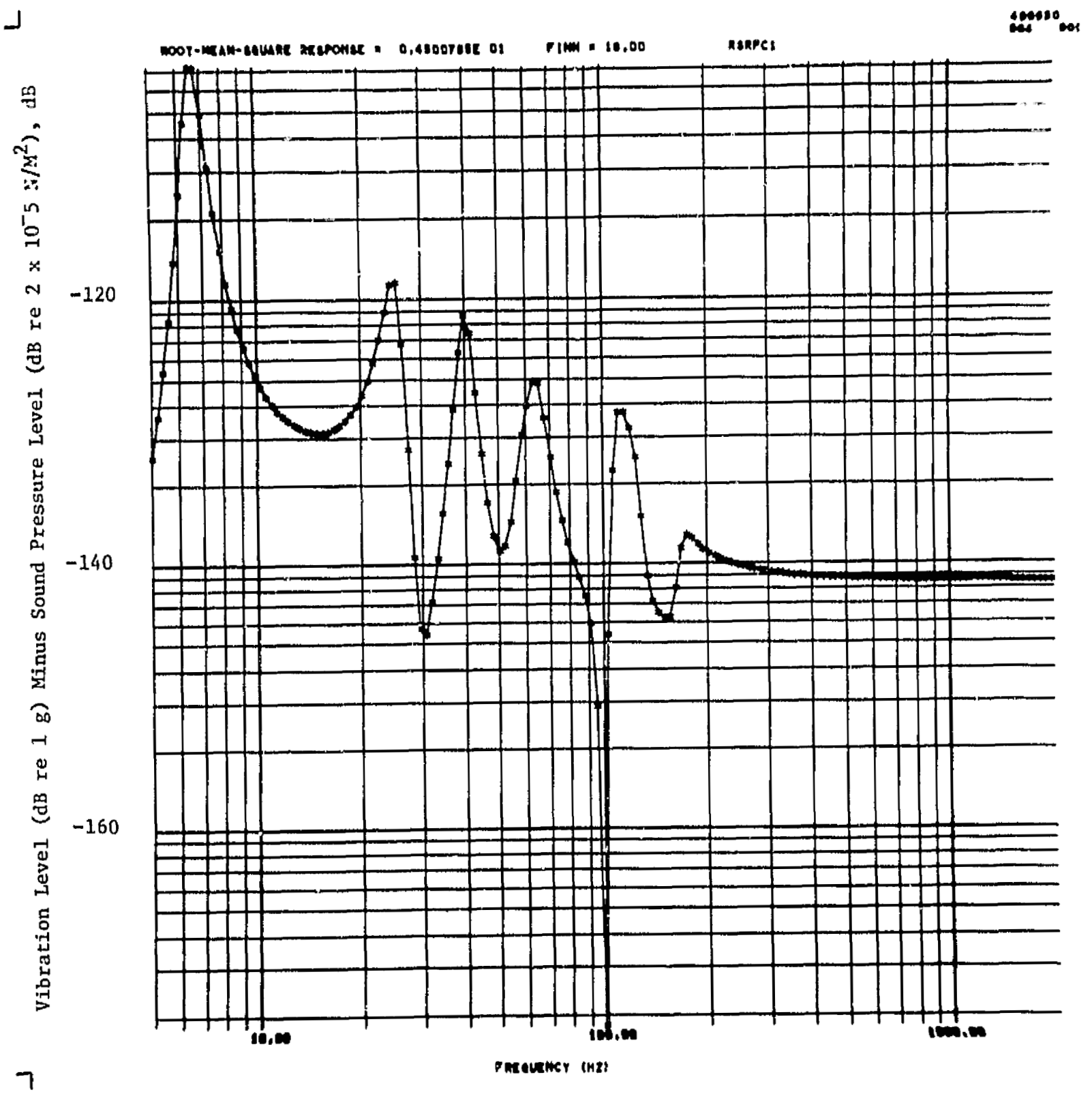

FIGURE 22. VIBRO-ACOUSTIC TRANSFER FUNCTION, CASE I.A.1

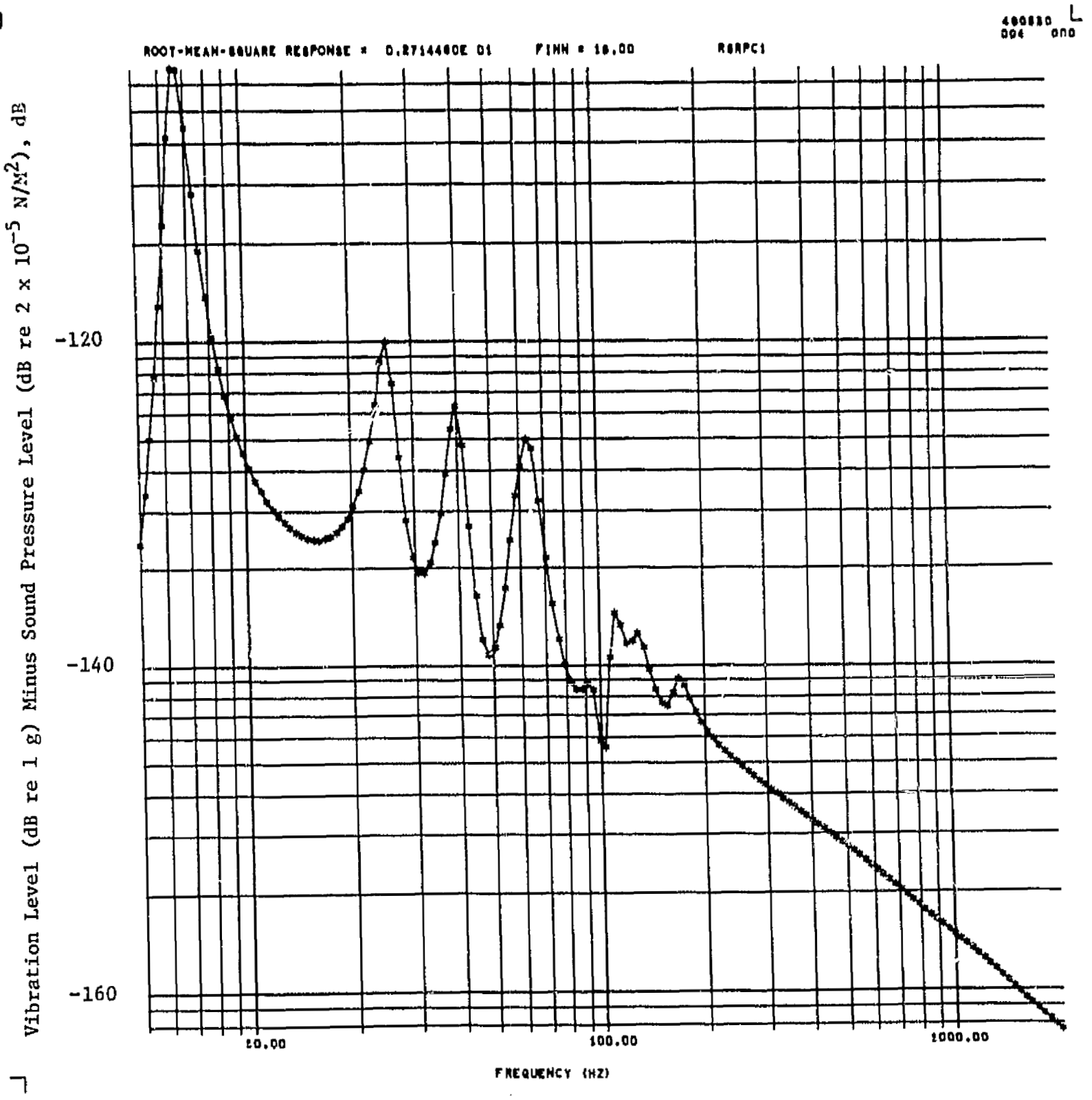

FIGURE 23. VIBRO-ACOUSTIC TRANSFER FUNCTION, CASE I.A.2

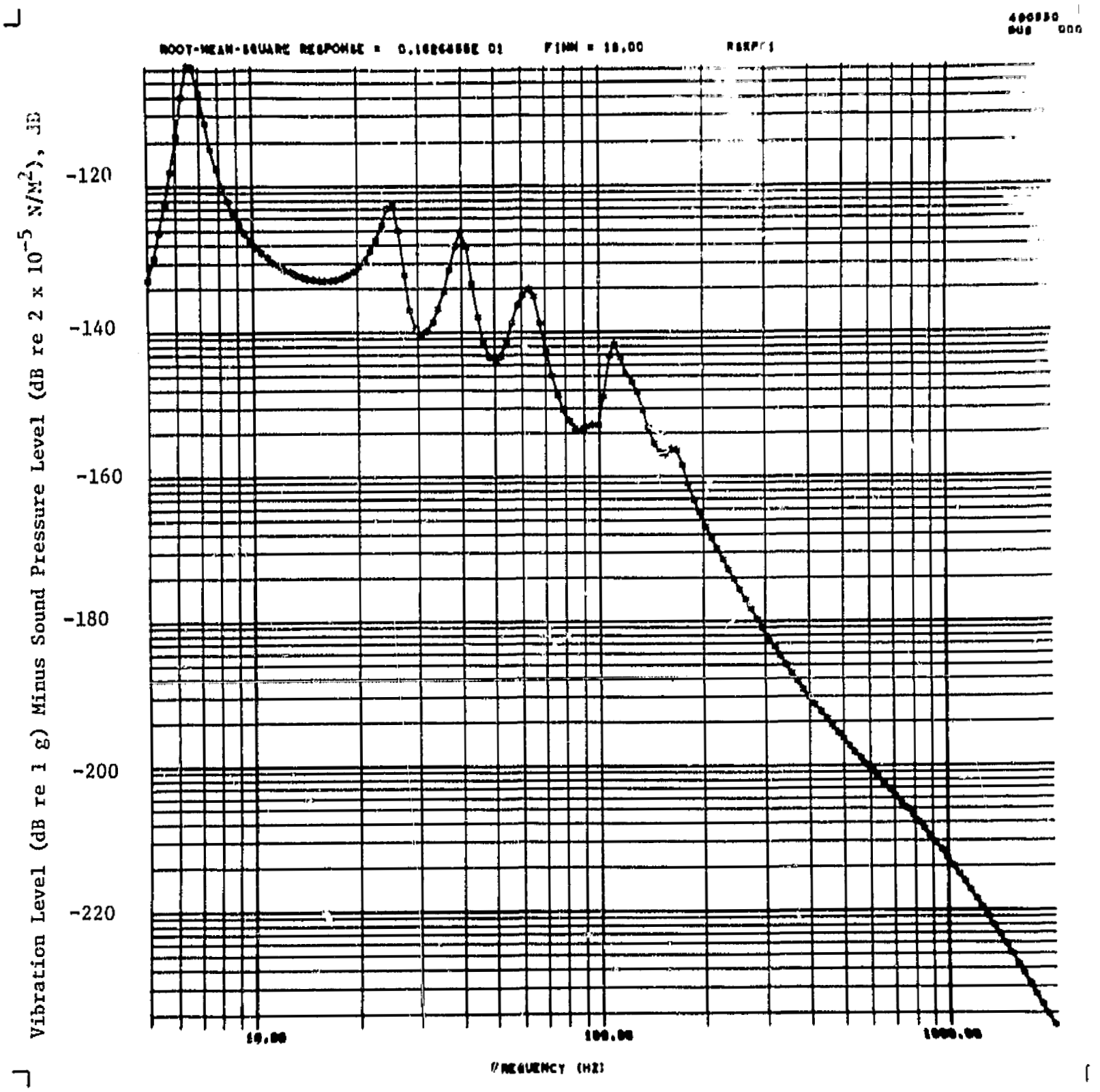

FIGURE 24. VIBRO-ACOUSTIC TRANSFER FUNCTION, CASE I.A.3

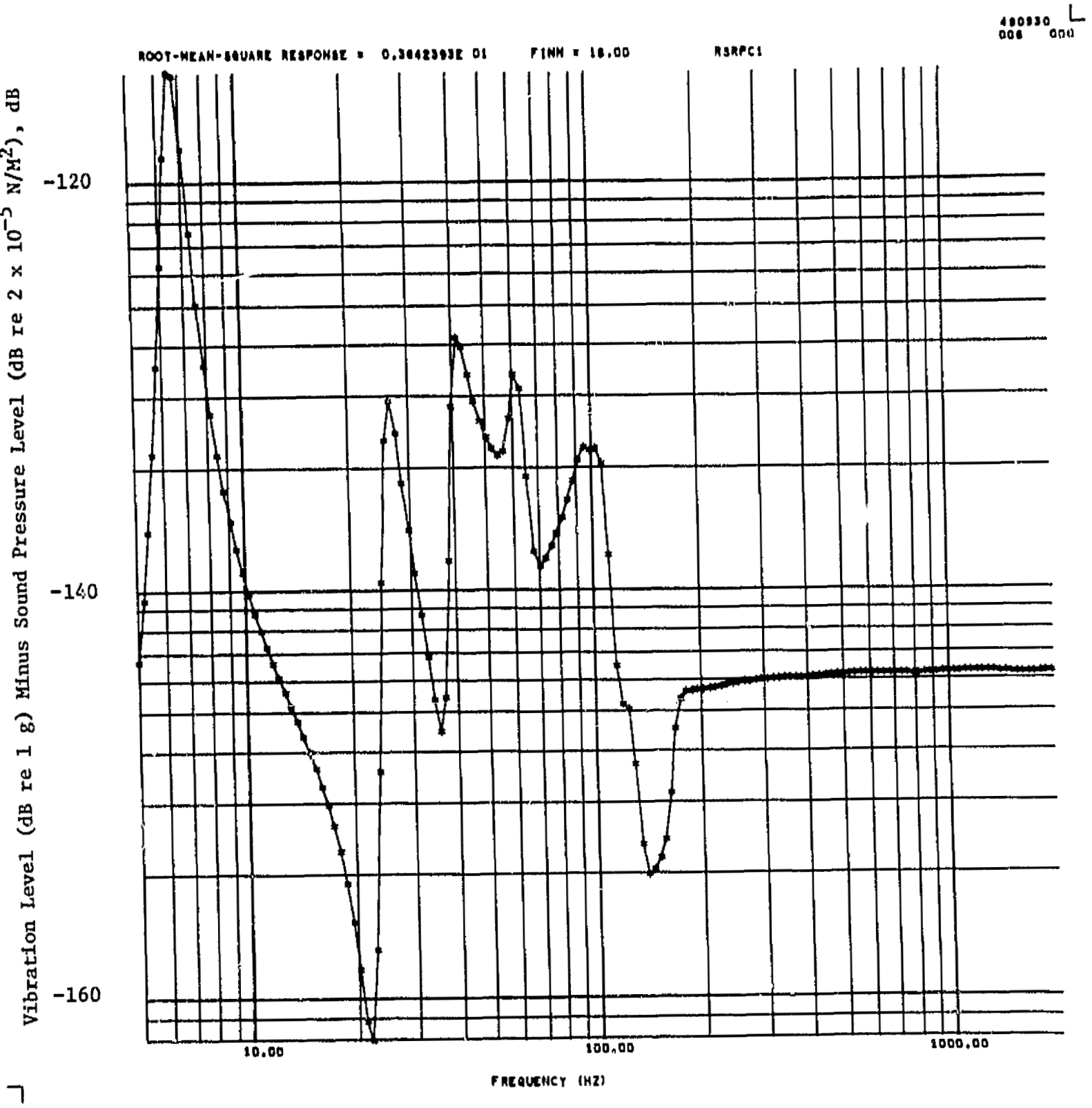

FIGURE 25. VIBRO-ACOUSTIC TRANSFER FUNCTION, CASE I.B.1

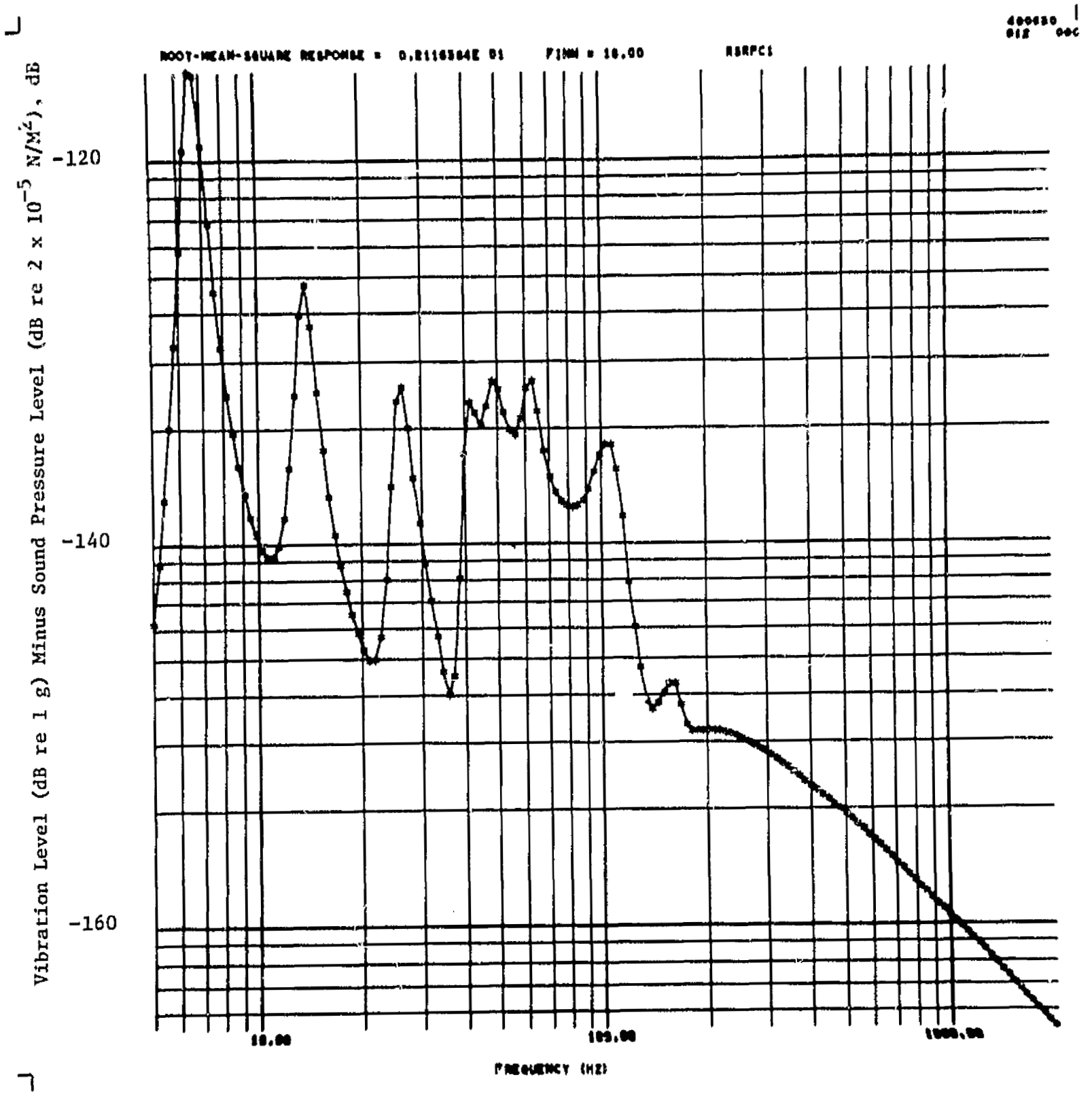

FIGURE 26. VIBRO-ACOUSTIC TRANSFER FUNCTION, CASE I.B.2

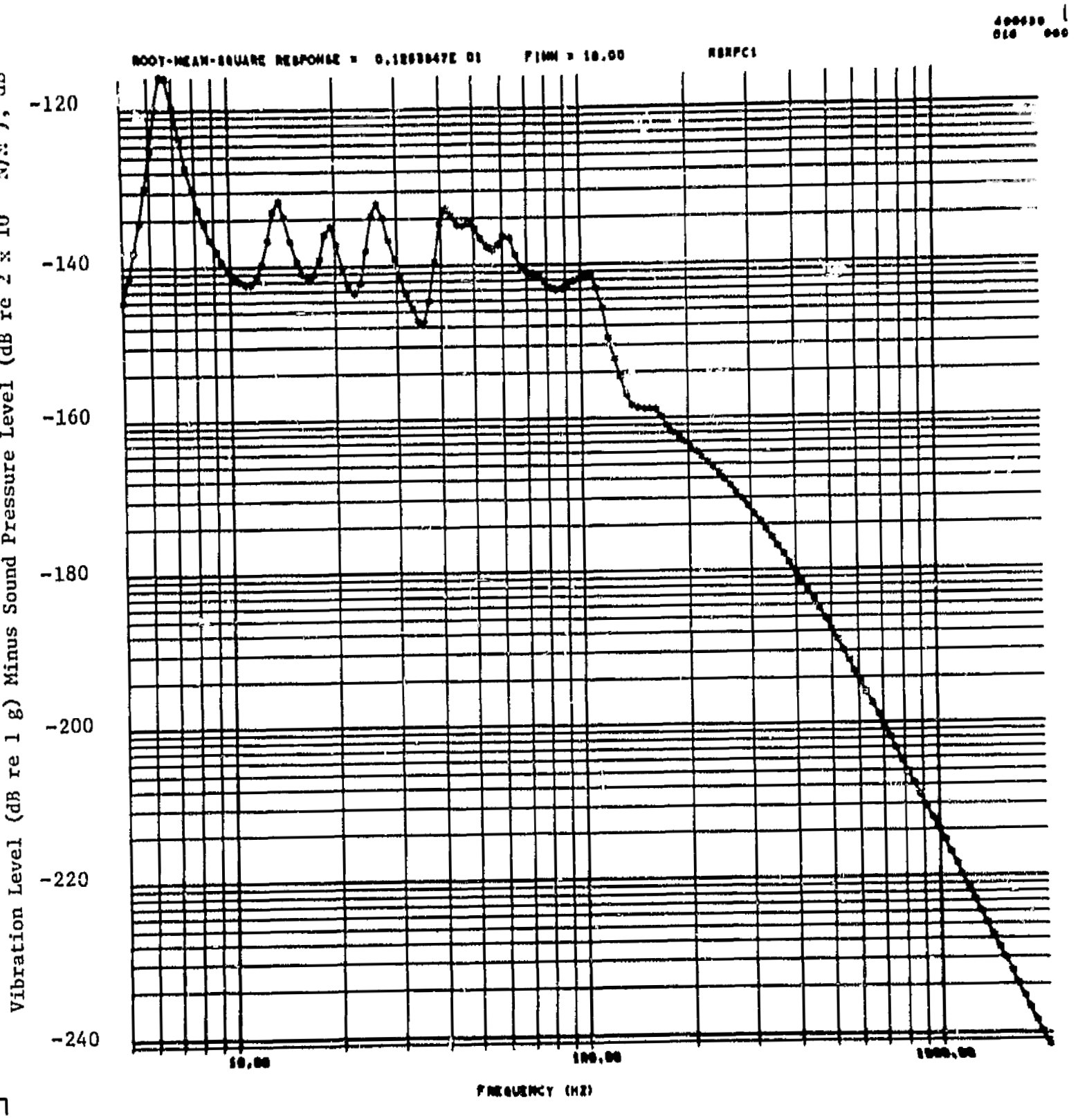

FIGURE 27. VIBRO-ACOUSTIC TRANSFER FUNCTION, CASE I.B.3

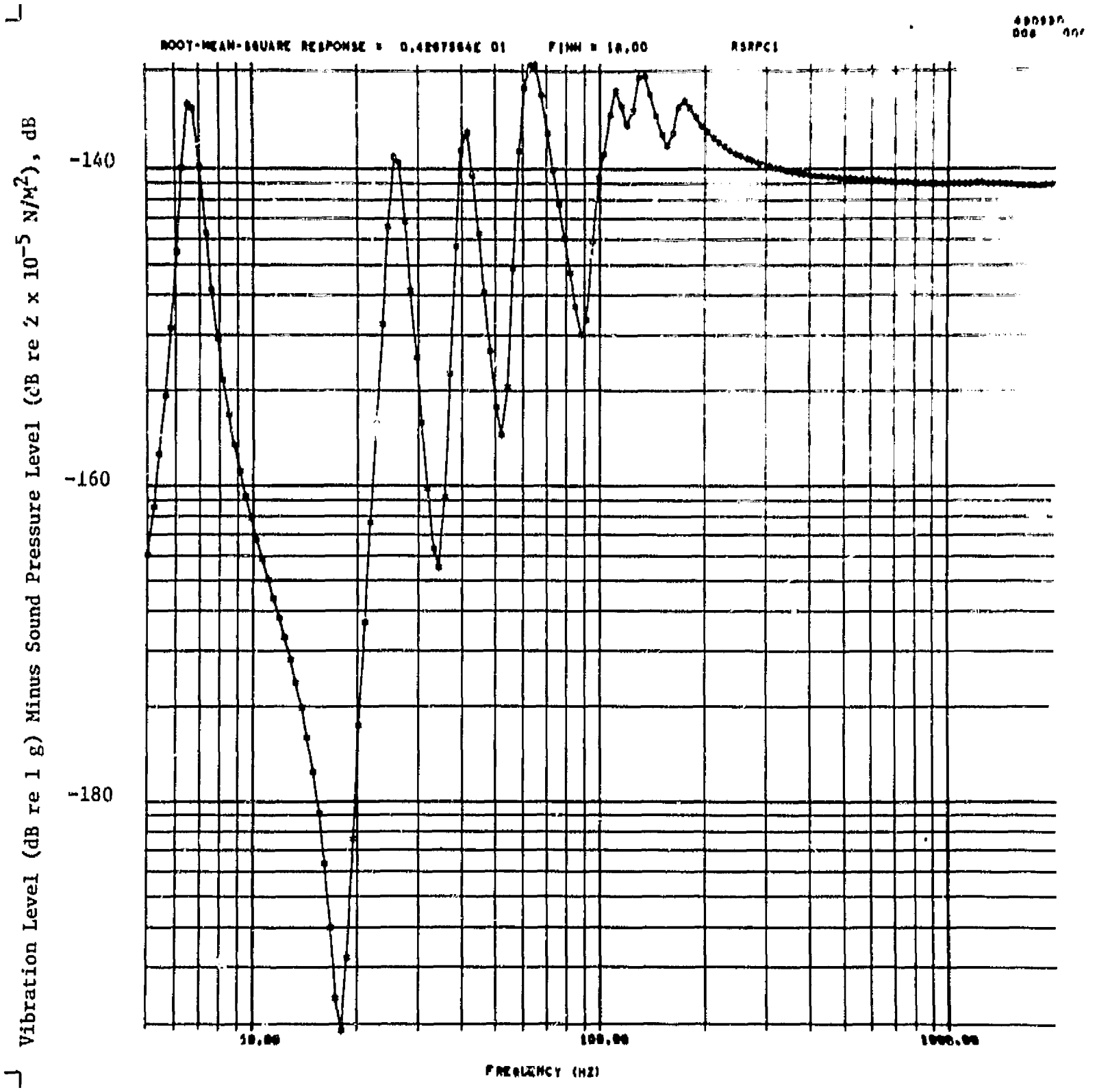

FIGURE 28. VIBRO-ACOUSTIC TRANSFER FUNCTION, CASE I.C.1

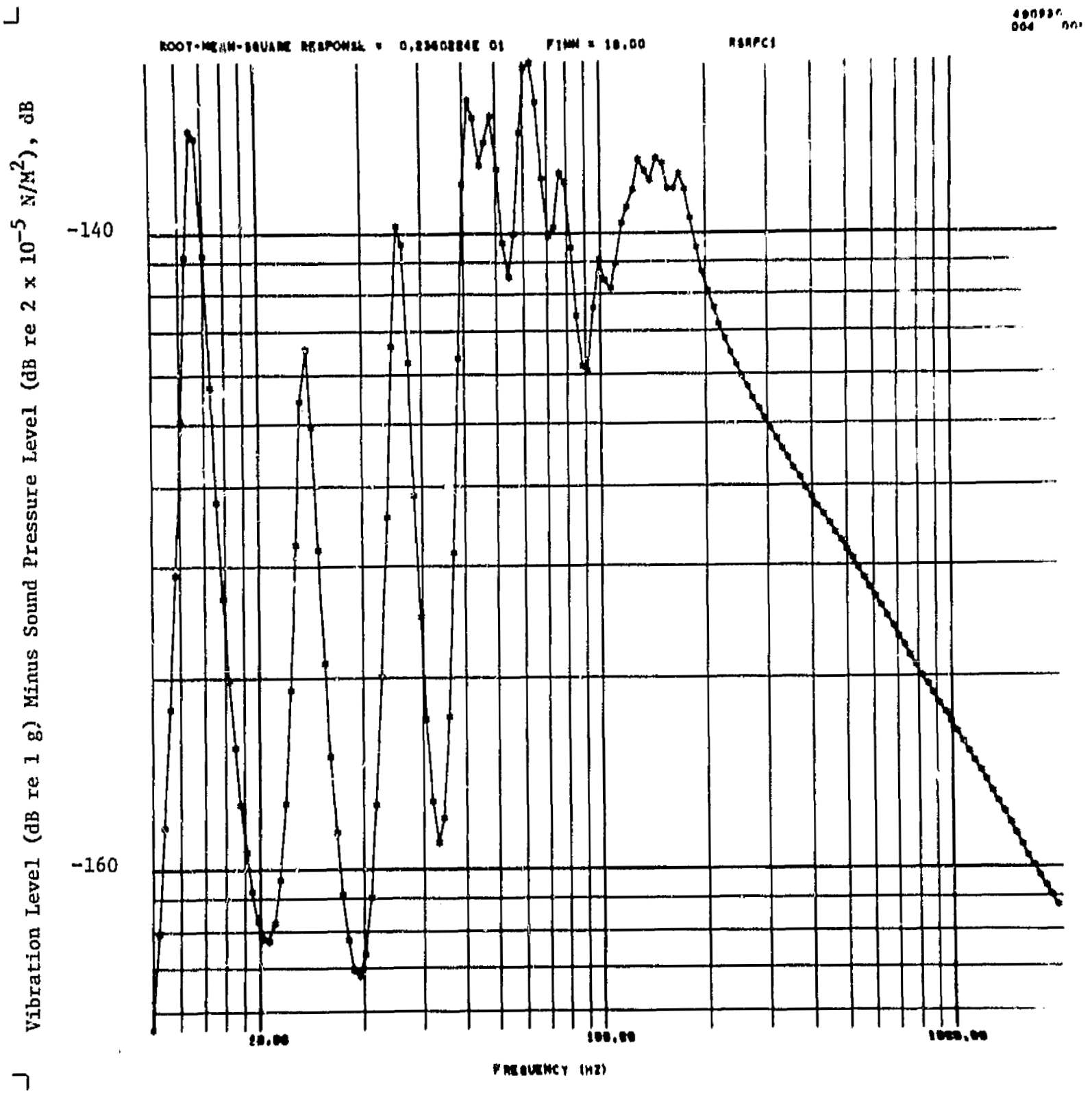

FIGURE 29. VIBRO-ACOUSTIC TRANSFER FUNCTION, CASE I.C.2

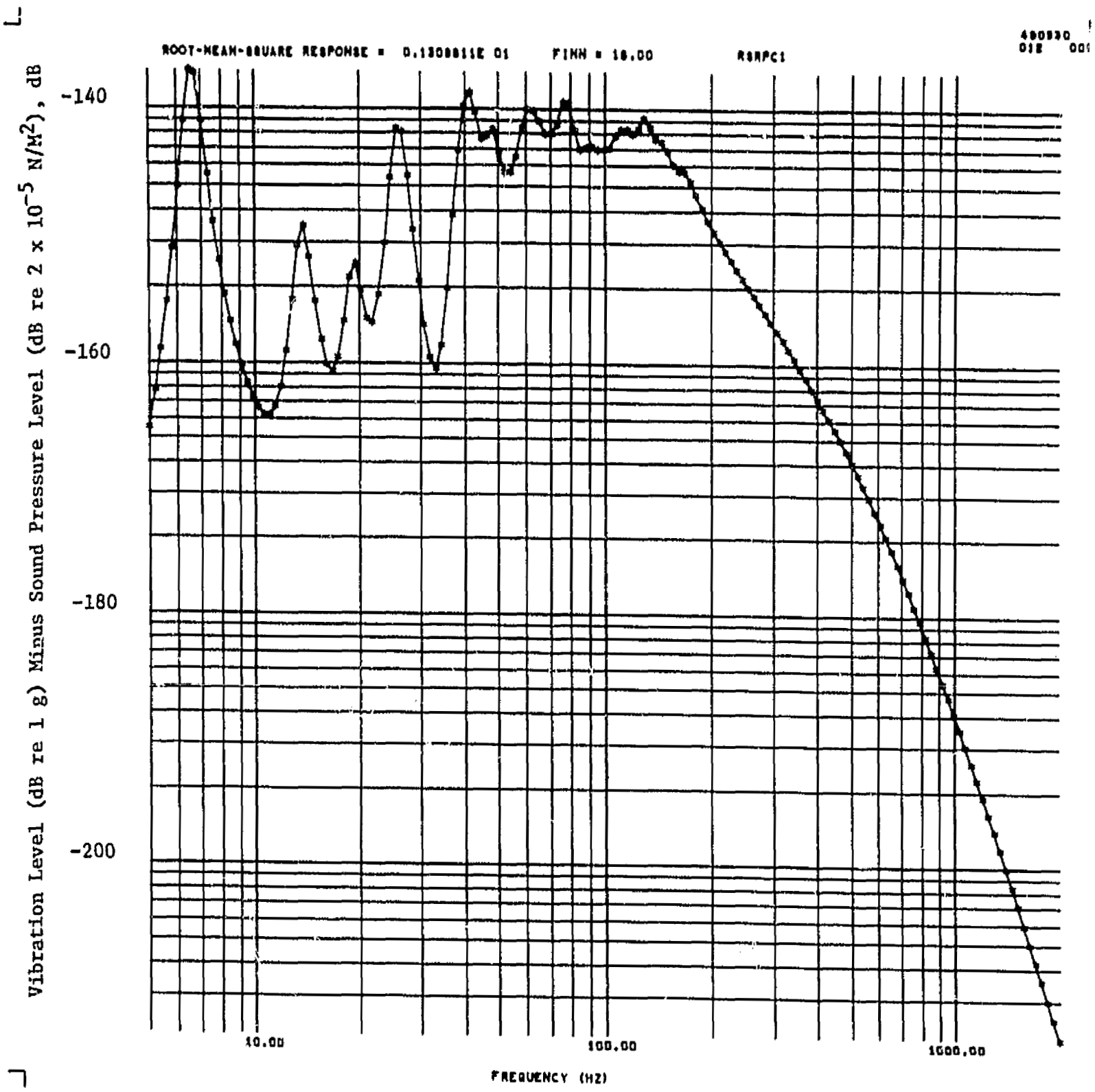

FIGURE 30. VIBRO-ACOUSTIC TRANSFER FUNCTION, CASE I.C.3

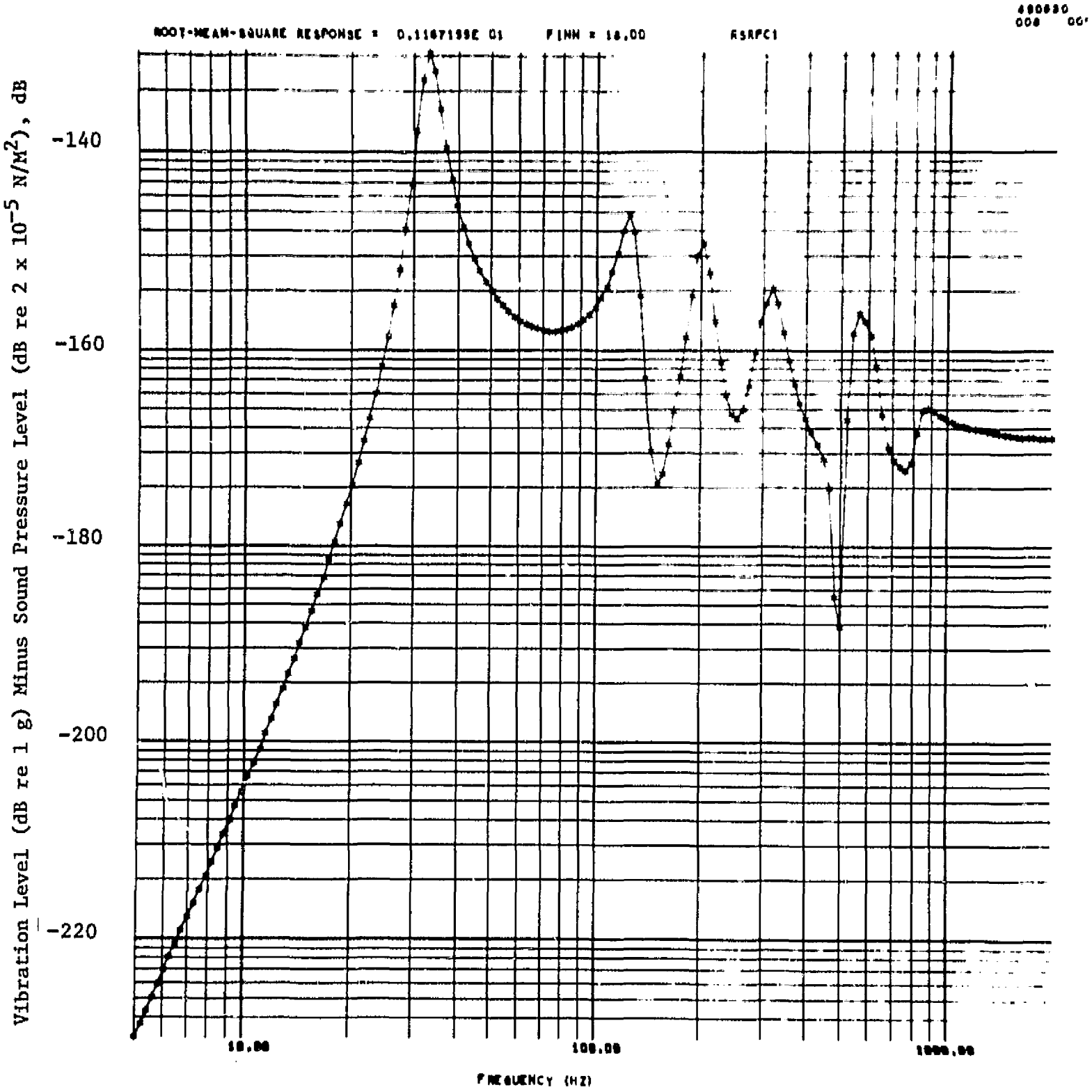

FIGURE 31. VIBRO-ACOUSTIC TRANSFER FUNCTION, CASE II.A.1

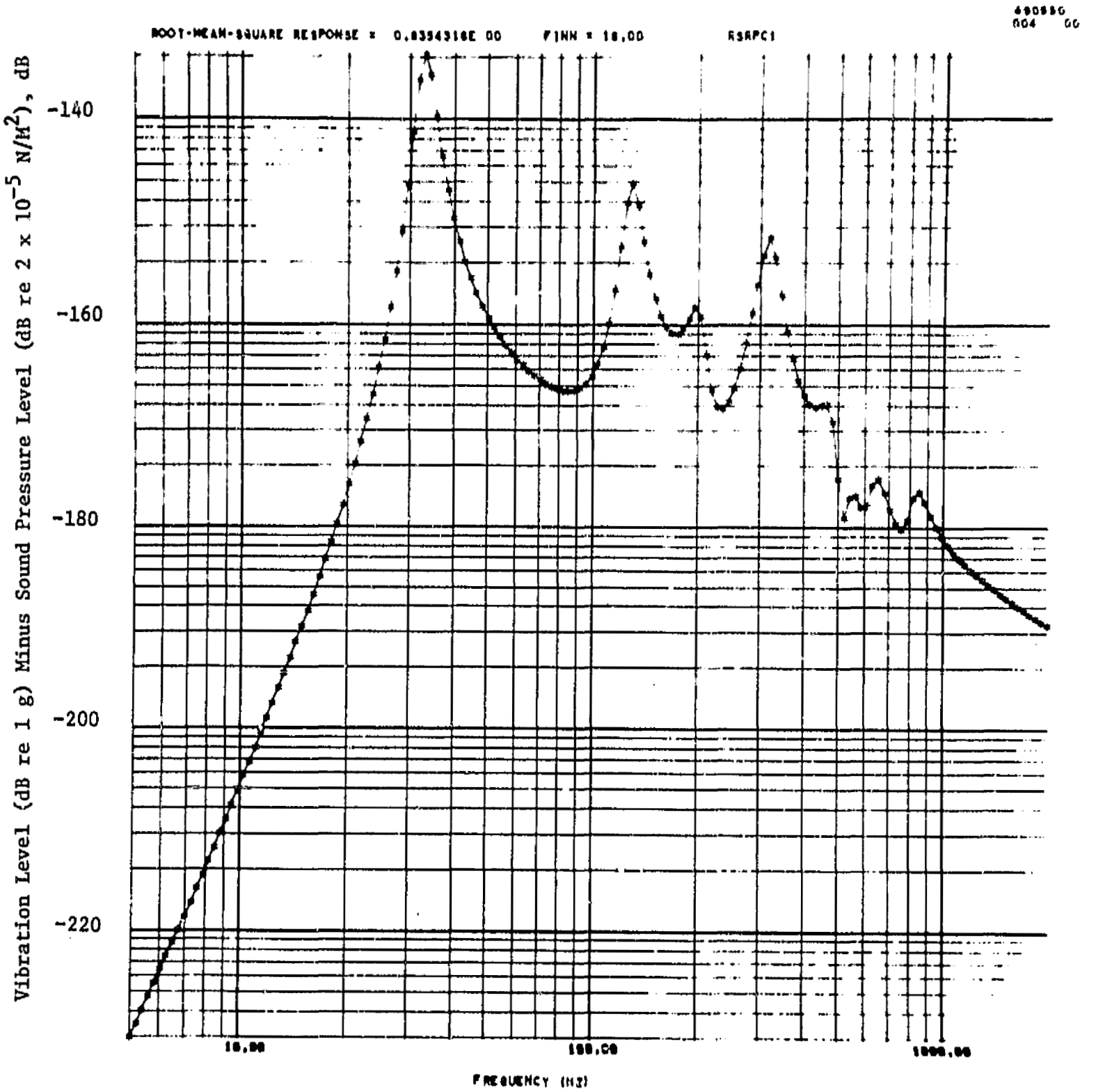

FIGURE 32. VIBRO-ACOUSTIC TRANSFER FUNCTION, CASE II.A.2

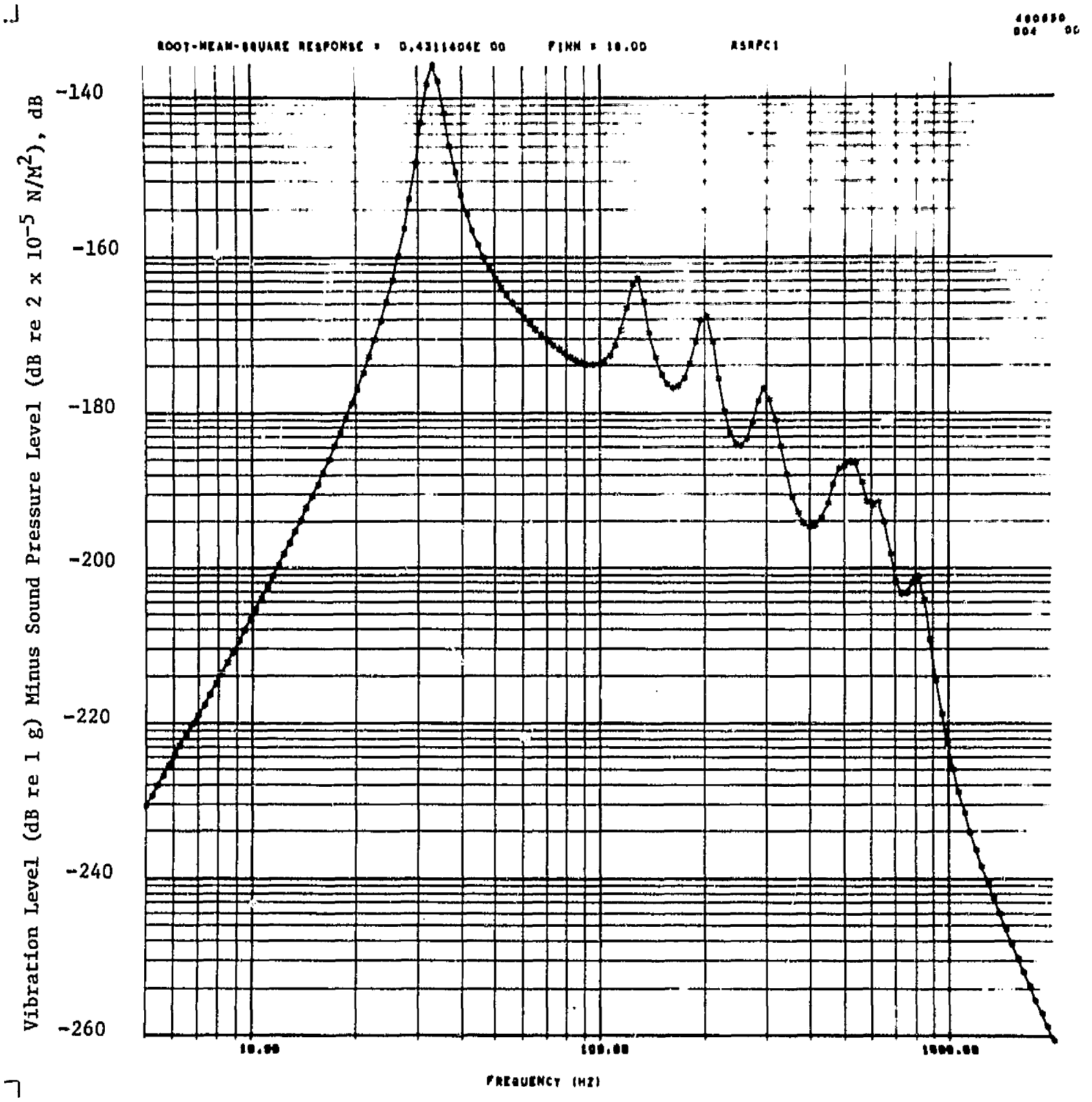

FIGURE 33. VIBRO-ACOUSTIC TRANSFER FUNCTION, CASE II.A.3

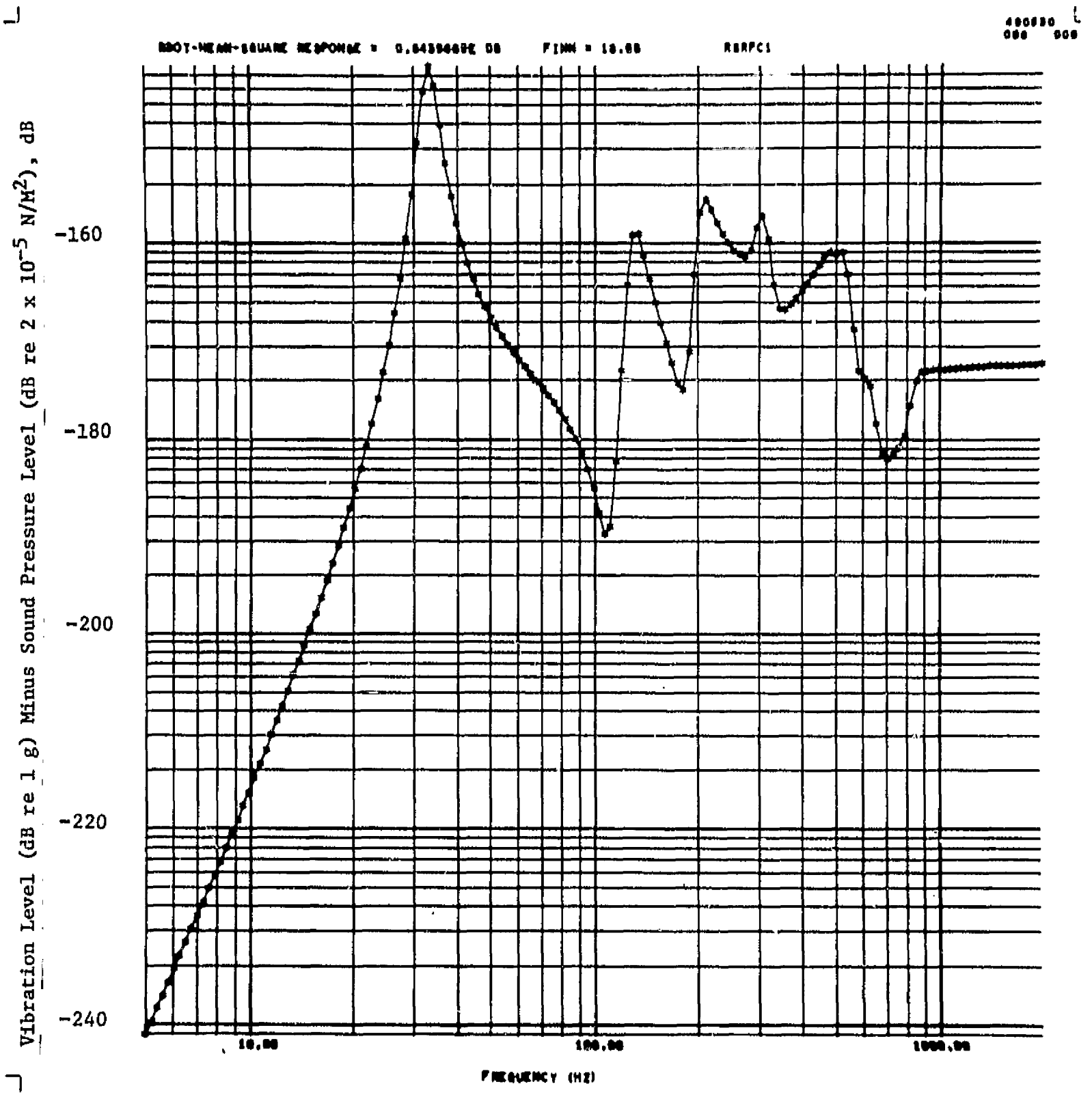

FIGURE 34. VIBRO-ACOUSTIC TRANSFER FUNCTION, CASE II.B.1

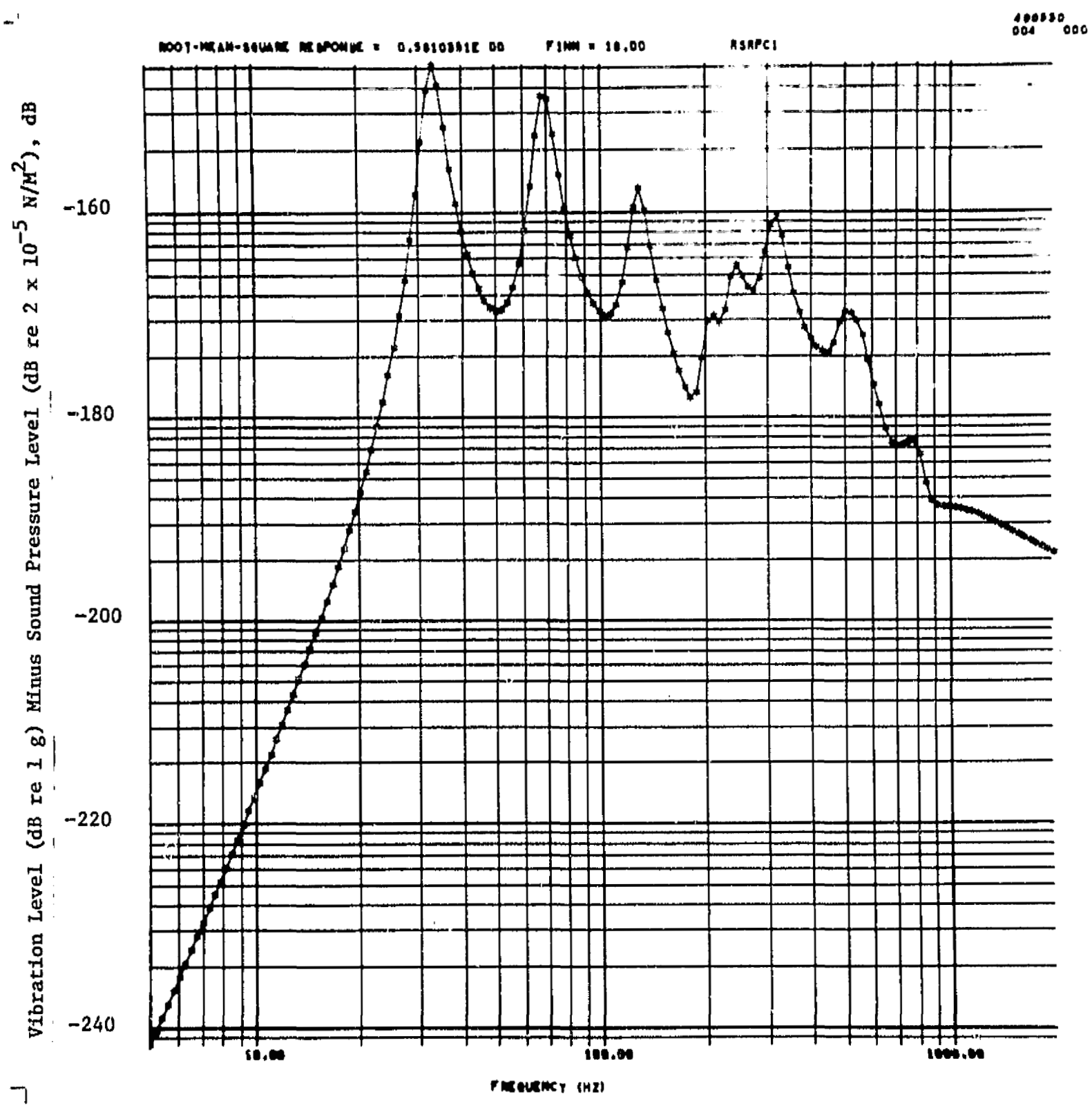

FIGURE 35. VIBRO-ACOUSTIC TRANSFER FUNCTION, CASE II.B.2

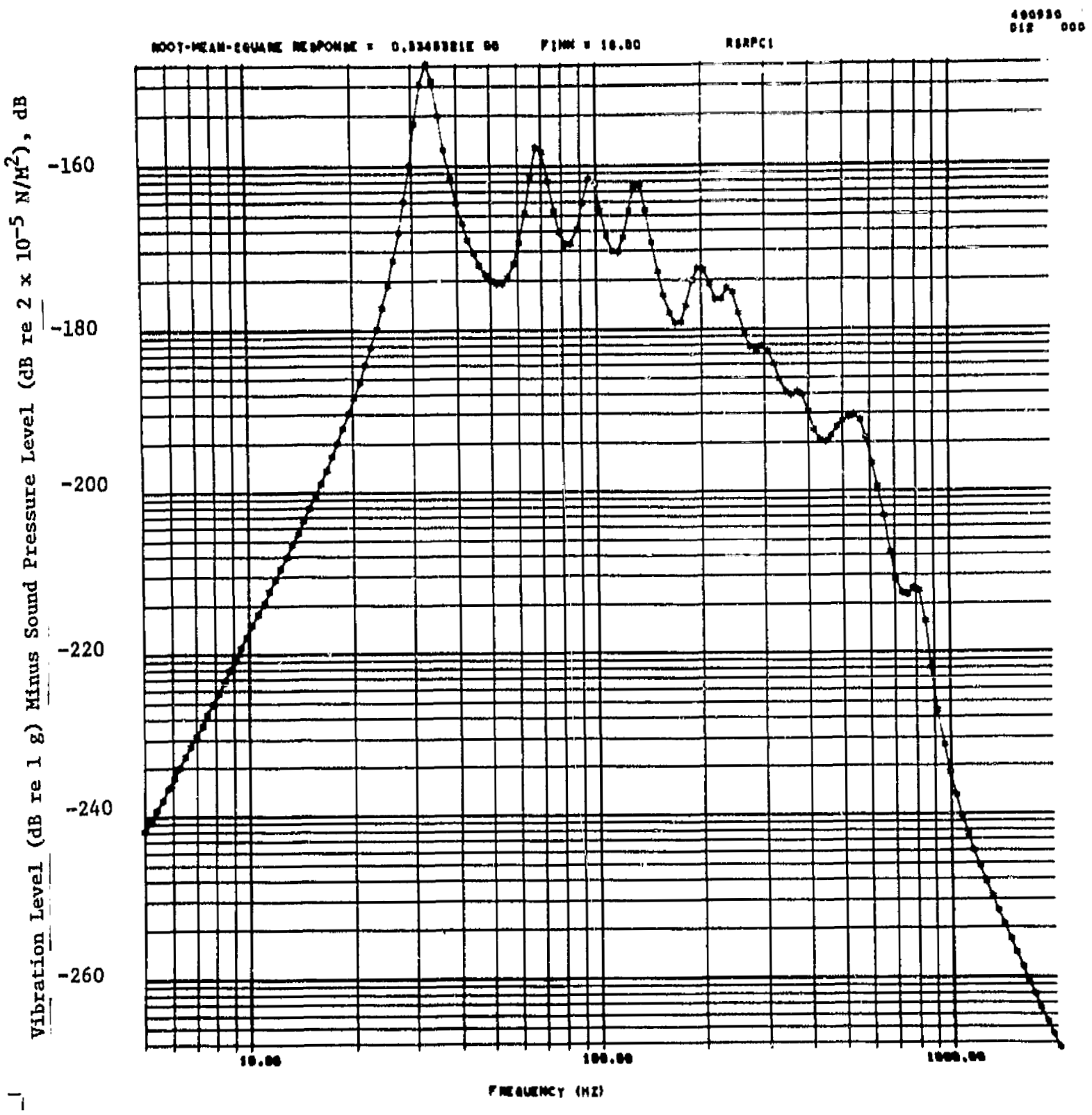

FIGURE 36. VIBRO-ACOUSTIC TRANSFER FUNCTION, CASE II.B.3

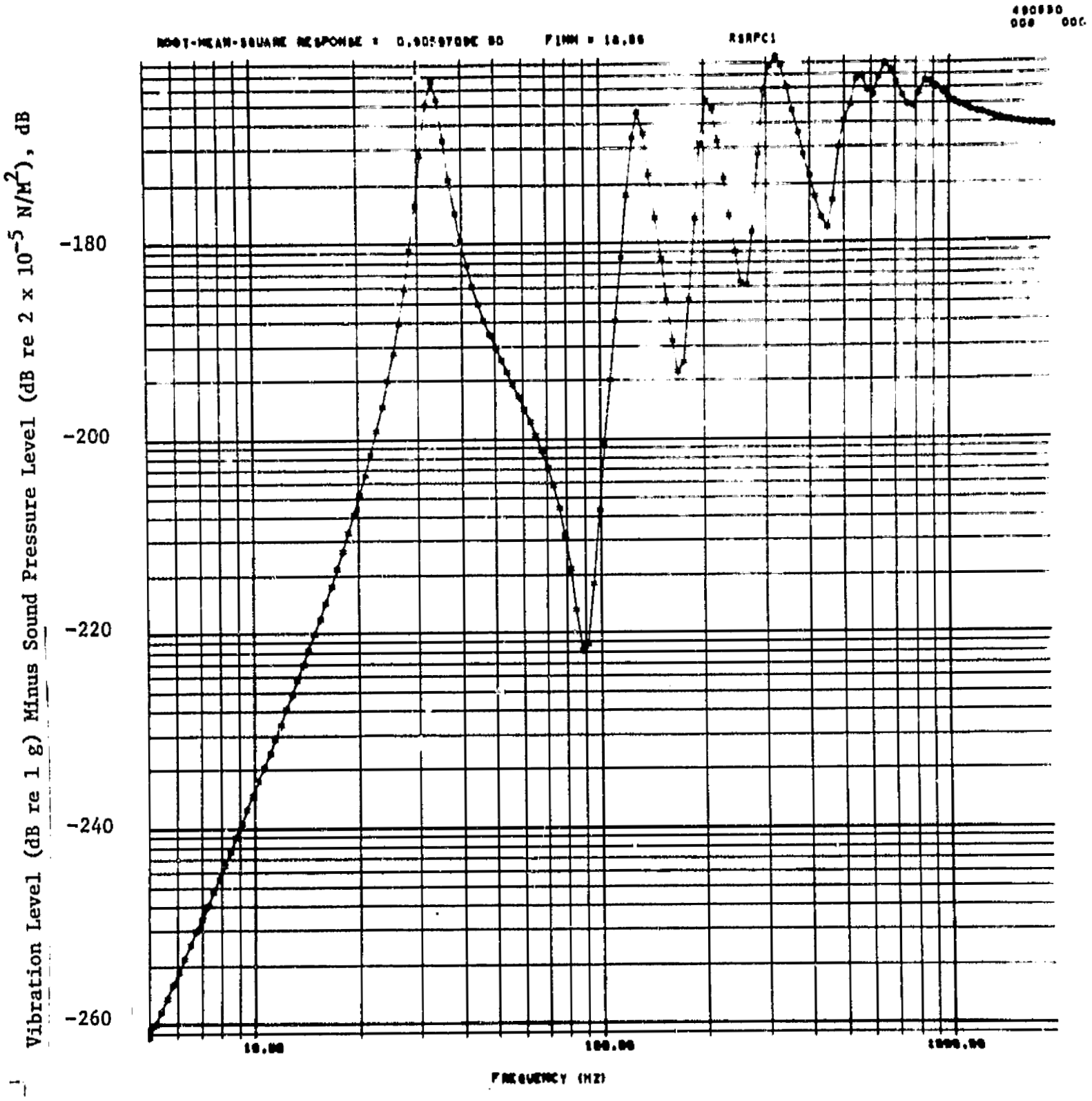

FIGURE 37. VIBRO-ACOUSTIC TRANSFER FUNCTION, CASE II.C.1

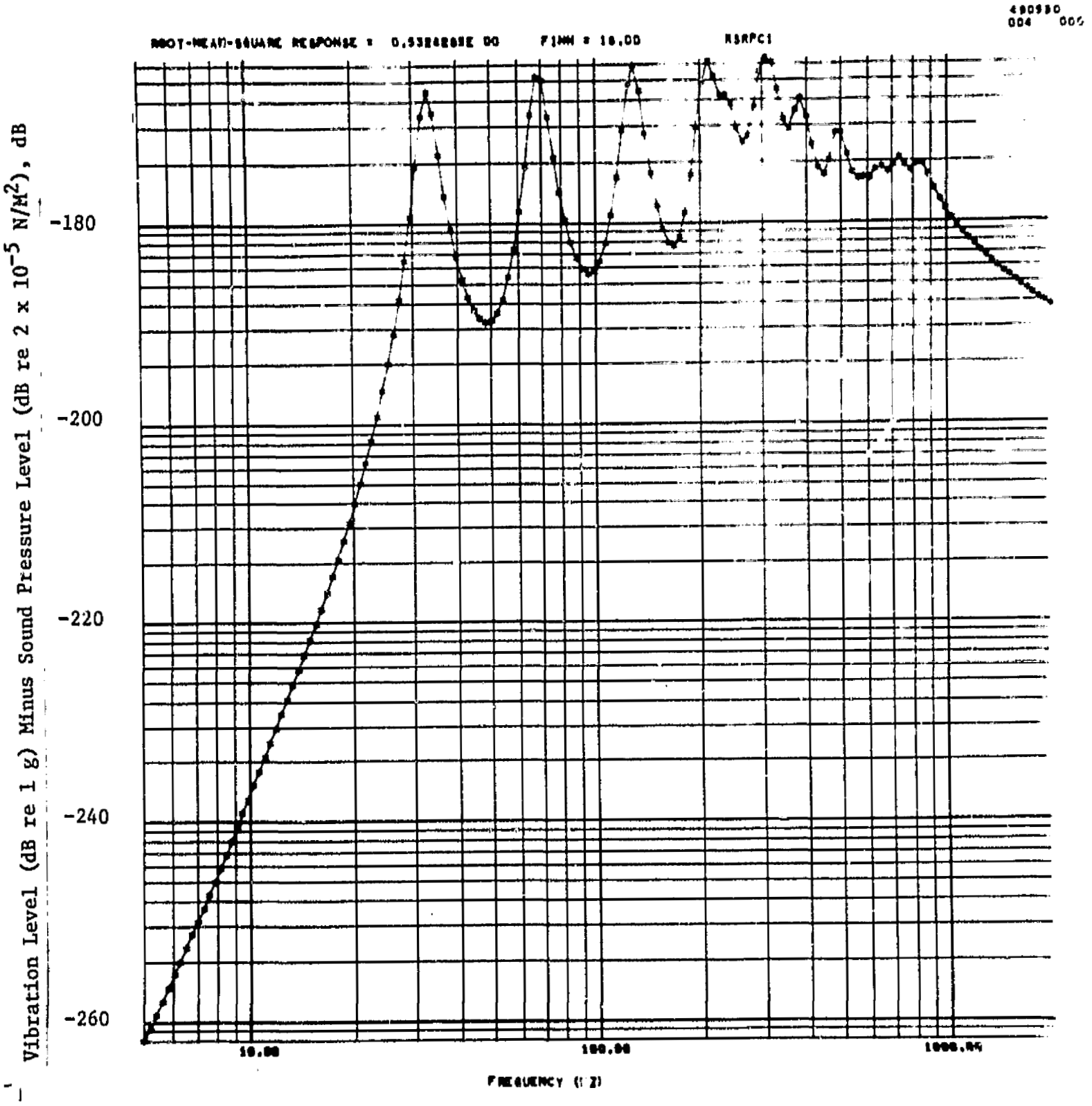

FIGURE 38. VIBRO-ACOUSTIC TRANSFER FUNCTION, CASE II.C.2

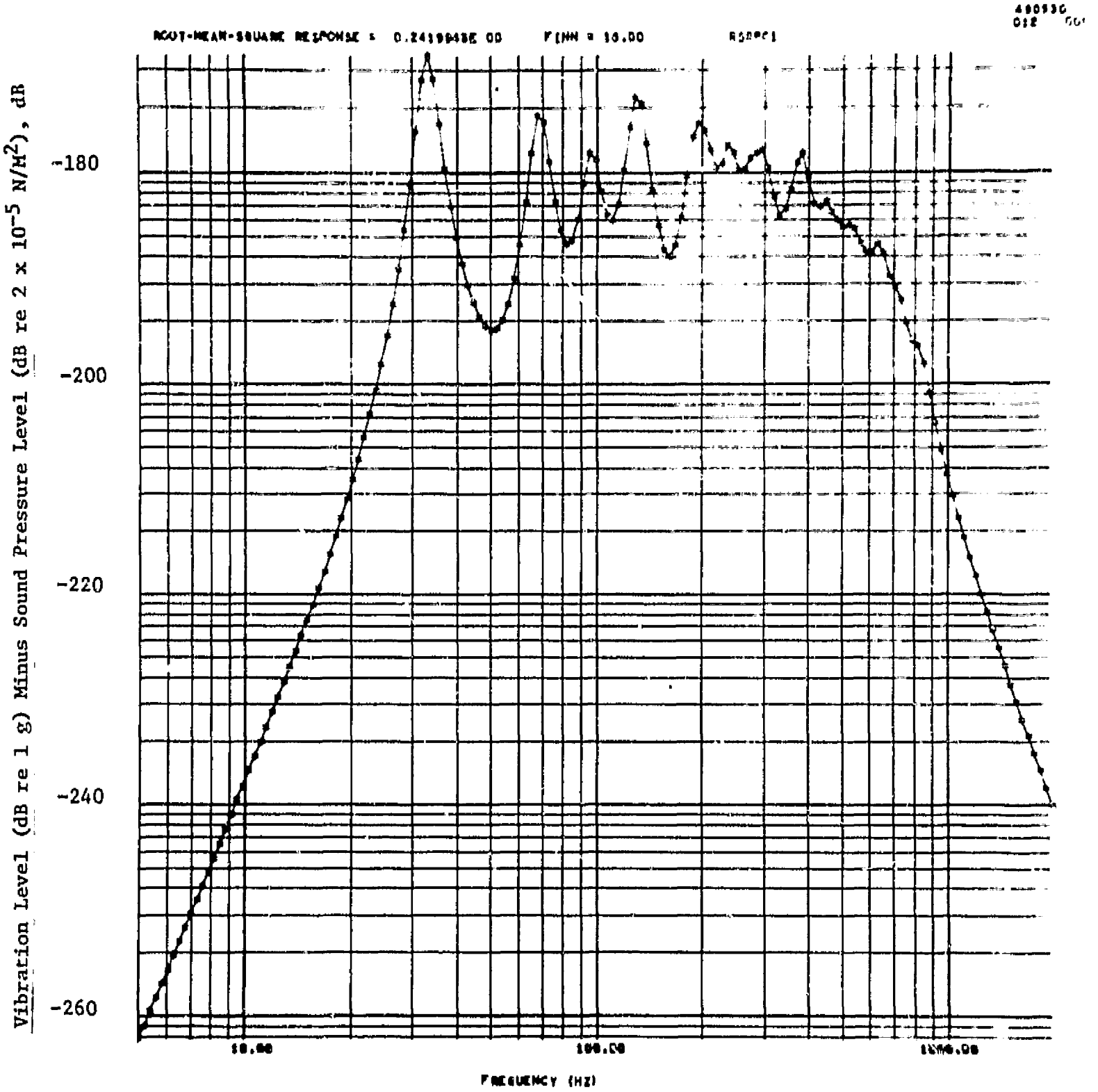

FIGURE 39. VIBRO-ACOUSTIC TRANSFER FUNCTION, CASE II.C.3

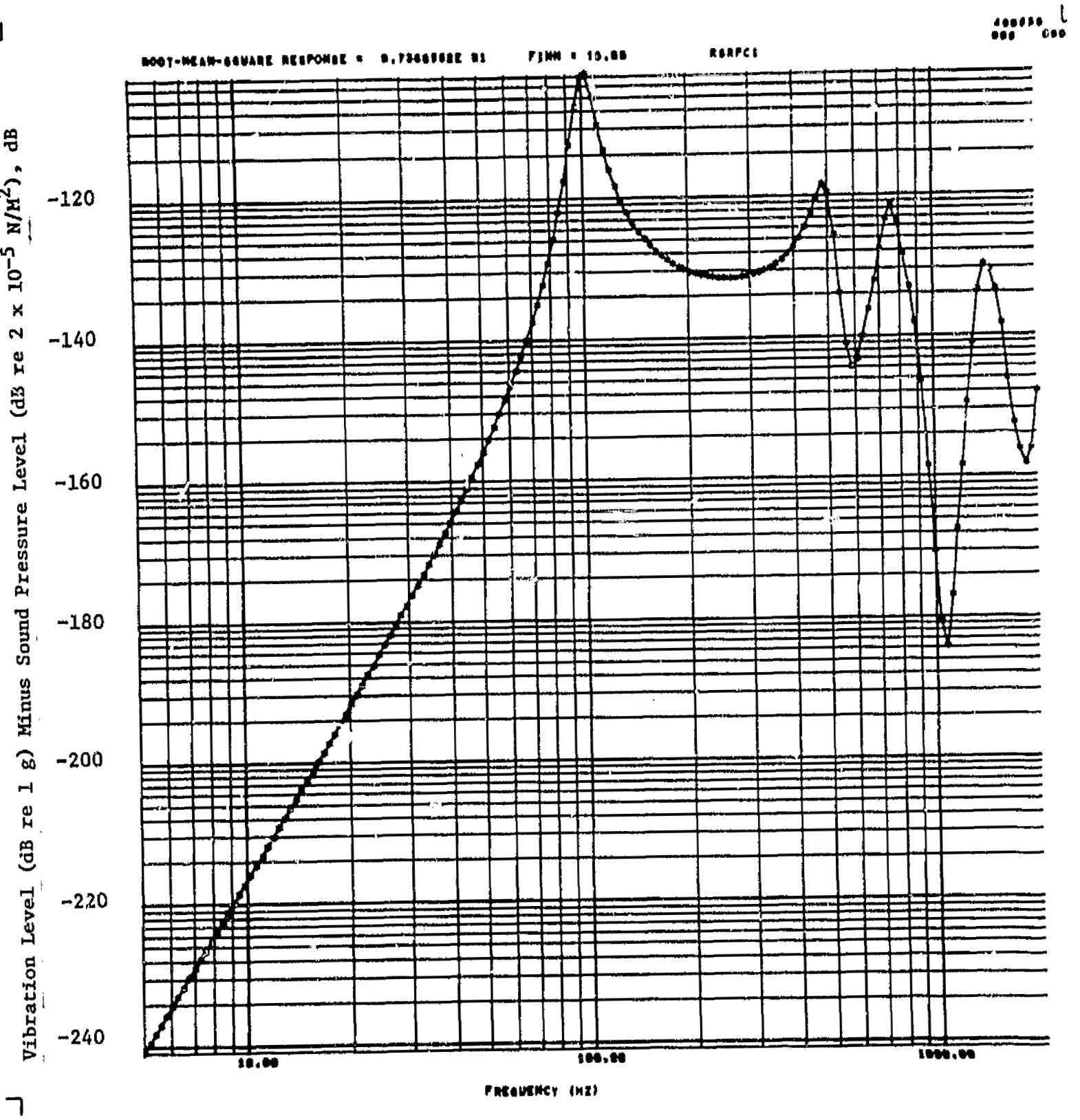

FIGURE 40. VIBRO-ACOUSTIC TRANSFER FUNCTION, CASE III.A.1

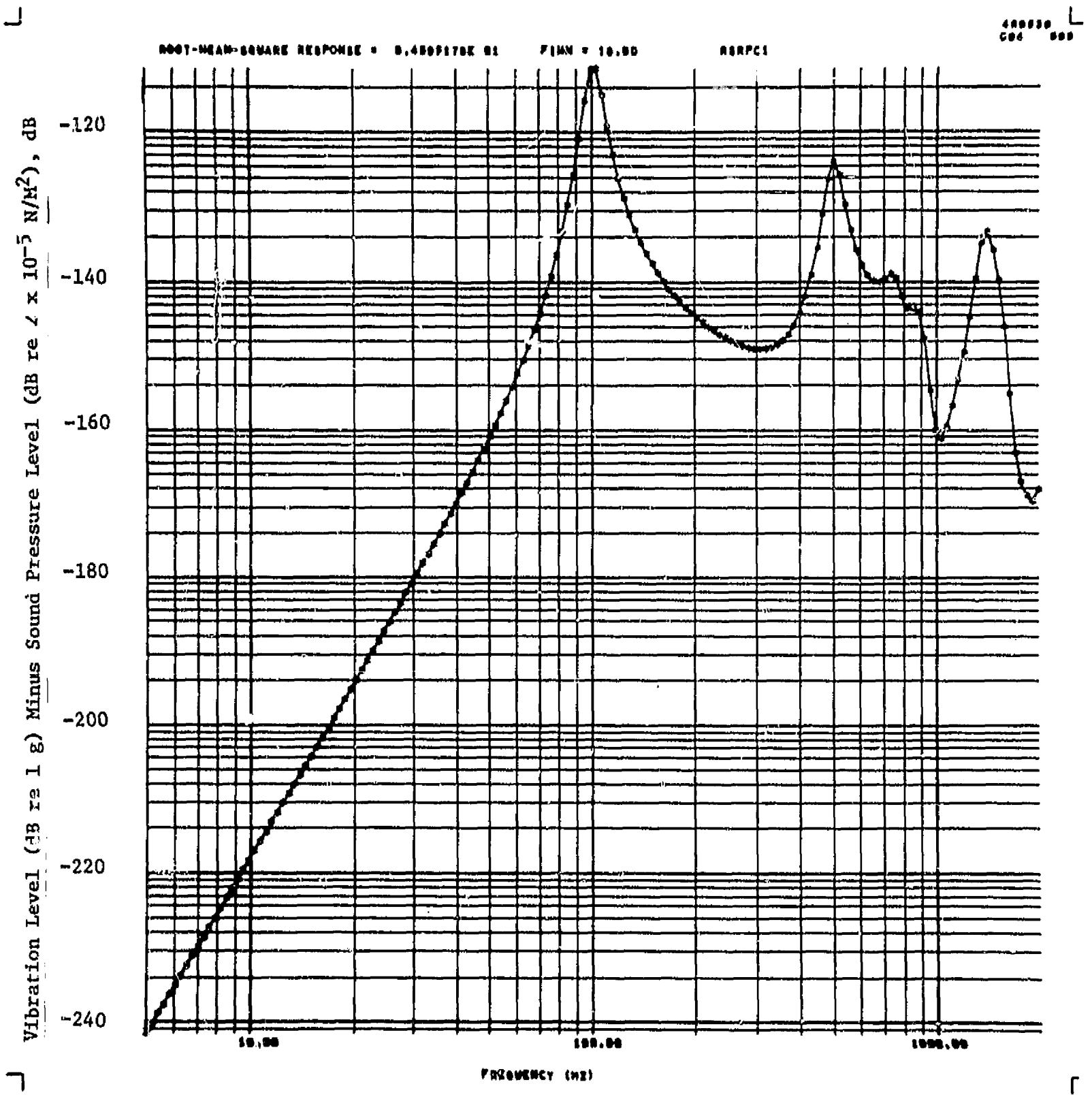

FIGURE 41. VIBRO-ACOUSTIC TRANSFER FUNCTION, CASE III.A.2

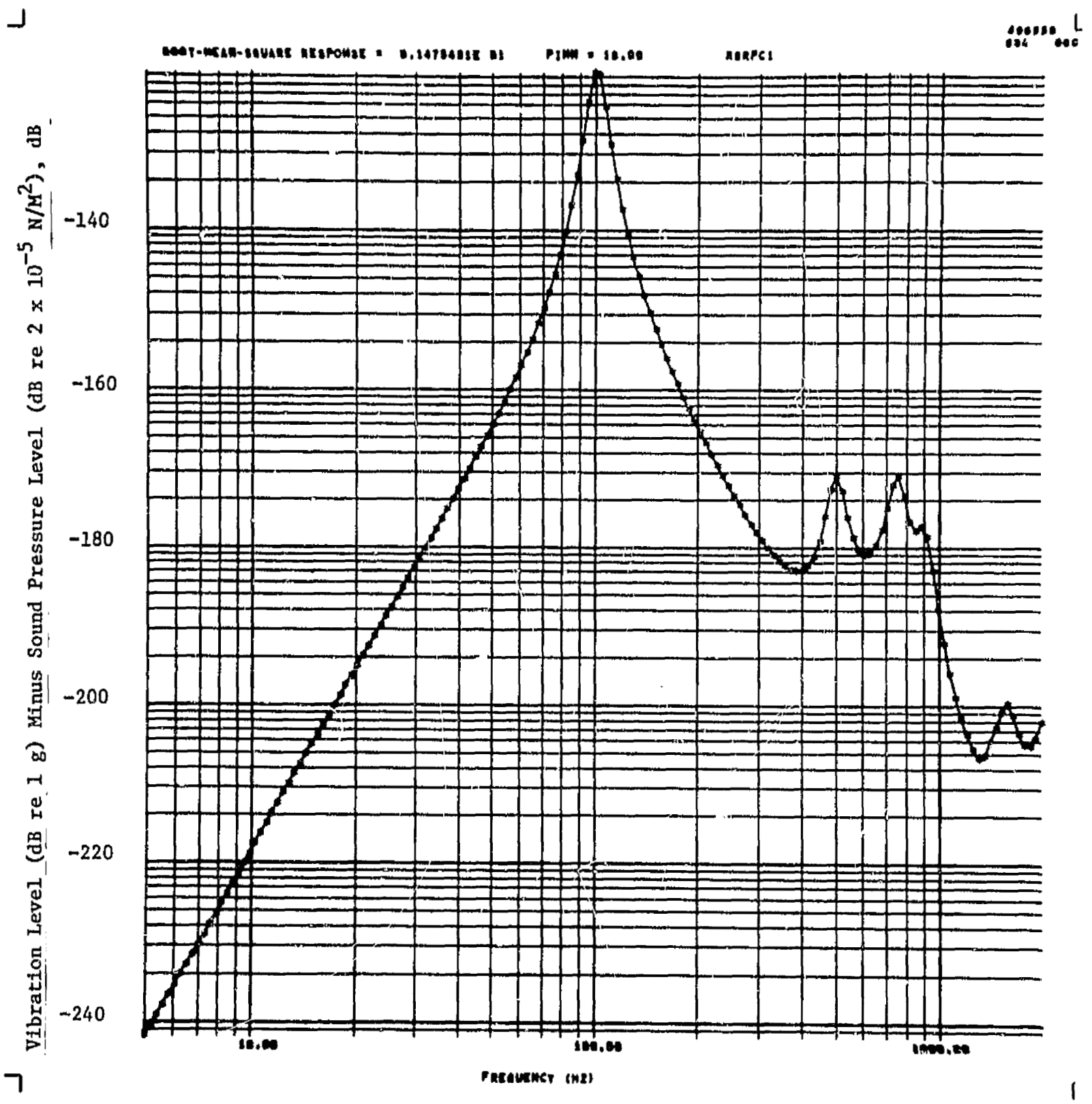

FIGURE 42. VIBRO-ACOUSTIC TRANSFER FUNCTION, CASE III.A.3

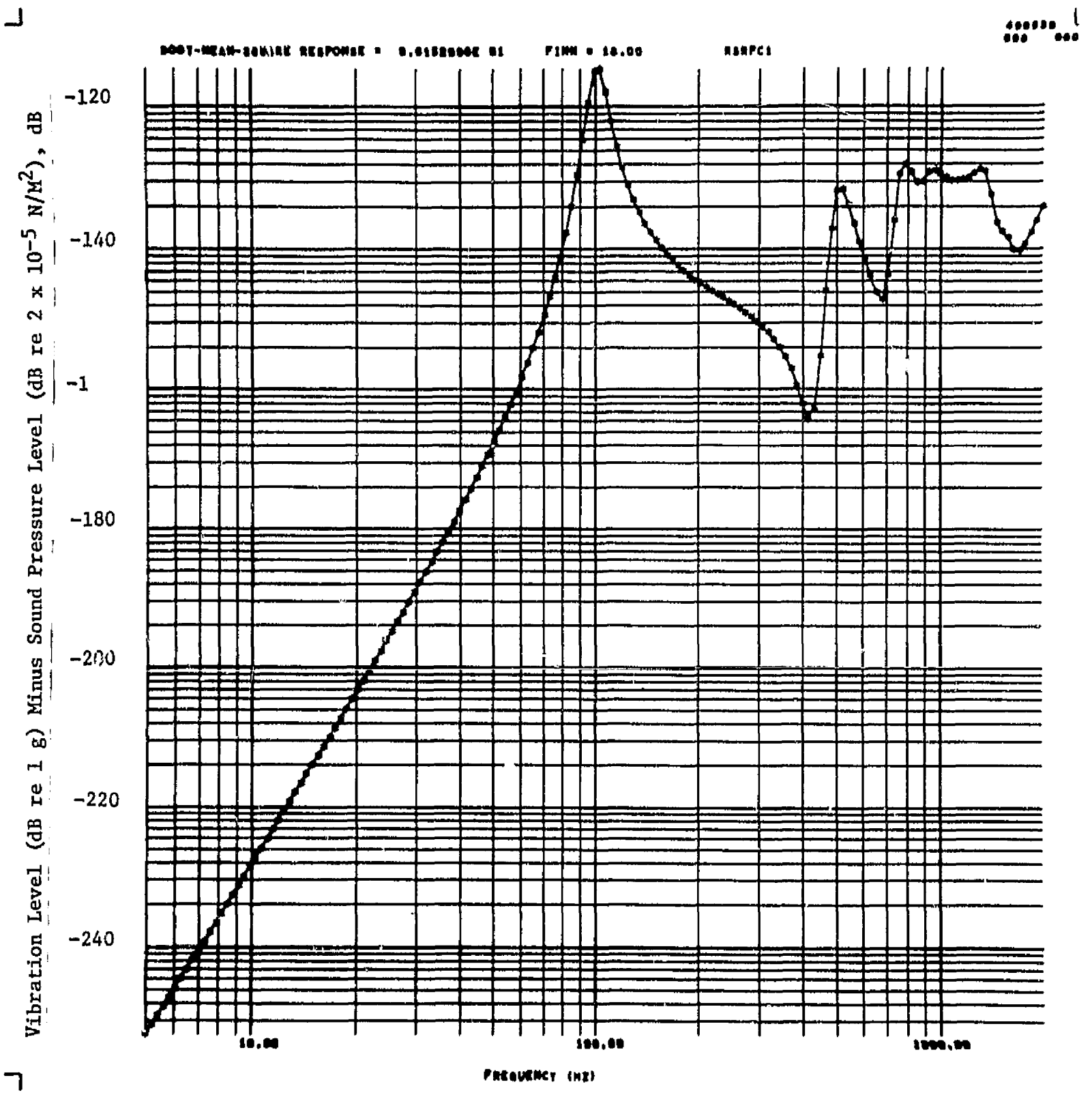

FIGURE 43. VIBRO-ACOUSTIC TRANSFER FUNCTION, CASE III.B.1

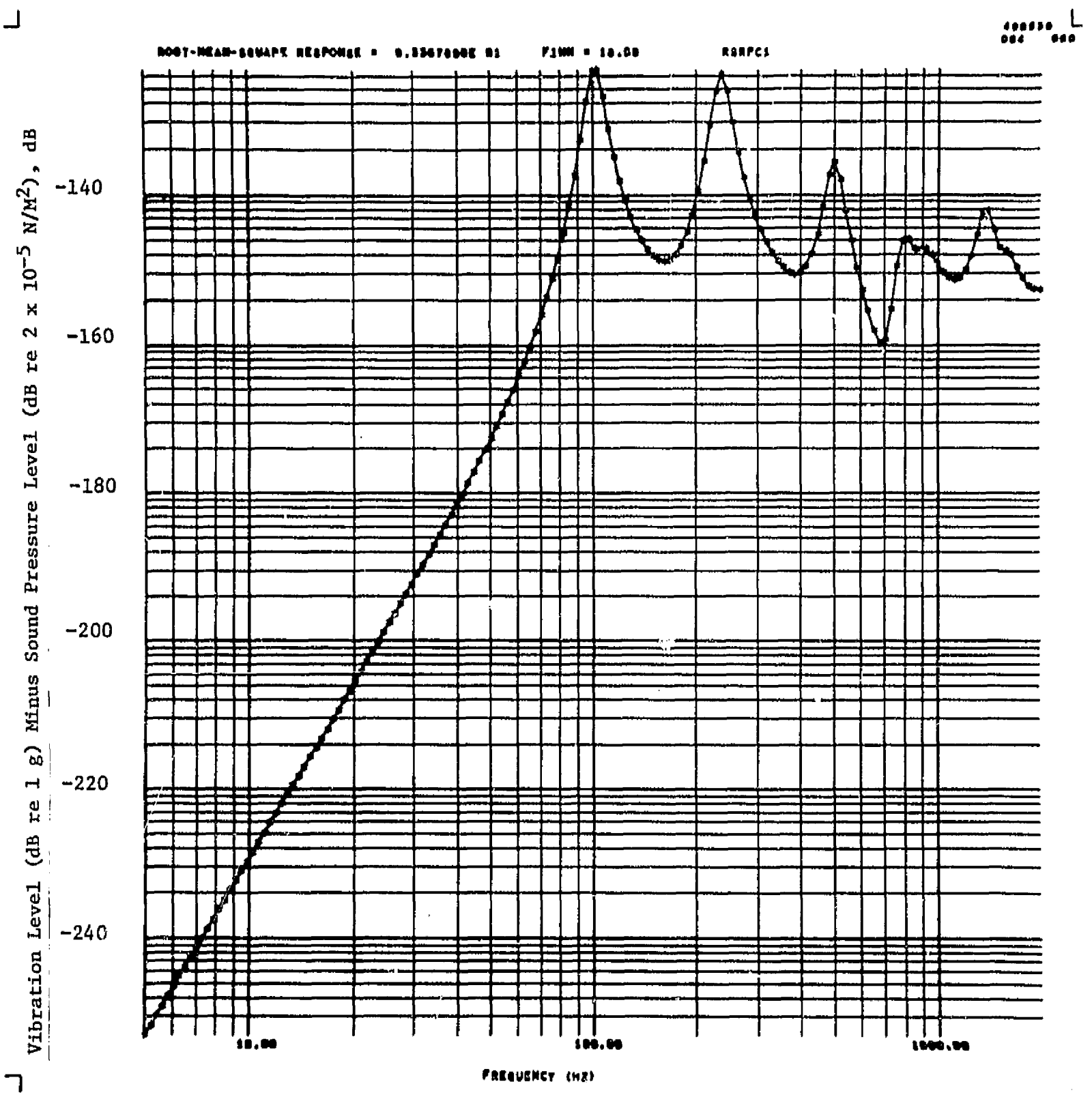

FIGURE 44. VIBRO-ACOUSTIC TRANSFER FUNCTION, CASE III.B.2

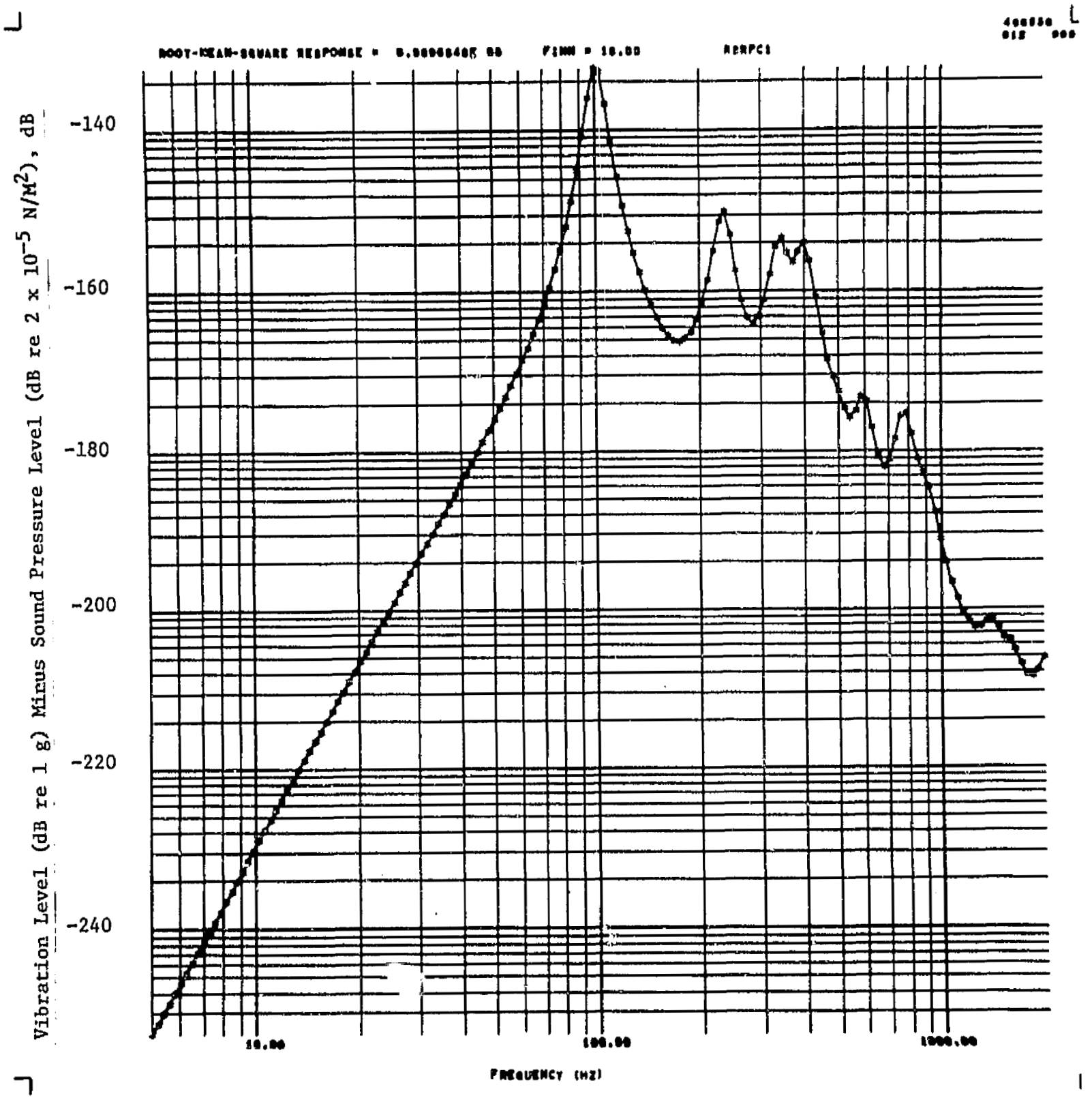

FIGURE 45. VIBRO-ACOUSTIC TRANSFER FUNCTION, CASE III.B.3

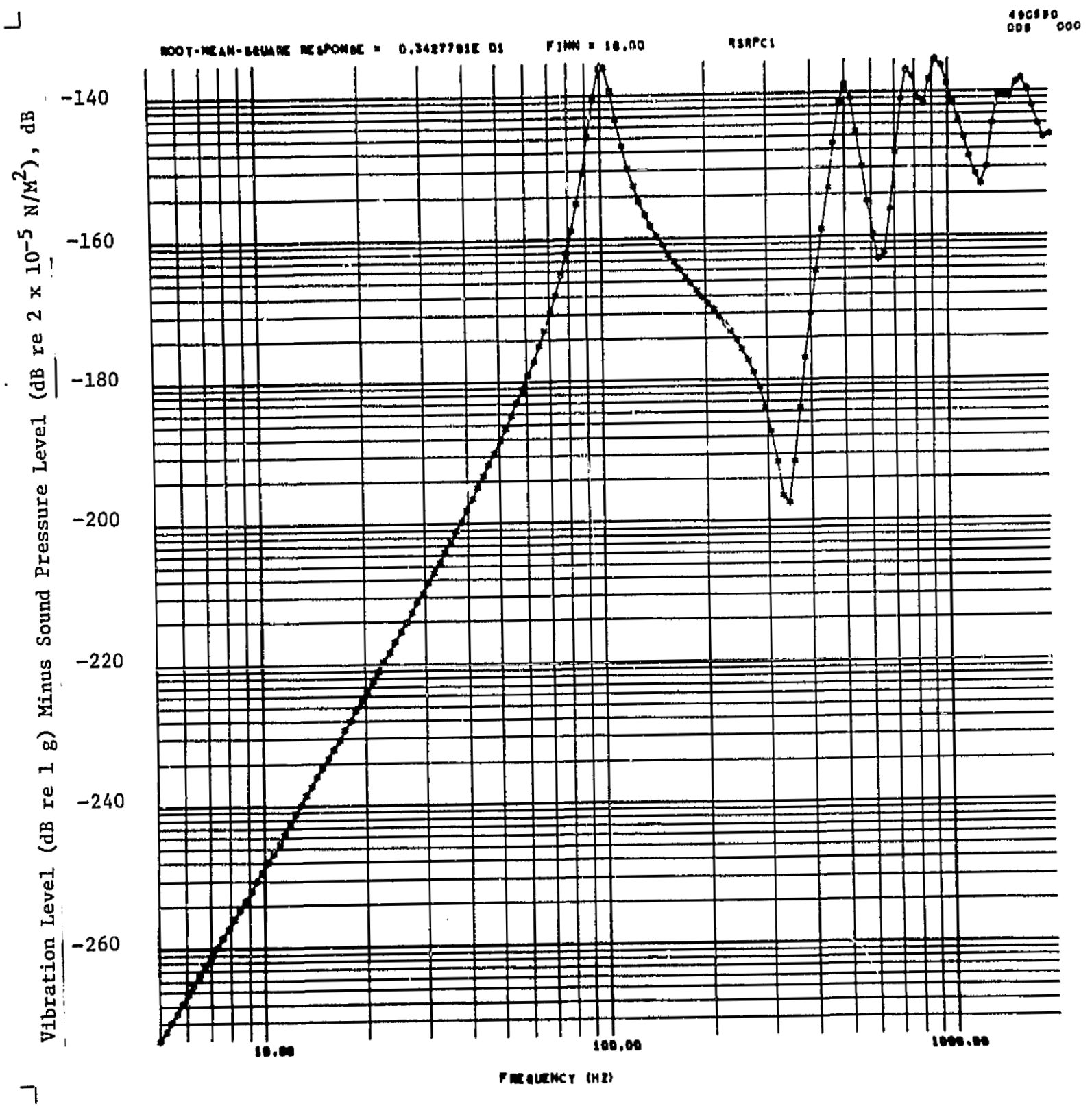

FIGURE 46. VIBRO-ACOUSTIC TRANSFER FUNCTION, CASE III.C.1

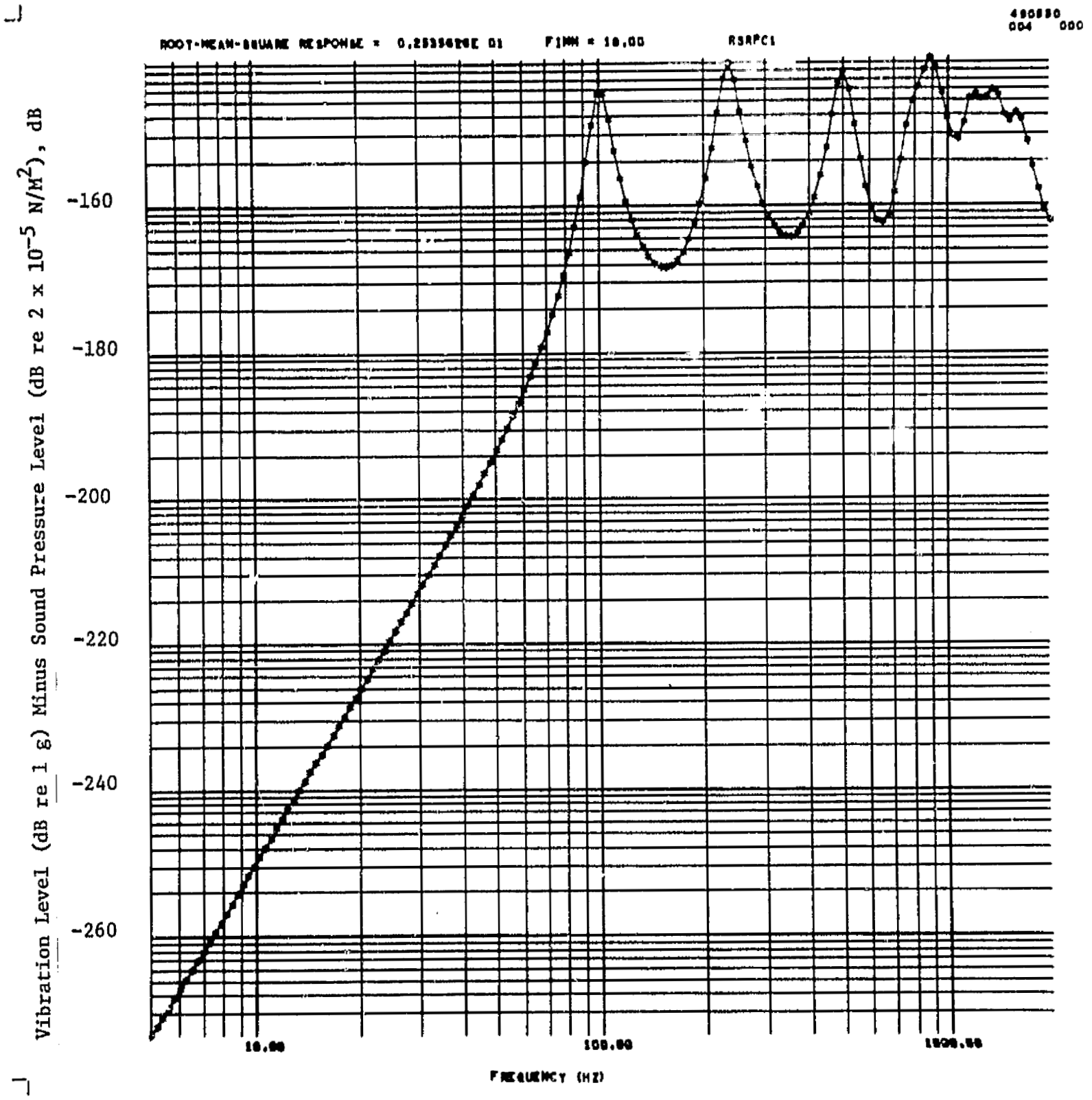

FIGURE 47. VIBRO-ACOUSTIC TRANSFER FUNCTION, CASE III.C.2

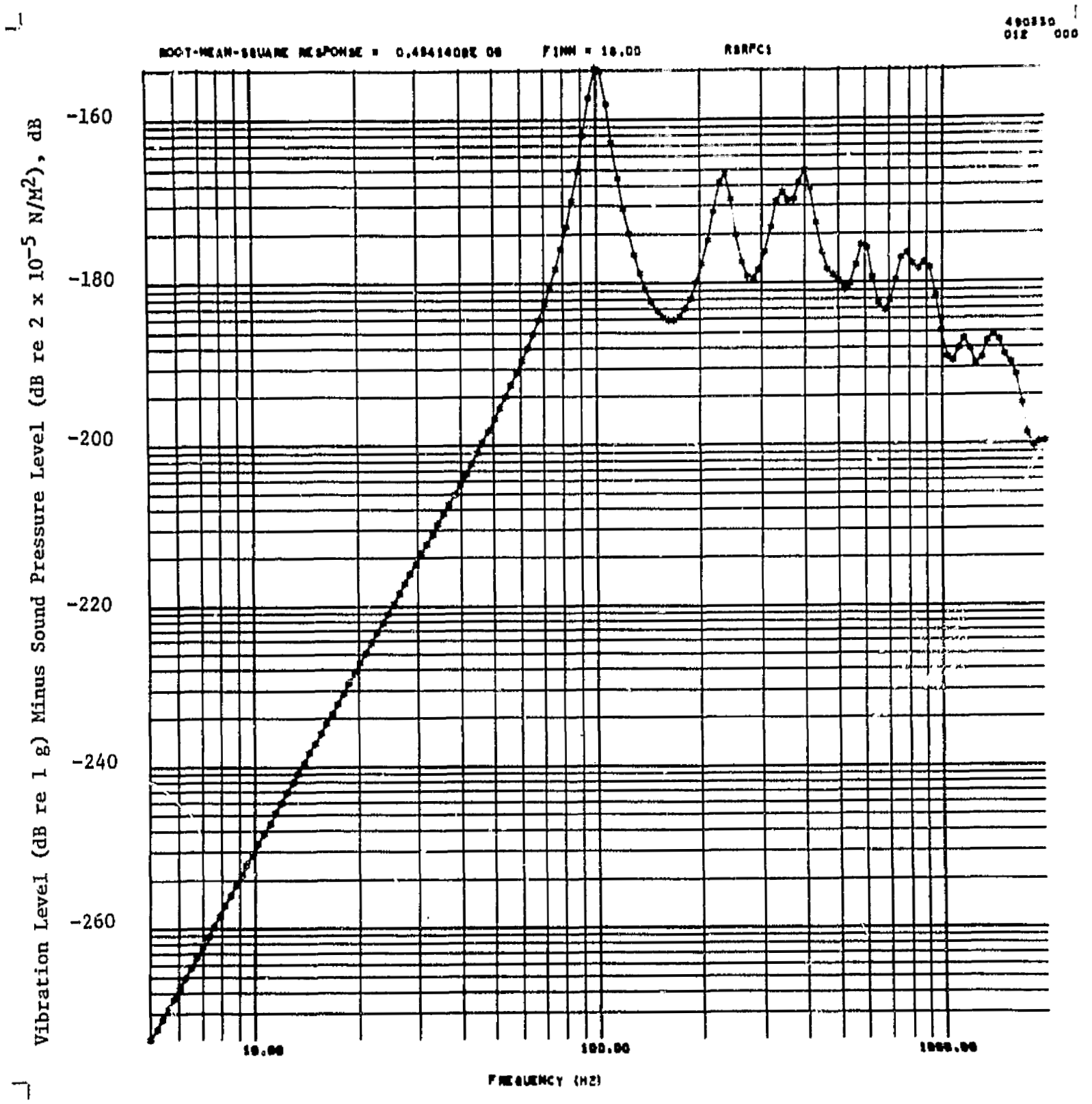

FIGURE 48. VIBRO-ACOUSTIC TRANSFER FUNCTION, CASE III.C.3

(a) less than the convection speed (The modes are classified hydrodynamically slow - HS.)

(b) equal to the convection speed (The modes are classified hydrodynamically coincident - HC.)

(c) greater than the convection speed (The modes are classifed hydrodynamically fast - HF.)

From reference 36, in the hydrodynamically slow region, $c_B < U_c$, (see figure 49 for c_B).

$$\Pi_{HS}\ (1/3 \text{ octave band}) = \frac{p_h^2\ G_\infty\ A_t\ (k_p\ \delta_1)}{\pi} \qquad \frac{\omega\theta}{1 + \omega^2\theta} \tag{71}$$

which becomes, using consistent nomenclature

$$\Pi_{HS}\ (1/3 \text{ octave band}) = P_{OA}^2\ \ G_\infty\ A_t\ \ \frac{\omega}{4\pi}\ W'(f) \tag{72}$$

and the input power spectral density is

$$\Pi(f) = 2.16\ \overline{P_{OA}^2}\ \ G_\infty\ A_t\ W'(f) \tag{73}$$

where

G_∞ = $(8\rho_s\ \kappa\ c_\ell^{-1}$ is the mechanical point input conductance of an infinite flat plate

κ = the radius of gyration $(h/\sqrt{12})$ for a flat panel of thickness h

c_ℓ = $(E/\rho_p(1-\sigma^2))^{1/2}$ is the speed of propagation of longitudinal waves in the panel

E = Young's modulus for the panel

ρ_p = panel density

σ = Poisson's ratio for the panel

A_t = the equivalent correlation area (figure 50) a function of the plate wave number (figure 51) and δ^*

Combining equations (70) and (73) and rearranging terms for the hydrodynamically slow modes,

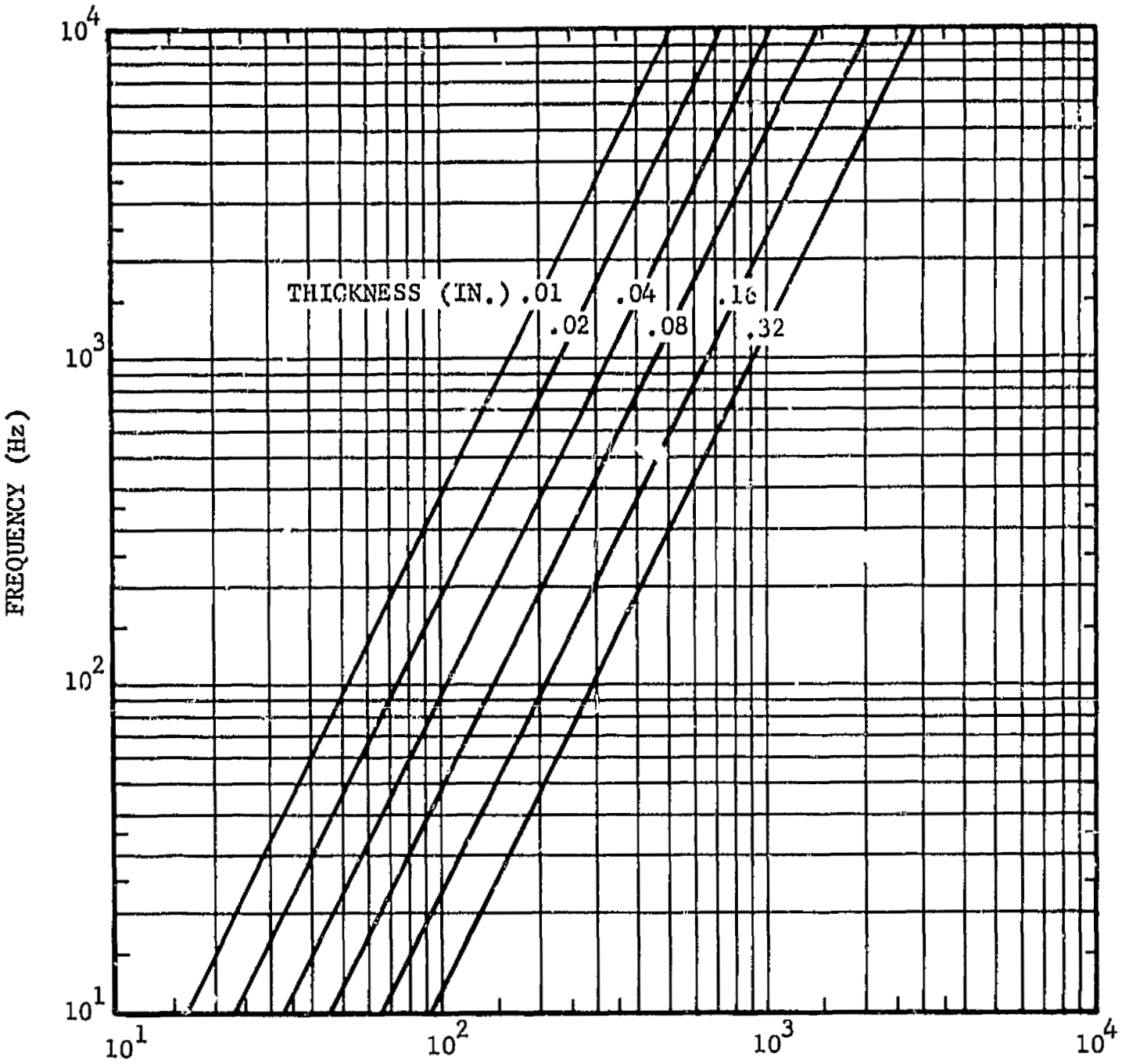

FIGURE 49. BENDING WAVE VELOCITY FOR PLATES OF ALUMINUM OR STEEL

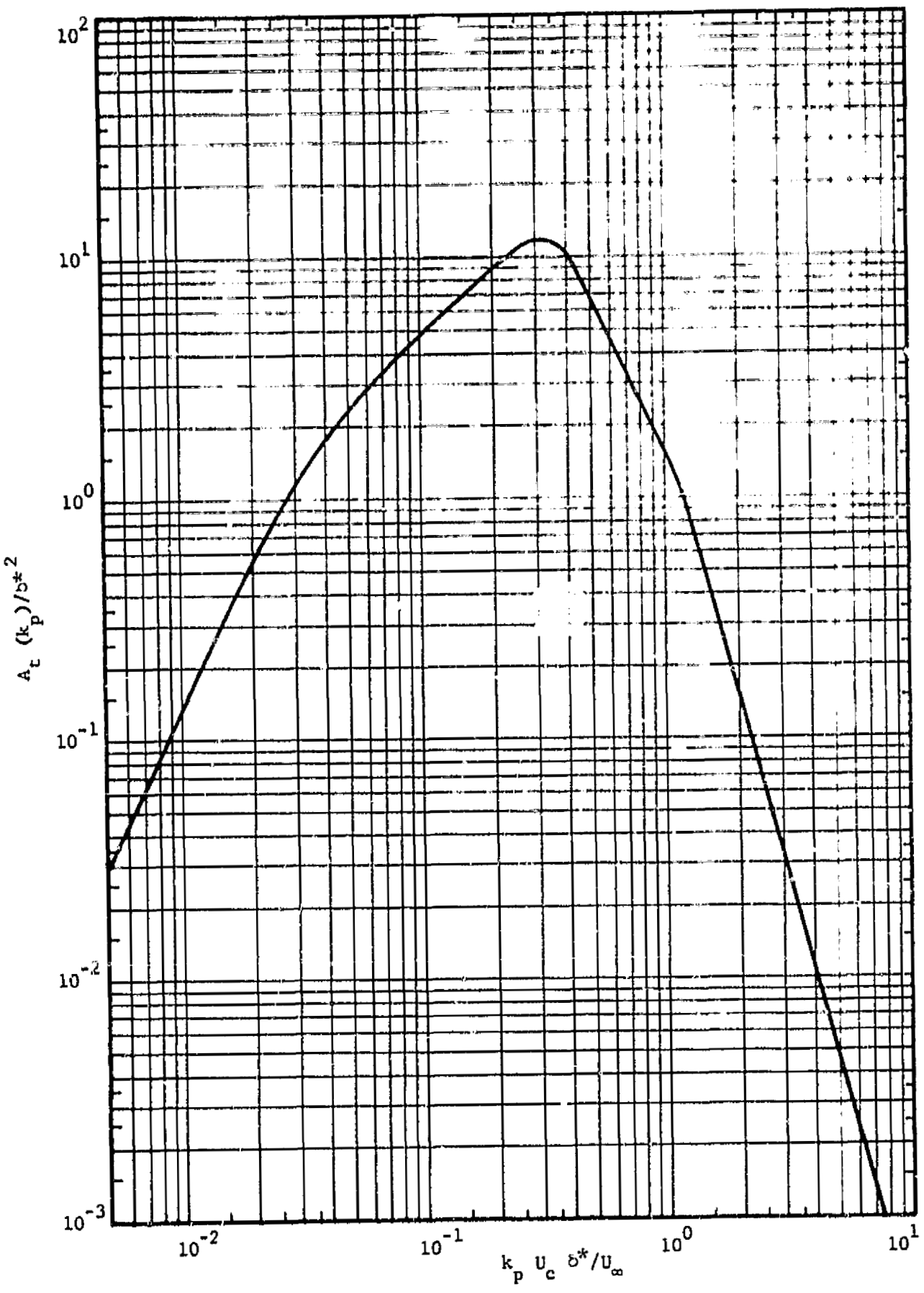

FIGURE 50. EFFECTIVE CORRELATION AREA OF TURBULENT BOUNDARY LAYER NOISE

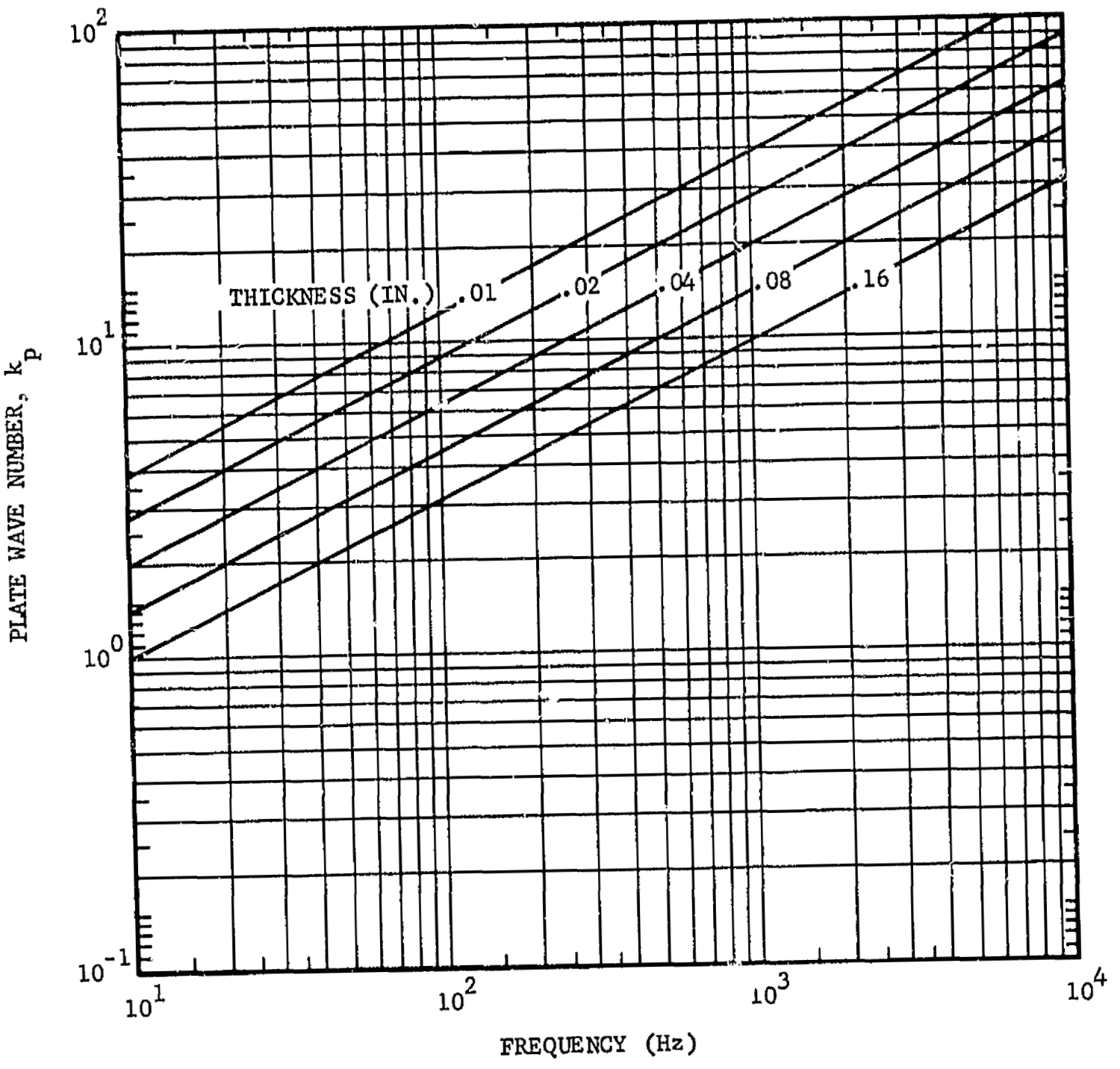

FIGURE 51. WAVE NUMBER FOR ALUMINUM OR STEEL PLATES

$$S_{ww}(f) = 13.57 \overline{P_{OA}^2} G_\infty A_t W'(f) f/\eta \rho_s \quad (74)$$

$$c_B \simeq U_c$$

For the hydrodynamically coincident region, $c_B \simeq U_c$, reference 36 gives for the input power per unit area in a bandwidth $\Delta\omega$,

$$\Pi_{HC} = \frac{p_h^2 G_\infty A_t (k_p \delta_1)\Delta\omega}{k_p U_c \sin \phi_c} \quad (75)$$

in consistent units the power in a unit bandwidth is,

$$\Pi_{HC}(f) = \overline{P_{OA}^2} G_\infty A_t/2\pi k_p U_c \sin \phi_c \quad (76)$$

and

$$S_{ww}(f) = \overline{P_{OA}^2} G_\infty A_t f/k_p U_c \sin \phi_c \eta\rho_s$$

where

$$\phi_c = \cos^{-1} (\omega/k_p U_c)$$

thus for the hydrodynamically coincident region,

$$S_{ww}(f) = 0.1592 \overline{P_{OA}^2} G_\infty A_t \cot \phi_c/\eta\rho_s \quad (77)$$

$$c_B \simeq U_c$$

In the hydrodynamically fast region $c_B > U_c$ the response spectral density is given (reference 37),

$$U(\omega) = p_h^2 G_\infty A_t P_\tau(\omega)/\omega\eta\rho_s \quad (78)$$

which becomes, in consistent units,

$$S_{ww}(f)_{HF} = \overline{P_{OA}^2} G_\infty A_t W'(f) / 8\pi^2 f\eta\rho_s$$

which yields

$$\Pi_{HF}(f) = \frac{1}{2} \overline{P_{OA}^2} G_\infty A_t W'(f) \quad (79)$$

and

$$S_{ww}(f) = 3.142 \overline{P_{OA}^2} G_\infty A_t W'(f) f/\eta\rho_s \quad (80)$$

The response of light-weight panels to acoustic fields can be obtained from references 37, 38

$$\overline{p^2} \approx a_d^2 \frac{R_{in} M_s}{2\pi^2 n_s(\omega) c^2 A_p \sigma_{rad} < D(\Omega) >} \tag{81}$$

which is re-written in consistent units

$$S_{ww}(f) = \frac{\overline{p^2(f)}\ 2\pi^2 n_s c^2 A_p \sigma_{rad} G_\infty < D(\Omega) >}{M_s} \tag{82}$$

and

$$\Pi(f)_a = \frac{\pi n_s c^2 \sigma_{rad} G_\infty \overline{p^2(f)}\ \eta < D(\Omega)}{fh} \tag{83}$$

where

A_p is the panel area

h is the panel thickness

M_s is the panel mass

$\overline{p^2(f)}$ is the excitation acoustic pressure spectral density

c is the speed of sound in air

n_s is the density of vibratory modes in the panel

For a simply supported cylindrical shell,

$$n_s = \frac{2\sqrt{3}\ A_p}{\pi\ c_\ell\ h} (k_\ell a)^{1/2} \qquad k_\ell a < 1 \tag{84}$$

$$= \frac{\sqrt{3}\ A_p}{c_\ell\ h} \qquad k_\ell a > 1$$

where

a is the cylinder radius

$k_\ell = (\omega/c_\ell)$ is the longitudinal wave number

The results for $k_\ell a > 1$ apply for a flat plate.

$\langle D(\Omega) \rangle$ is a directivity and correlation function,

$\langle D(\Omega) \rangle = 1$ for a reverberant field

and the radiation efficiency is given by

$$\sigma_{rad} = \frac{\pi (P_r)\ h(c_\ell)\ (f)^{1/2}}{\sqrt{3}\ (A_p)\ (c)\ (f_p)^{1/2}} \qquad f < \frac{f_p}{2} \tag{85}$$

and

$$\sigma_{rad} = 1 \qquad f > f_p$$

where P_r is the total panel edge perimeter and $f_p = 6.6\ c^2/h\ c_\ell$ is the critical frequency i.e., the lowest frequency for which wave coincidence occurs, that frequency for which $c = c_B$.

D. Transfer Function Level from Statistical Energy Analysis

The vibro-acoustic transfer function level, TFL, in dB is defined as the acceleration level AL in dB re 1g minus the sound pressure level SPL in dB re 20 $\mu N/M^2$.

$$TFL(f) = AL(f) - SPL(f) \tag{86}$$

$$AL(f) = 10 \log_{10} (S_{\ddot{w}\ddot{w}}(f)/1\ g^2) \tag{87}$$

$$1g^2 = (32.1740\ ft/sec)^2 = 1035.166\ ft^2/sec^4 \tag{88}$$

$$AL(f) = 10 \log S_{\ddot{w}\ddot{w}}(f) - 30.15\ dB \tag{89}$$

$$SPL(f) = 10 \log_{10} (\overline{P^2(f)}\ /(20\ \mu N/M^2)\ ) \tag{90}$$

$$= 10 \log \overline{P^2(f)} + 127.582\ \ dB \tag{91}$$

where $\overline{P^2(f)}$ is in $\#^2/ft^4$

and

$$\overline{P^2(f)} = \overline{P_{OA}^2}\ A_t\ W'(f), \quad \text{HS Turbulent Boundary Layer} \tag{92}$$

$$= \overline{P_{OA}^2}\ A_t\ , \quad \text{HC Turbulent Boundary Layer}$$

$$= \overline{P^2_{OA}}\, A_t\, W'(f), \text{ HF Turbulent Boundary Layer}$$

$$= \overline{P^2(f)}, \text{ Acoustical}$$

$$TFL = 10 \log_{10} (S_{ww}(f)/\overline{P^2(f)}) - 157.73 \text{ dB} \qquad (93)$$

Following are the pertinent parameters for test specimens (See also Section IV.):

Test Specimen I

$\rho_s = 1.732 \times 10^{-2}$ #-sec^2/ft^3

$G_\infty = 0.452$

$\eta = 0.04$

$\sigma_{rad} \simeq 1.1215 \times 10^{-5} f \qquad f < 5795$

$\simeq 1.0 \qquad f > 11590$

$n_s = 0.2608$

$f_p = 11590$

Test Specimen II

$\rho_s = 8.66 \times 10^{-2}$ #-sec^2/ft^3

$G_\infty = 0.0904$

$\eta = 0.04$

$\sigma_{rad} \simeq 2.804 \times 10^{-4} f \qquad f < 1159$

$\simeq 1.0 \qquad f > 2318$

$f_p = 2318$

$n_s = 0.05216$

Test Specimen III

$\rho_s = 3.5 \times 10^{-2}$ # - sec^2/ft^3

Other parameters utilized same as Test Specimen I

Utilizing equations (92) and (93) and the above parameters, the following results are obtained:

1. Hydrodynamically Slow Turbulent Boundary Layer

Specimen I:

$$TFL_{HS} = -118.3 + 10 \log f \qquad (94)$$

Specimen II:

$TFL_{HS} = -132.25 + 10 \log f$

Specimen III:

$TFL_{HS} = -121.3 + 10 \log f$

2. Hydrodynamically Coincident Turbulent Boundary Layer

Specimen I:

$TFL_{HS} = -137.57 + 10 \log (\cot \phi_c)$

Specimen II:

$$TFL_{HC} = -151.56 + 10 \log (\cot \phi_c) \qquad (95)$$

Specimen III:

$TFL_{HC} = -140.57 + 10 \log (\cot \phi_c)$

3. Hydrodynamically Fast Turbulent Boundary Layer

Specimen I:

$$TFL = -124.61 + 10 \log f \qquad (96)$$

Specimen II:

$TFL = -138.61 + 10 \log f$

Specimen III:

$TFL = -127.61 + 10 \log f$

4. Acoustic, Reverberant Field ($\langle D(\omega) \rangle = 1$)

Specimen I:

$$\begin{aligned} TFL &= -125.2 + 10 \log f && f < 5795 \\ &= -75.70 && f > 11590 \end{aligned}$$

Specimen II:

$$\begin{aligned} TFL &= 132.3 + 10 \log f && f < 1159 \\ &= -96.77 && f > 2318 \end{aligned} \qquad (97)$$

Specimen III:

$$\begin{aligned} TFL &= -128.2 + 10 \log f && f < 5795 \\ &= -78.70 && f > 11590 \end{aligned}$$

The transfer function levels for test specimens I, II, and III for the reverberant field acoustic excitation are shown in figure 52.

E. Damping Effects

The damping of a panel-type test specimen is due to material damping of the specimen, edge damping due to the test fixture and radiation damping. If fixture induced damping is negligible only the relative material damping and the radiation damping are of importance. Consideration of the damping is mandatory since the mean-square response at resonance is inversely proportional to damping squared. The problem arises from the desire to minimize cross-section area of a progressive wave test facility in order to maximize the acoustic forcing pressure for a given power source, and to maximize the frequency of cross modes. The radiation damping imposed on a simply supported test specimen, by a progressive wave section with cross-sectional area, S_r, is as follows (reference 39),

$$\zeta_{mn} = \frac{c_r}{c_c} = \frac{32\rho_o c_o}{\pi^6} \sqrt{\frac{12g}{E\gamma}} \left(\frac{ab}{S_r}\right) K \qquad (98)$$

For a homogeneous aluminum panel

$$\zeta_{mn} = 3.6 \times 10^{-6} \, (ab/S_r) \, K$$

where a, b are the panel dimensions, h is the thickness

$$K = \frac{a^2 b^2}{h^2 m^2 n^2 (b^2 m^2 + a^2 n^2)}$$

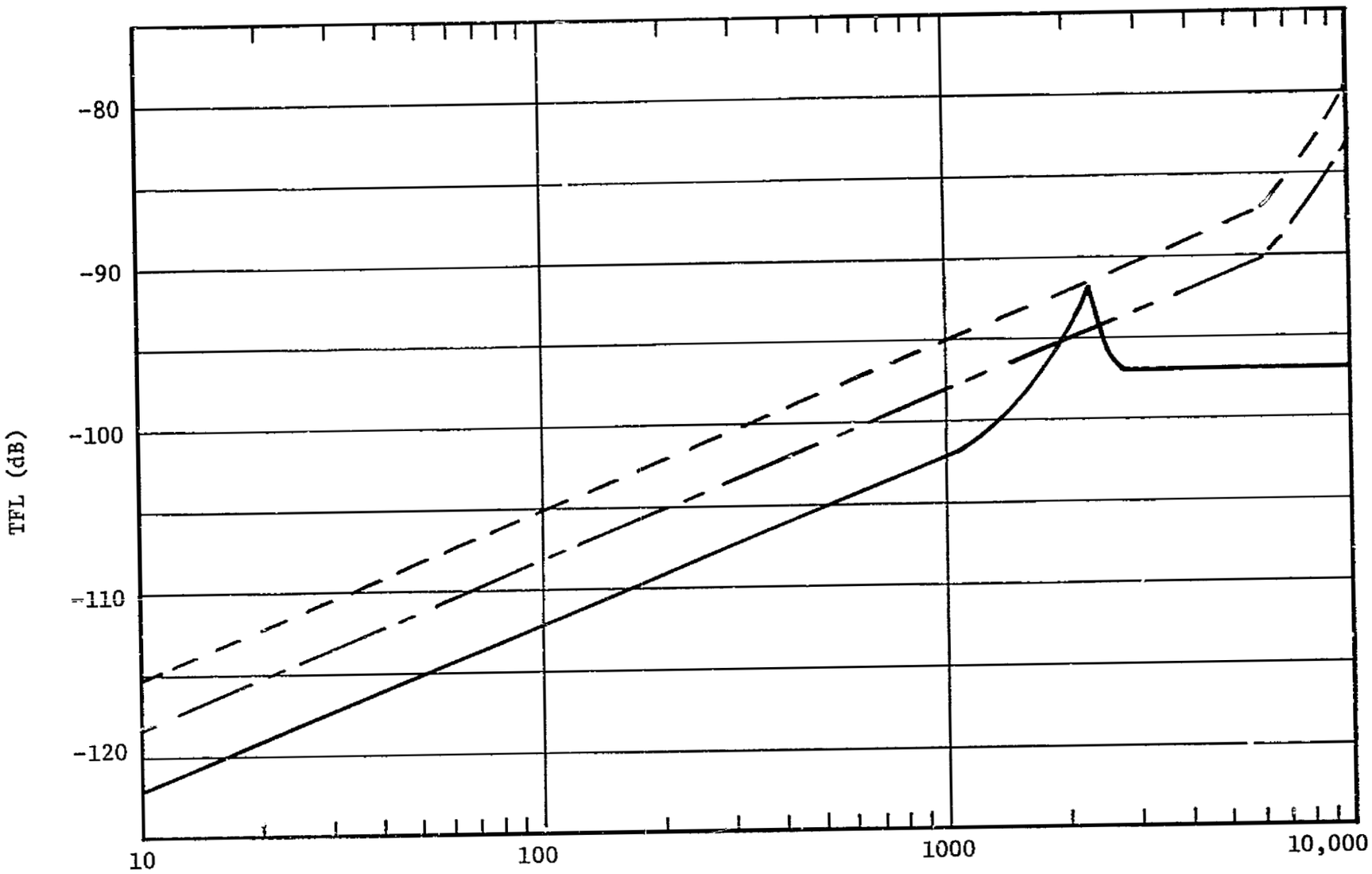

FIGURE 52. STATISTICAL VIBRO-ACOUSTIC TRANSFER FUNCTION LEVELS FOR REVERBERANT ACOUSTIC EXCITATION

m, n are modal indices in the a, b directions

F. Equipment Loading

Loading structural members with equipment will generally tend to reduce the vibratory amplitude and the resonant frequency. The following results are presented due to the inherent mathematical tractability and simplicity in form. Considering a single degree of freedom system analogy, it is clear that the mean square response is attenuated by a factor F_m.

where

$$F_m = (1 + \beta)^{-2} \tag{99}$$

$$\beta = m_e/m_s$$

m_e = equipment mass

m_s = structural mass

and the resonant frequency will be reduced by a factor

$$F_f = (1 + \beta)^{-1/2} \tag{100}$$

G. Exposed Area

When the excitation pressure field is homogeneous in space, the cross-spectral density of the excitation can be expressed

$$\Phi_{pp}(\vec{r}_1, \vec{r}_2, \omega) = \Phi_{pp}(\omega)\, R_{pp}(\xi, \omega) \tag{101}$$

where the spatial correlation function of the pressure field $R(\xi,\omega)$ is a function of frequency ω, and separation distance $(\vec{r}_1 - \vec{r}_2)$.

Under these conditions the response displacement spectral density, $\Phi_{ww}(\vec{r},\omega)$, is directly proportional to the area of the test specimen exposed to the homogeneous excitation pressure field. (See equation (52).)

Thus the response acceleration spectral density is also proportional to the square of the exposed area.

$$S_{ww}''''(f) \propto S_{ww}(f) \propto \Phi_{pp}(\vec{r}_1, \vec{r}_2, \omega) \propto S'^2 \tag{102}$$

SECTION IV. EMPIRICAL PROGRAM

Completion of the empirical program required utilization of an acoustical test facility, a progressive wave facility, a reverberation chamber, fabrication of test panels, performance of the test program and acquisition of vibration and acoustic data.

A. Test Facility

1. Progressive Wave Facility

The acoustic progressive wave test facility is shown in figure 53. The facility walls are a sandwich construction (two sheets of 3/4" plywood bonded to a cork compound designed to function as a constrained layer) with a steel frame. The necessary rigidity is furnished by the frame and the plywood members, the constrained cork layer provides high wall damping in resonant and coincident frequency ranges. The acoustic source is a Ling EPT-94B driver with a rated 4000 watt output. The driver is joined to a 50 Hz cutoff exponential transition section fabricated by Ling Electronics which converts the approximately 1.5 inch diameter circular exit at the transducer to a seven inch square cross-section. The Ling adapter is joined to a rectangular cross-section linearly-expanding horn with a cutoff frequency below 30 Hz. The horn is mated to an eight-foot long test section with internal dimensions of 1.98 feet deep by 3.69 feet high. The test section is joined to an anechoic termination section of the same dimension (i.e. 1.98' x 3.69; x 8'). The test section accommodates 30" x 40" and 13" x 13" plane test specimens in the simply-supported mode (see figure 54 for a sketch of the mounting arrangement) utilizing interchangeable fixtures.

The Beranek and Sleeper linear Harvard wedge termination is replaced by the more economical Gustin-Bacon (BB&N) laminated stair-step approximation (references 40 and 41). Figure 55 shows the appropriate design details for the two predominant wedge types with typical measured data. Both wedges act as quarter-wave length absorbers designed to reflect less than 10 percent of the incident energy above the cutoff frequency. The Gustin-Bacon wedge is fabricated from non-irritable glass fibers which are extremely resilient and durable. A standard model with a 75 Hz low frequency cutoff is utilized. Referring to the figure it is seen that a standing wave ratio of the order of two dB may be encountered at 50 Hz. Above 100 Hz, however, the ratio is on the order of 0.5 dB or less.

The sound power level capability of the Ling Modulator as limited by the exponential horn section is shown in figure 56. Figure 57 shows the maximum sound pressure levels in the vicinity of test specimens. The maximum capability of the facility is seen to be 157.5 dB sinusoidal or overall sound pressure level for a broad band random spectrum.

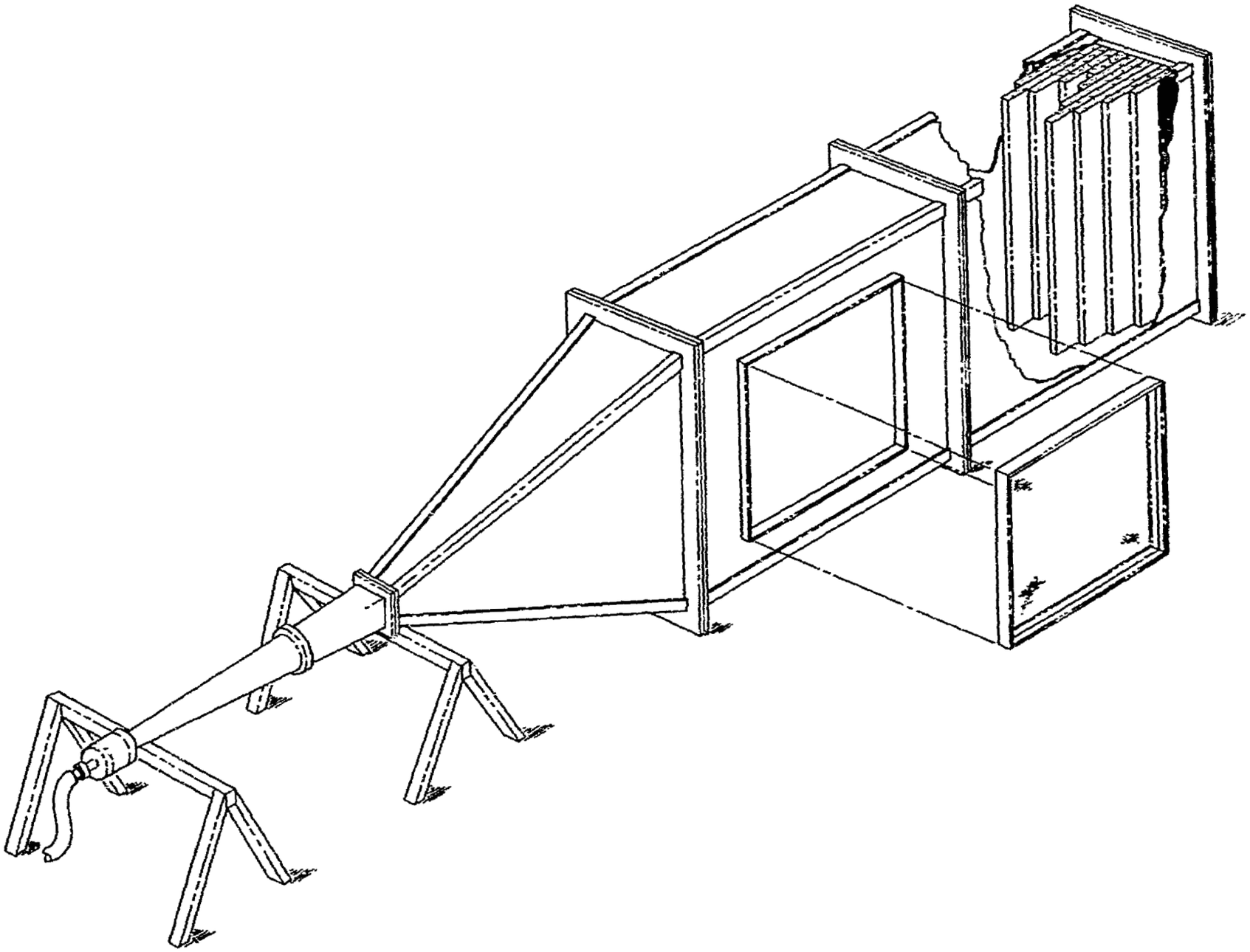

FIGURE 53. ACOUSTIC PROGRESSIVE WAVE FACILITY

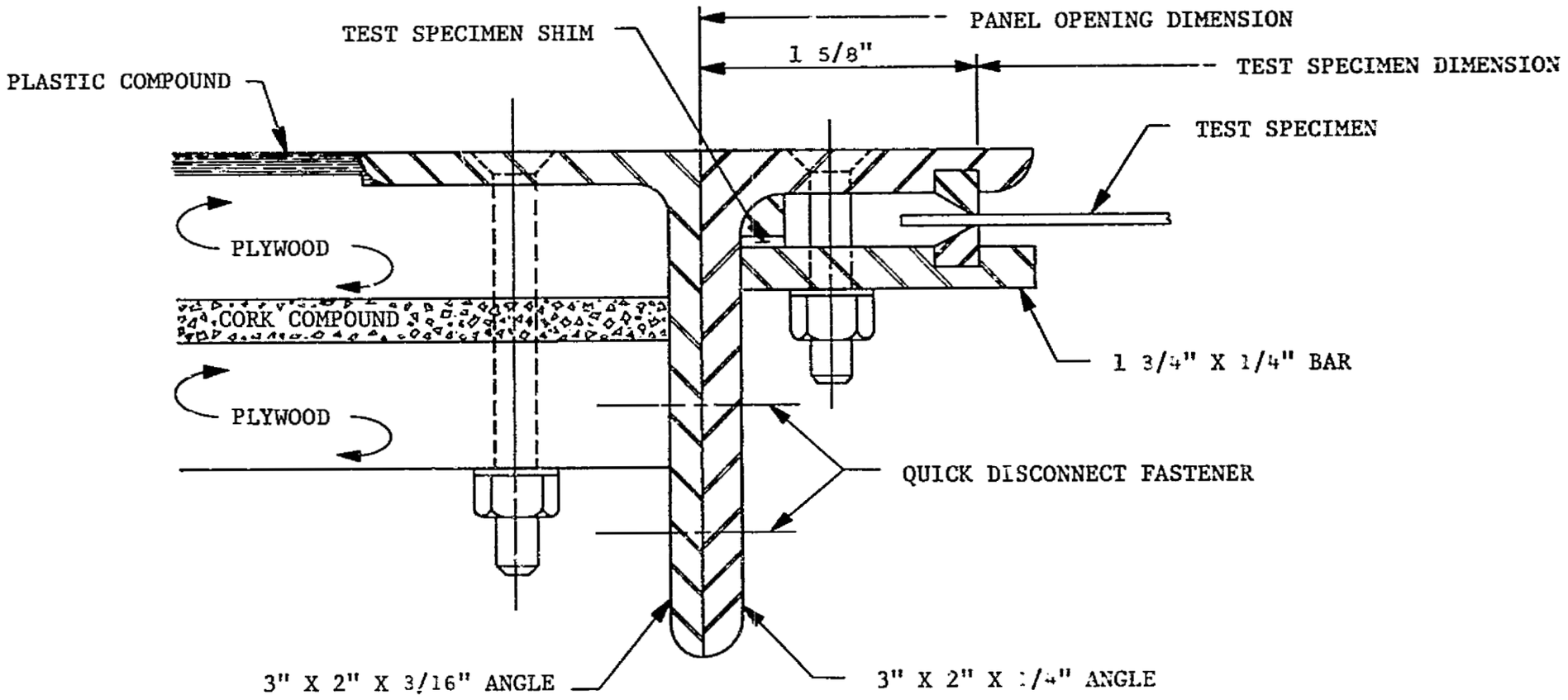

FIGURE 54. TYPICAL PANEL MOUNTING CONFIGURATION

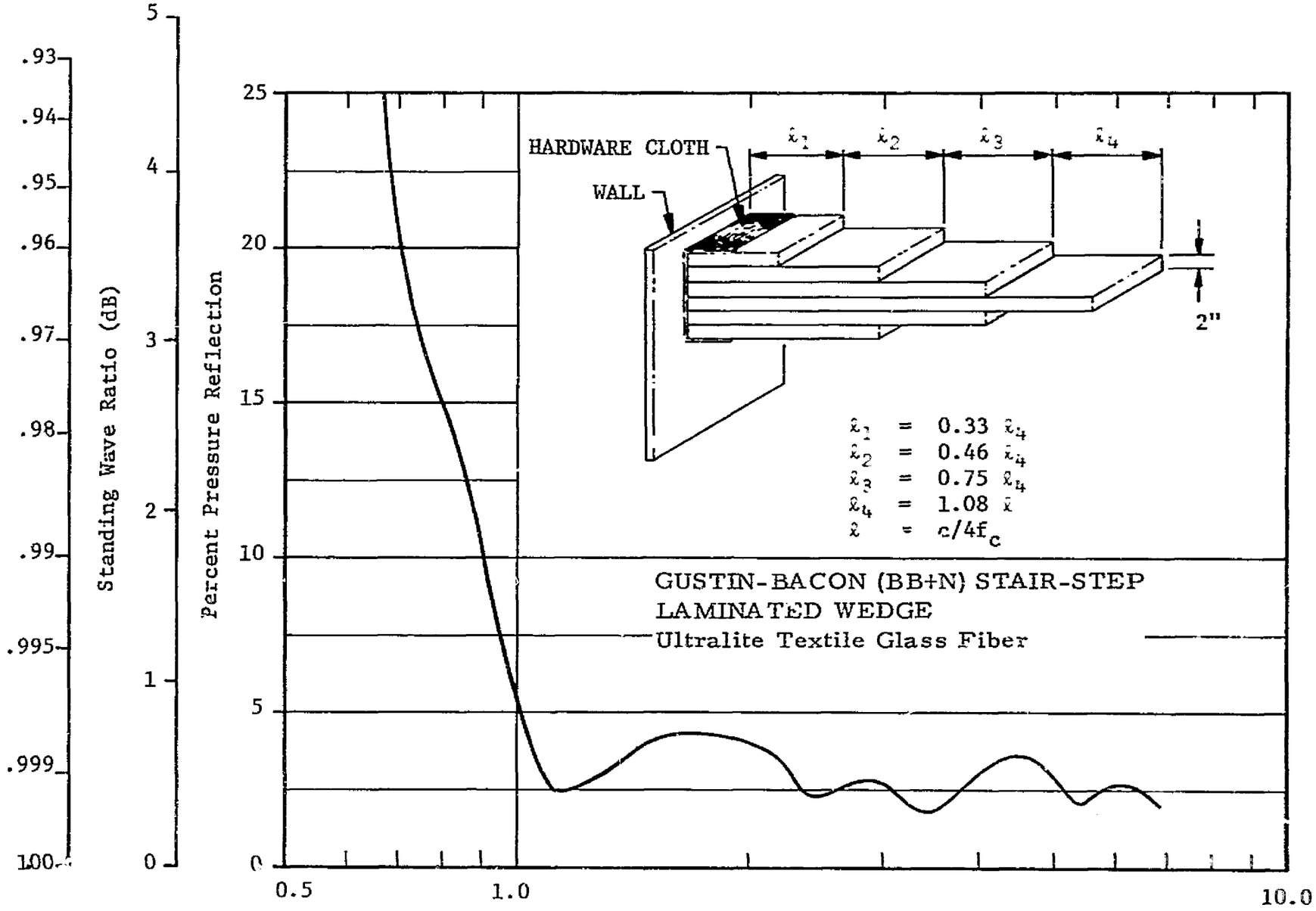

FIGURE 55. ANECHOIC WEDGE CHARACTERISTICS

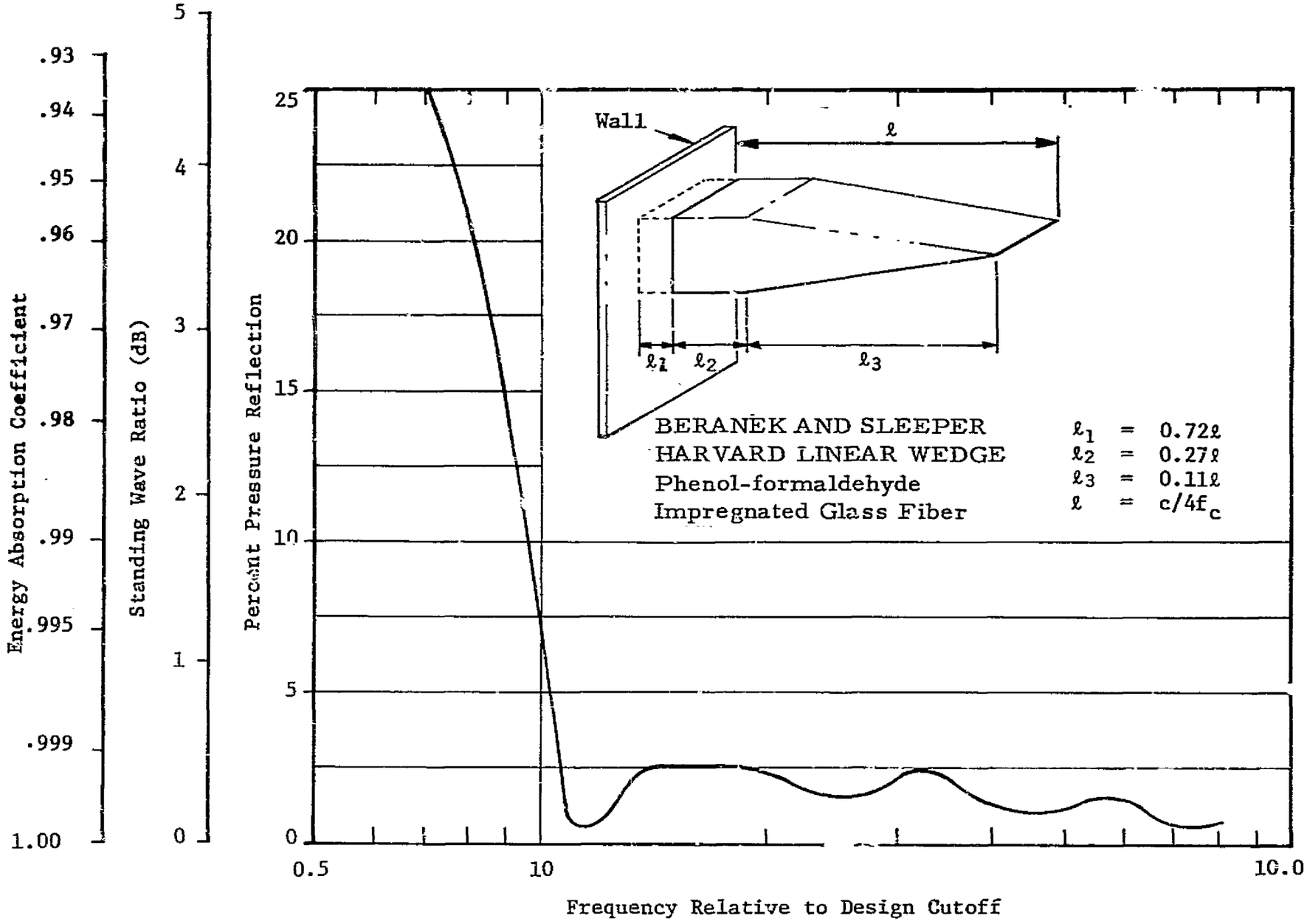

FIGURE 55. ANECHOIC WEDGE CHARACTERISTICS (Concluded)

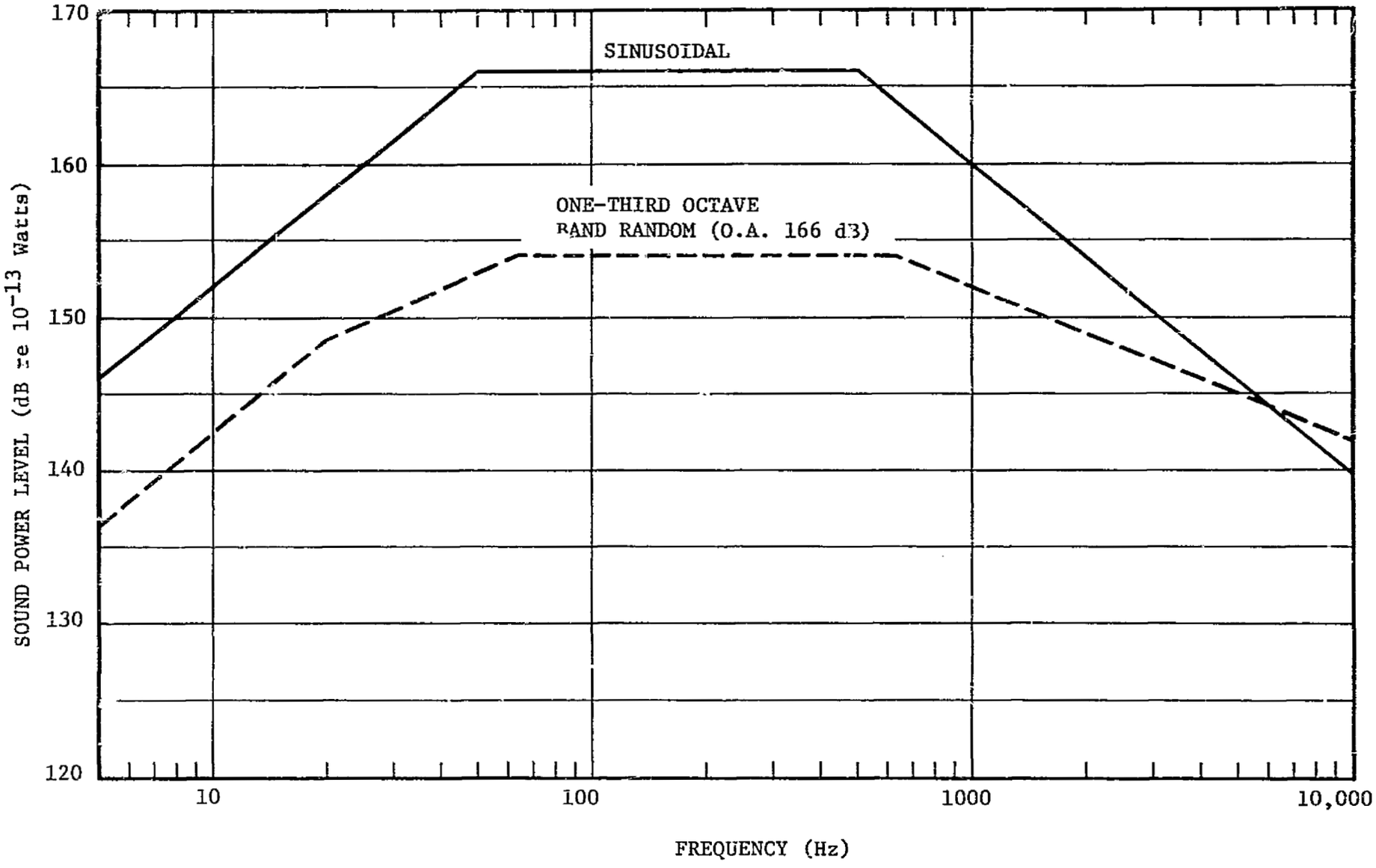

FIGURE 56. POWER CAPABILITY OF LING EPT-94B ACOUSTIC SOURCE WITH 50 Hz CUTOFF EXPONENTIAL HORN

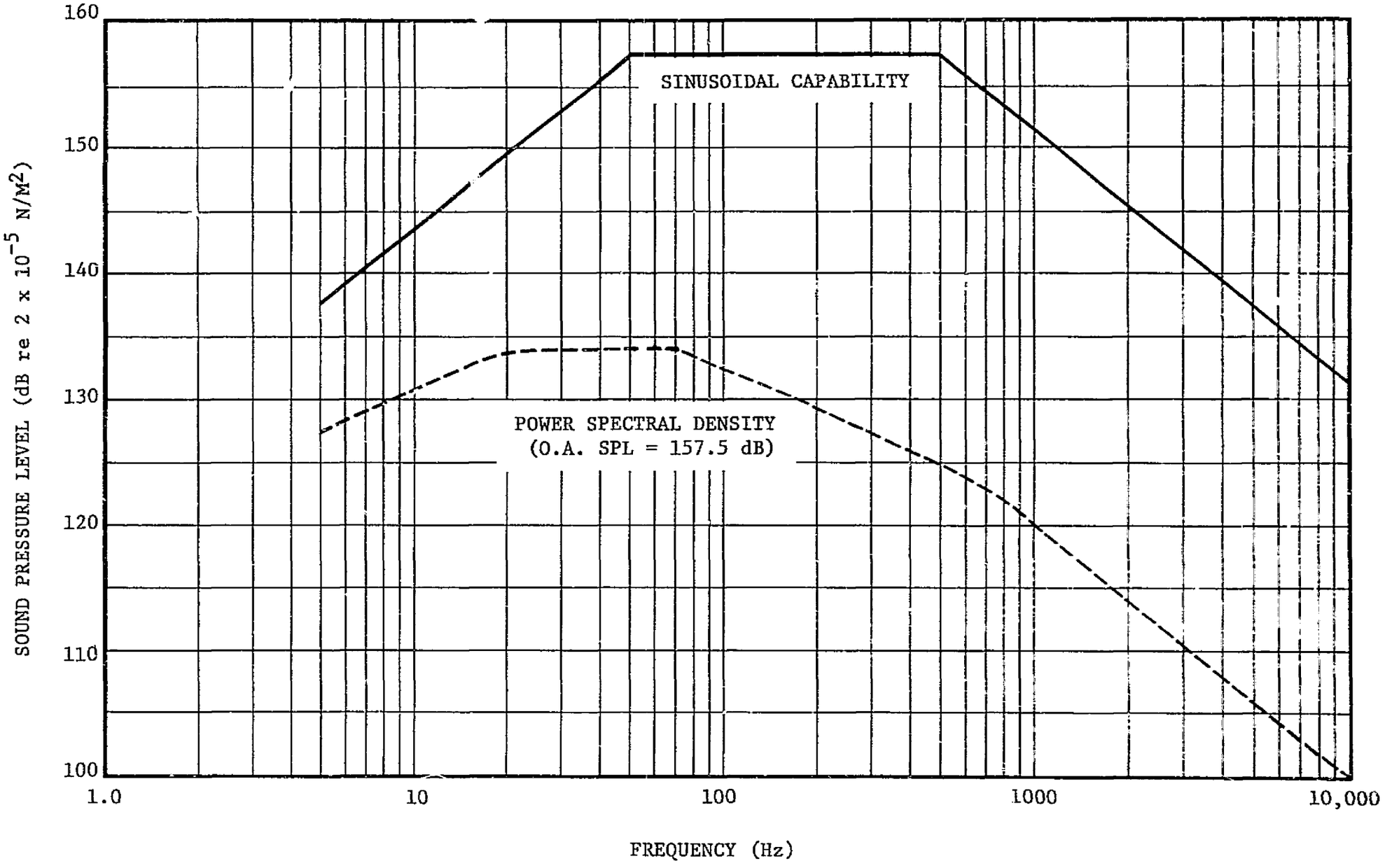

FIGURE 57. MAXIMUM SOUND PRESSURE LEVELS IN PROGRESSIVE WAVE ACOUSTIC TEST FACILITY

The facility has been equipped with a divider to enable the evaluation of radiation damping effects on specimen response. The divider may be located at 3,6, 12 and 18 inches from the test specimen. Acoustic cross-modes develop due to discontinuous wave expansion and minor surface discontinuities. The cross-modal frequencies are computed from the conventional equation for acoustic modal frequencies in a rectangular parallelopiped:

$$f_{n_x,n_y,n_z} = 0.5\ c\ [(n_x/\ell_x)^2 + (n_y/\ell_y)^2 + (n_z/\ell_z)^2]^{1/2} \quad (103)$$

where

ℓ_x is the facility length (essentially infinite above the cutoff frequency of the anechoic termination)

ℓ_y is the width

ℓ_z is the height

c is the speed of sound

and the modal indices

$n_x = 0$

$n_y = 0, 1, 2, 3, \ldots$

$n_z = 0, 1, 2, 3, \ldots$

except $n_y \neq n_z = 0$, simultaneously

The frequencies of the cross-modes have been calculated as described above for up to the 20 x 20 mode. The number of modal frequencies for which sound field interference (constructive and destructive may occur at the test specimen location is as follows for various divider spacings:

Distance from Divider to Test Specimen	Interference Frequencies (Below 2000 Hz)
0.25 ft.	13
0.50 ft.	24
0.75 ft.	35
1.00 ft.	47
1.50 ft.	65
1.98 ft.	84

Constructive interference occurs at approximately half of the above frequencies.

The driver air is exhausted via a plenum at the base of the wedges.

2. Reverberant Test Facility

Test Cell (2-20) at the Michoud Assembly Facility was chosen for use after refurbishing as the reverberation chamber for the evaluation of structural response to reverberant acoustic fields. The chamber is 10.0' x 16.0' x 42.5' with a total edge length 228 ft., total surface area 2758 ft^2, and volume 6763 ft^3. The fundamental acoustic mode occurs at 13.1 Hz.

Acoustic modes for a rectangular room $l_x \times l_y \times l_z$ are calculated from the equation (103). This equation has been utilized to calculate the acoustic modes for Test Cell 2-20 with l_x = 10.0', l_y = 16.0', and l_z = 42.5'. The modal indices have been varied from 0 to 20 producing 9260 calculated room resonances (Table 7).

The room modes may be separated into three categories - axial modes, tangential modes, and oblique modes (waves). Axial waves are parallel to a chamber axis and two modal indices are zero:

x - axial waves are parallel to the x axis (n_y, n_z = 0)

y - axial waves are parallel to the y axis (n_x, n_z = 0)

z - axial waves are parallel to the z axis (n_x, n_y = 0)

Tangential waves are parallel to a wall surface and have one modal index equal to zero:

x, y - tangential waves, parallel to the xy plane (n_z = 0)

y, z - tangential waves, parallel to the yz plane (n_x = 0)

x, z - tangential waves, parallel to the xz plane (n_y = 0)

Oblique waves have no modal indices equal to zero.

This distinction is important since the oblique waves are more highly damped than the tangential waves, and the axial waves are the least damped.

The number of each type of mode is calculated in Table 7:

	General	Test Cell 2-20
Axial Modes (Enclosed by solid lines)	$N_x + N_y + N_z$	60
Tangential Modes (Enclosed by dashed lines)	$2(N_xN_y + N_yN_z + N_zN_x)$	1200
Oblique Modes	$N_x N_y N_z$	8000

where $N_x = n_{x_{max}}$, $N_y = n_{y_{max}}$, $N_z = n_{z_{max}}$

TABLE 7. ACOUSTIC MODAL FREQUENCIES FOR REVERBERANT FACILITY (TEST CELL 2-20)

ACOUSTIC MODAL FREQUENCIES

FACILITY DIMENSIONS LX= 10.0 FEET, LY= 16.0 FEET, LZ= 42.5 FEET

SPEED OF SOUND = 1116.0 FEET PER SECOND

MODAL INDEX NSUBX = 0

MODAL INDEX NSUBY	MODAL INDEX NSUBZ=0	1	2	3	4	5	6	7	8	9	10	11	12	13	14	15	16	17	18	19	20
0		13.1	26.3	39.4	52.5	65.6	78.8	91.9	105.0	118.2	131.3	144.4	157.6	170.7	183.8	196.9	210.1	223.2	236.3	249.5	262.6
1	34.9	37.3	43.7	52.6	63.0	74.3	86.2	98.3	110.7	123.2	135.8	148.6	161.4	174.2	187.1	200.0	212.9	225.9	238.9	251.9	264.9
2	69.7	71.0	74.5	80.1	87.3	95.8	105.2	115.4	126.1	137.2	148.7	160.4	172.3	184.4	196.6	208.9	221.3	233.8	246.4	259.0	271.7
3	104.6	105.4	107.9	111.8	117.1	123.5	131.0	139.3	148.3	157.8	167.9	178.3	189.1	200.2	211.5	223.0	234.7	246.5	258.5	270.5	282.7
4	139.5	140.1	141.9	145.0	149.1	154.2	160.2	167.1	174.6	182.8	191.6	200.8	210.4	220.4	230.8	241.3	252.2	263.2	274.4	285.8	297.3
5	174.4	174.9	176.3	178.8	182.1	186.3	191.3	197.1	203.6	210.6	218.3	226.4	235.0	244.0	253.4	263.0	273.0	283.2	293.7	304.4	315.2
6	209.2	209.7	210.9	212.9	215.7	219.3	223.6	228.5	234.1	240.3	247.0	254.3	261.9	270.0	278.5	287.4	296.5	305.9	315.7	325.6	335.8
7	244.1	244.5	245.5	247.3	249.7	252.8	256.5	260.9	265.8	271.2	277.2	283.6	290.6	297.9	305.6	313.7	322.1	330.8	339.8	349.0	358.5
8	279.0	279.3	280.2	281.8	283.9	286.6	289.9	293.7	298.1	303.0	308.3	314.2	320.4	327.1	334.1	341.5	349.2	357.3	365.6	374.3	383.1
9	313.9	314.1	315.0	316.3	318.2	320.7	323.6	327.1	331.0	335.4	340.2	345.5	351.2	357.3	363.7	370.5	377.7	385.1	392.9	400.9	409.2
10	348.7	349.0	349.7	351.0	352.7	354.9	357.5	360.7	364.2	368.2	372.6	377.5	382.7	388.3	394.2	400.5	407.1	414.1	421.3	428.8	436.6
11	383.6	383.8	384.5	385.6	387.2	389.2	391.6	394.5	397.7	401.4	405.5	409.9	414.7	419.9	425.4	431.2	437.4	443.8	450.6	457.6	464.9
12	418.5	418.7	419.3	420.3	421.8	423.6	425.8	428.5	431.5	434.9	438.6	442.7	447.2	452.0	457.1	462.5	468.3	474.3	480.6	487.2	494.1
13	453.4	453.6	454.1	455.1	456.4	458.1	460.2	462.6	465.4	468.5	472.0	475.8	480.0	484.4	489.2	494.3	499.7	505.3	511.3	517.5	523.9
14	488.2	488.4	489.0	489.8	491.1	492.6	494.6	496.8	499.4	502.3	505.6	509.2	513.0	517.2	521.7	526.5	531.5	536.8	542.4	548.3	554.4
15	523.1	523.3	523.8	524.6	525.8	527.2	529.0	531.1	533.6	536.3	539.3	542.7	546.3	550.3	554.5	559.0	563.7	568.8	574.0	579.6	585.3
16	558.0	558.2	558.6	559.4	560.5	561.8	563.5	565.5	567.8	570.4	573.2	576.4	579.8	583.5	587.5	591.7	596.2	601.0	606.0	611.2	616.7
17	592.9	593.0	593.5	594.2	595.2	596.5	598.1	600.0	602.1	604.5	607.2	610.2	613.5	617.0	620.7	624.7	629.0	633.5	638.2	643.2	648.4
18	627.7	627.9	628.3	629.0	629.9	631.2	632.7	634.4	636.5	638.8	641.3	644.1	647.2	650.5	654.1	657.9	662.0	666.2	670.8	675.5	680.5
19	662.6	662.8	663.1	663.8	664.7	665.9	667.3	669.0	670.9	673.1	675.5	678.2	681.1	684.3	687.8	691.3	695.1	699.2	703.5	708.0	712.8
20	697.5	697.6	698.0	698.6	699.5	700.6	701.9	703.5	705.4	707.4	709.7	712.3	715.1	718.1	721.3	724.8	728.4	732.3	736.4	740.8	745.3

FACILITY DIMENSIONS LX= 10.0 FEET, LY= 14.0 FEET, LZ= 40.5 FEET

SPEED OF SOUND = 1116.0 FEET PER SECOND

MODAL INDEX NSUBX = 1

MODAL INDEX NSUBY / NSUBZ	0	1	2	3	4	5	6	7	8	9	10	11	12	13	14	15	16	17	18	19	20
0	55.8	57.3	61.7	68.3	76.6	86.2	96.5	107.5	118.9	130.7	142.7	154.8	167.1	179.6	192.1	204.7	217.4	230.1	242.8	255.6	268.5
1	65.8	67.1	70.8	76.7	84.2	92.9	102.6	113.0	123.9	135.3	146.9	158.7	170.7	182.9	195.2	207.6	220.1	232.7	245.3	258.0	270.7
2	89.3	90.3	93.1	97.6	103.6	110.9	119.1	128.2	137.9	148.1	158.8	169.8	181.1	192.6	204.4	216.3	228.3	240.4	252.6	265.0	277.4
3	118.6	119.3	121.4	124.9	129.7	135.5	142.4	150.0	158.4	167.4	176.9	186.9	197.2	207.8	218.7	229.9	241.2	252.7	264.4	276.2	288.1
4	150.2	150.8	152.5	155.3	159.2	164.0	169.6	176.1	183.3	191.1	199.5	208.4	217.7	227.4	237.4	247.7	258.3	269.1	280.0	291.2	302.5
5	183.1	183.6	185.0	187.3	190.5	194.5	199.2	204.9	211.1	217.9	225.3	233.2	241.5	250.3	259.4	268.9	278.7	288.7	299.0	309.4	320.1
6	216.6	217.0	218.1	220.1	222.8	226.3	230.4	235.3	240.7	246.7	253.3	260.3	267.8	275.7	284.1	292.7	301.7	311.0	320.5	330.3	340.4
7	250.4	250.8	251.9	253.5	255.9	258.9	262.5	266.6	271.2	276.9	282.3	289.1	295.9	303.1	310.6	318.6	326.9	335.5	344.3	353.5	362.9
8	284.5	284.8	285.7	287.2	289.3	292.0	295.2	299.0	303.3	308.1	313.4	319.1	325.2	331.8	338.7	346.0	353.7	361.6	369.9	378.4	387.2
9	318.8	319.1	319.9	321.2	323.1	325.5	328.4	331.8	335.7	340.0	344.8	350.0	355.6	361.6	368.0	374.7	381.8	389.2	396.8	404.8	413.0
10	353.2	353.4	354.2	355.4	357.1	359.2	361.9	364.9	368.5	372.4	376.8	381.6	386.7	392.3	398.2	404.4	410.9	417.8	425.0	432.4	440.1
11	387.7	387.9	388.6	389.7	391.2	393.2	395.6	398.4	401.6	405.3	409.3	413.7	418.5	423.6	429.1	434.8	440.9	447.3	454.0	461.0	468.2
12	422.2	422.4	423.0	424.0	425.5	427.3	429.5	432.1	435.1	438.4	442.1	446.2	450.6	455.4	460.5	465.9	471.6	477.6	483.8	490.4	497.2
13	456.8	457.0	457.6	458.5	459.8	461.5	463.5	465.9	468.7	471.8	475.4	479.1	483.2	487.6	492.2	497.4	502.8	508.4	514.3	520.5	526.9
14	491.4	491.6	492.1	493.0	494.2	495.8	497.7	499.9	502.5	505.4	508.7	512.2	516.1	520.2	524.7	529.4	534.4	539.7	545.3	551.1	557.2
15	526.1	526.3	526.7	527.6	528.7	530.2	532.0	534.1	536.5	539.2	542.2	545.6	549.2	553.1	557.3	561.7	566.5	571.5	576.7	582.2	588.0
16	560.8	560.9	561.4	562.2	563.2	564.6	566.3	568.3	570.5	573.1	575.9	579.1	582.5	586.2	590.1	594.4	598.9	603.6	608.5	613.8	619.2
17	595.5	595.6	596.1	596.8	597.8	599.1	600.7	602.5	604.7	607.1	609.8	612.8	616.0	619.5	623.2	627.2	631.5	636.0	640.7	645.6	650.8
18	630.2	630.4	630.9	631.5	632.4	633.6	635.1	636.9	638.9	641.2	643.8	646.6	649.6	652.9	656.5	660.3	664.3	668.6	673.1	677.8	682.7
19	665.0	665.1	665.5	666.1	667.0	668.2	669.6	671.3	673.2	675.4	677.8	680.5	683.4	686.5	689.9	693.5	697.4	701.4	705.7	710.2	714.9
20	699.7	699.9	700.2	700.8	701.7	702.8	704.1	705.7	707.6	709.6	711.9	714.5	717.2	720.2	723.5	726.9	730.5	734.5	738.6	742.9	747.4

ACOUSTIC MODAL FREQUENCIES

FACILITY DIMENSIONS LX= 10.0 FEET, LY= 14.0 FEET, LZ= 42.0 FEET

SPEED OF SOUND = 1116.0 FEET PER SECOND

MODAL INDEX NSUBX = 2

MODAL INDEX NSUBY / NSUBZ=0	1	2	3	4	5	6	7	8	9	10	11	12	13	14	15	16	17	18	19	20
0	111.6	112.4	114.6	118.3	123.3	129.5	136.6	144.6	153.3	162.5	172.3	182.5	193.1	203.9	215.0	226.4	237.9	249.5	261.4	273.3	285.3
1	116.9	117.7	119.8	123.4	128.2	134.1	141.0	148.7	157.2	166.2	175.6	185.8	196.2	206.9	217.8	229.0	240.4	252.0	263.7	275.5	287.4
2	131.6	132.3	134.2	137.4	141.7	147.1	153.4	160.5	168.4	176.9	185.9	195.4	205.3	215.5	226.1	236.9	247.9	259.1	270.5	282.0	293.7
3	153.0	153.5	155.2	158.0	161.7	166.5	172.1	178.5	185.6	193.3	201.6	210.4	219.6	229.2	239.1	249.4	259.9	270.6	281.5	292.6	303.9
4	178.6	179.1	180.6	182.9	186.2	190.3	195.2	200.9	207.2	214.2	221.7	229.7	238.2	247.1	256.3	265.9	275.8	285.9	296.3	306.8	317.6
5	207.0	207.4	208.7	210.7	213.6	217.2	221.5	226.5	232.1	238.4	245.2	252.4	260.2	268.3	276.9	285.7	294.9	304.4	314.2	324.2	334.4
6	237.1	237.5	238.6	240.4	242.9	246.1	249.9	254.3	259.4	265.0	271.1	277.7	284.7	292.2	300.0	308.3	316.8	325.7	334.8	344.2	353.8
7	268.4	268.7	269.7	271.3	273.5	276.3	279.7	283.7	288.2	293.3	298.8	304.8	311.2	318.1	325.3	332.9	340.9	349.1	357.6	366.4	375.5
8	300.5	300.8	301.6	303.1	305.0	307.6	310.6	314.2	318.3	322.9	327.9	333.4	339.3	345.6	352.3	359.3	366.6	374.3	382.3	390.5	399.1
9	333.1	333.4	334.2	335.4	337.2	339.5	342.3	345.6	349.3	353.5	358.1	363.1	368.5	374.3	380.5	387.0	393.8	401.0	408.4	416.2	424.2
10	366.2	366.4	367.1	368.3	369.9	372.0	374.5	377.5	380.9	384.8	389.0	393.6	398.6	404.0	409.7	415.8	422.2	428.8	435.8	443.1	450.6
11	399.5	399.7	400.4	401.5	403.0	404.9	407.2	410.0	413.1	416.6	420.5	424.8	429.5	434.5	439.8	445.4	451.4	457.6	464.2	471.0	478.1
12	433.1	433.3	433.8	434.9	436.3	438.1	440.2	442.8	445.7	449.0	452.6	456.6	461.0	465.5	470.5	475.8	481.4	487.3	493.4	499.8	506.5
13	466.9	467.1	467.6	468.6	469.9	471.5	473.5	475.9	478.6	481.6	485.0	488.7	492.8	497.1	501.8	506.7	512.0	517.5	523.3	529.4	535.7
14	500.8	501.0	501.5	502.4	503.6	505.1	507.0	509.2	511.7	514.6	517.9	521.2	525.0	529.1	533.5	538.2	543.1	548.3	553.8	559.5	565.5
15	534.9	535.1	535.5	536.3	537.5	538.9	540.7	542.7	545.1	547.8	550.8	554.1	557.6	561.5	565.6	570.0	574.7	579.6	584.8	590.2	595.9
16	569.1	569.2	569.7	570.4	571.5	572.8	574.5	576.4	578.7	581.2	584.0	587.1	590.5	594.1	598.0	602.2	606.6	611.3	616.2	621.3	626.7
17	603.3	603.4	603.8	604.6	605.6	606.8	608.4	610.2	612.4	614.8	617.4	620.3	623.5	627.0	630.7	634.6	638.8	643.3	647.9	652.8	658.0
18	637.6	637.7	638.1	638.8	639.8	641.0	642.4	644.2	646.2	648.5	651.0	653.7	656.8	660.1	663.6	667.3	671.3	675.5	680.0	684.7	689.5
19	672.0	672.1	672.5	673.1	674.0	675.2	676.6	678.2	680.1	682.3	684.7	687.3	690.2	693.3	696.6	700.2	704.0	708.1	712.3	716.8	721.4
20	706.4	706.5	706.9	707.5	708.3	709.4	710.8	712.3	714.1	716.2	718.5	721.0	723.7	726.7	729.9	733.3	736.9	740.8	744.9	749.1	753.6

ACOUSTIC MODAL FREQUENCIES

FACILITY DIMENSIONS LX= 10.0 FEET, LY= 16.0 FEET, LZ= 42.5 FEET

SPEED OF SOUND = 1116.0 FEET PER SECOND

MODAL INDEX NSUBX = 3

MODAL INDEX NSUBY / NSUBZ	0	1	2	3	4	5	6	7	8	9	10	11	12	13	14	15	16	17	18	19	20
0	167.4	167.9	169.4	172.0	175.4	179.8	185.0	191.0	197.6	204.9	212.7	221.1	229.9	239.1	248.6	258.5	268.6	279.0	289.6	300.4	311.4
1	171.0	171.5	173.0	175.5	178.9	183.2	188.3	194.1	200.7	207.9	215.6	223.8	232.5	241.6	251.0	260.8	270.9	281.2	291.7	302.4	313.4
2	181.3	181.8	183.2	185.6	188.8	192.9	197.7	203.3	209.6	216.5	223.9	231.8	240.2	249.0	258.2	267.7	277.5	287.6	297.9	308.4	319.1
3	197.4	197.8	199.1	201.3	204.3	208.0	212.5	217.8	223.6	230.1	237.1	244.6	252.6	261.0	269.7	278.8	288.3	298.0	307.9	318.1	328.5
4	217.9	218.3	219.5	221.4	224.1	227.6	231.7	236.5	241.9	247.9	254.4	261.4	268.9	276.8	285.1	293.7	302.7	311.9	321.5	331.2	341.2
5	241.7	242.1	243.3	244.9	247.4	250.5	254.2	258.6	263.6	269.1	275.1	281.6	288.5	295.9	303.7	311.8	320.2	329.0	338.1	347.4	356.9
6	268.0	268.3	269.3	270.9	273.1	275.9	279.3	283.3	287.8	292.9	298.4	304.4	310.9	317.7	325.0	332.6	340.5	348.7	357.3	366.1	375.2
7	296.0	296.3	297.2	298.6	300.6	303.2	306.3	309.9	314.1	318.7	323.8	329.4	335.3	341.7	348.4	355.5	363.0	370.7	378.8	387.1	395.7
8	325.4	325.6	326.4	327.7	329.6	331.9	334.8	338.1	341.9	346.2	350.9	356.0	361.5	367.4	373.7	380.3	387.3	394.6	402.1	410.0	418.1
9	355.7	356.0	356.7	357.9	359.6	361.7	364.3	367.4	370.9	374.8	379.2	383.9	389.1	394.6	400.4	406.6	413.1	420.0	427.1	434.5	442.1
10	386.8	387.1	387.7	388.8	390.4	392.4	394.8	397.6	400.9	404.5	408.5	412.9	417.7	422.8	428.3	434.1	440.2	446.6	453.3	460.3	467.5
11	418.6	418.8	419.4	420.4	421.8	423.7	425.9	428.5	431.5	434.9	438.7	442.8	447.2	452.0	457.1	462.6	468.3	474.4	480.7	487.3	494.1
12	450.7	450.9	451.5	452.5	453.8	455.5	457.6	460.0	462.8	466.0	469.5	473.3	477.5	482.1	486.8	491.9	497.3	503.0	508.9	515.2	521.6
13	483.5	483.5	484.1	484.9	486.1	487.7	489.7	492.0	494.6	497.5	500.8	504.4	508.3	512.5	517.1	521.9	527.0	532.3	538.0	543.9	550.0
14	516.1	516.3	516.8	517.7	518.8	520.3	522.1	524.3	526.7	529.5	532.6	536.0	539.7	543.6	547.9	552.4	557.3	562.3	567.7	573.3	579.1
15	549.3	549.4	549.9	550.7	551.8	553.2	554.9	556.9	559.2	561.8	564.7	567.9	571.4	575.2	579.2	583.5	588.1	592.9	597.9	603.3	608.8
16	582.6	582.7	583.2	583.9	584.9	586.3	587.9	589.8	592.0	594.4	597.2	600.2	603.5	607.1	611.0	615.0	619.3	623.9	628.7	633.7	639.0
17	616.1	616.2	616.6	617.3	618.3	619.5	621.1	622.9	624.9	627.3	629.9	632.8	635.9	639.3	643.0	646.8	650.9	655.2	659.8	664.6	669.7
18	649.7	649.8	650.2	650.9	651.8	653.0	654.4	656.2	658.1	660.3	662.8	665.5	668.5	671.7	675.2	678.9	682.8	687.0	691.3	695.9	700.7
19	683.4	683.6	683.9	684.6	685.5	686.6	688.0	689.6	691.5	693.6	695.9	698.5	701.4	704.4	707.7	711.3	715.0	719.0	723.2	727.5	732.2
20	717.3	717.4	717.8	718.4	719.2	720.3	721.6	723.2	725.0	727.0	729.2	731.7	734.4	737.3	740.5	743.9	747.5	751.2	755.2	759.4	763.9

ACOUSTIC MODAL FREQUENCIES

FACILITY DIMENSIONS LX= 10.0 FEET, LY= 16.0 FEET, LZ= 42.5 FEET

SPEED OF SOUND = [illegible] FEET PER SECOND

MODAL INDEX NSUBX = 0

MODAL INDEX NSUBY	MODAL INDEX NSUBZ=0	1	2	3	4	5	6	7	8	9	10	11	12	13	14	15	16	17	18	19	20
0	223.2	223.6	224.7	226.6	229.3	232.7	236.7	241.4	246.7	252.5	259.[illegible]	265.9	273.2	281.0	289.1	297.7	306.5	315.7	325.1	334.7	344.6
1	225.9	226.3	227.4	229.3	231.9	235.3	239.2	243.9	249.1	254.9	261.[illegible]	268.1	275.4	283.1	291.2	299.7	308.5	317.6	326.9	336.5	346.4
2	233.8	234.2	235.3	237.1	239.7	242.9	246.8	251.3	256.4	262.0	268.2	274.8	282.0	289.5	297.4	305.7	314.3	323.3	332.5	341.9	351.6
3	246.5	246.9	247.9	249.6	252.0	255.1	258.8	263.1	267.9	273.4	279.3	285.7	292.6	299.8	307.5	315.5	323.9	332.5	341.5	350.7	360.2
4	263.2	263.5	264.5	266.1	268.4	271.3	274.7	278.8	283.4	288.5	294.1	300.2	306.8	313.7	321.0	328.7	336.8	345.1	353.7	362.6	371.8
5	283.2	283.5	284.5	286.0	288.1	290.7	294.0	297.8	302.1	306.9	312.2	317.9	324.1	330.7	337.7	345.0	352.6	360.6	368.9	377.4	386.2
6	305.9	306.2	307.1	308.5	310.4	312.9	315.9	319.5	323.5	328.0	332.9	338.3	344.1	350.3	356.9	363.8	371.1	378.7	386.6	394.8	403.2
7	330.8	331.0	331.8	333.1	334.9	337.2	340.0	343.3	347.1	351.3	355.9	360.9	366.4	372.2	378.4	385.0	391.8	399.0	406.5	414.3	422.3
8	357.3	357.5	358.3	359.5	361.1	363.3	365.9	368.9	372.4	376.3	380.7	385.4	390.5	396.0	401.8	408.0	414.5	421.3	428.4	435.8	443.4
9	385.1	385.4	386.0	387.2	388.7	390.7	393.1	396.0	399.2	402.9	406.9	411.3	416.1	421.3	426.8	432.6	438.7	445.1	451.9	458.9	466.1
10	414.1	414.3	414.9	415.9	417.4	419.2	421.5	424.1	427.2	430.6	434.4	438.5	443.0	447.9	453.0	458.5	464.3	470.4	476.8	483.4	490.3
11	443.8	444.0	444.6	445.6	446.9	448.7	450.8	453.2	456.1	459.3	462.8	466.7	471.0	475.5	480.4	485.6	491.0	496.8	502.8	509.1	515.7
12	474.3	474.5	475.0	475.9	477.2	478.8	480.8	483.1	485.8	488.8	492.1	495.8	499.8	504.1	508.7	513.6	518.7	524.2	529.9	535.9	542.1
13	505.3	505.5	506.0	506.9	508.1	509.6	511.4	513.6	516.1	519.0	522.1	525.6	529.3	533.4	537.7	542.4	547.3	552.4	557.9	563.6	569.5
14	536.8	537.0	537.5	538.3	539.4	540.8	542.6	544.7	547.2	549.7	552.7	555.9	559.5	563.3	567.4	571.8	576.5	581.4	586.6	592.0	597.6
15	568.8	568.9	569.4	570.1	571.2	572.5	574.2	576.1	578.4	581.0	583.7	586.8	590.2	593.8	597.7	601.9	606.3	611.0	615.9	621.1	626.4
16	601.0	601.1	601.6	602.3	603.3	604.6	606.1	608.0	610.1	612.5	615.2	618.1	621.3	624.8	628.5	632.4	636.6	641.1	645.8	650.7	655.8
17	633.5	633.6	634.0	634.7	635.7	636.9	638.4	640.1	642.1	644.4	647.[illegible]	649.8	652.8	656.1	659.6	663.4	667.4	671.7	676.1	680.8	685.8
18	666.2	666.4	666.8	667.4	668.[illegible]	669.5	670.9	672.6	674.5	676.6	679.1	681.7	684.6	687.8	691.1	694.7	698.6	702.6	706.9	711.4	716.1
19	699.2	699.3	699.7	700.3	701.2	702.3	703.6	705.2	707.1	709.1	711.4	714.[illegible]	716.7	719.7	723.[illegible]	726.4	730.[illegible]	734.[illegible]	738.[illegible]	742.4	746.9
20	732.3	732.5	732.8	733.4	734.2	735.3	736.6	738.1	739.[illegible]	741.8	744.[illegible]	747.4	749.[illegible]	752.[illegible]	755.[illegible]	758.4	761.[illegible]	765.4	769.6	773.7	778.[illegible]

ACOUSTIC MODAL FREQUENCIES

FACILITY DIMENSIONS LX= 10.0 FEET, LY= 16.0 FEET, LZ= 42.5 FEET

SPEED OF SOUND = 1116.0 FEET PER SECOND

MODAL INDEX NSUBX = 5

MODAL INDEX NSUBY / MODAL INDEX NSUBZ=0	1	2	3	4	5	6	7	8	9	10	11	12	13	14	15	16	17	18	19	20
0	279.0	279.3	280.2	281.8	283.9	286.6	289.9	293.7	298.1	303.0	308.5	314.2	320.4	327.1	334.1	341.5	349.2	357.3	365.6	374.3	383.1
1	281.2	281.5	282.4	283.9	286.0	288.7	292.0	295.8	300.1	305.0	310.3	316.1	322.3	328.9	335.9	343.3	351.0	359.0	367.3	375.9	384.7
2	287.6	287.9	288.8	290.3	292.3	295.0	298.2	301.9	306.2	310.9	316.1	321.8	327.9	334.4	341.3	348.6	356.1	364.0	372.2	380.7	389.4
3	298.0	298.3	299.1	300.6	302.6	305.1	308.2	311.8	315.9	320.5	325.6	331.1	337.1	343.4	350.1	357.2	364.6	372.3	380.2	388.6	397.2
4	311.9	312.2	313.0	314.4	316.3	318.8	321.7	325.2	329.1	333.6	338.4	343.7	349.5	355.6	362.1	368.9	376.1	383.6	391.3	399.4	407.7
5	329.0	329.3	330.1	331.4	333.2	335.5	338.3	341.6	345.4	349.6	354.2	359.3	364.8	370.6	376.9	383.4	390.4	397.6	405.1	412.9	421.0
6	348.7	349.0	349.7	351.0	352.7	354.9	357.5	360.7	364.2	368.2	372.6	377.5	382.7	388.3	394.2	400.5	407.1	414.1	421.3	428.8	436.6
7	370.7	371.0	371.7	372.8	374.4	376.5	379.0	381.9	385.3	389.1	393.3	397.9	402.8	408.1	413.8	419.8	426.1	432.7	439.6	446.8	454.3
8	394.6	394.8	395.4	396.5	398.0	400.0	402.4	405.1	408.3	411.9	415.8	420.2	424.9	429.9	435.3	441.0	447.0	453.3	459.9	466.8	474.0
9	420.0	420.2	420.8	421.8	423.2	425.1	427.3	429.9	432.9	436.3	440.0	444.1	448.5	453.3	458.4	463.8	469.6	475.6	481.9	488.5	495.3
10	446.6	446.8	447.4	448.4	449.7	451.4	453.5	456.0	458.8	462.0	465.5	469.4	473.6	478.1	483.0	488.1	493.6	499.3	505.3	511.6	518.1
11	474.4	474.5	475.1	476.0	477.2	478.9	480.8	483.2	485.8	488.8	492.2	495.9	499.8	504.1	508.7	513.6	518.8	524.2	530.0	535.9	542.2
12	503.0	503.1	503.7	504.5	505.7	507.2	509.1	511.3	513.8	516.7	519.8	523.3	527.1	531.1	535.5	540.2	545.1	550.3	555.7	561.4	567.4
13	532.3	532.5	533.1	533.8	534.9	536.4	538.1	540.2	542.6	545.3	548.3	551.6	555.2	559.1	563.2	567.6	572.3	577.2	582.4	587.9	593.6
14	562.3	562.5	563.0	563.7	564.8	566.2	567.8	569.8	572.1	574.8	577.8	581.1	584.7	588.7	593.0	597.6	602.5	607.7	613.2	619.0	625.0
15	592.9	593.0	593.5	594.2	595.2	596.5	598.1	600.0	602.1	604.5	607.2	610.2	613.5	617.1	620.9	624.9	629.2	633.8	638.7	643.8	649.2
16	623.9	624.0	624.4	625.1	626.1	627.3	628.8	630.6	632.6	635.0	637.7	640.7	644.0	647.6	651.4	655.4	659.7	664.3	669.1	674.1	679.4
17	655.2	655.4	655.8	656.4	657.3	658.5	660.0	661.7	663.8	666.2	668.8	671.8	675.0	678.5	682.2	686.2	690.5	695.0	699.8	704.9	710.2
18	687.0	687.1	687.5	688.1	689.0	690.1	691.5	693.1	694.9	697.0	699.4	702.0	704.9	708.0	711.4	714.9	718.8	722.9	727.2	731.8	736.6
19	719.0	719.1	719.4	720.0	720.9	722.0	723.3	724.8	726.6	728.6	730.9	733.5	736.3	739.3	742.6	746.1	749.8	753.8	758.0	762.4	767.1
20	751.2	751.3	751.7	752.3	753.1	754.1	755.3	756.8	758.5	760.5	762.8	765.3	768.1	771.2	774.5	778.1	781.9	786.0	790.3	794.9	799.8

ACOUSTIC MODAL FREQUENCIES

FACILITY DIMENSIONS LX= 10.0 FEET, LY= 16.0 FEET, LZ= 42.5 FEET

SPEED OF SOUND = 1116.9 FEET PER SECOND

MODAL INDEX NSUBX = 6

MODAL INDEX NSUBY \ MODAL INDEX NSUBZ	0	1	2	3	4	5	6	7	8	9	10	11	12	13	14	15	16	17	18	19	20
0	334.8	335.1	335.8	337.1	338.9	341.2	343.9	347.2	350.9	355.0	359.4	364.6	370.0	375.8	381.9	388.4	395.2	402.4	409.8	417.5	425.5
1	336.6	336.9	337.6	338.9	340.7	343.0	345.7	348.9	352.6	356.7	361.3	366.3	371.7	377.4	383.5	390.0	396.8	403.9	411.3	419.0	426.9
2	342.0	342.2	343.0	344.2	346.0	348.2	350.9	354.1	357.8	361.8	366.3	371.2	376.5	382.2	388.3	394.6	401.4	408.4	415.7	423.3	431.2
3	350.8	351.0	351.7	353.0	354.7	356.9	359.5	362.6	366.2	370.1	374.5	379.3	384.5	390.1	396.0	402.3	408.9	415.8	423.0	430.4	438.2
4	362.7	362.9	363.4	364.8	366.5	368.6	371.2	374.2	377.6	381.5	385.7	390.4	395.4	400.9	406.6	412.7	419.1	425.9	432.9	440.2	447.8
5	377.5	377.7	378.4	379.5	381.1	383.2	385.6	388.5	391.8	395.6	399.7	404.2	409.0	414.3	419.9	425.8	432.0	438.5	445.4	452.5	459.8
6	394.8	395.0	395.7	396.8	398.3	400.2	402.6	405.4	408.5	412.1	416.1	420.4	425.1	430.1	435.5	441.2	447.2	453.5	460.1	467.0	474.2
7	414.4	414.6	415.2	416.2	417.7	419.5	421.8	424.4	427.5	430.9	434.7	438.8	443.3	448.1	453.3	458.8	464.6	470.6	477.0	483.7	490.6
8	435.8	436.0	436.6	437.6	439.0	440.7	442.9	445.4	448.3	451.5	455.2	459.1	463.4	468.0	473.0	478.2	483.8	489.6	495.8	502.2	508.8
9	458.9	459.1	459.7	460.6	461.9	463.6	465.6	468.0	470.8	473.9	477.3	481.1	485.2	489.6	494.4	499.4	504.7	510.3	516.2	522.3	528.7
10	483.4	483.6	484.2	485.0	486.3	487.9	489.8	492.1	494.7	497.7	501.0	504.6	508.5	512.7	517.2	522.0	527.1	532.5	538.2	544.0	550.2
11	509.2	509.3	509.9	510.7	511.9	513.4	515.2	517.4	519.9	522.7	525.8	529.3	533.0	537.0	541.3	545.9	550.8	555.9	561.3	567.0	572.9
12	535.9	536.1	536.6	537.4	538.5	539.9	541.7	543.8	546.1	548.8	551.8	555.1	558.6	562.5	566.6	571.0	575.6	580.5	585.7	591.2	596.8
13	563.6	563.7	564.2	565.0	566.0	567.4	569.1	571.0	573.3	575.8	578.7	581.8	585.2	588.9	592.8	597.0	601.5	606.2	611.1	616.3	621.8
14	592.0	592.2	592.6	593.3	594.3	595.6	597.2	599.1	601.3	603.7	606.4	609.4	612.6	616.1	619.9	623.9	628.2	632.7	637.4	642.4	647.6
15	621.1	621.2	621.6	622.3	623.3	624.5	626.1	627.9	629.9	632.2	634.8	637.7	640.8	644.1	647.7	651.6	655.7	660.1	664.8	669.8	674.3
16	650.7	650.9	651.3	651.9	652.9	654.0	655.5	657.2	659.2	661.4	663.8	666.6	669.5	672.7	676.2	679.9	683.8	687.9	692.3	696.9	701.7
17	680.9	681.0	681.4	682.0	682.9	684.0	685.4	687.1	688.9	691.1	693.4	696.0	698.9	701.9	705.3	708.8	712.5	716.5	720.7	725.1	729.8
18	711.4	711.6	711.9	712.5	713.4	714.5	715.8	717.4	719.2	721.2	723.5	726.0	728.7	731.6	734.8	738.2	741.8	745.6	749.7	753.9	758.4
19	742.4	742.5	742.9	743.4	744.3	745.3	746.6	748.1	749.8	751.7	753.9	756.3	758.9	761.8	764.9	768.1	771.6	775.3	779.2	783.2	787.5
20	773.7	773.8	774.1	774.7	775.5	776.5	777.7	779.1	780.8	782.7	784.8	787.1	789.6	792.3	795.2	798.4	801.7	805.3	809.1	813.2	817.5

ACOUSTIC MODAL FREQUENCIES

FACILITY DIMENSIONS LX= 16.0 FEET, LY= 15.0 FEET, LZ= 42.5 FEET

SPEED OF SOUND = 1116.0 FEET PER SECOND

MODAL INDEX NSUBX = 7

MODAL INDEX NSUBY / MODAL INDEX NSUBZ=0	1	2	3	4	5	6	7	8	9	10	11	12	13	14	15	16	17	18	19	20
0	390.6	390.8	391.5	392.6	394.1	396.1	398.5	401.3	404.5	408.1	412.1	416.4	421.2	426.3	431.7	437.4	443.5	449.9	456.5	463.5	470.7
1	392.2	392.4	393.0	394.1	395.7	397.6	400.0	402.8	406.0	409.6	413.5	417.9	422.6	427.7	433.1	438.8	444.9	451.2	457.9	464.8	472.0
2	396.8	397.0	397.6	398.7	400.2	402.2	404.5	407.3	410.4	414.0	417.9	422.2	426.9	431.9	437.3	443.0	449.0	455.2	461.8	468.7	475.8
3	404.4	404.6	405.2	406.3	407.8	409.7	412.0	414.7	417.8	421.3	425.2	429.4	434.0	438.9	444.2	449.8	455.7	461.9	468.4	475.1	482.1
4	414.8	415.0	415.6	416.6	418.1	419.9	422.2	424.8	427.9	431.3	435.0	439.2	443.7	448.5	453.7	459.1	464.9	471.0	477.4	484.0	490.9
5	427.8	428.0	428.6	429.6	431.0	432.8	434.9	437.5	440.5	443.8	447.5	451.5	455.8	460.6	465.6	470.9	476.6	482.5	488.7	495.2	501.9
6	443.1	443.3	443.9	444.9	446.2	448.0	450.1	452.5	455.4	458.6	462.2	466.1	470.3	474.9	479.7	484.9	490.4	496.2	502.2	508.5	515.1
7	460.6	460.8	461.4	462.3	463.6	465.3	467.3	469.7	472.4	475.5	479.0	482.7	486.8	491.2	495.9	501.0	506.3	511.8	517.7	523.8	530.2
8	480.0	480.2	480.7	481.6	482.9	484.5	486.4	488.7	491.4	494.3	497.6	501.3	505.2	509.5	514.0	518.8	524.0	529.4	535.0	541.0	547.1
9	501.1	501.3	501.8	502.6	503.8	505.4	507.2	509.4	512.0	514.8	518.0	521.5	525.3	529.4	533.7	538.4	543.3	548.5	554.0	559.7	565.7
10	523.6	523.8	524.3	525.1	526.3	527.7	529.5	531.6	534.1	536.8	539.8	543.2	546.8	550.8	555.0	559.4	564.2	569.1	574.5	580.0	585.8
11	547.5	547.6	548.1	548.9	550.0	551.4	553.1	555.1	557.5	560.1	563.0	566.2	569.7	573.5	577.5	581.8	586.4	591.2	596.3	601.6	607.2
12	572.5	572.6	573.1	573.8	574.9	576.2	577.9	579.8	582.1	584.5	587.3	590.4	593.7	597.4	601.2	605.4	609.8	614.5	619.4	624.5	629.8
13	598.4	598.6	599.0	599.7	600.7	602.0	603.6	605.4	607.6	610.0	612.7	615.6	618.8	622.3	626.0	630.0	634.2	638.7	643.4	648.3	653.5
14	625.3	625.4	625.8	626.5	627.5	628.7	630.2	632.0	634.0	636.3	638.9	641.7	644.8	648.1	651.7	655.5	659.6	663.9	668.4	673.2	678.2
15	652.9	653.0	653.4	654.0	655.0	656.2	657.6	659.3	661.3	663.5	665.9	668.6	671.6	674.8	678.2	681.9	685.8	690.0	694.3	698.9	703.7
16	681.1	681.3	681.6	682.3	683.1	684.3	685.7	687.3	689.2	691.3	693.7	696.3	699.1	702.2	705.5	709.0	712.8	716.8	721.0	725.4	730.0
17	710.0	710.1	710.5	711.1	711.9	713.0	714.3	715.9	717.7	719.7	722.0	724.5	727.2	730.2	733.4	736.8	740.4	744.2	748.3	752.5	757.0
18	739.3	739.5	739.8	740.4	741.2	742.3	743.5	745.0	746.8	748.7	750.9	753.3	756.0	758.8	761.9	765.1	768.6	772.3	776.2	780.3	784.6
19	769.2	769.3	769.6	770.2	771.0	772.0	773.2	774.7	776.3	778.2	780.3	782.6	785.2	787.9	790.9	794.0	797.4	800.9	804.7	808.6	812.8
20	799.4	799.5	799.9	800.4	801.1	802.1	803.3	804.7	806.3	808.1	810.1	812.4	814.8	817.4	820.2	823.2	826.4	829.8	833.4	837.2	841.4

ACOUSTIC MODAL FREQUENCIES

FACILITY DIMENSIONS LX= 10.0 FEET, LY= 16.0 FEET, LZ= 42.5 FEET

SPEED OF SOUND = 1116.0 FEET PER SECOND

MODAL INDEX NSUBX = 8

MODAL INDEX NSUBY	MODAL INDEX NSUBZ=0	1	2	3	4	5	6	7	8	9	10	11	12	13	14	15	16	17	18	19	20
0	446.4	446.6	447.2	448.1	449.5	451.2	453.3	455.8	458.6	461.8	465.3	469.2	473.4	477.9	482.8	487.9	493.4	499.1	505.1	511.4	517.9
1	447.8	448.0	448.5	449.5	450.8	452.5	454.6	457.1	459.9	463.1	466.6	470.5	474.7	479.2	484.0	489.2	494.6	500.3	506.3	512.6	519.1
2	451.8	452.0	452.6	453.5	454.9	456.6	458.6	461.1	463.9	467.0	470.5	474.3	478.5	483.0	487.8	492.9	498.3	503.9	509.7	516.1	522.6
3	458.5	458.7	459.2	460.2	461.5	463.2	465.2	467.6	470.4	473.5	476.9	480.7	484.8	489.2	494.0	499.0	504.3	509.9	515.8	522.0	528.4
4	467.7	467.9	468.4	469.3	470.6	472.3	474.3	476.6	479.3	482.4	485.8	489.5	493.5	497.9	502.5	507.5	512.7	518.2	524.0	530.1	536.4
5	479.2	479.4	480.0	480.9	482.1	483.7	485.7	488.0	490.6	493.6	496.9	500.5	504.5	508.7	513.3	518.1	523.3	528.7	534.4	540.3	546.5
6	493.8	493.2	493.7	494.6	495.8	497.4	499.3	501.5	504.1	507.0	510.2	513.7	517.6	521.7	526.2	530.9	535.9	541.2	546.7	552.5	558.6
7	508.8	509.0	509.5	510.3	511.5	513.0	514.9	517.0	519.5	522.3	525.5	528.9	532.6	536.7	541.0	545.6	550.5	555.6	561.0	566.7	572.6
8	526.4	526.6	527.1	527.9	529.0	530.5	532.3	534.4	536.8	539.5	542.5	545.9	549.5	553.4	557.6	562.0	566.8	571.8	577.0	582.5	588.3
9	545.7	545.9	546.3	547.1	548.2	549.6	551.4	553.4	555.7	558.3	561.3	564.5	568.0	571.8	575.8	580.2	584.7	589.6	594.7	600.0	605.6
10	566.5	566.6	567.1	567.8	568.9	570.3	571.9	573.9	576.1	578.7	581.5	584.6	588.0	591.6	595.6	599.7	604.2	608.9	613.8	619.0	624.4
11	588.6	588.7	589.2	589.9	590.9	592.2	593.8	595.7	597.9	600.3	603.1	606.1	609.3	612.8	616.6	620.7	625.1	629.5	634.3	639.3	644.5
12	611.9	612.0	612.5	613.2	614.1	615.4	616.9	618.8	620.8	623.2	625.8	628.7	631.9	635.3	638.9	642.8	647.1	651.3	655.9	660.8	666.0
13	636.3	636.4	636.8	637.5	638.4	639.6	641.1	642.9	644.9	647.1	649.7	652.4	655.5	658.8	662.3	666.0	670.0	674.3	678.7	683.4	688.3
14	661.6	661.7	662.1	662.7	663.6	664.8	666.2	667.9	669.8	672.0	674.5	677.1	680.1	683.2	686.6	690.3	694.2	698.2	702.5	707.0	711.8
15	687.7	687.8	688.2	688.8	689.7	690.8	692.2	693.8	695.7	697.8	700.1	702.7	705.5	708.6	711.8	715.3	719.1	723.1	727.3	731.5	736.1
16	714.6	714.7	715.1	715.7	716.5	717.6	718.9	720.5	722.3	724.3	726.6	729.0	731.6	734.7	737.9	741.2	744.8	748.6	752.7	756.9	761.3
17	742.1	742.3	742.6	743.2	744.0	745.0	746.3	747.8	749.5	751.5	753.7	756.1	758.7	761.5	764.6	767.8	771.3	775.0	778.9	782.9	787.2
18	770.3	770.4	770.7	771.3	772.1	773.1	774.3	775.8	777.4	779.3	781.4	783.7	786.2	788.9	791.8	795.1	798.4	802.0	805.7	809.7	813.8
19	799.0	799.1	799.4	799.9	800.7	801.7	802.8	804.2	805.8	807.7	809.7	811.9	814.4	817.0	819.8	822.9	826.1	829.6	833.2	837.0	841.0
20	828.1	828.2	828.5	829.1	829.8	830.7	831.9	833.2	834.8	836.5	838.5	840.6	843.0	845.5	848.3	851.2	854.4	857.7	861.2	864.9	868.8

ACOUSTIC MODAL FREQUENCIES

FACILITY DIMENSIONS LX= 10.0 FEET, LY= 16.0 FEET, LZ= 42.5 FEET

SPEED OF SOUND = 1116.0 FEET PER SECOND

MODAL INDEX NSUBX = 9

MODAL INDEX NSUBY	MODAL INDEX NSUBZ=0	1	2	3	4	5	6	7	8	9	10	11	12	13	14	15	16	17	18	19	20
0	502.2	502.4	502.9	503.7	504.9	506.5	508.3	510.5	513.1	515.9	519.1	522.6	526.3	530.4	534.8	539.4	544.4	549.6	555.0	560.7	566.7
1	503.4	503.6	504.1	504.9	506.1	507.7	509.5	511.7	514.3	517.1	520.2	523.7	527.5	531.6	535.9	540.6	545.5	550.7	556.1	561.8	567.8
2	507.0	507.2	507.7	508.5	509.7	511.3	513.1	515.3	517.8	520.6	523.7	527.2	530.9	535.0	539.3	543.9	548.8	554.0	559.4	565.1	571.0
3	513.0	513.2	513.7	514.5	515.7	517.2	519.0	521.2	523.6	526.4	529.5	532.9	536.6	540.6	544.9	549.5	554.3	559.4	564.8	570.4	576.3
4	521.2	521.4	521.9	522.7	523.9	525.3	527.1	529.3	531.7	534.4	537.5	540.9	544.5	548.5	552.7	557.2	562.0	567.0	572.3	577.8	583.6
5	531.6	531.8	532.3	533.1	534.2	535.7	537.4	539.5	541.9	544.6	547.6	550.9	554.5	558.3	562.5	566.9	571.6	576.6	581.8	587.2	592.9
6	544.0	544.2	544.7	545.5	546.6	548.0	549.7	551.8	554.1	556.7	559.7	562.9	566.4	570.2	574.3	578.6	583.2	588.1	593.2	598.5	604.1
7	558.4	558.5	559.0	559.8	560.9	562.2	563.9	565.9	568.2	570.8	573.6	576.8	580.2	583.9	587.9	592.1	596.6	601.3	606.3	611.6	617.1
8	574.5	574.6	575.1	575.8	576.9	578.2	579.9	581.8	584.0	586.5	589.3	592.4	595.7	599.3	603.2	607.3	611.7	616.3	621.2	626.3	631.7
9	592.2	592.4	592.8	593.5	594.5	595.8	597.4	599.3	601.5	603.9	606.6	609.6	612.8	616.3	620.1	624.1	628.4	632.9	637.6	642.6	647.8
10	611.4	611.6	612.0	612.7	613.7	614.9	616.5	618.3	620.4	622.7	625.4	628.2	631.4	634.8	638.4	642.4	646.5	650.9	655.5	660.3	665.4
11	632.0	632.1	632.5	633.2	634.1	635.4	636.9	638.6	640.6	642.9	645.5	648.3	651.3	654.6	658.1	661.9	666.0	670.2	674.7	679.4	684.3
12	653.7	653.8	654.2	654.9	655.8	657.0	658.4	660.1	662.1	664.3	666.8	669.5	672.4	675.6	679.1	682.7	686.6	690.8	695.1	699.7	704.5
13	676.6	676.7	677.1	677.7	678.6	679.8	681.1	682.8	684.7	686.8	689.2	691.8	694.7	697.8	701.1	704.7	708.4	712.4	716.7	721.1	725.7
14	700.4	700.5	700.9	701.5	702.4	703.5	704.8	706.4	708.3	710.3	712.6	715.2	717.9	720.9	724.1	727.6	731.2	735.1	739.2	743.5	748.0
15	725.2	725.3	725.6	726.2	727.1	728.1	729.4	731.0	732.7	734.7	737.0	739.4	742.1	745.0	748.1	751.4	755.0	758.7	762.7	766.9	771.2
16	750.7	750.8	751.2	751.7	752.5	753.4	754.8	756.3	758.0	760.0	762.1	764.5	767.1	769.9	772.9	776.1	779.6	783.2	787.0	791.1	795.3
17	777.0	777.1	777.4	778.0	778.8	779.8	781.0	782.4	784.1	785.9	788.0	790.3	792.8	795.5	798.4	801.6	804.9	808.4	812.1	816.0	820.2
18	803.9	804.0	804.3	804.9	805.6	806.6	807.8	809.1	810.7	812.6	814.6	816.8	819.2	821.8	824.7	827.7	830.9	834.3	837.9	841.7	845.7
19	831.4	831.5	831.9	832.4	833.1	834.0	835.2	836.5	838.0	839.8	841.7	843.9	846.2	848.8	851.5	854.4	857.6	860.9	864.4	868.0	871.9
20	859.5	859.6	859.9	860.4	861.1	862.0	863.1	864.4	865.9	867.6	869.5	871.5	873.7	876.3	878.9	881.8	884.9	[illegible]	891.4	895.0	898

ACOUSTIC MODAL FREQUENCIES

FACILITY DIMENSIONS LX= 10.0 FEET, LY= 16.0 FEET, LZ= 42.5 FEET

SPEED OF SOUND = 1116.0 FEET PER SECOND

MODAL INDEX NSUBX = 10

MODAL INDEX NSUBY	MODAL INDEX NSUBZ=0	1	2	3	4	5	6	7	8	9	10	11	12	13	14	15	16	17	18	19	20
0	556.0	558.2	558.6	559.4	560.5	561.8	563.5	565.5	567.8	570.4	573.2	576.4	579.8	583.5	587.5	591.7	596.2	601.0	606.0	611.2	616.7
1	559.1	559.2	559.7	560.5	561.5	562.9	564.6	566.6	568.9	571.4	574.3	577.4	580.9	584.6	588.5	592.8	597.3	602.0	607.0	612.2	617.7
2	562.3	562.5	563.0	563.7	564.8	566.2	567.8	569.8	572.1	574.6	577.5	580.6	584.0	587.7	591.6	595.8	600.3	605.0	610.0	615.2	620.6
3	567.7	567.9	568.3	569.1	570.1	571.5	573.2	575.1	577.4	579.9	582.7	585.8	589.2	592.8	596.7	600.9	605.3	610.0	614.9	620.1	625.5
4	575.2	575.3	575.8	576.5	577.6	578.9	580.5	582.5	584.7	587.2	590.0	593.0	596.4	600.0	603.8	608.0	612.3	617.0	621.8	626.9	632.3
5	584.6	584.8	585.2	585.9	587.0	588.3	589.9	591.8	594.0	596.4	599.2	602.2	605.5	609.0	612.8	616.9	621.2	625.8	630.6	635.6	640.9
6	595.9	596.1	596.5	597.2	598.3	599.5	601.1	603.0	605.1	607.5	610.2	613.2	616.4	619.9	623.6	627.6	631.9	636.4	641.1	646.0	651.2
7	609.1	609.2	609.6	610.3	611.3	612.6	614.1	616.0	618.1	620.4	623.1	626.0	629.1	632.5	636.2	640.1	644.3	648.7	653.3	658.2	663.3
8	623.9	624.0	624.4	625.1	626.1	627.3	628.8	630.6	632.6	635.0	637.5	640.4	643.5	646.8	650.4	654.2	658.3	662.6	667.1	671.9	676.9
9	640.2	640.4	640.8	641.4	642.4	643.6	645.0	646.8	648.8	651.0	653.5	656.3	659.3	662.6	666.1	669.8	673.8	678.0	682.4	687.1	692.0
10	658.0	658.2	658.5	659.2	660.1	661.3	662.7	664.4	666.4	668.5	671.0	673.7	676.6	679.8	683.2	686.9	690.7	694.8	699.2	703.7	708.5
11	677.2	677.3	677.7	678.3	679.2	680.3	681.7	683.4	685.2	687.4	689.8	692.4	695.2	698.3	701.7	705.3	709.1	713.1	717.3	721.6	726.3
12	697.5	697.6	698.0	698.6	699.5	700.6	701.9	703.5	705.4	707.4	709.7	712.3	715.1	718.1	721.3	724.8	728.6	732.5	736.4	740.8	745.3
13	719.0	719.1	719.4	720.0	720.9	722.0	723.3	724.8	726.6	728.6	730.9	733.3	736.0	738.9	742.1	745.5	749.[illegible]	[illegible]2.8	756.5	761.0	765.4
14	741.5	741.6	741.9	742.5	743.3	744.4	745.6	747.1	748.9	750.8	753.0	755.4	758.0	760.8	763.9	767.2	770.8	774.3	778.2	782.3	786.6
15	764.9	765.0	765.3	765.9	766.7	767.7	768.9	770.4	772.0	773.9	776.1	778.4	780.9	783.7	786.6	789.8	793.2	796.8	800.5	804.5	808.7
16	789.1	789.2	789.5	790.1	790.9	791.9	793.1	794.5	796.1	797.9	800.0	802.2	804.7	807.4	810.3	813.3	816.6	820.1	823.8	827.6	831.7
17	814.2	814.3	814.6	815.1	815.9	816.8	818.0	819.3	820.9	822.7	824.7	826.9	829.3	831.9	834.7	837.6	840.8	844.2	847.8	851.5	855.5
18	839.9	840.0	840.3	840.8	841.5	842.5	843.6	844.9	846.4	848.2	850.1	852.2	854.6	857.1	859.8	862.7	865.8	869.1	872.5	876.2	880.0
19	866.3	866.4	866.7	867.2	867.9	868.8	869.9	871.1	872.6	874.3	876.2	878.2	880.5	882.9	885.6	888.4	891.4	894.6	897.9	901.5	905.2
20	893.2	893.3	893.6	894.1	894.8	895.6	896.7	898.0	899.4	901.0	902.8	904.8	907.0	[illegible]	[illegible]	[illegible]	[illegible]	[illegible]	[illegible]	927.4	931.0

ACOUSTIC MODAL FREQUENCIES

FACILITY DIMENSIONS LX= 10.0 FEET, LY= 16.0 FEET, LZ= 42.5 FEET

SPEED OF SOUND = 1116.0 FEET PER SECOND

MODAL INDEX NSUBX = 11

MODAL INDEX NSUBY	MODAL INDEX NSUBZ=0	1	2	3	4	5	6	7	8	9	10	11	12	13	14	15	16	17	18	19	20
0	613.8	613.9	614.4	615.1	616.0	617.3	618.8	620.6	622.7	625.1	627.7	630.6	633.7	637.1	640.7	644.6	648.8	653.1	657.7	662.6	667.6
1	614.8	614.9	615.4	616.1	617.0	618.3	619.8	621.6	623.7	626.0	628.7	631.5	634.7	638.0	641.7	645.6	649.7	654.1	658.6	663.5	668.5
2	617.8	617.9	618.3	619.0	620.0	621.2	622.8	624.5	626.6	629.0	631.5	634.4	637.5	641.0	644.5	648.4	652.5	656.8	661.4	666.2	671.2
3	622.7	622.8	623.2	623.9	624.9	626.1	627.6	629.4	631.5	633.8	636.3	639.2	642.3	645.6	649.2	653.1	657.1	661.4	666.0	670.8	675.8
4	629.5	629.6	630.0	630.7	631.6	632.9	634.4	636.1	638.2	640.4	643.0	645.8	648.9	652.2	655.7	659.5	663.4	667.9	672.4	677.1	682.0
5	638.1	638.2	638.6	639.3	640.2	641.5	642.9	644.7	646.7	648.9	651.5	654.2	657.3	660.5	664.0	667.8	671.8	676.0	680.4	685.1	690.0
6	648.5	648.6	649.0	649.7	650.6	651.8	653.3	655.0	656.9	659.2	661.6	664.4	667.4	670.6	674.0	677.7	681.7	685.8	690.2	694.8	699.6
7	660.6	660.7	661.1	661.7	662.7	663.8	665.2	666.9	668.9	671.1	673.5	676.2	679.1	682.3	685.7	689.3	693.2	697.3	701.6	706.1	710.8
8	674.2	674.4	674.7	675.4	676.3	677.4	678.8	680.5	682.4	684.5	686.9	689.5	692.4	695.5	698.8	702.4	706.2	710.2	714.5	718.9	723.6
9	689.4	689.5	689.9	690.5	691.4	692.5	693.9	695.5	697.4	699.5	701.8	704.4	707.2	710.2	713.5	717.0	720.7	724.6	728.8	733.1	737.7
10	706.0	706.1	706.4	707.1	707.9	709.0	710.3	711.9	713.7	715.8	718.1	720.6	723.3	726.3	729.5	732.9	736.6	740.5	744.5	748.7	753.2
11	723.8	723.9	724.3	724.9	725.7	726.8	728.1	729.6	731.4	733.4	735.6	738.1	740.8	743.7	746.8	750.1	753.7	757.5	761.4	765.6	770.0
12	742.9	743.0	743.4	743.9	744.7	745.8	747.1	748.6	750.3	752.2	754.4	756.8	759.4	762.3	765.3	768.6	772.0	775.7	779.6	783.7	787.9
13	763.1	763.2	763.5	764.1	764.9	765.9	767.1	768.6	770.3	772.2	774.3	776.6	779.2	781.9	784.9	788.1	791.5	795.1	798.9	802.8	807.0
14	784.3	784.4	784.7	785.3	786.1	787.1	788.3	789.7	791.3	793.2	795.2	797.5	800.0	802.7	805.6	808.7	812.0	815.4	819.1	823.0	827.1
15	806.5	806.6	806.9	807.4	808.2	809.1	810.3	811.7	813.3	815.1	817.1	819.3	821.7	824.3	827.2	830.2	833.4	836.8	840.4	844.2	848.2
16	829.5	829.6	829.9	830.5	831.2	832.1	833.3	834.6	836.2	837.9	839.9	842.0	844.4	846.9	849.6	852.6	855.7	859.0	862.5	866.2	870.1
17	853.4	853.5	853.8	854.3	855.0	855.9	857.0	858.3	859.8	861.5	863.4	865.5	867.8	870.3	873.0	875.9	878.9	882.1	885.5	889.1	892.9
18	878.0	878.1	878.4	878.8	879.5	880.4	881.5	882.8	884.2	885.9	887.7	889.8	892.0	894.4	897.0	899.8	902.7	905.9	909.2	912.7	916.4
19	903.2	903.3	903.6	904.1	904.8	905.6	906.7	907.9	909.3	910.9	912.7	914.7	916.9	919.2	921.7	924.5	927.5	930.4	933.6	937.0	940.6
20	929.1	929.2	929.5	930.0	930.6	931.4	932.4	933.7	935.2	936.6	938.3	940.3	942.4	944.7	947.1	949.8	952.8	955.5	958.7	962.0	965.5

ACOUSTIC MODAL FREQUENCIES

FACILITY DIMENSIONS LX= 10.0 FEET, LY= 16.0 FEET, LZ= 42.5 FEET

SPEED OF SOUND = 1116.0 FEET PER SECOND

MODAL INDEX NSUBX = 12

MODAL INDEX NSUBY / NSUBZ	0	1	2	3	4	5	6	7	8	9	10	11	12	13	14	15	16	17	18	19	20
0	669.6	669.7	670.1	670.8	671.7	672.8	674.2	675.9	677.8	679.9	682.4	685.0	687.9	691.0	694.4	698.0	701.8	705.8	710.1	714.6	719.2
1	670.5	670.6	671.0	671.7	672.6	673.7	675.1	676.8	678.7	680.8	683.2	685.9	688.8	691.9	695.2	698.8	702.6	706.7	710.9	715.4	720.1
2	673.2	673.4	673.7	674.4	675.3	676.4	677.8	679.5	681.4	683.5	685.9	688.5	691.4	694.5	697.9	701.4	705.2	709.3	713.5	718.0	722.6
3	677.7	677.9	678.2	678.9	679.8	680.9	682.3	683.9	685.8	687.9	690.3	692.9	695.8	698.9	702.2	705.8	709.5	713.5	717.7	722.2	726.8
4	684.0	684.1	684.5	685.1	686.0	687.1	688.5	690.1	692.0	694.1	696.5	699.1	701.9	705.0	708.2	711.8	715.5	719.5	723.7	728.0	732.7
5	691.9	692.1	692.4	693.1	693.9	695.0	696.4	698.0	699.9	701.9	704.3	706.8	709.6	712.7	715.9	719.4	723.1	727.0	731.2	735.5	740.1
6	701.5	701.7	702.0	702.6	703.5	704.6	705.9	707.5	709.4	711.4	713.7	716.2	719.0	722.0	725.2	728.7	732.3	736.2	740.3	744.6	749.1
7	712.7	712.8	713.2	713.8	714.6	715.7	717.1	718.6	720.4	722.4	724.7	727.2	729.9	732.9	736.0	739.4	743.0	746.8	750.9	755.1	759.5
8	725.4	725.5	725.9	726.5	727.3	728.4	729.7	731.2	733.0	735.0	737.2	739.6	742.3	745.2	748.3	751.7	755.2	759.0	762.9	767.1	771.5
9	739.5	739.6	740.0	740.6	741.4	742.4	743.7	745.2	746.9	748.9	751.1	753.5	756.1	759.0	762.0	765.3	768.8	772.5	776.4	780.5	784.8
10	755.0	755.1	755.4	756.0	756.8	757.8	759.1	760.6	762.2	764.2	766.3	768.7	771.2	774.0	777.0	780.2	783.7	787.3	791.1	795.1	799.3
11	771.7	771.8	772.2	772.7	773.5	774.5	775.7	777.2	778.8	780.7	782.8	785.1	787.6	790.4	793.3	796.4	799.8	803.3	807.1	811.0	815.2
12	789.6	789.7	790.1	790.6	791.4	792.3	793.5	795.0	796.6	798.4	800.5	802.7	805.2	807.9	810.7	813.8	817.1	820.6	824.2	828.1	832.1
13	808.6	808.8	809.1	809.6	810.4	811.3	812.5	813.9	815.4	817.2	819.2	821.4	823.9	826.5	829.3	832.3	835.5	838.9	842.5	846.3	850.2
14	828.7	828.8	829.1	829.6	830.4	831.3	832.4	833.8	835.3	837.1	839.0	841.2	843.5	846.1	848.8	851.8	854.9	858.2	861.7	865.4	869.3
15	849.7	849.8	850.1	850.6	851.3	852.3	853.4	854.7	856.2	857.9	859.8	861.9	864.2	866.7	869.4	872.2	875.3	878.5	882.0	885.6	889.4
16	871.6	871.7	872.0	872.5	873.2	874.1	875.2	876.5	877.9	879.6	881.5	883.5	885.7	888.2	890.8	893.6	896.6	899.7	903.1	906.6	910.3
17	894.4	894.4	894.7	895.2	895.9	896.8	897.8	899.1	900.5	902.1	903.9	905.9	908.1	910.5	913.0	915.8	918.7	921.8	925.0	928.5	932.1
18	917.8	917.9	918.2	918.7	919.3	920.2	921.2	922.4	923.8	925.4	927.2	929.1	931.3	933.6	936.1	938.7	941.6	944.6	947.8	951.1	954.7
19	942.0	942.1	942.4	942.9	943.5	944.3	945.3	946.5	947.9	949.4	951.1	953.0	955.1	957.4	959.8	962.4	965.2	968.1	971.2	974.5	978.0
20	966.9	967.0	967.2	967.7	968.3	969.1	970.1	971.2	972.6	974.1	975.8	977.6	979.6	981.8	984.2	986.7	989.4	992.3	995.4	998.7	1001.9

ACOUSTIC MODAL FREQUENCIES

FACILITY DIMENSIONS LX= 10.0 FEET, LY= 16.[illegible] FEET, LZ= 42.5 FEET

SPEED OF SOUND = 1116.0 FEET PER SECOND

MODAL INDEX NSUBX = 13

MODAL INDEX NSUBY	MODAL INDEX NSUBZ=0	1	2	3	4	5	6	7	8	9	10	11	12	13	14	15	16	17	18	19	20
0	725.4	725.5	725.9	726.5	727.3	728.4	729.7	731.2	733.0	735.0	737.2	739.6	742.3	745.2	748.3	751.7	755.2	759.0	762.9	767.1	771.5
1	726.2	726.4	726.7	727.3	728.1	729.2	730.5	732.0	733.8	735.8	738.0	740.5	743.1	746.0	749.1	752.5	756.0	759.8	763.7	767.9	772.3
2	728.7	728.9	729.2	729.8	730.6	731.7	733.0	734.5	736.3	738.3	740.5	742.9	745.6	748.5	751.6	754.9	758.4	762.2	766.1	770.3	774.6
3	732.9	733.0	733.4	734.0	734.8	735.8	737.1	738.6	740.4	742.4	744.6	747.0	749.6	752.5	755.6	758.9	762.4	766.1	770.1	774.2	778.5
4	738.7	738.8	739.2	739.7	740.6	741.6	742.9	744.4	746.1	748.1	750.3	752.7	755.3	758.2	761.2	764.5	768.0	771.7	775.6	779.7	784.0
5	746.1	746.2	746.5	747.1	747.9	748.9	750.2	751.7	753.4	755.4	757.5	759.9	762.5	765.3	768.4	771.6	775.1	778.7	782.6	786.7	790.9
6	755.0	755.1	755.4	756.0	756.8	757.8	759.1	760.6	762.2	764.2	766.3	768.7	771.2	774.0	777.0	780.2	783.7	787.3	791.1	795.1	799.3
7	765.4	765.5	765.8	766.4	767.2	768.2	769.4	770.9	772.6	774.4	776.6	778.9	781.4	784.2	787.1	790.3	793.7	797.3	801.2	805.0	809.2
8	777.2	777.3	777.6	778.2	779.0	780.0	781.2	782.6	784.3	786.1	788.2	790.5	793.0	795.7	798.6	801.8	805.1	808.6	812.3	816.3	820.4
9	790.4	790.5	790.8	791.4	792.1	793.1	794.3	795.7	797.3	799.2	801.2	803.5	805.9	808.6	811.5	814.6	817.8	821.3	825.0	828.8	832.9
10	804.9	805.0	805.3	805.8	806.6	807.6	808.7	810.1	811.7	813.5	815.5	817.7	820.2	822.8	825.6	828.6	831.8	835.3	838.9	842.7	846.8
11	820.6	820.7	821.0	821.5	822.3	823.2	824.4	825.7	827.3	829.1	831.[illegible]	833.2	835.6	838.2	840.9	843.9	847.1	850.4	853.9	857.7	861.8
12	837.5	837.6	837.9	838.4	839.1	840.0	841.2	842.5	844.[illegible]	845.8	847.7	849.8	852.2	854.7	857.4	860.3	863.[illegible]	866.[illegible]	[illegible]	[illegible]	[illegible]
13	855.4	855.5	855.8	856.3	857.0	857.9	859.0	860.3	861.9	863.5	865.4	867.5	869.8	872.3	875.[illegible]	877.8	880.[illegible]	884.[illegible]	[illegible]	891.1	894.8
14	874.4	874.5	874.8	875.3	876.0	876.9	878.0	879.2	880.7	882.4	884.2	886.3	[illegible].5	890.9	893.5	896.3	899.3	902.6	906.1	909.8	913.8
15	894.4	894.4	894.7	895.2	895.9	896.8	897.8	899.1	900.5	902.1	903.9	905.9	908.1	910.5	913.0	915.8	918.7	921.8	[illegible]25.[illegible]	928.5	932.1
16	915.2	915.3	915.6	916.0	916.7	917.5	918.6	919.8	921.2	922.8	924.6	926.5	928.7	931.0	933.5	936.1	939.0	942.0	945.2	948.6	952.1
17	936.9	937.0	937.2	937.7	938.3	939.2	940.2	941.4	942.7	944.3	946.0	947.9	950.[illegible]	952.3	954.7	957.3	960.1	963.[illegible]	966.2	969.5	973.0
18	959.3	959.4	959.7	960.1	960.7	961.6	962.5	963.7	965.0	966.6	968.3	970.1	972.2	974.4	976.9	979.3	982.[illegible]	984.9	988.[illegible]	991.2	995.6
19	982.5	982.6	982.8	983.3	983.9	984.7	985.6	986.8	988.1	989.6	991.2	993.0	995.[illegible]	997.2	999.5	1002.[illegible]	1004.7	1007.5	1010.5	13.71	17.0
20	1006.3	1006.4	1006.7	1007.1	1007.7	1008.5	1009.4	1010.5	1011.8	1013.2	1014.[illegible]	1016.[illegible]	1018.[illegible]	1020.[illegible]	1023.[illegible]	1025.4	1028.[illegible]	1030.[illegible]	34.[illegible]	38.[illegible]	42.[illegible]

FACILITY DIMENSIONS LX= 10.0 FEET, LY= 16.[illegible] FEET, LZ= 42.5 FEET

SPEED OF SOUND = 1116.0 FEET PER SECOND

MODAL INDEX NSUBX = 14

MODAL INDEX NSUBY / NSUBZ	0	1	2	3	4	5	6	7	8	9	10	11	12	13	14	15	16	17	18	19	20
0	781.2	781.3	781.6	782.2	783.0	784.0	735.2	786.6	788.2	790.1	792.2	794.4	796.9	799.6	802.5	805.6	809.0	812.5	816.2	820.1	824.2
1	782.0	782.1	782.4	783.0	783.7	784.7	785.9	787.4	789.0	790.9	792.9	795.2	797.7	800.4	803.3	806.4	809.7	813.2	816.9	820.8	824.9
2	784.3	784.4	784.7	785.3	786.1	787.1	788.3	789.7	791.3	793.2	795.2	797.5	800.0	802.7	805.6	808.7	812.0	815.4	819.1	823.0	827.1
3	788.2	788.3	788.6	789.2	789.9	790.9	792.1	793.5	795.1	797.0	799.0	801.3	803.8	806.4	809.3	812.4	815.7	819.2	822.9	826.7	830.8
4	793.6	793.7	794.0	794.5	795.3	796.3	797.5	798.9	800.5	802.3	804.3	806.6	809.0	811.7	814.6	817.6	820.9	824.3	828.0	831.8	835.9
5	800.4	800.5	800.9	801.4	802.1	803.1	804.3	805.7	807.3	809.1	811.1	813.4	815.8	818.4	821.3	824.3	827.5	831.0	834.6	838.4	842.4
6	808.7	808.8	809.2	809.7	810.4	811.4	812.6	813.9	815.5	817.3	819.3	821.5	823.9	826.6	829.4	832.4	835.6	839.0	842.6	846.3	850.3
7	818.5	818.6	818.9	819.4	820.1	821.1	822.2	823.6	825.2	826.9	828.9	831.1	833.5	836.1	838.8	841.8	845.0	848.3	851.9	855.6	859.5
8	829.5	829.6	829.9	830.5	831.2	832.1	833.3	834.6	836.2	837.9	839.9	842.0	844.4	846.9	849.6	852.6	855.7	859.0	862.5	866.2	870.1
9	841.9	842.0	842.3	842.8	843.5	844.5	845.6	846.9	848.4	850.1	852.1	854.2	856.5	859.0	861.7	864.6	867.7	871.0	874.4	878.1	881.9
10	855.5	855.6	855.9	856.4	857.1	858.0	859.1	860.4	861.9	863.6	865.5	867.6	869.9	872.4	875.0	877.9	880.9	884.1	887.6	891.1	894.9
11	870.3	870.4	870.7	871.2	871.9	872.8	873.9	875.2	876.6	878.3	880.2	882.2	884.5	886.9	889.6	892.5	895.6	898.8	902.4	905.4	909.1
12	886.2	886.3	886.6	887.1	887.8	888.7	889.7	891.0	892.4	894.1	895.9	897.9	900.1	902.5	905.1	907.9	911.0	914.3	917.9	921.7	925.7	924.3
13	903.2	903.3	903.6	904.1	904.8	905.6	906.7	907.9	909.3	910.9	912.7	914.7	916.9	919.2	921.7	924.5	927.5	930.8	934.3	938.0	941.9	940.6
14	921.2	921.3	921.6	922.1	922.7	923.6	924.6	925.8	927.2	928.8	930.5	932.5	934.6	936.9	939.4	942.0	944.9	947.9	951.1	954.4	957.9
15	940.2	940.3	940.5	941.0	941.6	942.5	943.5	944.7	946.0	947.6	949.3	951.2	953.3	955.5	958.0	960.6	963.4	966.3	969.4	972.7	976.2
16	960.0	960.1	960.4	960.8	961.5	962.3	963.2	964.4	965.7	967.3	969.0	971.0	972.9	975.1	977.5	980.0	982.7	985.6	988.7	991.9	995.3
17	980.7	980.8	981.1	981.5	982.1	982.9	983.9	985.0	986.3	987.8	989.5	991.3	993.3	995.4	997.8	1000.3	1002.9	1005.8	1008.8	1011.9	1015.2
18	1002.2	1002.3	1002.5	1002.9	1003.5	1004.3	1005.3	1006.4	1007.7	1009.1	1010.7	1012.5	1014.5	1016.6	1018.9	1021.3	1023.9	1026.7	1029.7	1032.8	1036.0
19	1024.4	1024.5	1024.7	1025.1	1025.7	1026.5	1027.4	1028.5	1029.7	1031.2	1032.8	1034.5	1036.4	1038.5	1040.7	1043.1	1045.7	1048.4	1051.3	1054.3	1057.5
20	1047.3	1047.4	1047.6	1048.0	1048.6	1049.3	1050.2	1051.3	1052.5	1053.9	1055.5	1057.2	1059.1	1061.1	1063.3	1065.6	1068.1	1070.8	1073.6	1076.6	1079.

ACOUSTIC MODAL FREQUENCIES

FACILITY DIMENSIONS LX= 10.0 FEET, LY= 16.0 FEET, LZ= 42.5 FEET

SPEED OF SOUND = 1116.0 FEET PER SECOND

MODAL INDEX NSUBX = 15

MODAL INDEX NSUBY / MODAL INDEX NSUBZ=0	1	2	3	4	5	6	7	8	9	10	11	12	13	14	15	16	17	18	19	20
0	837.0	837.1	837.4	837.9	838.6	839.6	840.7	842.0	843.6	845.3	847.2	849.4	851.7	854.2	856.9	859.9	863.0	866.2	869.7	873.4	877.2
1	837.7	837.8	838.1	838.7	839.4	840.3	841.4	842.8	844.3	846.0	848.0	850.1	852.4	854.9	857.7	860.6	863.7	867.0	870.4	874.1	877.9
2	839.9	840.0	840.3	840.8	841.5	842.5	843.6	844.9	846.4	848.2	850.1	852.2	854.6	857.1	859.8	862.7	865.8	869.1	872.5	876.2	880.0
3	843.5	843.6	843.9	844.4	845.1	846.1	847.2	848.5	850.0	851.8	853.7	855.8	858.1	860.6	863.3	866.2	869.3	872.5	876.0	879.6	883.4
4	848.5	848.6	849.0	849.5	850.2	851.1	852.2	853.5	855.0	856.7	858.6	860.7	863.0	865.5	868.2	871.1	874.2	877.4	880.8	884.5	888.2
5	855.0	855.1	855.4	855.9	856.6	857.5	858.6	859.9	861.4	863.1	865.0	867.1	869.4	871.8	874.5	877.4	880.4	883.6	887.0	890.6	894.4
6	862.8	862.9	863.2	863.7	864.4	865.3	866.3	867.6	869.1	870.8	872.7	874.8	877.0	879.5	882.1	885.0	888.0	891.2	894.5	898.1	901.8
7	871.9	872.0	872.3	872.8	873.5	874.3	875.4	876.7	878.2	879.8	881.7	883.8	886.0	888.4	891.0	893.8	896.8	900.0	903.3	906.9	910.6
8	882.3	882.4	882.7	883.2	883.8	884.7	885.8	887.0	888.5	890.2	892.0	894.0	896.2	898.6	901.2	904.0	906.9	910.1	913.4	916.9	920.5
9	893.9	894.0	894.3	894.8	895.5	896.3	897.4	898.6	900.1	901.7	903.5	905.5	907.7	910.1	912.6	915.4	918.3	921.4	924.6	928.1	931.7
10	906.7	906.8	907.1	907.6	908.3	909.1	910.2	911.4	912.8	914.4	916.2	918.2	920.3	922.7	925.2	927.9	930.8	933.9	937.	940.4	944.0
11	920.7	920.8	921.1	921.6	922.2	923.1	924.1	925.3	926.7	928.3	930.0	932.0	934.1	936.4	938.9	941.6	944.4	947.	950.6	953.9	957.
12	935.8	935.9	936.2	936.6	937.3	938.1	939.1	940.3	941.7	943.2	945.0	946.9	949.0	951.2	953.7	956.3	959.1	962.	965.2	968.5	972.
13	951.9	952.0	952.3	952.7	953.3	954.2	955.2	956.3	957.7	959.2	960.9	962.8	964.9	967.1	969.5	972.1	974.9	977.7	980.8	984.0	987.5
14	969.0	969.1	969.4	969.8	970.4	971.2	972.2	973.3	974.7	976.2	977.9	979.7	981.7	983.9	986.3	988.8	991.5	994.4	997.4	1000.6	1003.9
15	987.0	987.1	987.4	987.8	988.4	989.2	990.2	991.3	992.6	994.1	995.7	997.5	999.5	1001.7	1004.0	1006.5	1009.1	1012.0	1014.9	1018.1	1021.4
16	1005.9	1006.0	1006.3	1006.7	1007.3	1008.1	1009.0	1010.1	1011.4	1012.9	1014.5	1016.3	1018.2	1020.3	1022.6	1025.0	1027.6	1030.4	1033.3	1036.4	1039.7
17	1025.7	1025.8	1026.0	1026.5	1027.0	1027.8	1028.7	1029.8	1031.1	1032.5	1034.1	1035.8	1037.7	1039.8	1042.0	1044.4	1047.0	1049.7	1052.6	1055.6	1058.8
18	1046.2	1046.3	1046.6	1047.0	1047.6	1048.3	1049.2	1050.3	1051.5	1052.9	1054.5	1056.2	1058.0	1060.1	1062.3	1064.6	1067.1	1069.8	1072.6	1075.6	1078.7
19	1067.5	1067.6	1067.9	1068.3	1068.8	1069.4	1070.4	1071.5	1072.7	1074.1	1075.6	1077.3	1079.1	1081.1	1083.2	1085.6	1088.1	1090.8	1093.6	1096.7	1099.9
20	1089.5	1089.6	1089.8	1090.2	1090.8	1091.5	1092.4	1093.4	1094.6	1095.9	1097.4	1099.1	1100.9	1102.9	1105.1	1107.4	1109.9	1112.6	1115.4	1118.4	1121.7

ACOUSTIC MODAL FREQUENCIES

FACILITY DIMENSIONS LX= 10.0 FEET, LY= 16.0 FEET, LZ= 42.5 FEET

SPEED OF SOUND = 1116.0 FEET PER SECOND

MODAL INDEX NSUBX = 16

MODAL INDEX NSUBY	MODAL INDEX NSUBZ=0	1	2	3	4	5	6	7	8	9	10	11	12	13	14	15	16	17	18	19	20
0	892.8	892.9	893.2	893.7	894.3	895.2	896.3	897.5	899.0	900.6	902.4	904.4	906.6	909.0	911.5	914.3	917.2	920.3	923.5	927.0	930.6
1	893.5	893.6	893.9	894.3	895.0	895.9	896.9	898.2	899.6	901.3	903.1	905.1	907.3	909.6	912.2	914.9	917.8	920.9	924.2	927.7	931.3
2	895.5	895.6	895.9	896.4	897.1	897.9	899.0	900.2	901.7	903.3	905.1	907.1	909.3	911.6	914.2	916.9	919.8	922.9	926.2	929.6	933.2
3	898.9	899.0	899.3	899.8	900.4	901.3	902.4	903.6	905.0	906.6	908.4	910.4	912.6	915.0	917.5	920.2	923.1	926.2	929.5	932.9	936.5
4	903.6	903.7	904.0	904.5	905.2	906.0	907.1	908.3	909.7	911.3	913.1	915.1	917.3	919.6	922.1	924.8	927.7	930.8	934.0	937.4	941.0
5	909.7	909.8	910.0	910.5	911.2	912.0	913.1	914.3	915.7	917.3	919.1	921.1	923.2	925.5	928.1	930.7	933.6	936.7	939.9	943.3	946.8
6	917.0	917.1	917.4	917.8	918.5	919.3	920.4	921.6	923.0	924.6	926.3	928.3	930.4	932.7	935.2	937.9	940.7	943.8	947.0	950.3	953.9
7	925.6	925.7	925.9	926.4	927.1	927.9	928.9	930.1	931.5	933.1	934.8	936.8	938.9	941.2	943.7	946.3	949.1	952.1	955.3	958.6	962.1
8	935.4	935.5	935.7	936.2	936.9	937.7	938.7	939.9	941.3	942.8	944.5	946.5	948.6	950.8	953.3	955.9	958.7	961.6	964.8	968.1	971.5
9	946.4	946.5	946.7	947.2	947.8	948.6	949.6	950.8	952.2	953.7	955.4	957.3	959.4	961.6	964.1	966.6	969.4	972.3	975.4	978.7	982.1
10	958.5	958.6	958.9	959.3	959.9	960.7	961.7	962.9	964.2	965.8	967.4	969.3	971.4	973.6	976.0	978.5	981.2	984.1	987.2	990.4	993.8
11	971.7	971.8	972.1	972.5	973.1	973.9	974.9	976.1	977.4	978.9	980.6	982.4	984.4	986.6	989.0	991.5	994.2	997.0	1000.0	1003.2	1006.6
12	986.0	986.1	986.4	986.8	987.4	988.2	989.2	990.3	991.6	993.1	994.7	996.5	998.5	1000.7	1003.1	1005.5	1008.1	1011.0	1014.1	1017.4	1020.9
13	1001.3	1001.4	1001.7	1002.1	1002.7	1003.5	1004.4	1005.5	1006.8	1008.3	1009.9	1011.7	1013.6	1015.8	1018.2	1020.5	1023.1	1025.9	1028.8	1031.9	1035.2
14	1017.6	1017.7	1017.9	1018.3	1018.9	1019.7	1020.6	1021.7	1023.0	1024.4	1026.0	1027.8	1029.7	1031.8	1034.2	1036.5	1039.0	1041.8	1044.7	1047.7	1050.9
15	1034.8	1034.9	1035.1	1035.5	1036.1	1036.9	1037.8	1038.8	1040.1	1041.5	1043.1	1044.8	1046.7	1048.8	1051.0	1053.3	1055.9	1058.6	1061.4	1064.4	1067.6
16	1052.8	1052.9	1053.2	1053.6	1054.1	1054.9	1055.8	1056.8	1058.1	1059.4	1061.0	1062.7	1064.6	1066.6	1068.8	1071.1	1073.6	1076.4	1079.3	1082.3	1085.5
17	1071.7	1071.8	1072.0	1072.4	1073.0	1073.7	1074.6	1075.7	1076.9	1078.2	1079.7	1081.4	1083.2	1085.2	1087.4	1089.7	1092.1	1094.7	1097.5	1100.4	1103.4
18	1091.4	1091.5	1091.7	1092.1	1092.7	1093.4	1094.2	1095.3	1096.4	1097.8	1099.3	1101.0	1102.7	1104.7	1106.8	1109.0	1111.4	1114.0	1116.7	1119.5	1122.5
19	1111.8	1111.9	1112.1	1112.5	1113.1	1113.8	1114.6	1115.6	1116.8	1118.1	1119.6	1121.2	1122.9	1124.9	1126.9	1129.1	1131.5	1134.0	1136.7	1139.5	1142.4
20	1133.0	1133.0	1133.3	1133.6	1134.2	1134.9	1135.7	1136.7	1137.8	1139.1	1140.5	1142.1	1143.9	1145.7	1147.6	1149.9	1152.3	1154.9	1157.7	1160.6	1163.7

ACOUSTIC MODAL FREQUENCIES

FACILITY DIMENSIONS LX= 10.0 FEET, LY= 16.0 FEET, LZ= 42.5 FEET

SPEED OF SOUND = 1116.0 FEET PER SECOND

MODAL INDEX NSUBX = 17

MODAL INDEX NSUBY	MODAL INDEX NSUBZ=0	1	2	3	4	5	6	7	8	9	10	11	12	13	14	15	16	17	18	19	20
0	948.6	948.7	949.0	949.4	950.1	950.9	951.9	953.0	954.4	955.9	957.6	959.5	961.6	963.8	966.2	968.8	971.6	974.5	977.6	980.9	984.3
1	949.2	949.3	949.6	950.1	950.7	951.5	952.5	953.7	955.0	956.6	958.3	960.2	962.2	964.5	966.9	969.5	972.2	975.1	978.2	981.5	984.9
2	951.2	951.3	951.5	952.0	952.6	953.4	954.4	955.6	956.9	958.5	960.2	962.1	964.1	966.4	968.8	971.3	974.1	977.0	980.1	983.3	986.7
3	954.4	954.4	954.7	955.2	955.8	956.6	957.6	958.8	960.1	961.6	963.3	965.2	967.3	969.5	971.9	974.5	977.2	980.1	983.2	986.4	989.8
4	958.8	958.9	959.2	959.6	960.2	961.0	962.0	963.2	964.5	966.1	967.8	969.6	971.7	973.9	976.3	978.8	981.5	984.4	987.5	990.7	994.1
5	964.5	964.6	964.9	965.3	965.9	966.7	967.7	968.9	970.2	971.7	973.4	975.2	977.3	979.5	981.9	984.4	987.1	990.0	993.0	996.2	999.6
6	971.4	971.5	971.8	972.2	972.8	973.6	974.6	975.7	977.1	978.6	980.2	982.1	984.1	986.3	988.6	991.2	993.9	996.7	999.7	1002.9	1006.3
7	979.5	979.6	979.9	980.3	980.9	981.7	982.7	983.8	985.1	986.6	988.3	990.1	992.1	994.3	996.6	999.1	1001.8	1004.6	1007.6	1010.8	1014.1
8	988.8	988.9	989.1	989.6	990.2	991.0	991.9	993.0	994.3	995.8	997.5	999.3	1001.3	1003.4	1005.7	1008.2	1010.8	1013.7	1016.6	1019.8	1023.1
9	999.2	999.3	999.5	1000.0	1000.6	1001.3	1002.3	1003.4	1004.7	1006.1	1007.8	1009.6	1011.5	1013.7	1015.9	1018.4	1021.0	1023.8	1026.7	1029.8	1033.1
10	1010.7	1010.8	1011.0	1011.4	1012.0	1012.8	1013.7	1014.8	1016.1	1017.6	1019.2	1020.9	1022.9	1025.0	1027.3	1029.7	1032.3	1035.0	1037.9	1041.0	1044.2
11	1023.2	1023.3	1023.6	1024.0	1024.6	1025.3	1026.3	1027.4	1028.6	1030.0	1031.6	1033.4	1035.3	1037.4	1039.6	1042.0	1044.6	1047.3	1050.2	1053.2	1056.4
12	1036.8	1036.9	1037.1	1037.6	1038.1	1038.9	1039.8	1040.9	1042.1	1043.5	1045.1	1046.8	1048.7	1050.8	1053.0	1055.4	1057.9	1060.6	1063.4	1066.4	1069.5
13	1051.4	1051.5	1051.7	1052.1	1052.7	1053.4	1054.3	1055.4	1056.6	1058.0	1059.5	1061.2	1063.1	1065.1	1067.3	1069.7	1072.2	1074.8	1077.6	1080.6	1083.7
14	1066.9	1067.0	1067.2	1067.6	1068.2	1068.9	1069.8	1070.8	1072.0	1073.4	1074.9	1076.6	1078.4	1080.4	1082.6	1084.9	1087.4	1090.0	1092.7	1095.7	1098.7
15	1083.3	1083.4	1083.6	1084.0	1084.6	1085.3	1086.1	1087.2	1088.4	1089.7	1091.2	1092.9	1094.7	1096.6	1098.8	1101.0	1103.5	1106.0	1108.8	1111.6	1114.7
16	1100.5	1100.6	1100.9	1101.3	1101.8	1102.5	1103.4	1104.4	1105.5	1106.9	1108.4	1110.0	1111.8	1113.7	1115.8	1118.0	1120.4	1123.0	1125.6	1128.5	1131.4
17	1118.6	1118.7	1118.9	1119.3	1119.9	1120.6	1121.4	1122.4	1123.6	1124.9	1126.3	1127.9	1129.7	1131.6	1133.6	1135.8	1138.2	1140.7	1143.3	1146.1	1149.0
18	1137.5	1137.6	1137.8	1138.2	1138.7	1139.4	1140.2	1141.2	1142.3	1143.6	1145.1	1146.8	1148.4	1150.2	1152.3	1154.4	1156.7	1159.2	1161.8	1164.5	1167.4
19	1157.1	1157.2	1157.4	1157.8	1158.3	1159.0	1159.8	1160.8	1161.9	1163.1	1164.5	1166.1	1167.8	1169.6	1171.6	1173.8	1176.0	1178.4	1181.0	1183.7	1186.5
20	1177.4	1177.5	1177.7	1178.1	1178.6	1179.3	1180.1	1181.0	1182.1	1183.3	1184.7	1186.3	1187.9	1189.7	1191.7	1193.8	1196.0	1198.4	1200.9	1203.6	1206.4

ACOUSTIC MODAL FREQUENCIES

FACILITY DIMENSIONS LX= 10.0 FEET, LY= 16.0 FEET, LZ= 42.5 FEET

SPEED OF SOUND = 1116.0 FEET PER SECOND

MODAL INDEX NSUBX = 18

MODAL INDEX NSUBY	MODAL INDEX NSUBZ=0	1	2	3	4	5	6	7	8	9	10	11	12	13	14	15	16	17	18	19	20
0	1004.4	1004.5	1004.7	1005.2	1005.8	1006.5	1007.5	1008.6	1009.9	1011.3	1012.9	1014.7	1016.7	1018.8	1021.1	1023.5	1026.1	1028.9	1031.8	1034.9	1038.2
1	1005.0	1005.1	1005.3	1005.8	1006.4	1007.1	1008.1	1009.2	1010.5	1011.9	1013.5	1015.3	1017.3	1019.4	1021.7	1024.1	1026.7	1029.5	1032.4	1035.5	1038.7
2	1006.8	1006.9	1007.2	1007.6	1008.2	1009.0	1009.9	1011.0	1012.3	1013.7	1015.3	1017.1	1019.1	1021.2	1023.5	1025.9	1028.5	1031.3	1034.2	1037.3	1040.5
3	1009.8	1009.9	1010.2	1010.6	1011.2	1012.0	1012.9	1014.0	1015.3	1016.7	1018.3	1020.1	1022.1	1024.2	1026.4	1028.9	1031.5	1034.2	1037.1	1040.2	1043.4
4	1014.0	1014.1	1014.4	1014.8	1015.4	1016.2	1017.1	1018.2	1019.5	1020.9	1022.5	1024.3	1026.2	1028.3	1030.6	1033.0	1035.6	1038.3	1041.2	1044.3	1047.5
5	1019.4	1019.5	1019.8	1020.2	1020.8	1021.5	1022.5	1023.6	1024.8	1026.2	1027.8	1029.6	1031.5	1033.6	1035.9	1038.3	1040.8	1043.6	1046.5	1049.5	1052.7
6	1026.0	1026.0	1026.3	1026.7	1027.3	1028.1	1029.0	1030.1	1031.3	1032.7	1034.3	1036.1	1038.0	1040.1	1042.3	1044.7	1047.3	1050.0	1052.8	1055.9	1059.0
7	1033.6	1033.7	1034.0	1034.4	1035.0	1035.7	1036.6	1037.7	1039.0	1040.4	1041.9	1043.7	1045.6	1047.6	1049.9	1052.2	1054.8	1057.5	1060.3	1063.3	1066.5
8	1042.4	1042.5	1042.8	1043.2	1043.8	1044.5	1045.4	1046.5	1047.7	1049.1	1050.7	1052.4	1054.3	1056.3	1058.5	1060.9	1063.4	1066.1	1068.9	1071.9	1075.0
9	1052.3	1052.4	1052.6	1053.0	1053.6	1054.3	1055.2	1056.3	1057.5	1058.9	1060.5	1062.2	1064.0	1066.1	1068.2	1070.6	1073.1	1075.7	1078.5	1081.5	1084.6
10	1063.2	1063.3	1063.5	1064.0	1064.5	1065.2	1066.1	1067.2	1068.4	1069.8	1071.3	1073.0	1074.8	1076.8	1078.9	1081.3	1083.8	1086.4	1089.2	1092.1	1095.2
11	1075.2	1075.2	1075.5	1075.9	1076.5	1077.2	1078.1	1079.1	1080.3	1081.6	1083.2	1084.8	1086.7	1088.6	1090.8	1093.1	1095.5	1098.1	1100.8	1103.7	1106.8
12	1088.1	1088.2	1088.4	1088.8	1089.4	1090.1	1090.9	1092.0	1093.2	1094.5	1096.0	1097.6	1099.4	1101.4	1103.5	1105.8	1108.2	1110.7	1113.5	1116.3	1119.3
13	1102.0	1102.1	1102.3	1102.7	1103.2	1103.9	1104.8	1105.8	1107.0	1108.3	1109.8	1111.4	1113.2	1115.1	1117.2	1119.4	1121.8	1124.4	1127.1	1129.9	1132.8
14	1116.8	1116.9	1117.1	1117.5	1118.0	1118.7	1119.6	1120.6	1121.7	1123.0	1124.5	1126.1	1127.8	1129.8	1131.8	1134.0	1136.4	1138.9	1141.5	1144.3	1147.2
15	1132.5	1132.5	1132.8	1133.2	1133.7	1134.4	1135.2	1136.2	1137.3	1138.6	1140.1	1141.6	1143.4	1145.3	1147.3	1149.5	1151.8	1154.3	1156.9	1159.6	1162.5
16	1149.0	1149.1	1149.3	1149.7	1150.2	1150.9	1151.7	1152.7	1153.8	1155.1	1156.5	1158.0	1159.7	1161.6	1163.6	1165.7	1168.0	1170.5	1173.0	1175.8	1178.6
17	1166.3	1166.4	1166.6	1167.0	1167.5	1168.2	1169.0	1169.9	1171.0	1172.3	1173.7	1175.2	1176.9	1178.8	1180.8	1182.8	1185.1	1187.5	1190.0	1192.7	1195.5
18	1184.4	1184.5	1184.7	1185.1	1185.6	1186.3	1187.1	1188.0	1189.1	1190.3	1191.7	1193.2	1194.9	1196.7	1198.6	1200.7	1202.9	1205.3	1207.8	1210.4	1213.2
19	1203.3	1203.4	1203.6	1203.9	1204.4	1205.1	1205.9	1206.8	1207.9	1209.1	1210.4	1211.9	1213.6	1215.3	1217.2	1219.3	1221.5	1223.8	1226.3	1228.9	1231.6
20	1222.8	1222.9	1223.1	1223.5	1224.0	1224.6	1225.4	1226.3	1227.3	1228.5	1229.9	1231.3	1232.9	1234.7	1236.6	1238.6	1240.7	1242.9	1245.2	1247.6	1250.1

ACOUSTIC MODAL FREQUENCIES

FACILITY DIMENSIONS LX= 10.0 FEET, LY= 16.0 FEET, LZ= 42.5 FEET

SPEED OF SOUND = 1116.0 FEET PER SECOND

MODAL INDEX NSUBX = 19

MODAL INDEX NSUBY	MODAL INDEX NSUBZ=0	1	2	3	4	5	6	7	8	9	10	11	12	13	14	15	16	17	18	19	20
0	1060.2	1060.3	1060.5	1060.9	1061.5	1062.2	1063.1	1064.2	1065.4	1066.8	1068.3	1070.0	1071.8	1073.9	1076.0	1078.3	1080.8	1083.4	1086.2	1089.2	1092.2
1	1060.8	1060.9	1061.1	1061.5	1062.1	1062.8	1063.7	1064.7	1066.0	1067.3	1068.9	1070.6	1072.4	1074.4	1076.6	1078.9	1081.4	1084.0	1086.8	1089.7	1092.8
2	1062.5	1062.6	1062.8	1063.2	1063.8	1064.5	1065.4	1066.5	1067.7	1069.0	1070.6	1072.3	1074.1	1076.1	1078.3	1080.6	1083.1	1085.7	1088.5	1091.4	1094.5
3	1065.3	1065.4	1065.7	1066.1	1066.6	1067.4	1068.3	1069.3	1070.5	1071.9	1073.4	1075.1	1076.9	1078.9	1081.1	1083.4	1085.9	1088.5	1091.2	1094.2	1097.2
4	1069.3	1069.4	1069.7	1070.1	1070.6	1071.4	1072.2	1073.3	1074.5	1075.8	1077.4	1079.0	1080.9	1082.9	1085.0	1087.3	1089.8	1092.4	1095.1	1098.1	1101.1
5	1074.4	1074.5	1074.8	1075.2	1075.7	1076.4	1077.3	1078.4	1079.6	1080.9	1082.4	1084.1	1085.9	1087.9	1090.0	1092.3	1094.8	1097.4	1100.1	1103.0	1106.1
6	1080.7	1080.7	1081.0	1081.4	1081.9	1082.6	1083.5	1084.6	1085.7	1087.1	1088.6	1090.3	1092.1	1094.0	1096.2	1098.5	1100.9	1103.5	1106.2	1109.1	1112.1
7	1087.9	1088.0	1088.3	1088.7	1089.2	1089.9	1090.8	1091.8	1093.0	1094.3	1095.8	1097.5	1099.3	1101.3	1103.4	1105.6	1108.0	1110.6	1113.3	1116.2	1119.2
8	1096.3	1096.4	1096.6	1097.0	1097.6	1098.3	1099.1	1100.1	1101.3	1102.6	1104.1	1105.8	1107.6	1109.5	1111.6	1113.8	1116.2	1118.8	1121.5	1124.3	1127.3
9	1105.7	1105.8	1106.0	1106.4	1106.9	1107.6	1108.5	1109.5	1110.7	1112.0	1113.5	1115.1	1116.9	1118.8	1120.9	1123.1	1125.5	1128.0	1130.7	1133.5	1136.4
10	1116.1	1116.2	1116.4	1116.8	1117.3	1118.0	1118.9	1119.9	1121.0	1122.3	1123.8	1125.4	1127.2	1129.1	1131.1	1133.3	1135.7	1138.2	1140.8	1143.6	1146.6
11	1127.5	1127.5	1127.8	1128.2	1128.7	1129.4	1130.2	1131.2	1132.4	1133.6	1135.1	1136.7	1138.4	1140.3	1142.4	1144.5	1146.9	1149.4	1152.1	1154.9	1157.
12	1139.8	1139.9	1140.1	1140.5	1141.0	1141.7	1142.5	1143.5	1144.6	1145.9	1147.3	1148.9	1150.6	1152.5	1154.5	1156.7	1159.0	1161.5	1164.1	1166.8	1169.
13	1153.1	1153.1	1153.4	1153.7	1154.3	1154.9	1155.8	1156.7	1157.	159.1	1160.5	1162.1	1163.8	1165.6	1167.6	1169.8	1172.1	1174.5	1177.0	1179.7	1182.
14	1167.2	1167.3	1167.5	1167.9	1168.4	1169.1	1169.9	1170.8	1171.9	1173.2	1174.6	1176.	1177.8	1179.6	1181.6	1183.7	1186.0	1188.4	1190.9	1193.6	1196.4
15	1182.2	1182.3	1182.5	1182.9	1183.4	1184.1	1184.9	1185.8	1186.9	1188.1	1189.5	1191.0	1192.7	1194.5	1196.4	1198.5	1200.8	1203.1	1205.6	1208.3	1211.
16	1198.1	1198.1	1198.4	1198.7	1199.2	1199.9	1200.7	1201.6	1202.7	1203.9	1205.2	1206.8	1208.4	1210.	1212.1	1214.2	1216.4	1218.7	1221.2	1223.8	1226.5
17	1214.7	1214.8	1215.0	1215.4	1215.8	1216.5	1217.3	1218.2	1219.2	1220.4	1221.8	1223.3	1224.9	1226.8	1228.5	1230.6	1232.7	1235.0	1237.5	1240.1	1242.8
18	1232.1	1232.2	1232.4	1232.7	1233.2	1233.9	1234.6	1235.5	1236.6	1237.8	1239.1	1240.6	1242.1	1243.9	1245.7	1247.7	1249.9	1252.2	1254.6	1257.1	1259.8
19	1250.2	1250.3	1250.5	1250.9	1251.3	1252.0	1252.7	1253.6	1254.6	1255.8	1257.1	1258.6	1260.1	1261.8	1263.7	1265.7	1267.8	1270.0	1272.4	1274.9	1277.5
20	1269.1	1269.1	1269.3	1269.7	1270.2	1270.8	1271.5	1272.4	1273.4	1274.6	1275.8	1277.3	1278.8	1280.5	1282.3	1284.3	1286.3	1288.5	1290.9	1293.4	1295.9

ACOUSTIC MODAL FREQUENCIES

FACILITY DIMENSIONS LX= 10.0 FEET, LY= 16.0 FEET, LZ= 42.5 FEET

SPEED OF SOUND = 1116.0 FEET PER SECOND

MODAL INDEX NSUBX = 20

MODAL=MODAL
INDEX=INDEX
NSUBY=NSUBZ=0

	0	1	2	3	4	5	6	7	8	9	10	11	12	13	14	15	16	17	18	19	20
0	1116.0	1116.1	1116.3	1116.7	1117.2	1117.9	1118.8	1119.8	1120.9	1122.2	1123.7	1125.3	1127.1	1129.0	1131.0	1133.2	1135.6	1138.1	1140.7	1143.5	1146.5
1	1116.5	1116.6	1116.9	1117.2	1117.8	1118.5	1119.3	1120.3	1121.5	1122.8	1124.2	1125.8	1127.6	1129.5	1131.6	1133.8	1136.1	1138.6	1141.3	1144.1	1147.0
2	1118.2	1118.3	1118.5	1118.9	1119.4	1120.1	1120.9	1121.9	1123.1	1124.4	1125.9	1127.5	1129.2	1131.1	1133.2	1135.4	1137.7	1140.2	1142.9	1145.7	1148.6
3	1120.9	1121.0	1121.2	1121.6	1122.1	1122.8	1123.7	1124.7	1125.8	1127.1	1128.6	1130.2	1131.9	1133.8	1135.9	1138.1	1140.4	1142.9	1145.5	1148.3	1151.2
4	1124.7	1124.8	1125.0	1125.4	1125.9	1126.6	1127.4	1128.4	1129.6	1130.9	1132.3	1133.9	1135.7	1137.6	1139.6	1141.8	1144.1	1146.6	1149.2	1152.0	1154.9
5	1129.5	1129.6	1129.8	1130.2	1130.8	1131.4	1132.3	1133.3	1134.4	1135.7	1137.1	1138.7	1140.5	1142.4	1144.4	1146.6	1148.9	1151.4	1154.0	1156.8	1159.7
6	1135.4	1135.5	1135.8	1136.1	1136.7	1137.3	1138.2	1139.2	1140.3	1141.6	1143.0	1144.6	1146.3	1148.2	1150.2	1152.4	1154.7	1157.2	1159.8	1162.5	1165.4
7	1142.4	1142.5	1142.7	1143.1	1143.6	1144.3	1145.1	1146.1	1147.2	1148.5	1149.9	1151.5	1153.2	1155.1	1157.1	1159.2	1161.5	1164.0	1166.6	1169.3	1172.2
8	1150.3	1150.4	1150.6	1151.0	1151.5	1152.2	1153.0	1154.0	1155.1	1156.4	1157.8	1159.4	1161.1	1162.9	1164.9	1167.1	1169.4	1171.8	1174.4	1177.1	1179.9
9	1159.3	1159.4	1159.6	1160.0	1160.5	1161.2	1162.0	1162.9	1164.0	1165.3	1166.7	1168.3	1170.0	1171.8	1173.8	1175.9	1178.2	1180.6	1183.1	1185.8	1188.7
10	1169.2	1169.3	1169.5	1169.9	1170.4	1171.1	1171.9	1172.8	1173.9	1175.2	1176.6	1178.1	1179.8	1181.6	1183.6	1185.7	1187.9	1190.3	1192.9	1195.5	1198.3
11	1180.1	1180.2	1180.4	1180.8	1181.3	1181.9	1182.7	1183.7	1184.8	1186.0	1187.4	1188.9	1190.6	1192.4	1194.3	1196.4	1198.6	1201.0	1203.5	1206.2	1209.0
12	1191.9	1192.0	1192.2	1192.5	1193.0	1193.7	1194.5	1195.4	1196.5	1197.7	1199.1	1200.6	1202.3	1204.0	1206.0	1208.0	1210.3	1212.7	1215.3	1217.7	1220.5
13	1204.6	1204.6	1204.9	1205.2	1205.7	1206.4	1207.1	1208.1	1209.1	1210.4	1211.7	1213.2	1214.8	1216.6	1218.5	1220.6	1222.8	1225.1	1227.5	1230.1	1232.9
14	1218.1	1218.2	1218.4	1218.8	1219.3	1219.9	1220.7	1221.6	1222.7	1223.8	1225.2	1226.7	1228.3	1230.0	1231.9	1233.9	1236.1	1238.4	1240.8	1243.4	1246.1
15	1232.5	1232.6	1232.8	1233.2	1233.6	1234.3	1235.0	1235.9	1237.0	1238.2	1239.5	1241.0	1242.6	1244.3	1246.2	1248.2	1250.3	1252.6	1255.0	1257.5	1260.2
16	1247.7	1247.8	1248.0	1248.3	1248.8	1249.5	1250.2	1251.1	1252.1	1253.3	1254.6	1256.1	1257.6	1259.3	1261.2	1263.2	1265.3	1267.5	1269.9	1272.4	1275.1
17	1263.7	1263.8	1264.0	1264.3	1264.8	1265.4	1266.2	1267.0	1268.1	1269.2	1270.5	1271.9	1273.5	1275.2	1277.0	1279.0	1281.0	1283.3	1285.6	1288.1	1290.7
18	1280.4	1280.5	1280.7	1281.0	1281.5	1282.1	1282.9	1283.7	1284.7	1285.9	1287.2	1288.6	1290.1	1291.8	1293.6	1295.5	1297.6	1299.7	1302.1	1304.5	1307.1
19	1297.9	1298.0	1298.2	1298.5	1299.0	1299.6	1300.3	1301.1	1302.1	1303.3	1304.5	1305.9	1307.4	1309.1	1310.8	1312.8	1314.8	1316.9	1319.2	1321.6	1324.2
20	1316.0	1316.1	1316.3	1316.6	1317.1	1317.7	1318.4	1319.2	1320.2	1321.3	1322.6	1323.9	1325.4	1327.1	1328.8	1330.7	1332.7	1334.8	1337.1	1339.5	1342.0

The number of modes may be counted in frequency space utilizing a statistical approach.

$$N \simeq 4\pi Vf^3/3c^3 + \pi Af^2/4c^2 + Lf/8c \qquad (104)$$

where N is the total number of standing wave modes of all types up to frequency f. The modal density is simply

$$dN/df = 4\pi Vf^2/c^3 + \pi Af/2c^2 + L/8c \qquad (105)$$

For Test Cell 2-20 utilizing the above dimensions and sonic velocity of 1116.0 ft/sec., equations (104) and (105) become:

$$N = 2.037 \times 10^{-5}f^3 + 1.74 \times 10^{-3}f^2 + 3.07 \times 10^{-2}f \qquad (106)$$

and

$$dN/df = 6.11 \times 10^{-5}f^2 + 3.48 \times 10^{-3}f^2 + 3.07 \times 10^{-2} \qquad (107)$$

Equation (107) is graphically displayed in figure 58 showing the modal density for the reverberant facility as well as the components due to edge length, surface area, and volume. The frequency at which the statistical modal density equals 1 can be determined from equation (107).

$$f = 99.6 \text{ Hz} \quad \text{if} \quad dN/df = 1$$

Figure 59 shows the calculated modal density for frequencies up to 200 Hz, as calculated from equation (103). The amplitude is shown with a non-zero bandwidth since each mode has an associated magnification factor and response bandwidth.

The classical approach provides a deterministic, exact result whereas the statistical technique is only approximate. For frequencies whose modal density is greater than one, the statistical method may be used with confidence. For example, the total number of modal occurrences on figure 59 is 237 as compared with 238.7 from equation (106).

A figure of merit or quality for a reverberation room is the frequency above which the modal response of the room becomes continuous and every source frequency component will be amplified. If the wall absorption coefficient is 0.02 then the magnification factor is 50 and the modal response bandwidth is 0.02 times the modal frequency. (In actuality $\alpha_{axial} \simeq 0.02$, $\alpha_{oblique} \simeq 0.04$ and $\alpha_{tangential} \simeq 0.03$ for lower frequencies.) A uniform coefficient of 0.02 which would yield minimum modal overlap is utilized for mathematical expediency. The number of modes per room response bandwidth βf can thus be calculated from:

$$N_r = 4\pi\beta Vf^3/c^3 + \pi\beta Af^2/2c^2 + \beta Lf/8c \qquad (108)$$

and for Test Cell 2-20,

$$N_r = 1.223 \times 10^{-6}f^3 + 6.956 \times 10^{-5}f^2 + 6.14 \times 10^{-4}f \qquad (109)$$

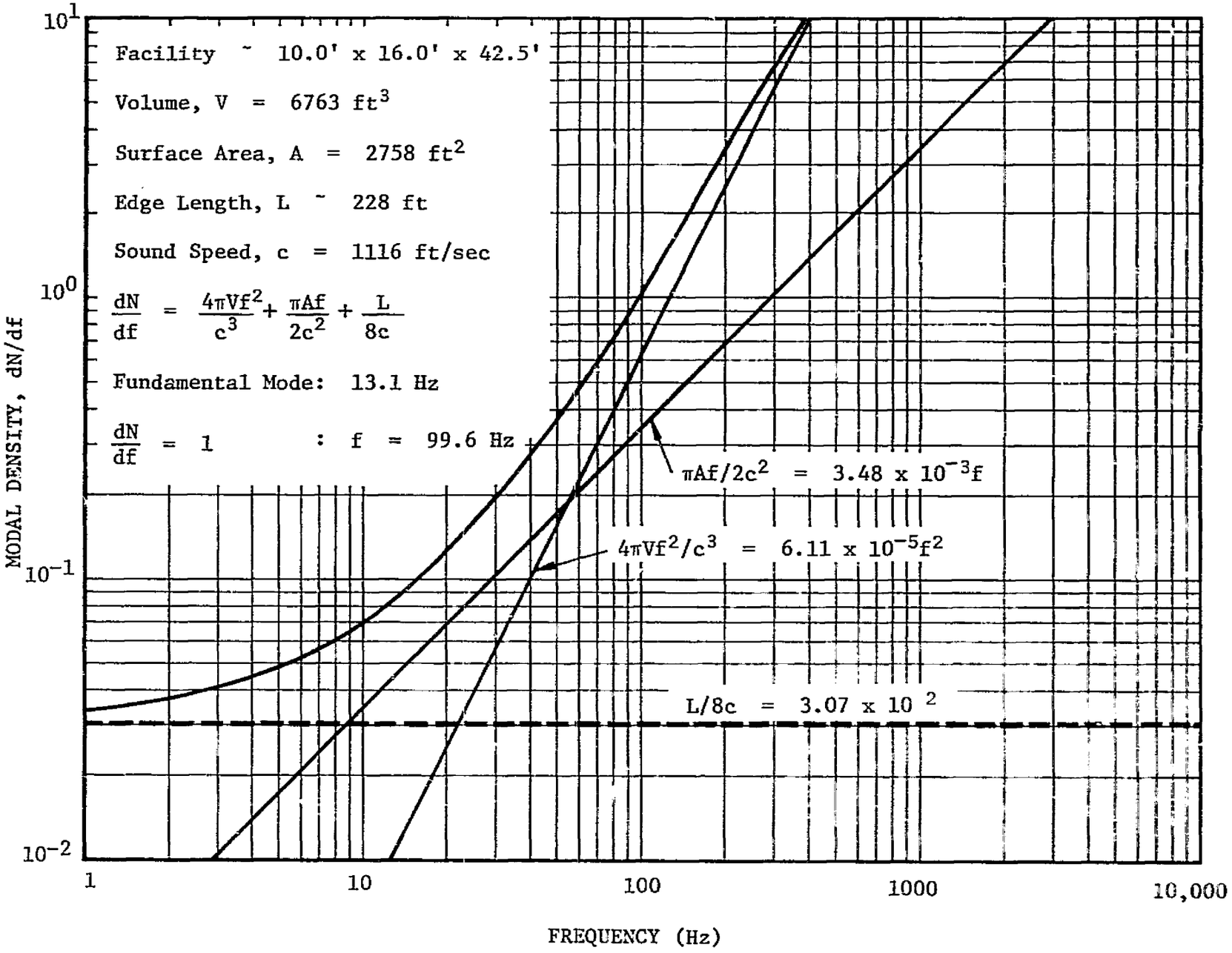

FIGURE 58. STATISTICAL MODAL DENSITY FOR ACOUSTIC REVERBERANT FACILITY (TEST CELL 2-20)

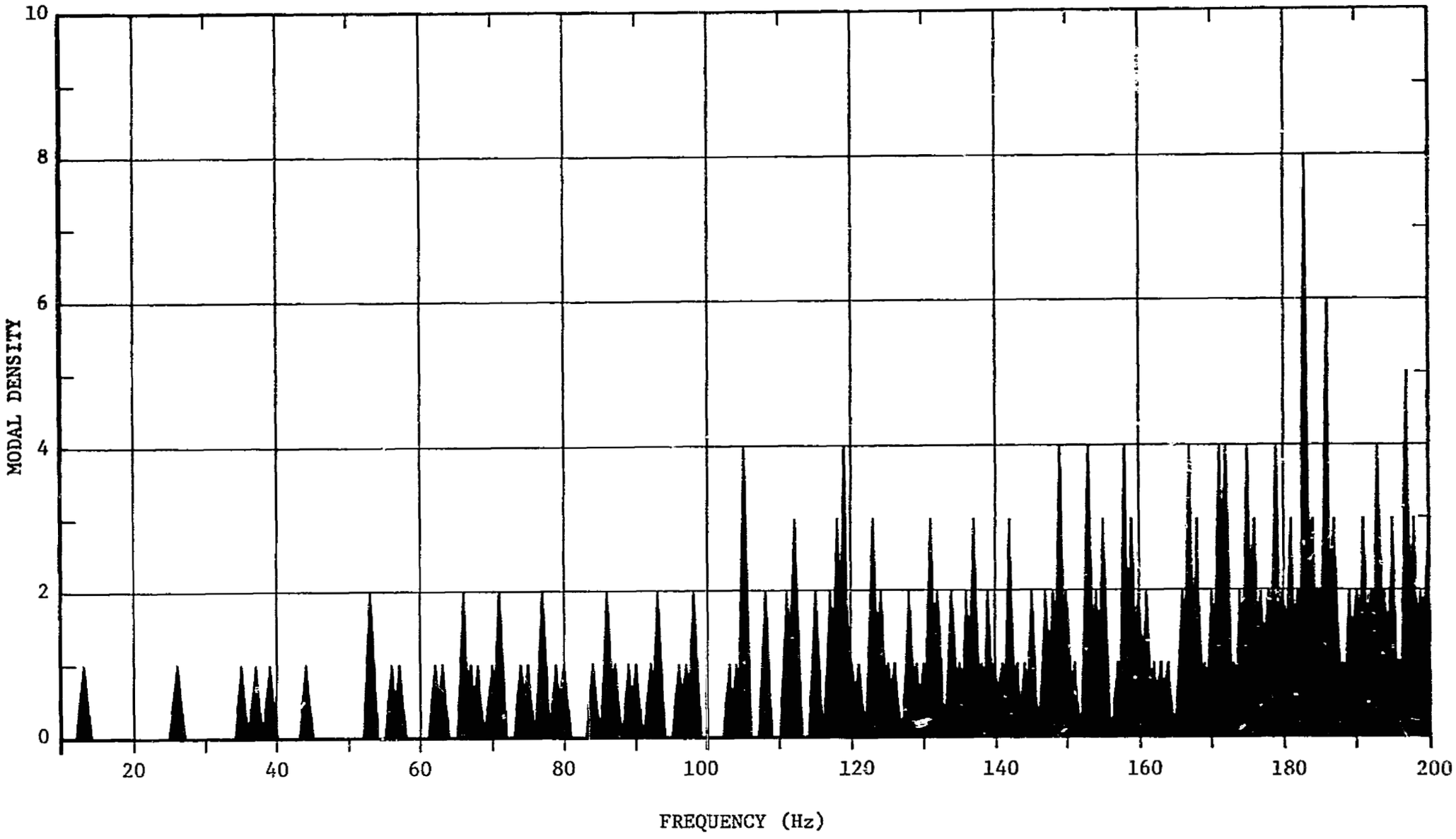

FIGURE 59. CLASSICAL MODAL DENSITY FOR ACOUSTIC REVERBERANT FACILITY (TEST CELL 2-20)

This function, with the volume, area, and length components is shown graphically in figure 60. Figure 60 shows the chamber efficiency to be good for frequencies above 76 Hz. Referring to figure 59, the modal response is observed to be relatively dense above 65 Hz except in the immediate vicinity of 86 and 100 Hz.

The absorption coefficient is shown in figure 61. Absorption is shown, sub-divided into three categories, wall absorption which is proportional to the square root of frequency, molecular energy absorption which is strongly dependent upon relative humidity effects on molecular relaxation processes, and classical energy absorption due to heat conduction and radiation, viscosity and diffusion processes. Wall absorption occurs only at chamber boundaries, but molecular and classical absorption occur during normal propagation of sound in air.

An estimated lower limit of 0.02 is provided in figure 61. Wall absorption is estimated from previous measured data, reference 42 is utilized as a basis for prediction of molecular absorption, and reference 43 is developed to provide classical absorption values. Molecular and classical absorption are dependent upon the chamber volume, but are shown as psuedo-areal coefficients in figure 61.

Figure 62 is obtained directly from figure 61 by multiplying the total surface area times the total effective surface absorption coefficient. The EPT-94B source and horn increases the total absorption above that for an empty chamber. The increase is estimated to be 6 Sabins (6 square feet of totally absorbing area).

Figure 63 presents the reverberation time of Test Cell 2-20 determined from the following equation:

$$T_{60} = 0.049\ V / \sum A_s \alpha_s \qquad (110)$$

Equation (110) utilizes an approximation $\overline{\alpha} \approx -2.30 \log_{10} (1 - \overline{\alpha})$, however this approximation yields an over estimation of the reverberation time by less than 16% at 10,000 Hz, 6% at 2000 Hz and 5% at 500 Hz, the relative error approaching zero as the absorption coefficient approaches zero. Figure 63 is very important in the empirical evaluation of the reverberant facility since the reverberation time is measured relatively easily. (The reverberation time is the time in seconds for the chamber response to decay by 60 dB when the input signal is instantaneously terminated.)

Figure 64 presents the maximum sound pressure levels near the center of the reverberant facility utilizing the Ling EPT-94B acoustic source. The sound pressure levels are calculated from the conventional formula,

$$SPL = PWL + 10 \log (4) - 10 \log \left(\sum A_i \alpha_i + 4mV\right) \qquad (111)$$

where $\sum A_i \alpha_i + 4$ mV is the total absorption as presented in figure 62.

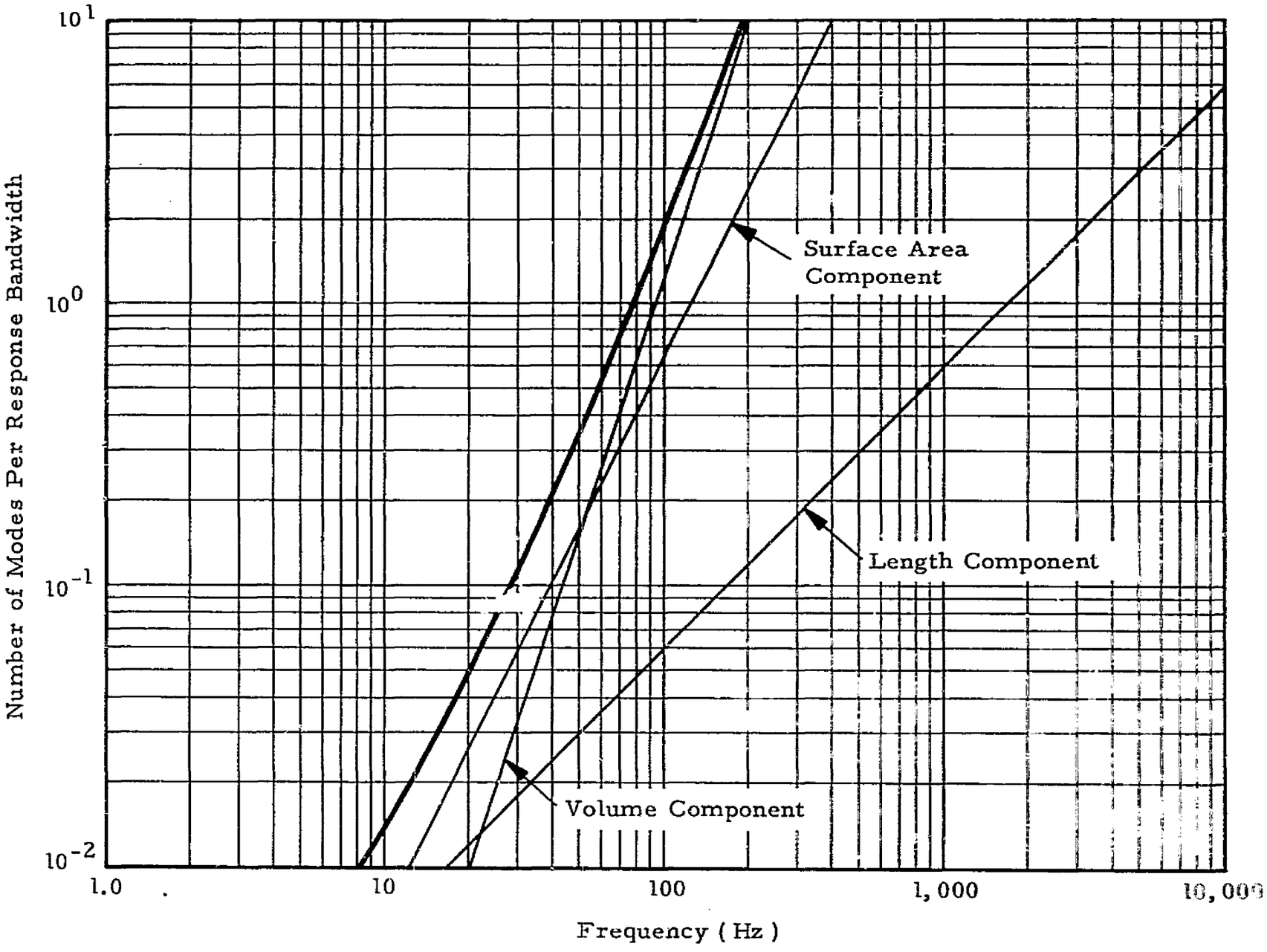

FIGURE 60. STATISTICAL RESPONSE FOR ACOUSTIC REVERBERANT FACILITY (TEST CELL 2-20)

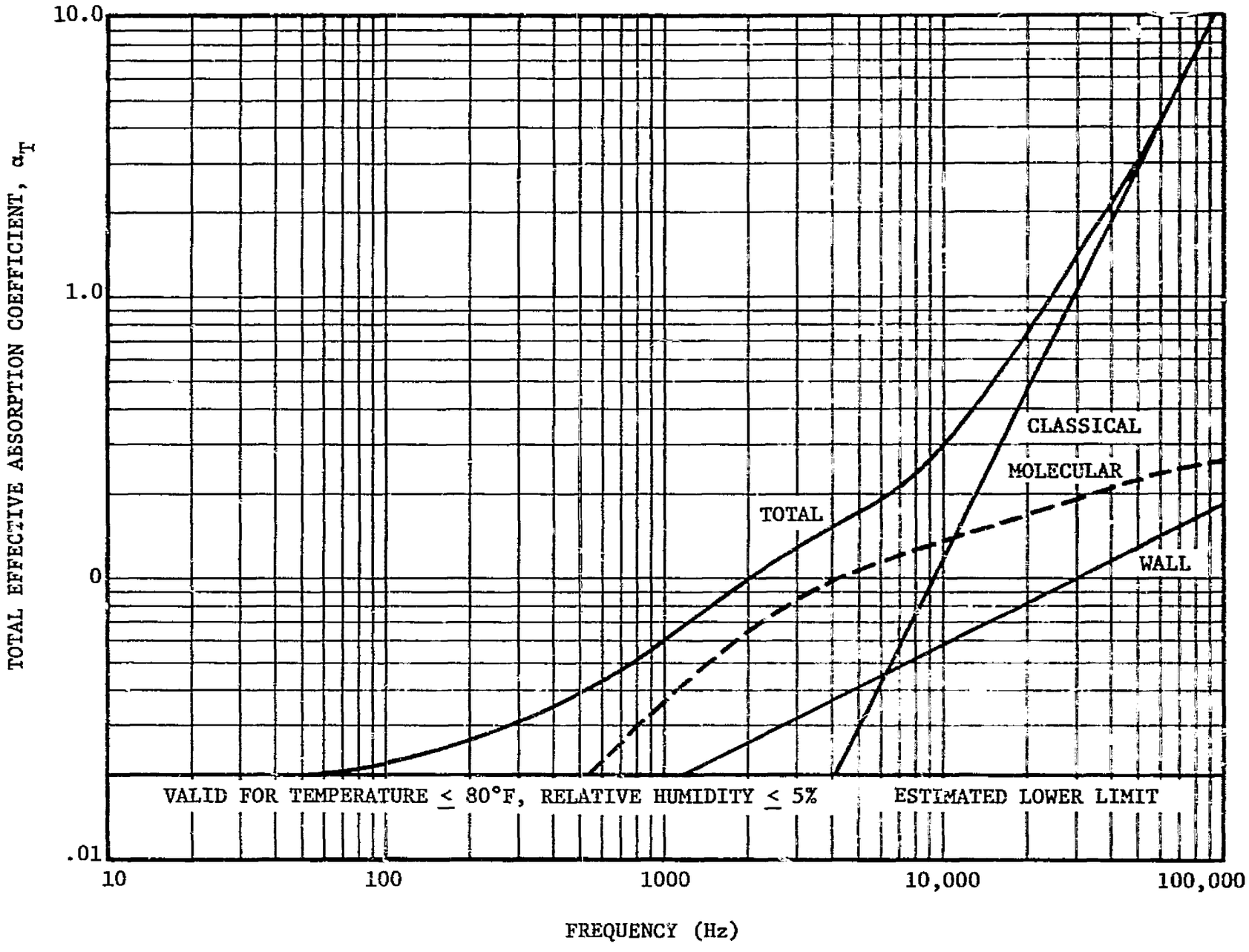

FIGURE 61. EFFECTIVE WALL ABSORPTION COEFFICEINT FOR ACOUSTIC REVERBERANT FACILITY (TEST CELL 2-20)

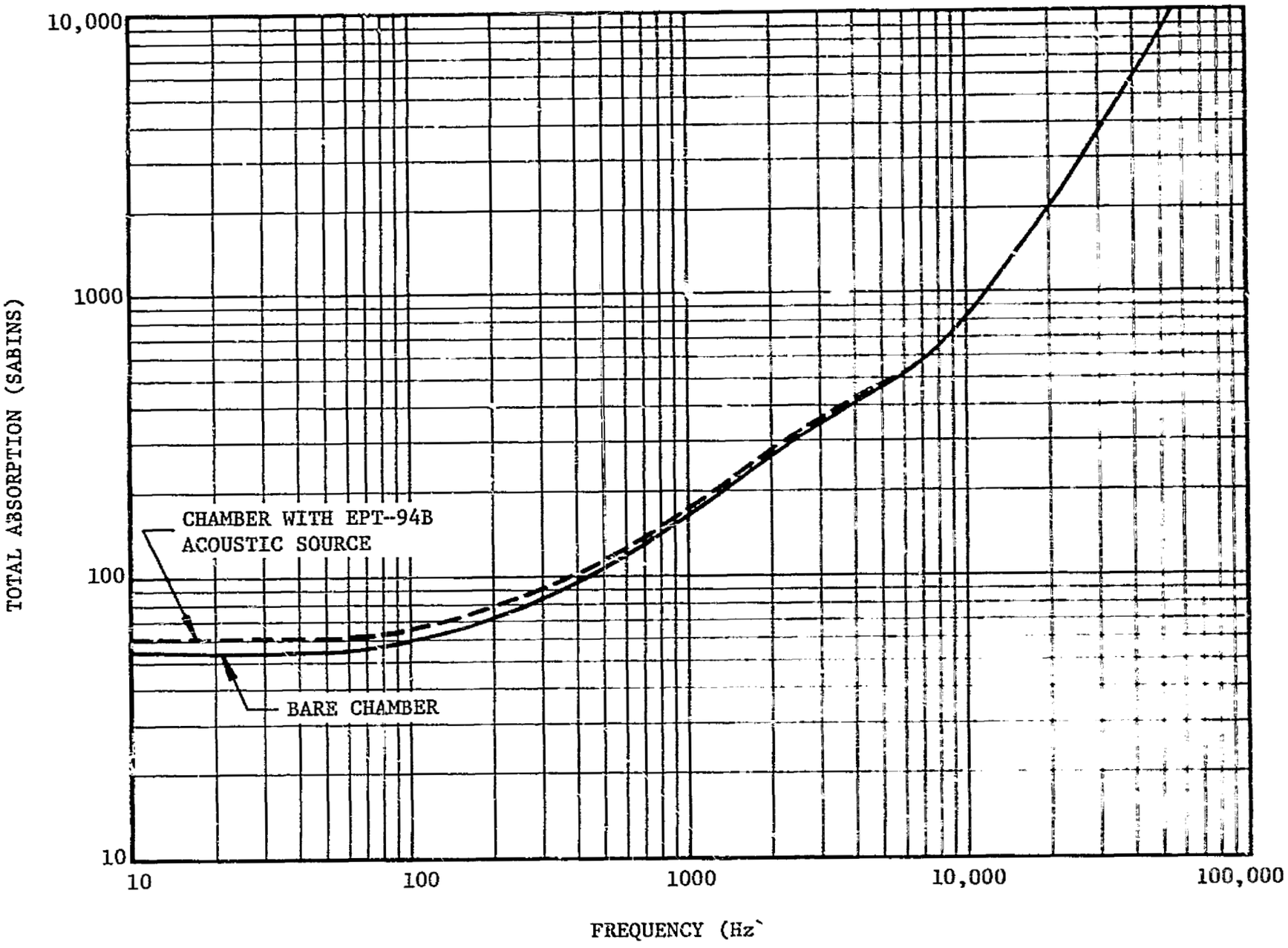

FIGURE 62. TOTAL ABSORPTION FOR ACOUSTIC REVERBERANT FACILITY (TEST CELL 2-20)

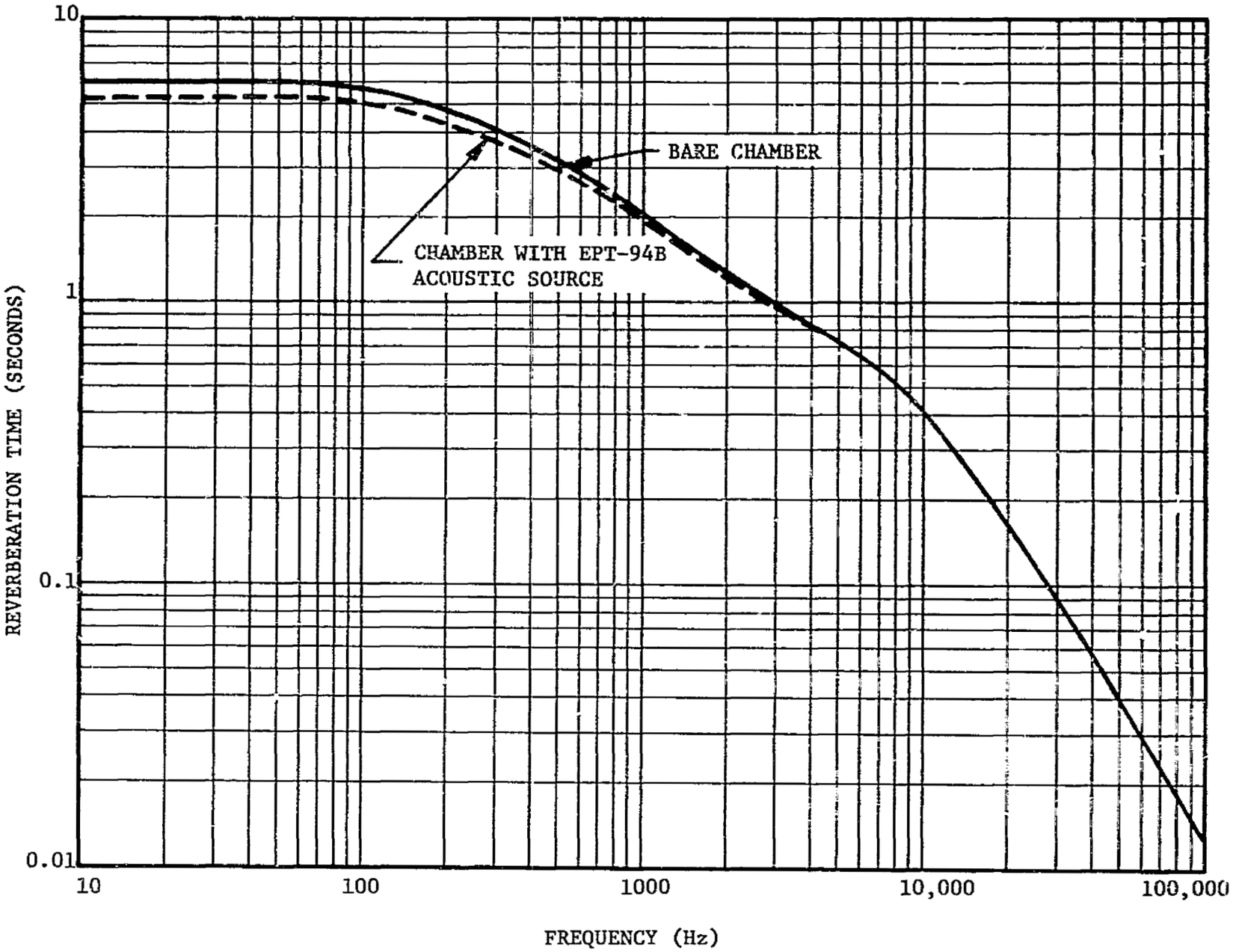

FIGURE 63. REVERBERATION TIME FOR ACOUSTIC REVERBERANT FACILITY (TEST CELL 2-20)

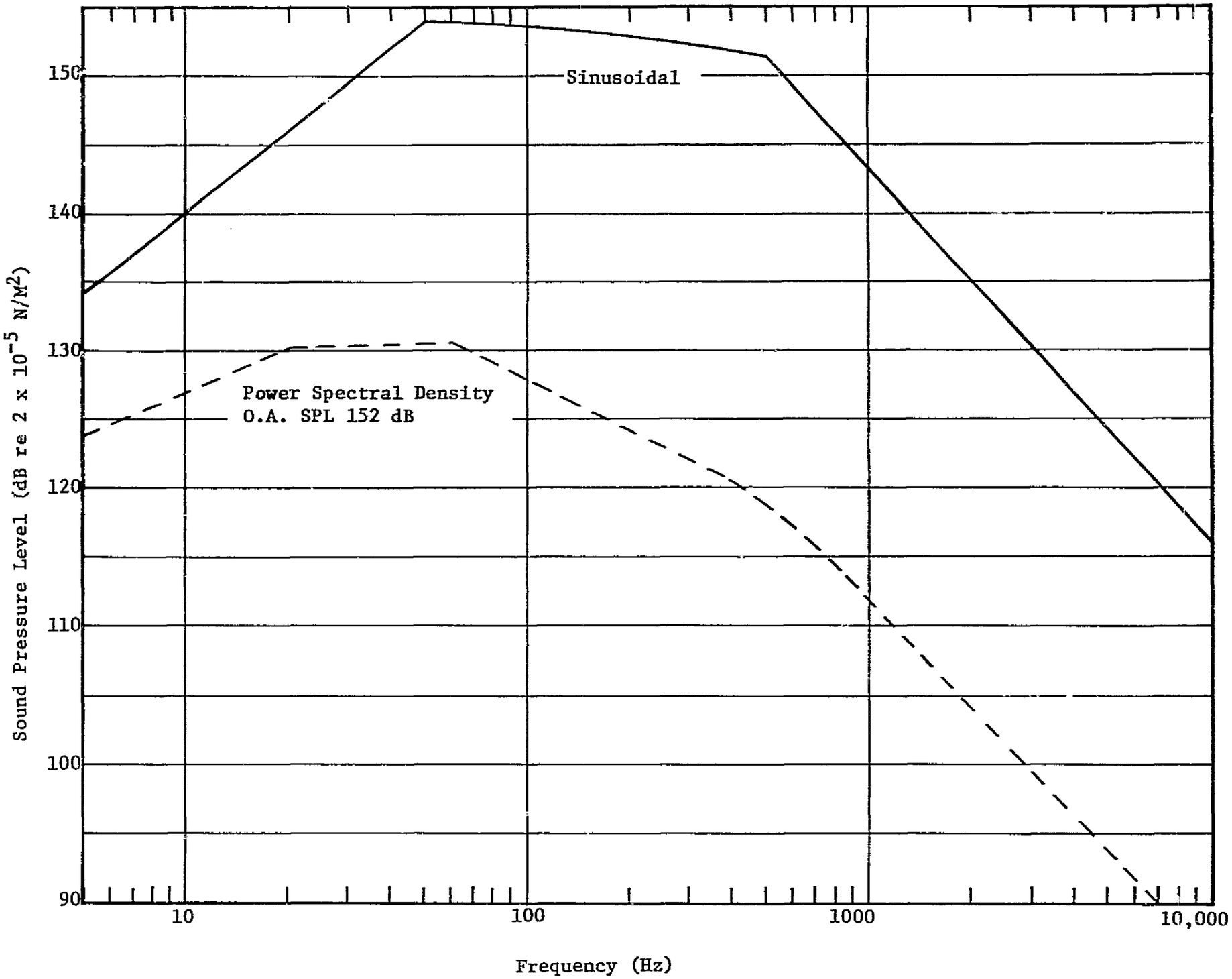

FIGURE 64. MAXIMUM SOUND PRESSURE LEVELS IN ACOUSTIC REVERBERANT FACILITY (TEST CELL 2-20)

Above 100 Hz the cross-correlation coefficient of the acoustic field should approach sin (kr)/kr where k is the wave number and r is the distance relative to the origin.

B. Test Specimens

Four test specimens were exposed to the specified acoustic excitations, the response being monitored by a complement of accelerometers. The four specimens are flat panels, two homogeneous aluminum panels and one stiffened panel with and without an attached mass loading system. These specimens are illustrated in figure 65 and are detailed below:

1. Test Specimen I -

Homogeneous aluminum panel with test dimensions of 30" x 40" and 0.04" thickness. The fundamental mode of vibration for this specimen is in the neighborhood of 6 to 10 Hz. The acoustic critical frequency should occur at 12 kHz. Thus within the frequency range of the acoustic source panel motion will be primarily of the reverberant vibration type (i.e. composed of high vibratory modal indices). This specimen has been designed to study the characteristics of reverberant vibration. (See figure 66 for measurement locations.)

2. Test Specimen II -

Homogeneous aluminum panel with test dimensions of 30" x 40" and 0.2" thickness (fabricated using .190 Al). The fundamental vibratory mode of this panel is 31 to 50 Hz and the acoustic critical frequency should occur at approximately 2300 Hz. Panel response in the modal, reverberant and coincidence frequency domains is monitored for this specimen. (See figure 67 for measurement locations.)

3. Test Specimen III -

A flat aluminum panel as in I above (fabricated with .05 Al skin), but with two stiffeners in each direction, dividing the panel into nine bays. The fundamental mode of the sub-panels is in the range of 60 to 100 Hz; the acoustic critical frequency should be 9.6 kHz for the 0.05 thickness sheet. Panel motion of the modal and reverberant types is evaluated for this structure. (See figure 68 for measurement locations.)

4. Test Specimen IV -

Test specimen III as described above, but with simulated equipment loading. The alteration of the amplitude and modal frequencies is examined in terms of shifted resonant frequencies, mass attenuation and coupling interaction. (See figure 69 for measurement locations.)

FIGURE 65. TEST SPECIMENS FOR COMPARATIVE ANALYSIS OF ACOUSTIC TESTING TECHNIQUES

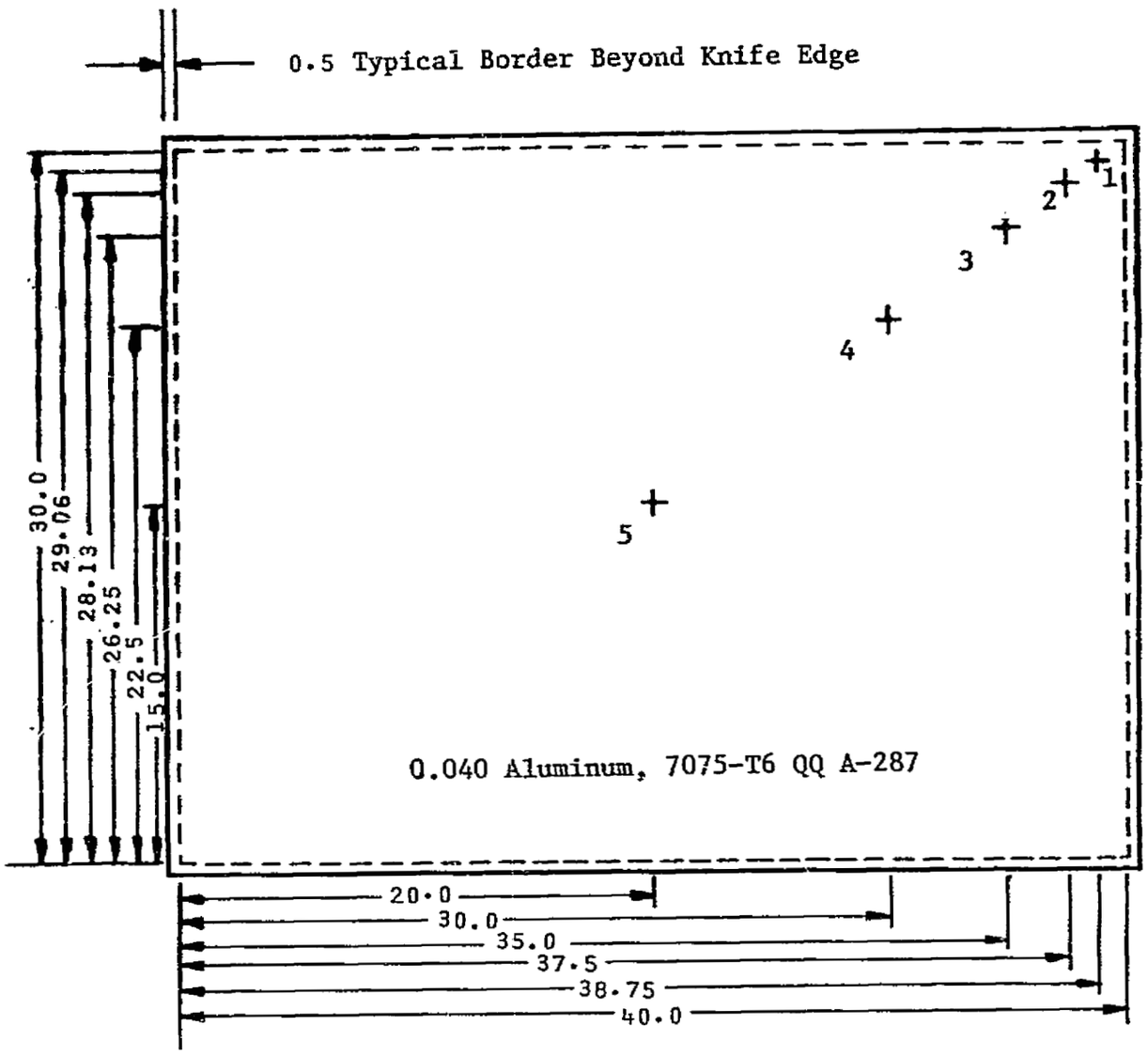

Notes:
1. All Dimensions In Inches
2. Test Location 5 Corresponds to Location A, Table 6
3. Test Location 4 corresponds to Location B, Table 6
4. Test Location 3 Corresponds to Location C, Table 6

FIGURE 66. ACCELEROMETER LOCATIONS FOR TEST SPECIMEN I

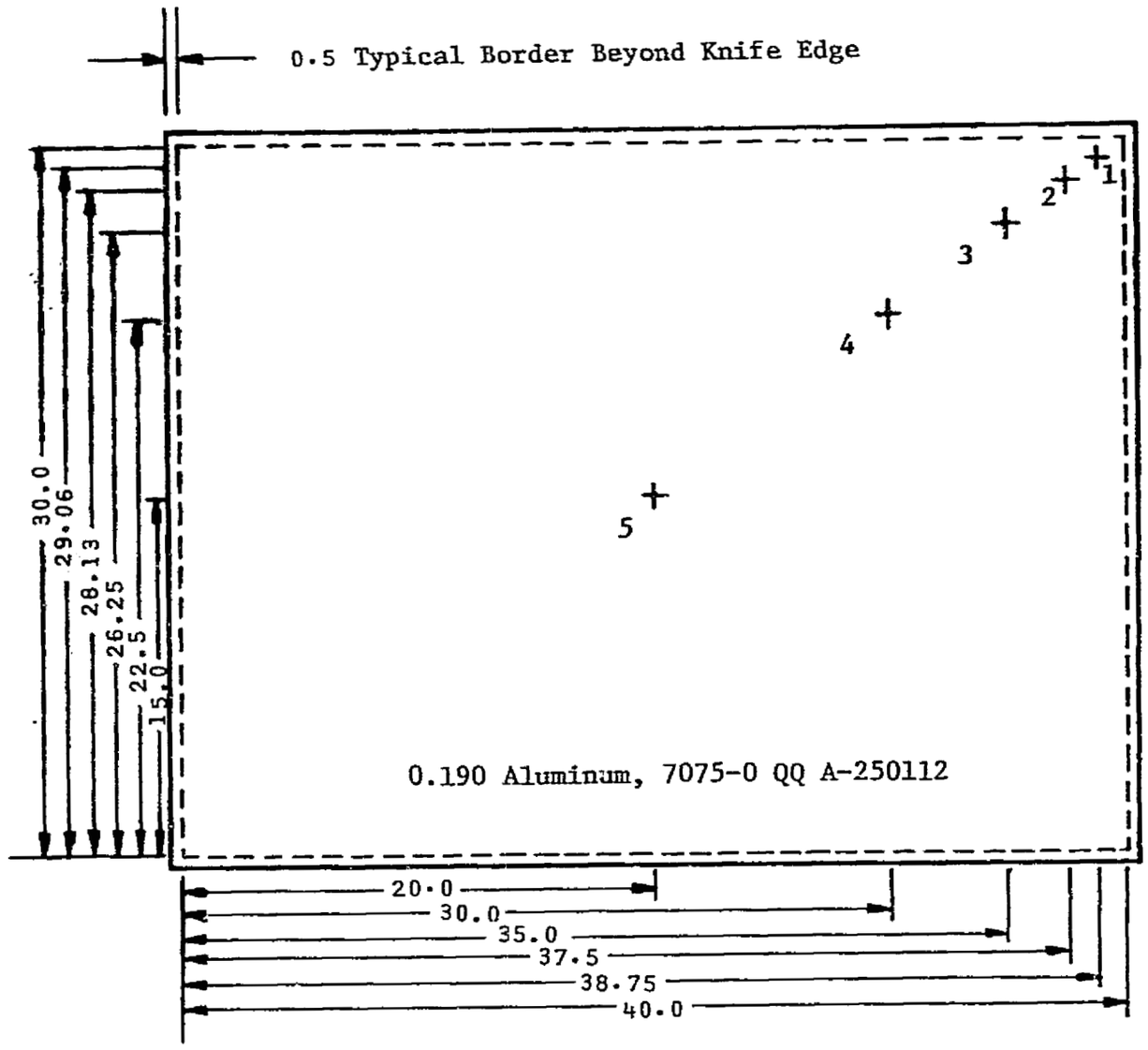

Notes:
1. All Dimensions In Inches
2. Test Location 5 Corresponds to Location A, Table 6
3. Test Location 4 corresponds to Location B, Table 6
4. Test Location 3 Corresponds to Location C, Table 6

FIGURE 67. ACCELEROMETER LOCATIONS FOR TEST SPECIMEN II

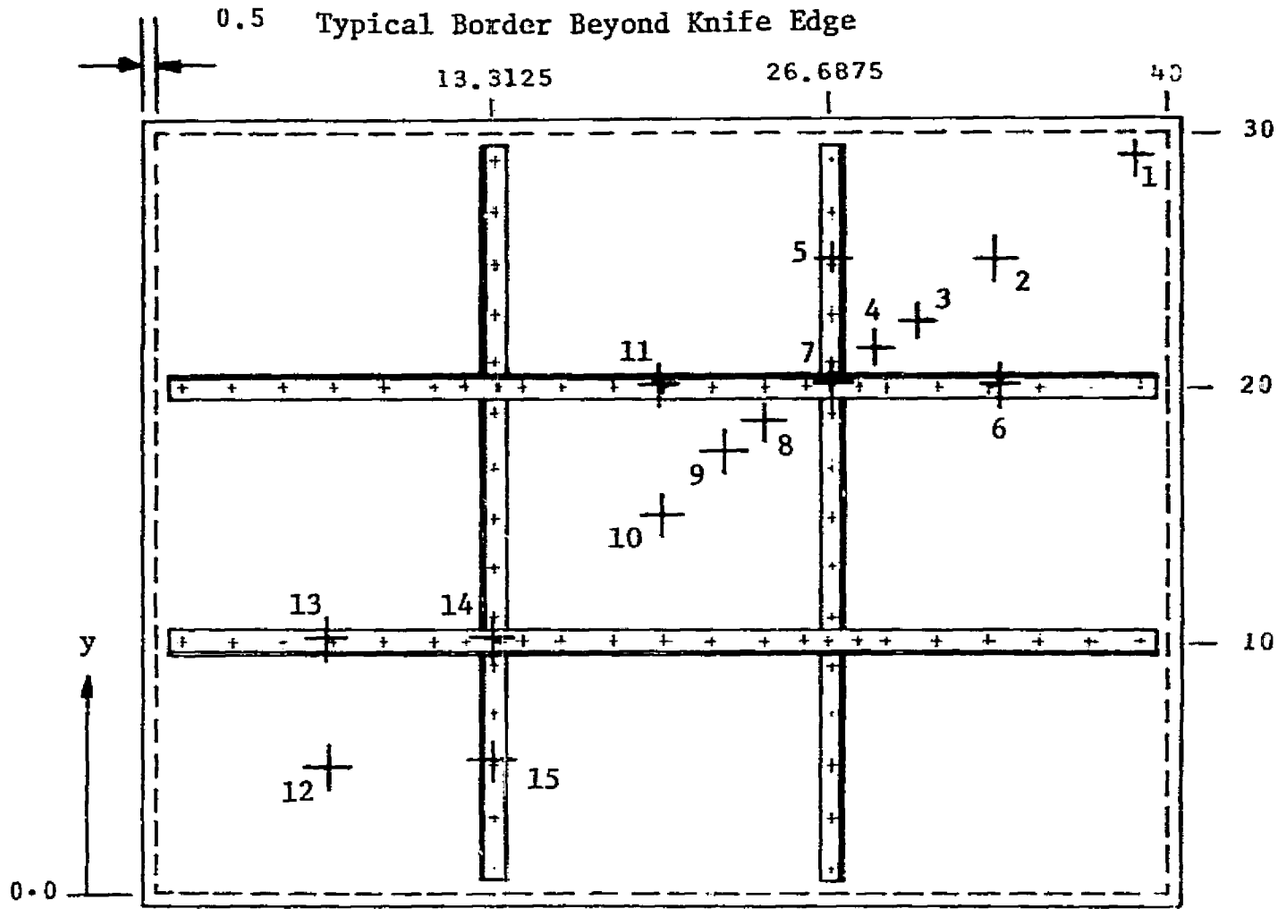

(0.05 Aluminum stiffened by 1 x 1 x 1/8 Angle)

Loc	x	y	Loc	x	y	Loc	x	y
1	38.75	29.05	6	33.25	20.0	11	19.875	20.0
2	33.125	25.0	7	26.6875	20.0	12	6.875	5.0
3	29.9375	22.5	8	25.0	18.75	13	6.750	10.0
4	28.3125	21.25	9	23.375	17.5	14	13.3125	10.0
5	26.6875	24.825	10	20.0	15.0	15	13.3125	5.125

Notes:
1. All dimensions in Inches
2. Test Location 10 Corresponds to Location A, Table 6
3. Test Location 4 Corresponds to Location B, Table 6
4. Test Location 3 Corresponds to Location C, Table 6

FIGURE 68. ACCELEROMETER LOCATIONS FOR TEST SPECIMEN III

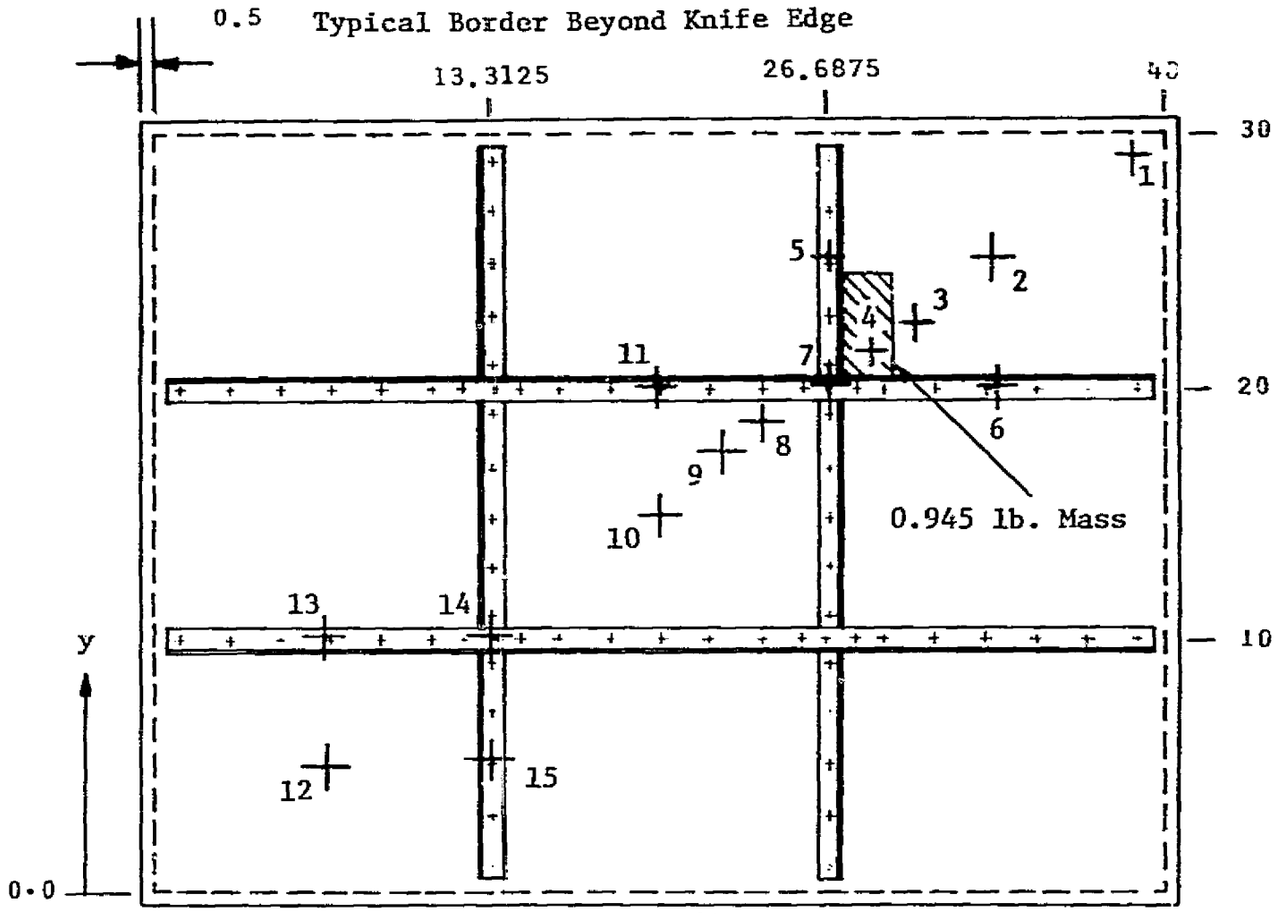

0.0 → x

(0.05 Aluminum stiffened by 1 x 1 x 1/8 Angle)

Loc	x	y	Loc	x	y	Loc	x	y
1	38.75	29.05	6	33.25	20.0	11	19.875	20.0
2	33.125	25.0	7	26.6875	20.0	12	6.875	5.0
3	29.9375	22.5	8	25.0	18.75	13	6.750	10.0
4	28.3125	21.25	9	23.375	17.5	14	13.3125	10.0
5	26.6875	24.825	10	20.0	15.0	15	13.3125	5.125

Notes:
1. All dimensions in Inches
2. Test Location 10 Corresponds to Location A, Table 6
3. Test Location 4 Corresponds to Location B, Table 6
4. Test Location 3 Corresponds to Location C, Table 6

FIGURE 69. ACCELEROMETER LOCATIONS FOR TEST SPECIMEN IV

C. Test Configurations

A matrix was constructed (figure 70) to facilitate planning, execution and analysis of simulation testing. Each required test is assigned a test number. Figures 71 - 73 portray photographically test apparatus and supporting instrumentation.

Tests 1, 5, 10, and 14 were performed with a reverberant field incident on one side of the test specimen. The test section was placed near a room wall such that the plane of the test panel was not parallel or perpendicular to any room surface. For all tests in the reverberant facility, the Ling EPT-94B with the model 5756 hypex horn and the Chrysler linear expansion horn was utilized as the acoustic source.

Flat test panels were installed in the test section of the progressive wave facility with the smooth surface inward for testing with the acoustic progressive wave at parallel incidence (tests 3, 7, 12, and 16). Acoustic testing at normal incidence (tests 2, 6, 11 and 15) was completed with the panels mounted in the progressive wave test section but with the acoustic source-horn axis positioned normal to the test panel, 1.5 feet from the mouth of the horn to the test panel, with the 2' horn dimension paralleling the 30" panel dimension and the horn axis at the center of the test specimen surface. Normal incidence testing was performed in a central position of the reverberant facility or under quasi-free field conditions. It was estimated that the direct field was 16 to 20 dB greater than the reverberant field.

Localized excitation of the flat panels (tests 4, 8, 13 and 17) was accomplished by utilization of a Chrysler wave guide. The test panels were mounted (smooth side inward) in the progressive wave test section with the source end sealed. The wave guide was attached to the internal side of the progressive wave test section along one of the 40" test specimen sides.

In each simulation test, testing was performed utilizing a broad band random noise source. Data recording was performed after the testing conditions had stabilized (two minutes were allowed for stabilization). An instrumentation block diagram is shown in figure 74. Instrumentation was situated in a manner to measure structural response of test specimens in the modal, coincidence and reverberant response regions, to implement measurement of the acoustic field.

Light-weight accelerometers (approximately 2 gram weight - 4 gram weight with mounting block) with a frequency response to 10 kHz were utilized for vibration measurements. High frequency response was corrected as applicable for the accelerometer mass.

Environmental excitation and response data were reduced in the form of constant bandwidths, log amplitude vs log frequency by a Spectral Dynamics analog system. Acoustic excitation was monitored for each test condition.

TEST CONDITIONS / TEST SPECIMENS (Section IV,B)	REVERBERANT ACOUSTIC FIELD (Excitation 3)	PROGRESSIVE WAVE NORMAL INCIDENCE (Excitation 1)	PROGRESSIVE WAVE PARALLEL INCIDENCE (Excitation 2)	LOCALIZED EXCITATION (Excitation 4)	RADIATION DAMPING
IV.B.1 FLAT PLATE - TEST SPECIMEN I (Reverberant Response)	1	2	3	4	9B
IV.B.2 FLAT PLATE - TEST SPECIMEN II (Coincidence and Modal Response)	5	6	7	8	9
IV.B.3 FLAT PLATE - TEST SPECIMEN III (Stiffened)	10	11	12	13	
IV.B.4 FLAT PLATE - TEST SPECIMEN IV (Stiffened and Mass Loaded)	14	15	16	17	

NOTE: ARABIC NUMBERS IN THE TEST MATRIX REFER TO ASSIGNED TEST NUMBERS FOR THE APPROPRIATE COMBINATION OF TEST SPECIMEN AND EXCITATION

FIGURE 70. TEST MATRIX

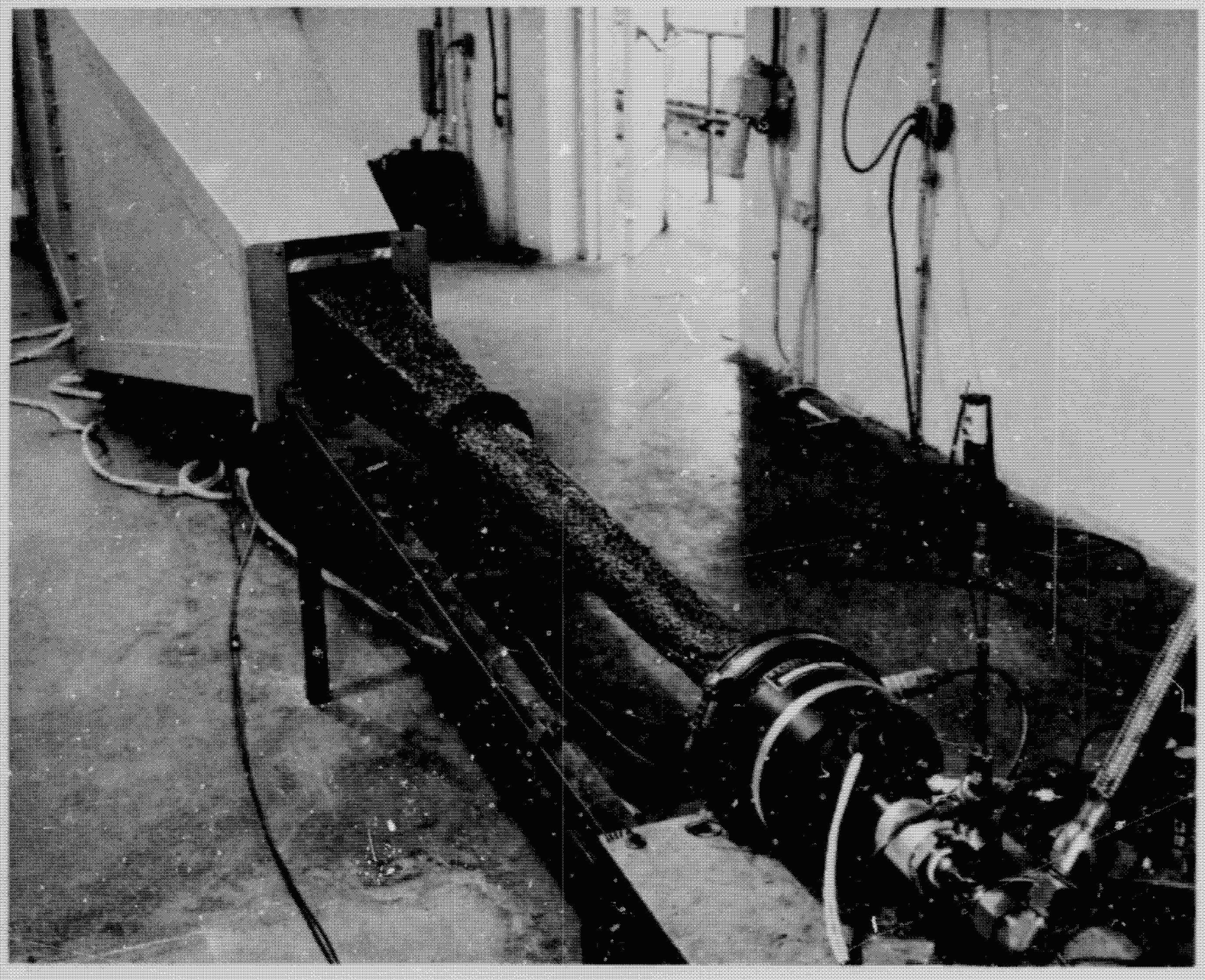

FIGURE 71. ACOUSTIC TEST FACILITY

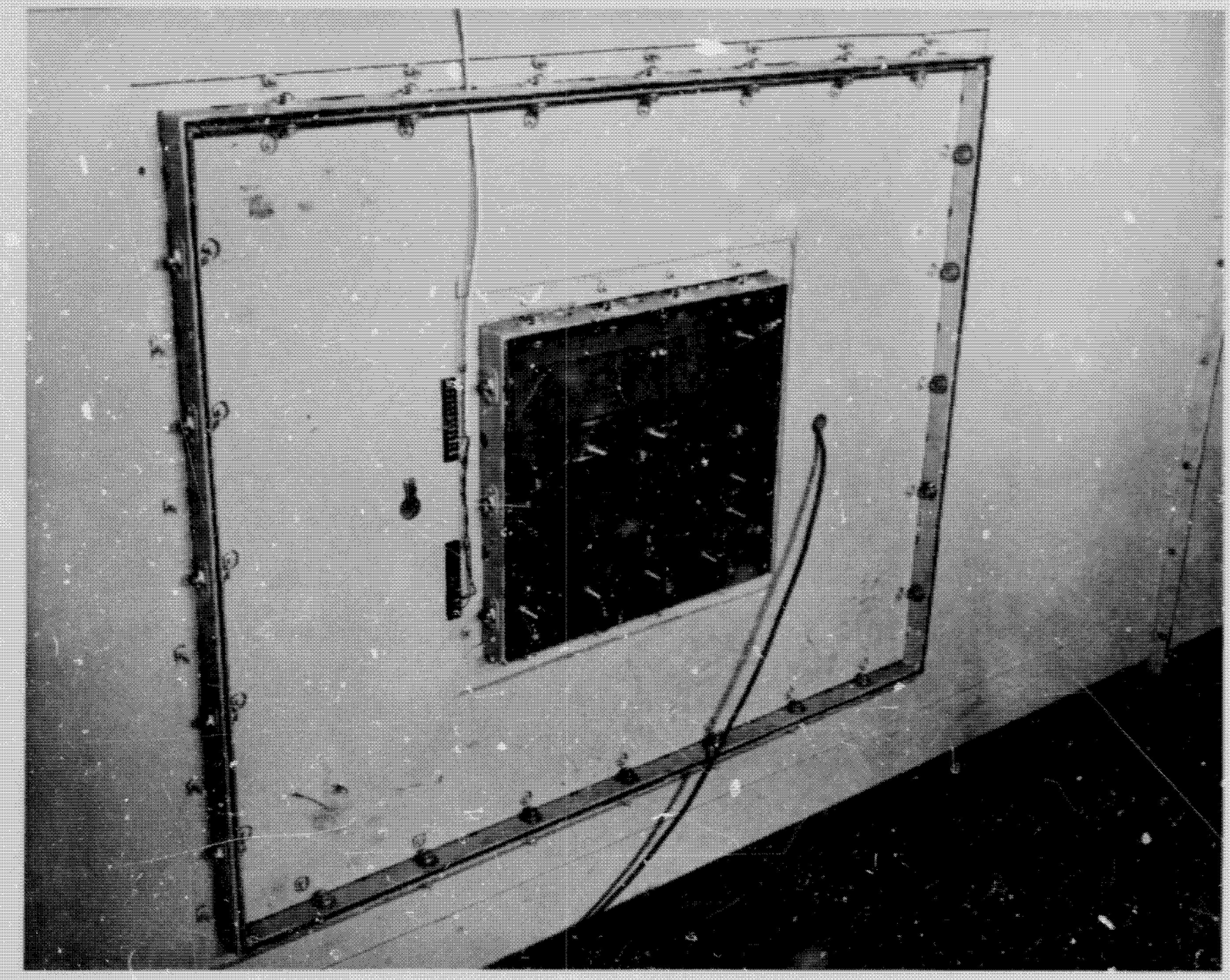

FIGURE 72. SMALL PANEL INSTALLATION

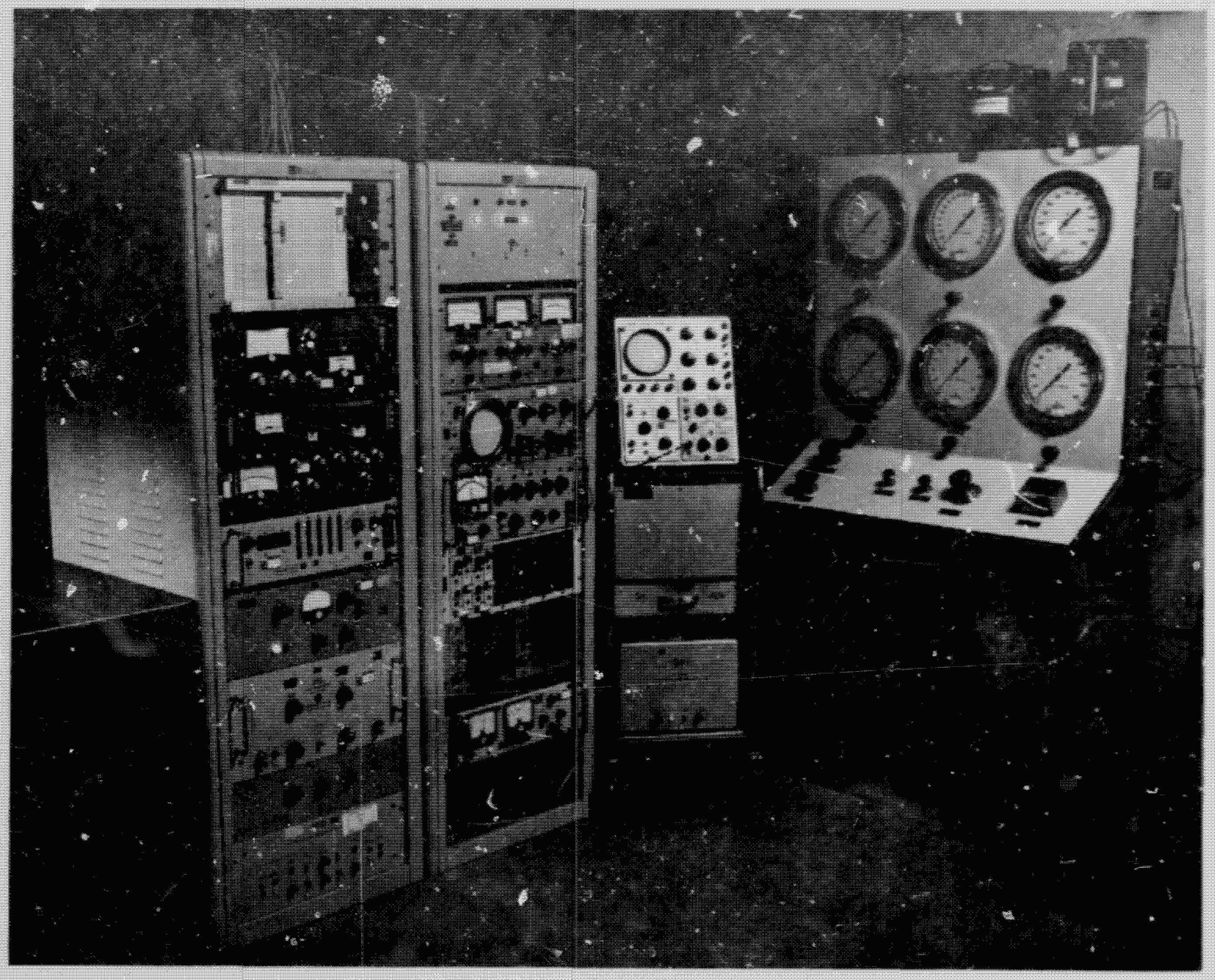

FIGURE 73. SUPPORTING INSTRUMENTATION

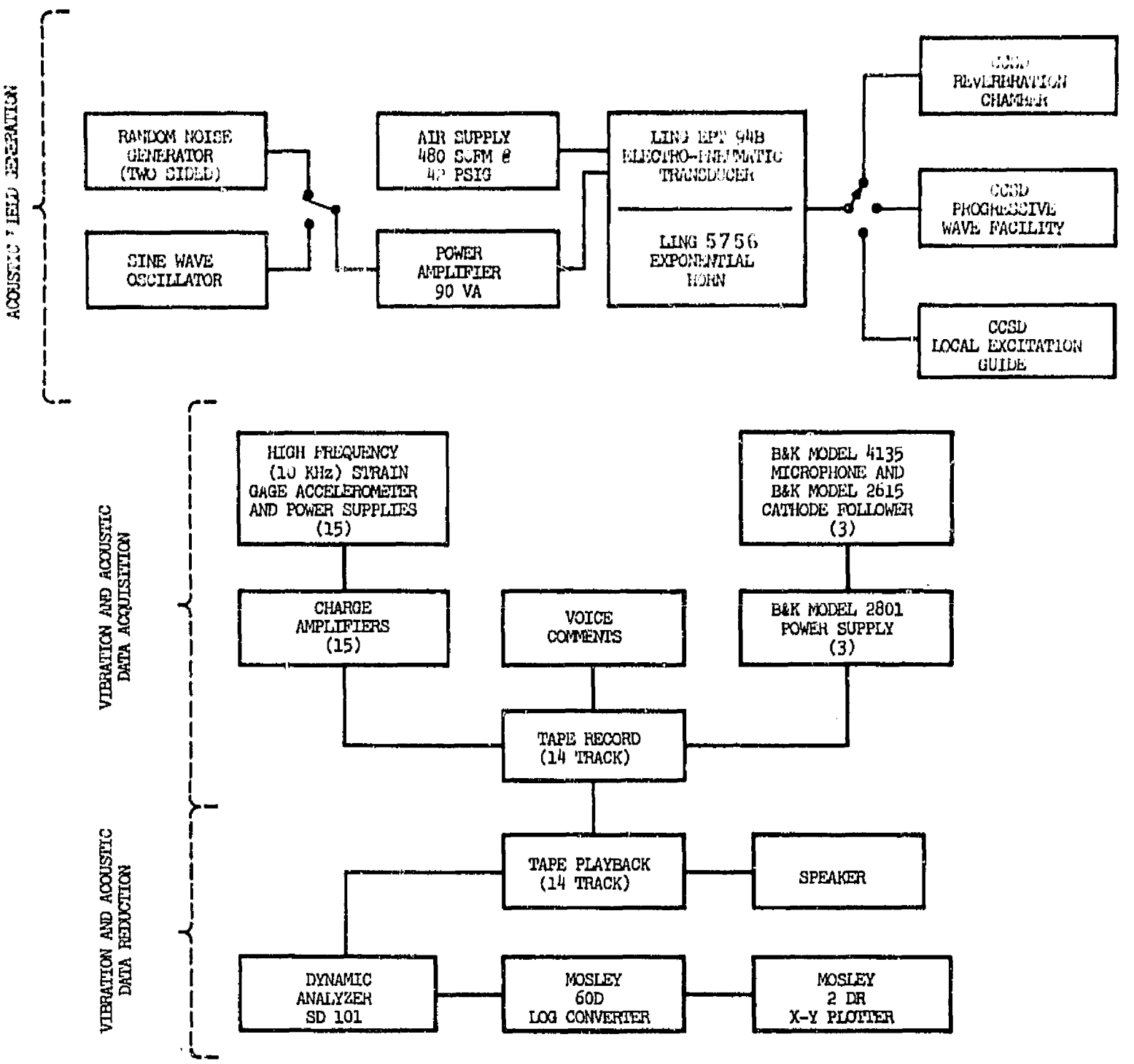

FIGURE 74. INSTRUMENTATION BLOCK DIAGRAM FOR DETERMINATION OF ACOUSTIC EXCITATION AND VIBRATORY RESPONSE

Test configuration sketches are provided in figures 75, 76, 77 and 78 for progressive wave excitation at normal incidence, progressive wave excitation at parallel incidence, reverberant acoustic field excitation and localized excitation with a progressive acoustic wave at parallel incidence. The sketches are approximately 1/50 scale, the cross-section of the acoustic progressive wave apparatus was approximately 2' x 4'. The test section and termination section were each eight feet long. The reverberation room had dimensions of 10' x 16' x 42.5'. The cross sectional area of the localized incidence wave guide was approximately 0.48 ft^2. The excited area of the panels was 500 $in.^2$ as compared to the whole panel area of 1200 $in.^2$.

Typical acoustic spectral densities of the excitation are shown in figures 79, 80, 81 and 82 for the progressive wave testing at normal incidence, progressive wave testing at parallel incidence, the reverberant acoustic field, and the localized acoustic progressive wave excitation at parallel incidence. Figures 8 84, 85 and 86 are smoothed spectra acquired by averaging the acoustic excitation from each test run for the four test configurations. The overall sound pressure level was nominally 140 dB re 2 x 10^{-5} N/M^2 for testing with progressive wave at normal incidence, progressive wave at parallel incidence and reverberant field excitation. The overall sound pressure level for the localized progressive wave excitation was 150 dB.

D. Test Data

Vibratory response data is organized in numerical order (figures 87 - 104) by test number (figure 70) and within a given test by accelerometer location (figures 66 - 69). The data is produced in power spectral density format, log amplitude vs log frequency. Test locations and composite levels (where available) are indicated.

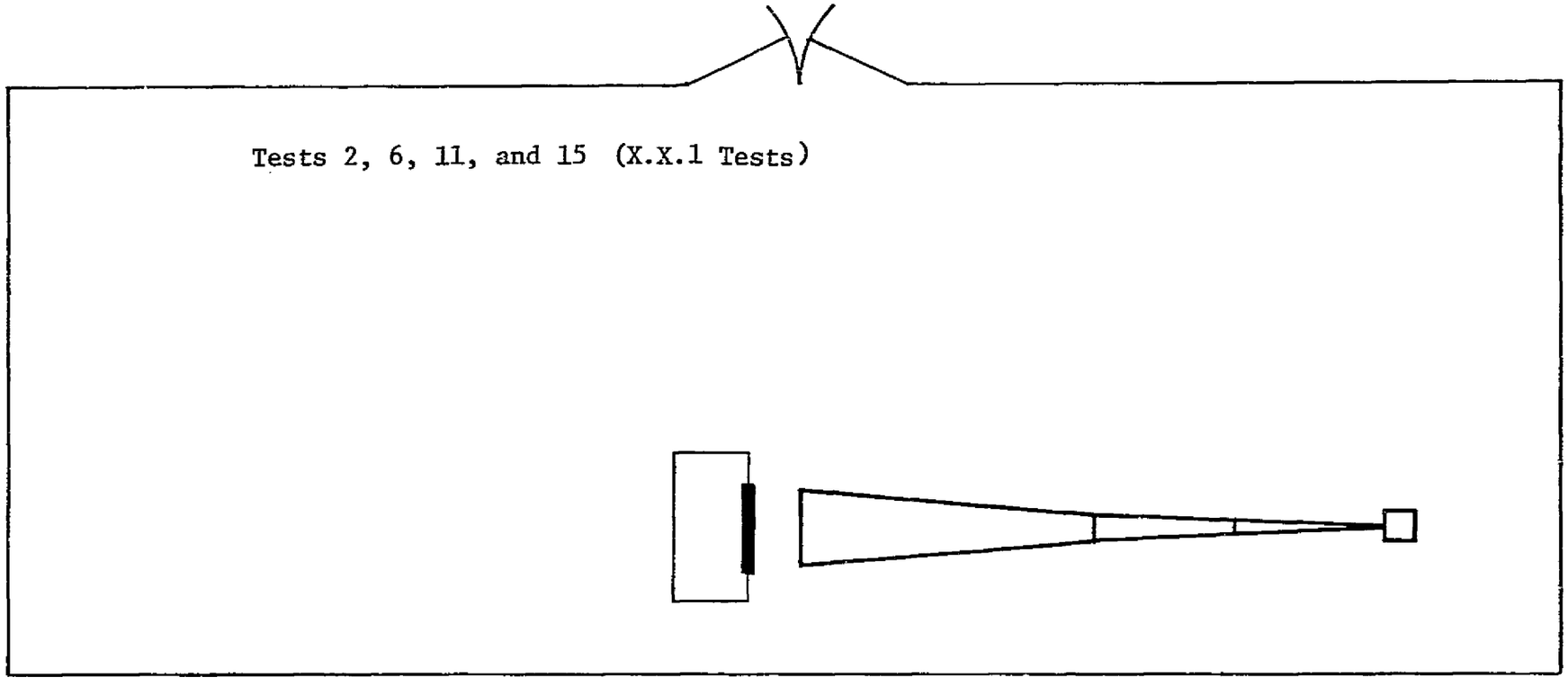

NOTES:

1. Test section on end as described in the test plan.
2. Test panel is located 1.5 feet from the horn.
3. Microphone 6 inches in front of center of test panel.

FIGURE 75. TEST CONFIGURATION I - PROGRESSIVE WAVE TESTING AT NORMAL INCIDENCE

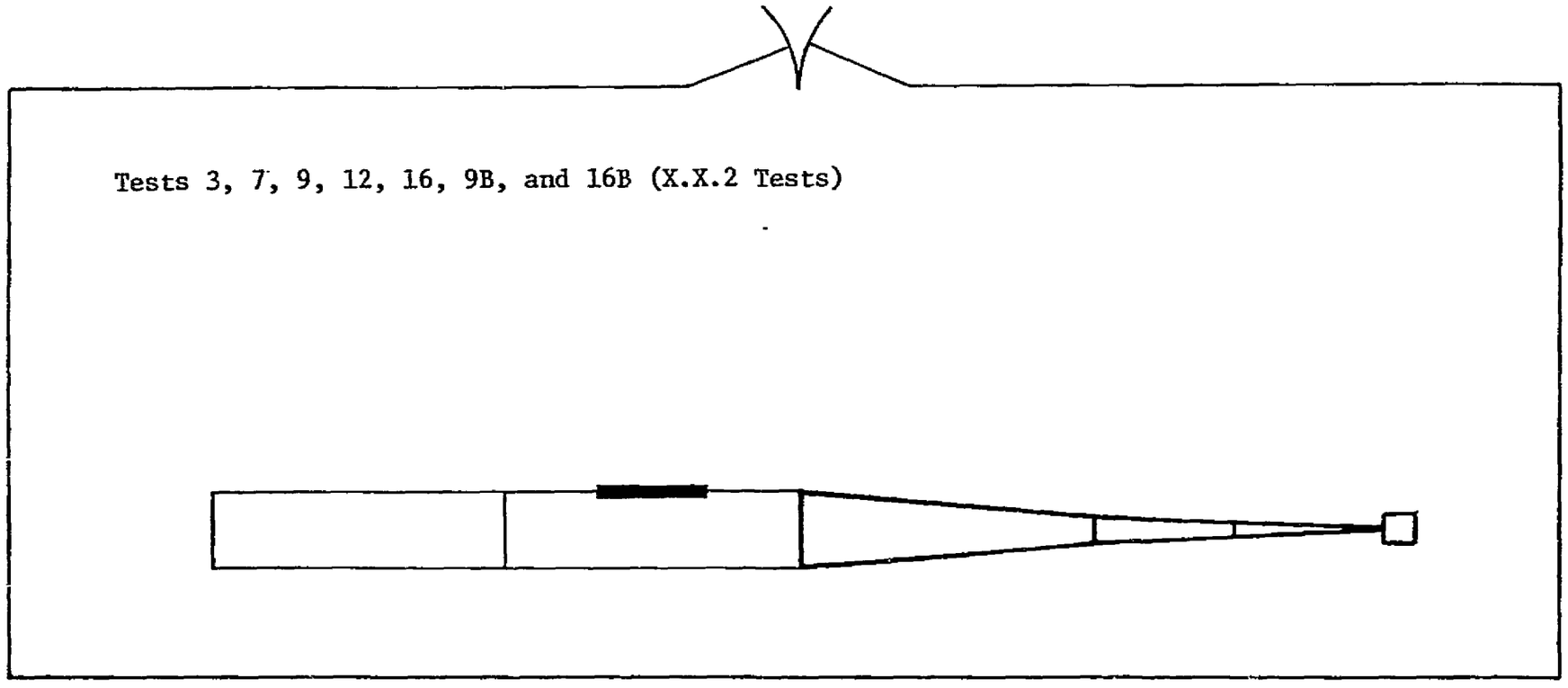

Notes:

1. Microphone diaphram located flush with inside surface immediately ahead of test specimen.

FIGURE 76. TEST CONFIGURATION II - PROGRESSIVE WAVE TESTING AT PARALLEL INCIDENCE

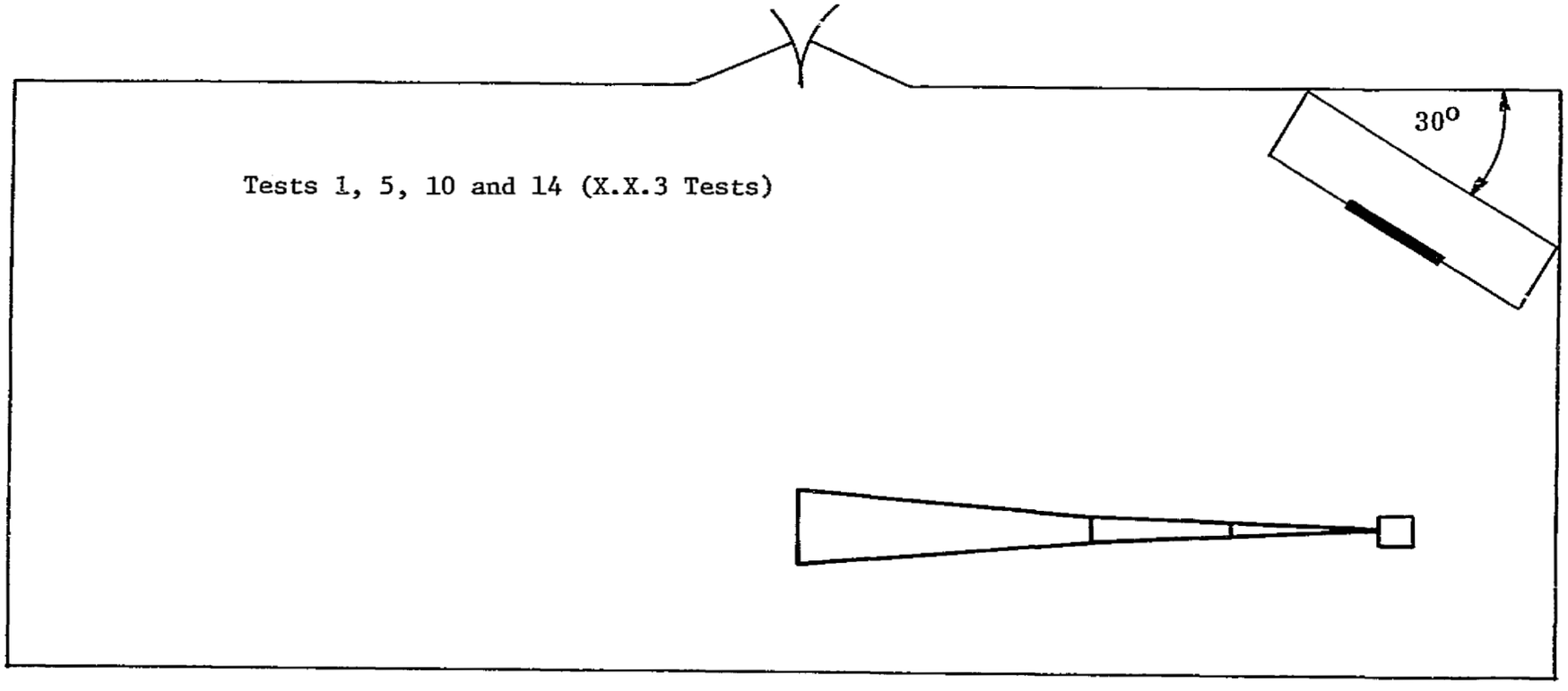

NOTES:

1. Test section in corner behind mouth of horn at a nominal 30° angle with longer side of test cell.
2. Microphone six inches in front of center of test panel.

FIGURE 77. TEST CONFIGURATION III - REVERBERANT ACOUSTIC FIELD

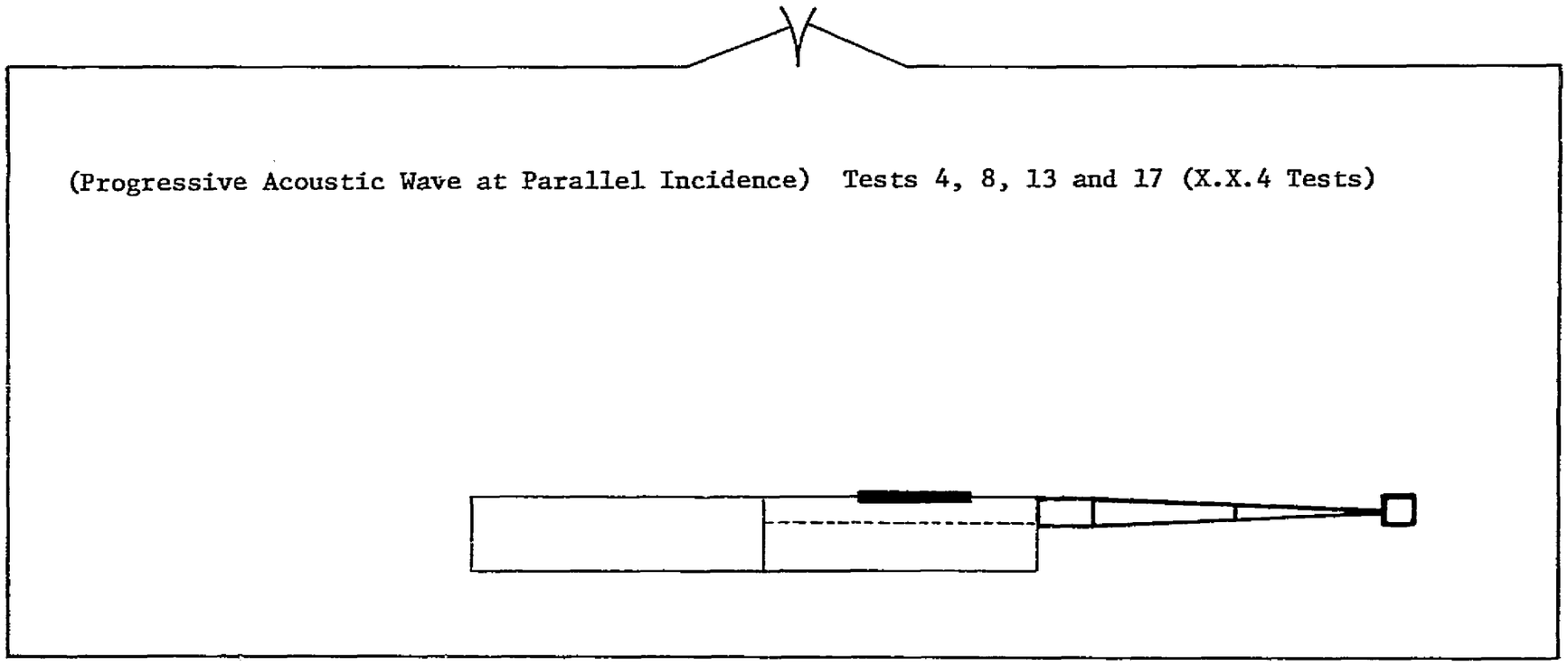

NOTES:

1. Microphone as for progressive wave testing at parallel incidence.

FIGURE 78. TEST CONFIGURATION IV - LOCALIZED EXCITATION

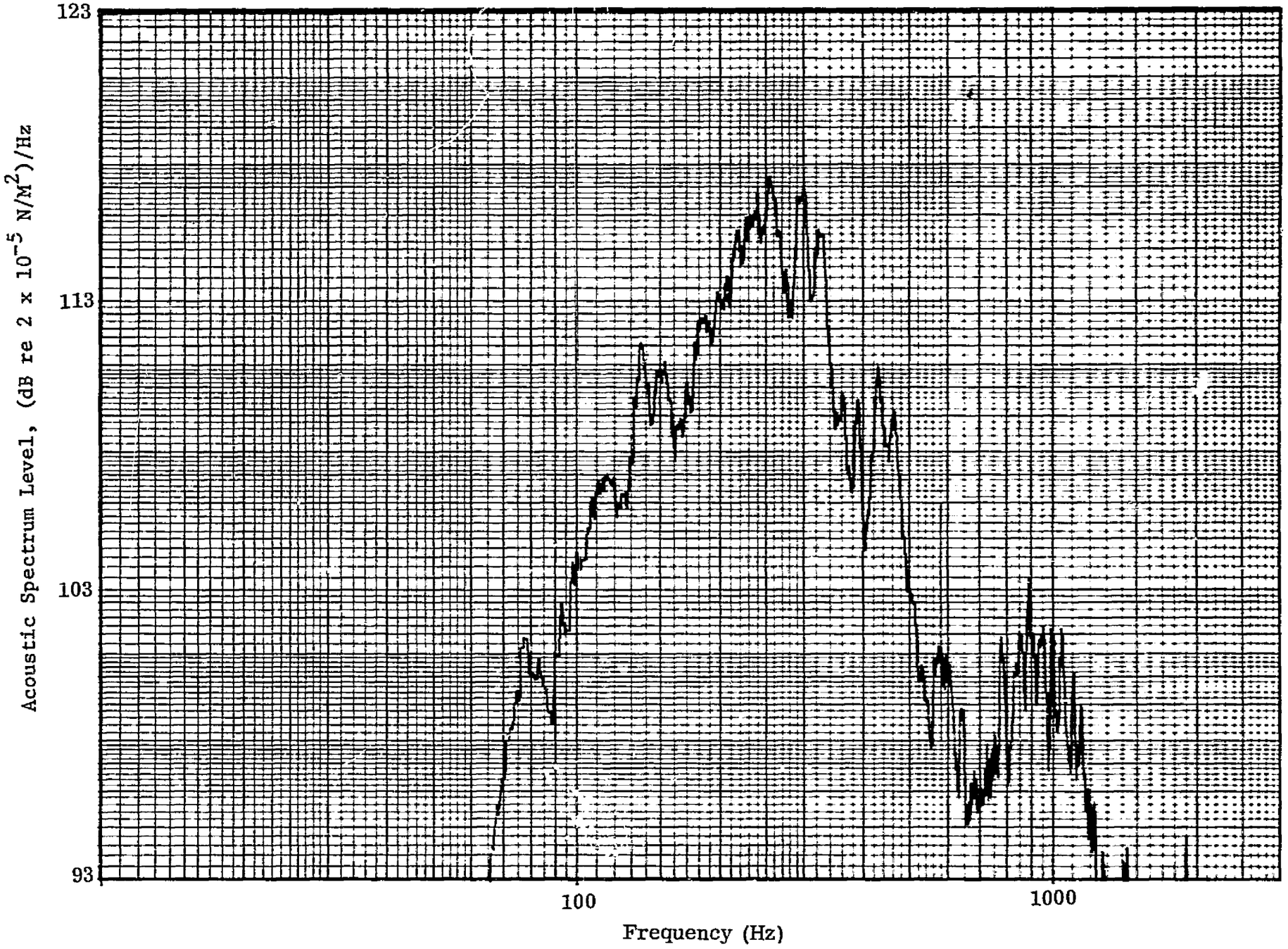

FIGURE 79. TYPICAL ACOUSTIC SPECTRUM FOR NORMAL INCIDENCE PROGRESSIVE WAVE TESTING

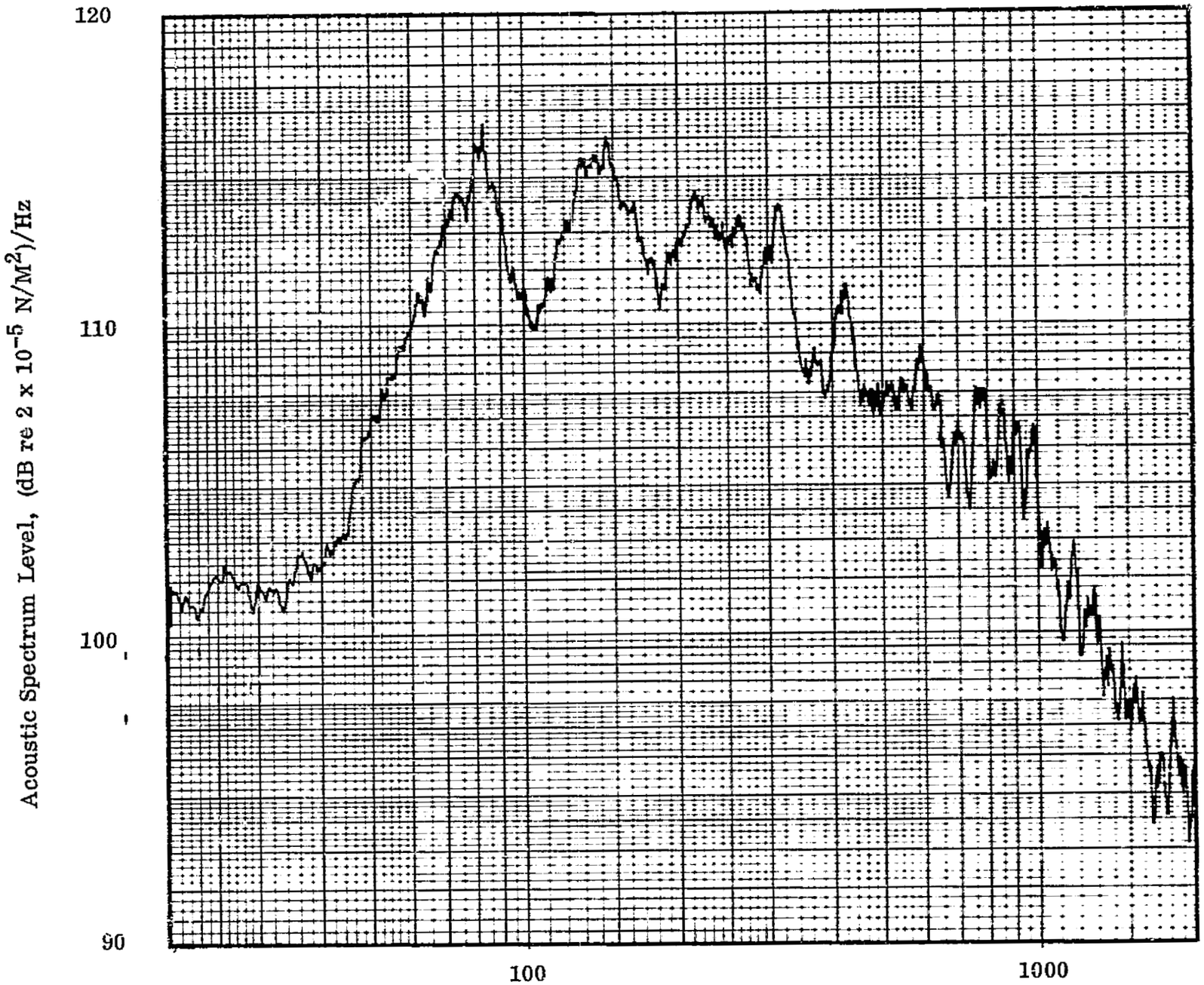

FIGURE 80. TYPICAL ACOUSTIC SPECTRUM FOR PARALLEL INCIDENCE PROGRESSIVE WAVE TESTING

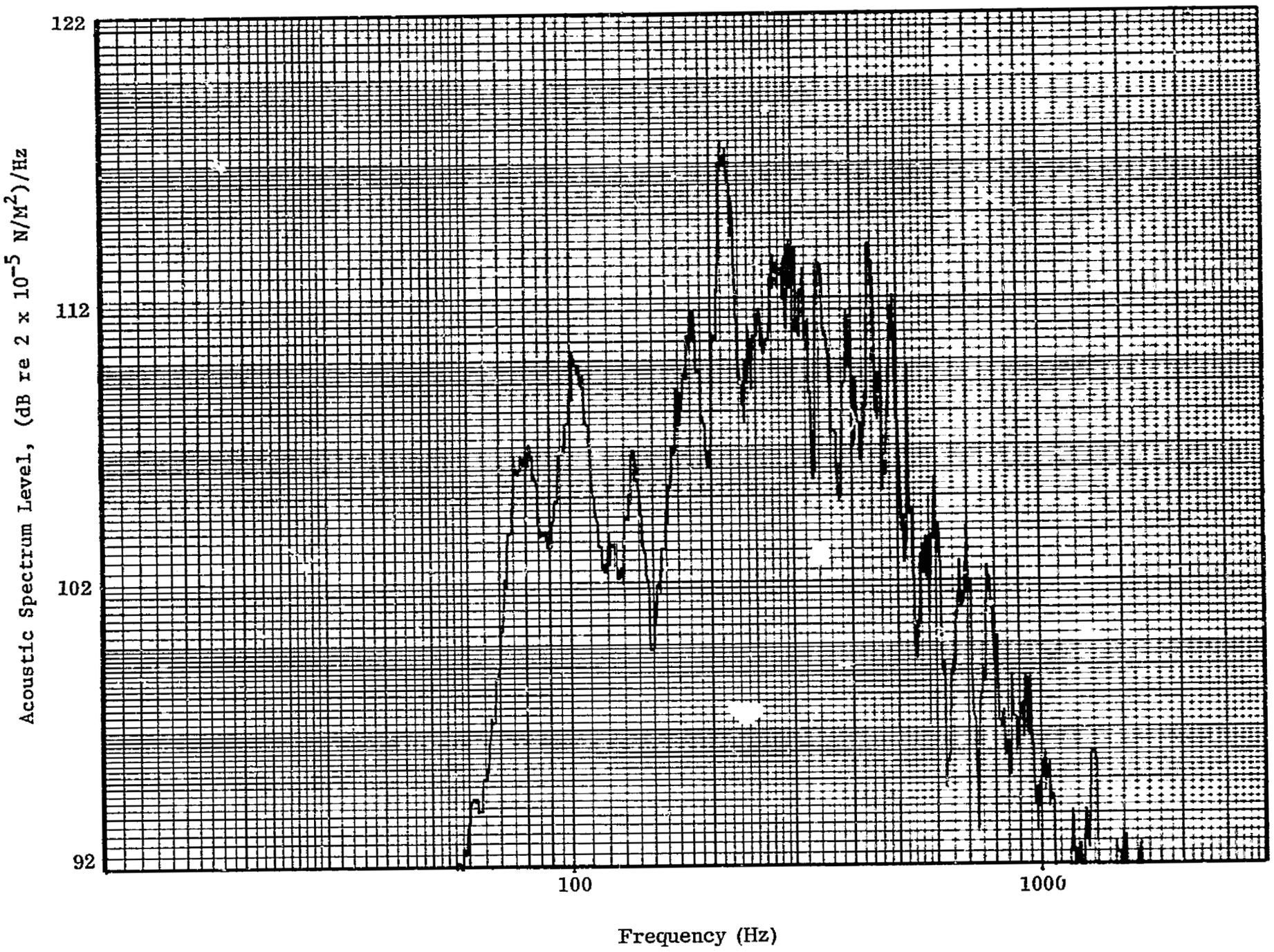

FIGURE 81. TYPICAL ACOUSTIC SPECTRUM FOR REVERBERANT FIELD TESTING

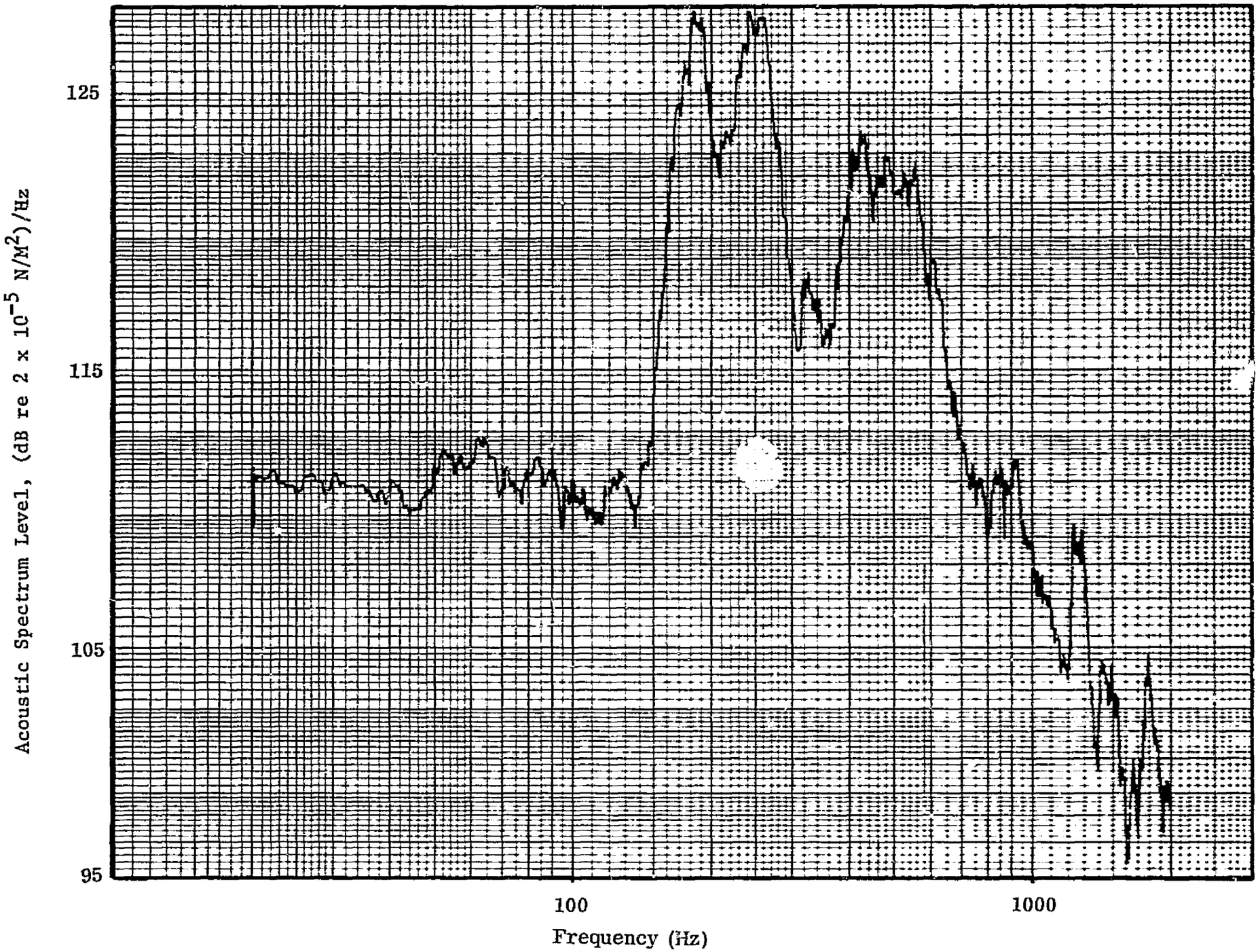

FIGURE 82. TYPICAL ACOUSTIC SPECTRUM FOR LOCALIZED EXCITATION TESTING

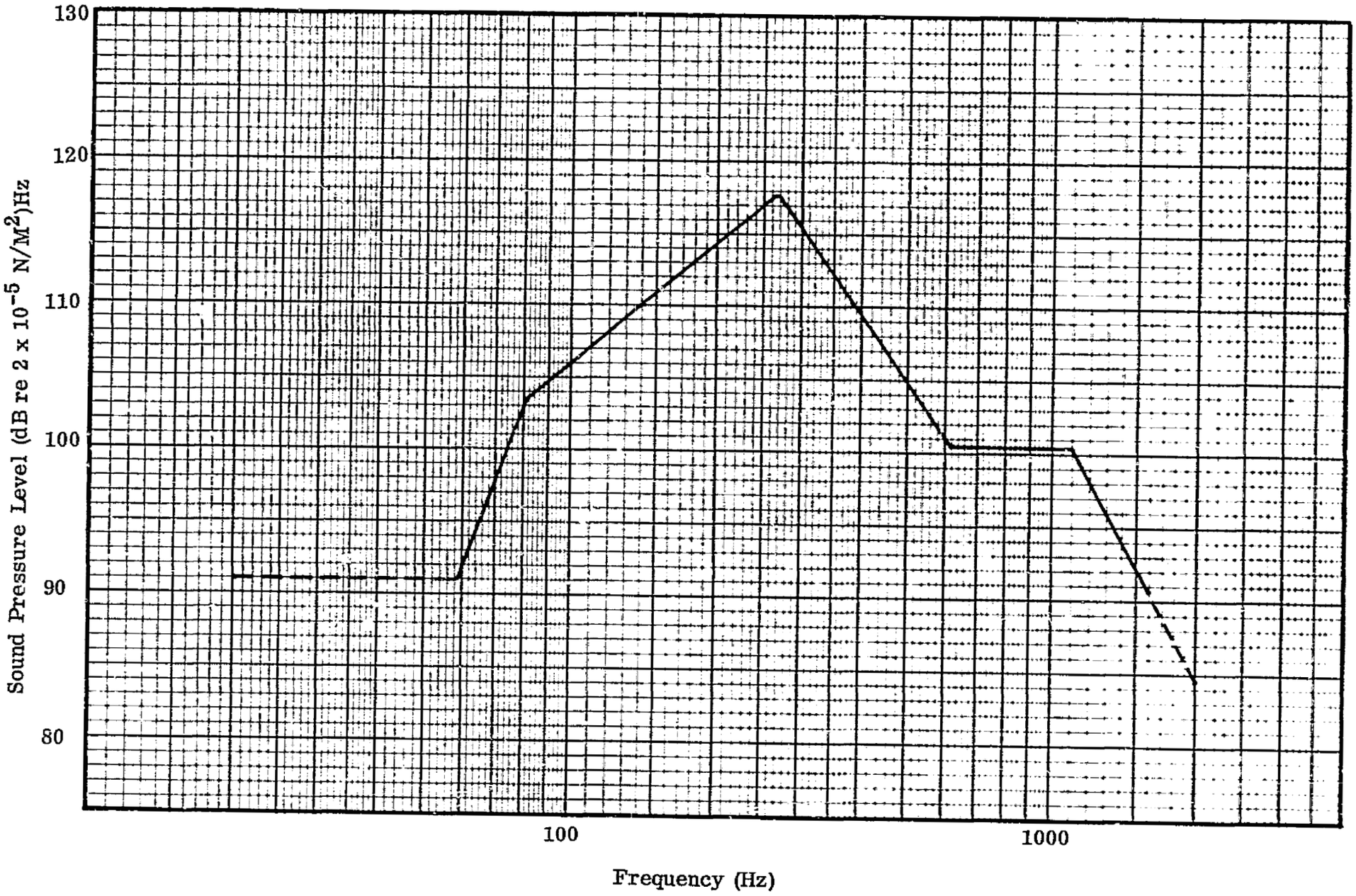

FIGURE 83. SMOOTHED PSD OF ACOUSTIC EXCITATION FOR PLANE PROGRESSIVE WAVE TESTING AT NORMAL INCIDENCE (OA SPL 140 dB)

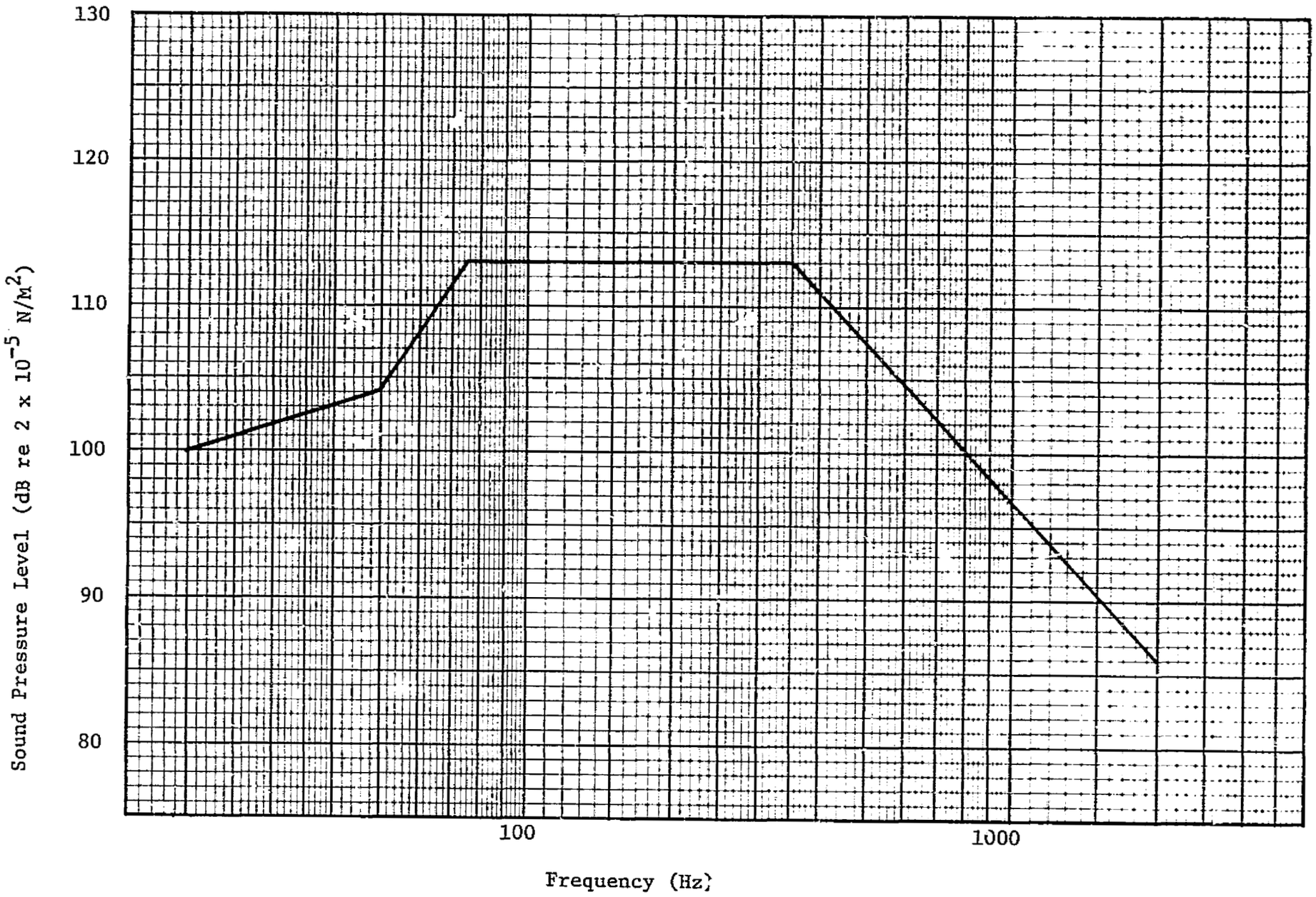

FIGURE 84. SMOOTHED PSD OF ACOUSTIC EXCITATION FOR PLANE PROGRESSIVE WAVE TESTING AT PARALLEL INCIDENCE (OA SPL 140 dB)

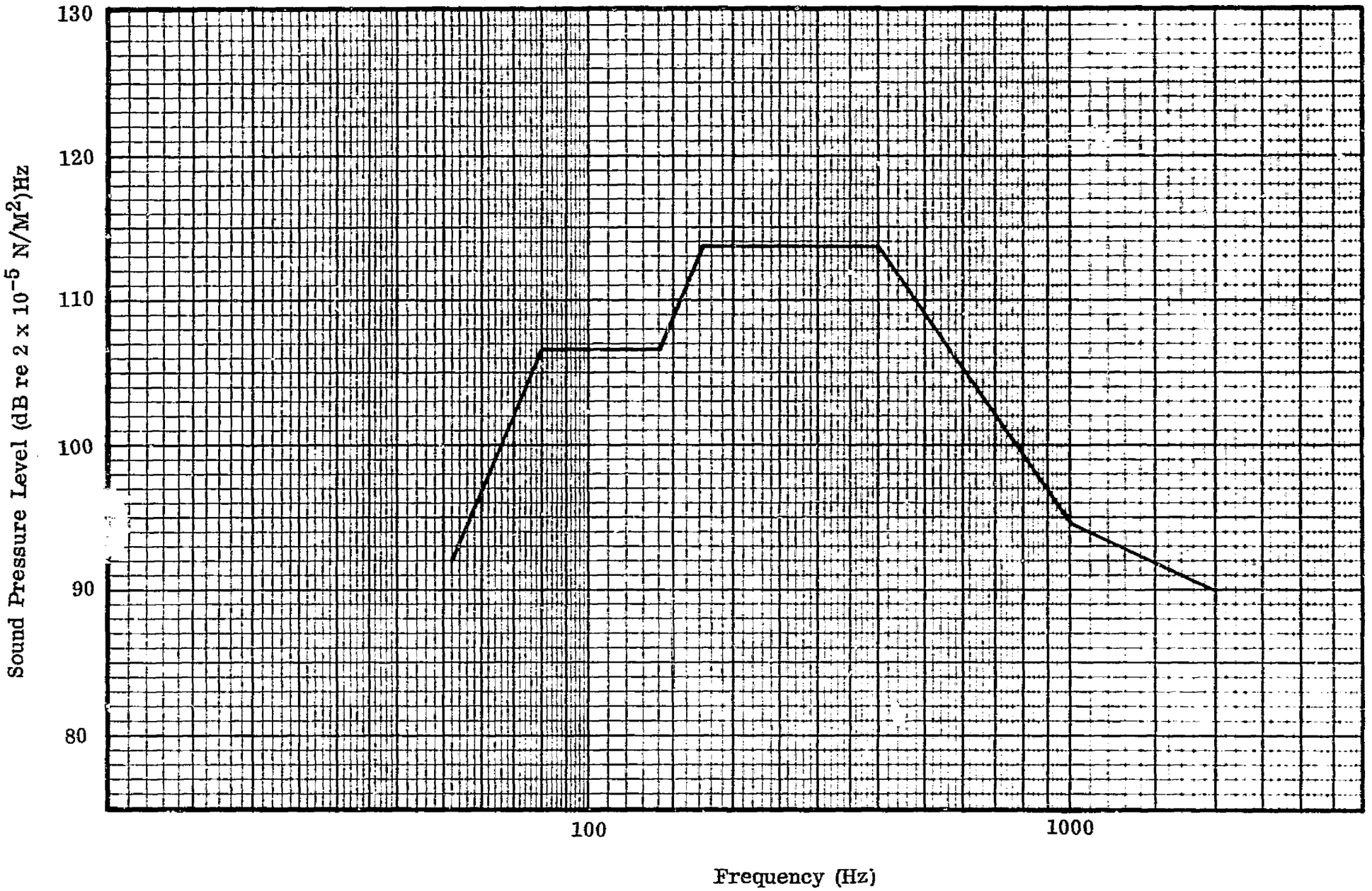

FIGURE 85. SMOOTHED PSD OF ACOUSTIC EXCITATION FOR REVERBERANT ACOUSTIC TESTING (OA SPL 140 dB)

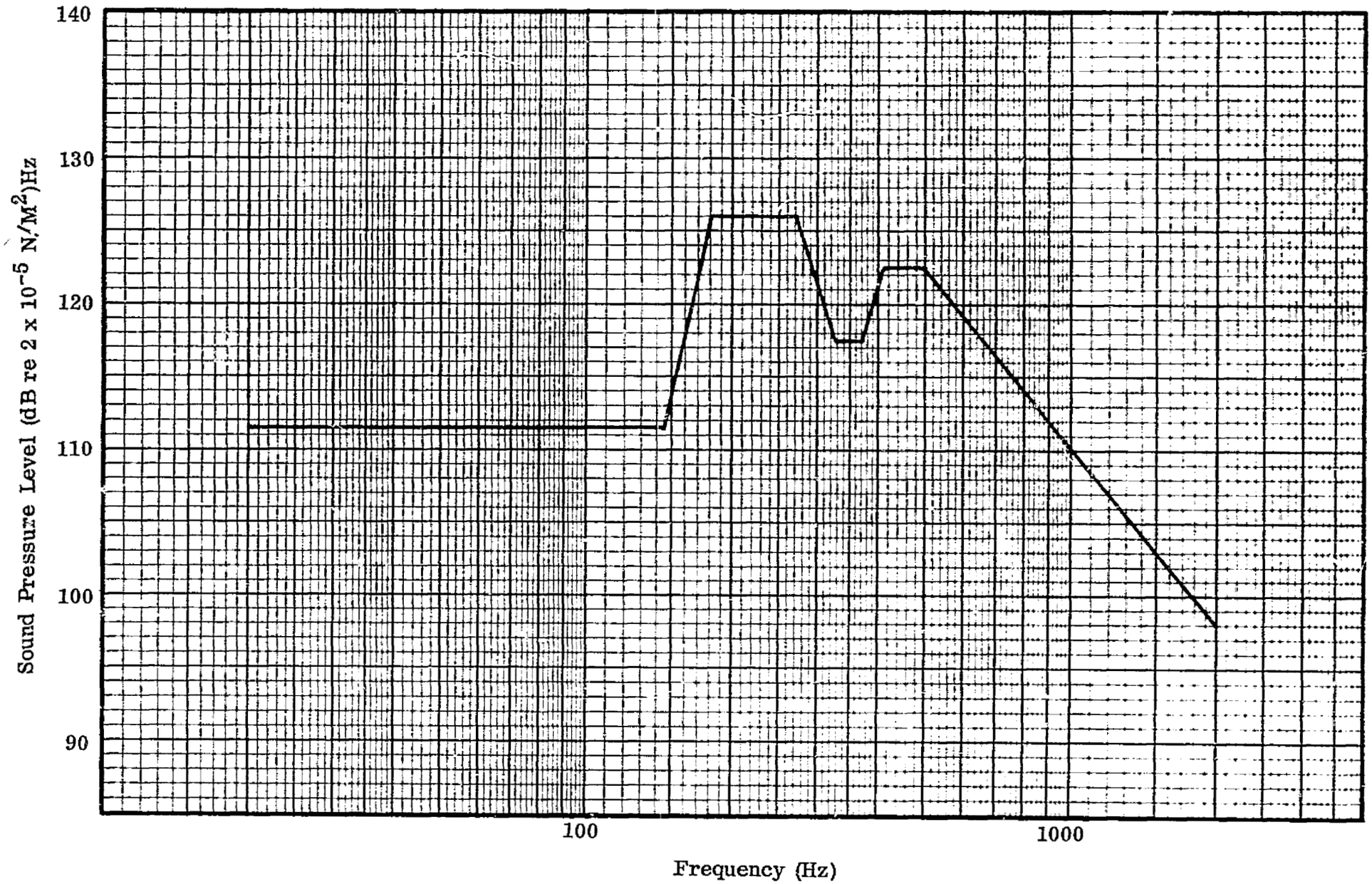

FIGURE 86. SMOOTHED PSD OF ACOUSTIC EXCITATION FOR LOCALIZED EXCITATION PROGRESSIVE WAVE TESTING AT PARALLEL INCIDENCE (OA SPL 150 dB)

Location 1 32.4 G_{rms}

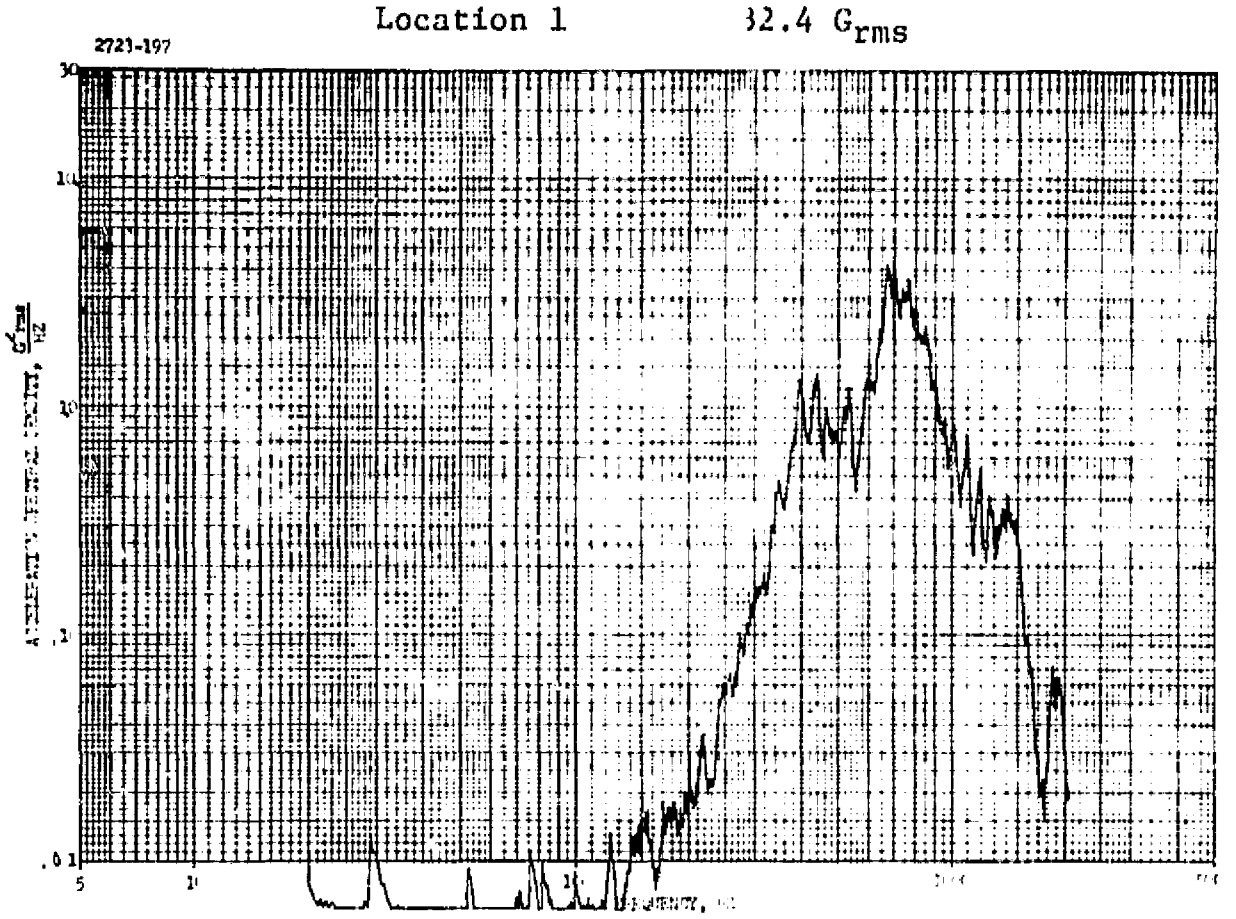

Location 2 38.3 G_{rms}

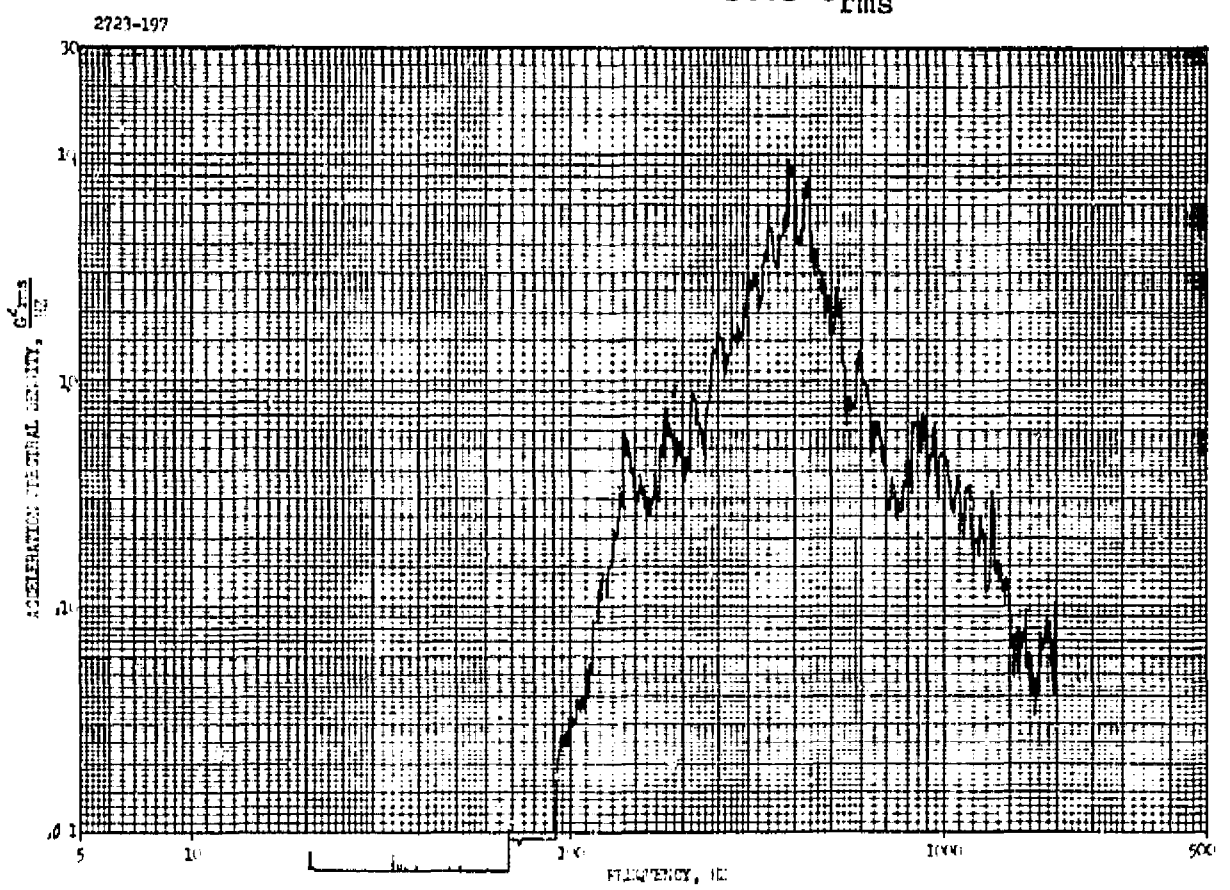

FIGURE 87. TEST # 1 DATA

Location 3 41.2 G_{rms}

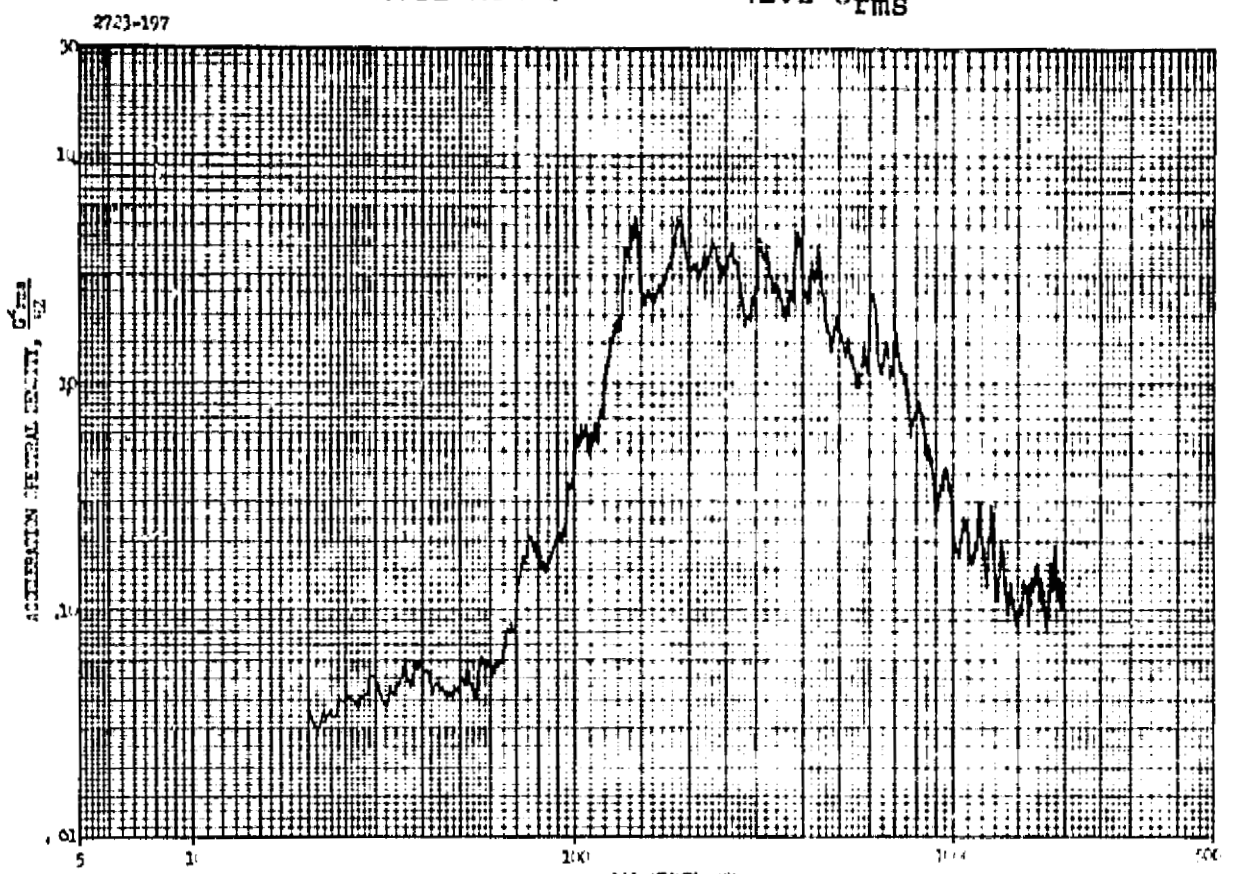

Location 4 38.2 G_{rms}

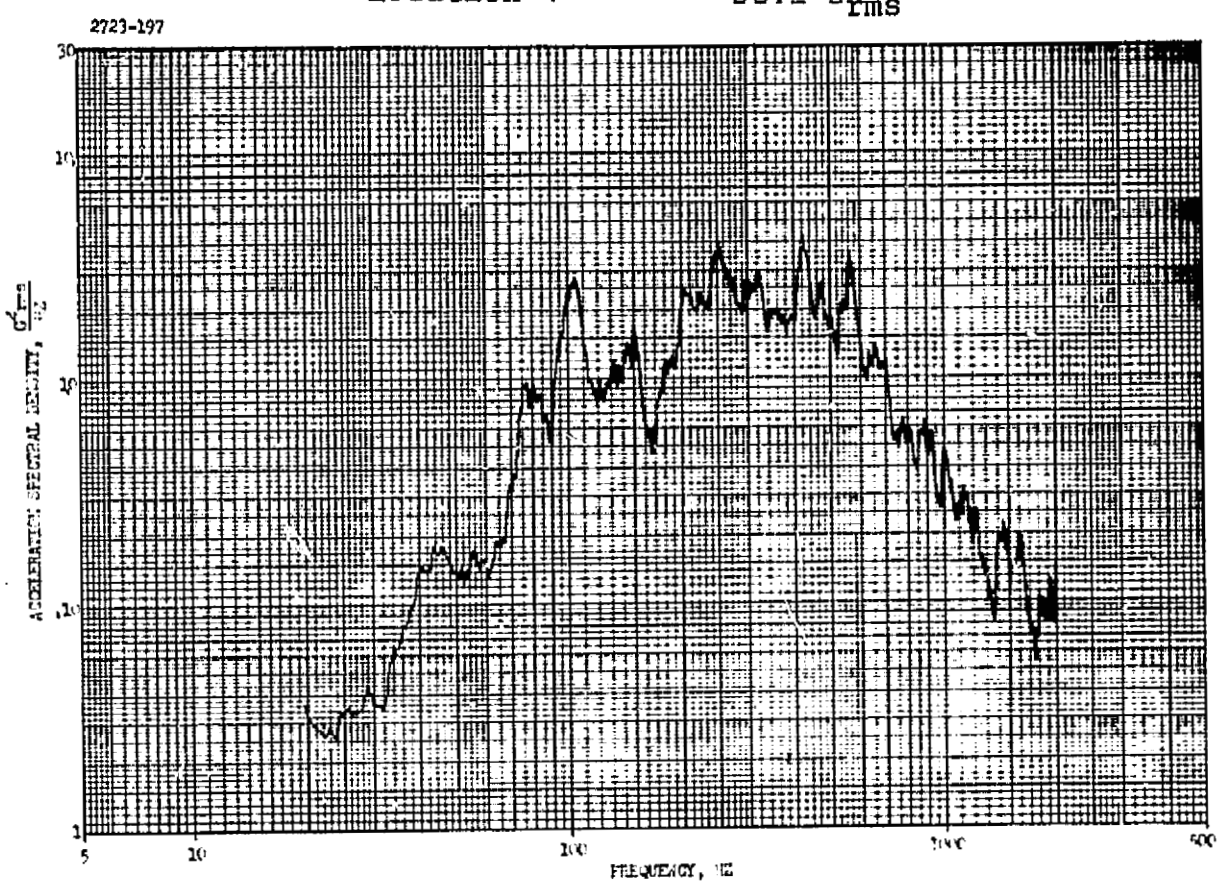

FIGURE 87. TEST #1 DATA (Continued)

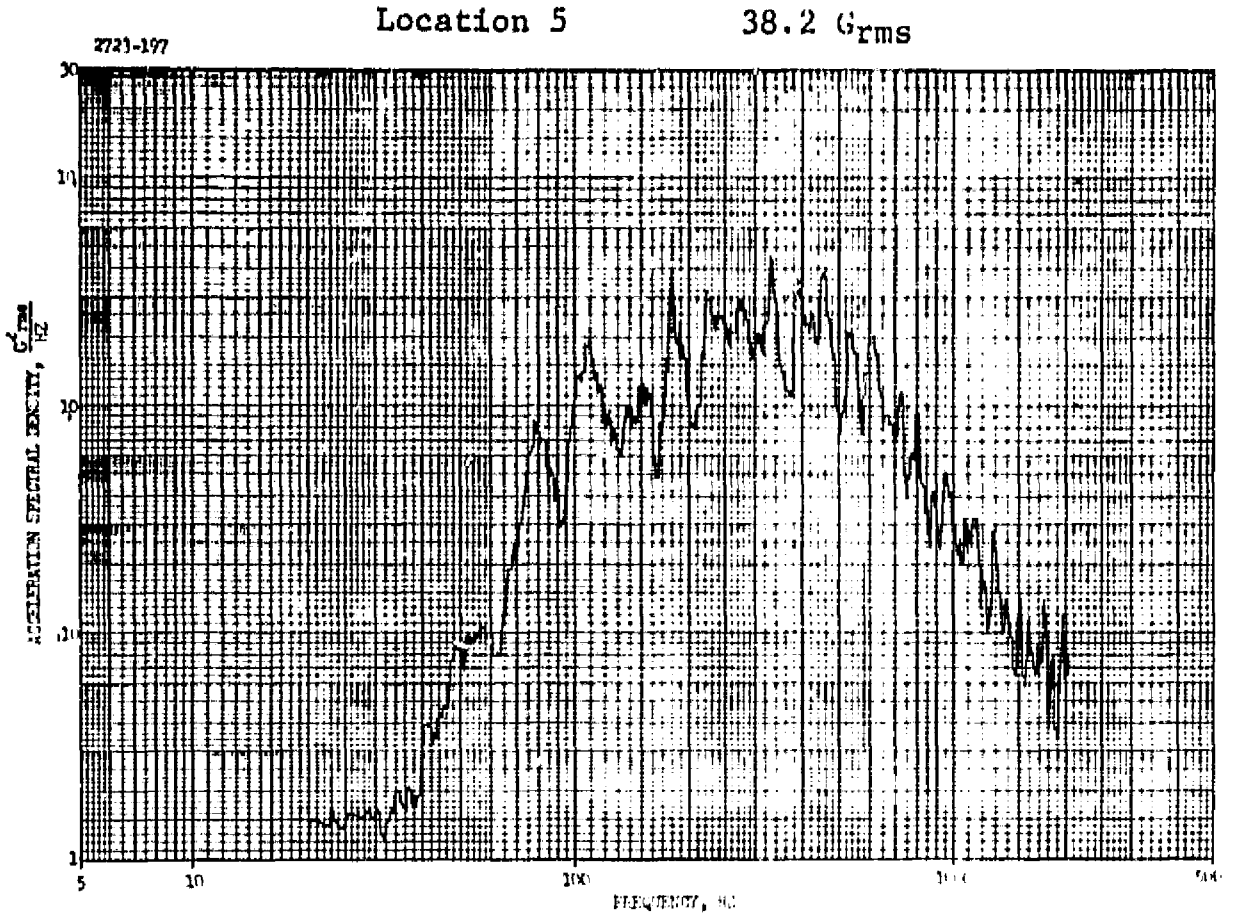

FIGURE 87. TEST #1 DATA (Concluded)

Location 1 20.6 G_{rms}

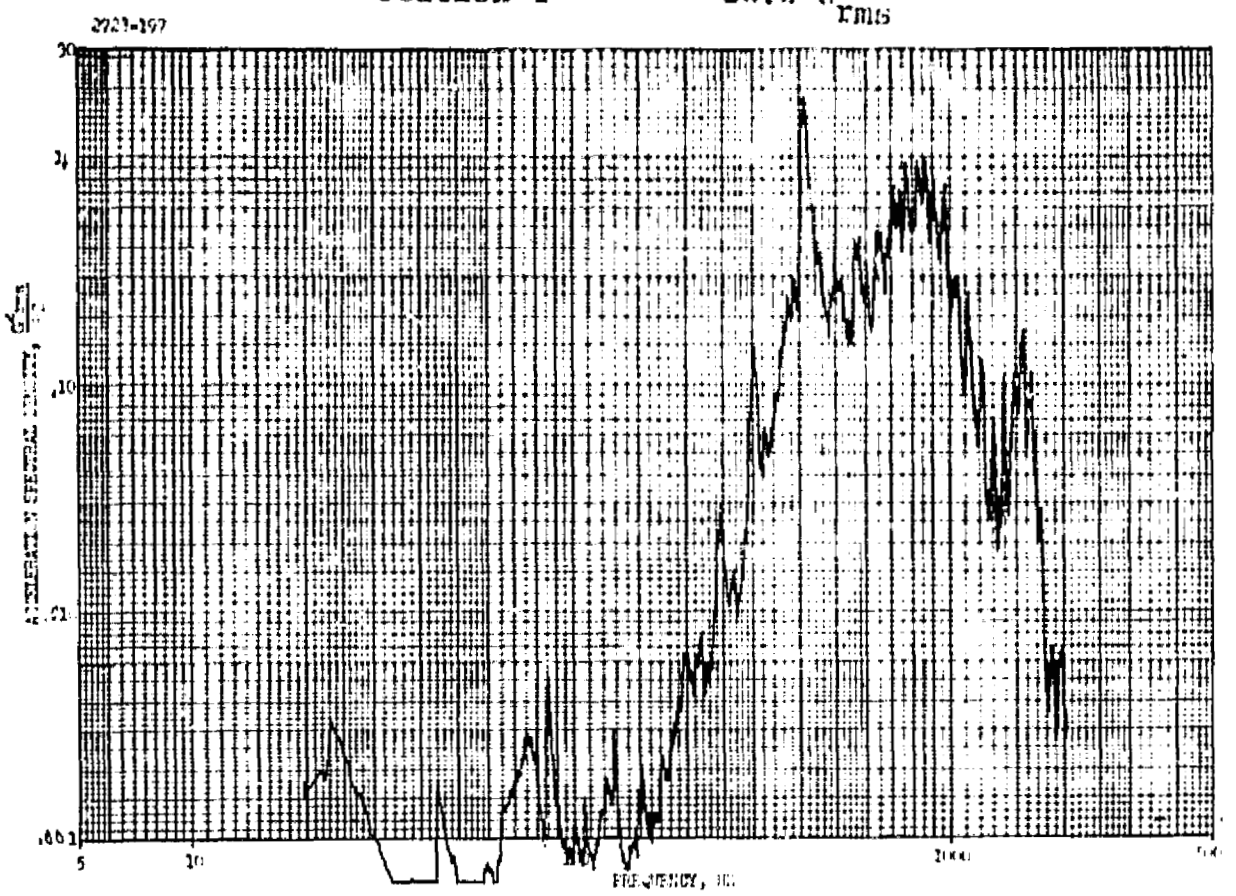

Location 2 32.4 G_{rms}

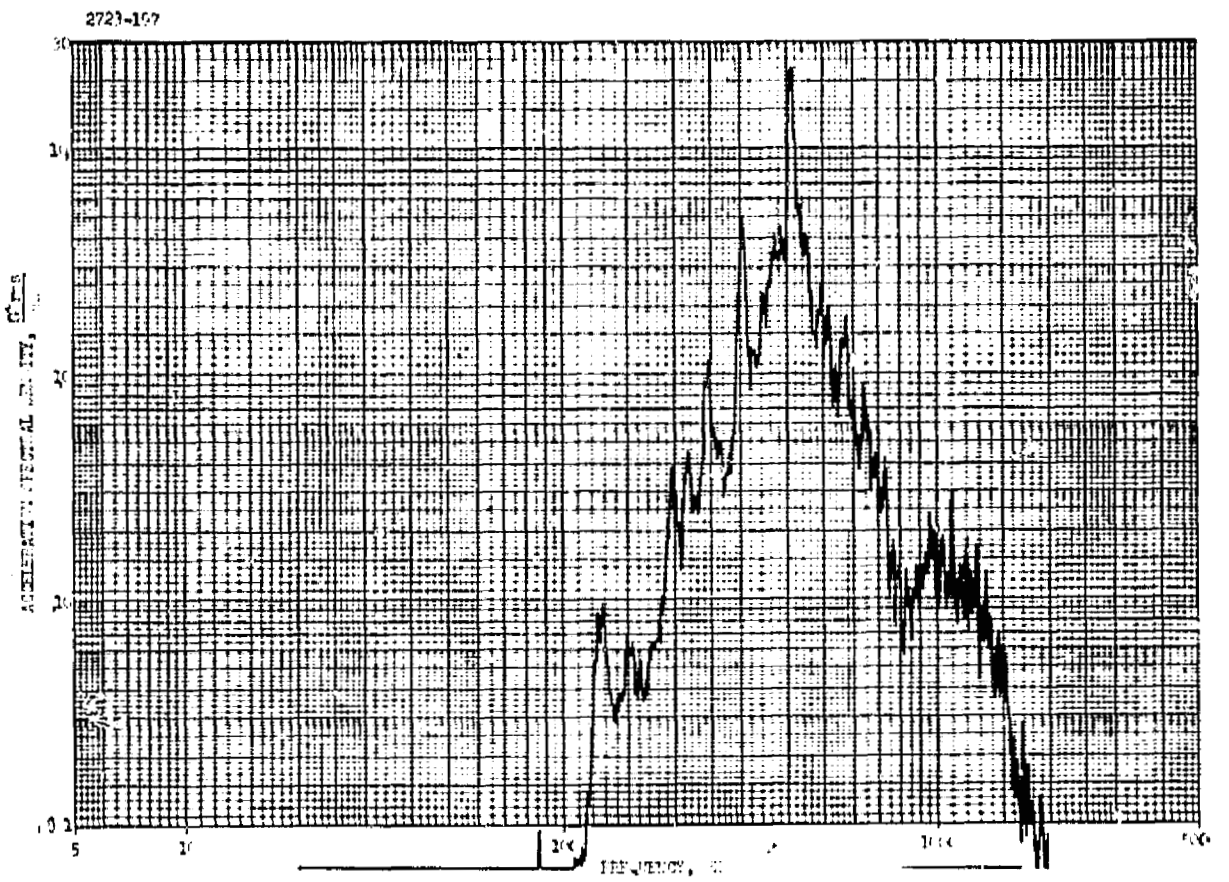

FIGURE 88. TEST # 2 DATA

Location 3 35.3 G_{rms}

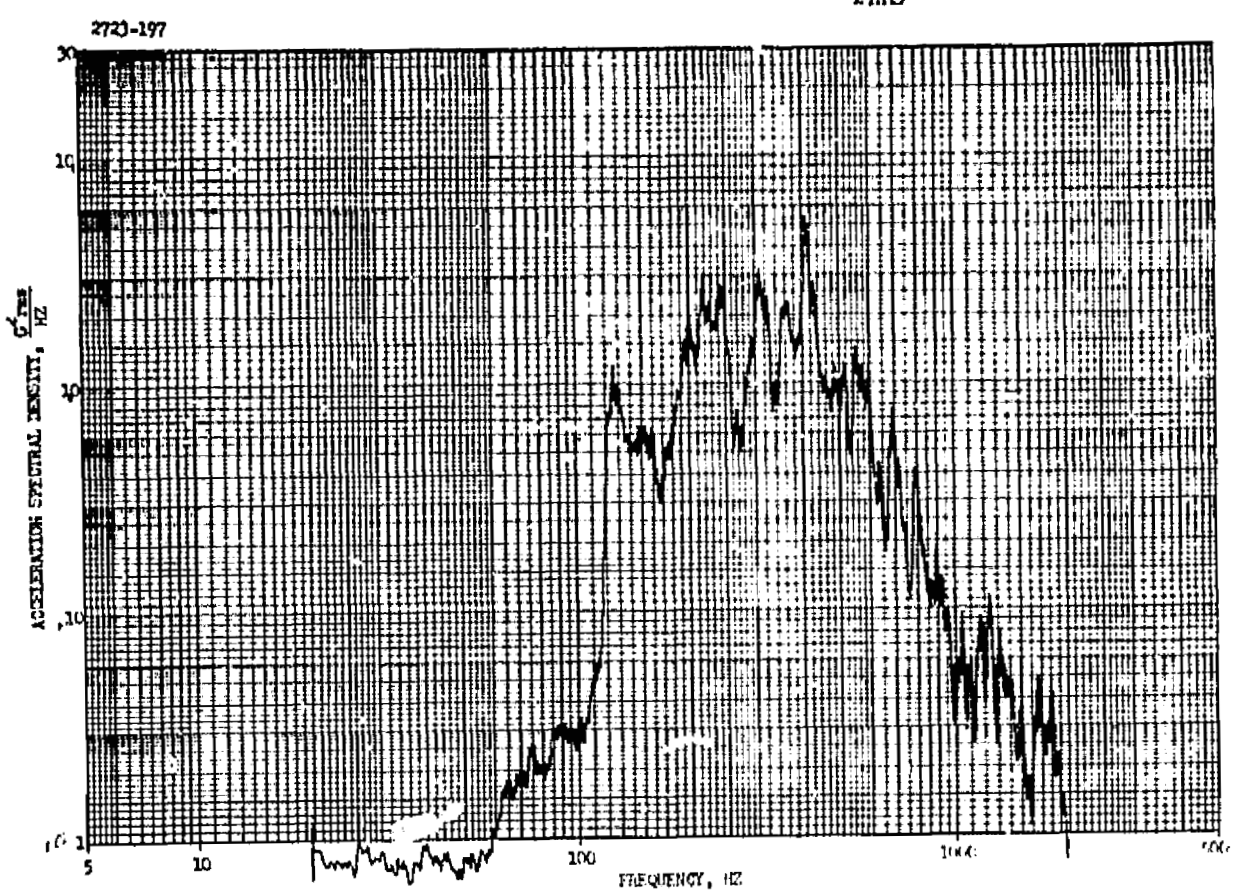

Location 4 28.2 G_{rms}

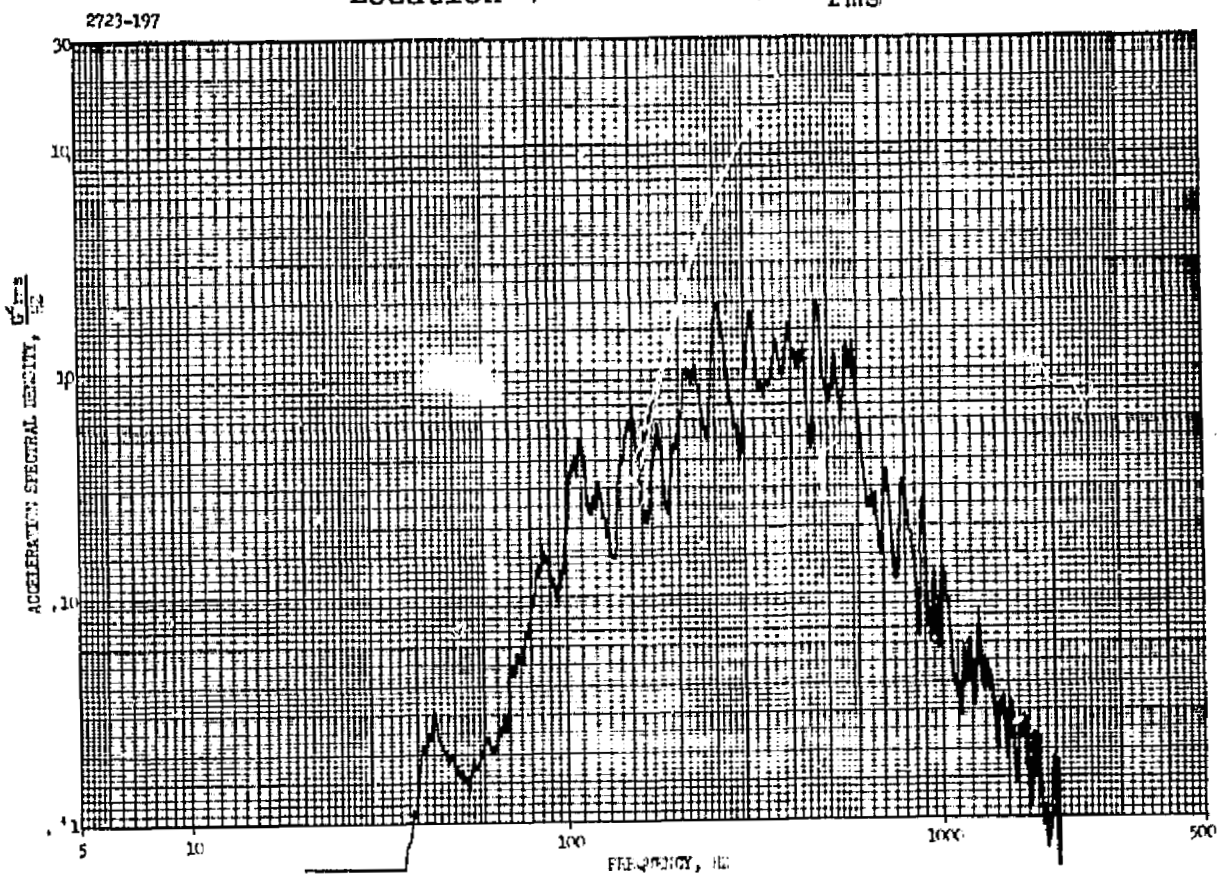

FIGURE 88. TEST #2 DATA (Continued)

Location 5 35.3 G_{rms}

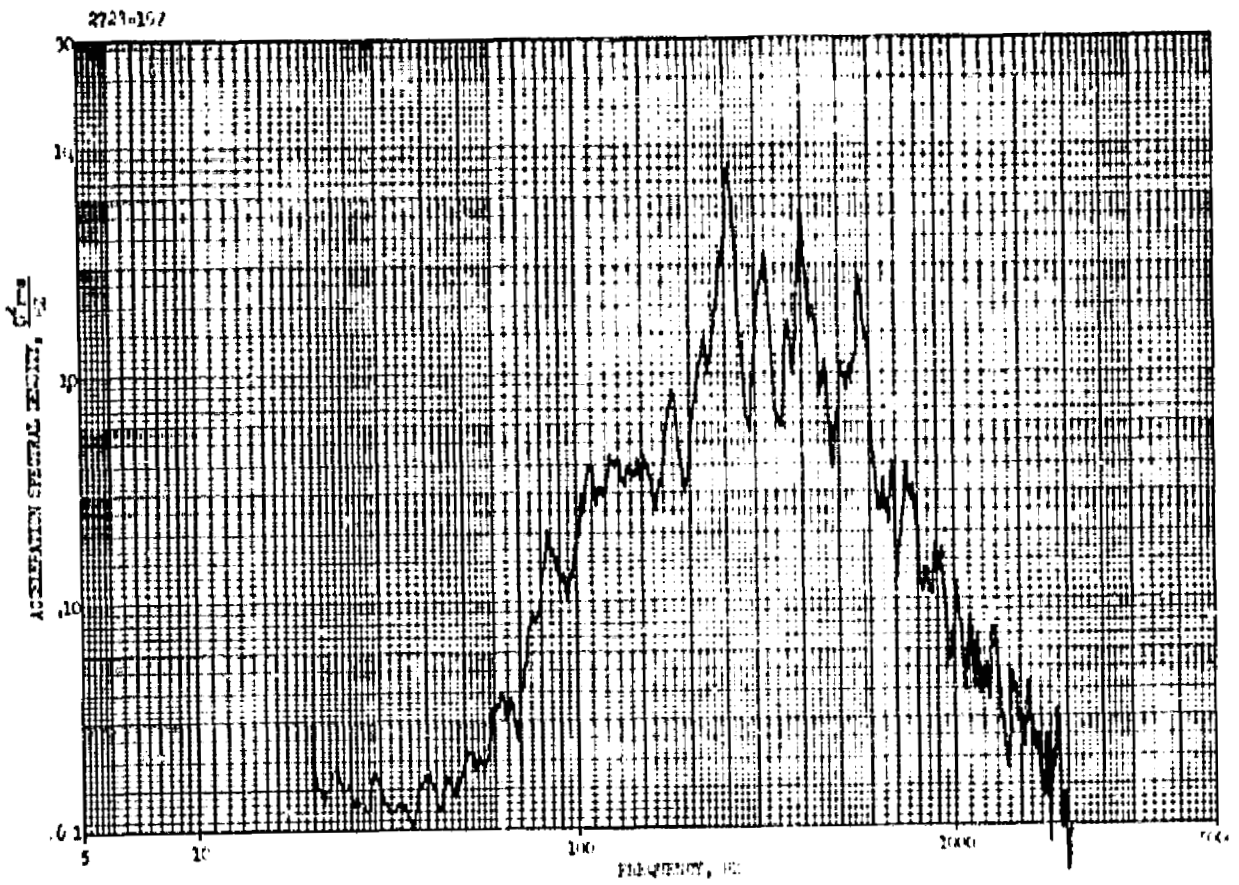

FIGURE 88. TEST #2 DATA (Concluded)

Location 1 19.4 G_{rms}

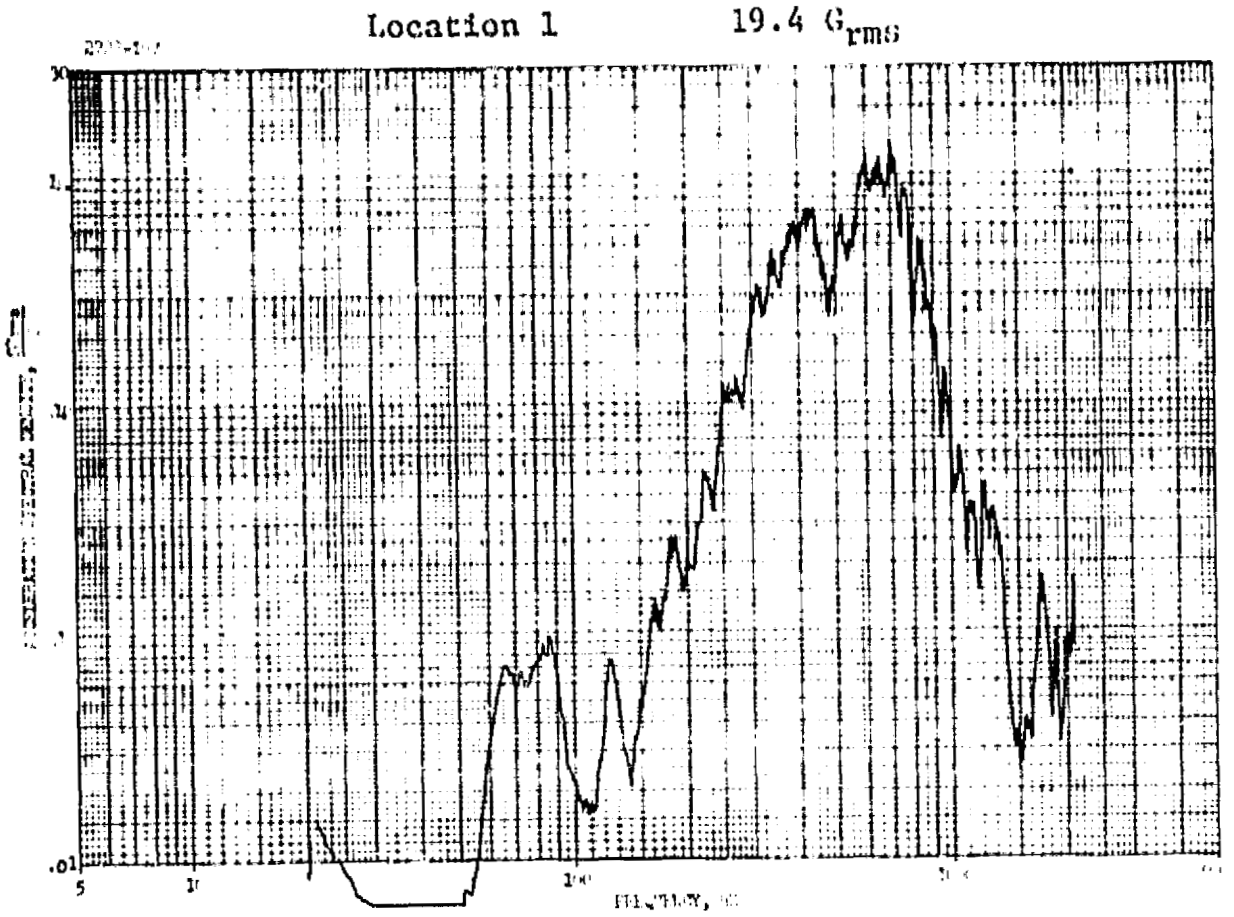

Location 2 26.5 G_{rms}

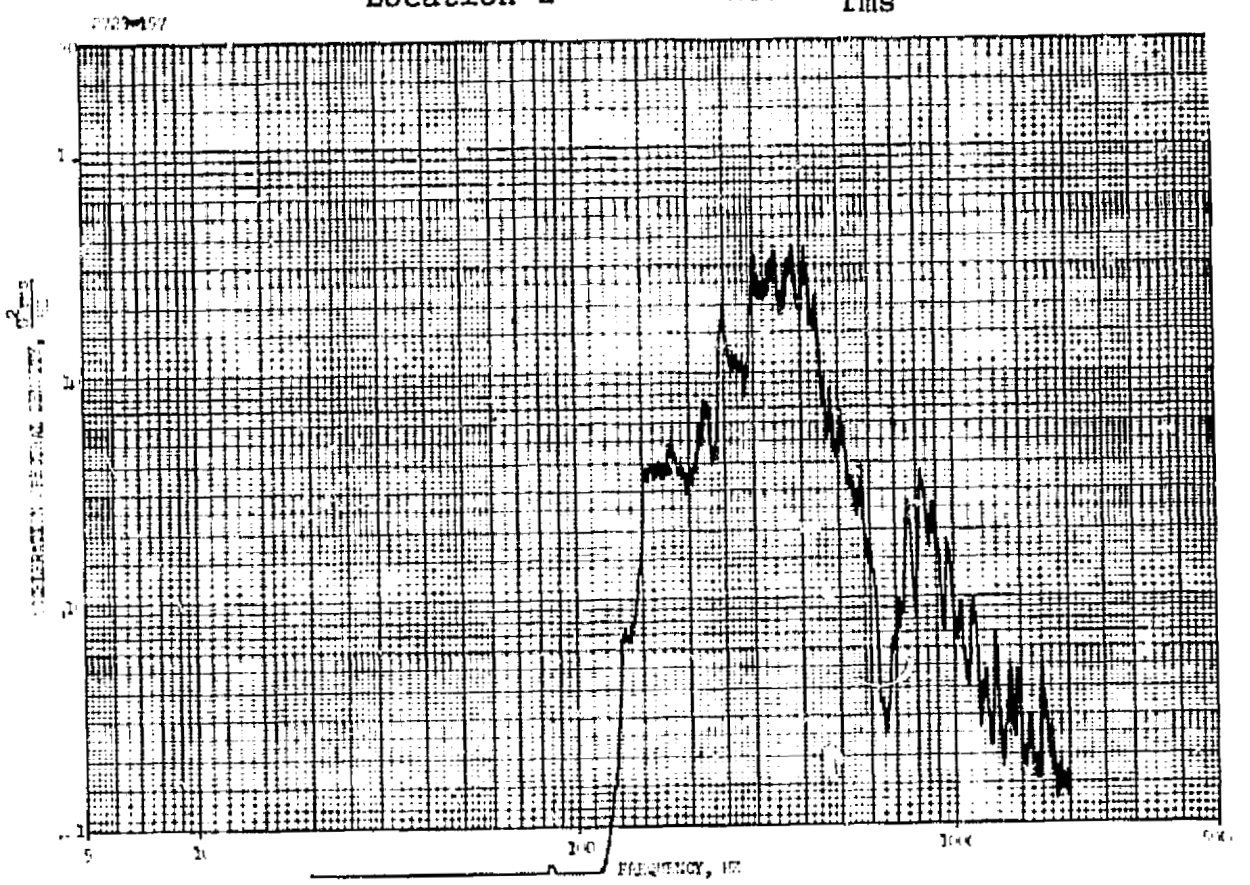

FIGURE 89. TEST # 3 DATA

Location 3 23.5 G_{rms}

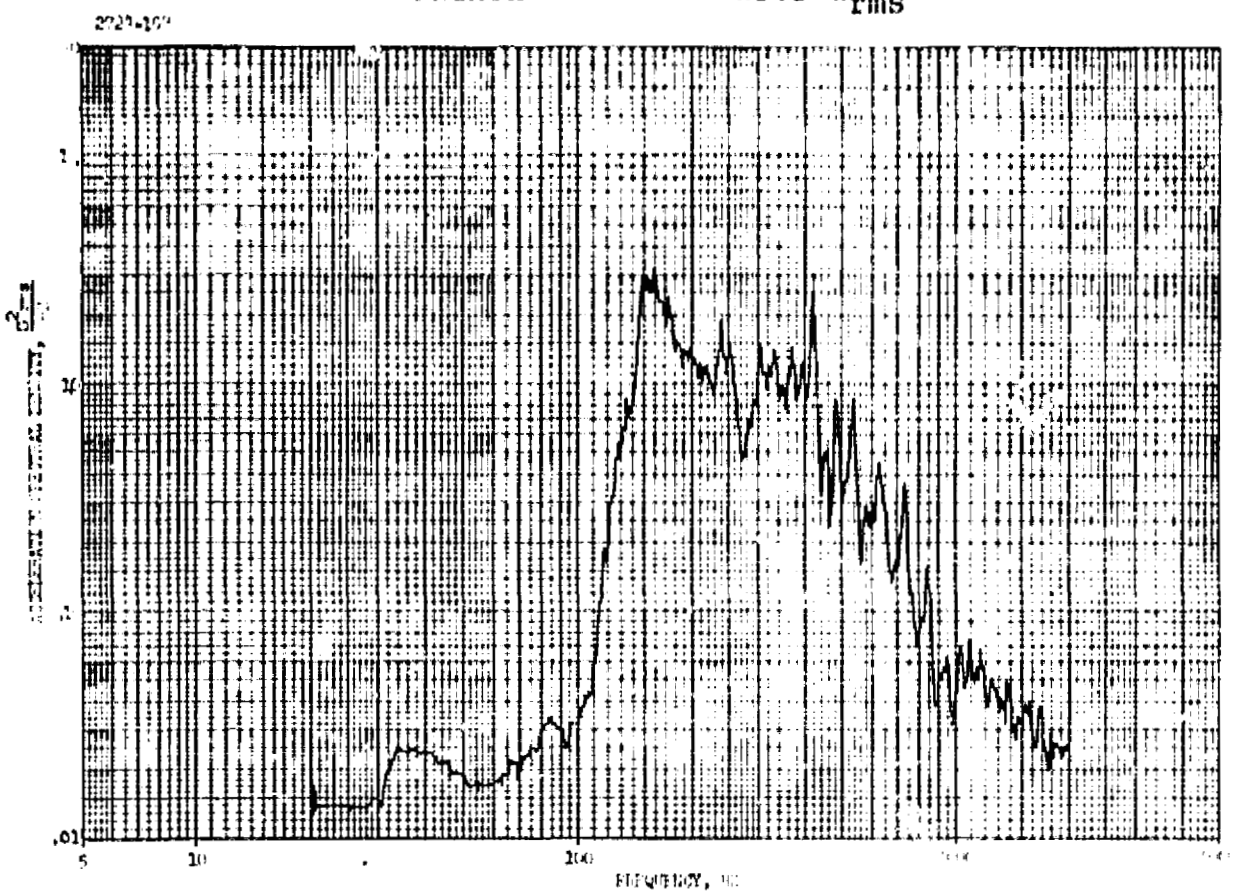

Location 4 23.5 G_{rms}

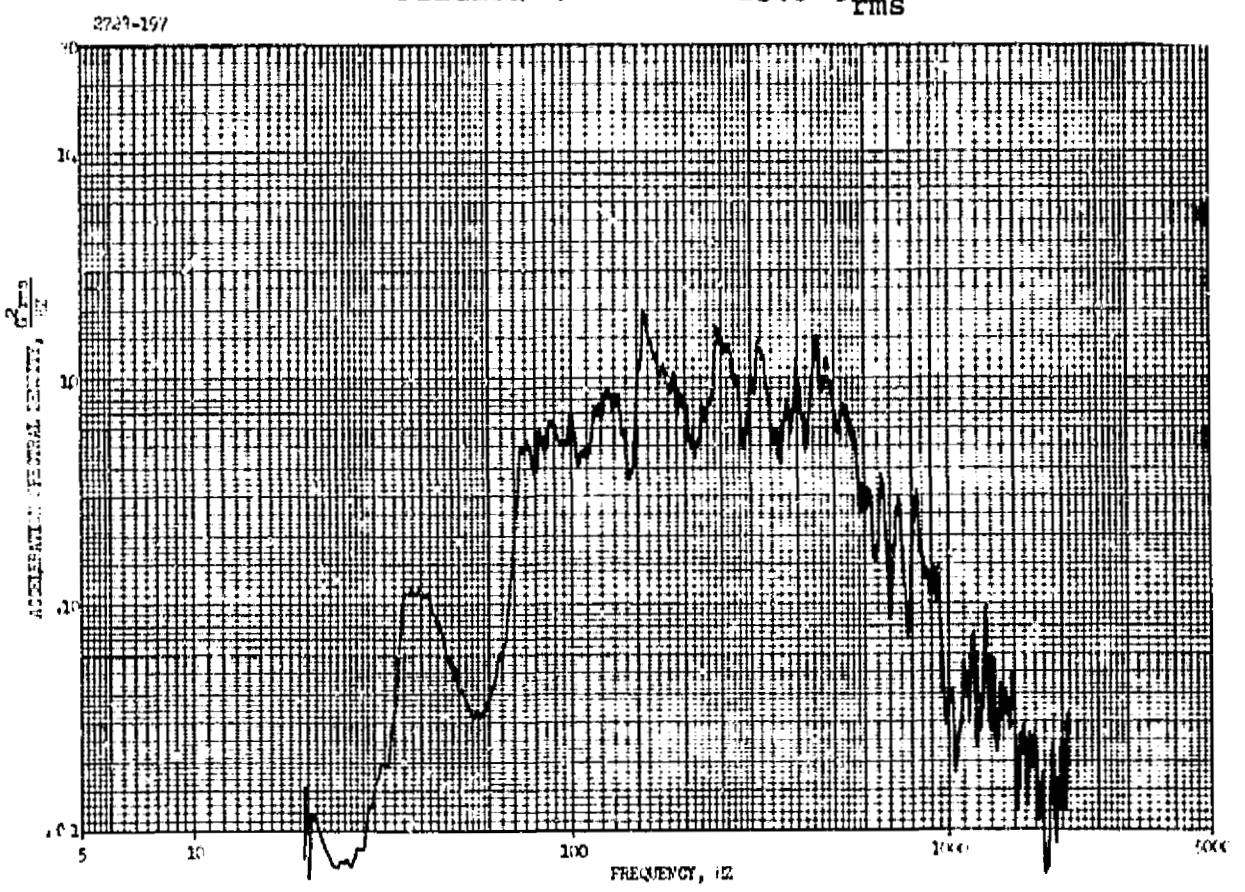

FIGURE 89. TEST #3 DATA (Continued)

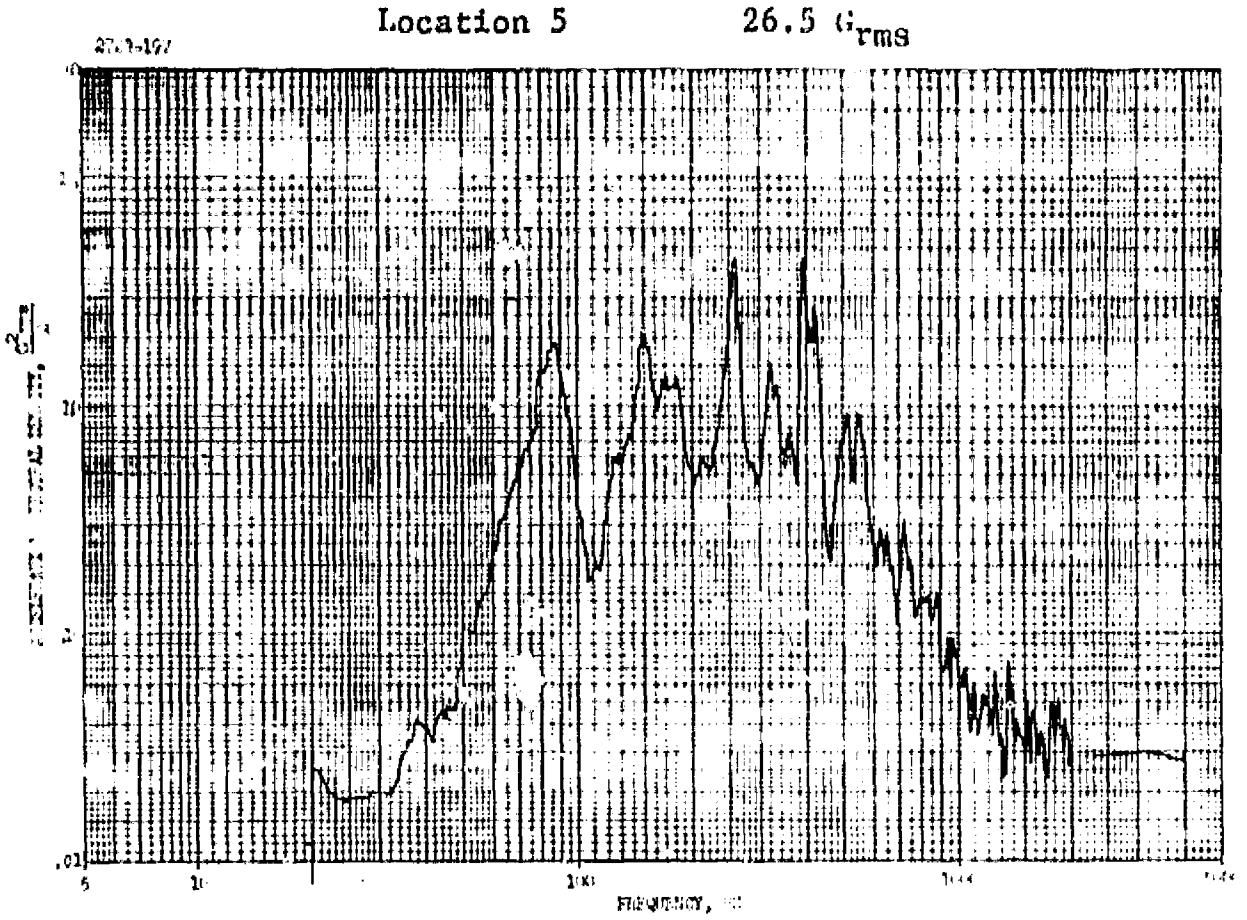

FIGURE 89. TEST #3 DATA (Concluded)

Location 1 64.7 G_{rms}

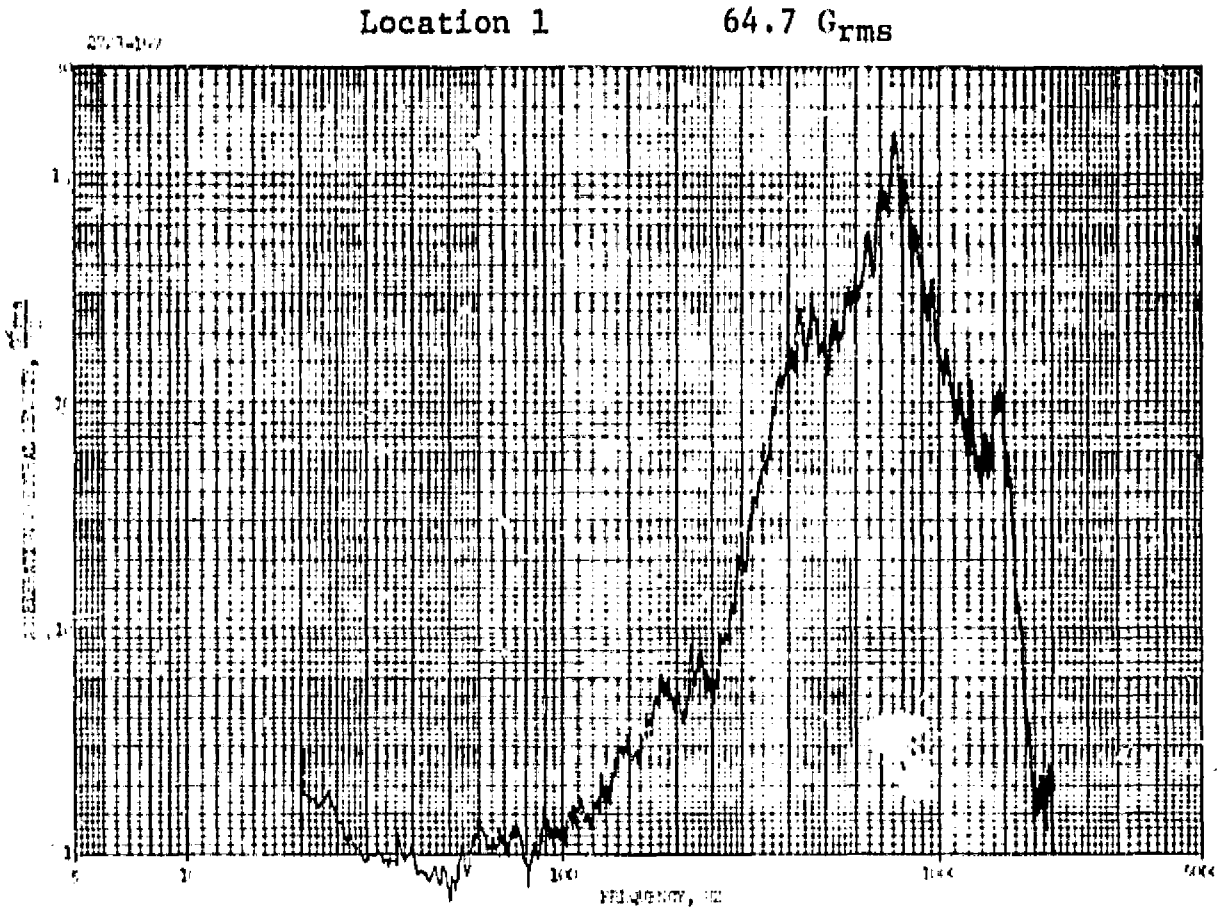

Location 2 70.6 G_{rms}

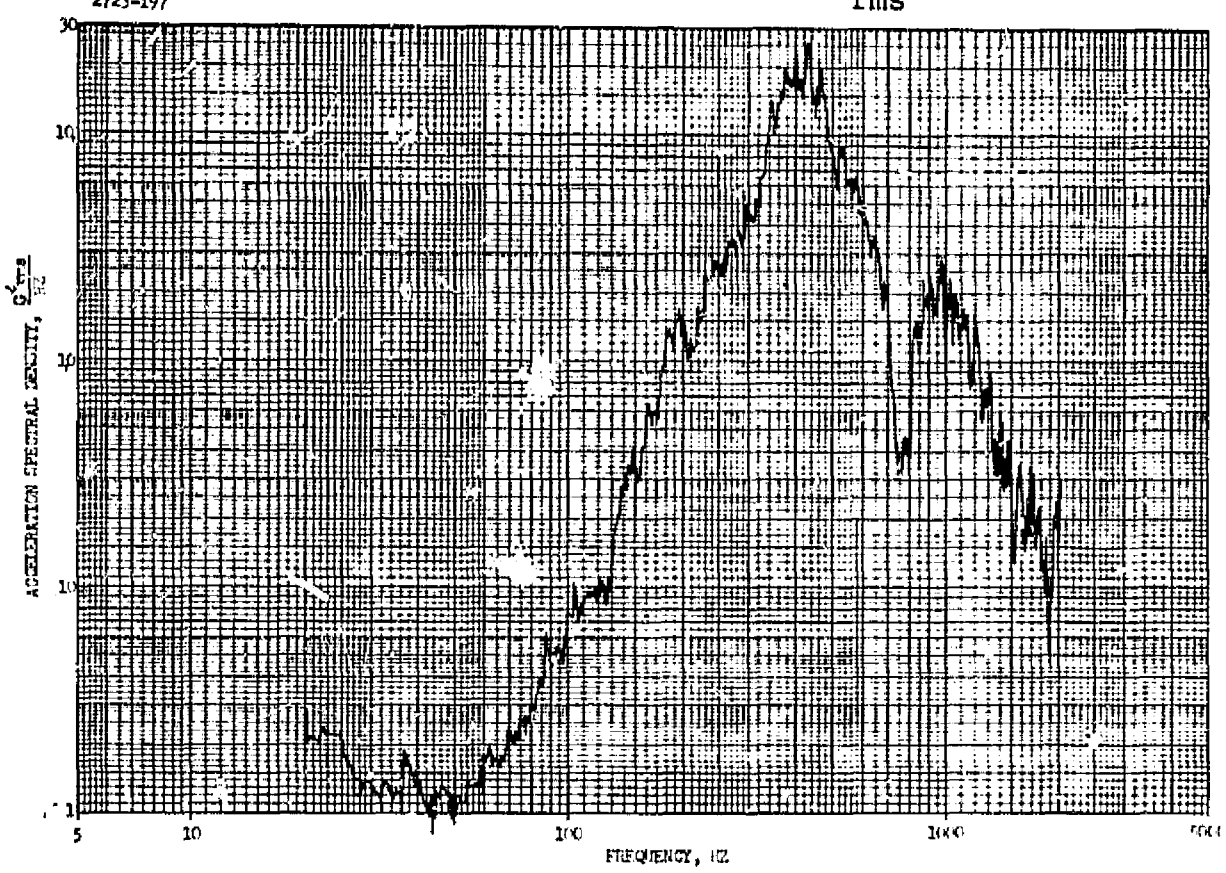

FIGURE 90. TEST # 4 DATA

Location 3 61.8 G_{rms}

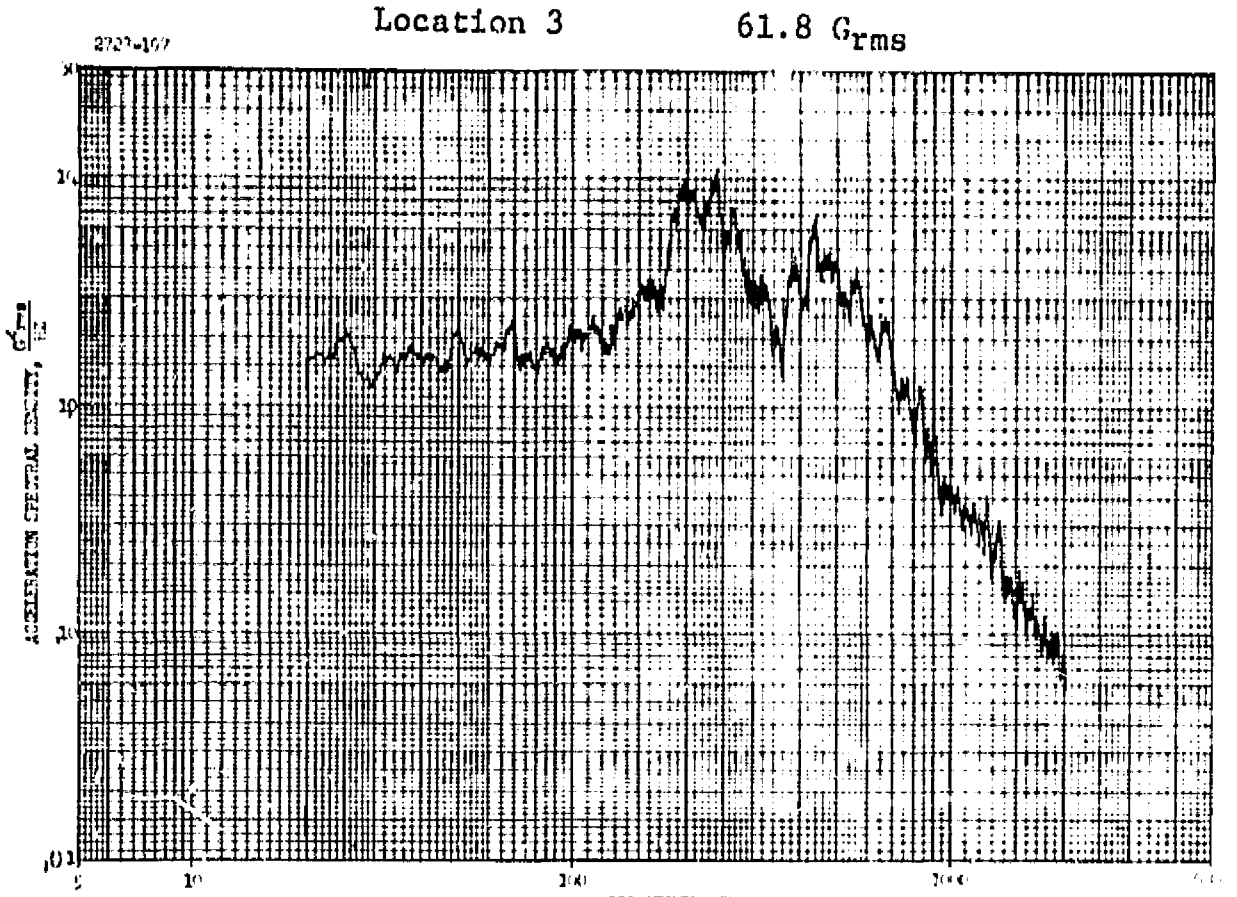

Location 4 67.7 G_{rms}

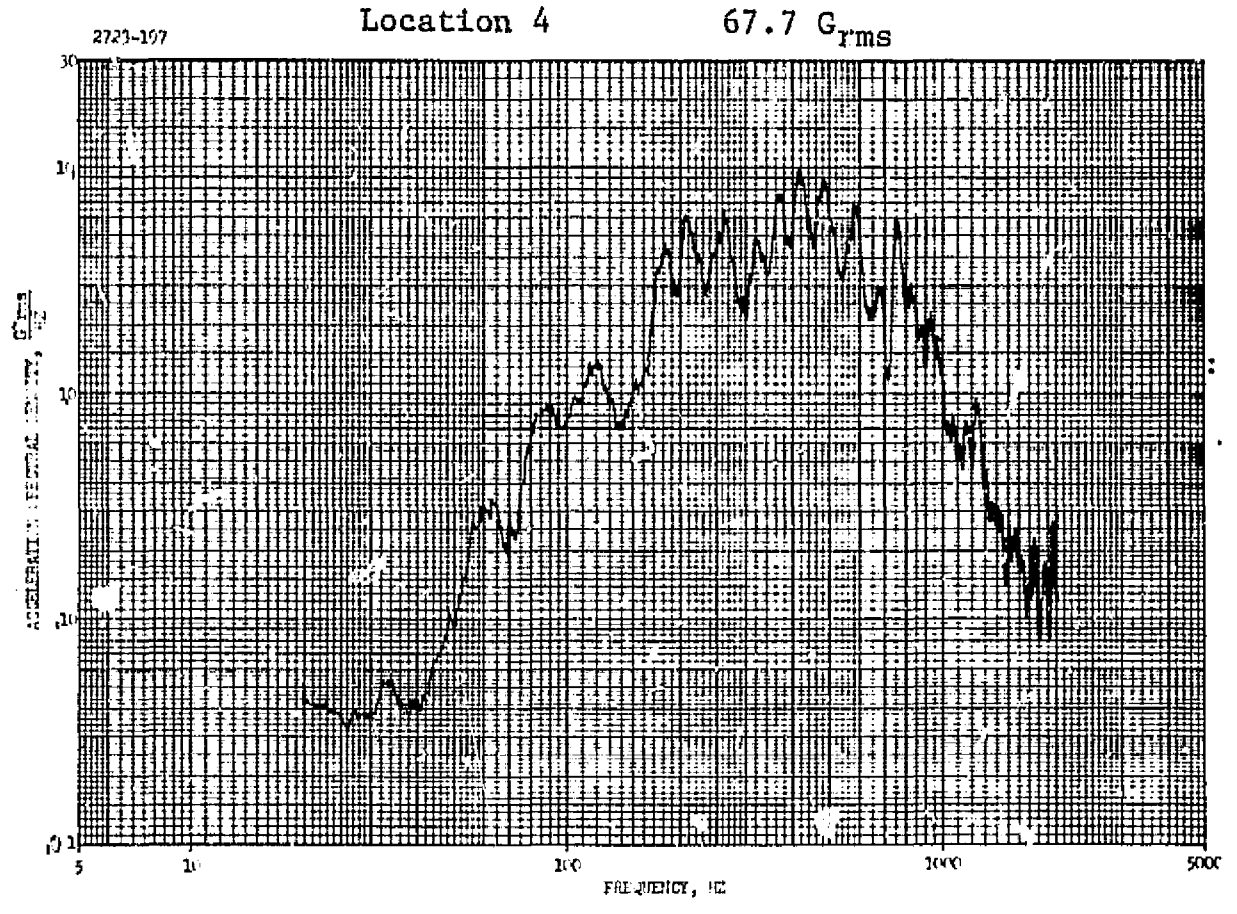

FIGURE 90. TEST #4 DATA (Continued)

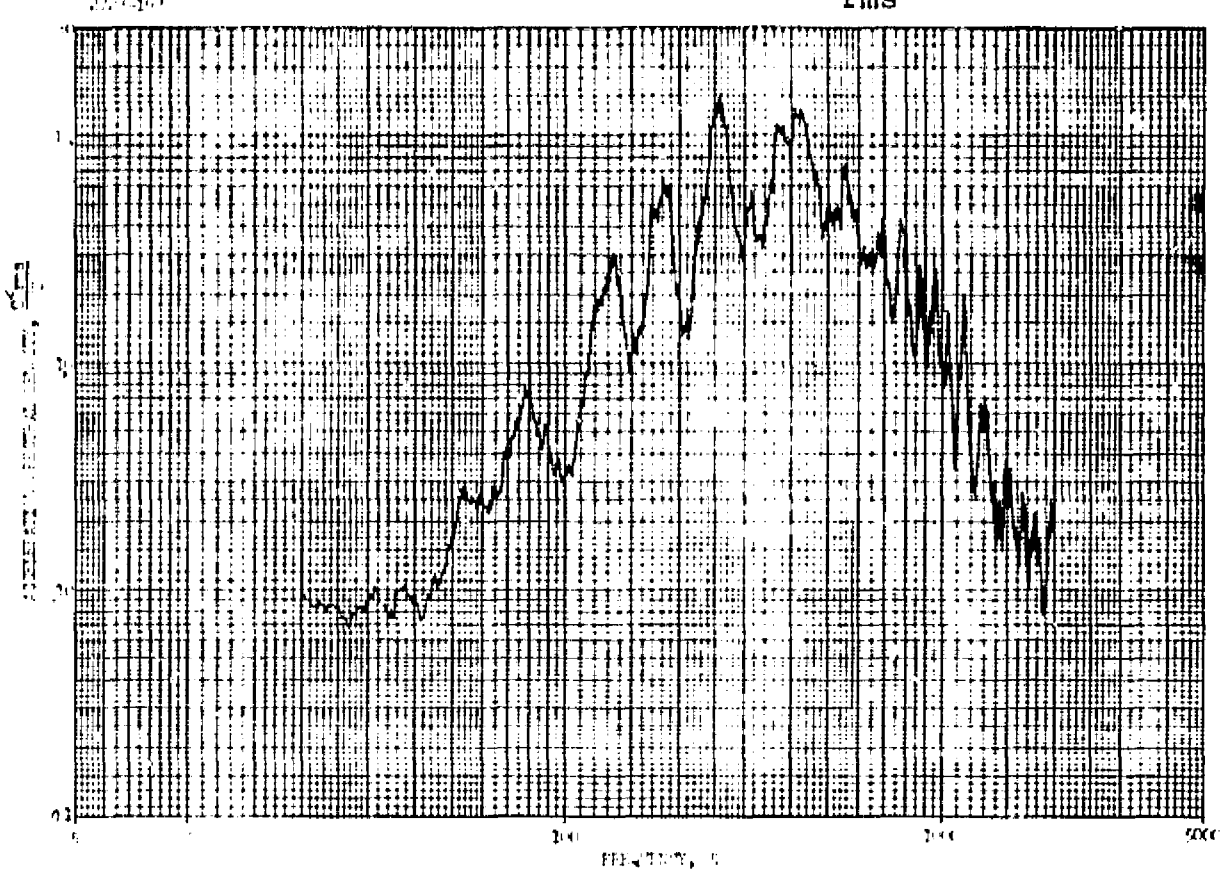

FIGURE 90. TEST #4 DATA (Concluded)

Location 1 3.22 G_{rms}

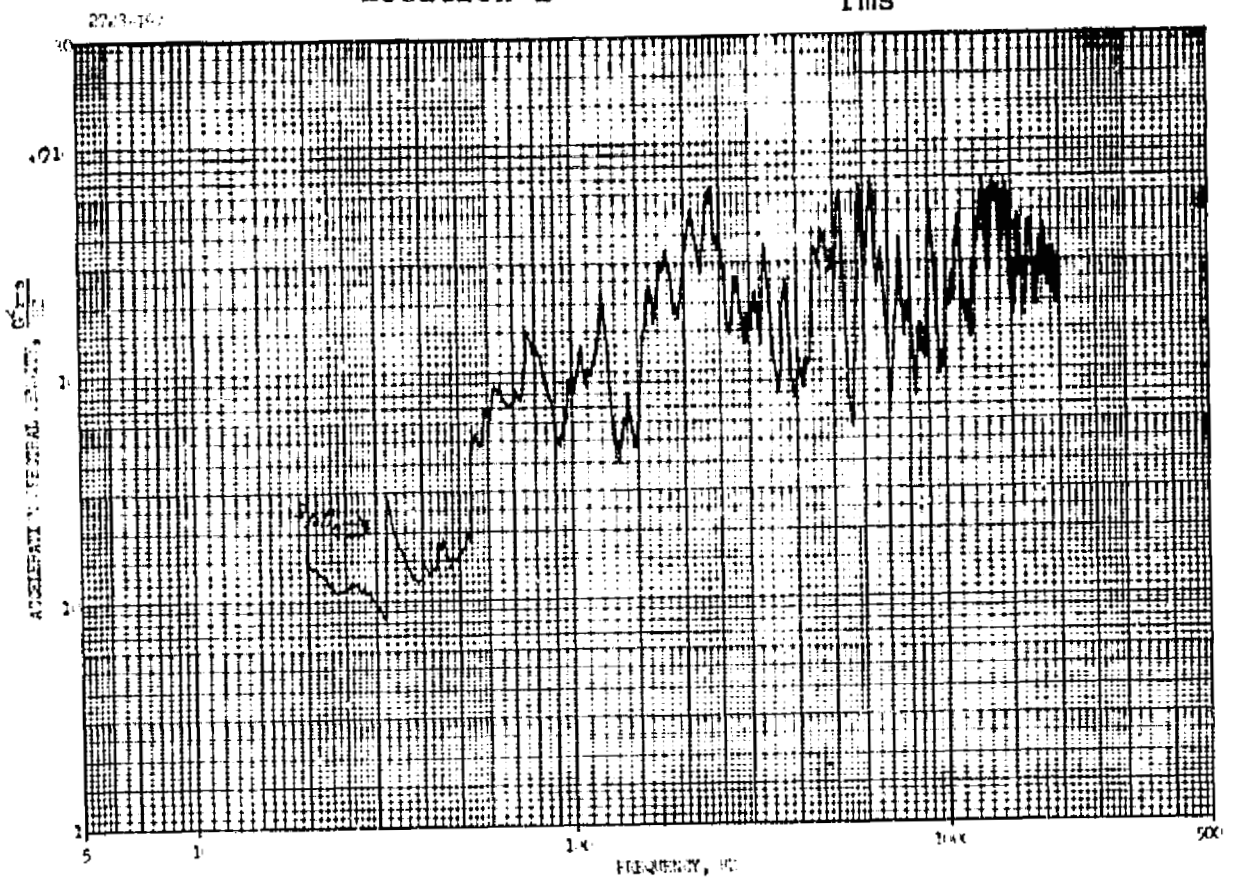

Location 2 6.6 G_{rms}

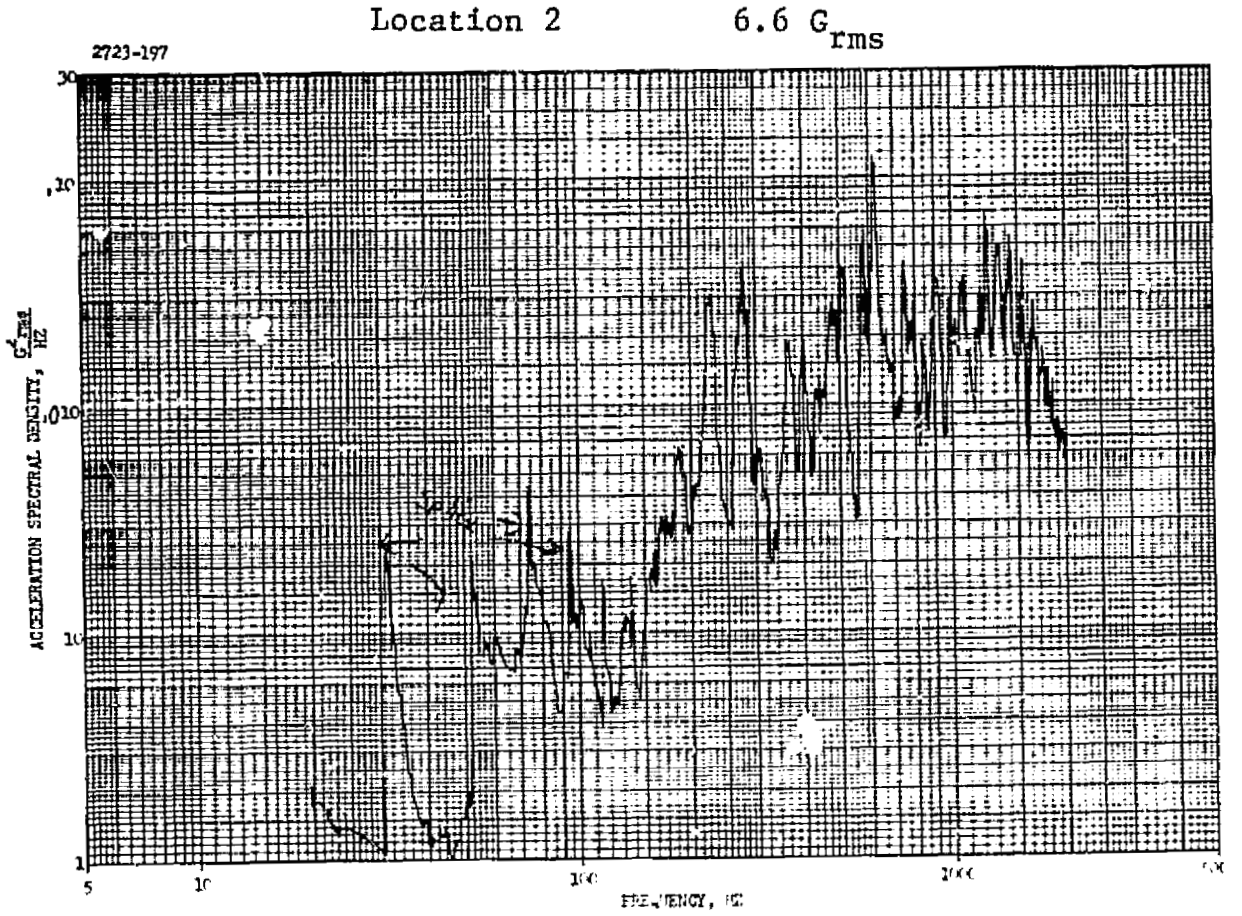

FIGURE 91. TEST # 5 DATA

Location 3 9.8 G_{rms}

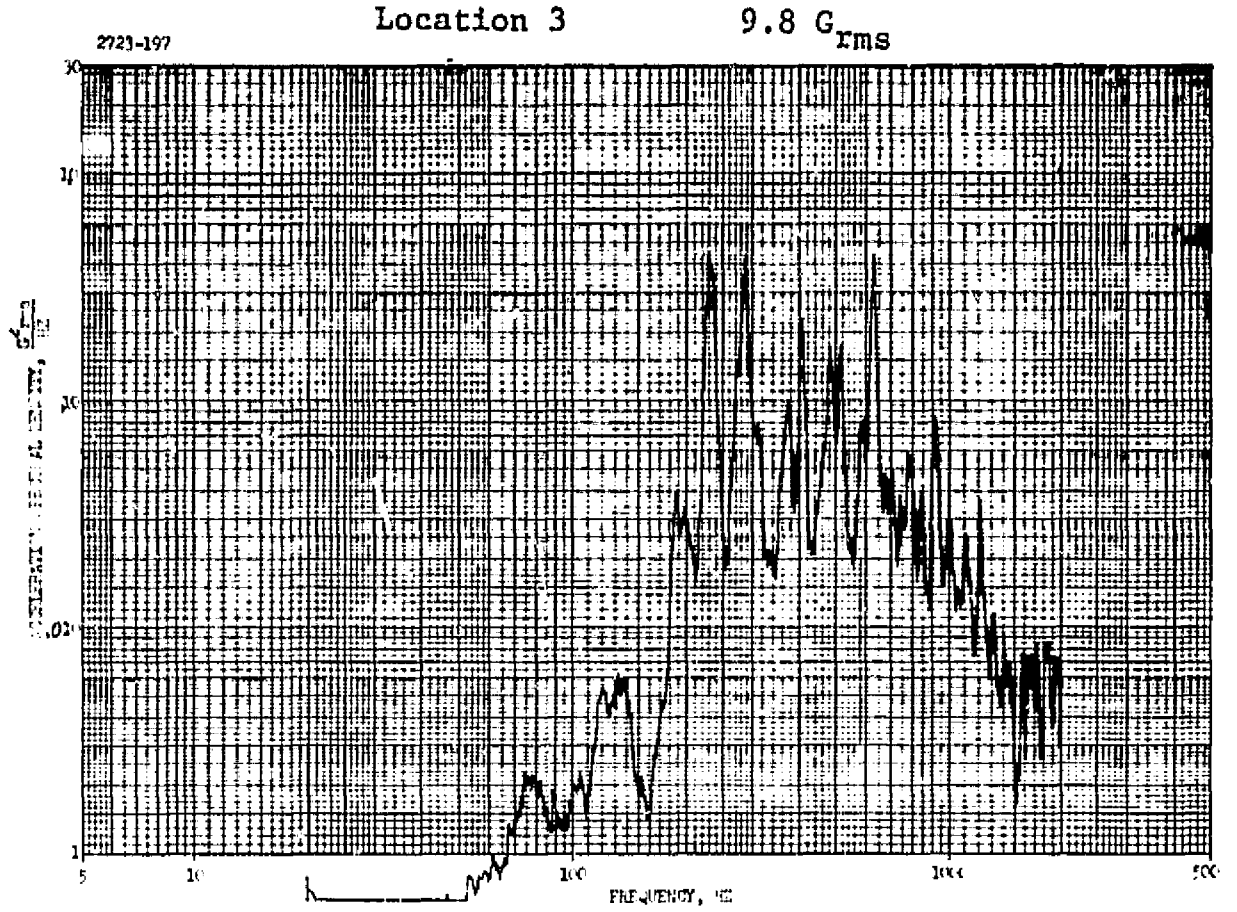

Location 4 9.8 G_{rms}

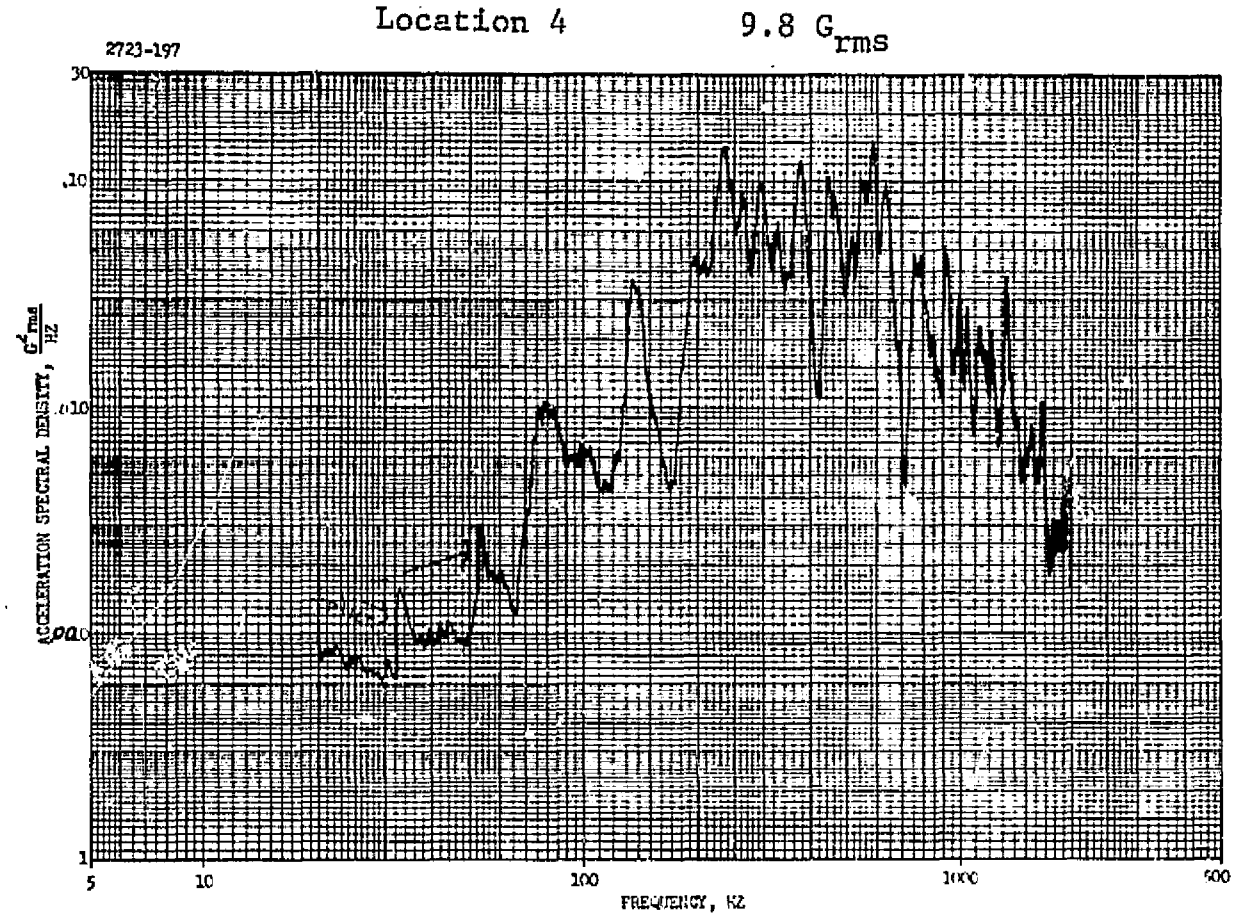

FIGURE 91. TEST #5 DATA (Continued)

Location 5 9.8 G_{rms}

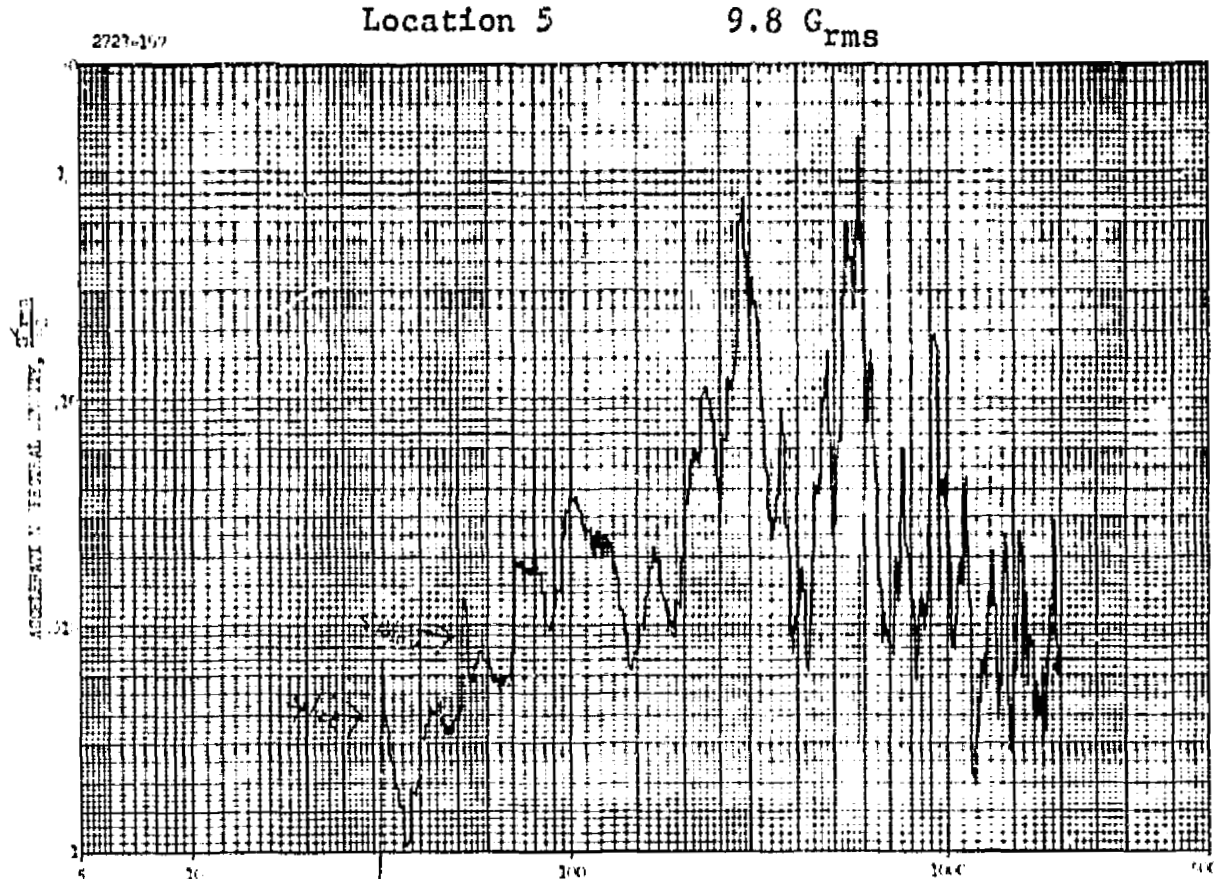

FIGURE 91. TEST #5 DATA (Concluded)

Location 1 1.32 G_{rms}

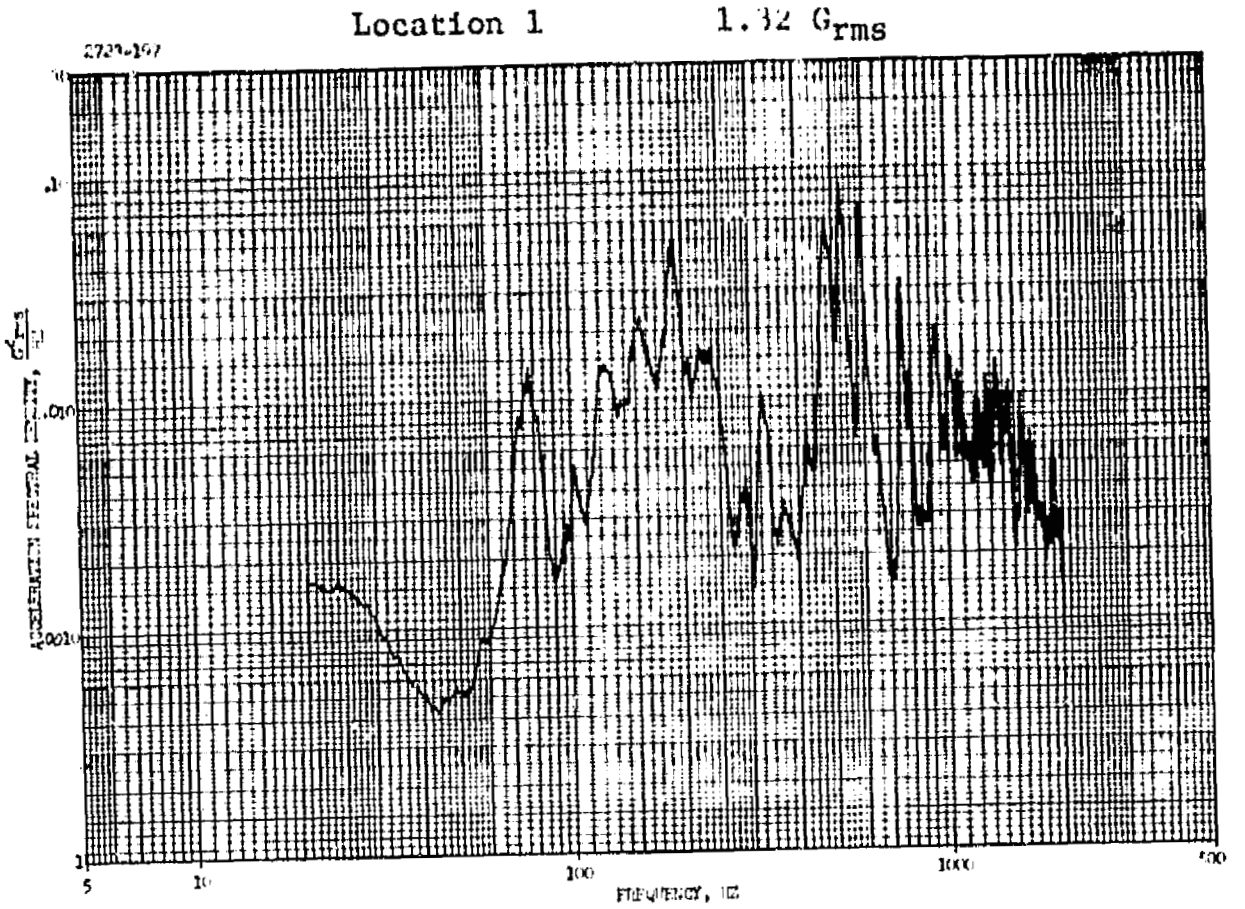

Location 2 2.83 G_{rms}

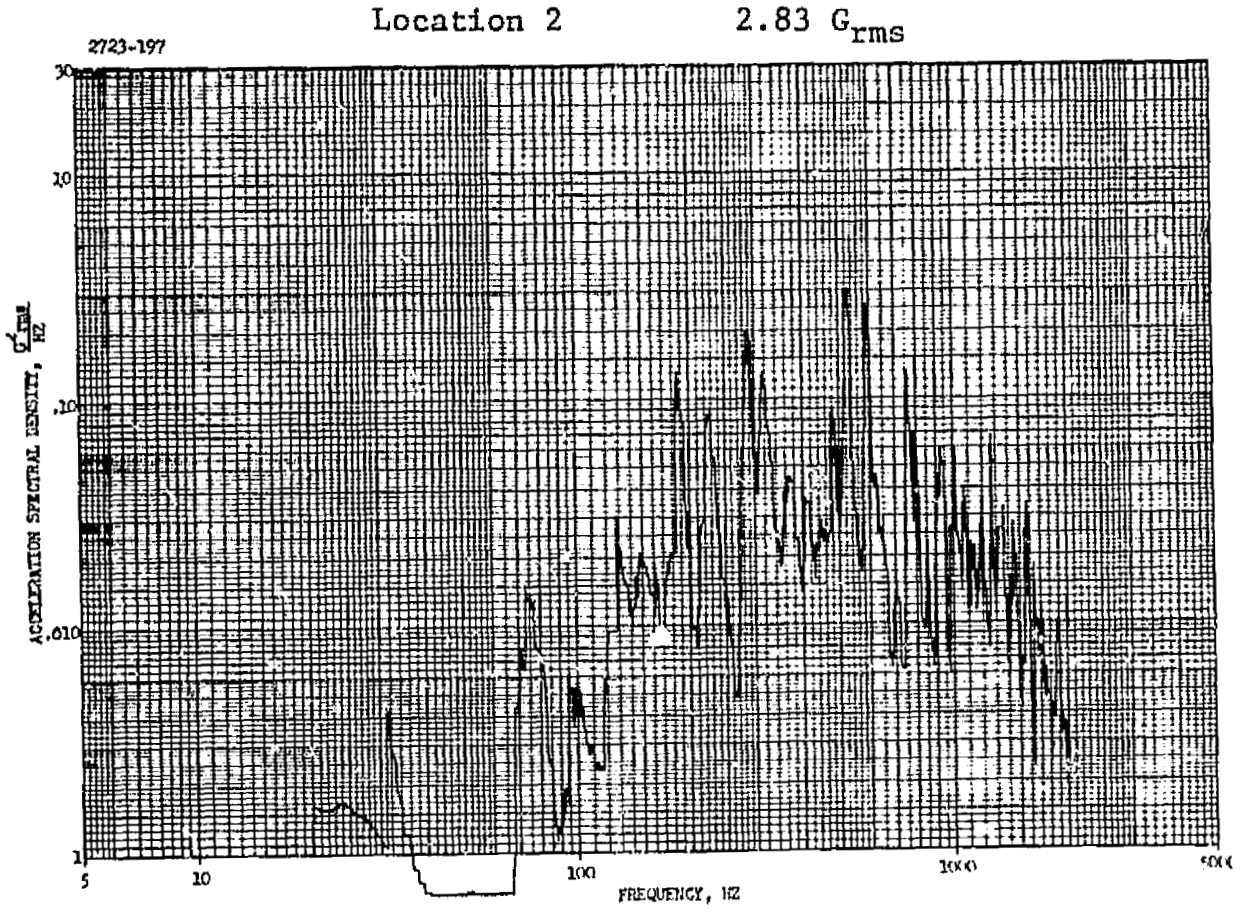

FIGURE 92. TEST # 6 DATA

Location 3 4.4 G_{rms}

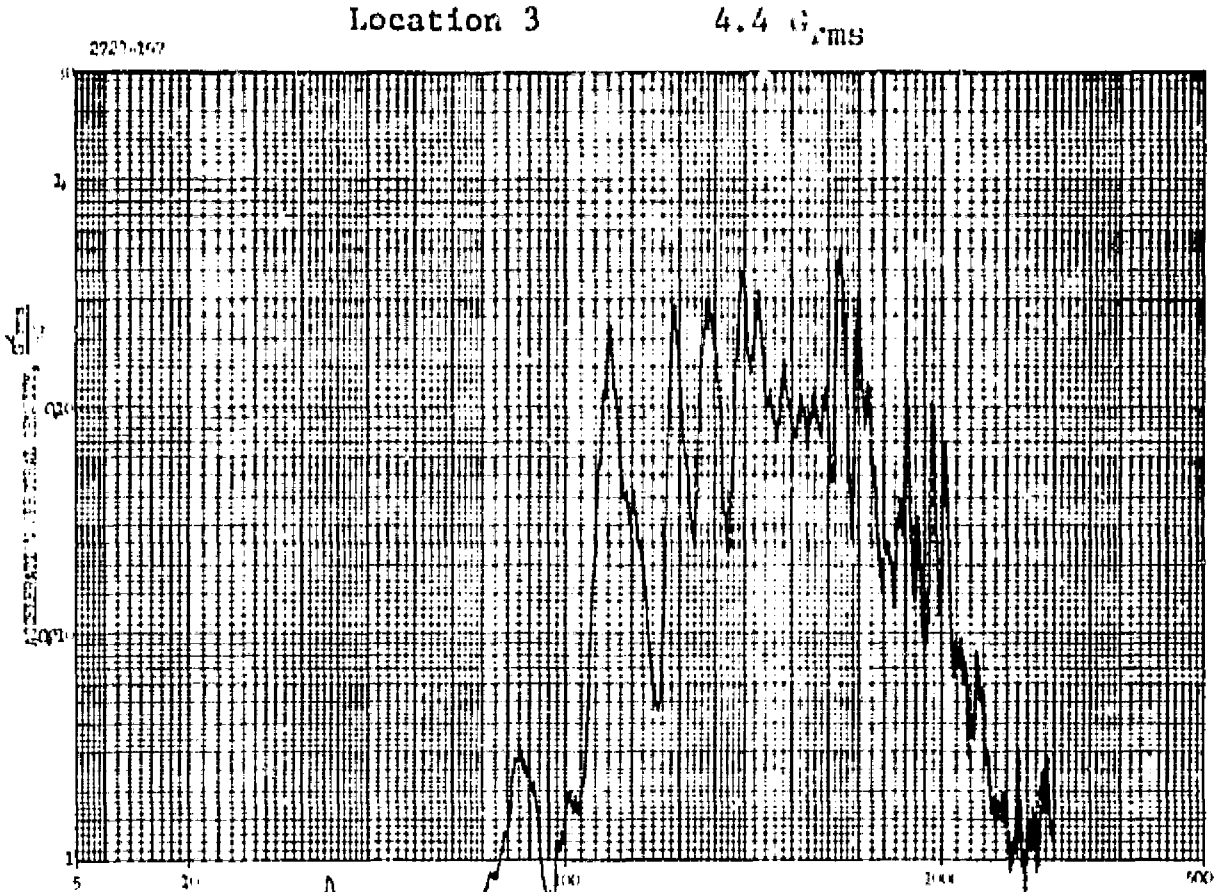

Location 4 5.3 G_{rms}

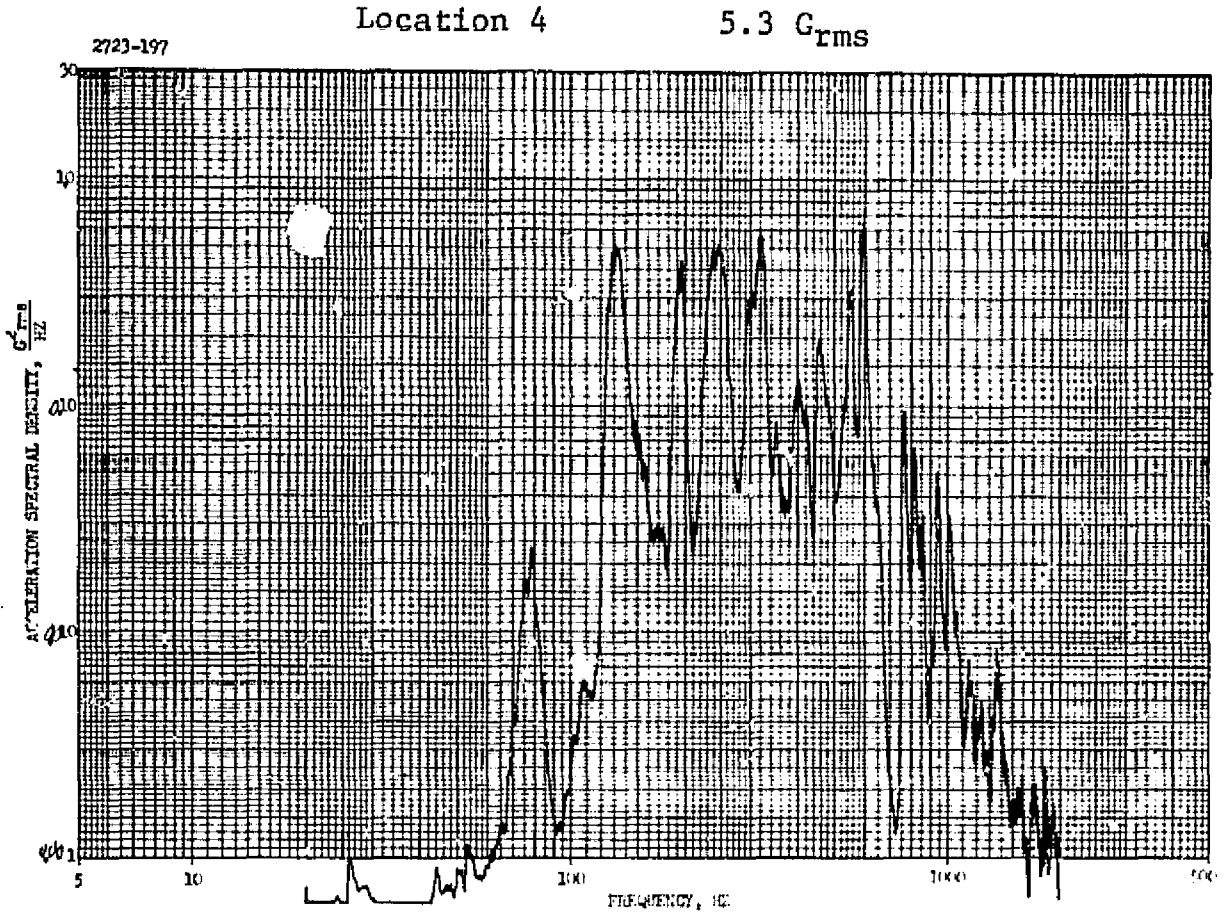

FIGURE 92. TEST #6 DATA (Continued)

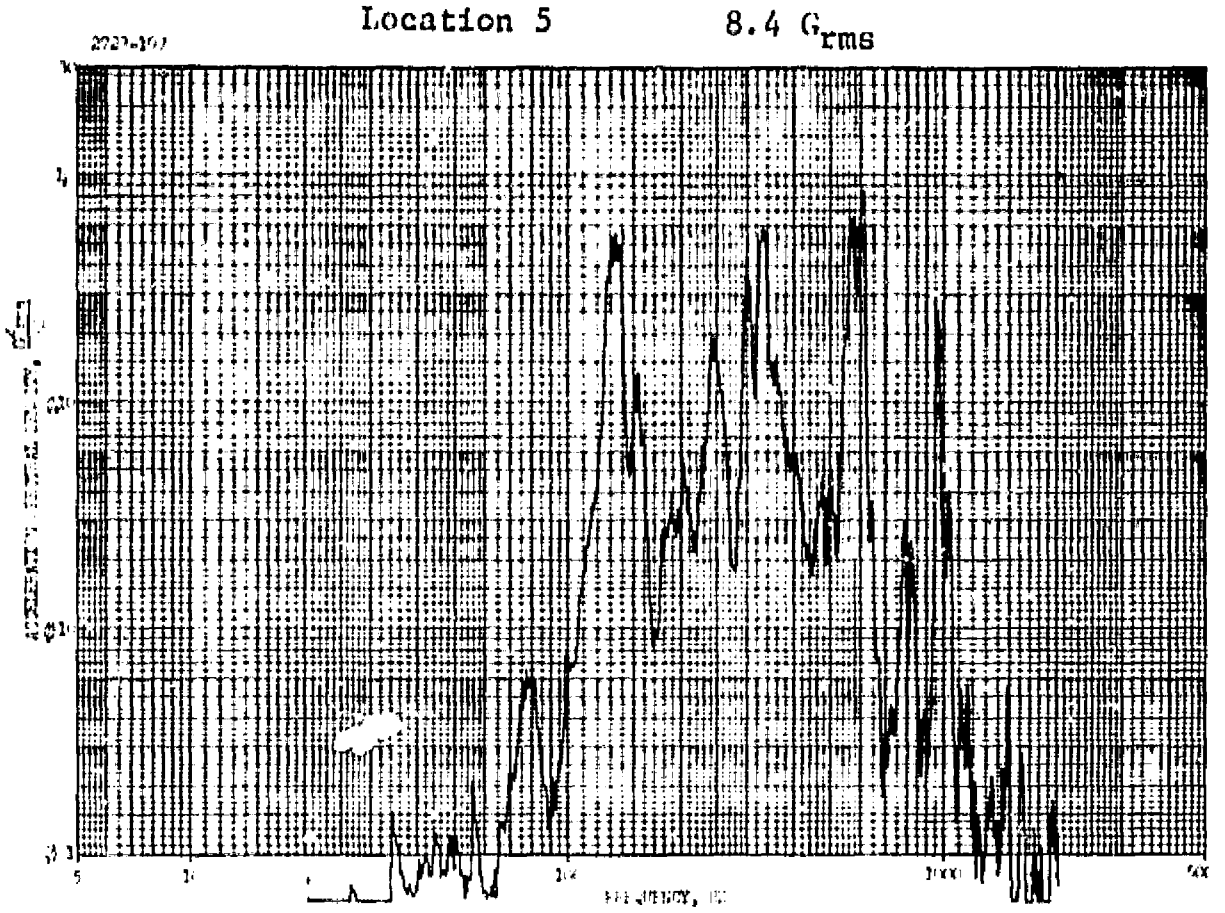

FIGURE 92. TEST #6 DATA (Concluded)

Location 1 3.15 G_{rms}

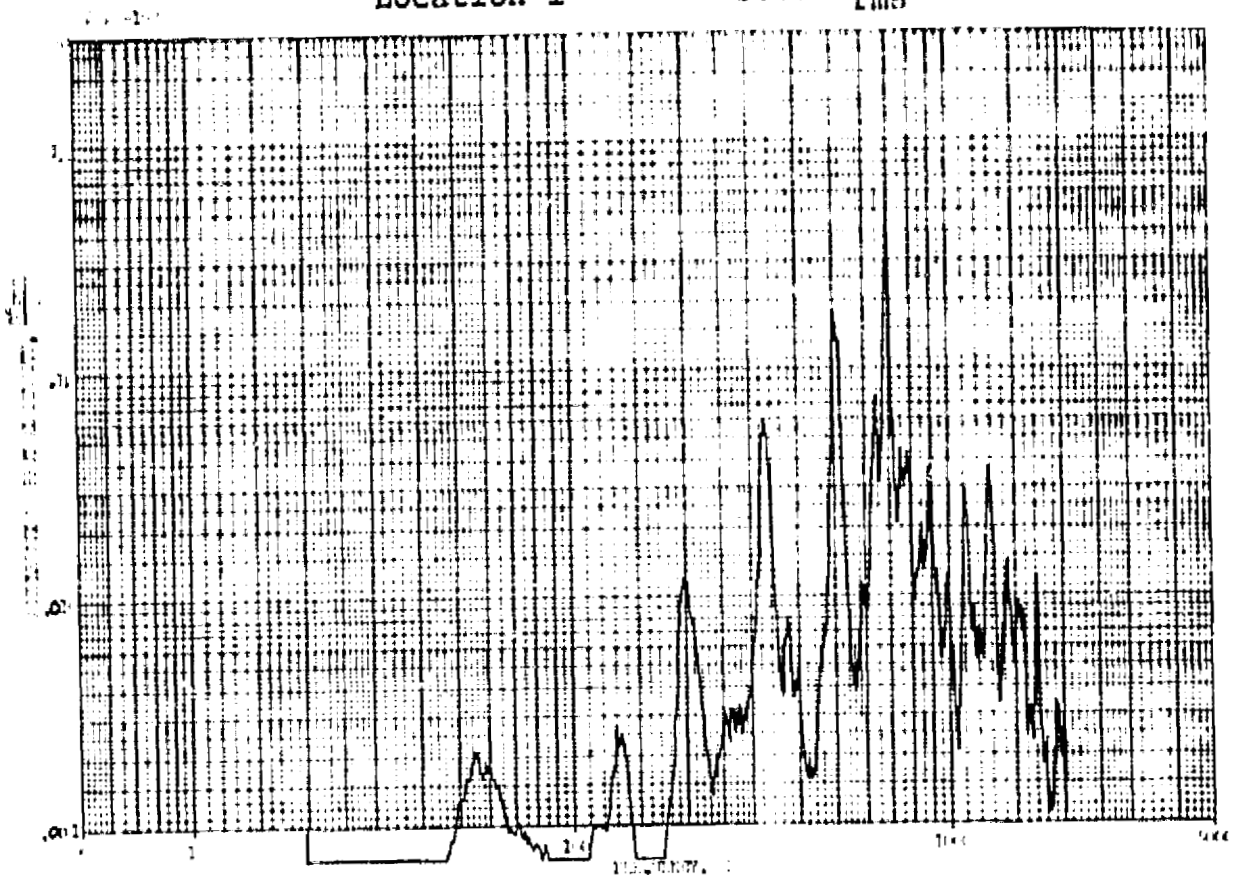

Location 2 8.8 G_{rms}

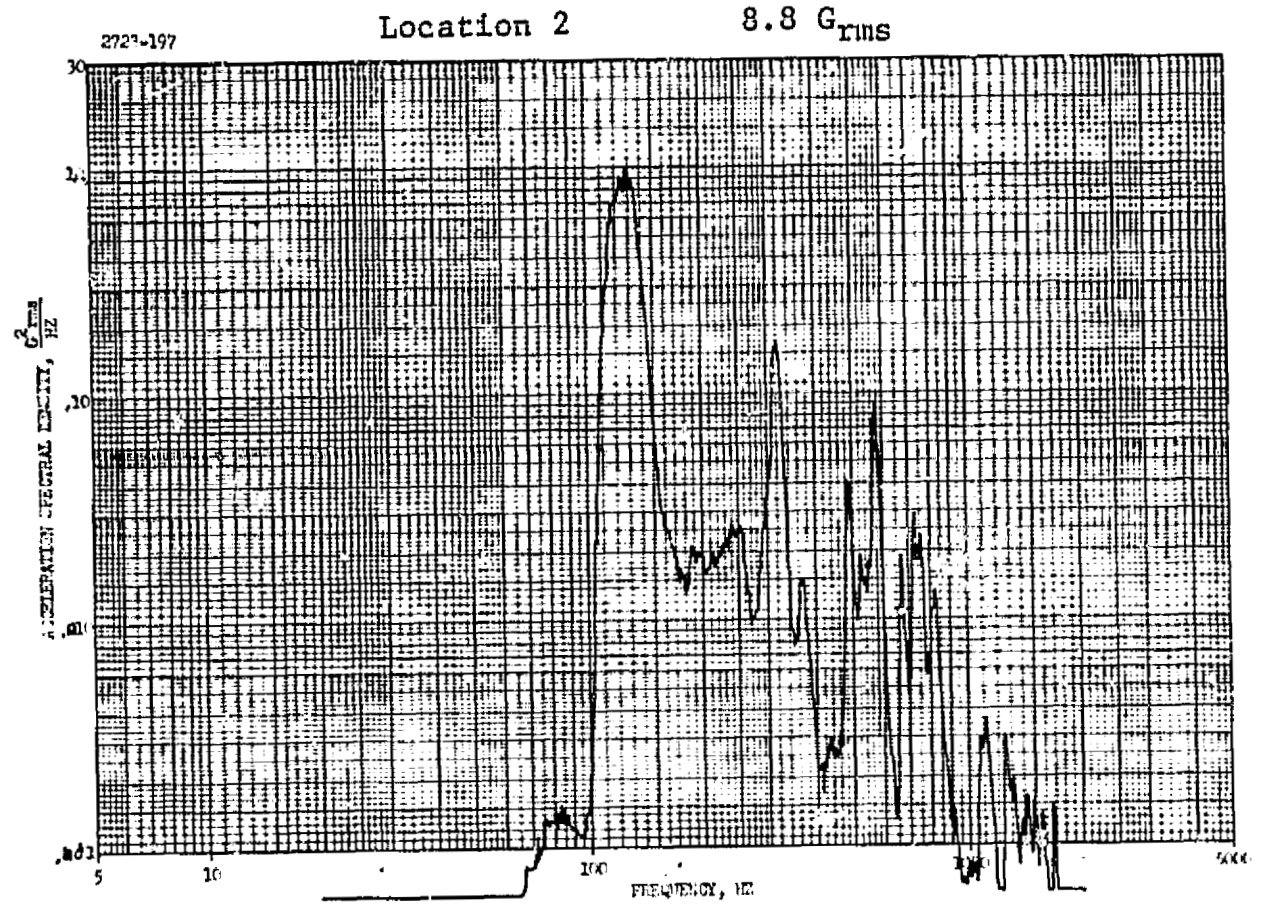

FIGURE 93. TEST # 7 DATA

Location 3 9.31 G_{rms}

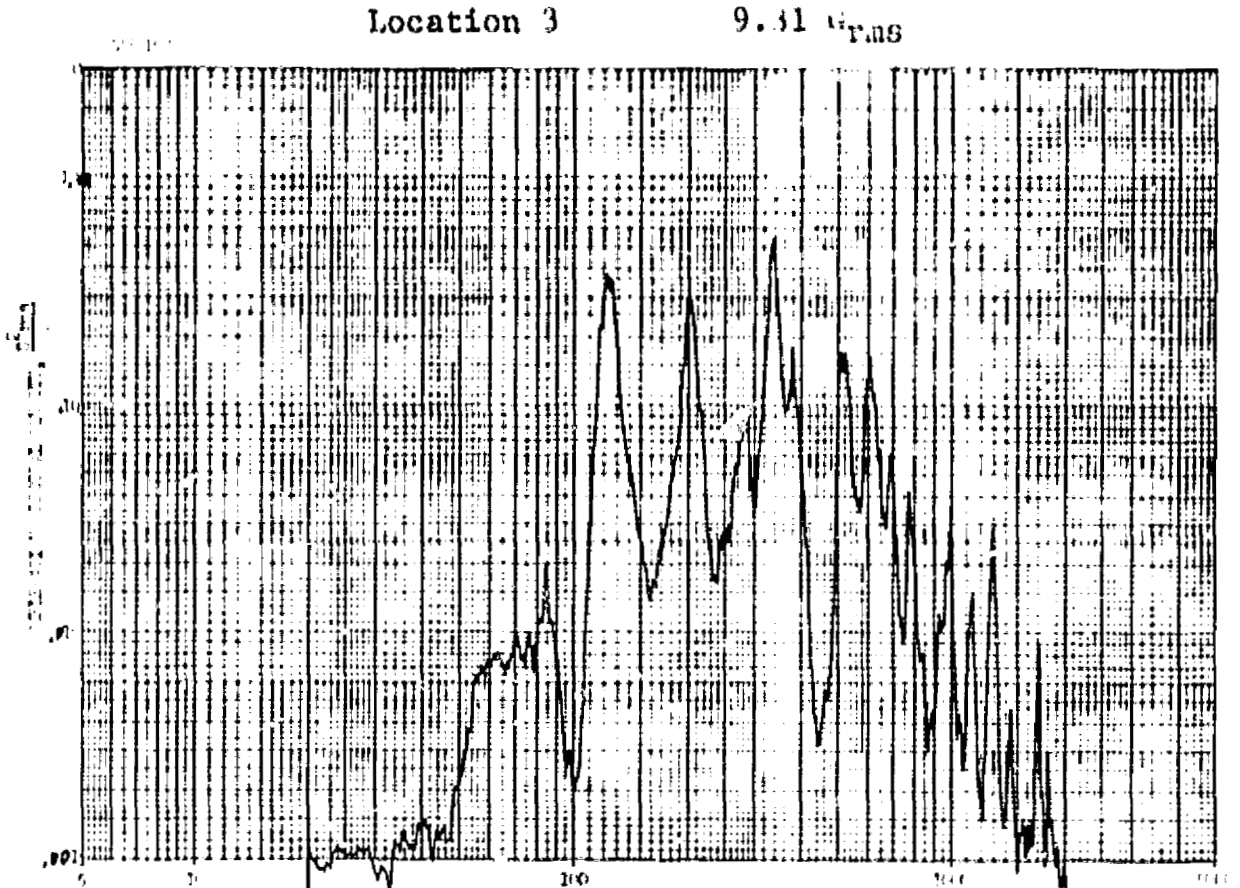

Location 4 6.18 G_{rms}

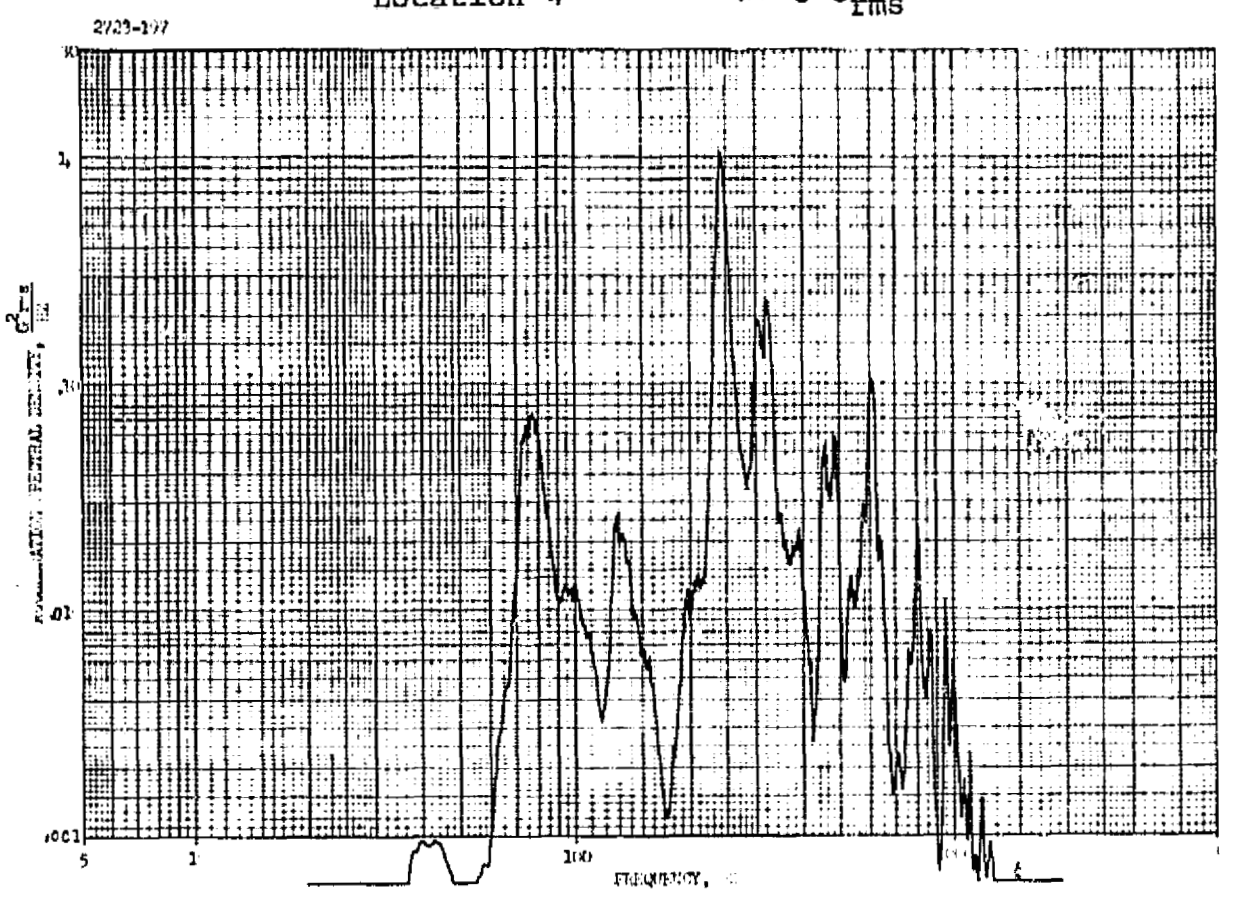

FIGURE 93. TEST #7 DATA (Continued)

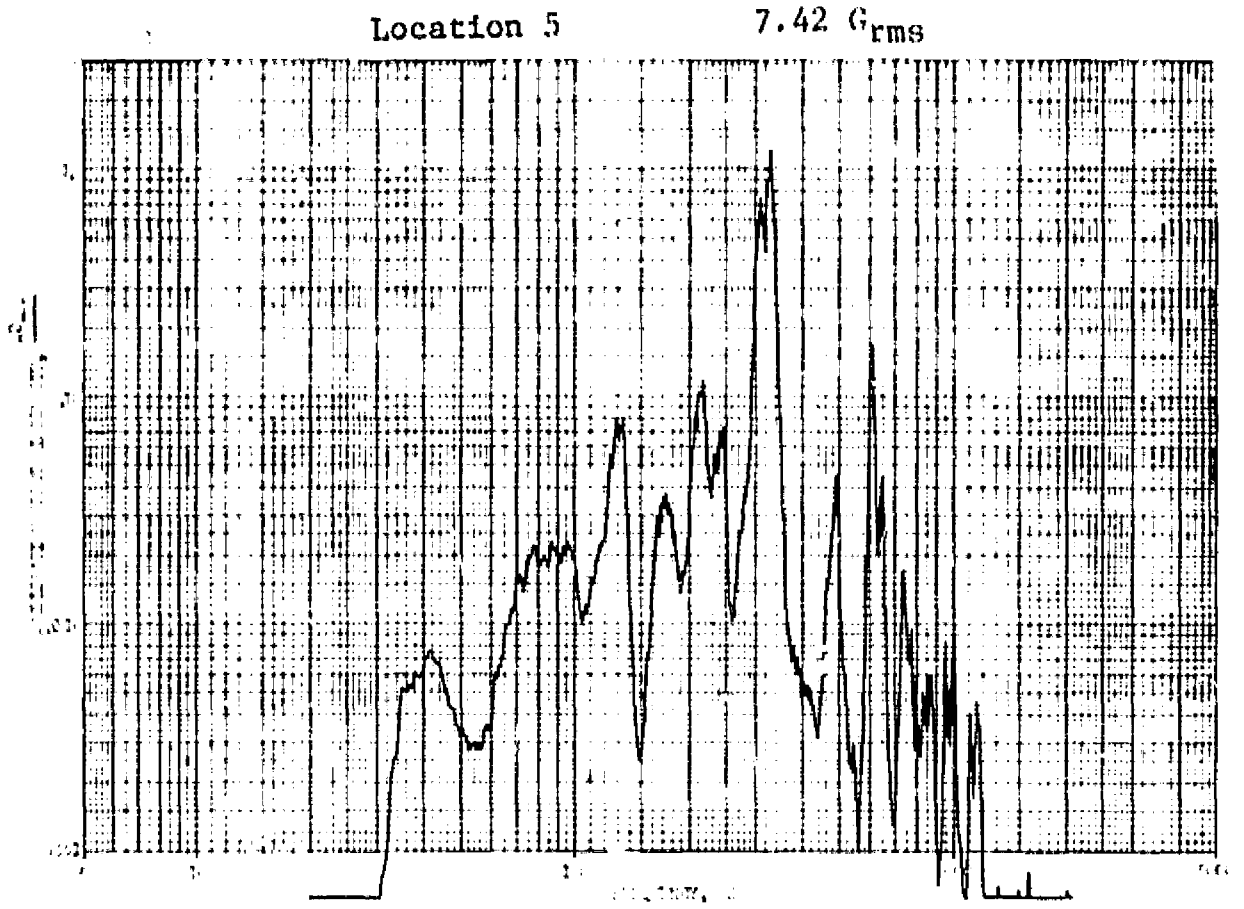

FIGURE 93. TEST #7 DATA (Concluded)

Location 1 3.81 G_{rms}

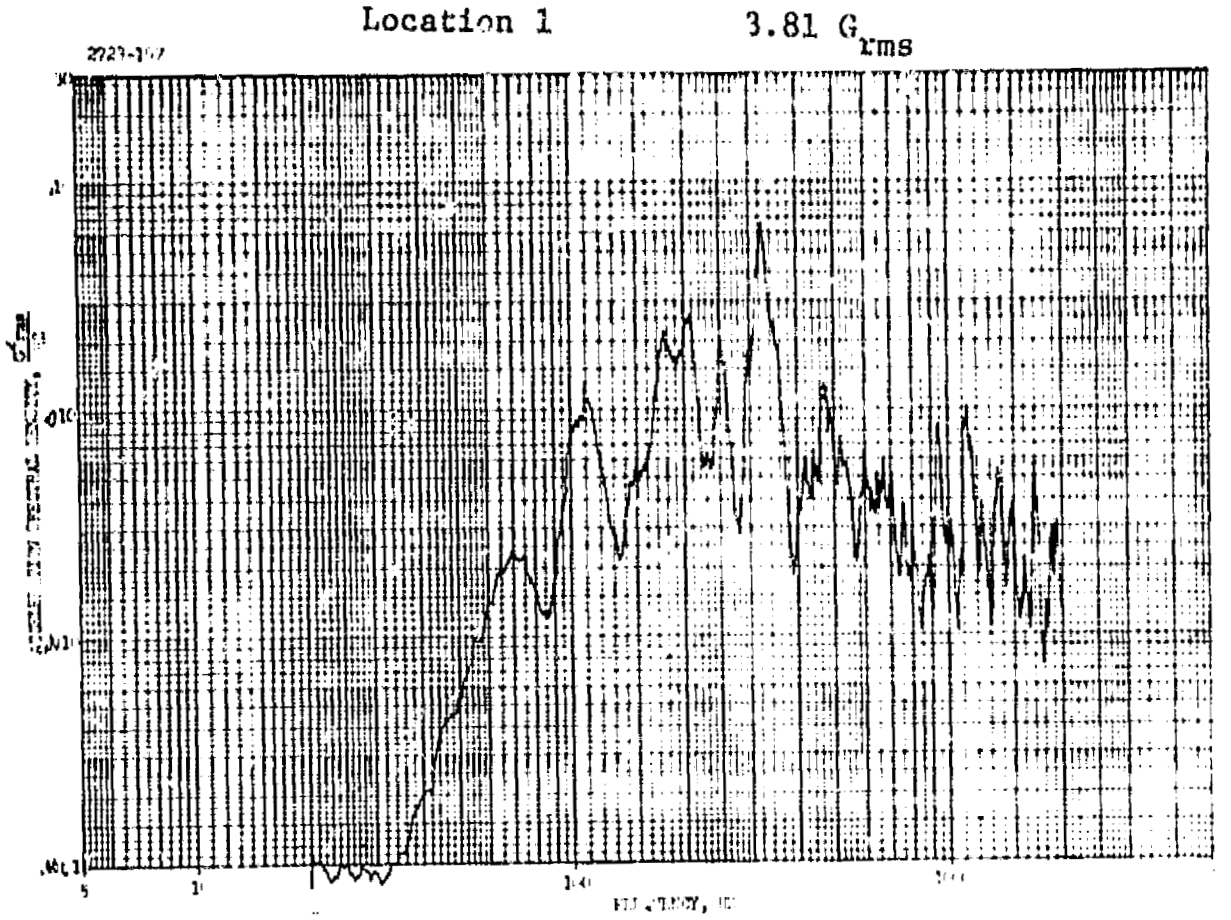

Location 2 7.96 G_{rms}

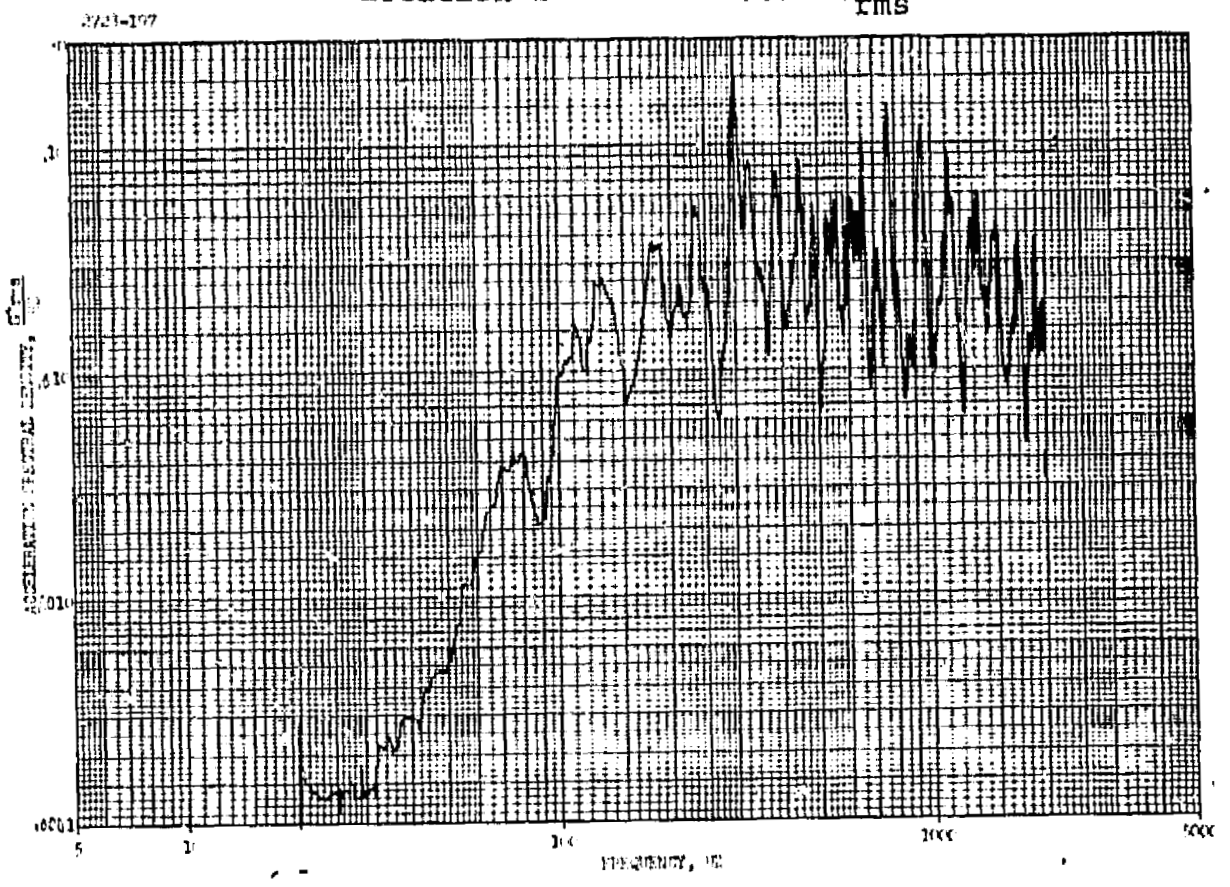

FIGURE 94. TEST # 8 DATA

Location 3 7.52 G_{rms}

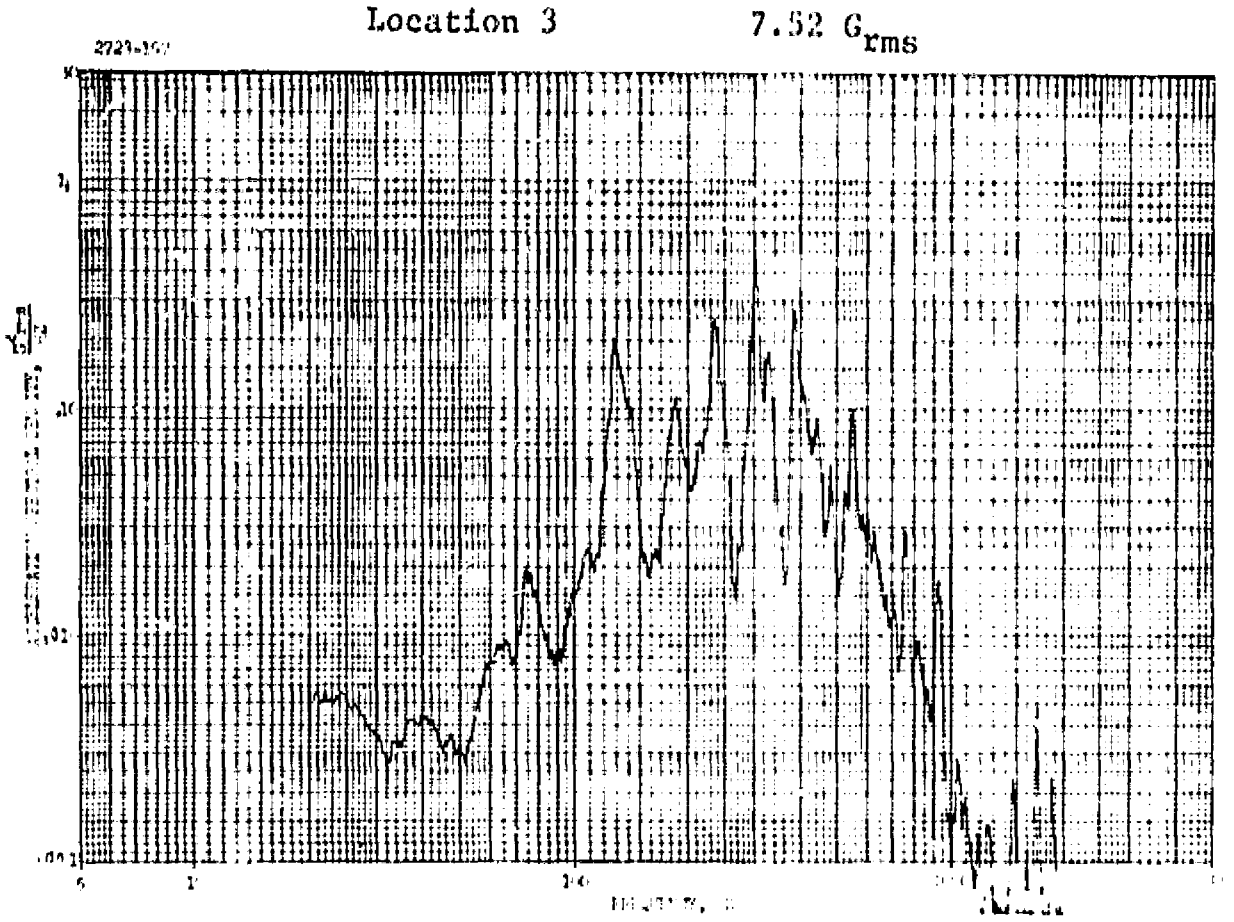

Location 4 15.65 G_{rms}

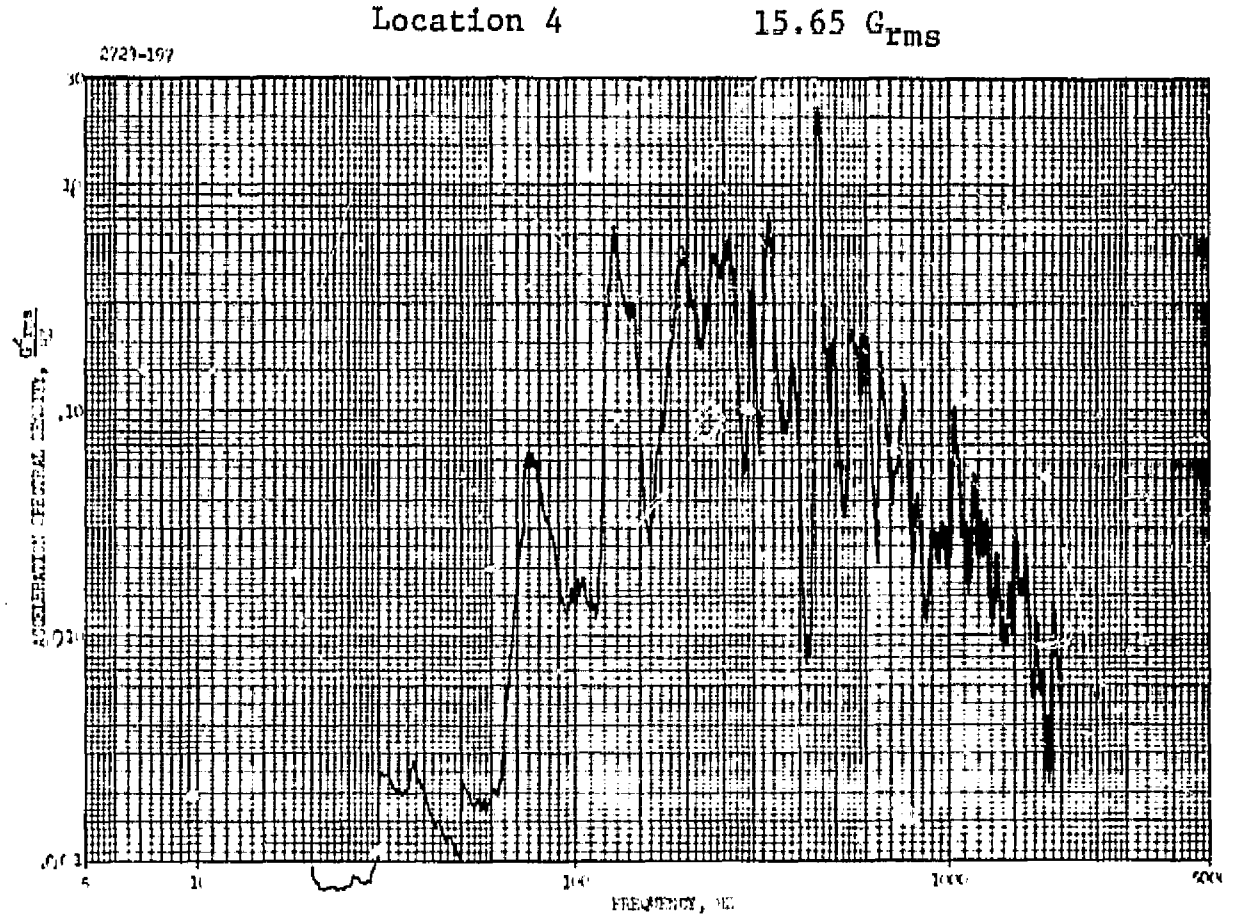

FIGURE 94. TEST #8 DATA (Continued)

Location 5 22.1 G_{rms}

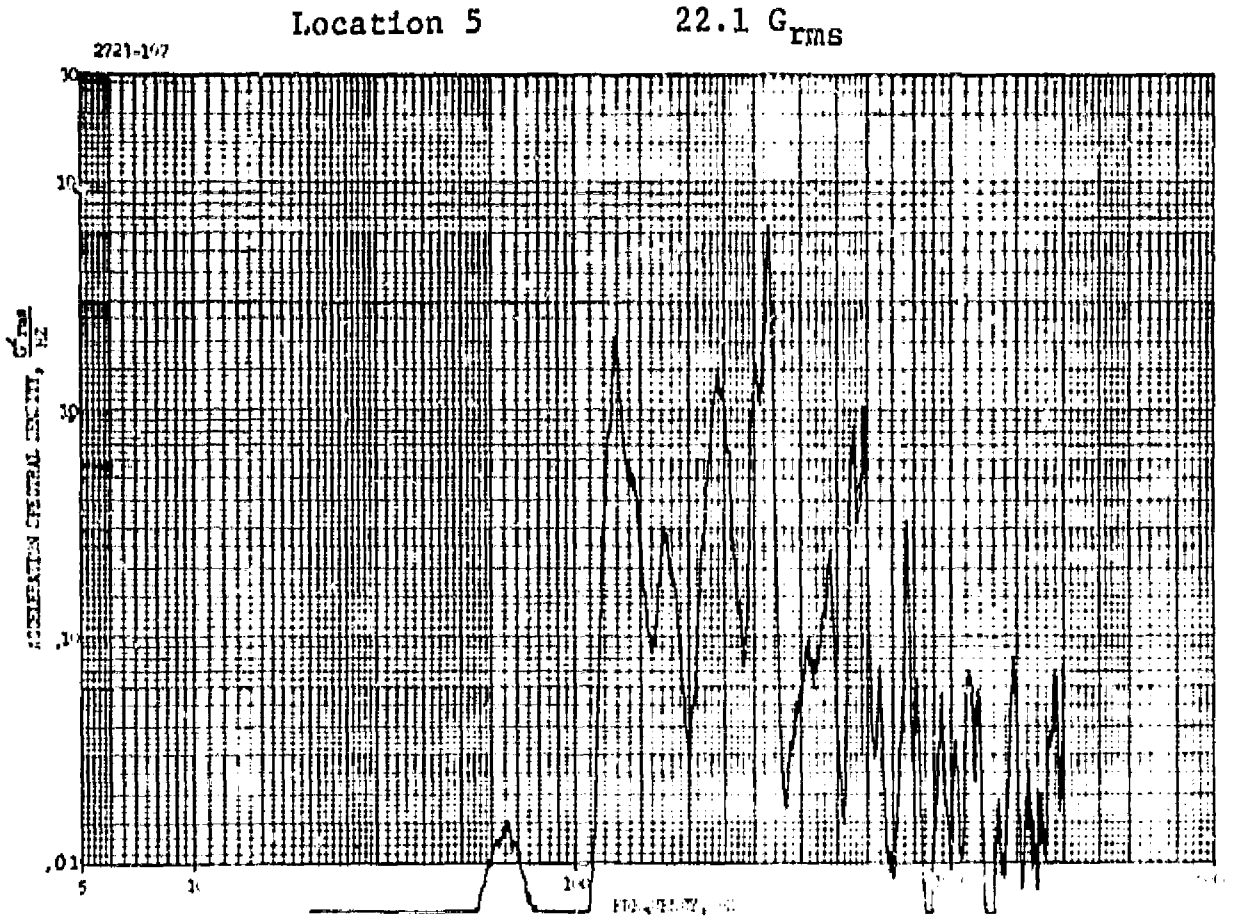

FIGURE 94. TEST #8 DATA (Concluded)

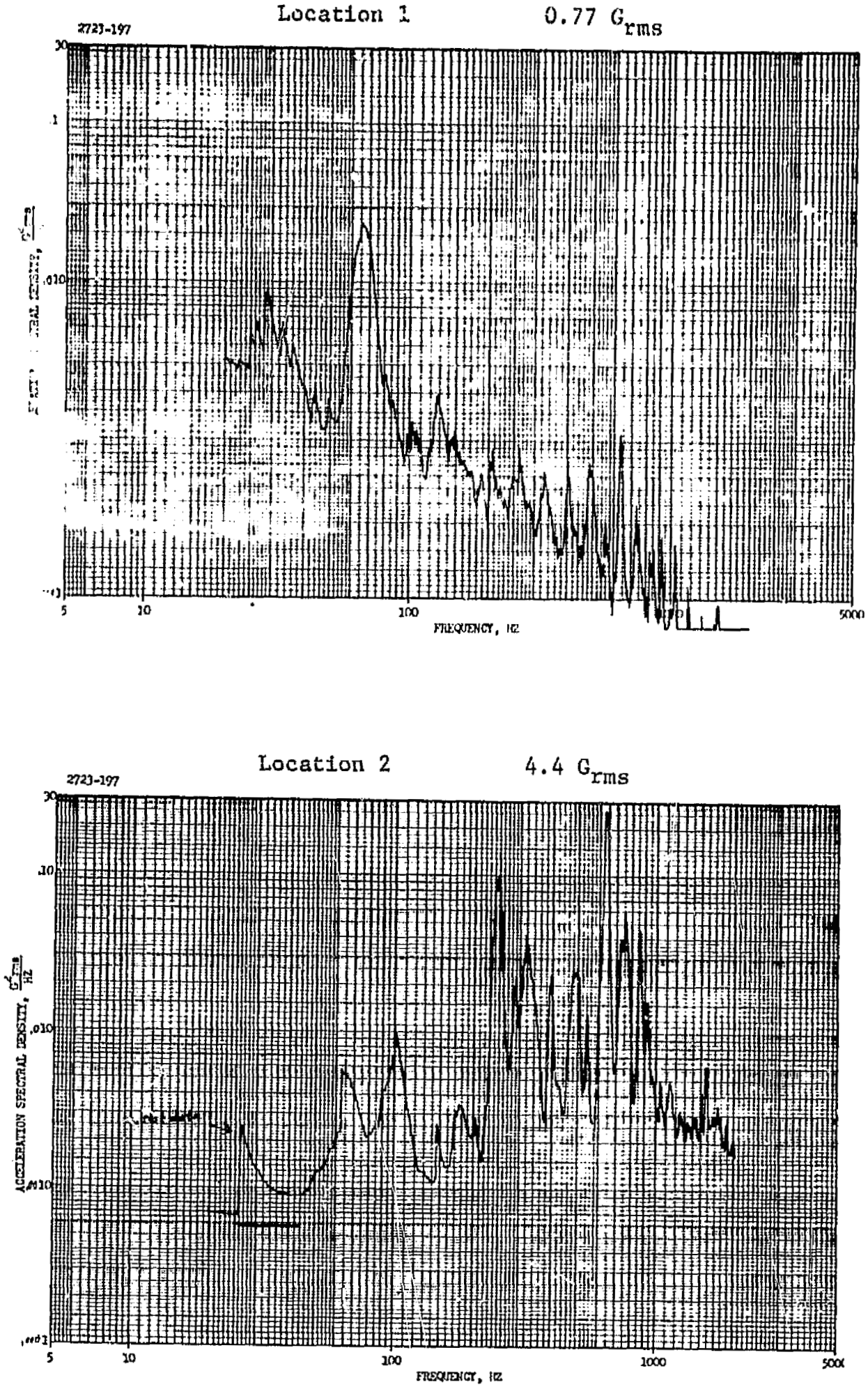

FIGURE 95. TEST #9 DATA - 3" SPACING

Location 3 6.18 G_{rms}

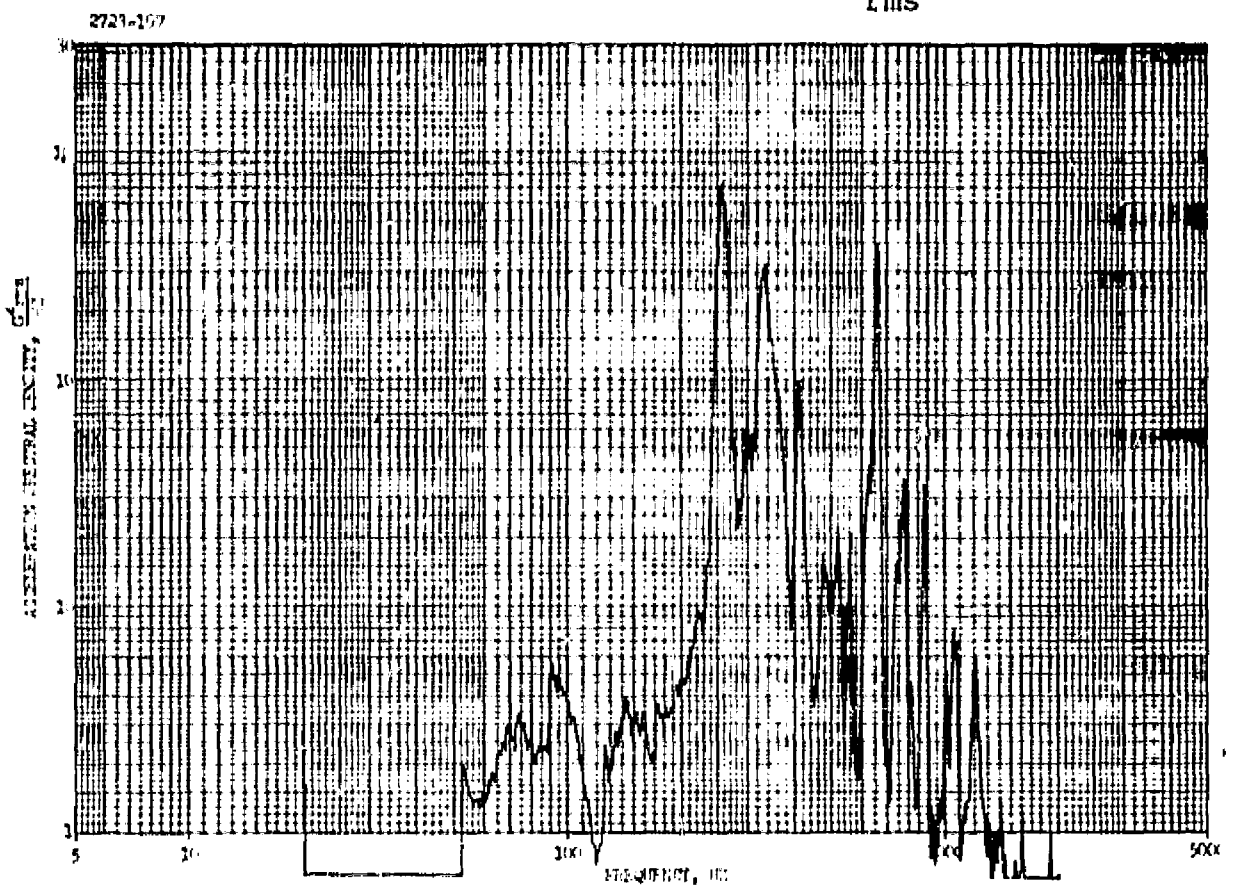

Location 4 5.7 G_{rms}

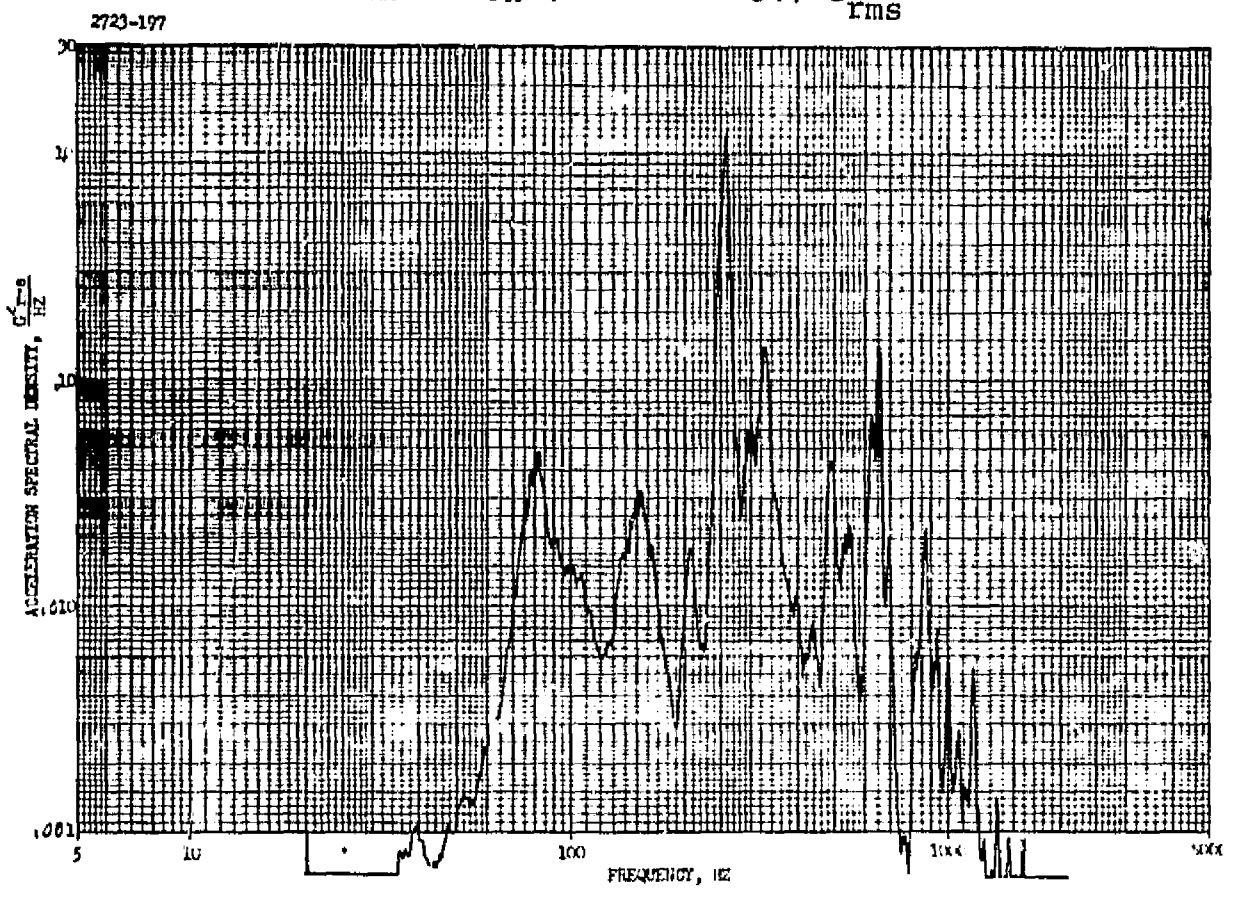

FIGURE 95. TEST #9 DATA - 3" SPACING (Continued)

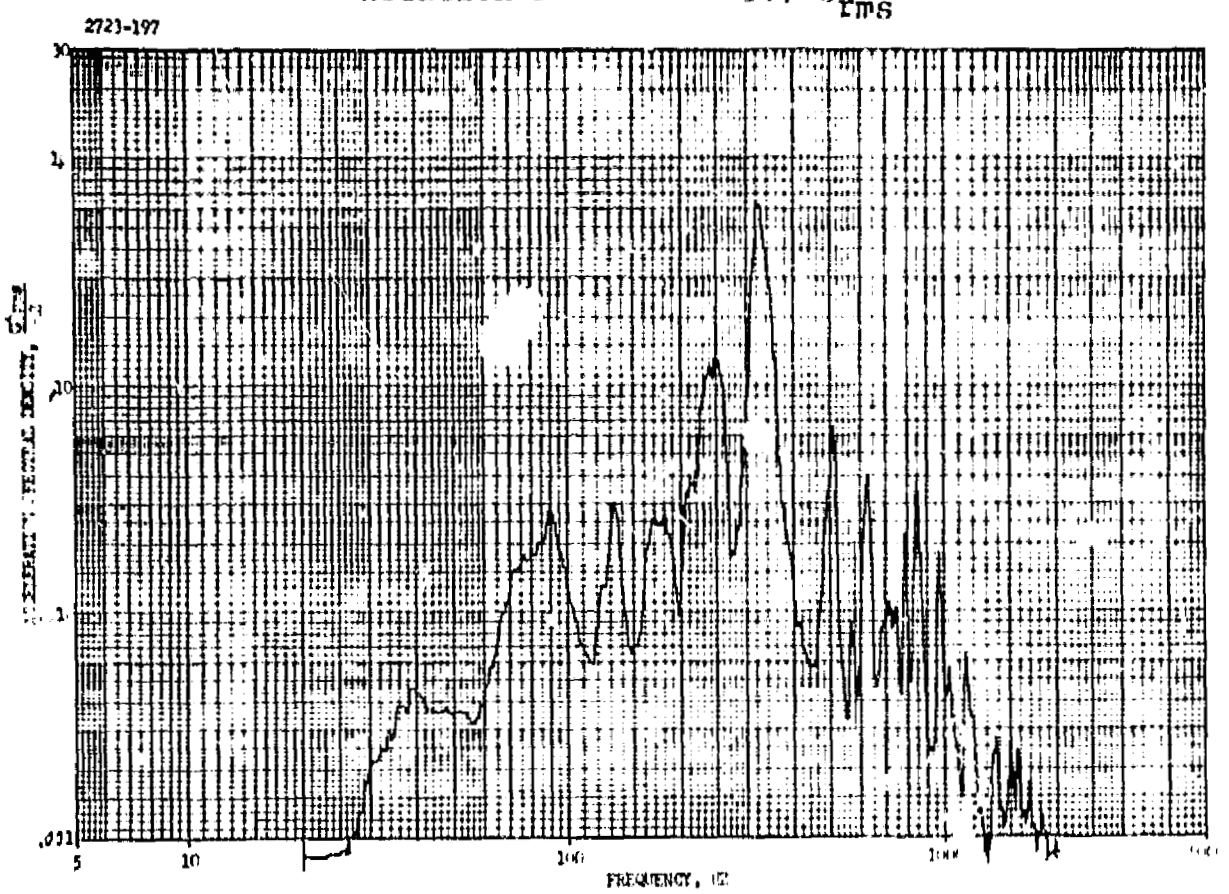

FIGURE 95. TEST #9 DATA - 3" SPACING (Concluded)

Location 1 1.6 G_{rms}

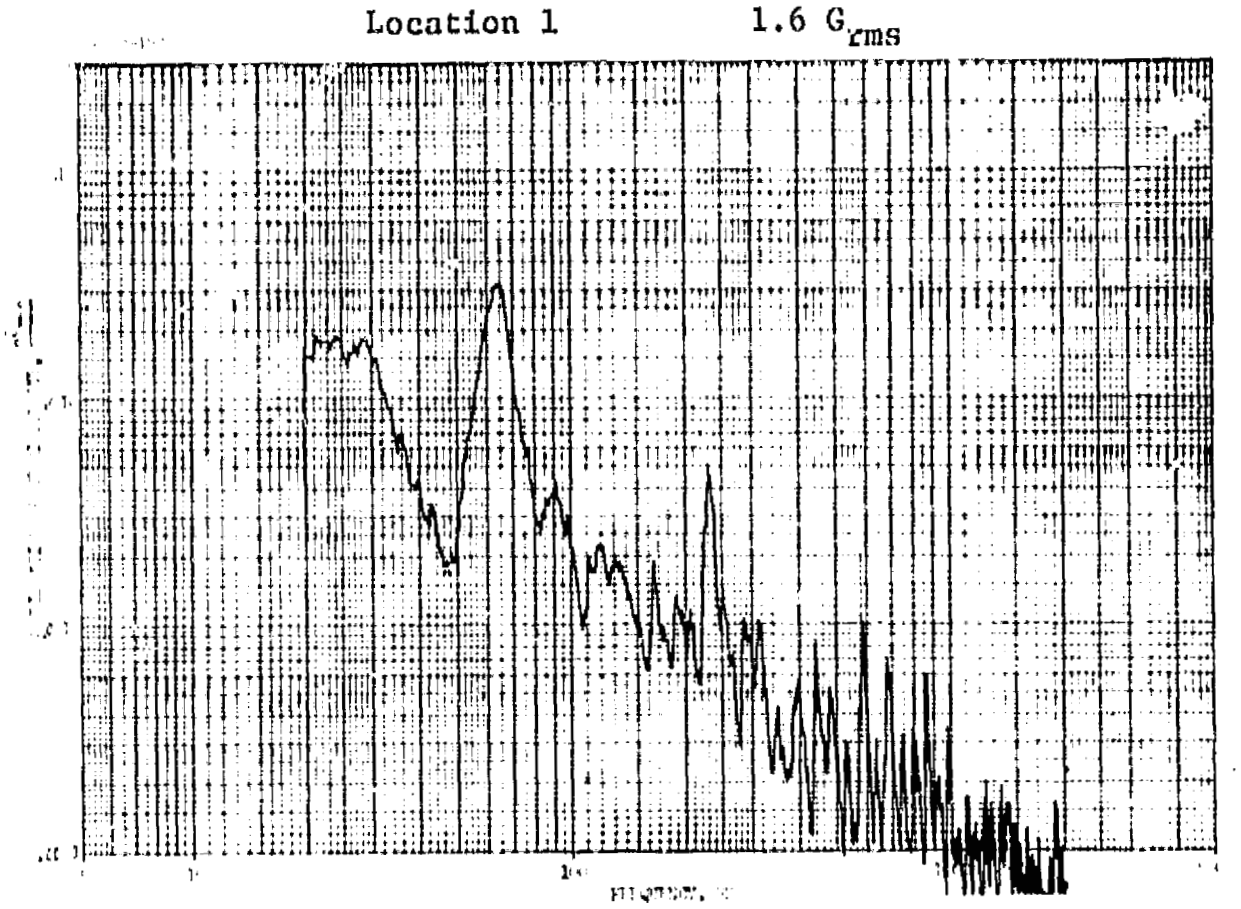

Location 2 3.9 G_{rms}

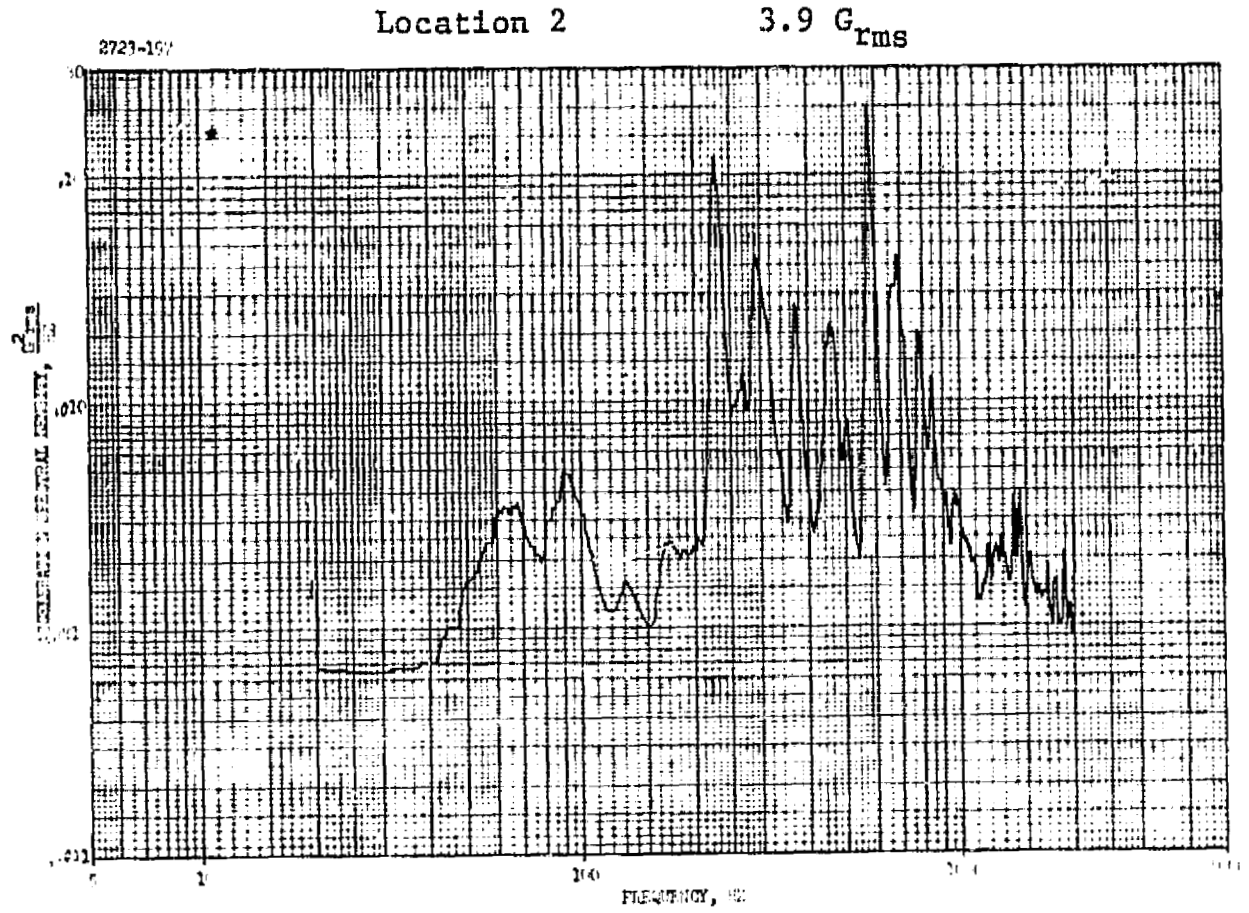

FIGURE 95. TEST #9 DATA - 6" SPACING

Location 3 6.18 G_{rms}

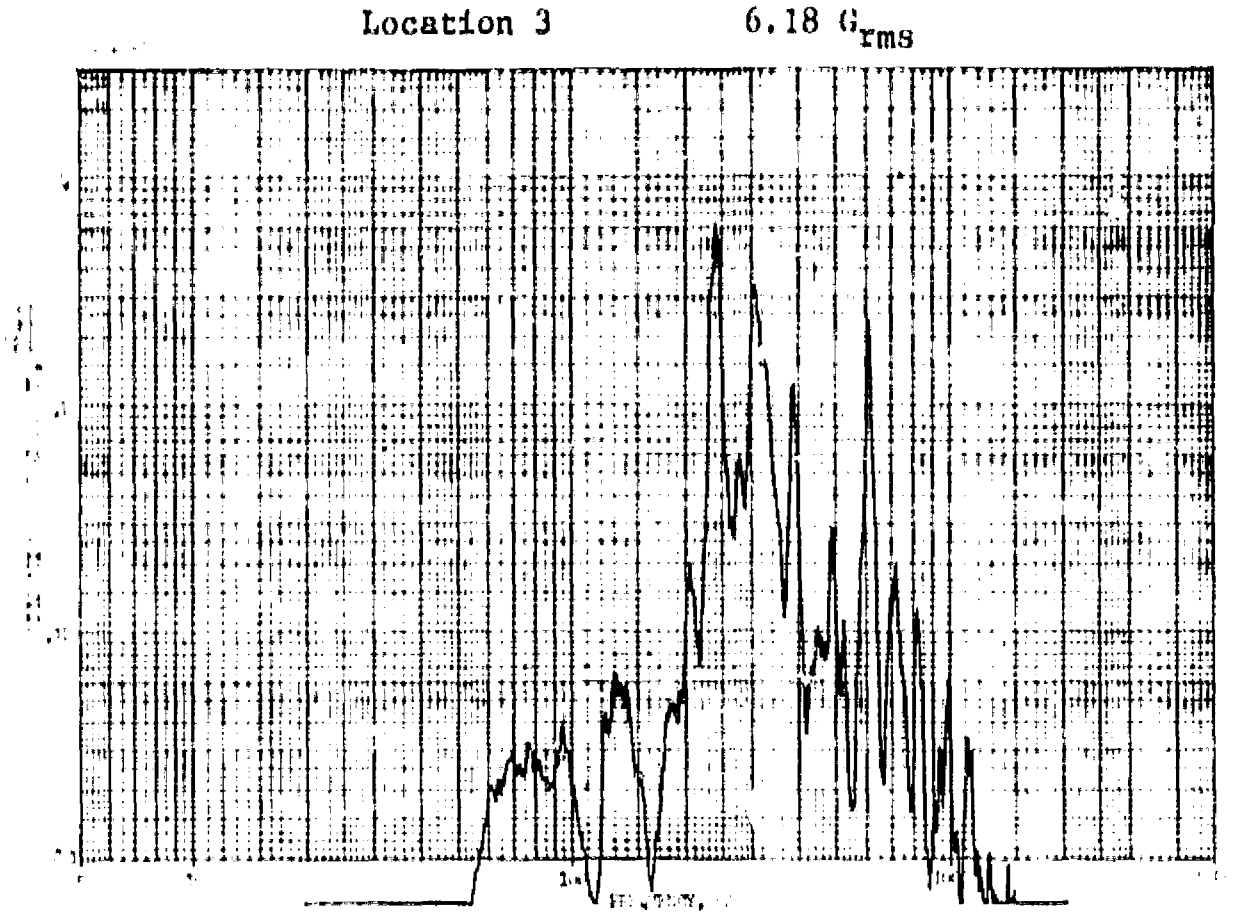

Location 4 5.7 G_{rms}

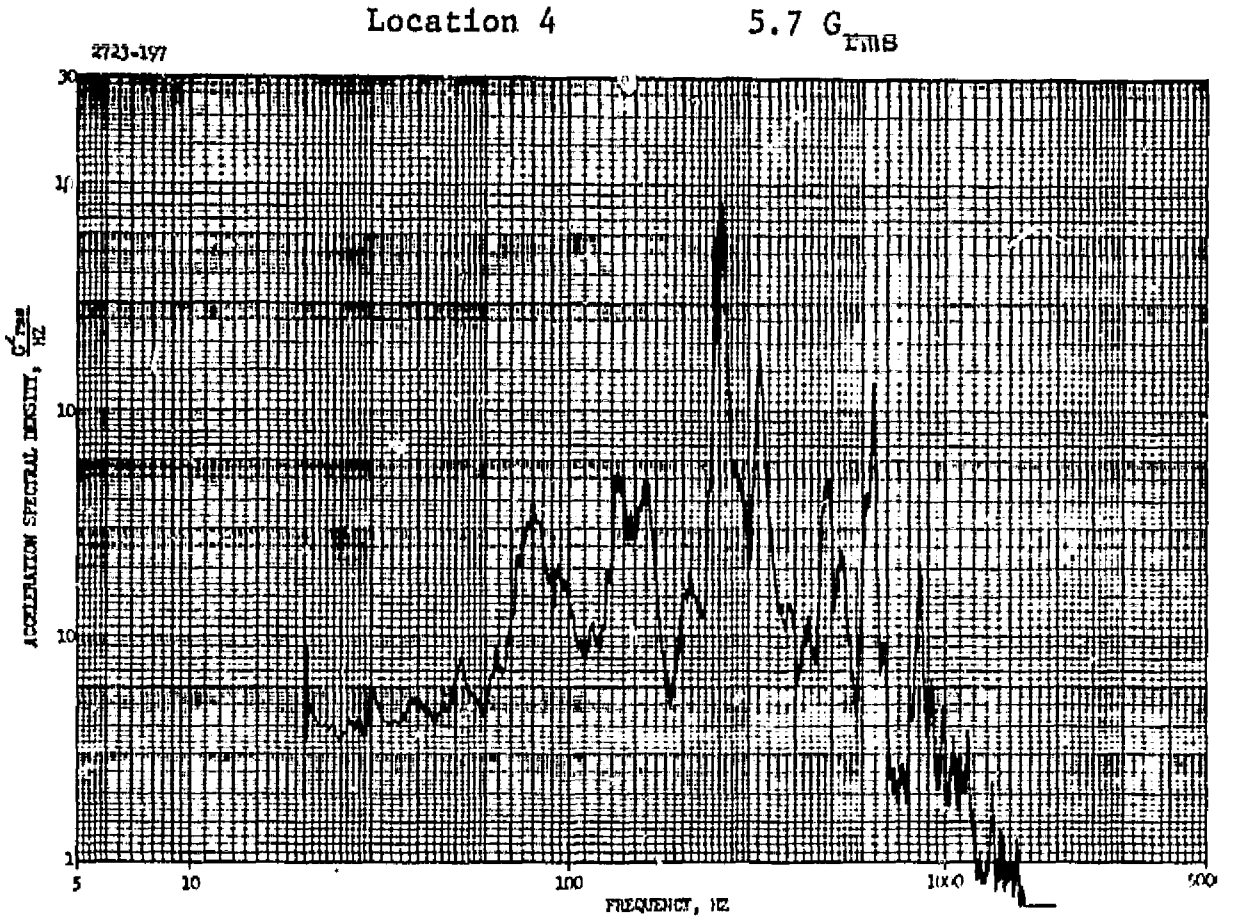

FIGURE 95. TEST #9 DATA - 6" SPACING (Continued)

Location 5 6.18 G_{rms}

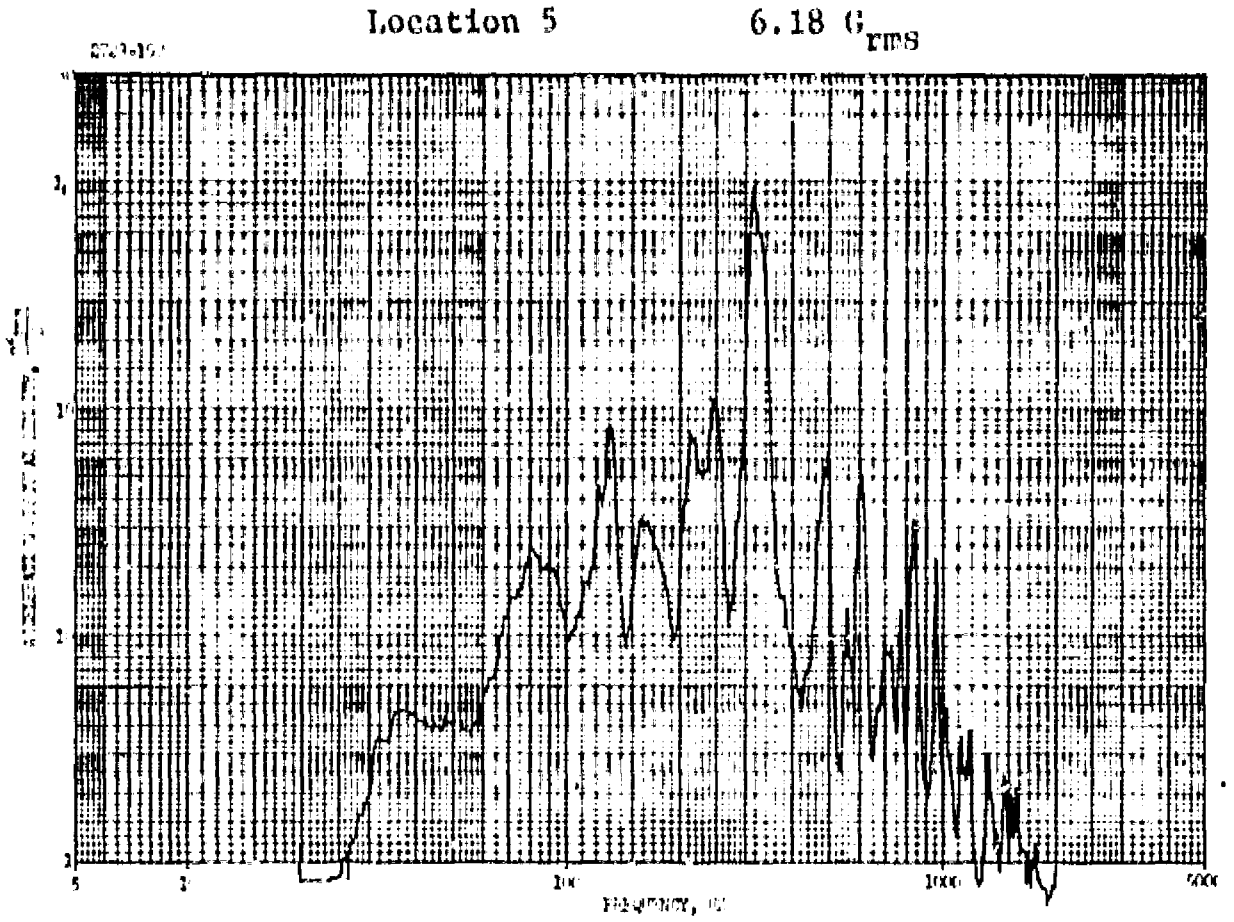

FIGURE 95. TEST #9 DATA - 6" SPACING (Concluded)

Location 1 2.1 G_{rms}

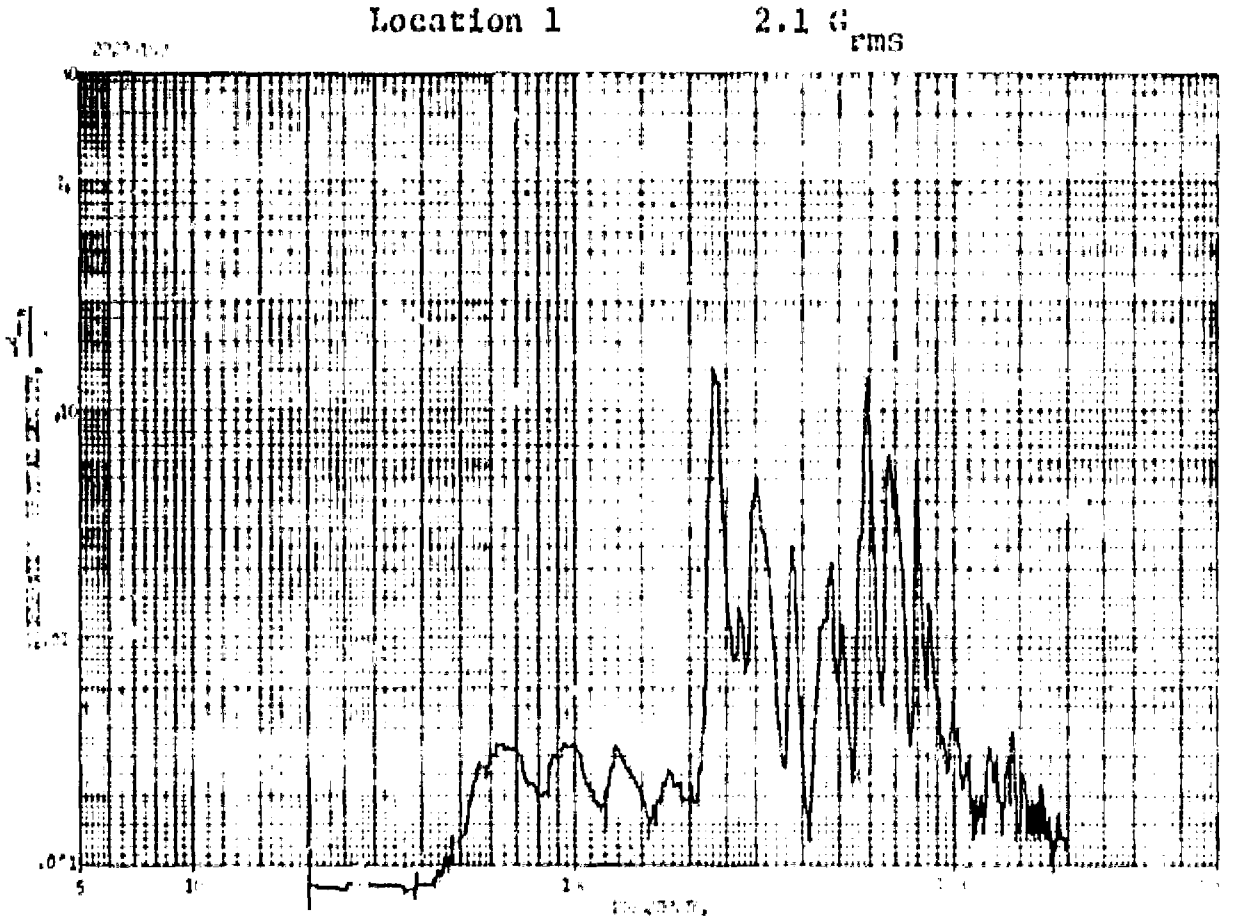

Location 2 3.7 G_{rms}

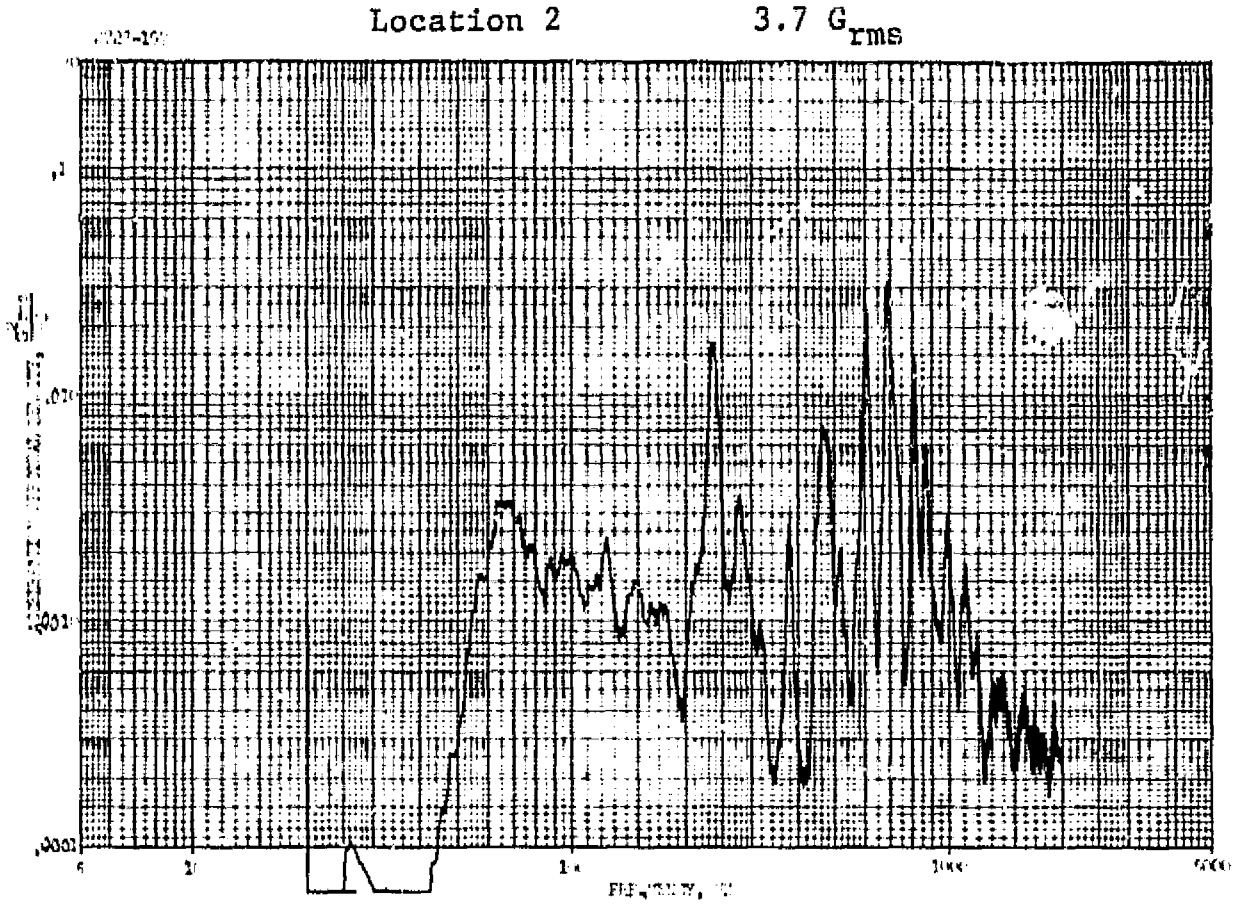

FIGURE 95. TEST #9 DATA - 12 1/2" SPACING

Location 3 7 G_{rms}

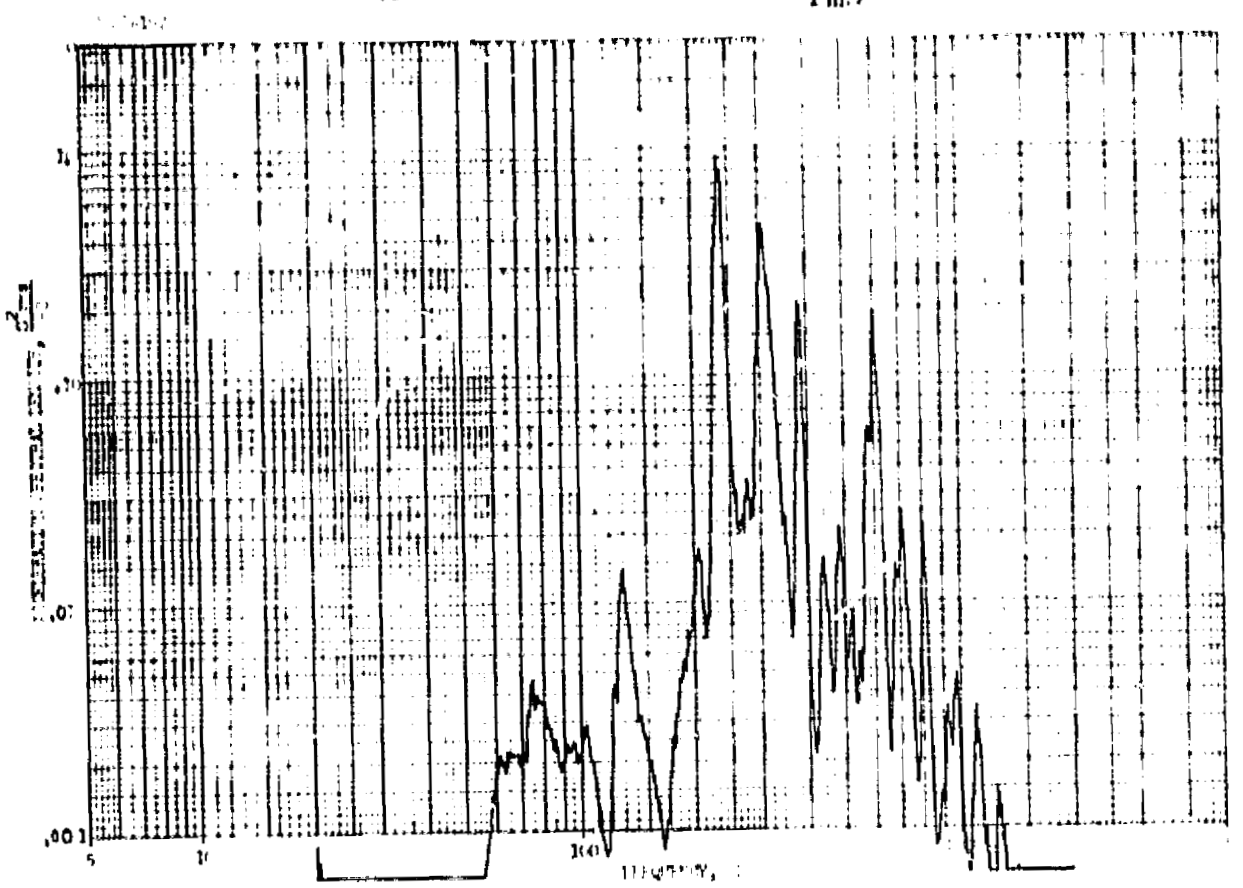

Location 4 6.7 G_{rms}

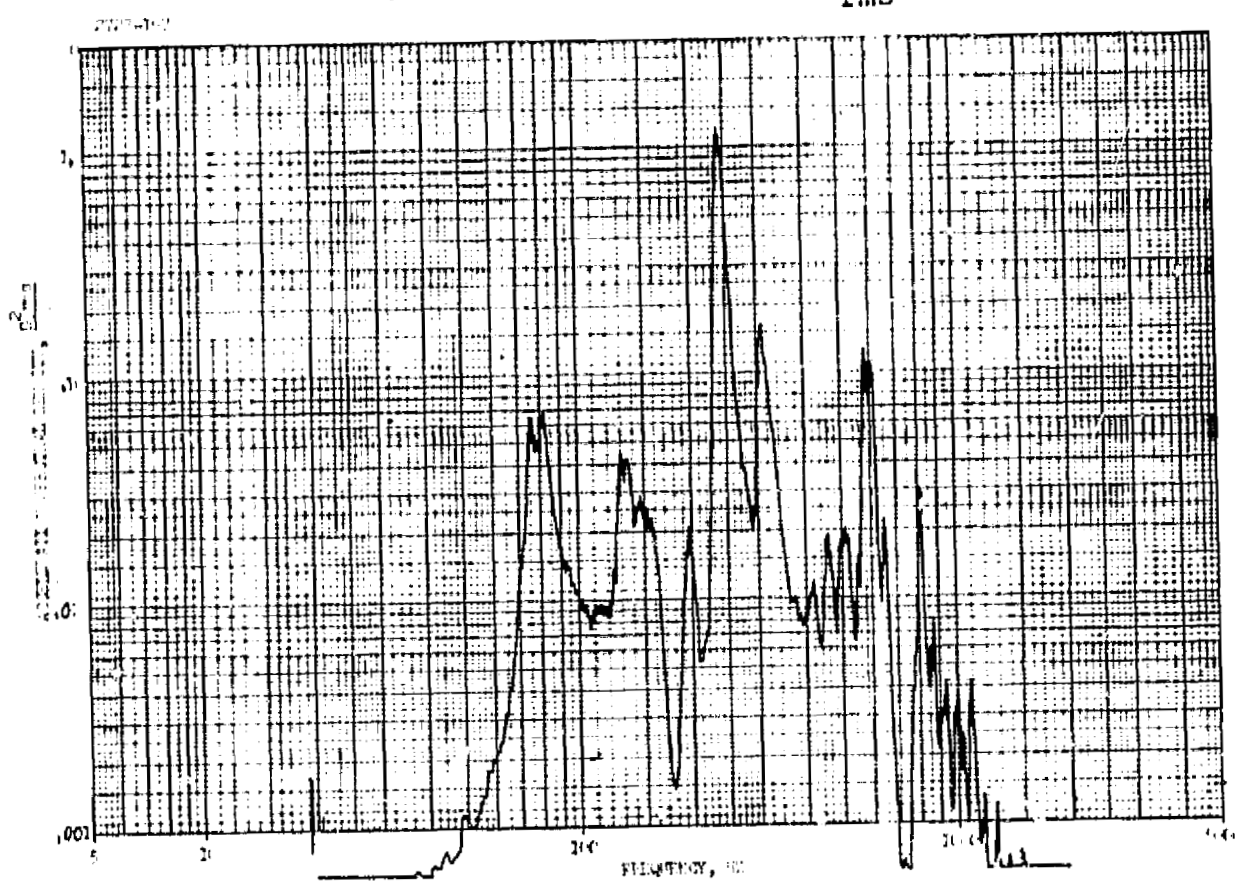

FIGURE 95. TEST #9 DATA - 12 1/2" SPACING (Continued)

Location 5 7.3 G_{rms}

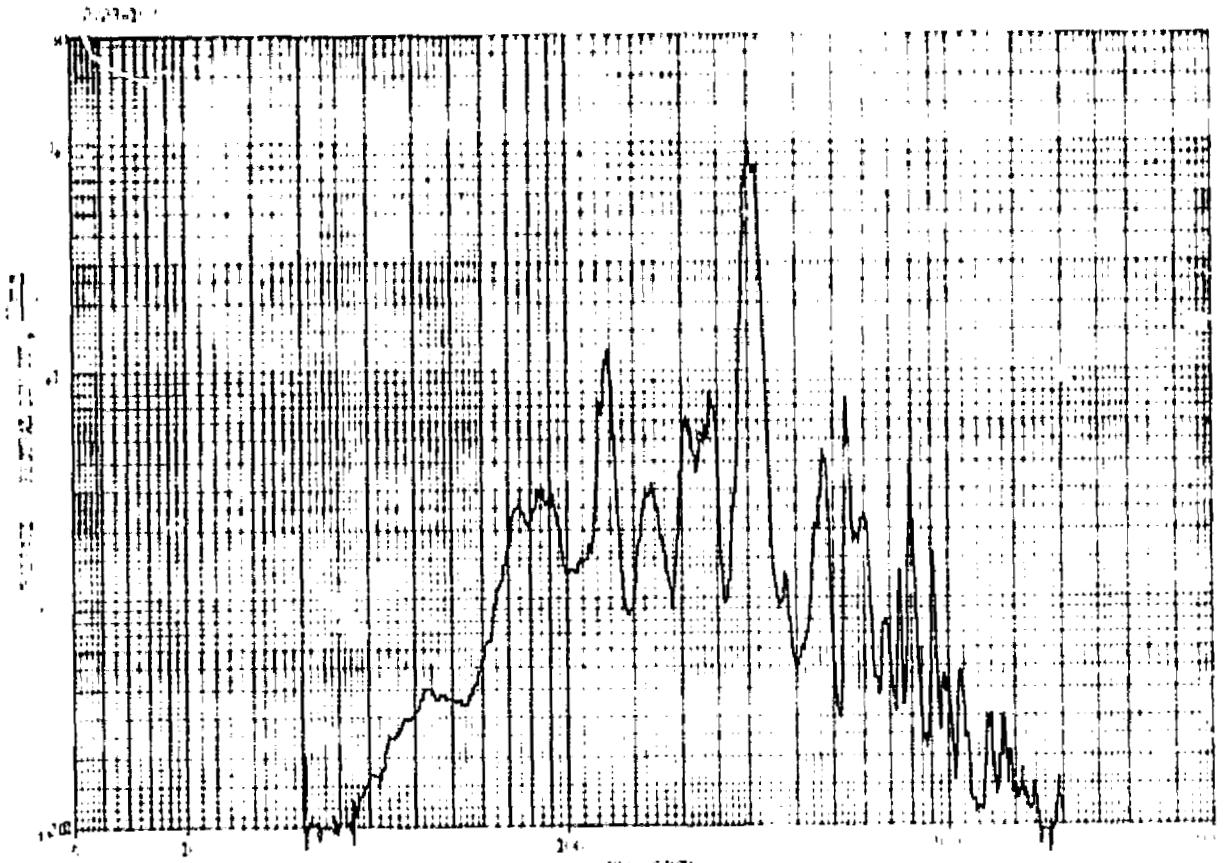

FIGURE 95. TEST #9 DATA - 12 1/2" SPACING (Concluded)

Location 1 1.93 G_{rms}

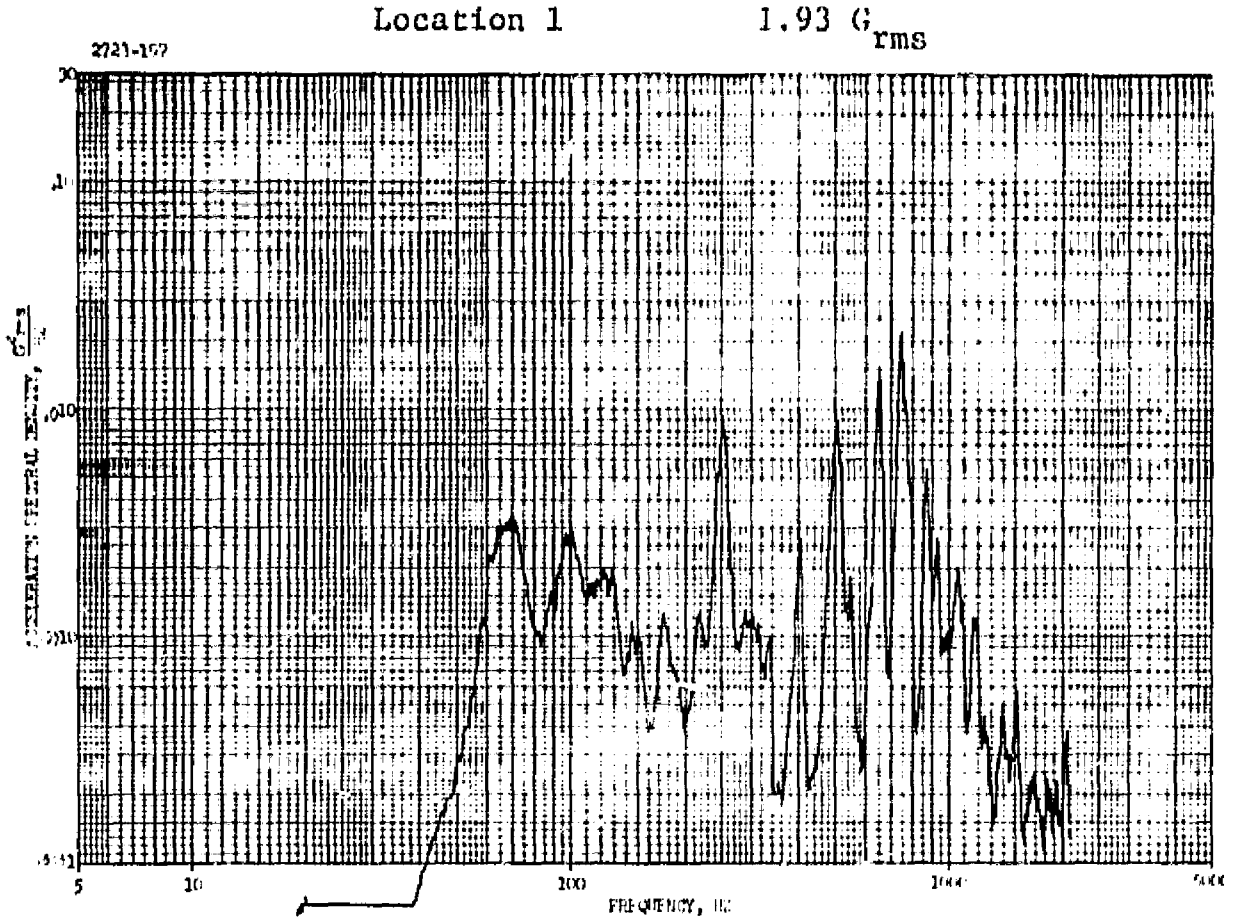

Location 2 4.4 G_{rms}

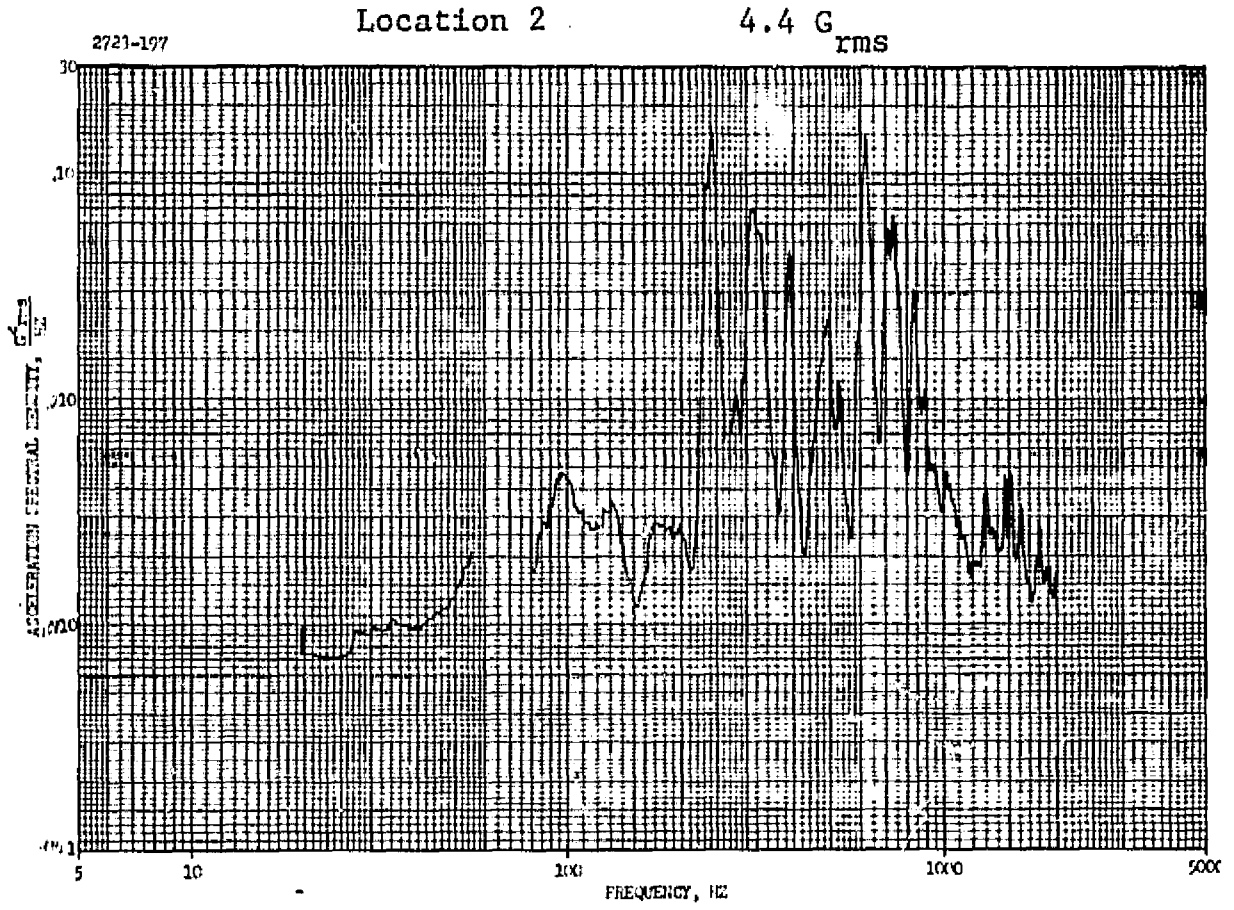

FIGURE 95. TEST #9 DATA - DIVIDER REMOVED

Location 3 6.18 G_{rms}

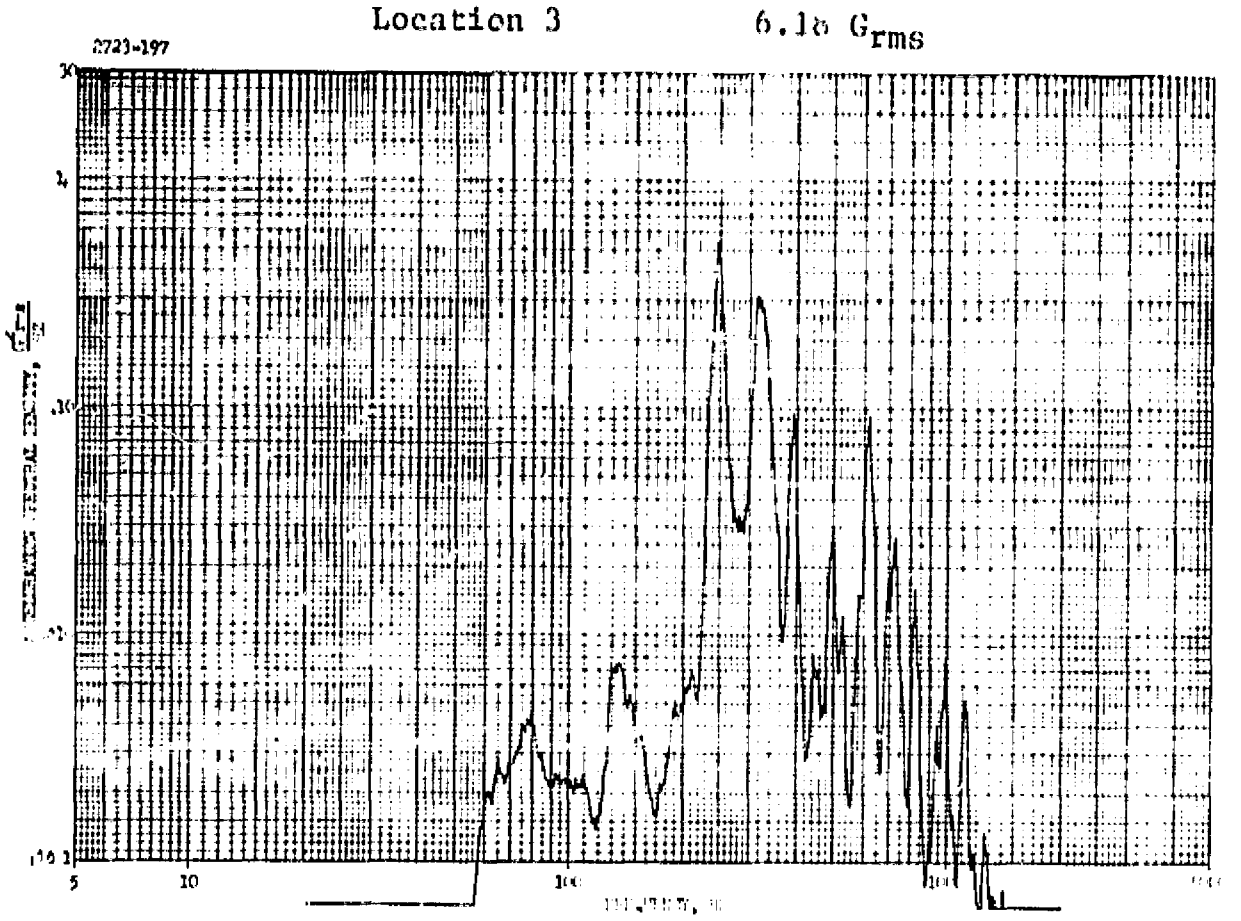

Location 4 6.18 G_{rms}

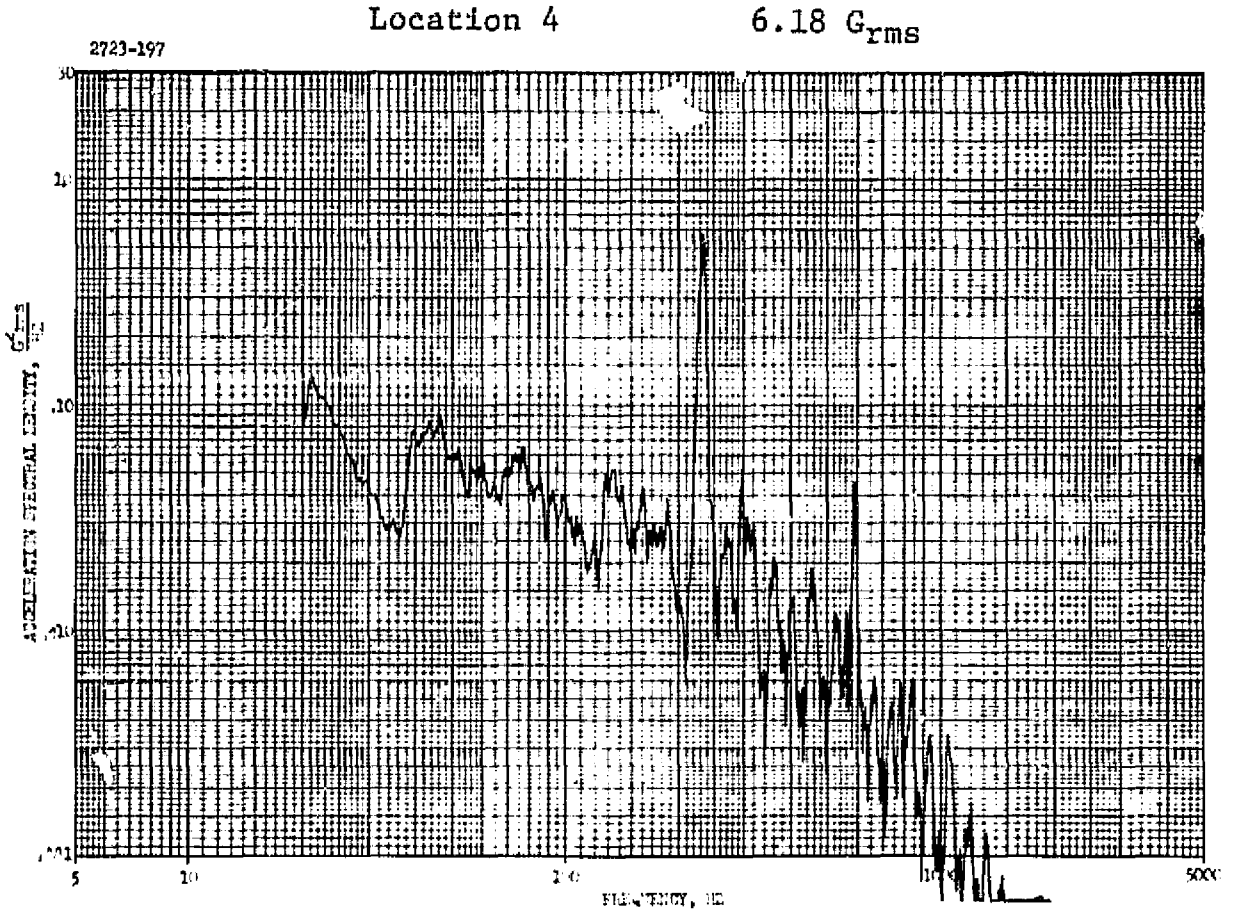

FIGURE 95. TEST #9 DATA - DIVIDER REMOVED (Continued)

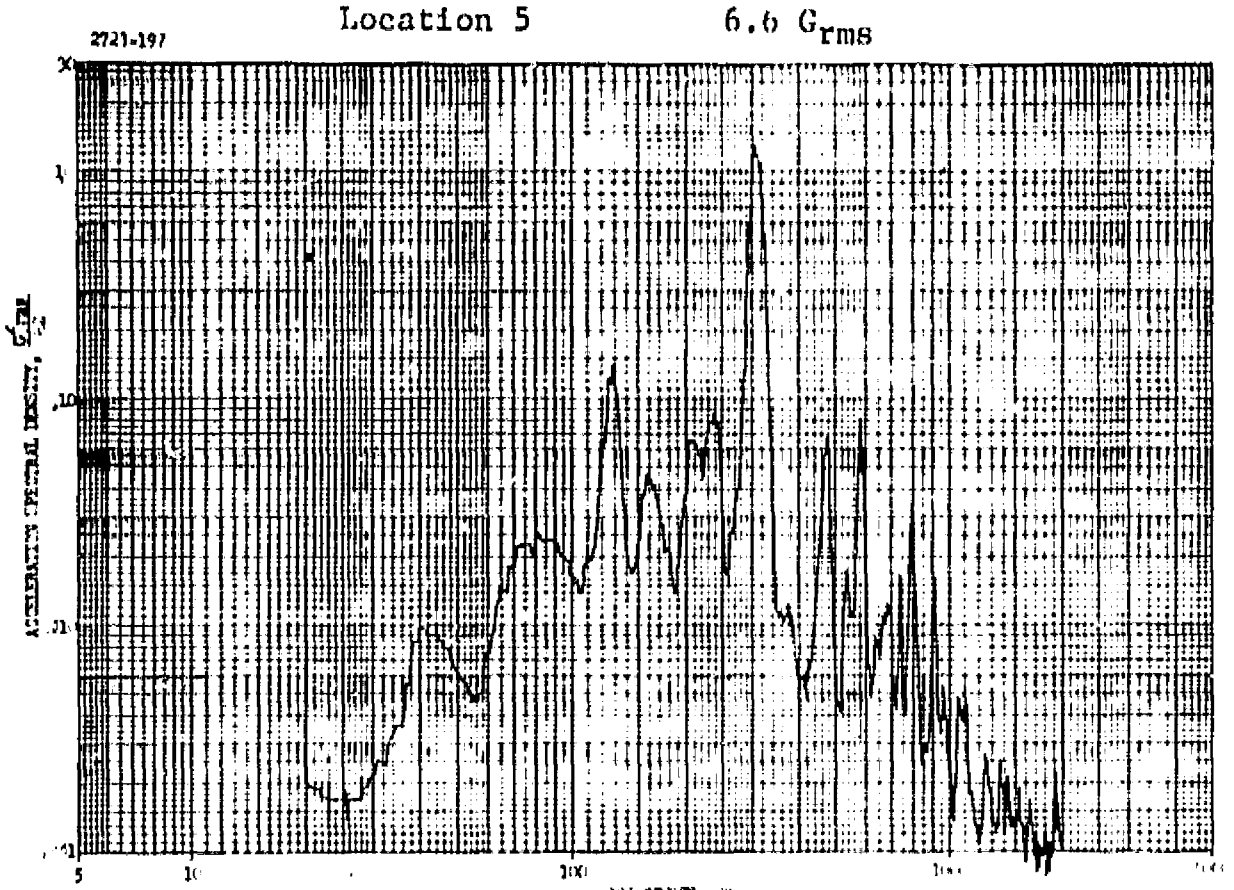

FIGURE 95. TEST #9 DATA - DIVIDER REMOVED (Concluded)

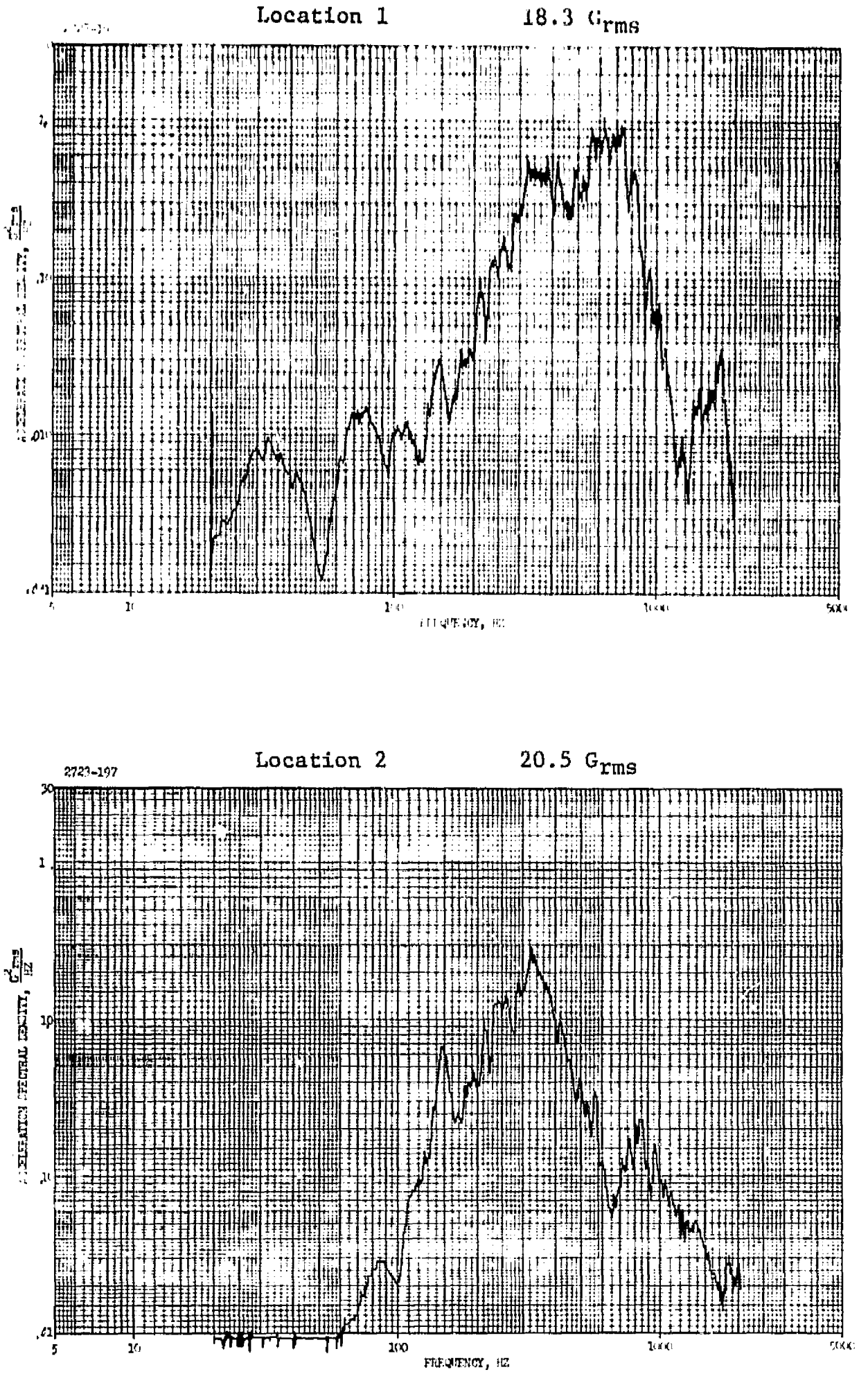

FIGURE 96. TEST #9B DATA

Location 3 20.5 G_{rms}

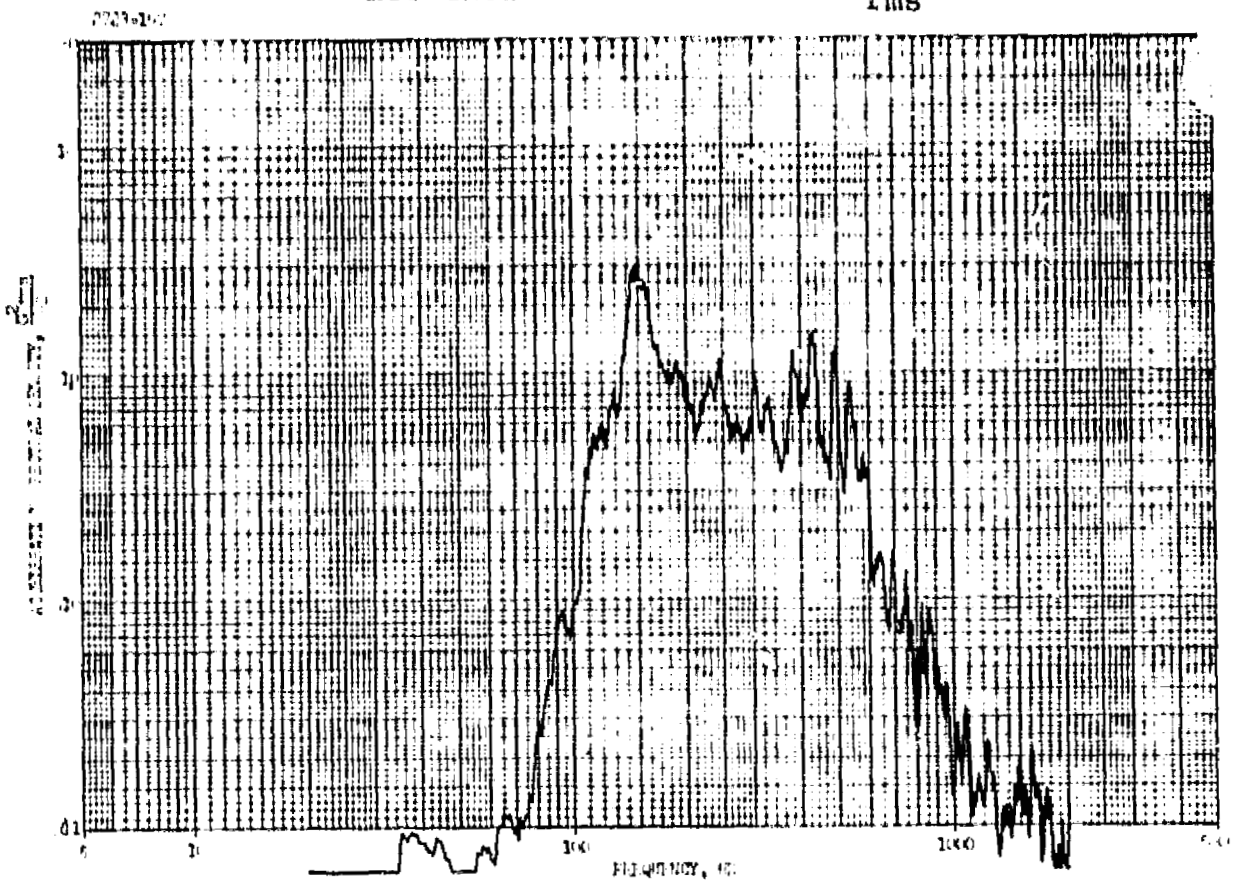

Location 4 19.3 G_{rms}

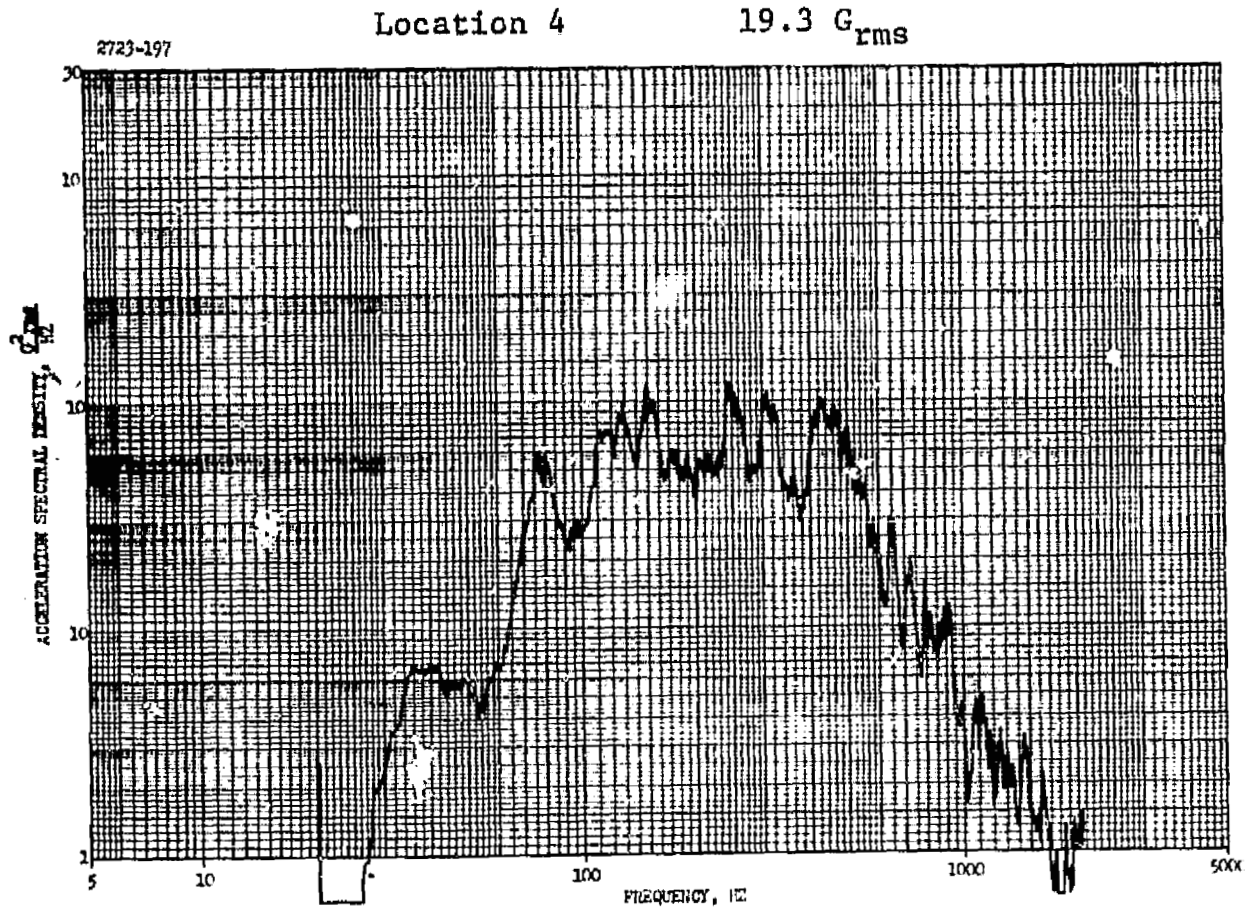

FIGURE 96. TEST #9B DATA (Continued)

Location 5 24.7 G_{rms}

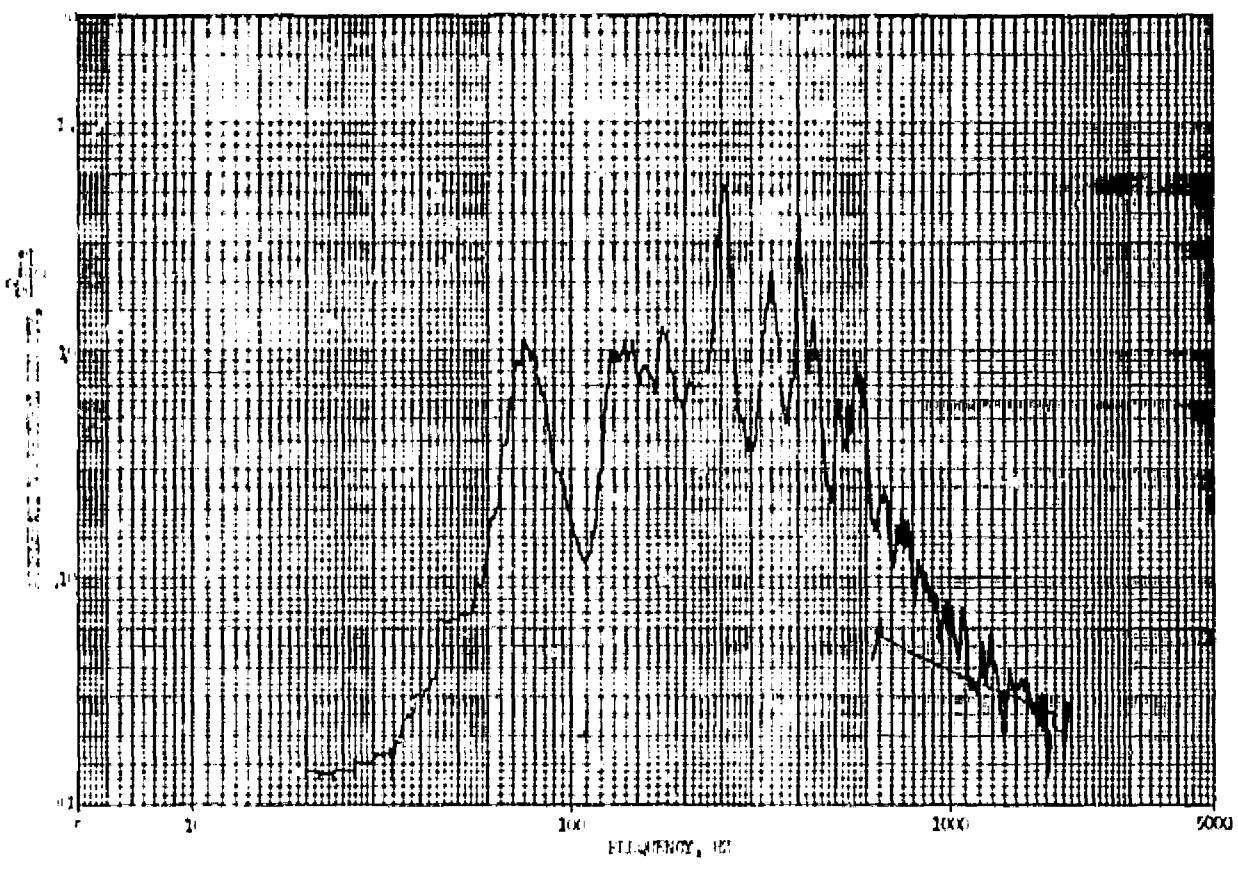

FIGURE 96. TEST #9B DATA (Concluded)

Location 1 14.7 G_{rms}

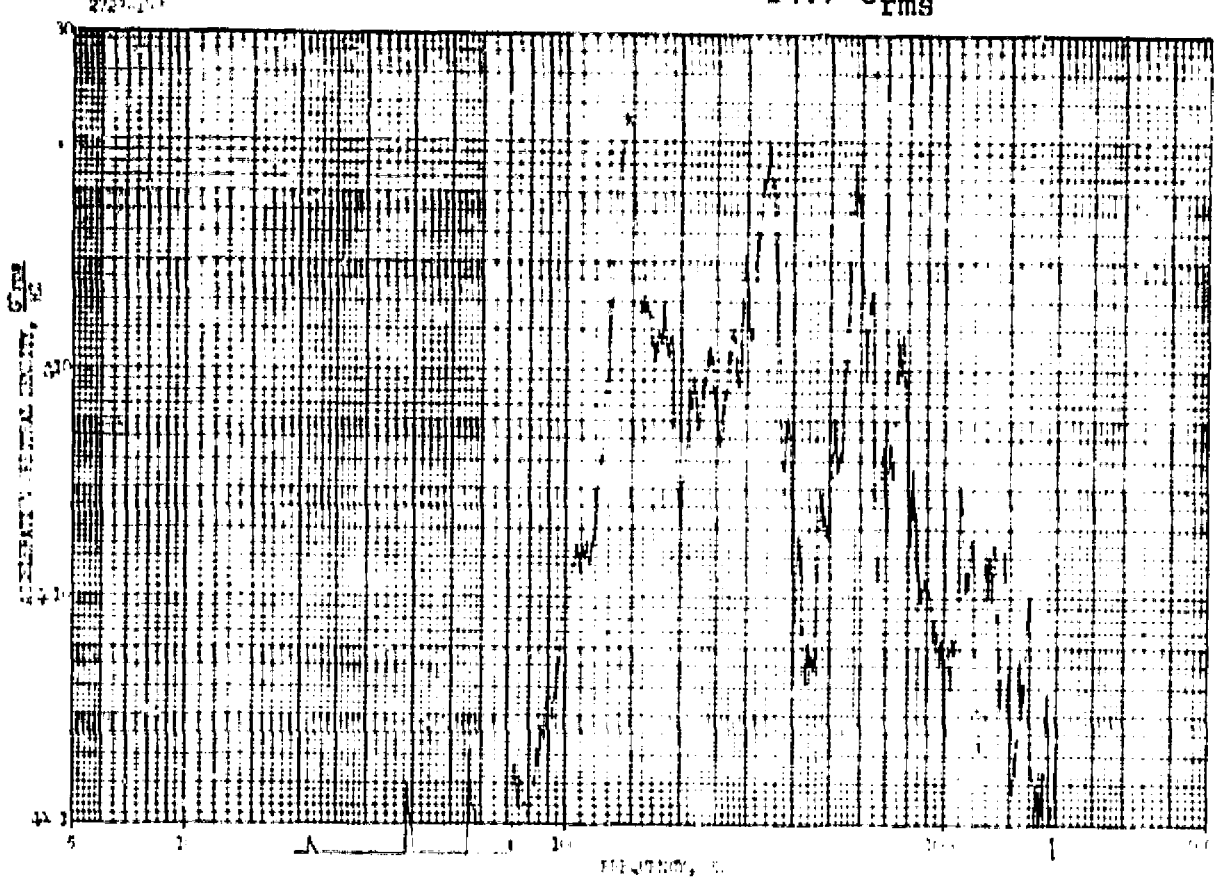

Location 2 35.3 G_{rms}

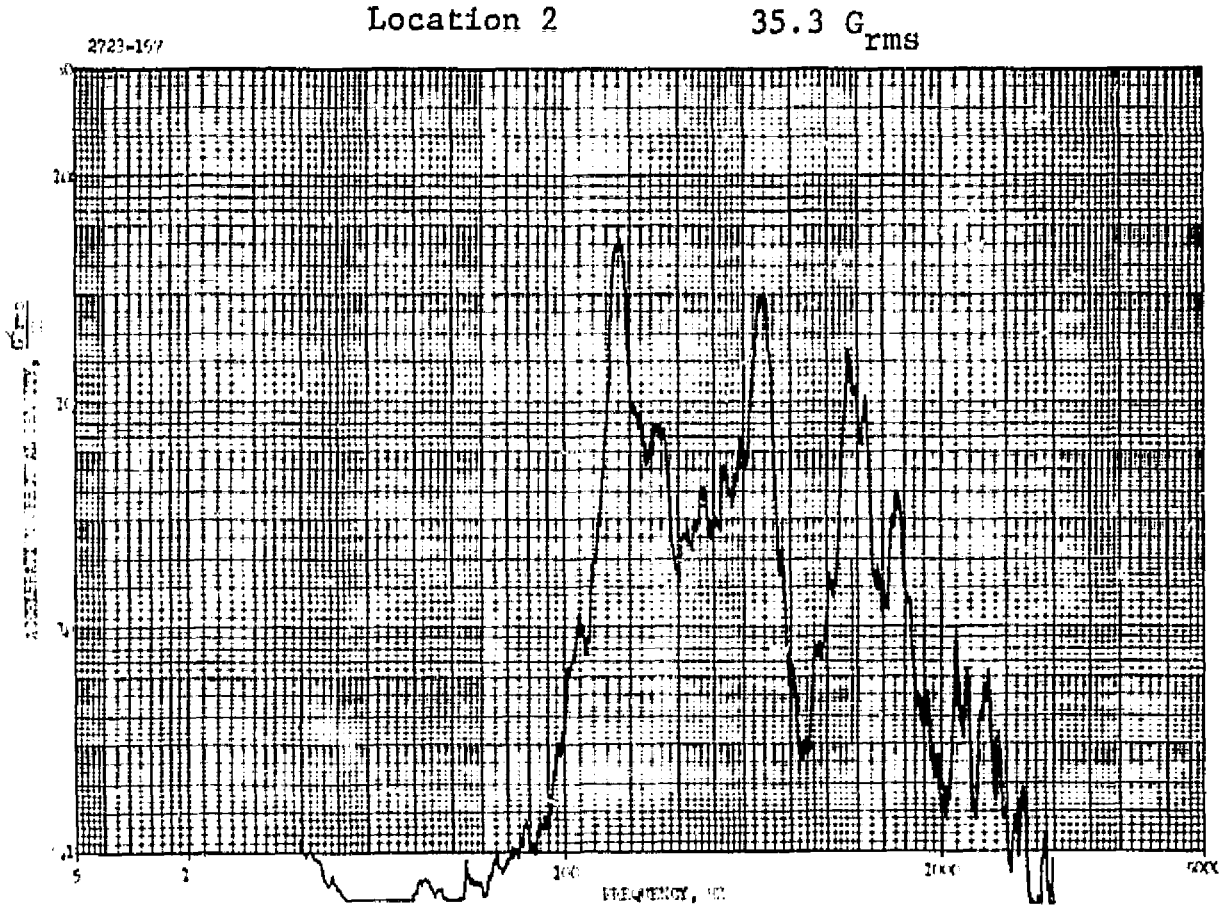

FIGURE 97. TEST # 10 DATA

Location 3 32.4 G_{rms}

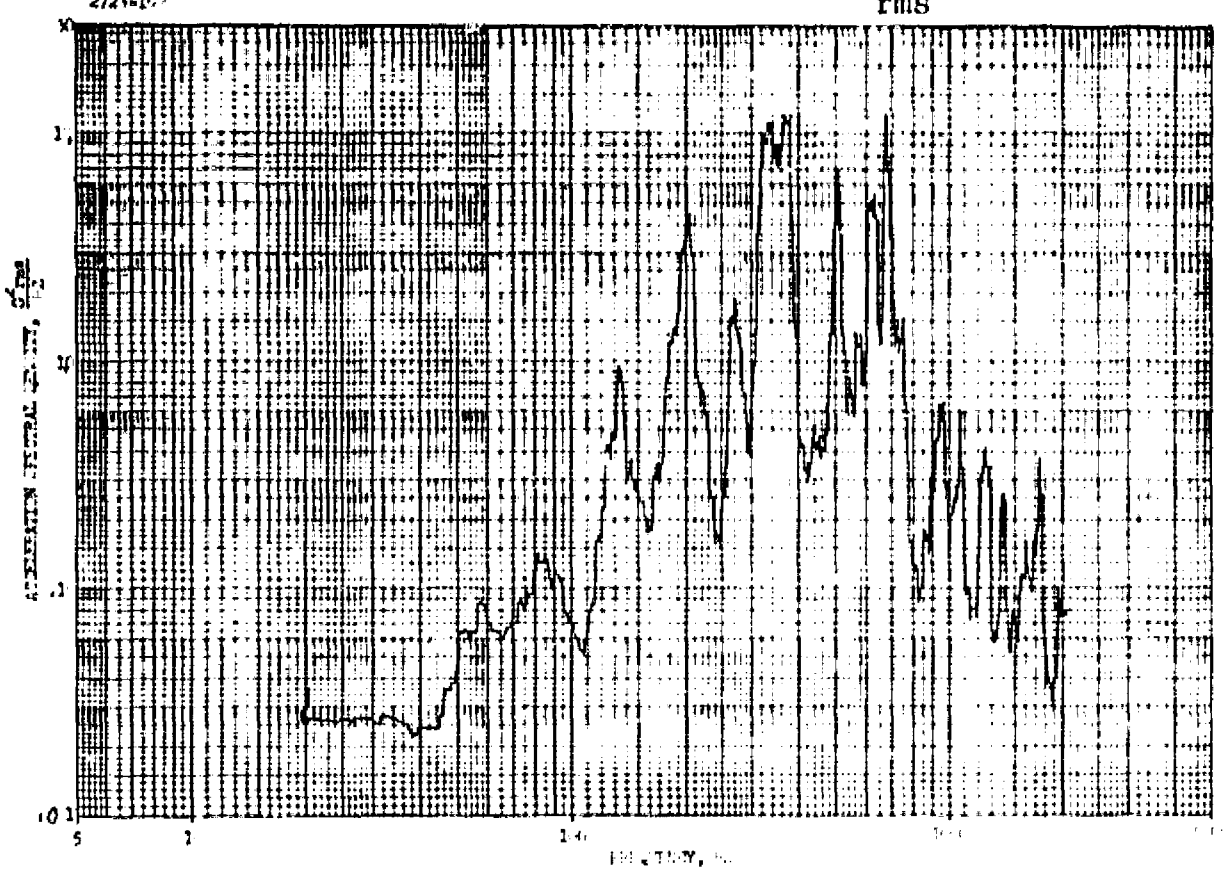

Location 4 14.7 G_{rms}

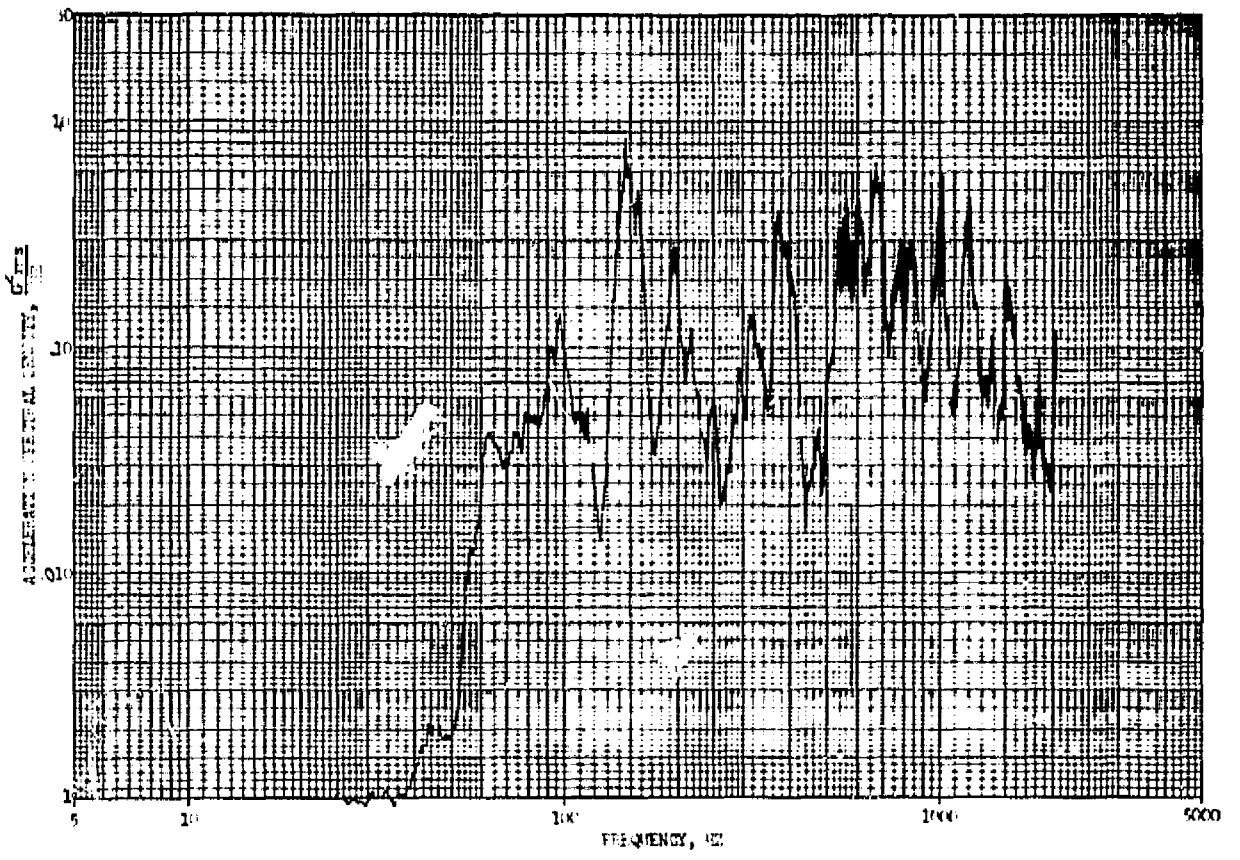

FIGURE 97. TEST #10 DATA (Continued)

Location 5 9.44 G_{rms}

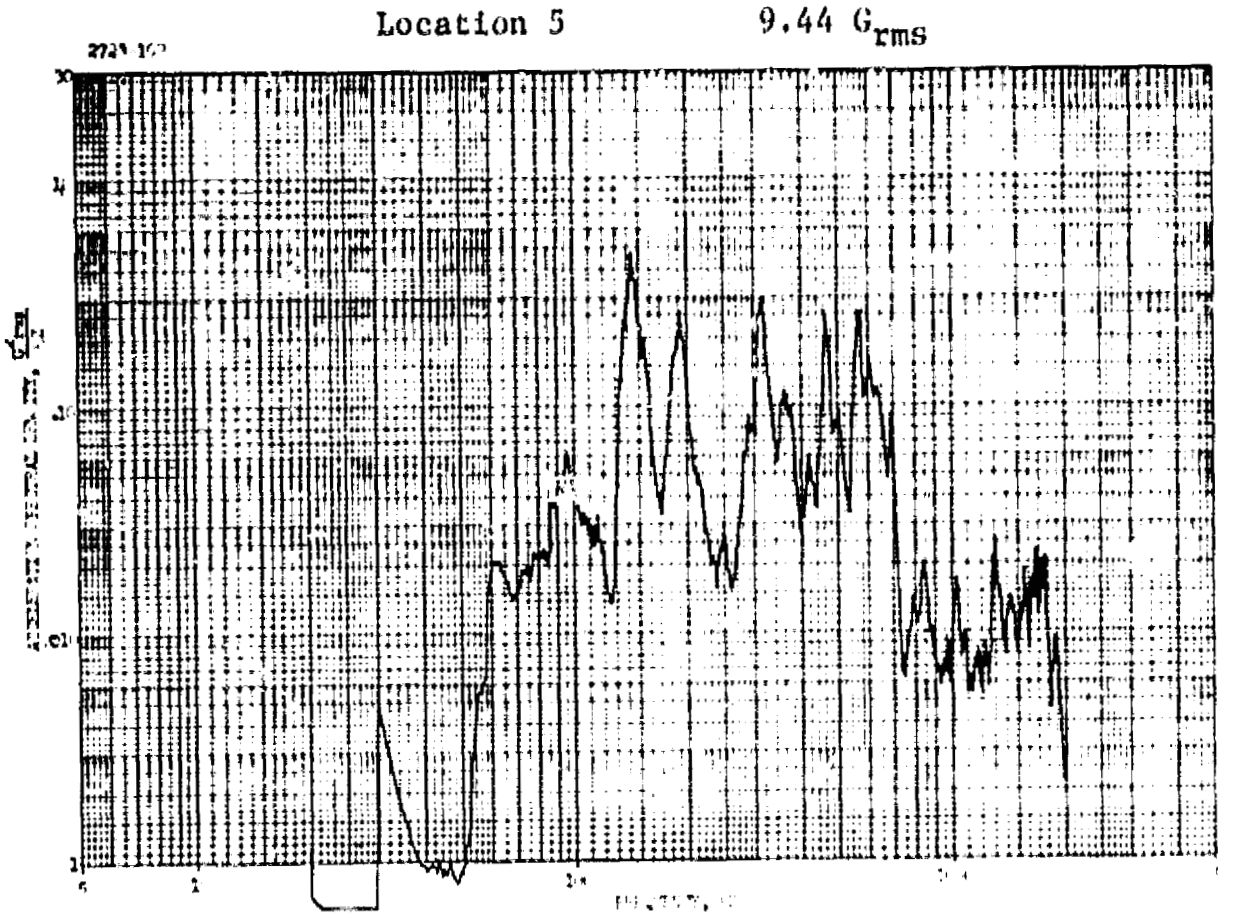

Location 6 11.8 G_{rms}

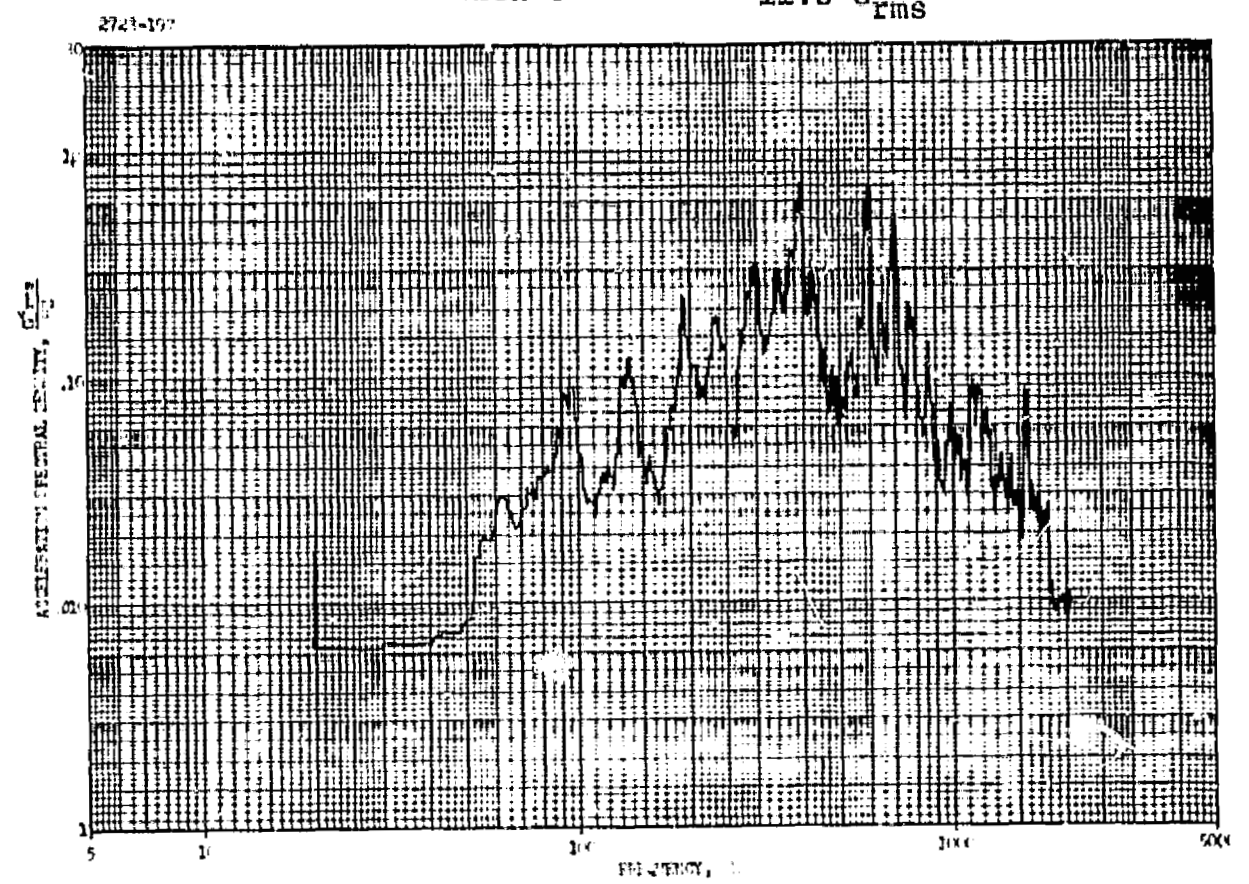

FIGURE 97. TEST #10 DATA (Continued)

Location 7 8.25 G_{rms}

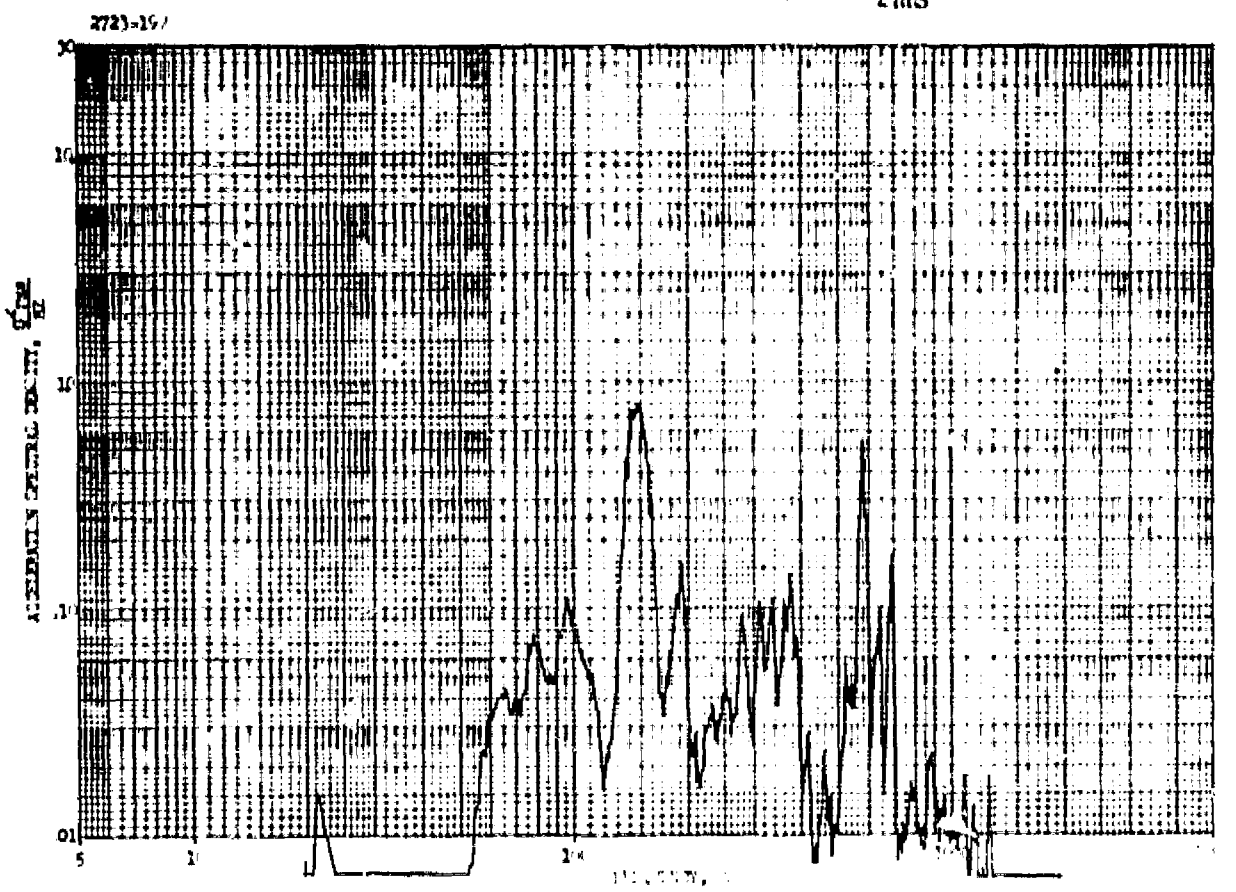

Location 8 22.4 G_{rms}

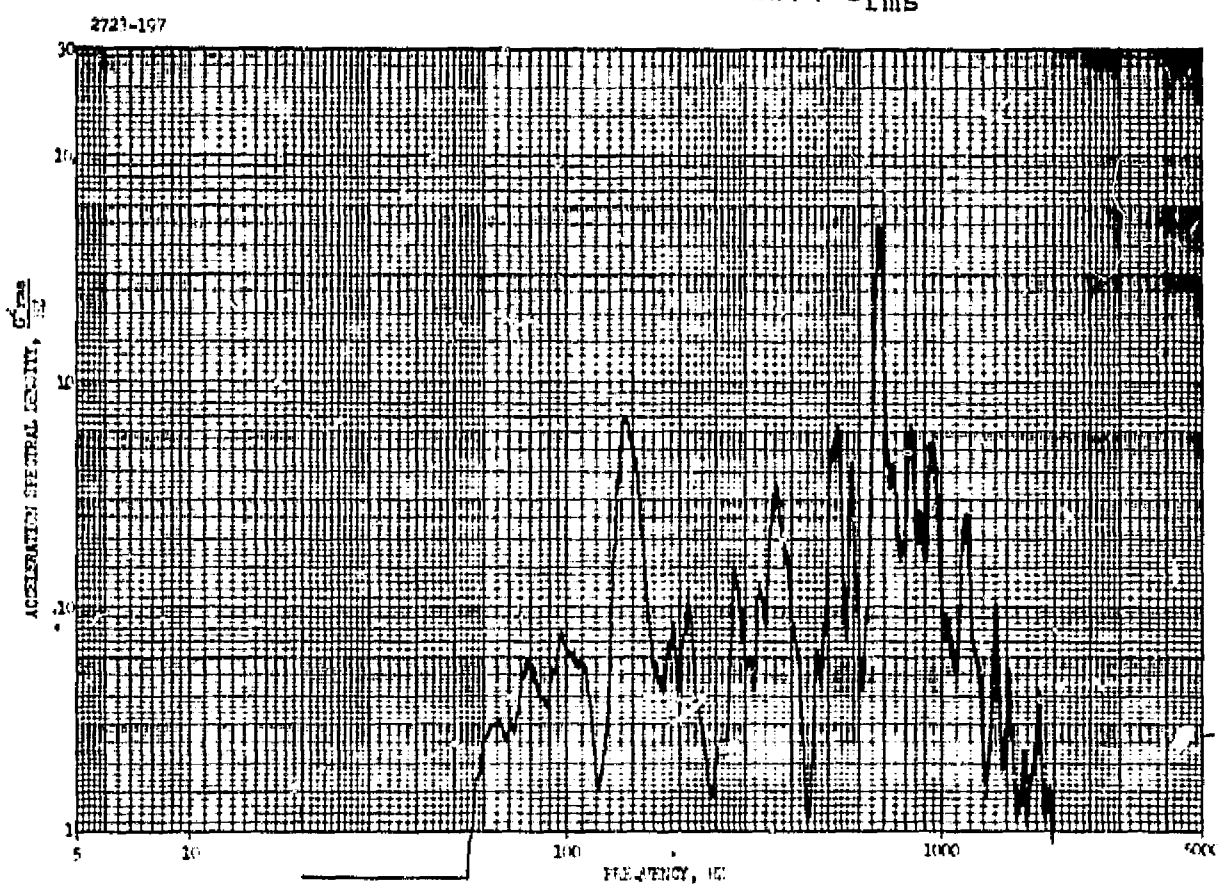

FIGURE 97. TEST #10 DATA (Continued)

Location 9 33.5 G_{rms}

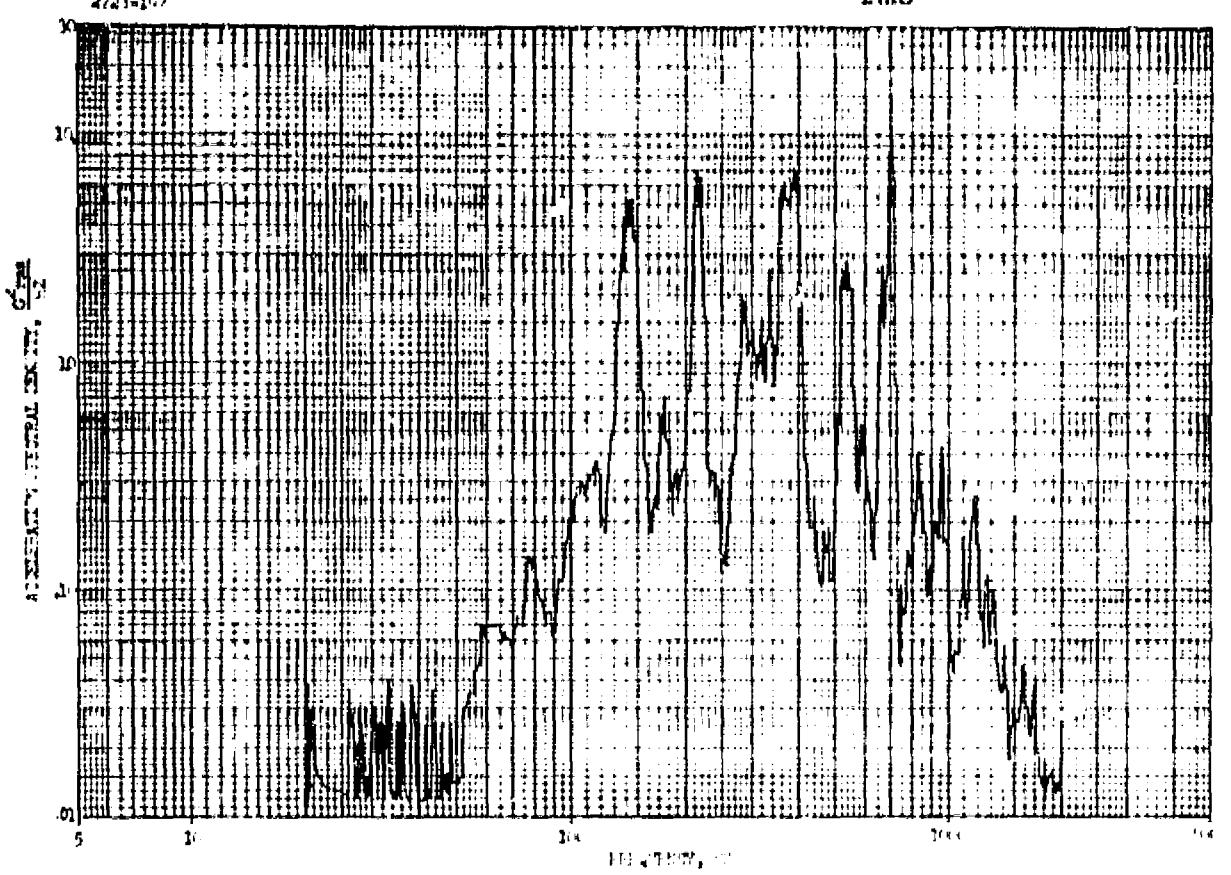

Location 10 35.3 G_{rms}

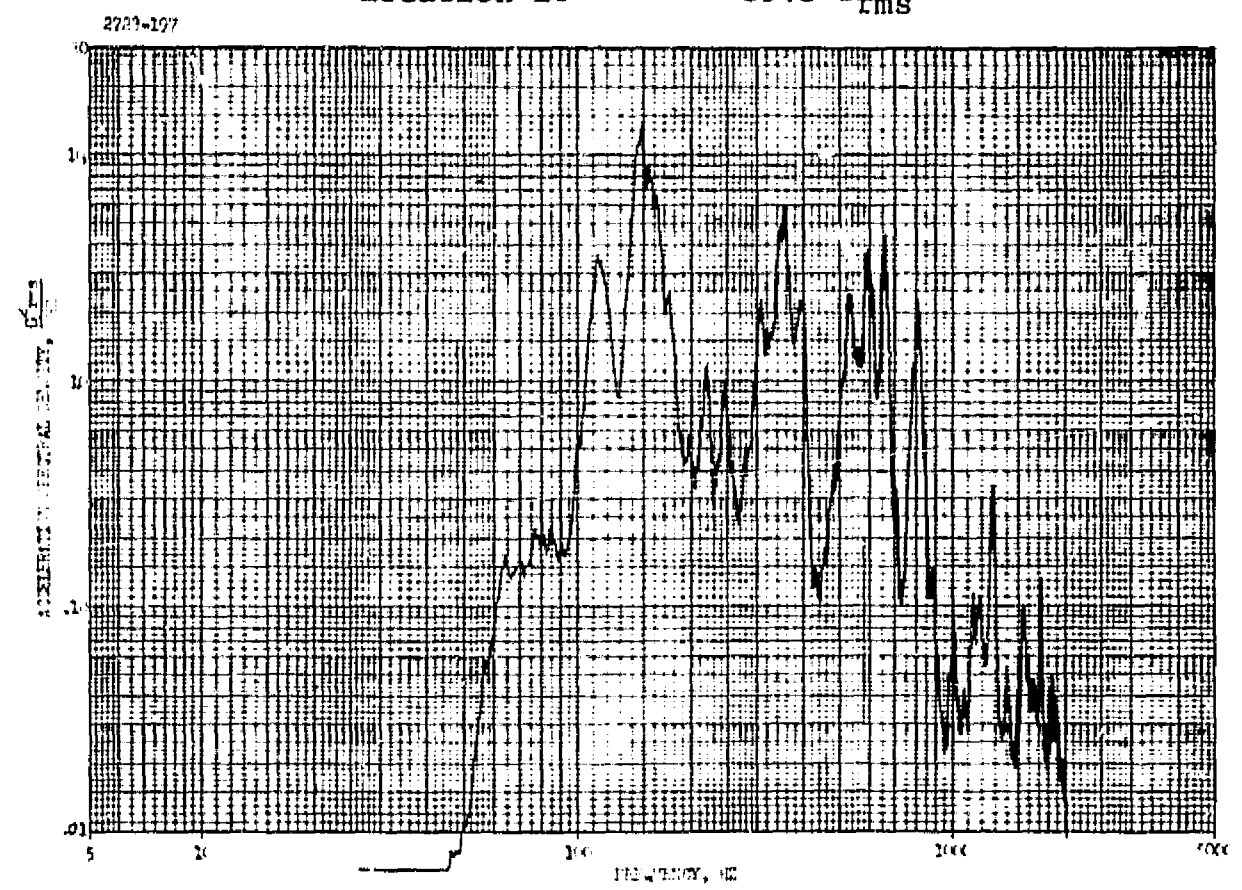

FIGURE 97. TEST #10 DATA (Continued)

Location 11 14.7 G_{rms}

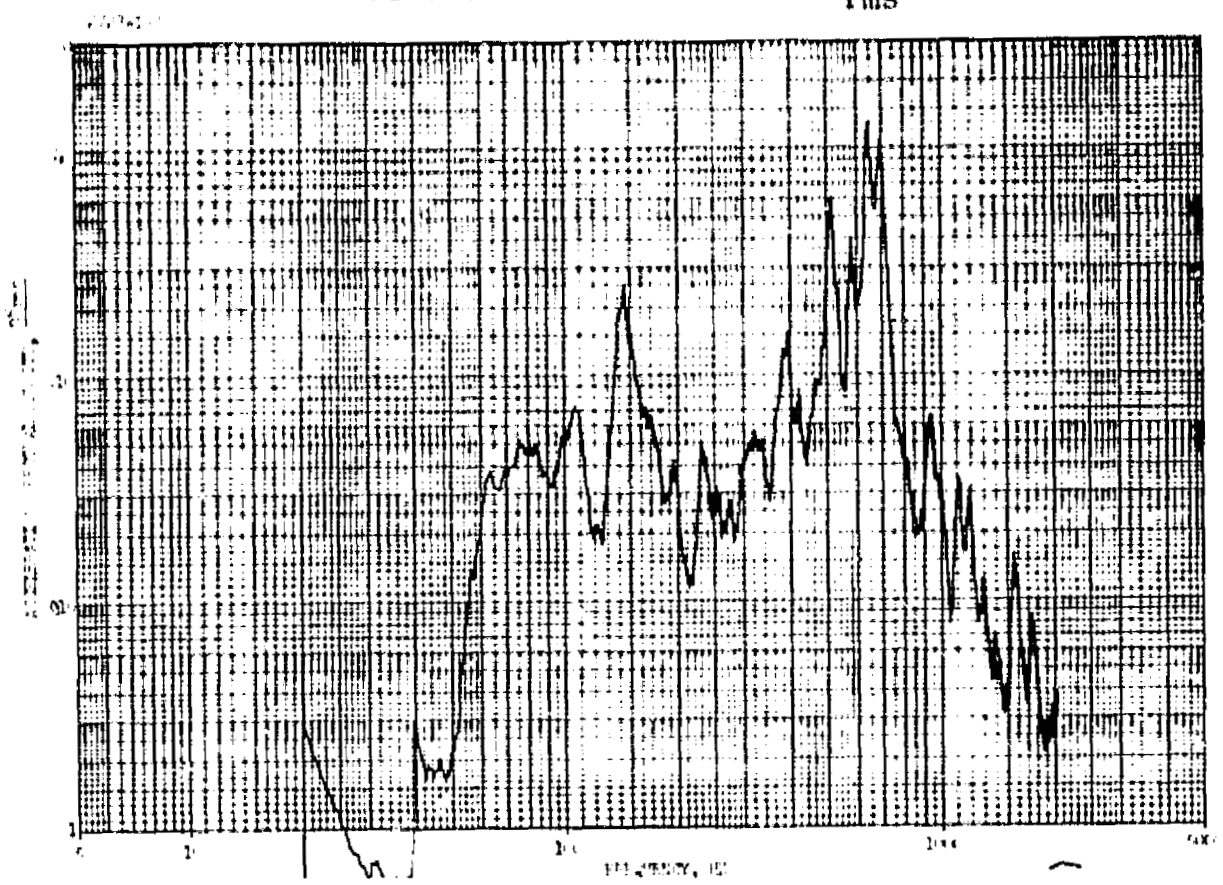

FIGURE 97. TEST #10 DATA (Concluded)

Location 1 9.43 G_{rms}

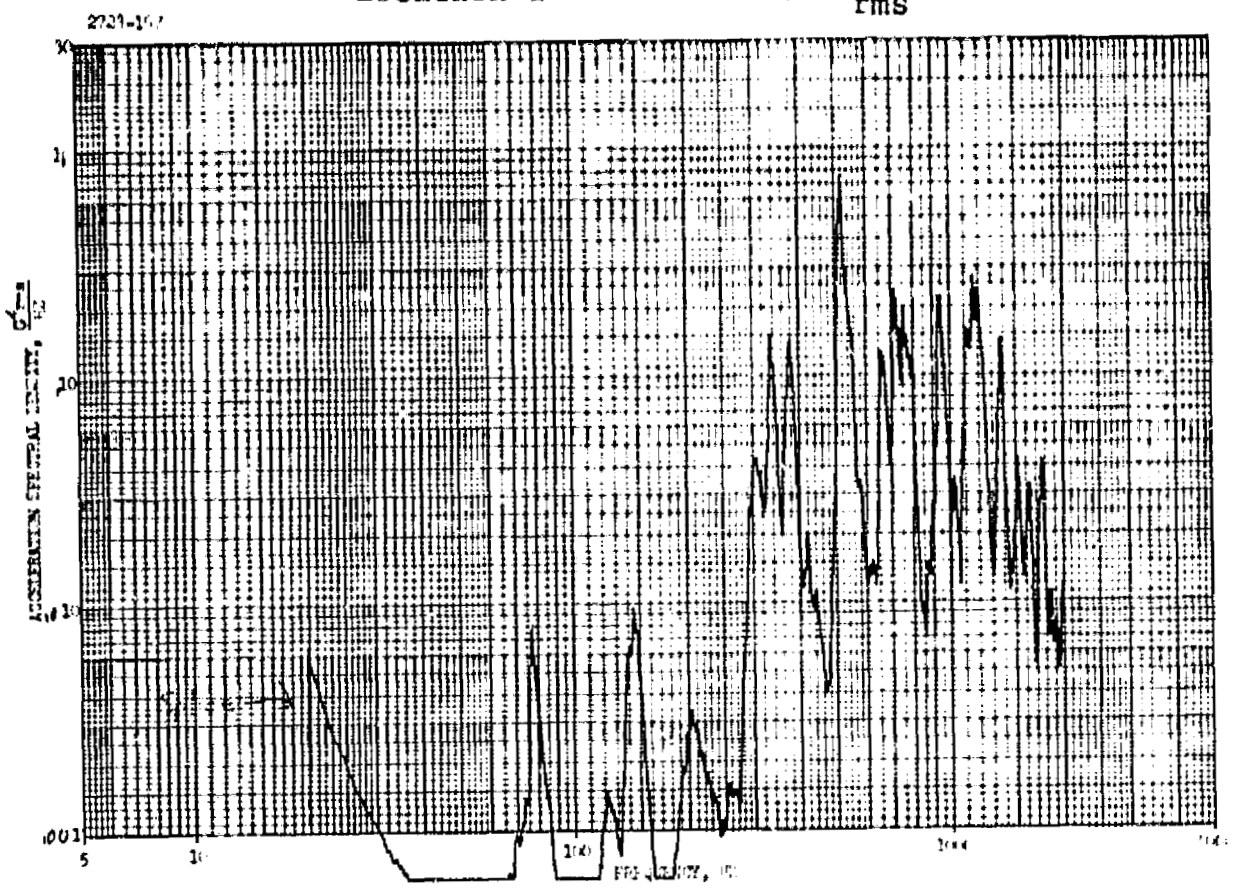

Location 2 32.4 G_{rms}

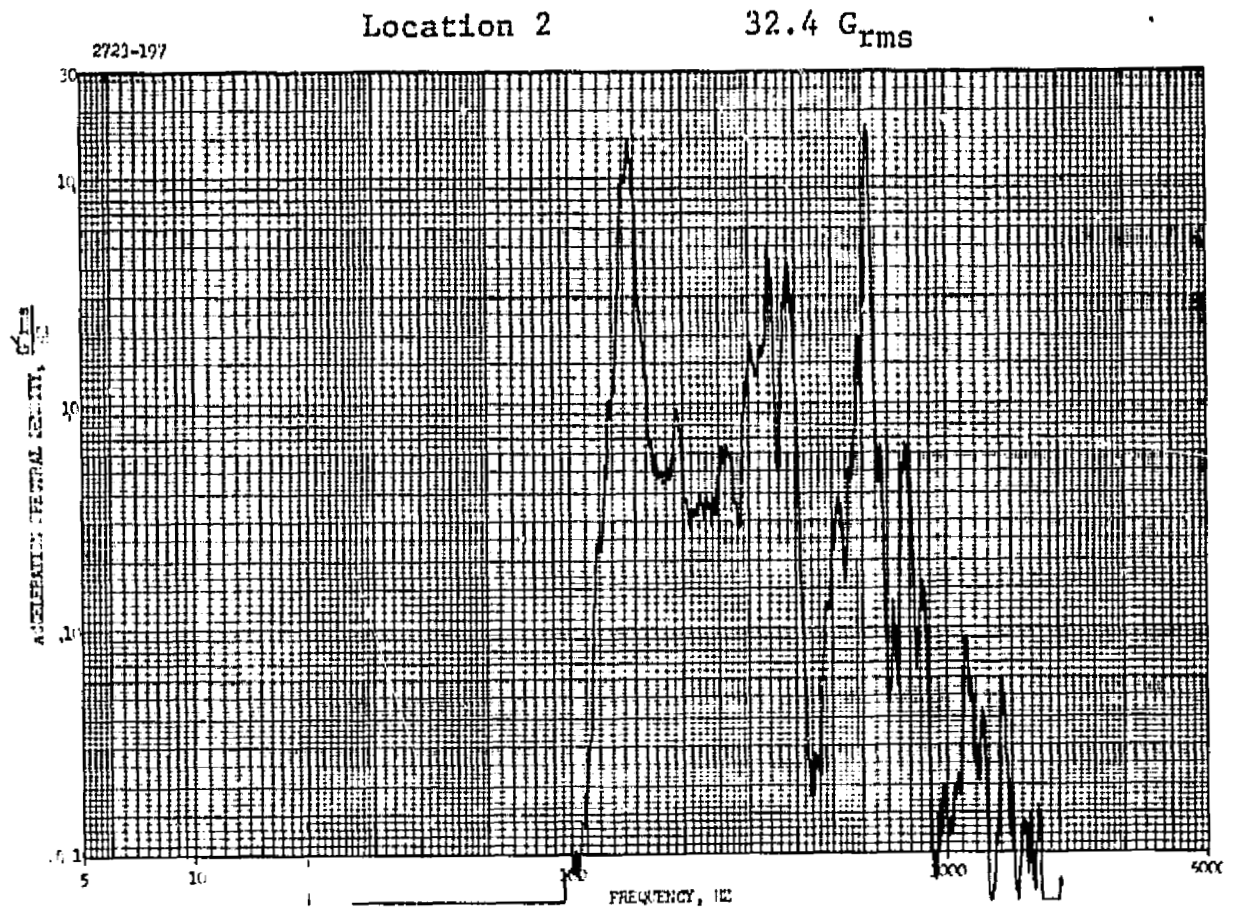

FIGURE 98. TEST # 11 DATA

Location 3 26.5 G_{rms}

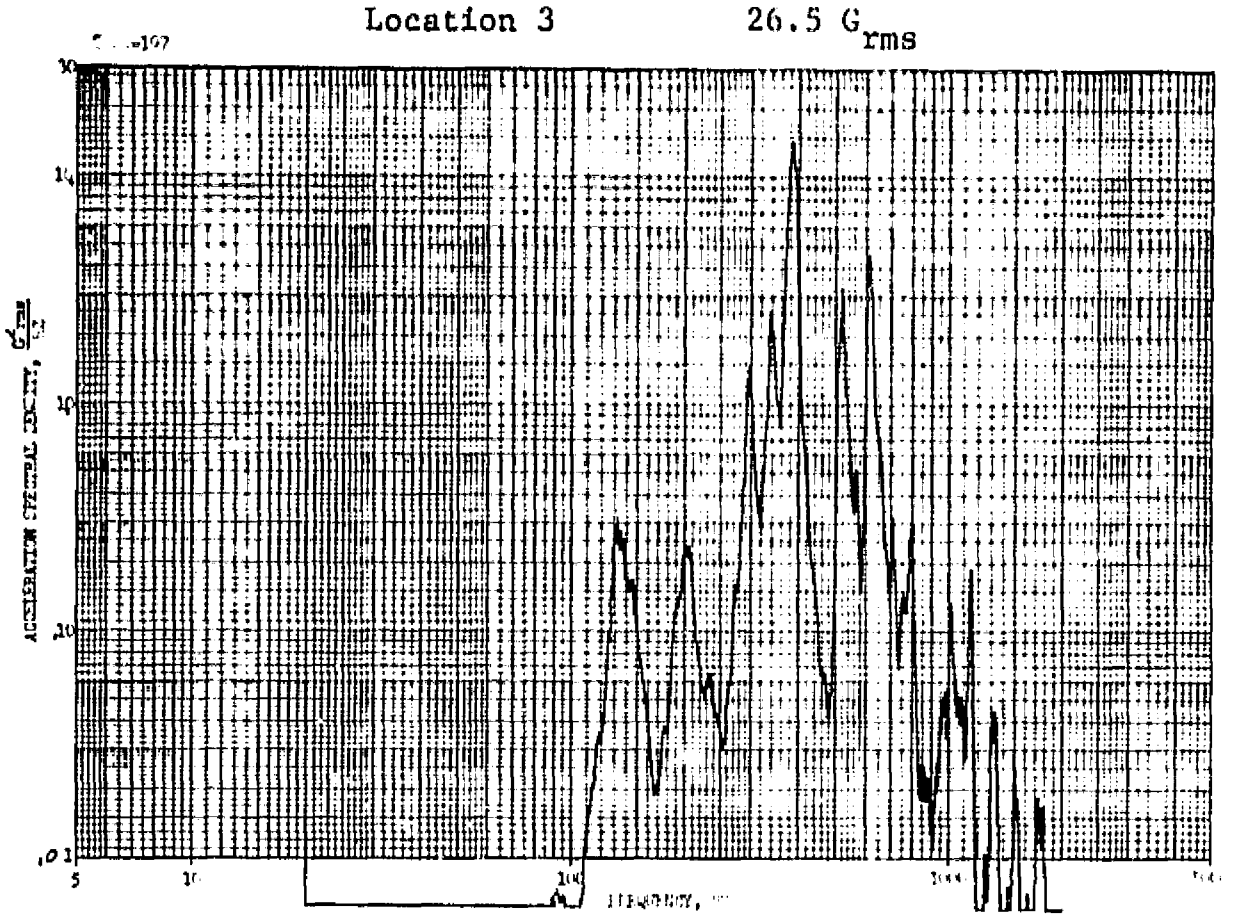

Location 4 8.24 G_{rms}

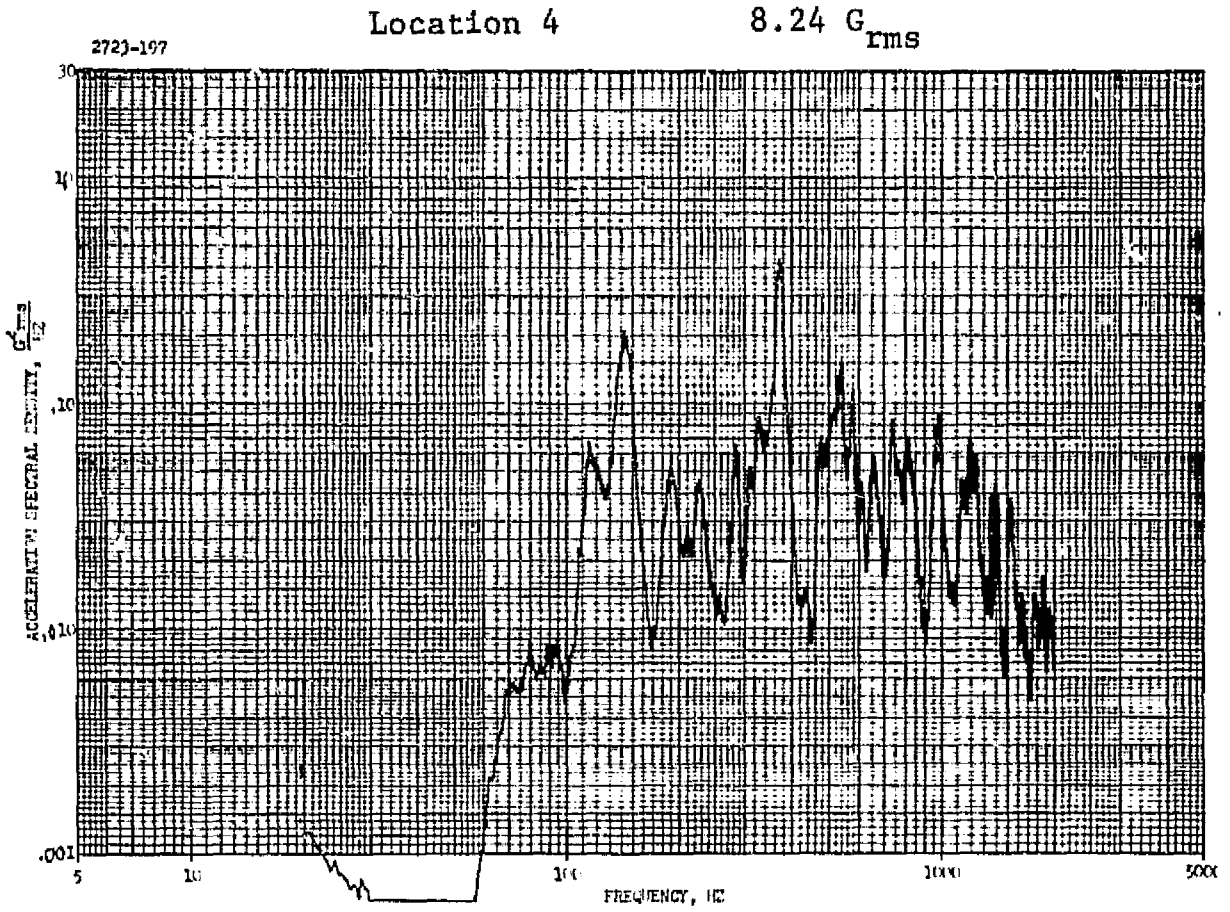

FIGURE 98. TEST #11 DATA (Continued)

Location 5 8.83 G_{rms}

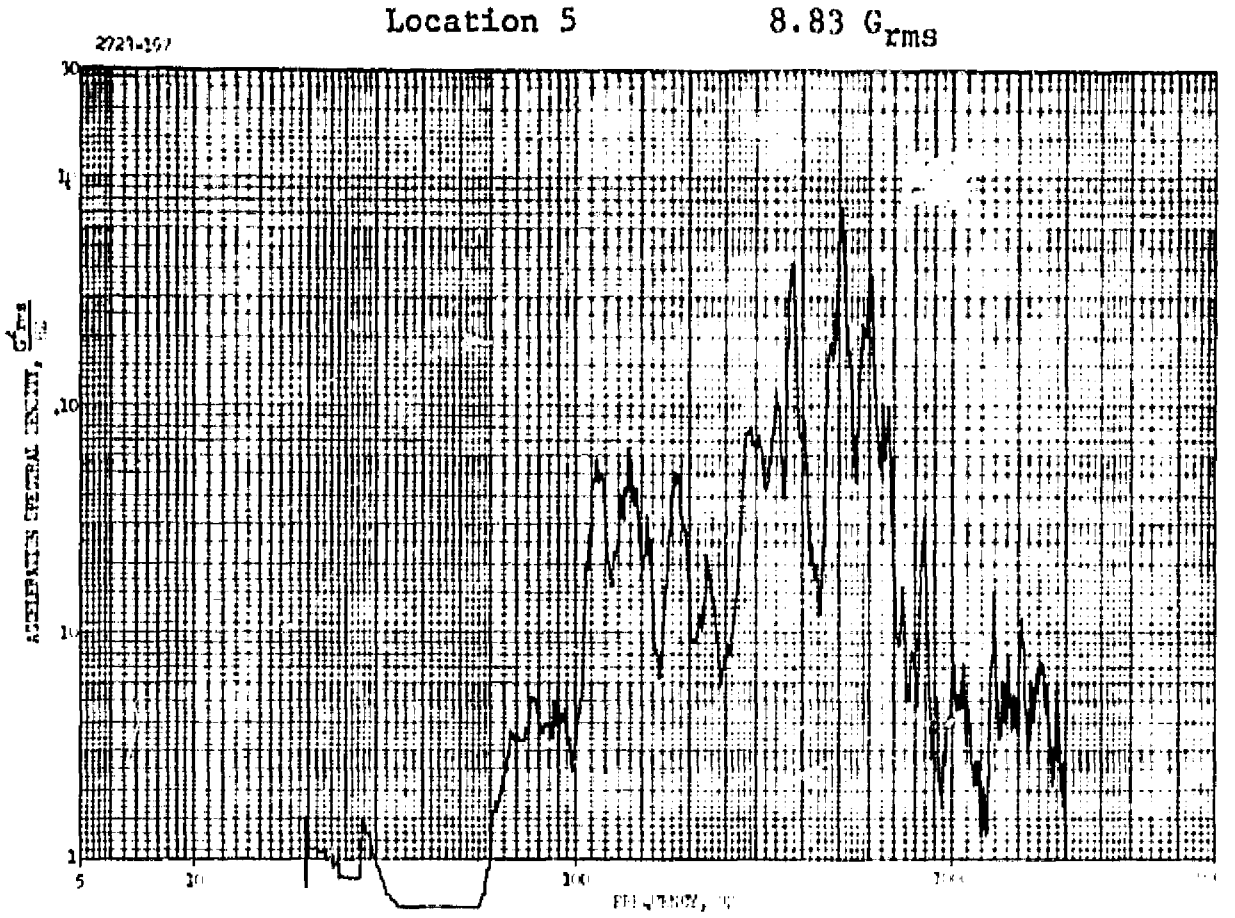

Location 6 11.75 G_{rms}

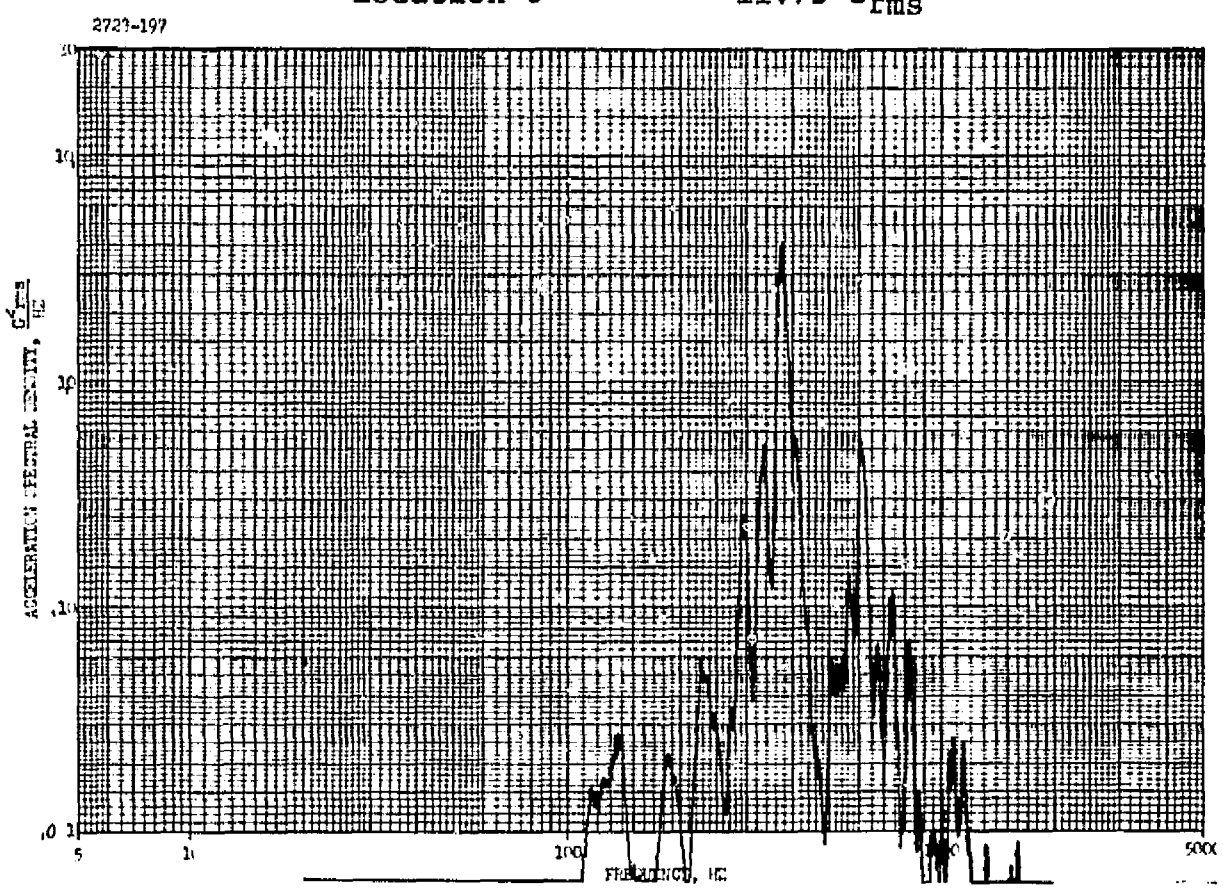

FIGURE 98. TEST #11 DATA (Continued)

Location 7 6.43 G_{rms}

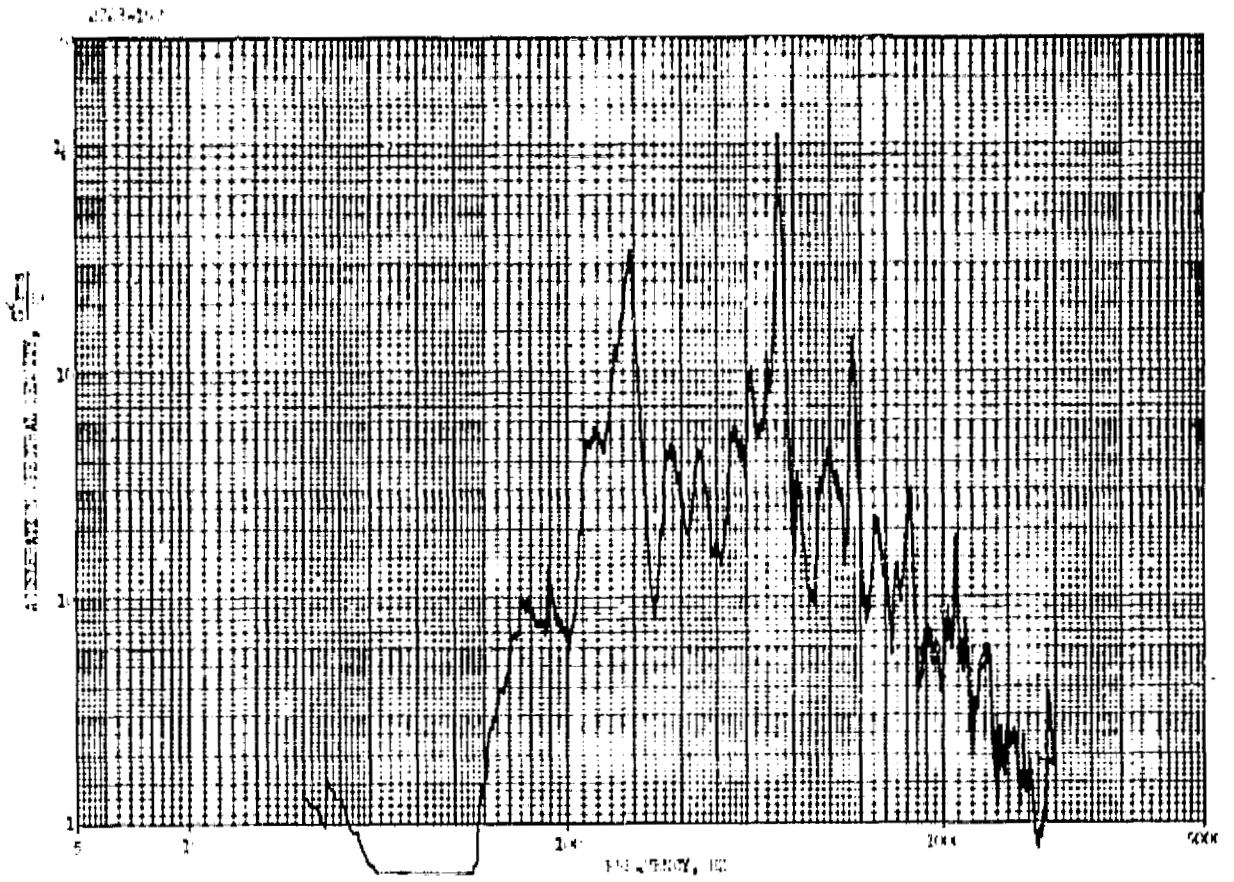

Location 8 17.65 G_{rms}

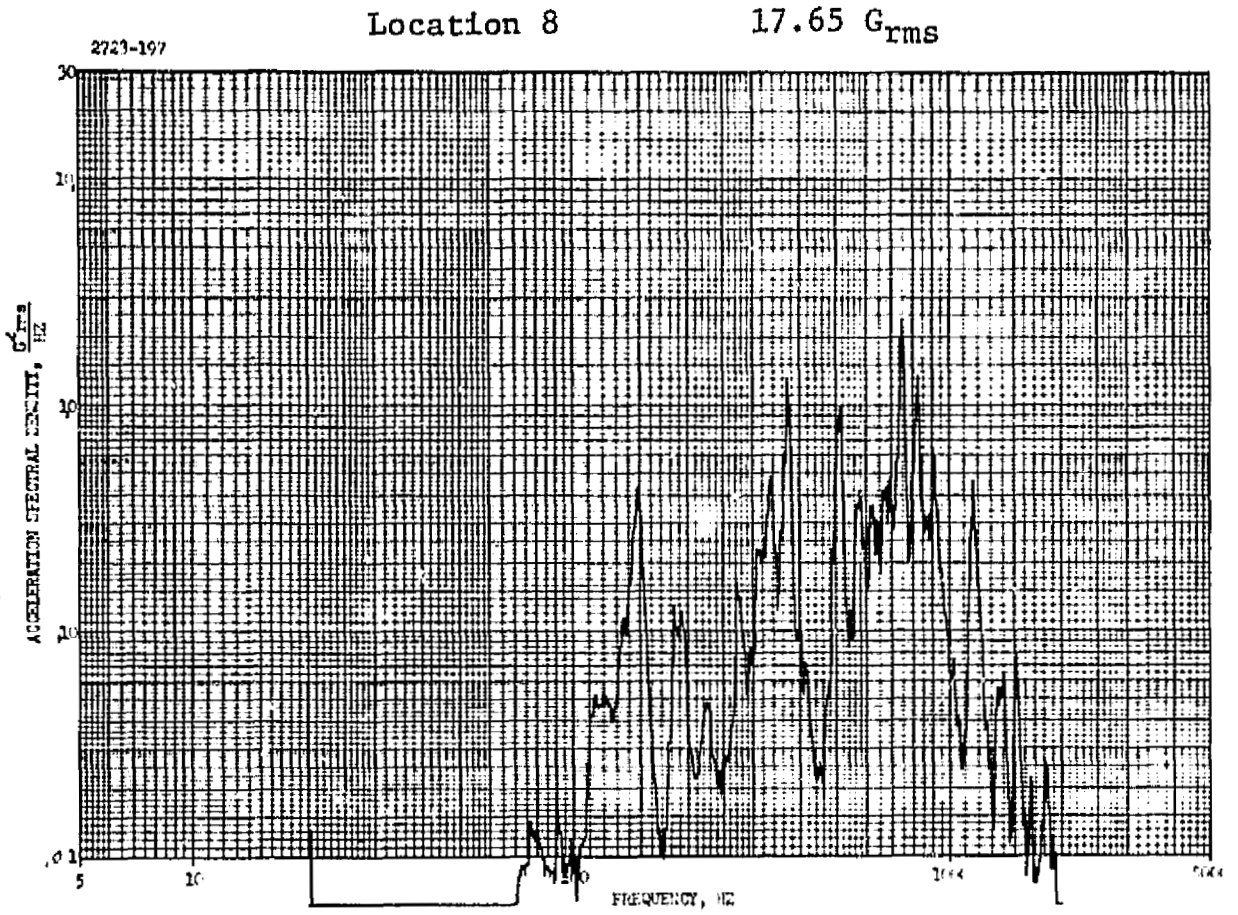

FIGURE 98. TEST #11 DATA (Continued)

Location 9 30.9 G_{rms}

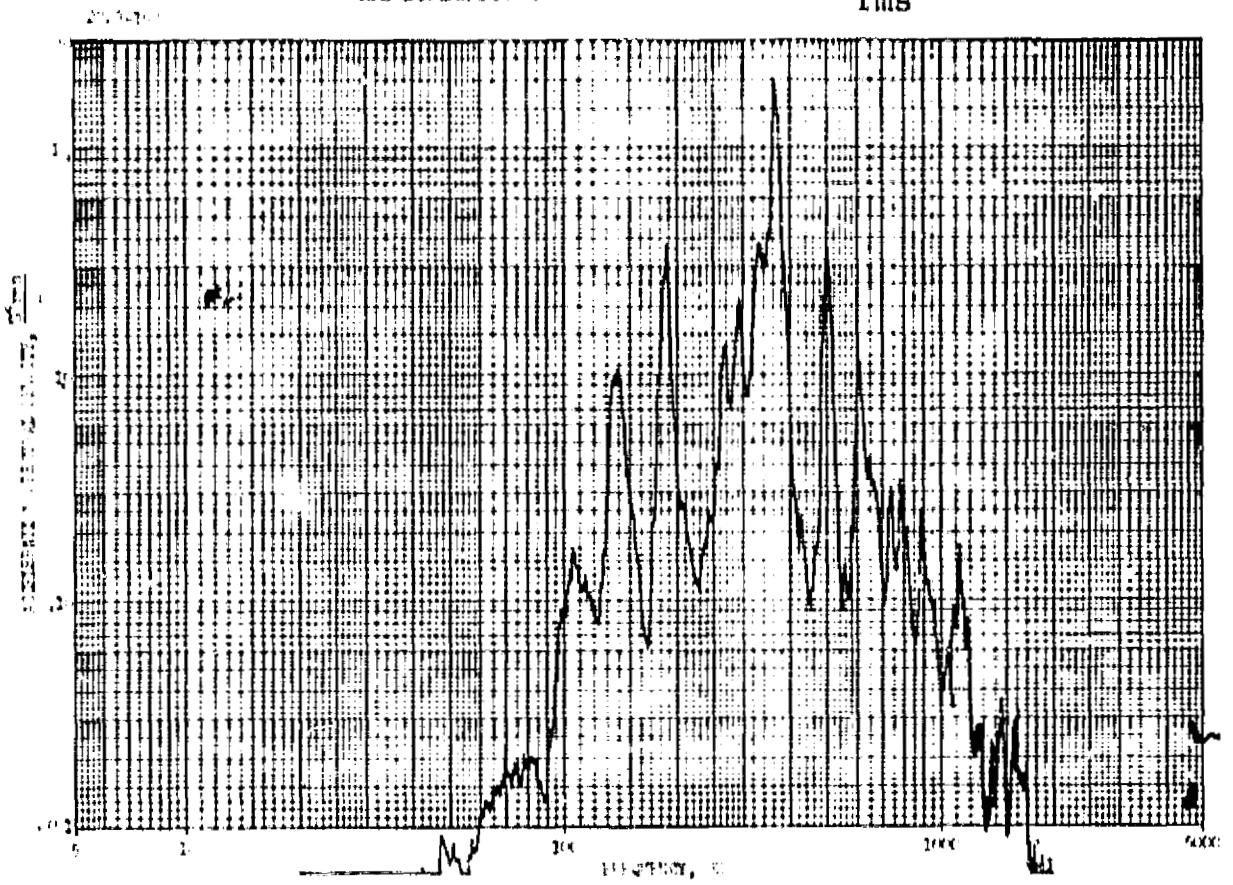

Location 10 41.2 G_{rms}

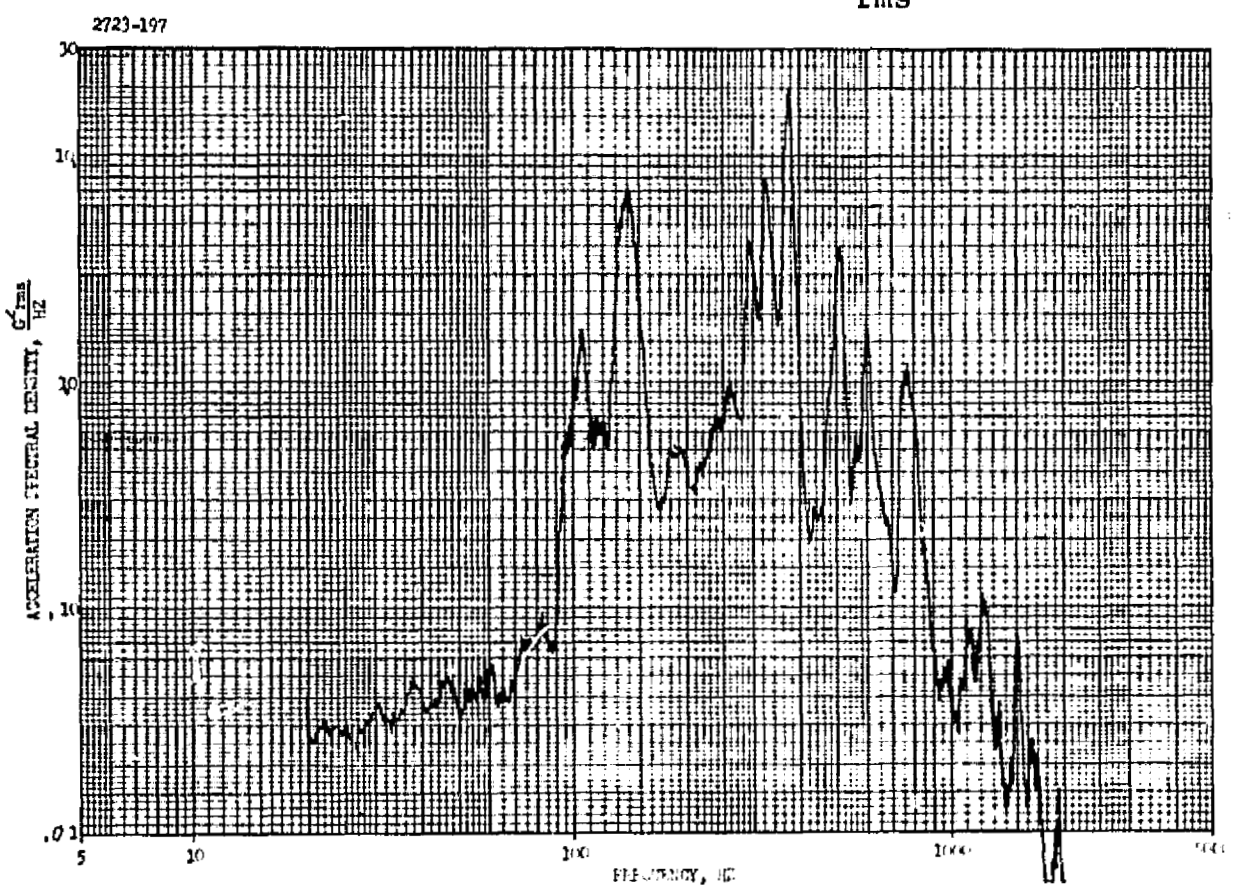

FIGURE 98. TEST #11 DATA (Continued)

Location 11 13.25 G_{rms}

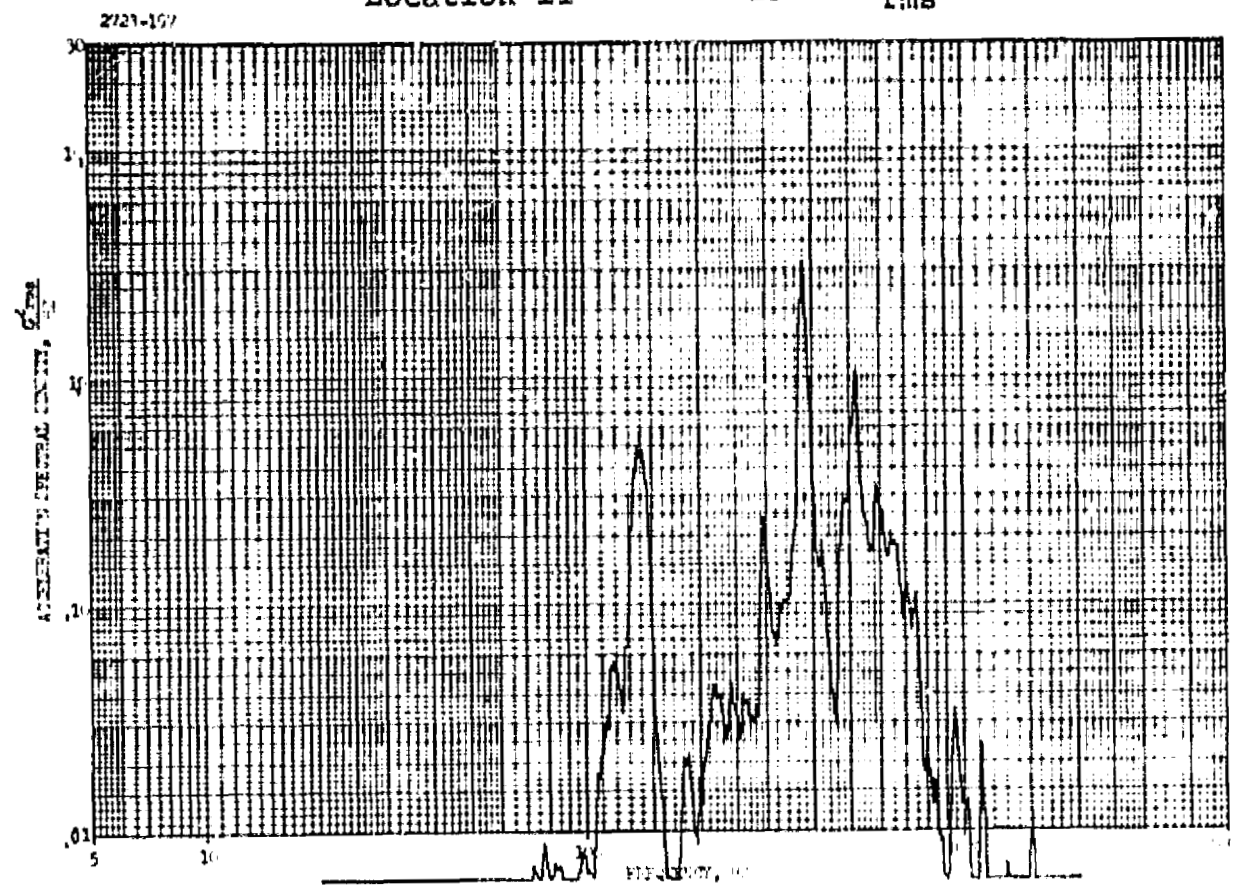

FIGURE 98. TEST #11 DATA (Concluded)

Location 1 4.62 G_{rms}

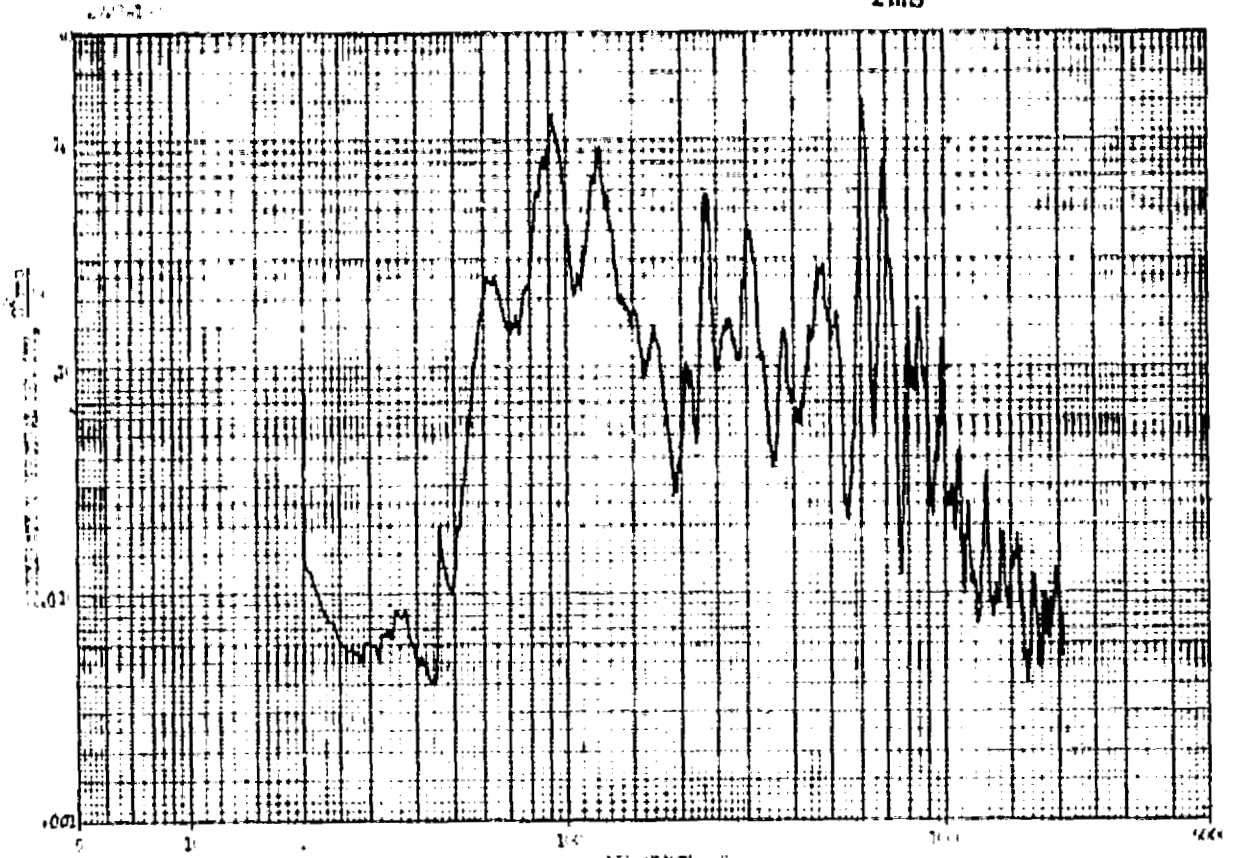

Location 2 11. 06 G_{rms}

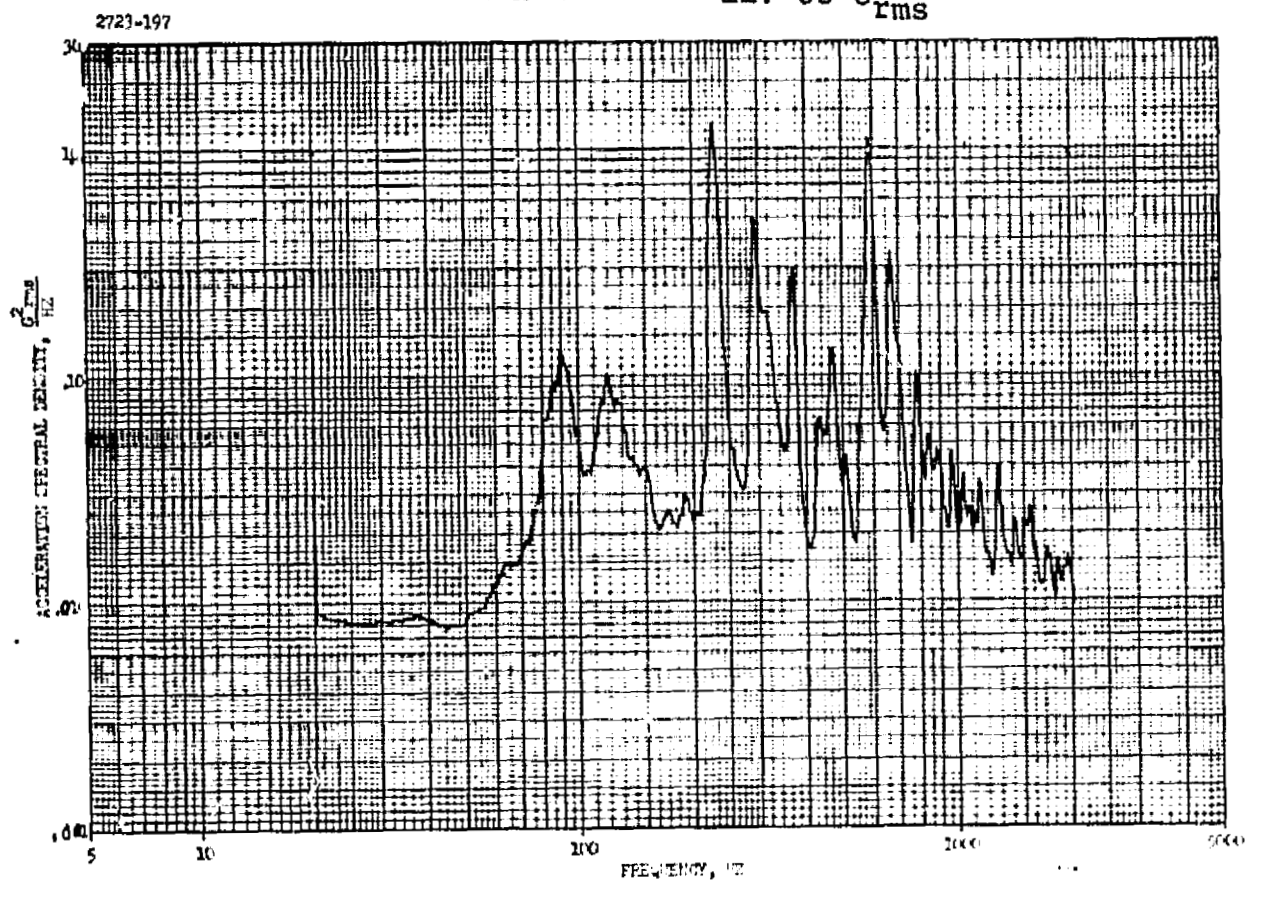

FIGURE 99. TEST # 12 DATA

Location 3

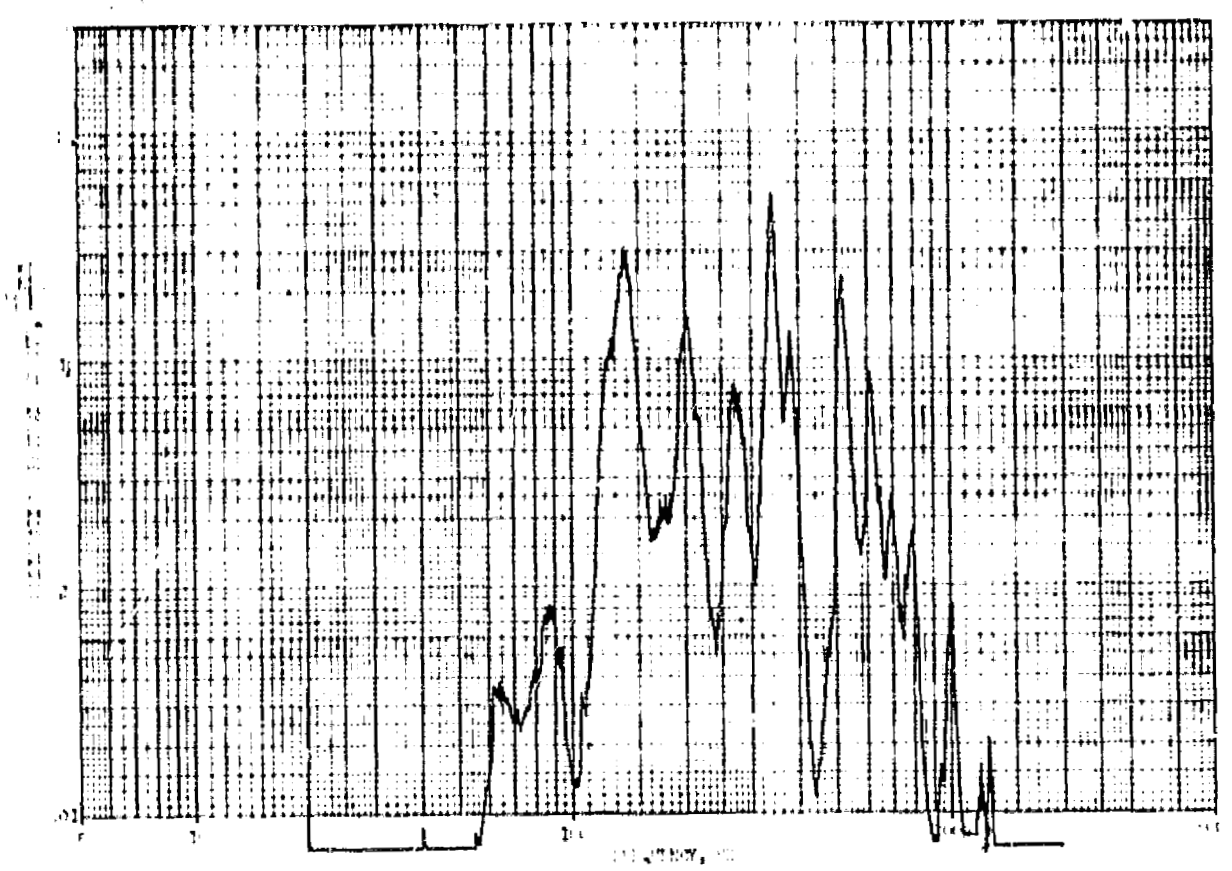

Location 4 11.53 G_{rms}

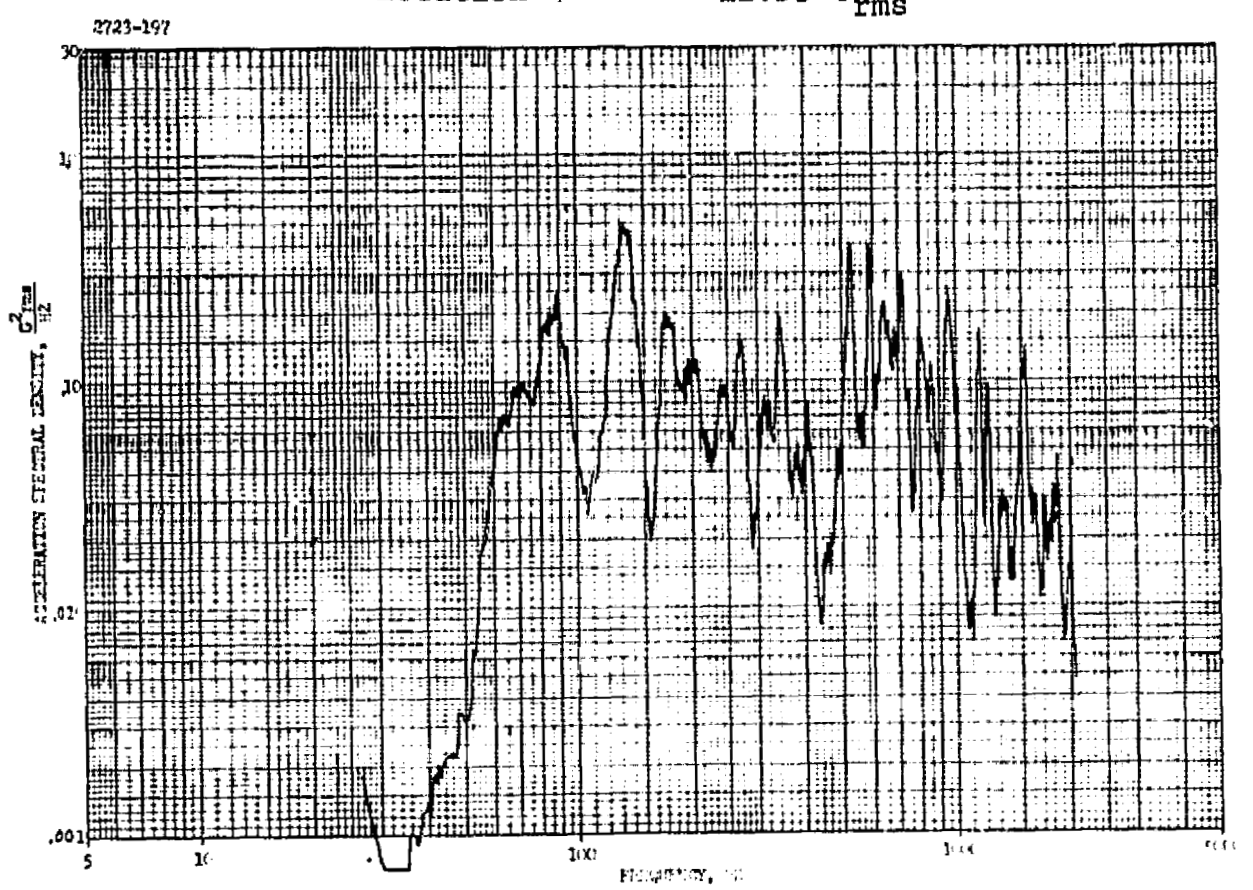

FIGURE 99. TEST #12 DATA (Continued)

Location 5 7.6 G_{rms}

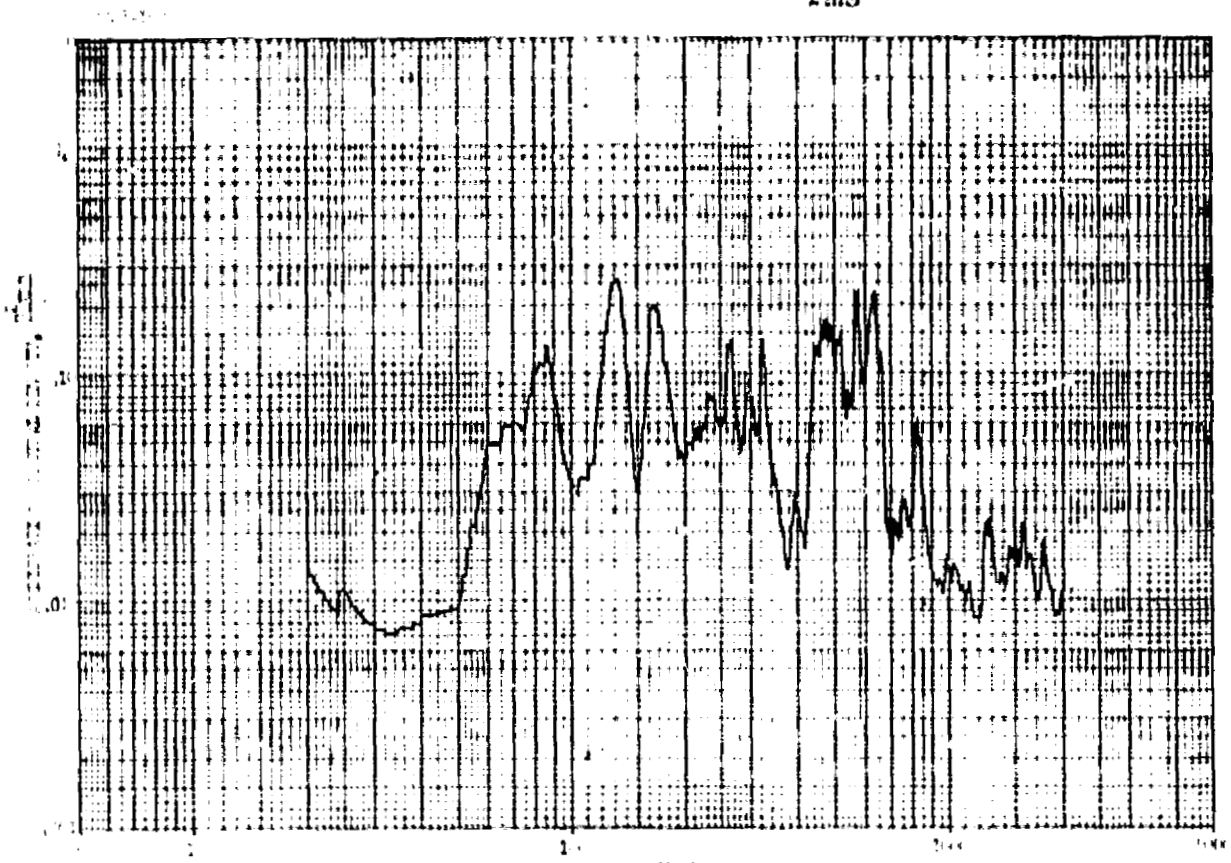

Location 6 6.4 G_{rms}

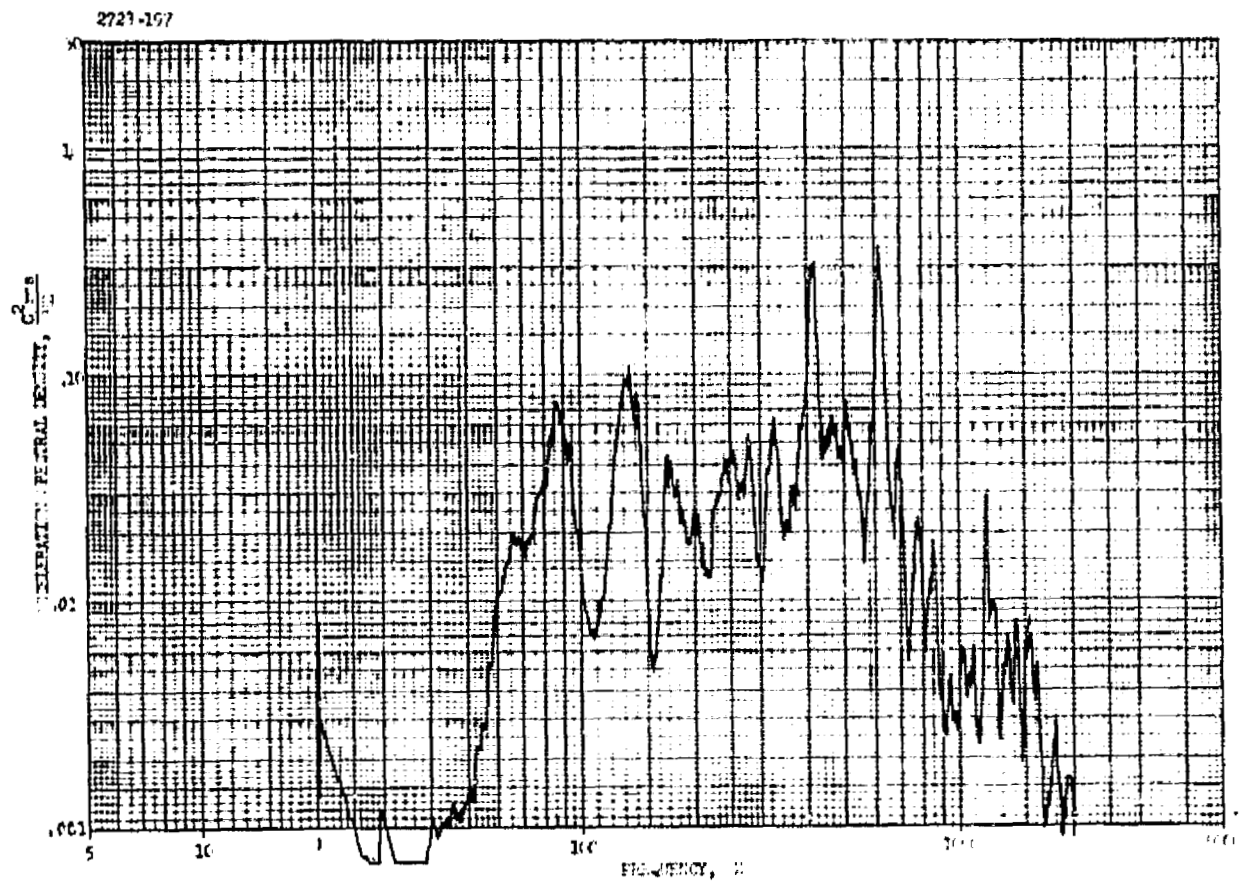

FIGURE 99. TEST #12 DATA (Continued)

Location 7 20.2 G_{rms}

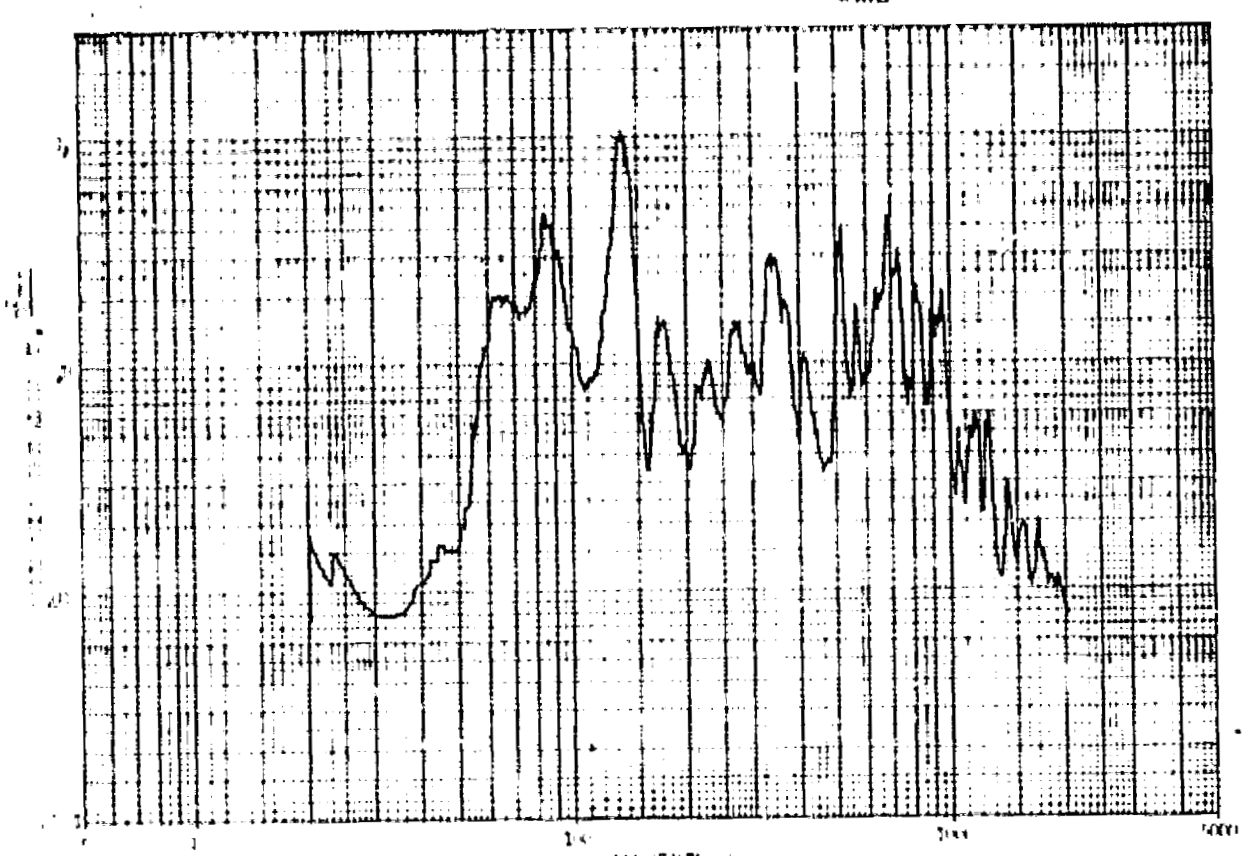

Location 8 11.06 G_{rms}

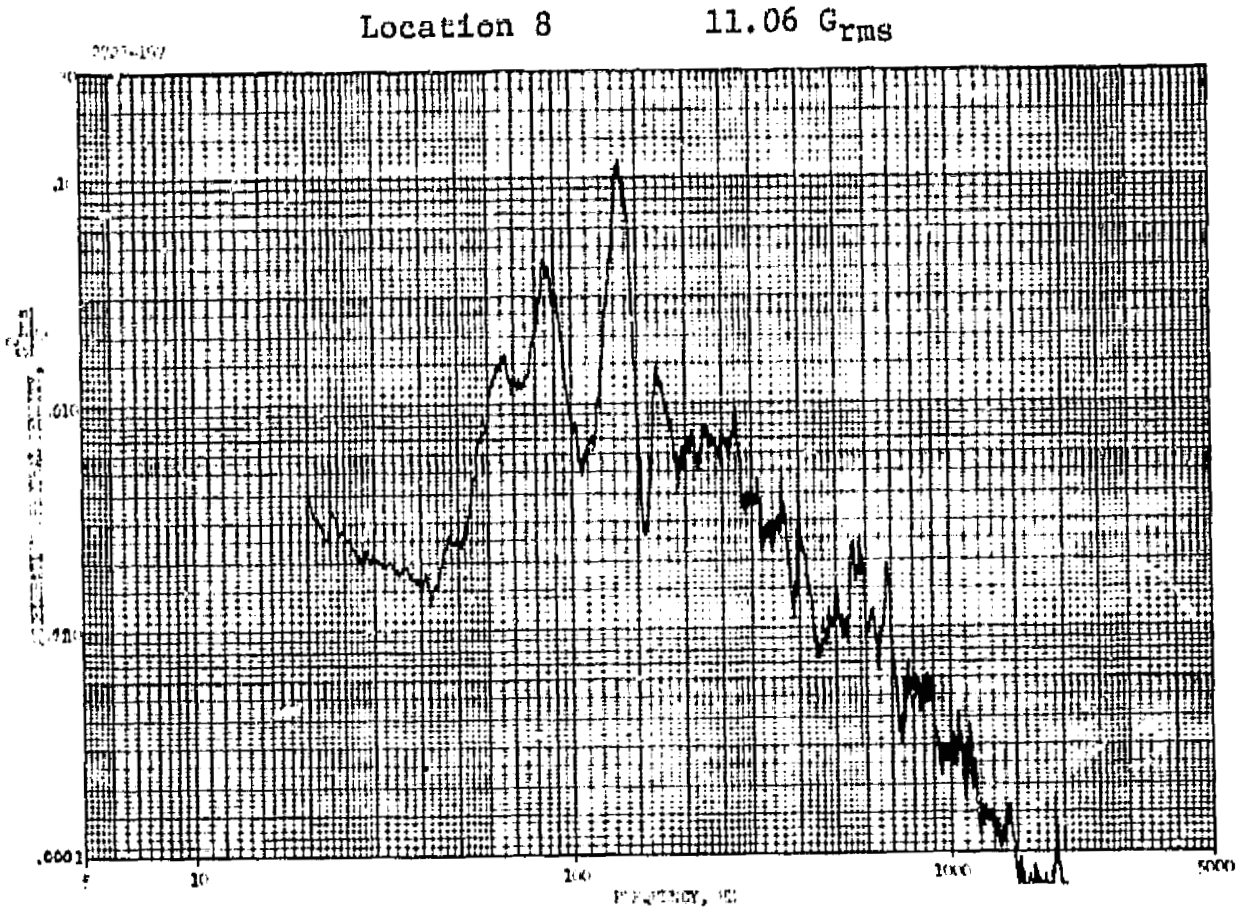

FIGURE 99. TEST #12 DATA (Continued)

Location 9 19.2 G_{rms}

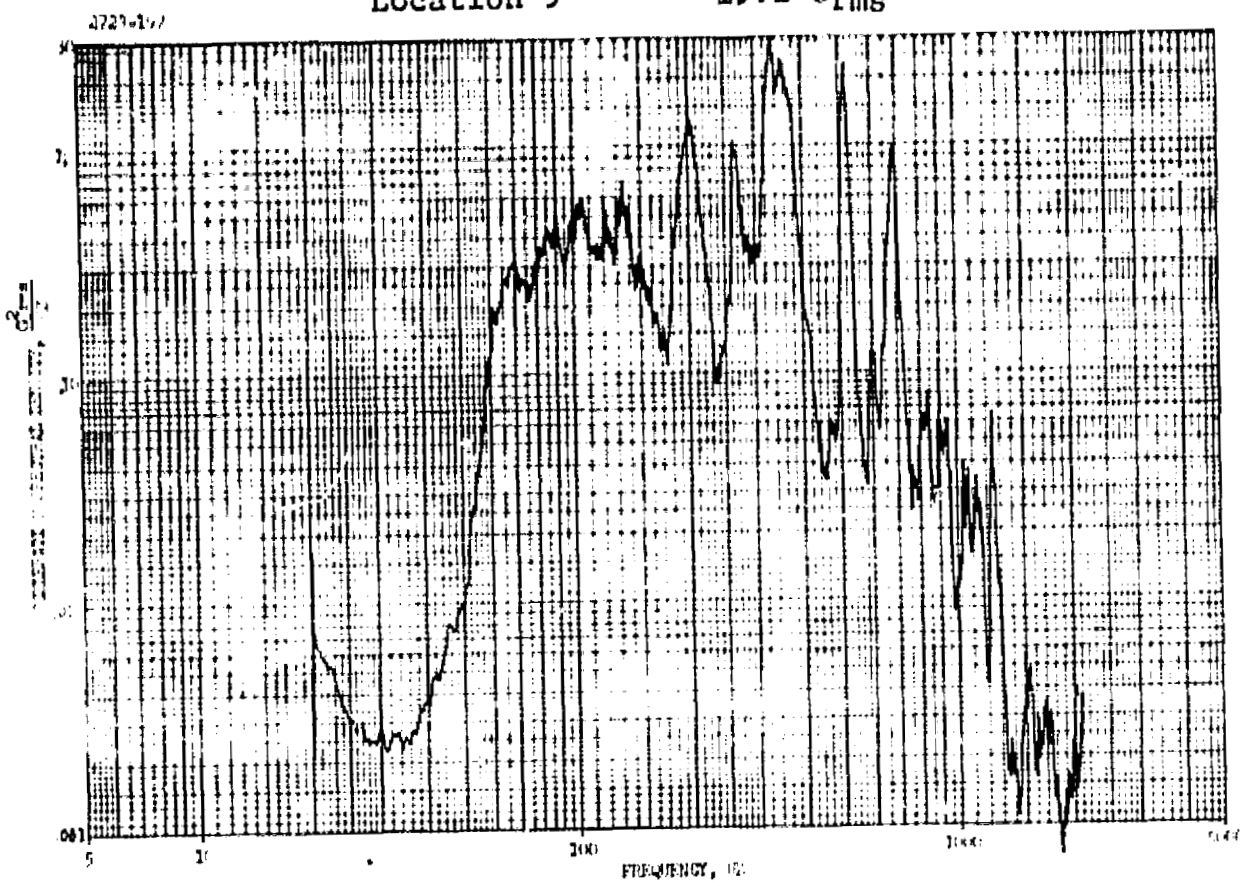

Location 10

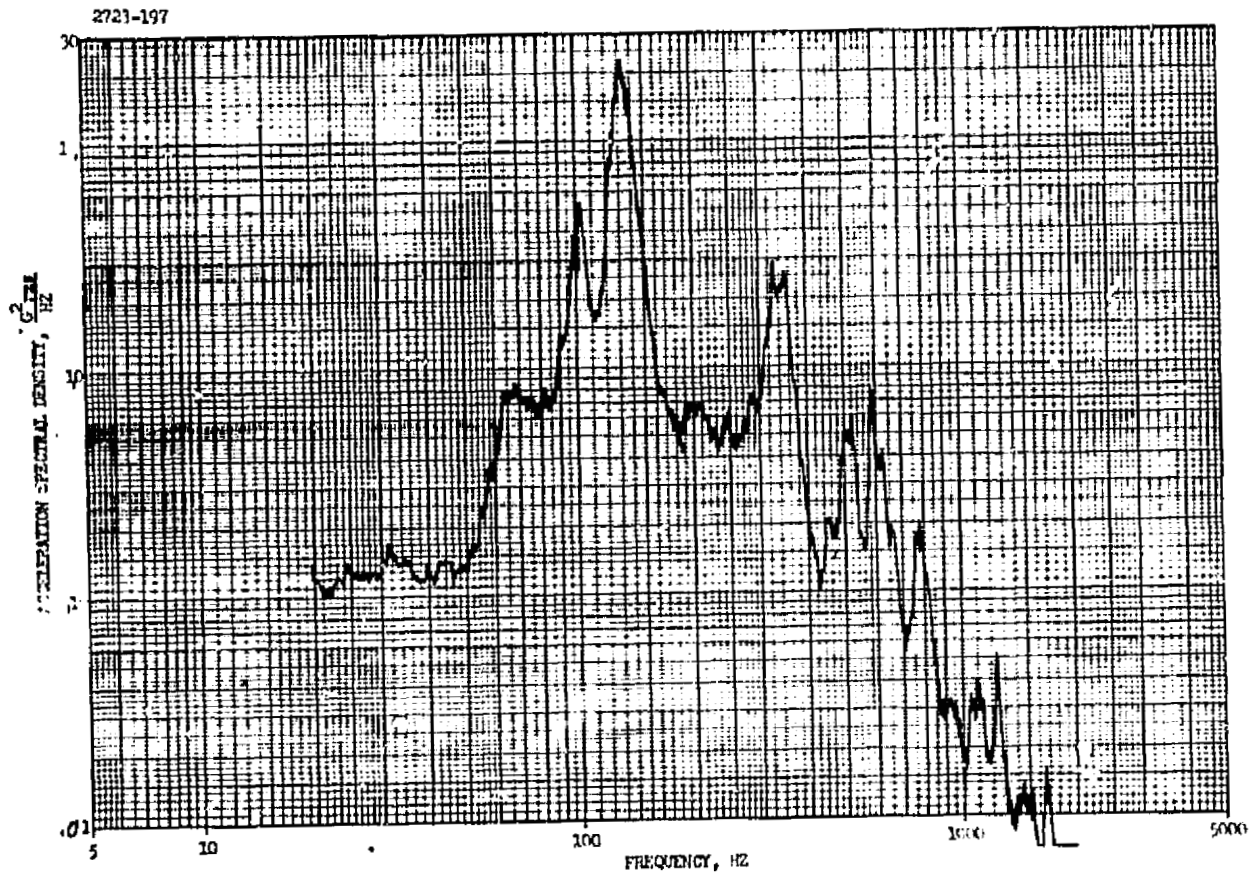

FIGURE 99. TEST #12 DATA (Continued)

Location 11

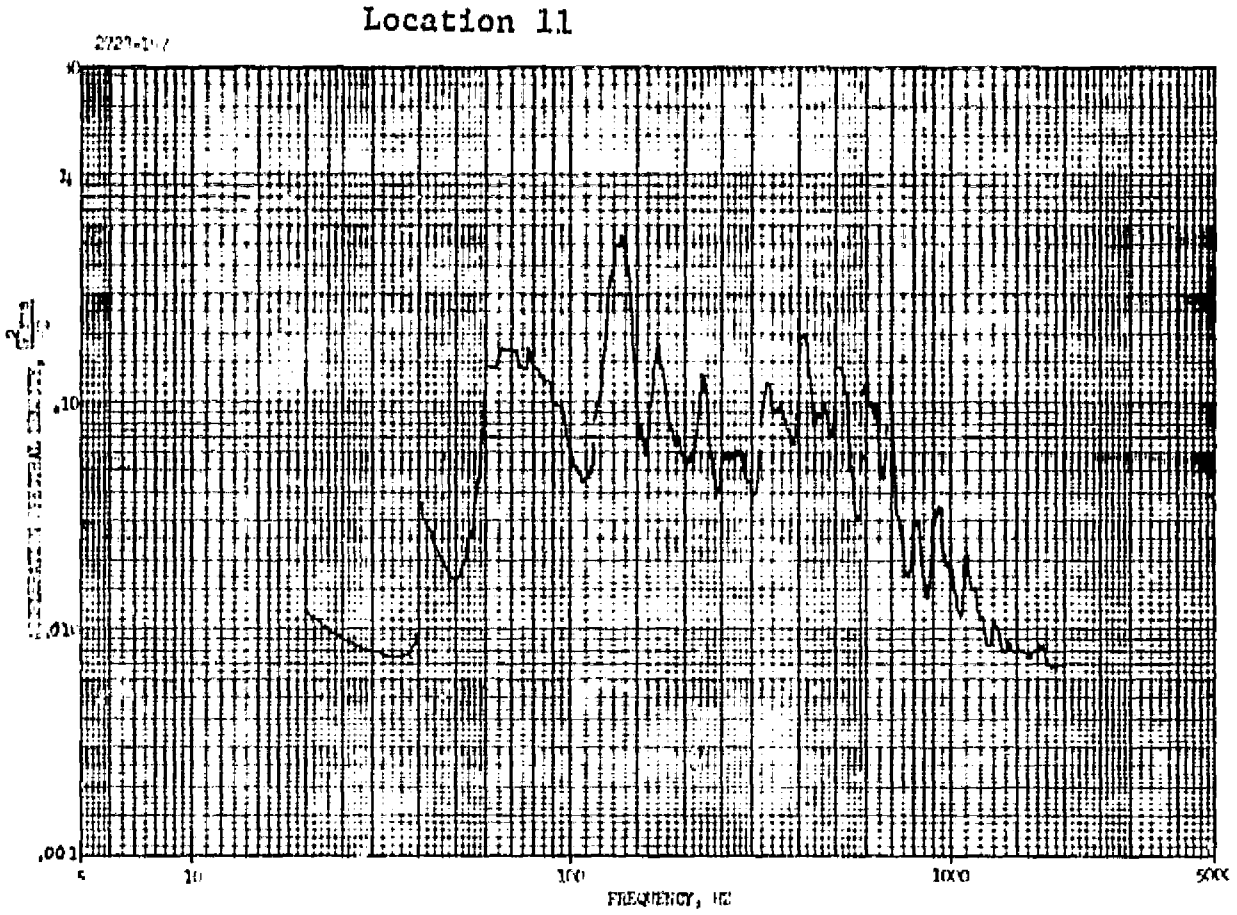

FIGURE 99. TEST #12 DATA (Concluded)

Location 1 27.0 G_{rms}

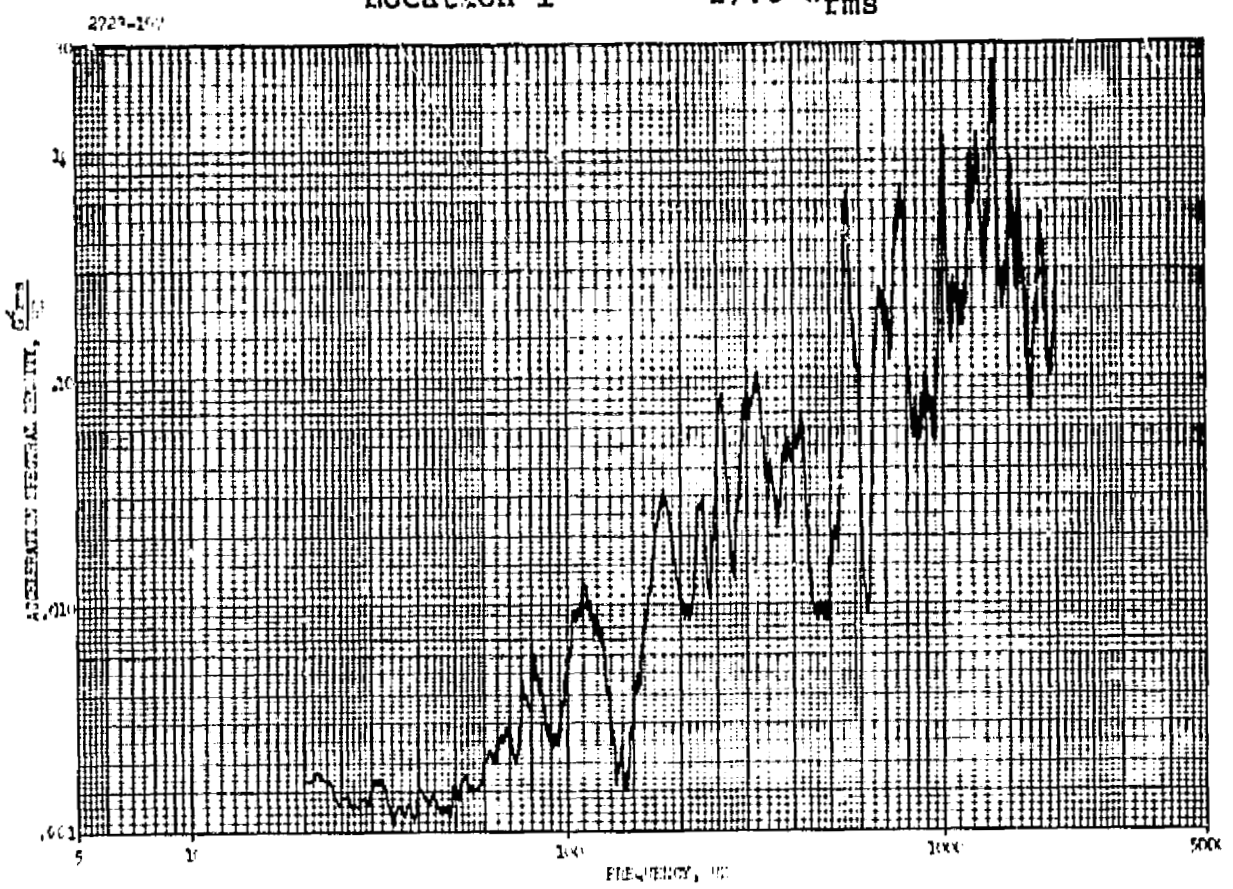

Location 2 47.0 G_{rms}

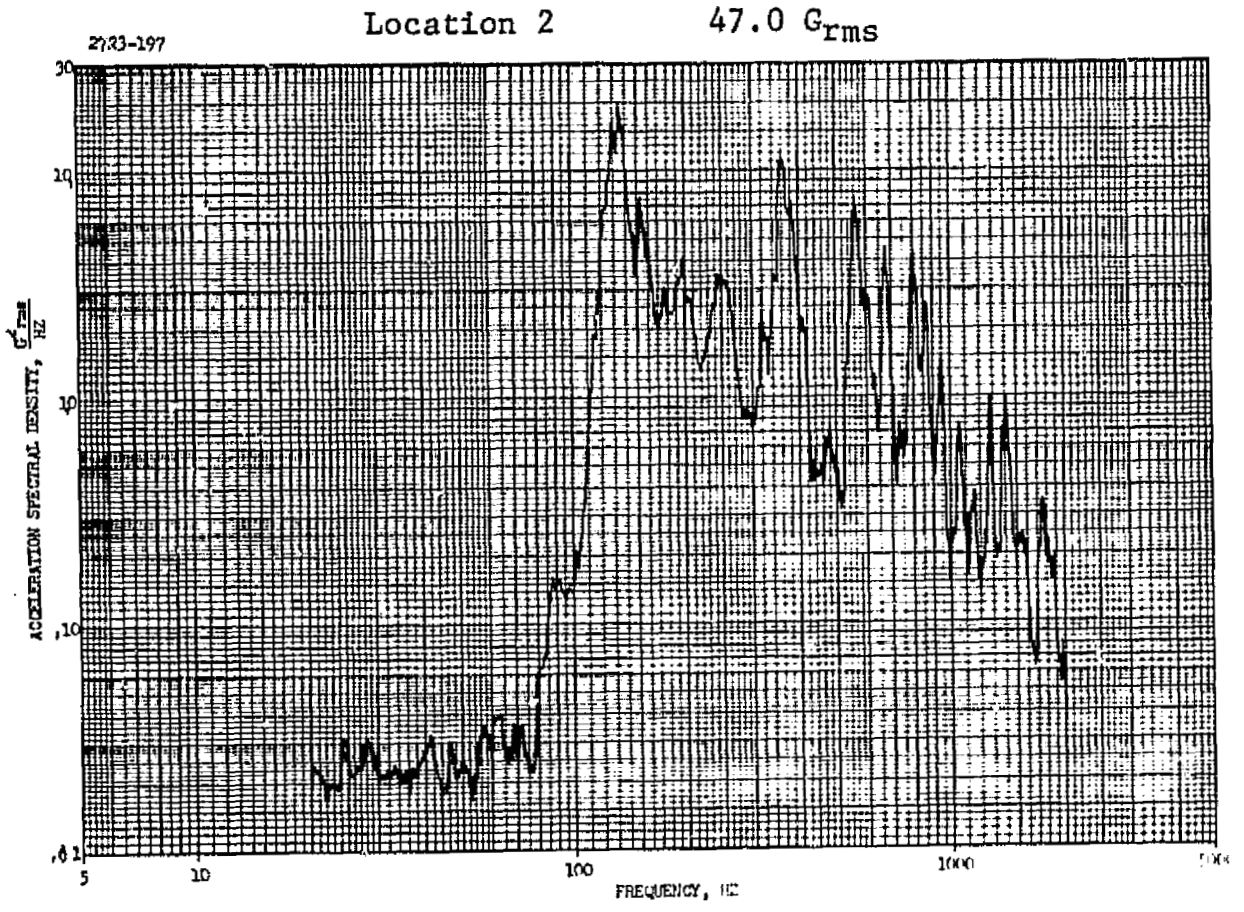

FIGURE 100. TEST # 13 DATA

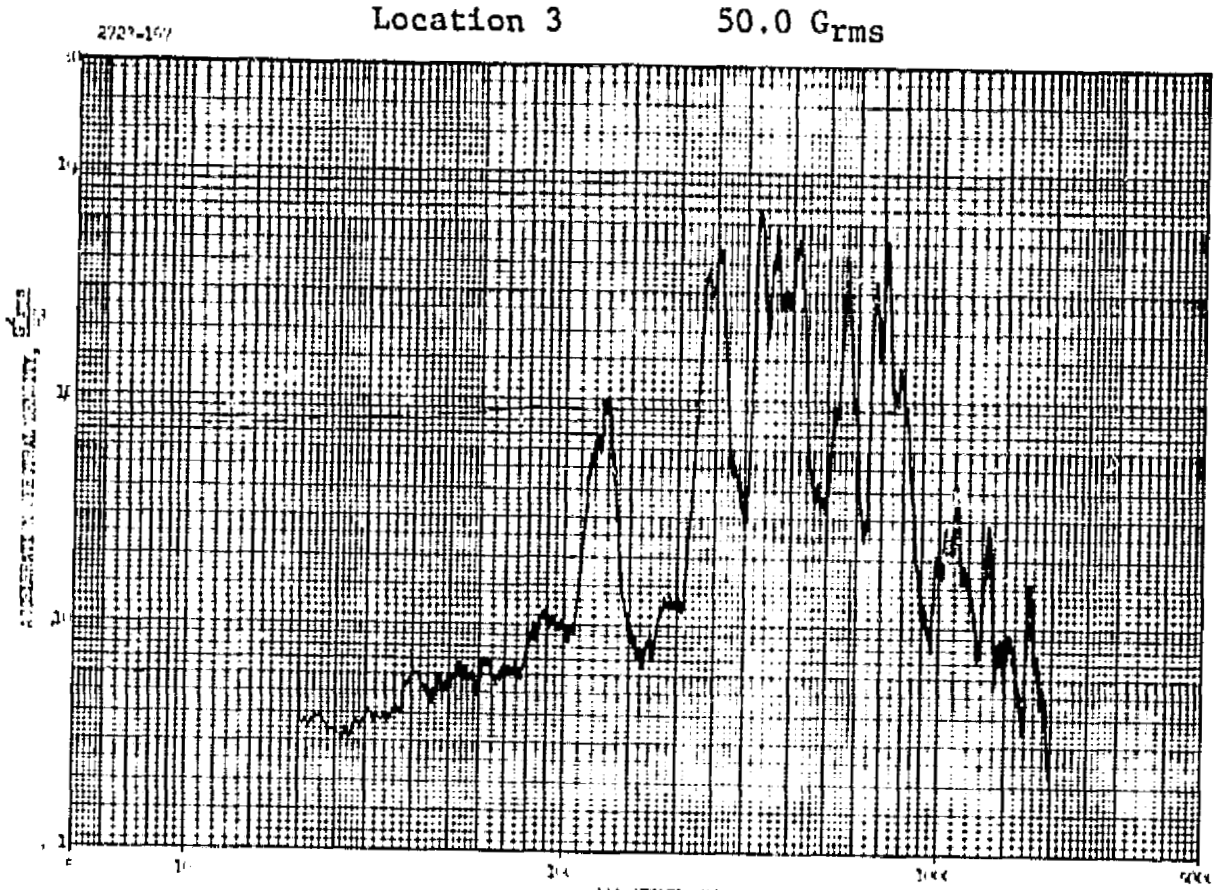

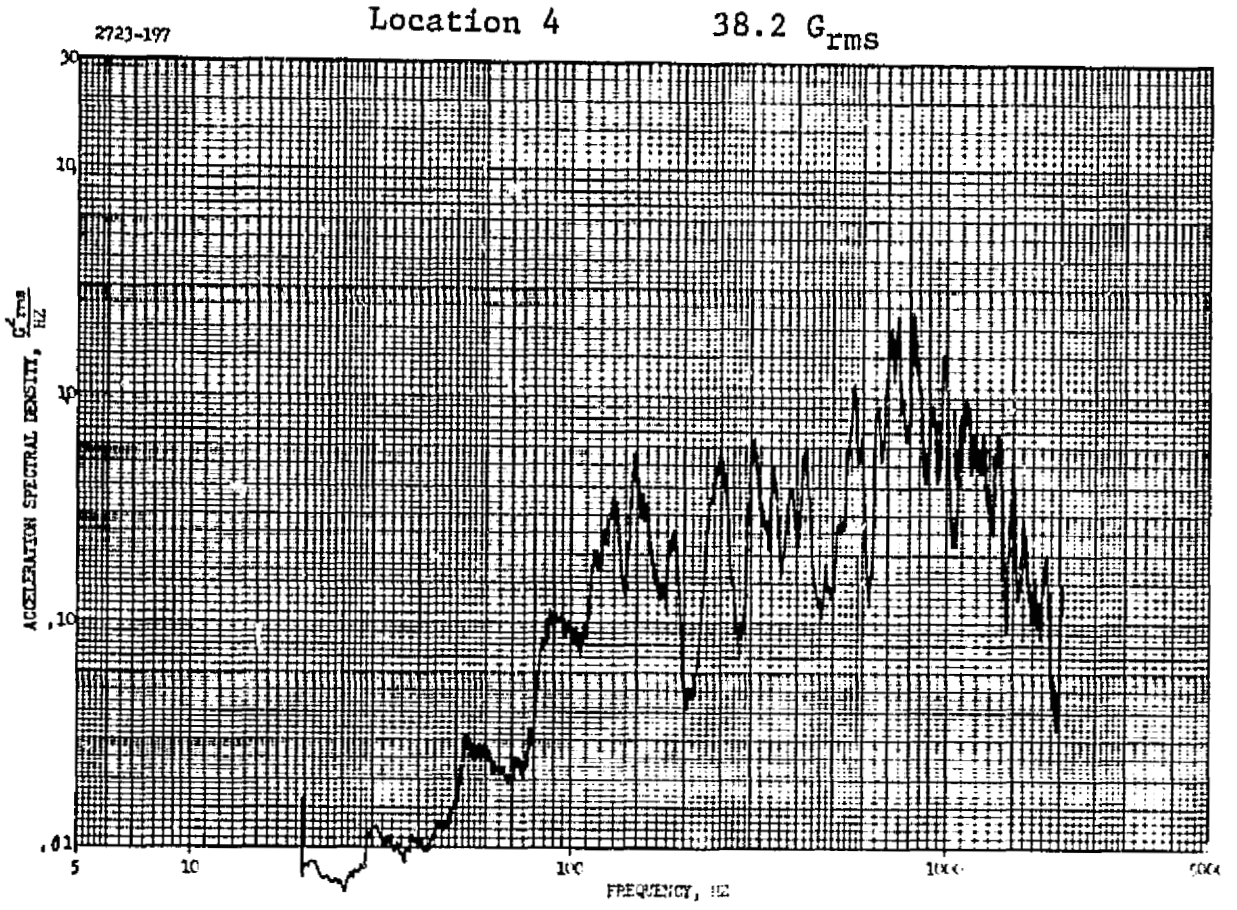

FIGURE 100. TEST #13 DATA (Continued)

Location 5 22.4 G_{rms}

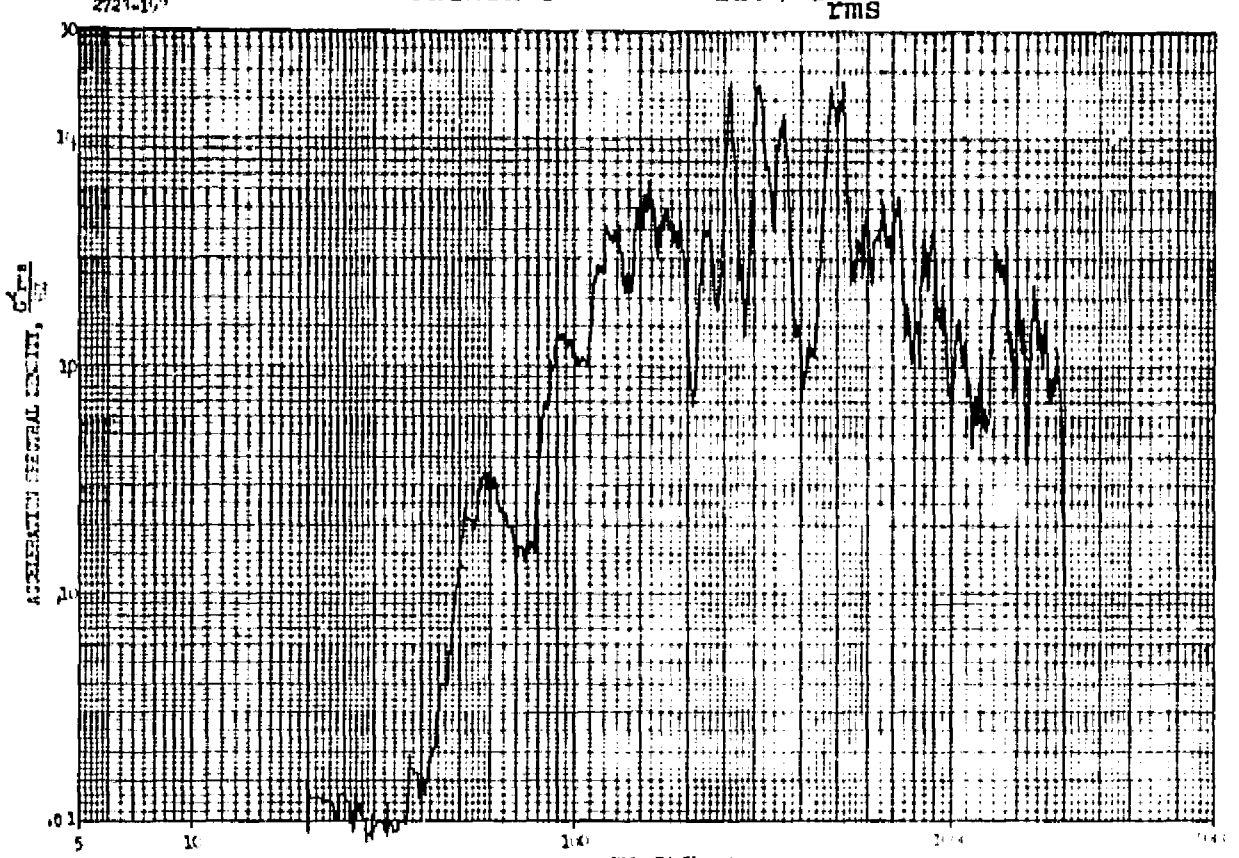

Location 6 24.1 G_{rms}

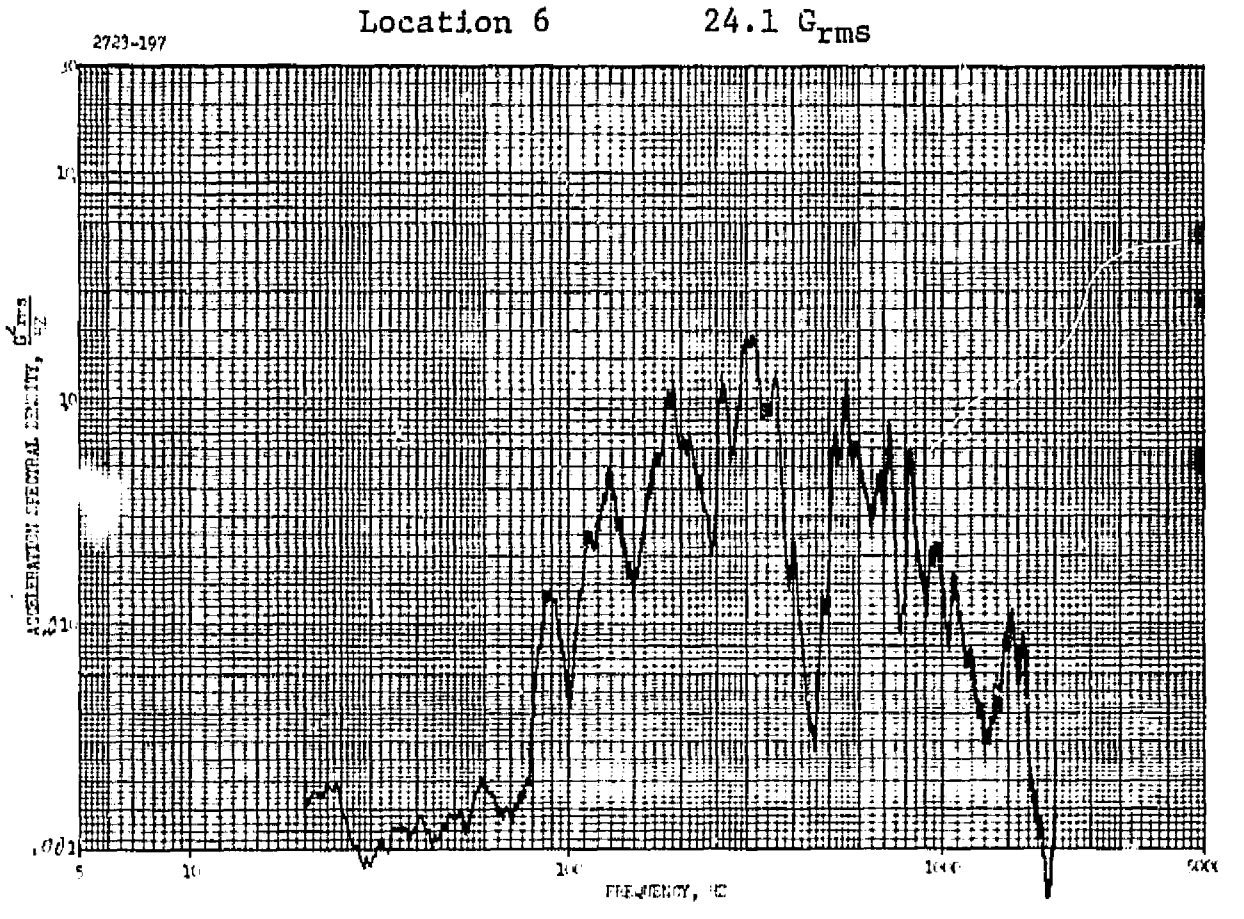

FIGURE 100. TEST #13 DATA (Continued)

Location 7 17.0 G_{rms}

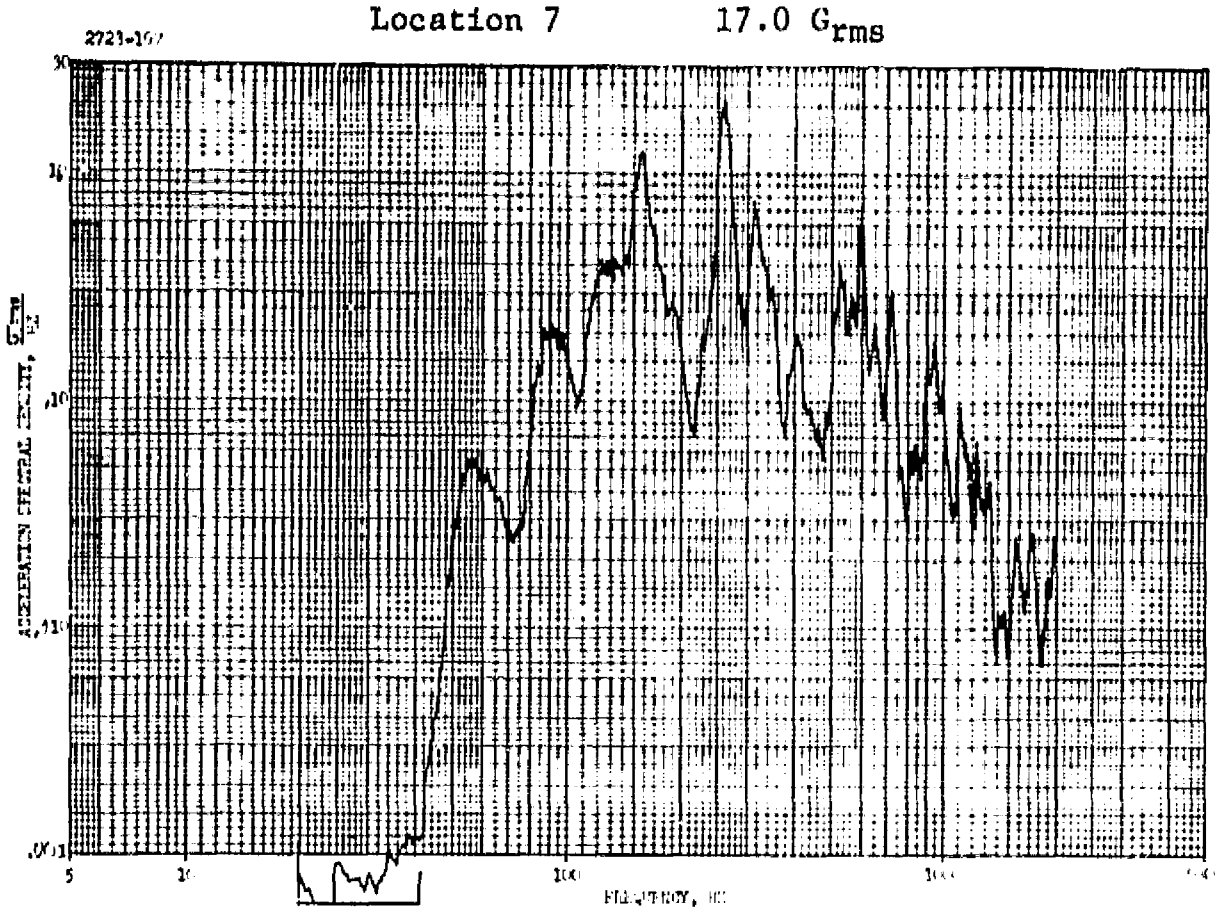

Location 8 47.0 G_{rms}

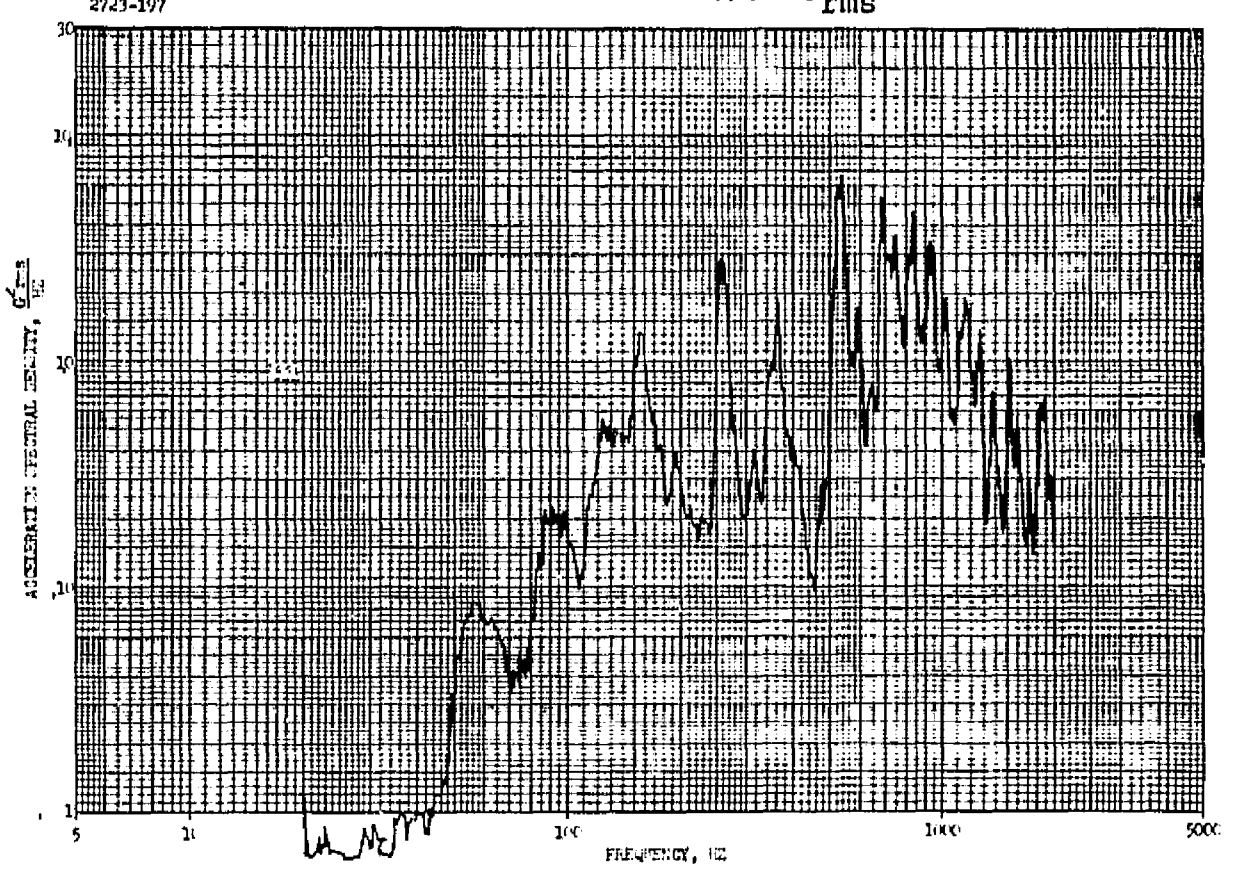

FIGURE 100. TEST #13 DATA (Continued)

Location 9 47.0 G_{rms}

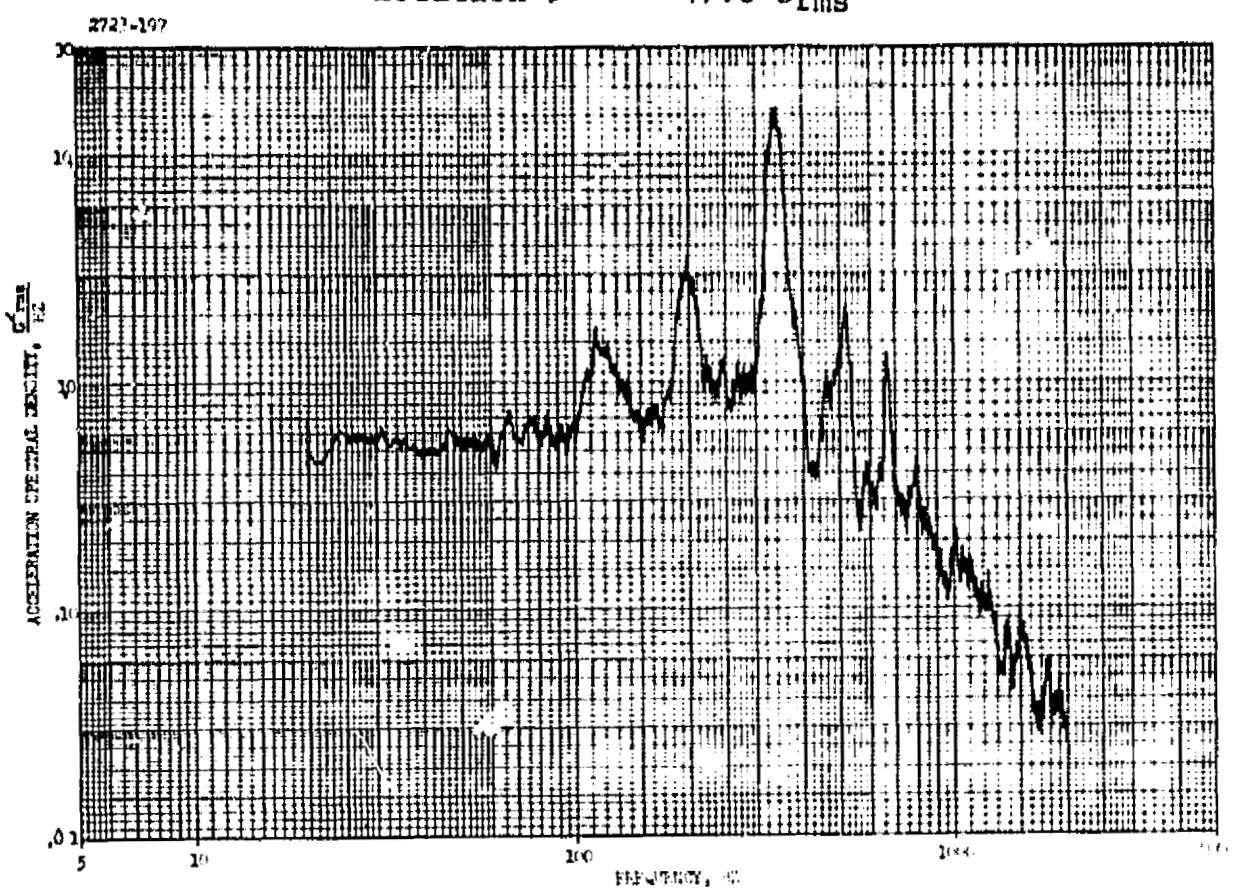

Location 10 73.5 G_{rms}

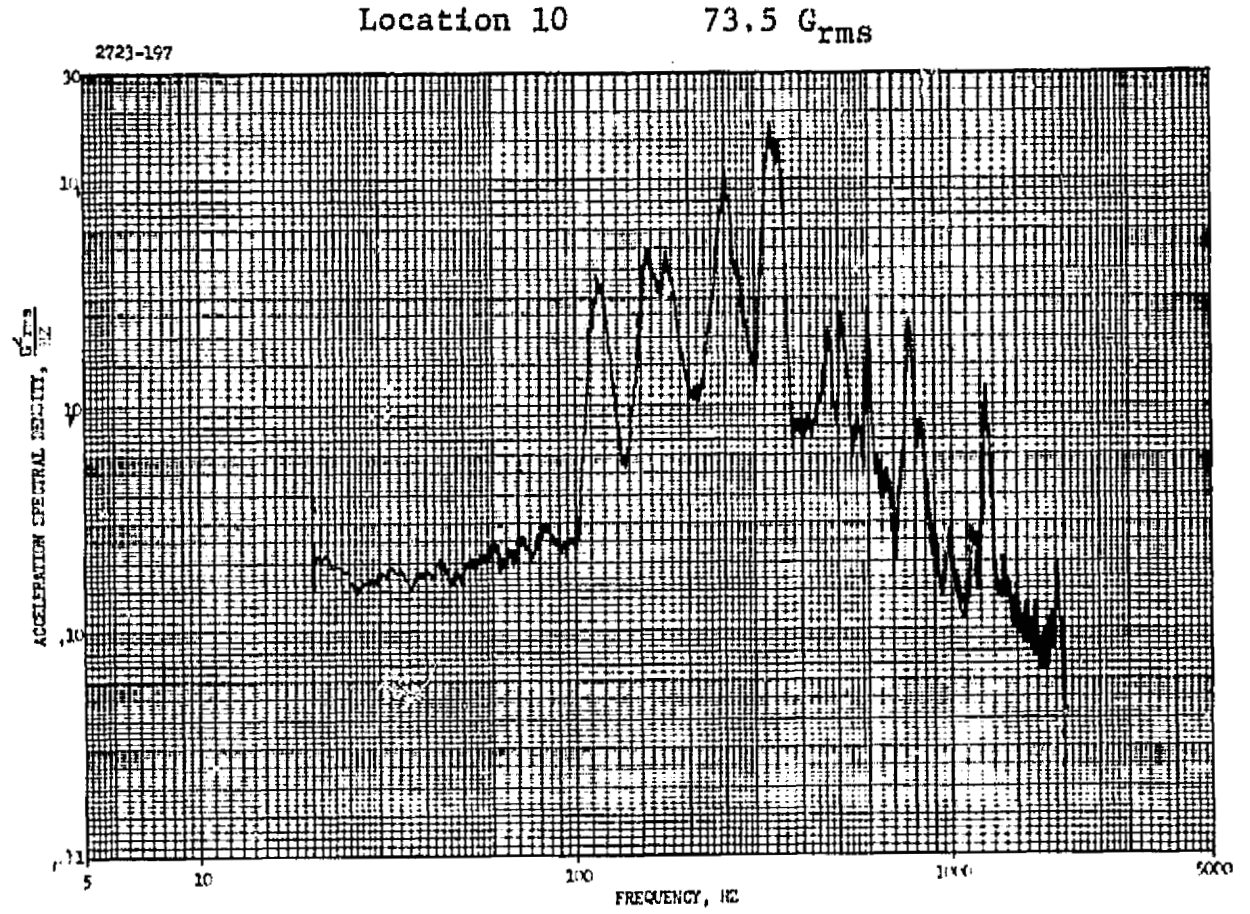

FIGURE 100. TEST #13 DATA (Continued)

Location 11 26.5 G_{rms}

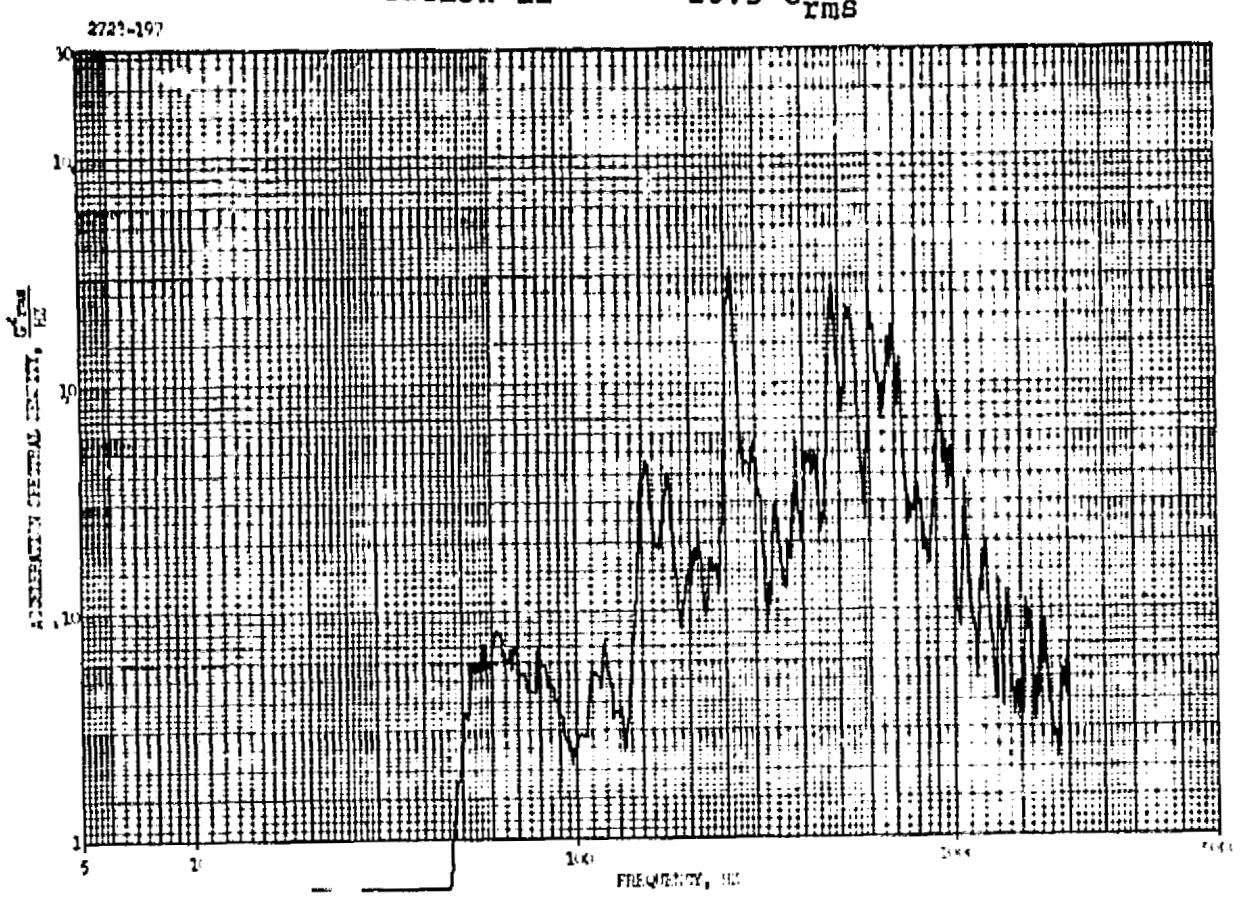

FIGURE 100. TEST #13 DATA (Concluded)

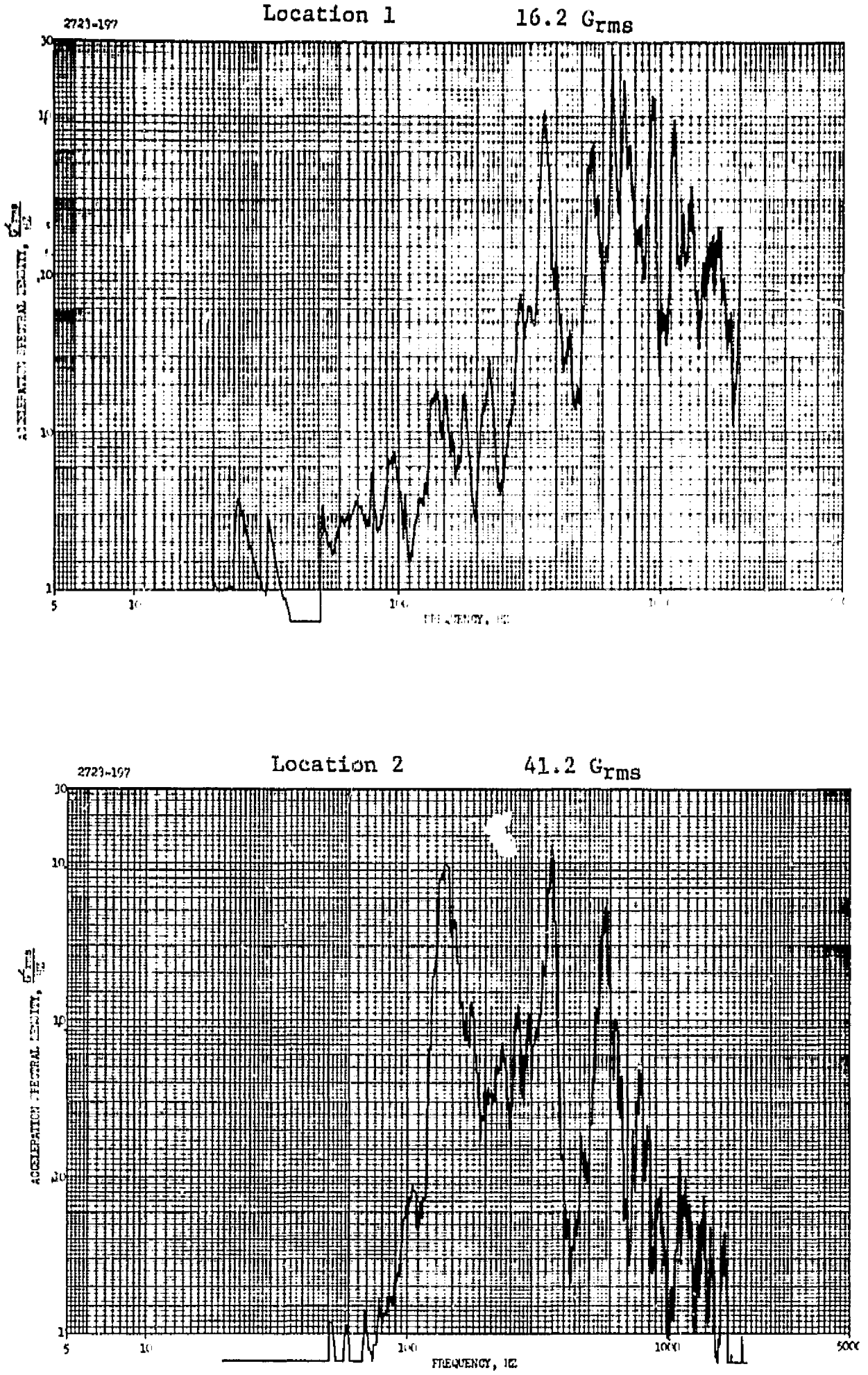

FIGURE 101. TEST # 14 DATA

Location 3 28.2 G_{rms}

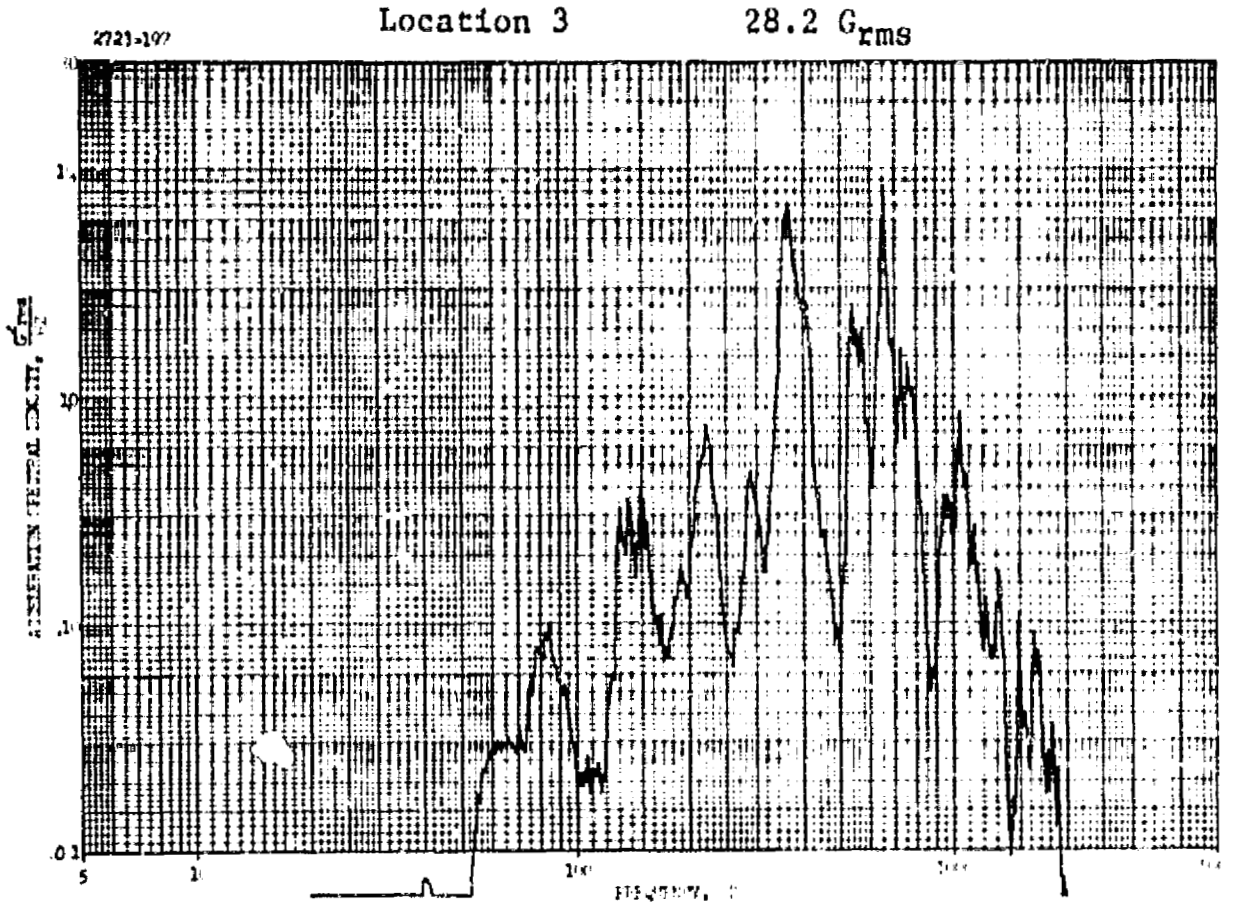

Location 4 5.0 G_{rms}

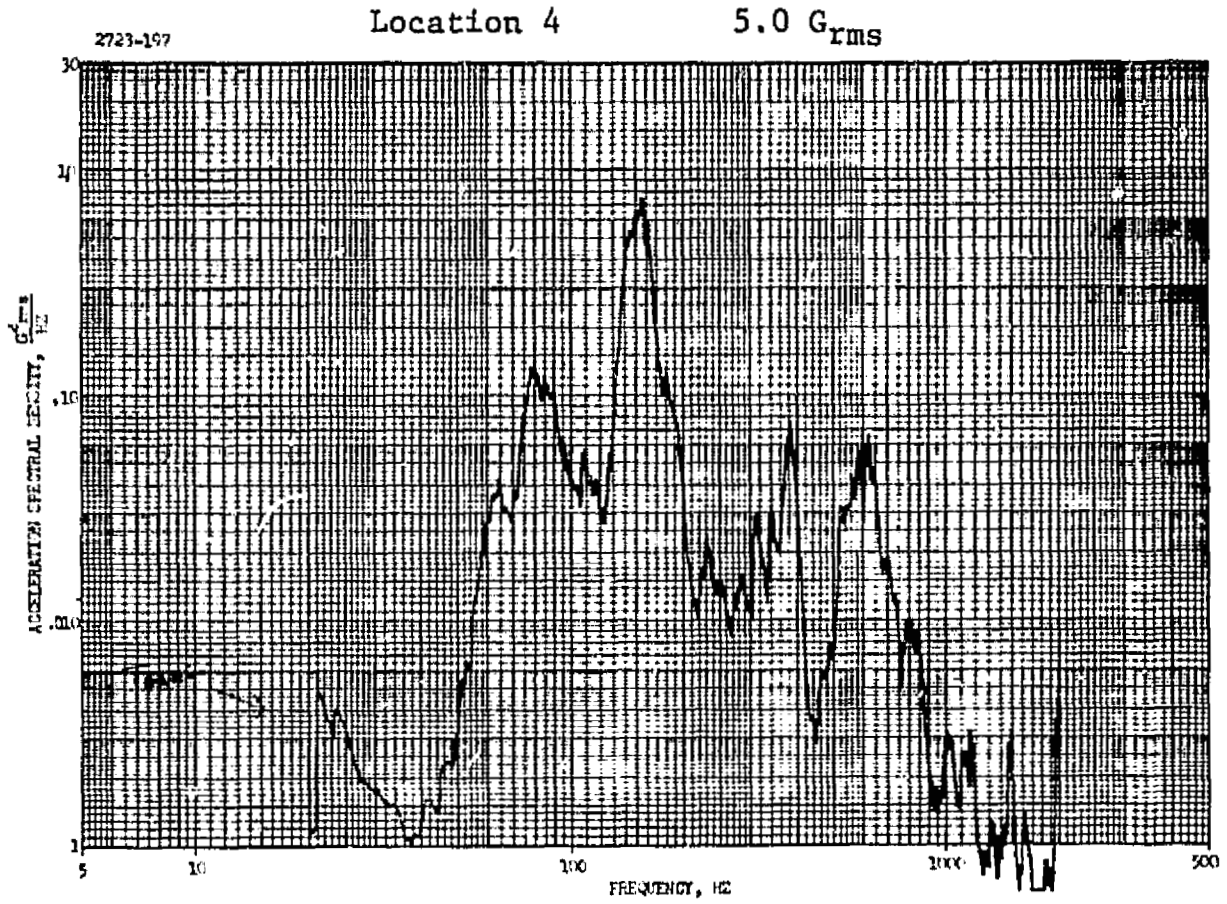

FIGURE 101. TEST #14 DATA (Continued)

Location 5 7.65 G_{rms}

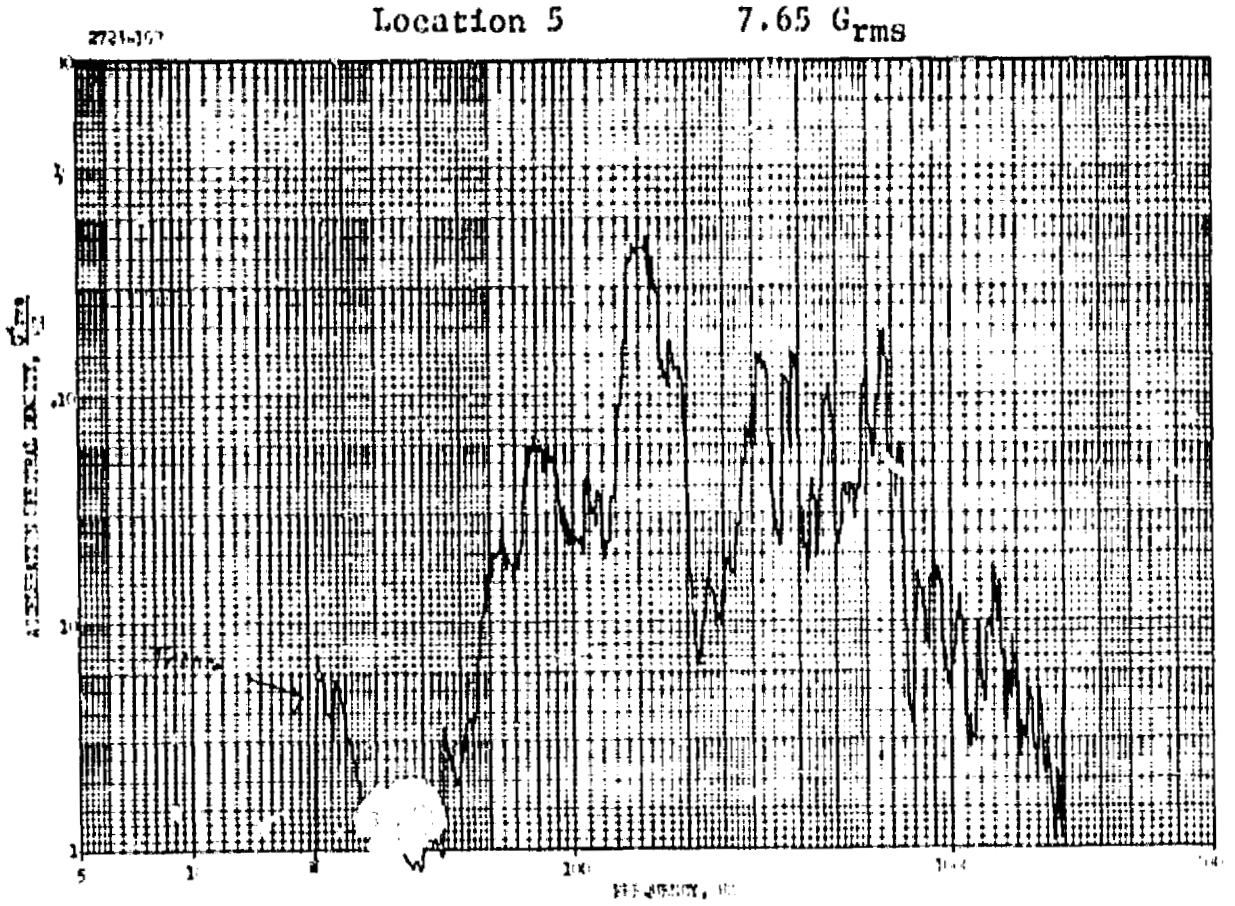

Location 6 10.6 G_{rms}

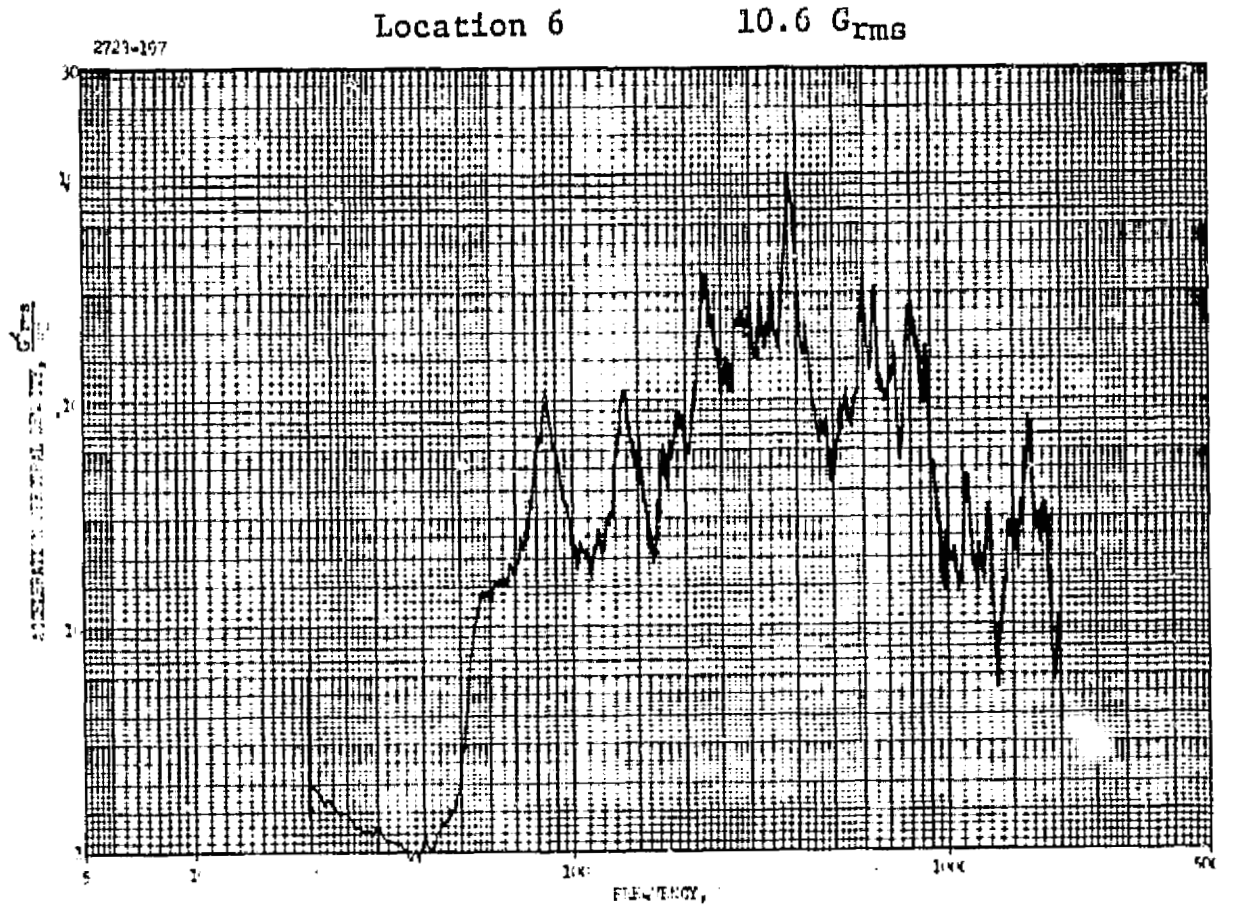

FIGURE 101. TEST #14 DATA (Continued)

Location 7 6.5 G_{rms}

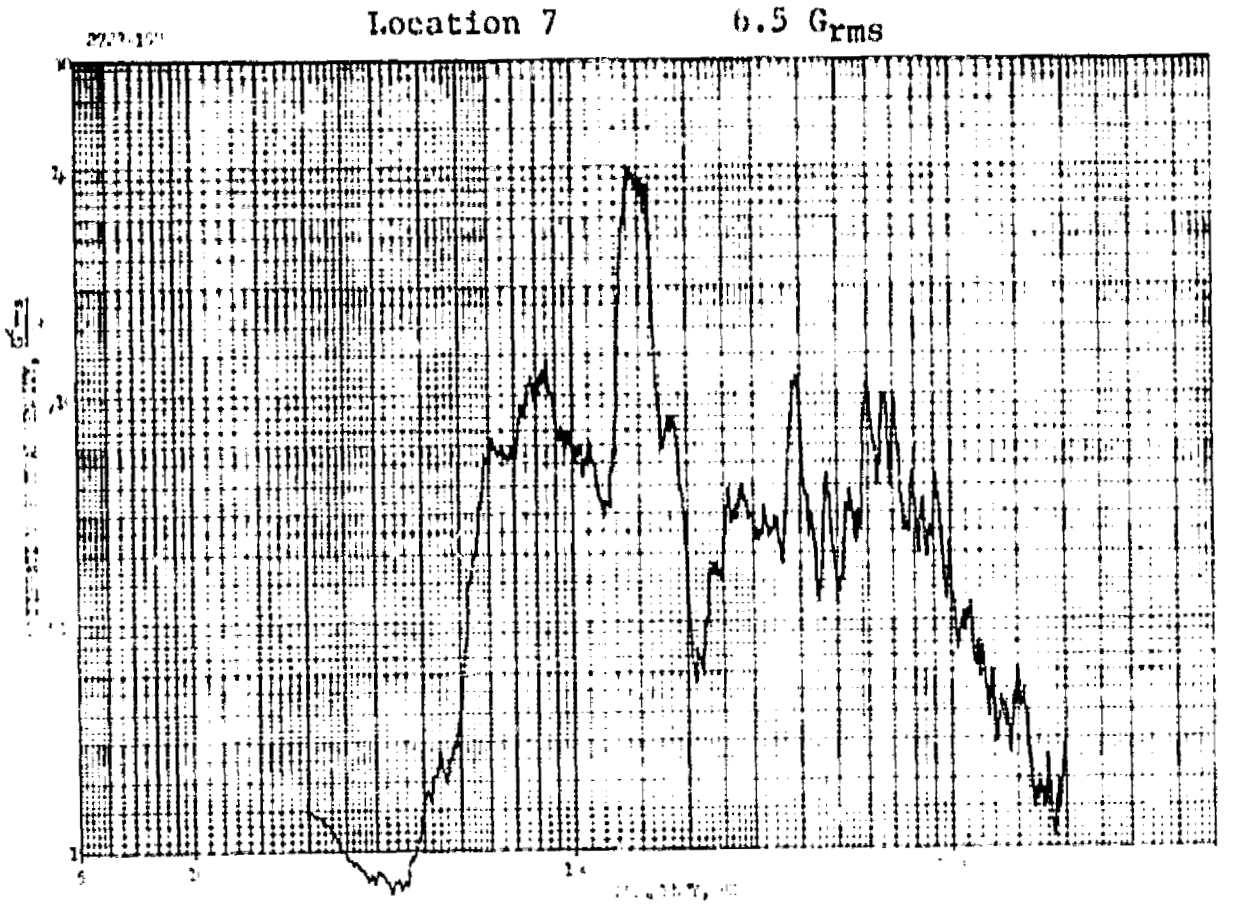

Location 8 20.6 G_{rms}

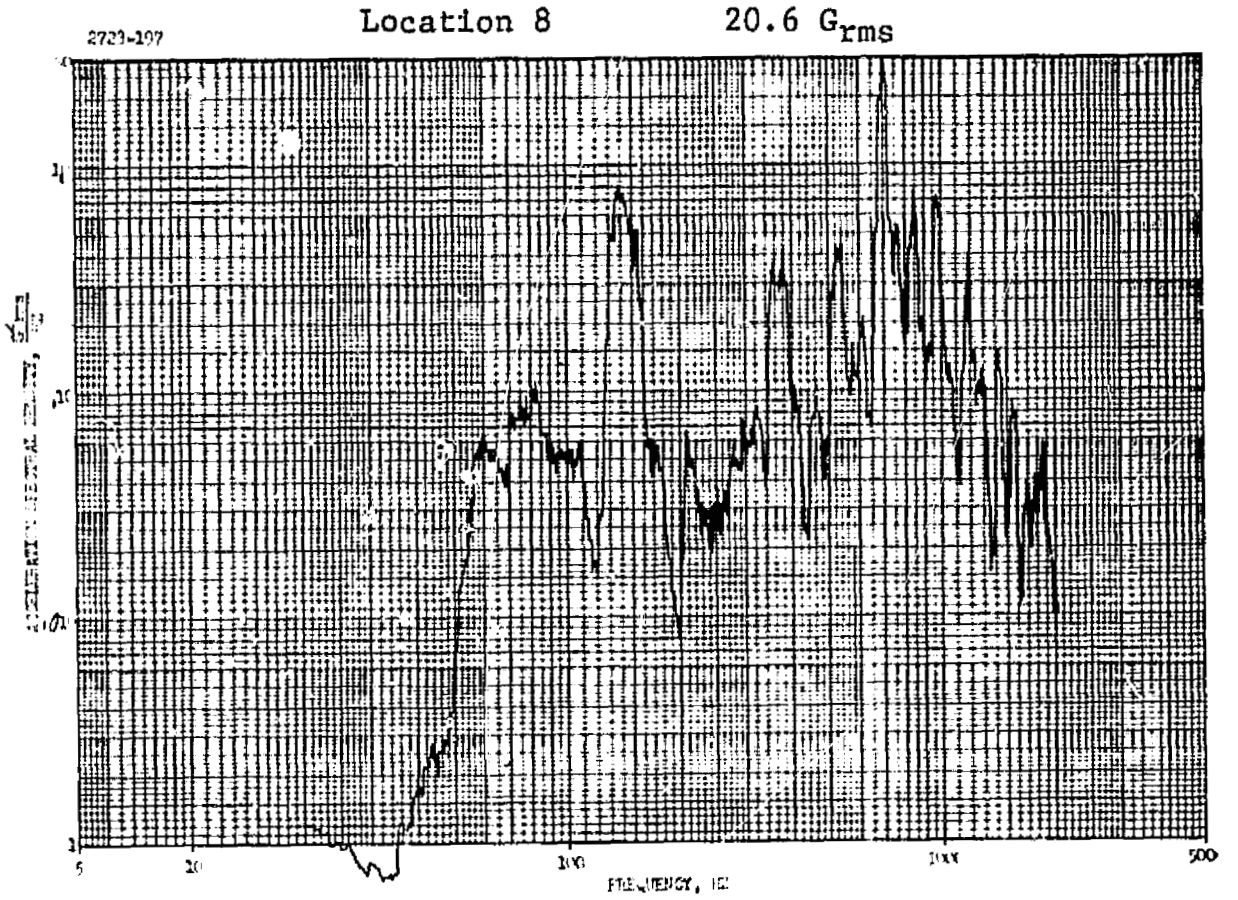

FIGURE 101. TEST #14 DATA (Continued)

Location 9 35.3 G_{rms}

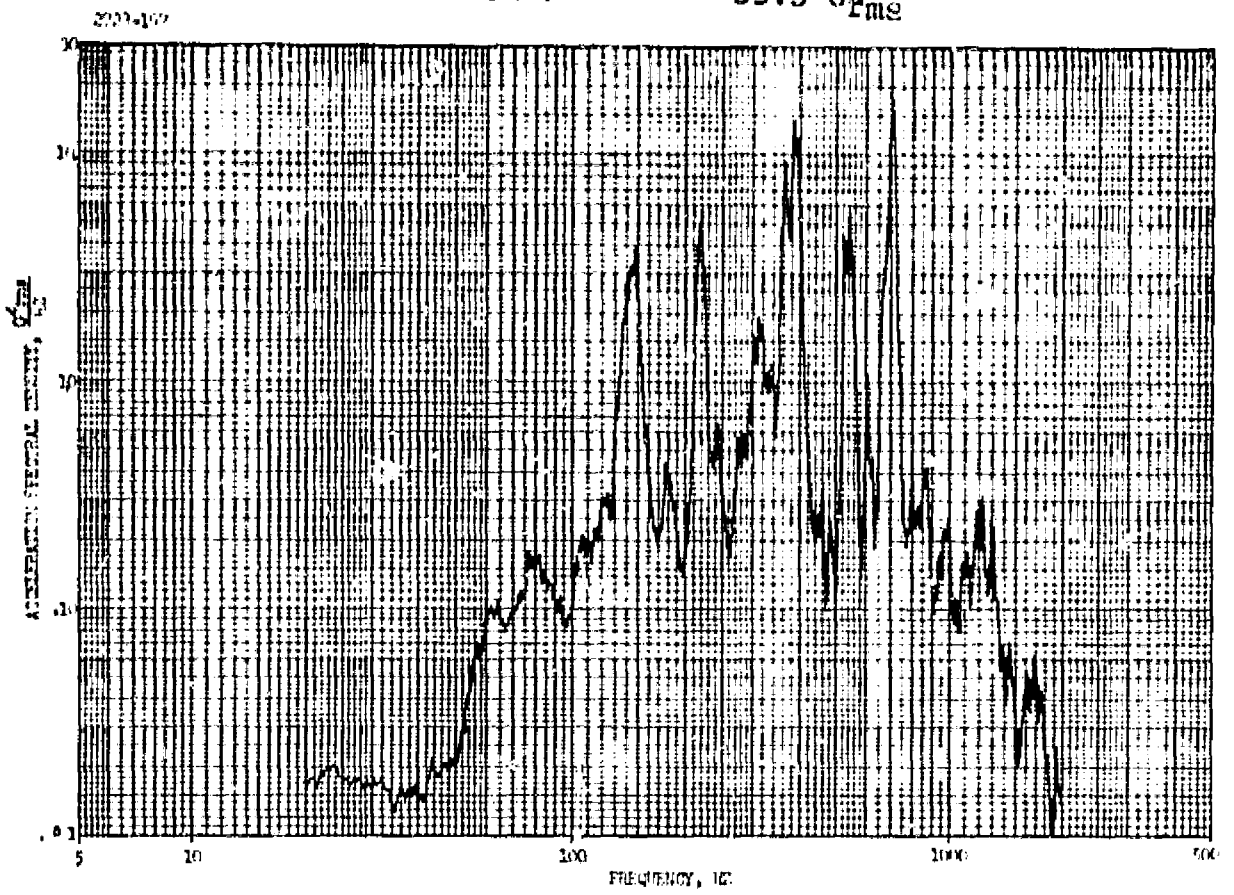

Location 10 38.2 G_{rms}

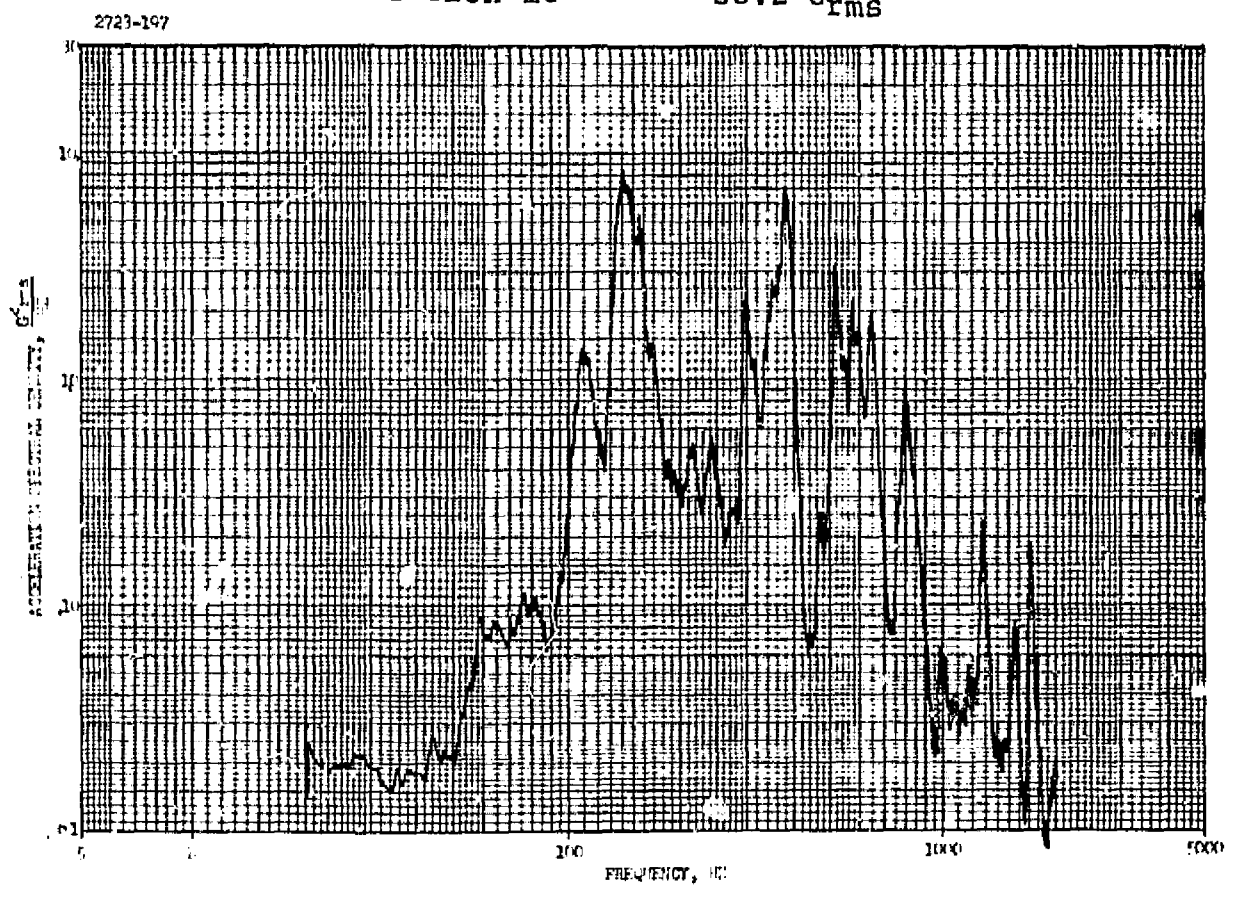

FIGURE 101. TEST #14 DATA (Continued)

Location 11 12.8 G_{rms}

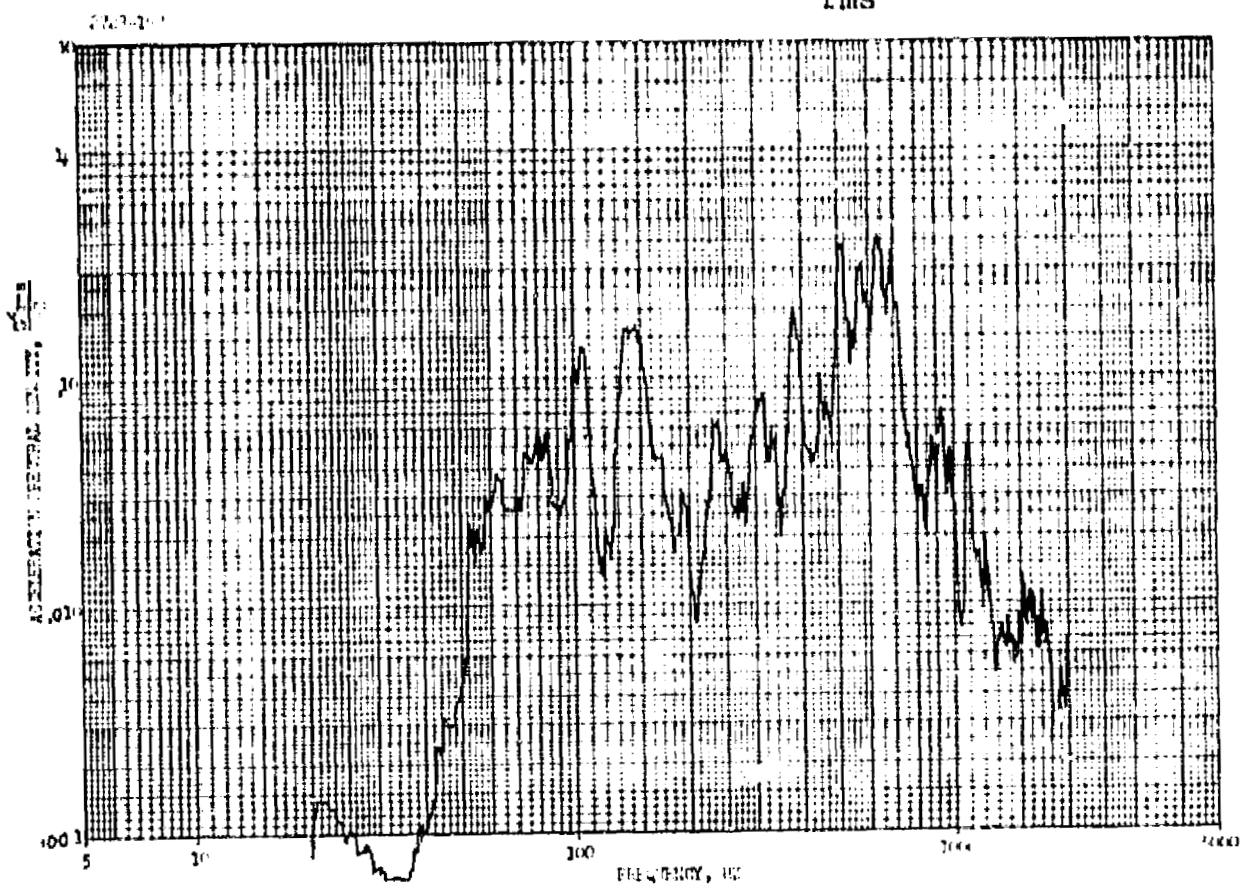

Location 12 50.0 G_{rms}

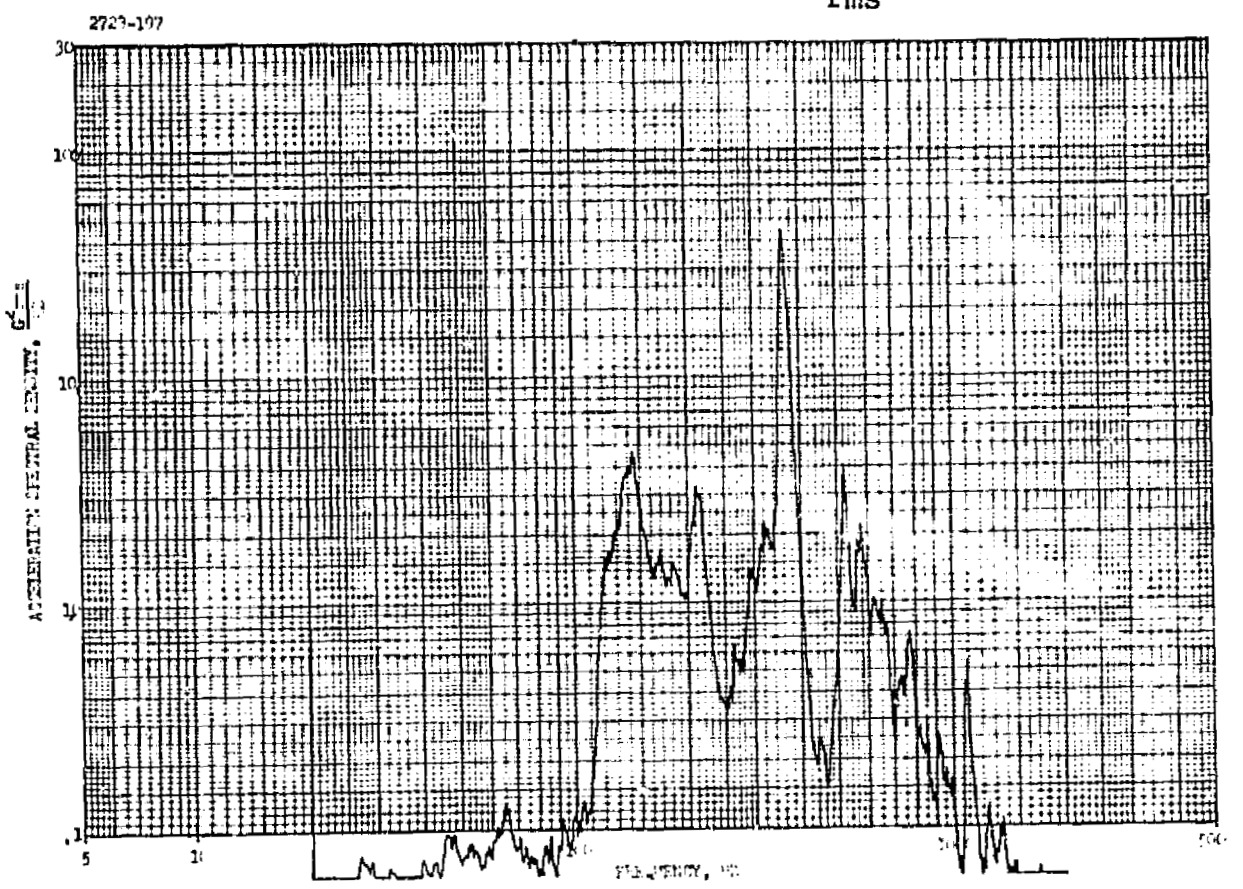

FIGURE 10 ST #14 DATA (Continued)

Location 13 11.2 G_{rms}

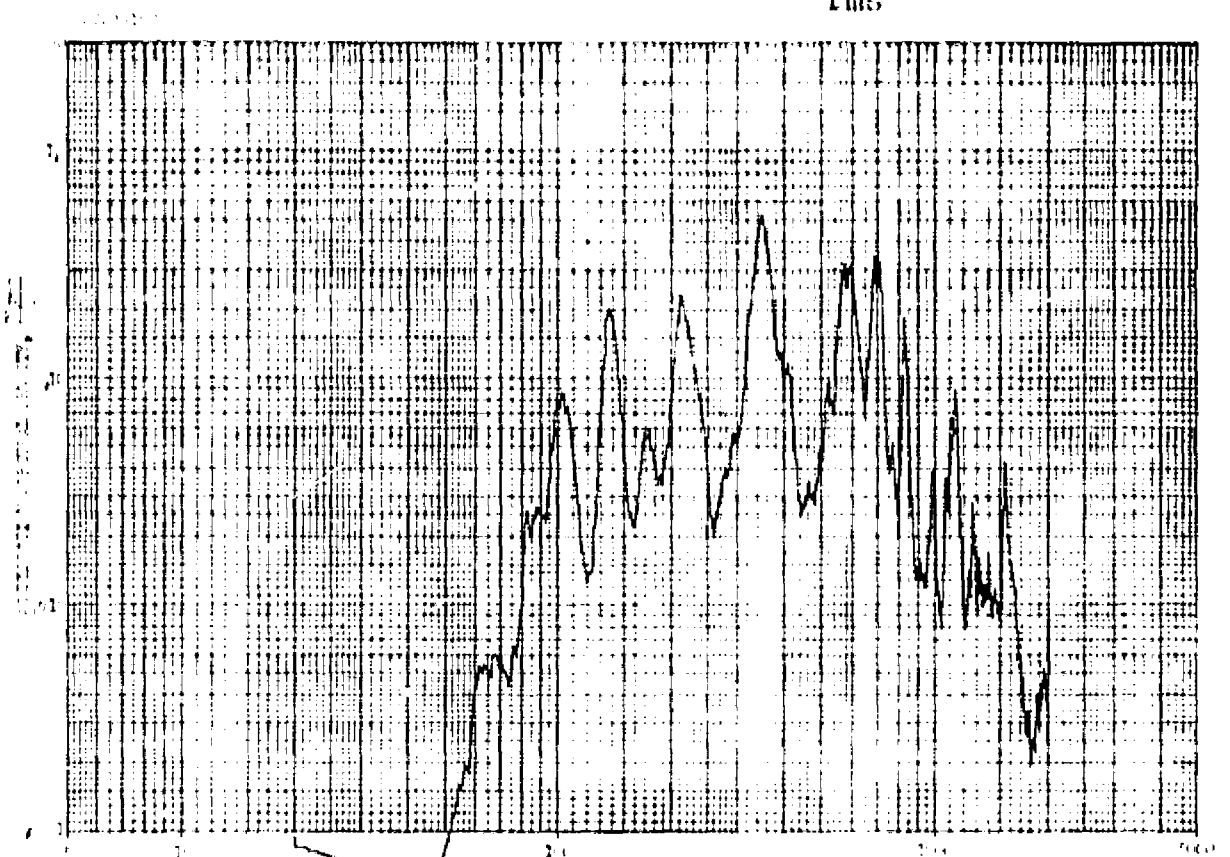

Location 14 8.54 G_{rms}

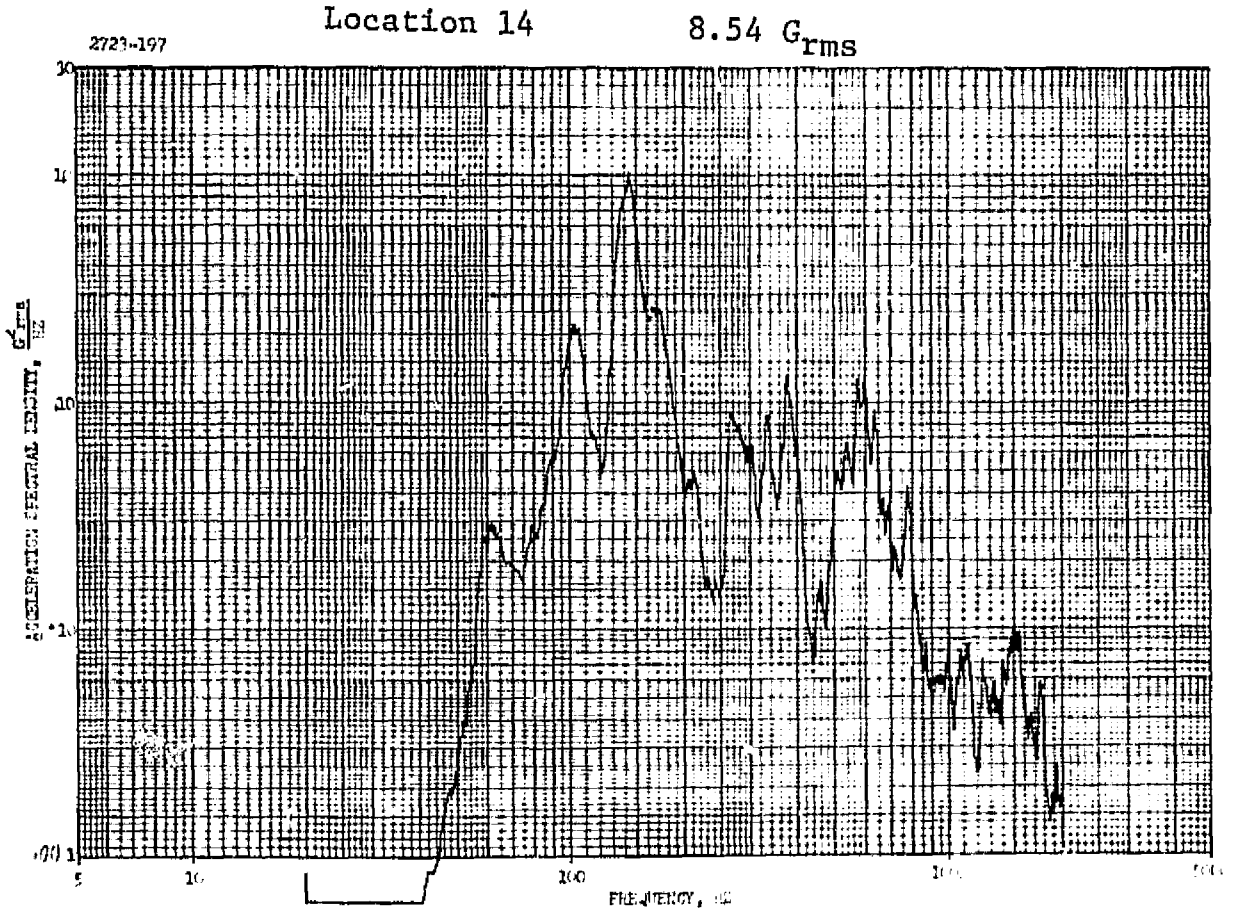

FIGURE 101. TEST #14 DATA (Continued)

Location 15 8.24 G_{rms}

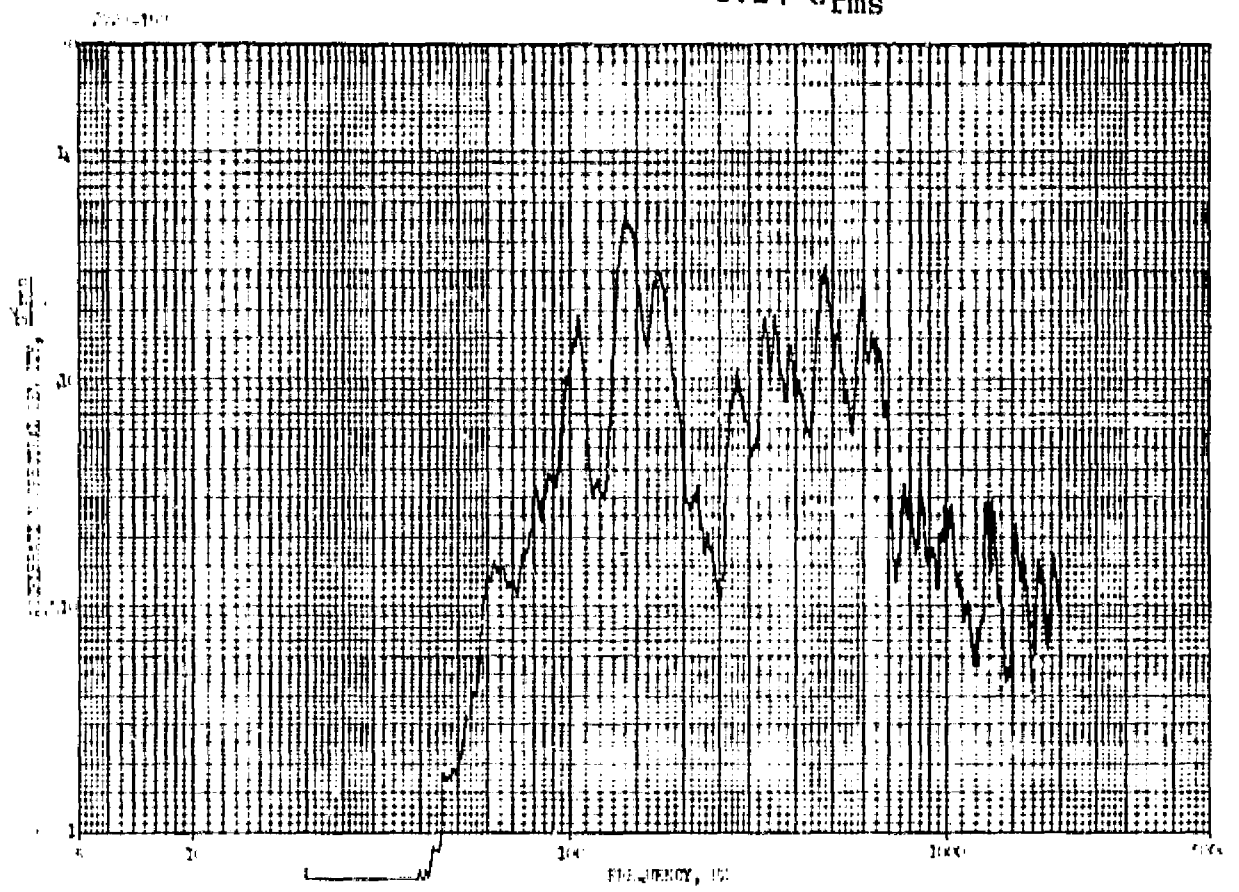

FIGURE 101. TEST #14 DATA (Concluded)

Location 1 10.0 G_{rms}

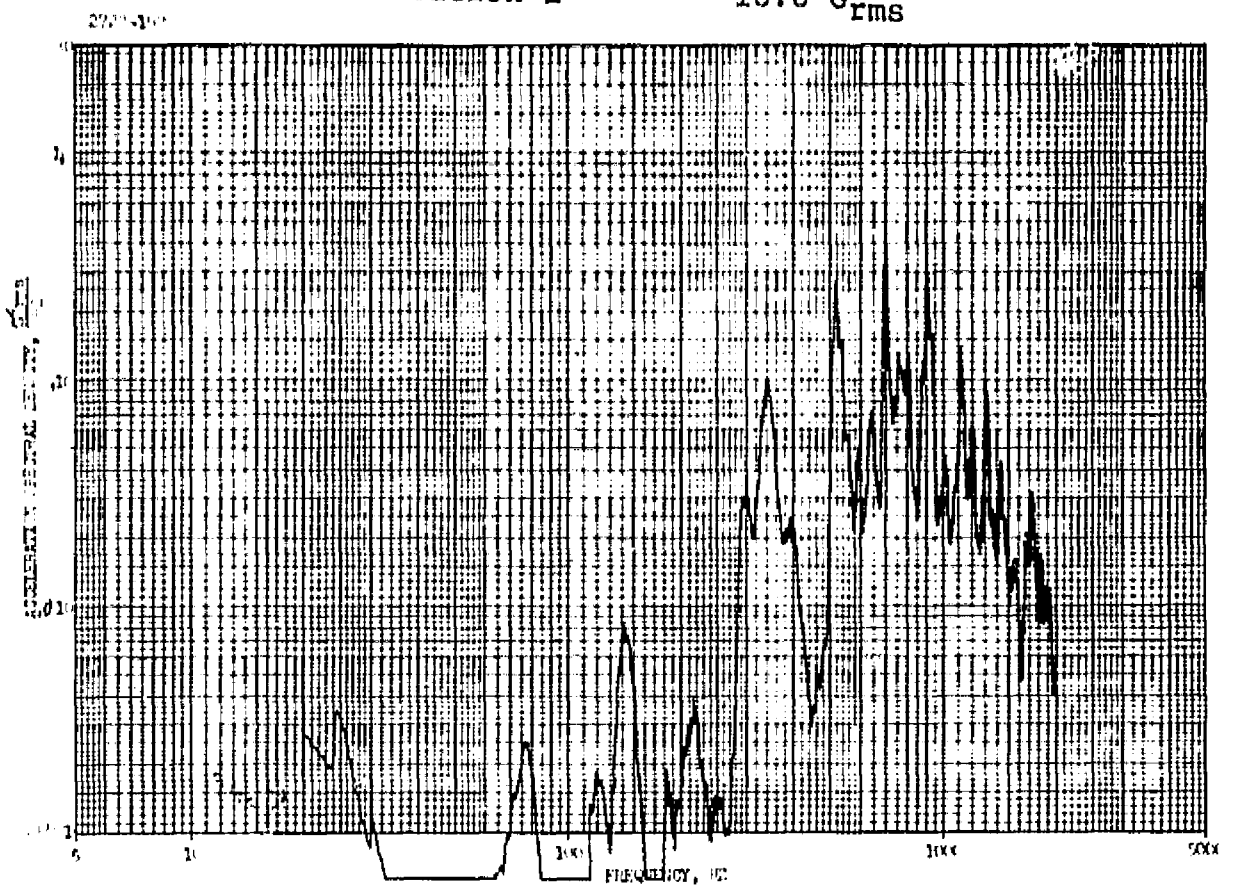

Location 2 33.8 G_{rms}

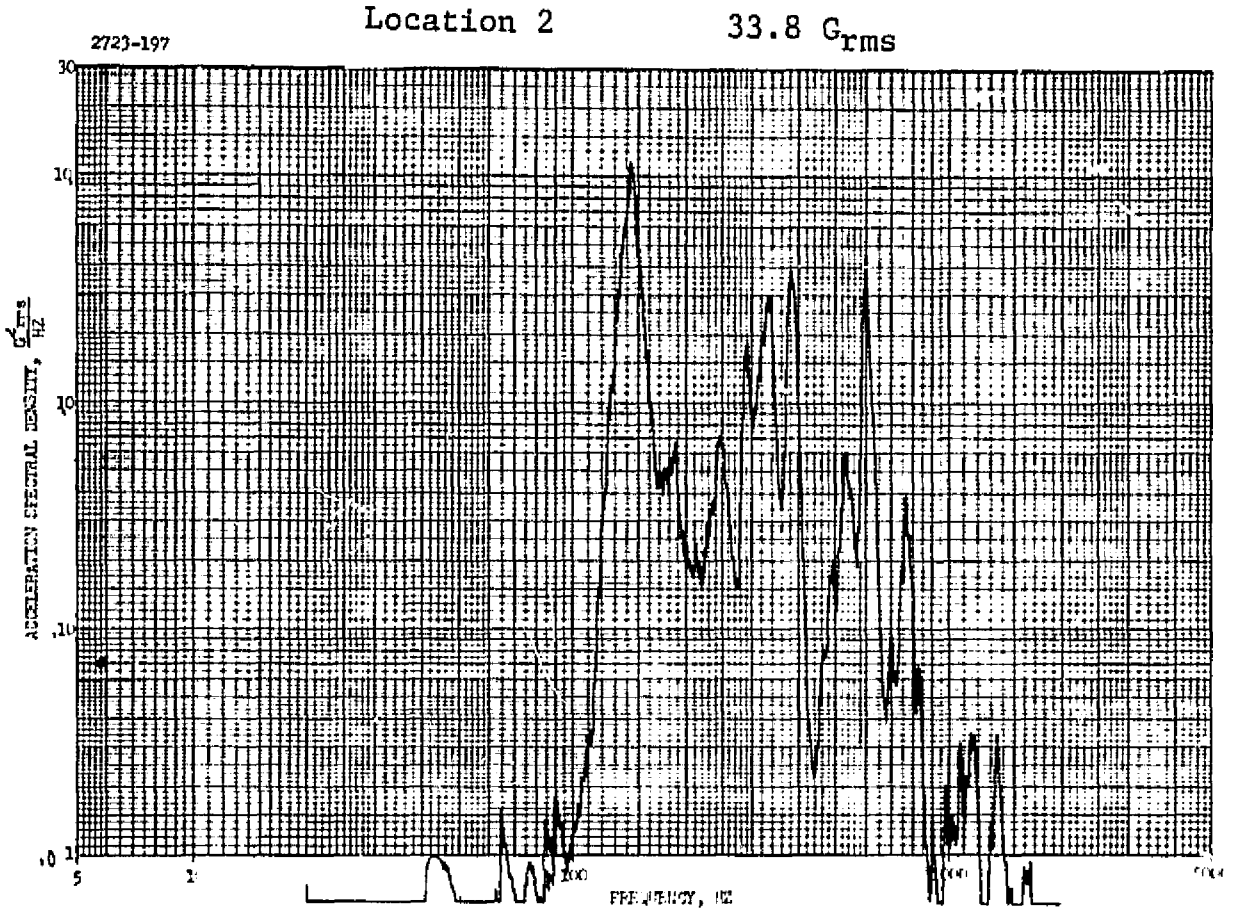

FIGURE 102. TEST # 15 DATA

Location 3 29.4 G_{rms}

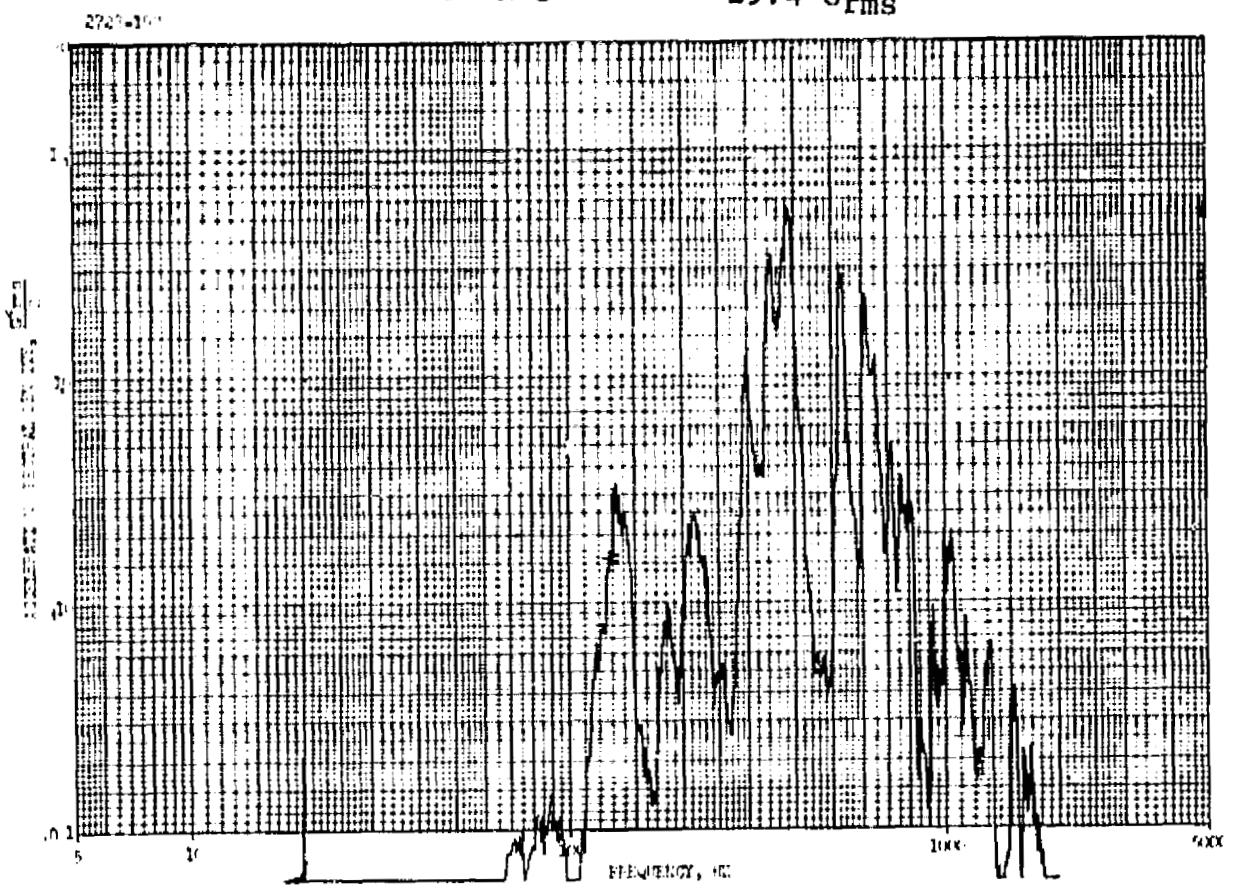

Location 4 4.7 G_{rms}

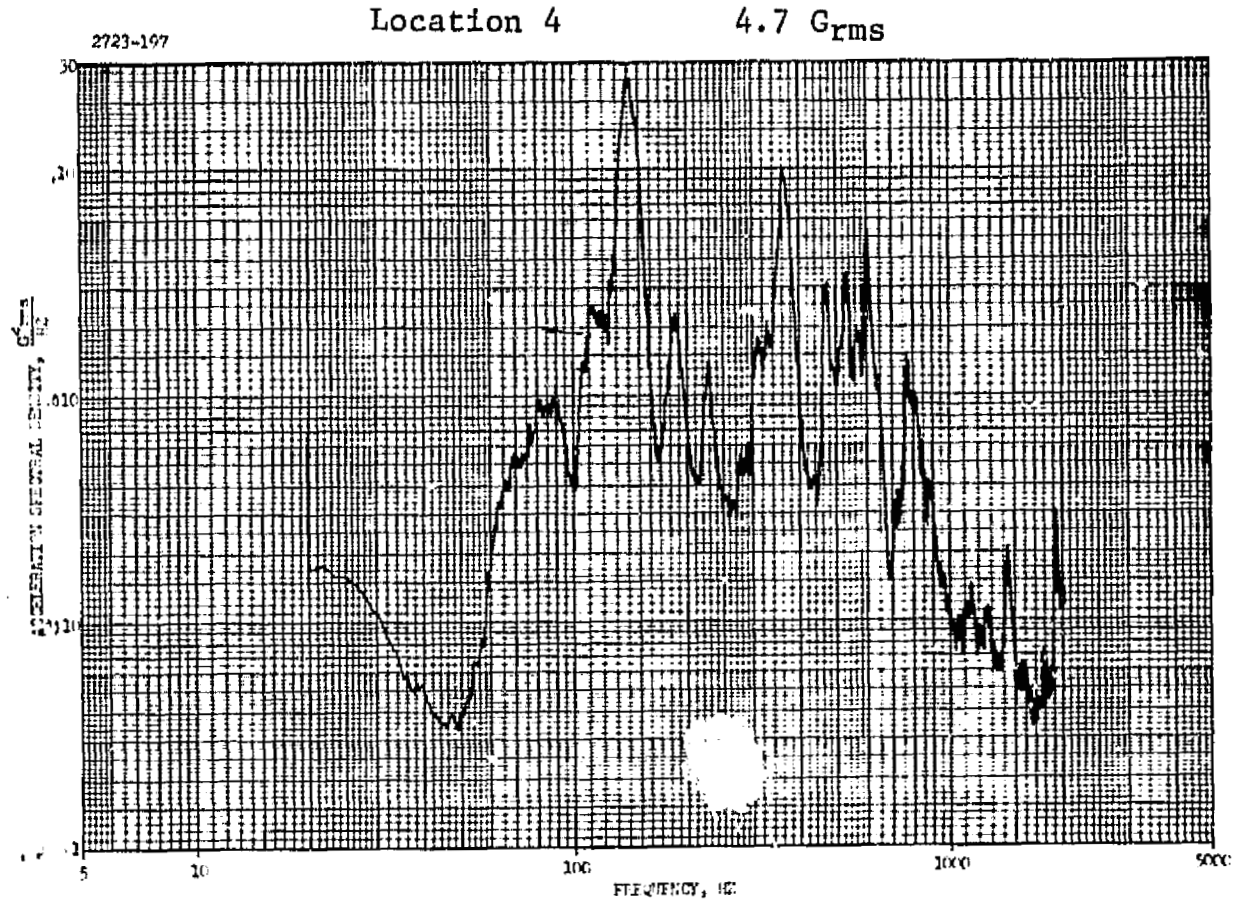

FIGURE 102. TEST #15 DATA (Continued)

Location 5 6.5 G_{rms}

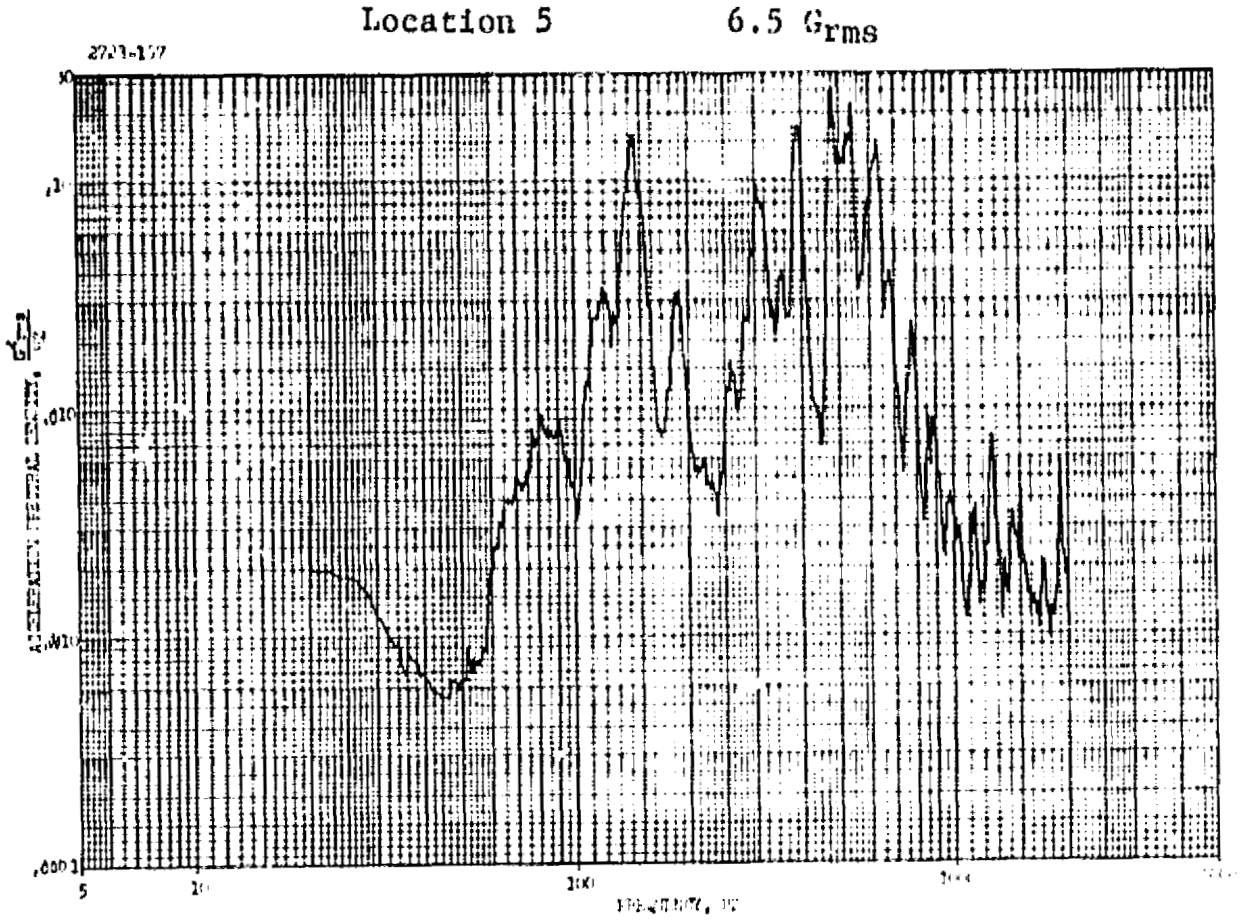

Location 6 10.6 G_{rms}

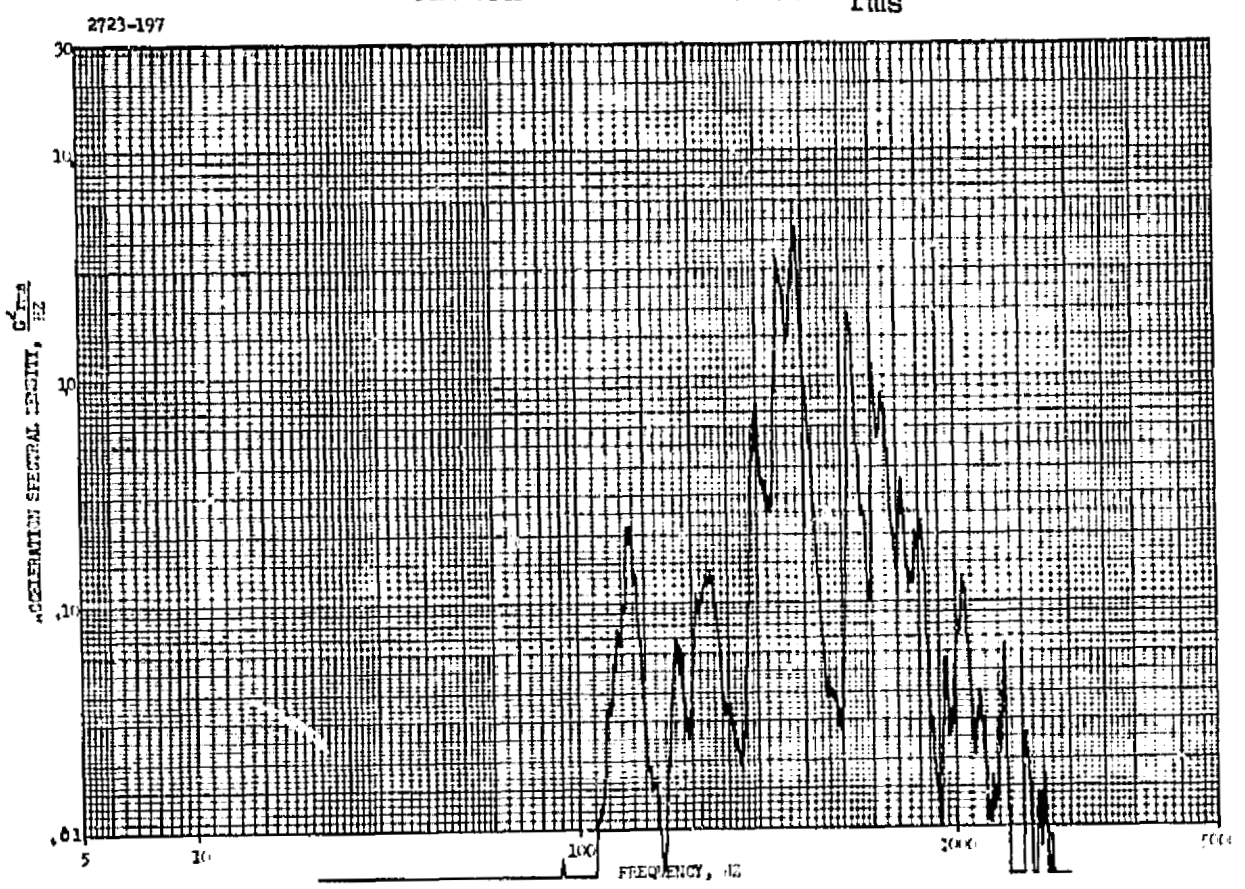

FIGURE 102. TEST #15 DATA (Continued)

Location 7 5.88 G_{rms}

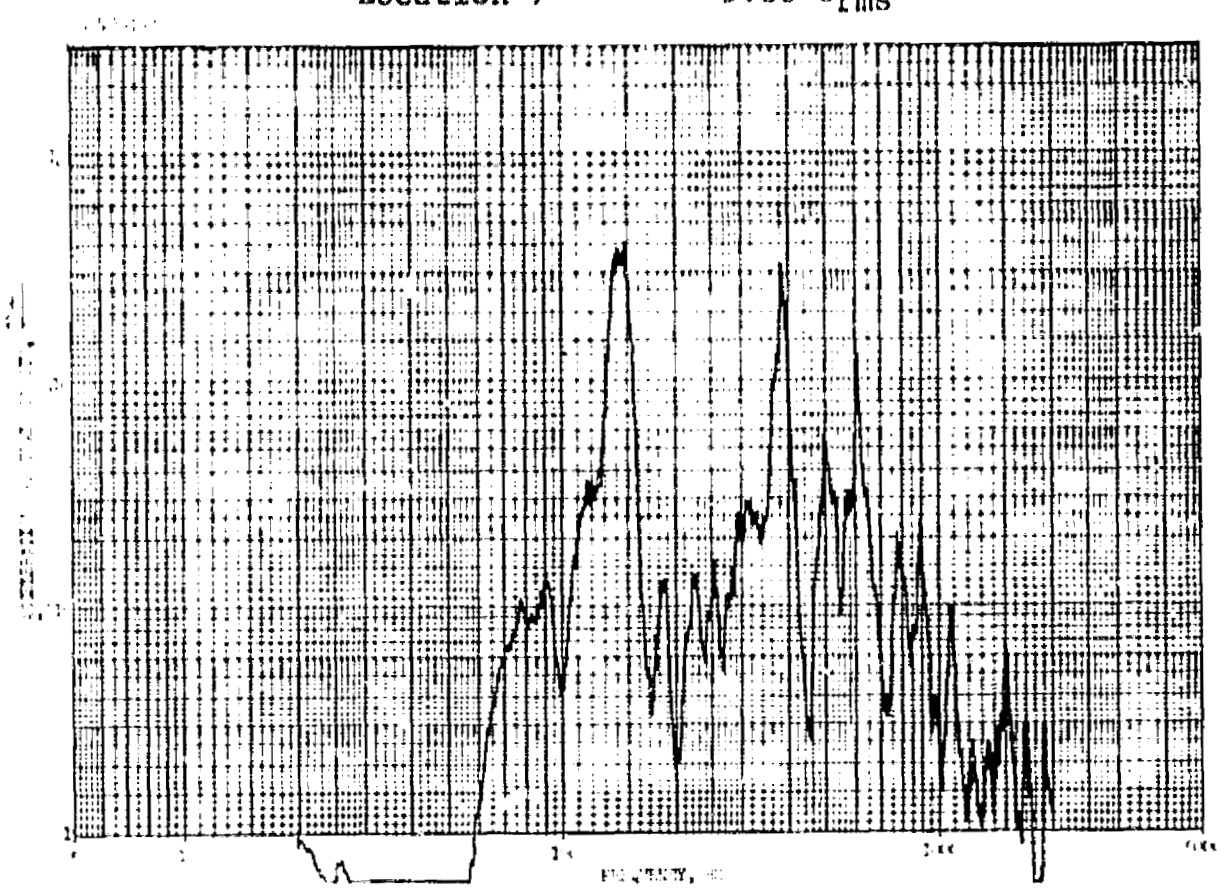

Location 8 17.6 G_{rms}

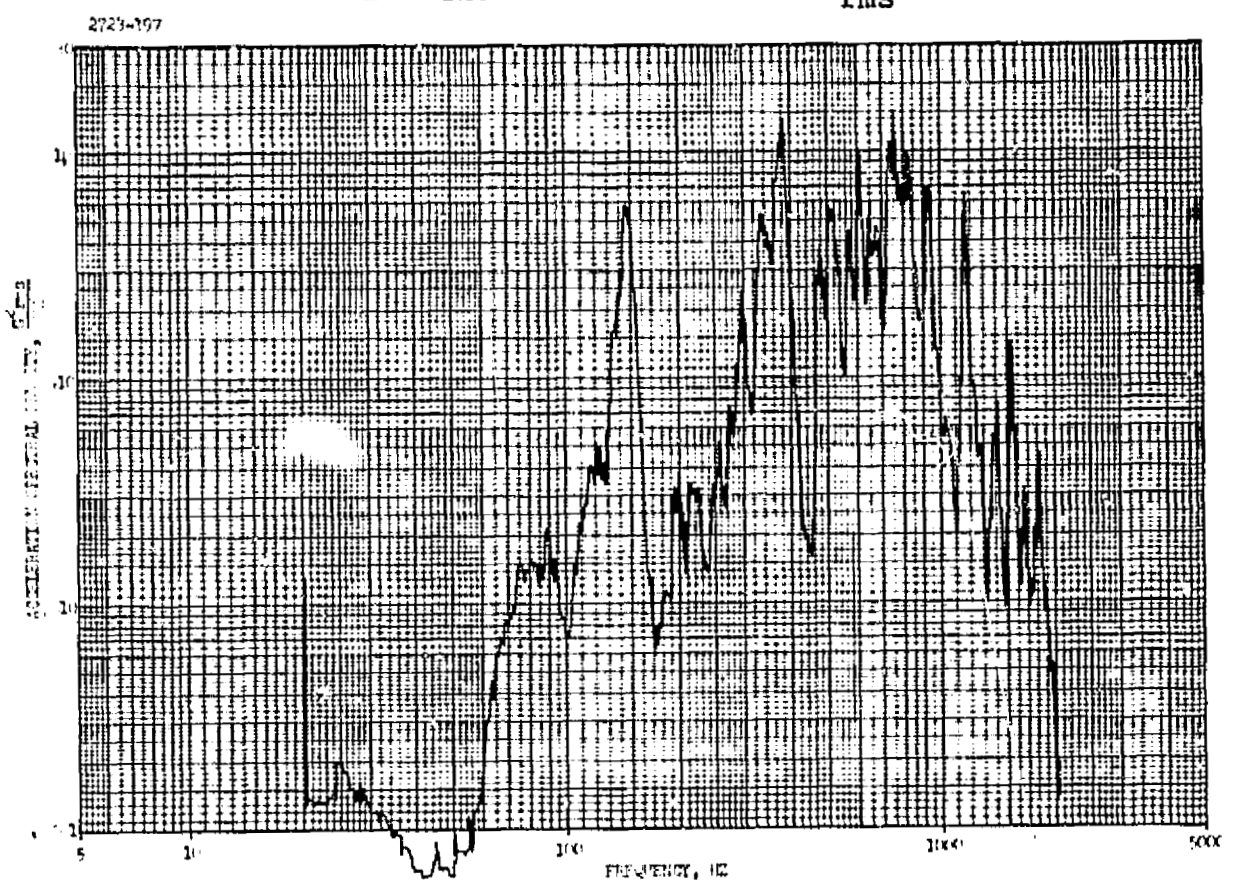

FIGURE 102. TEST #15 DATA (Continued)

Location 9 29.4 G_{rms}

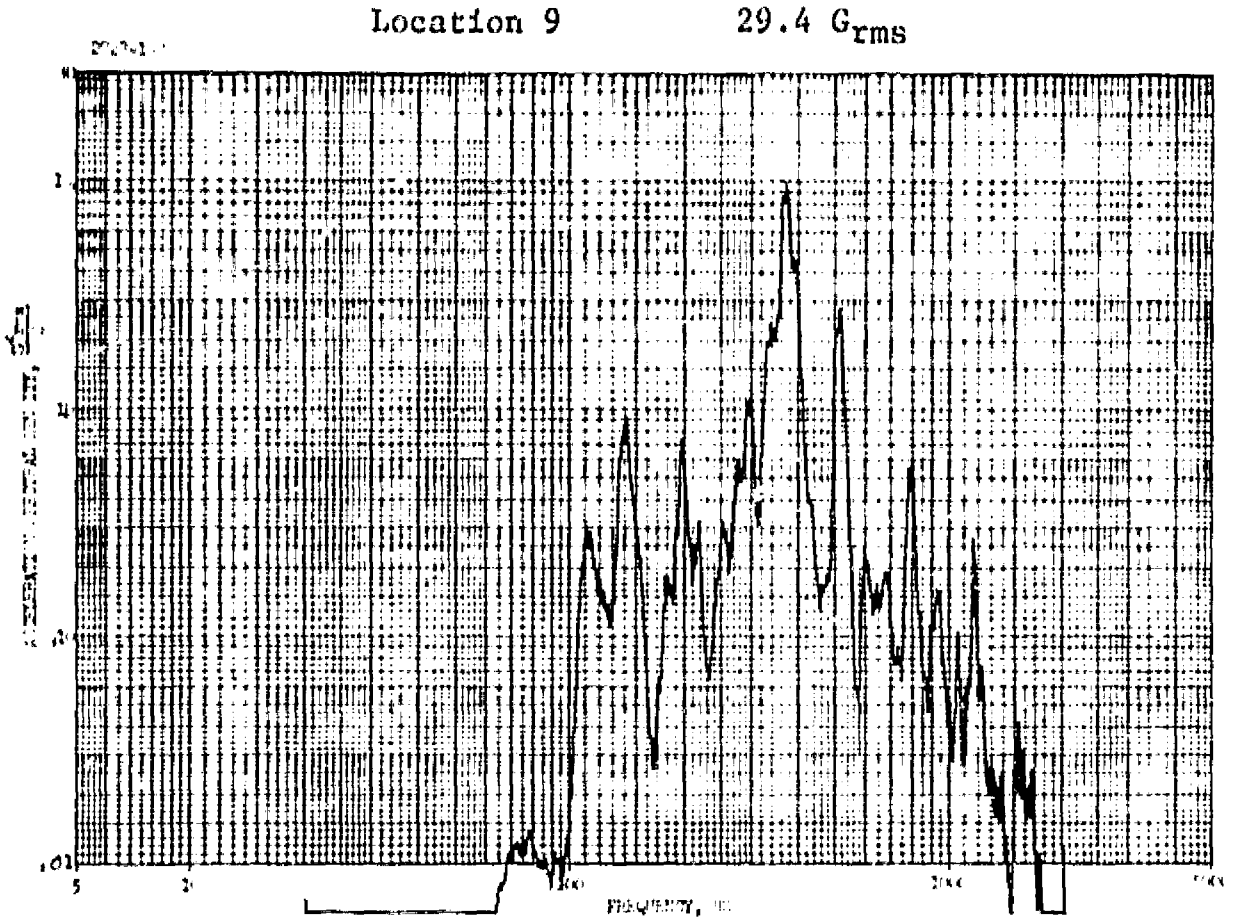

Location 10 41.2 G_{rms}

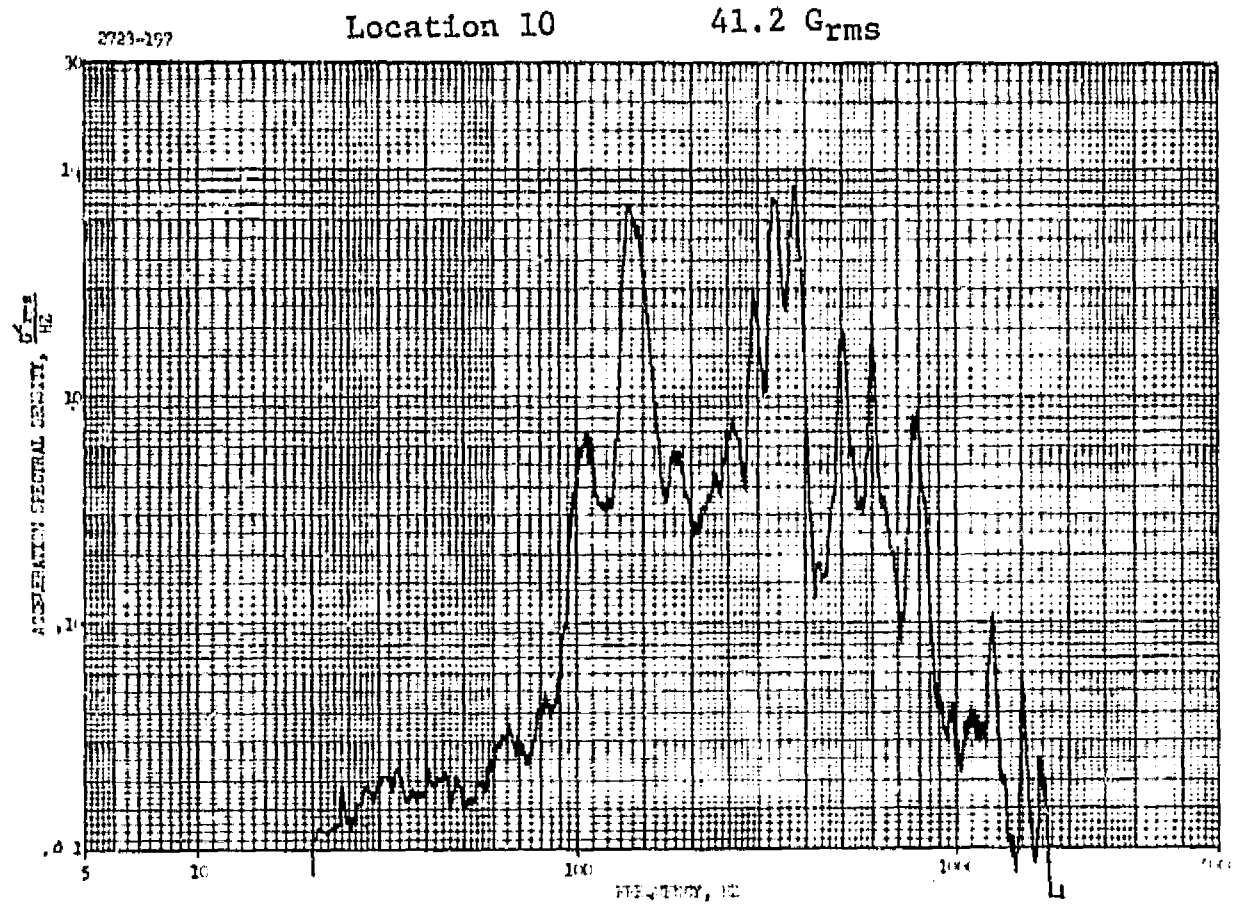

FIGURE 102. TEST #15 DATA (Continued)

Location 11 12.9 G_{rms}

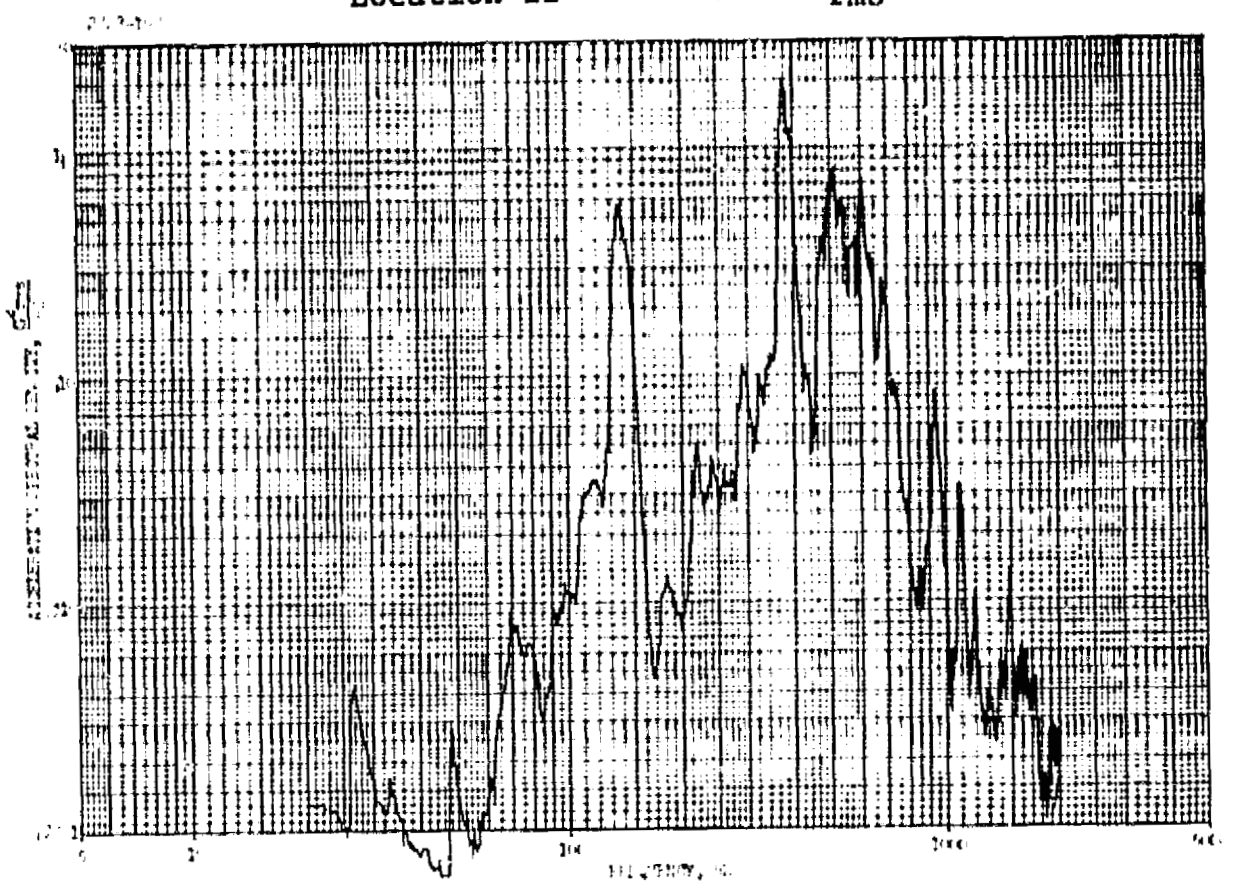

Location 12 35.3 G_{rms}

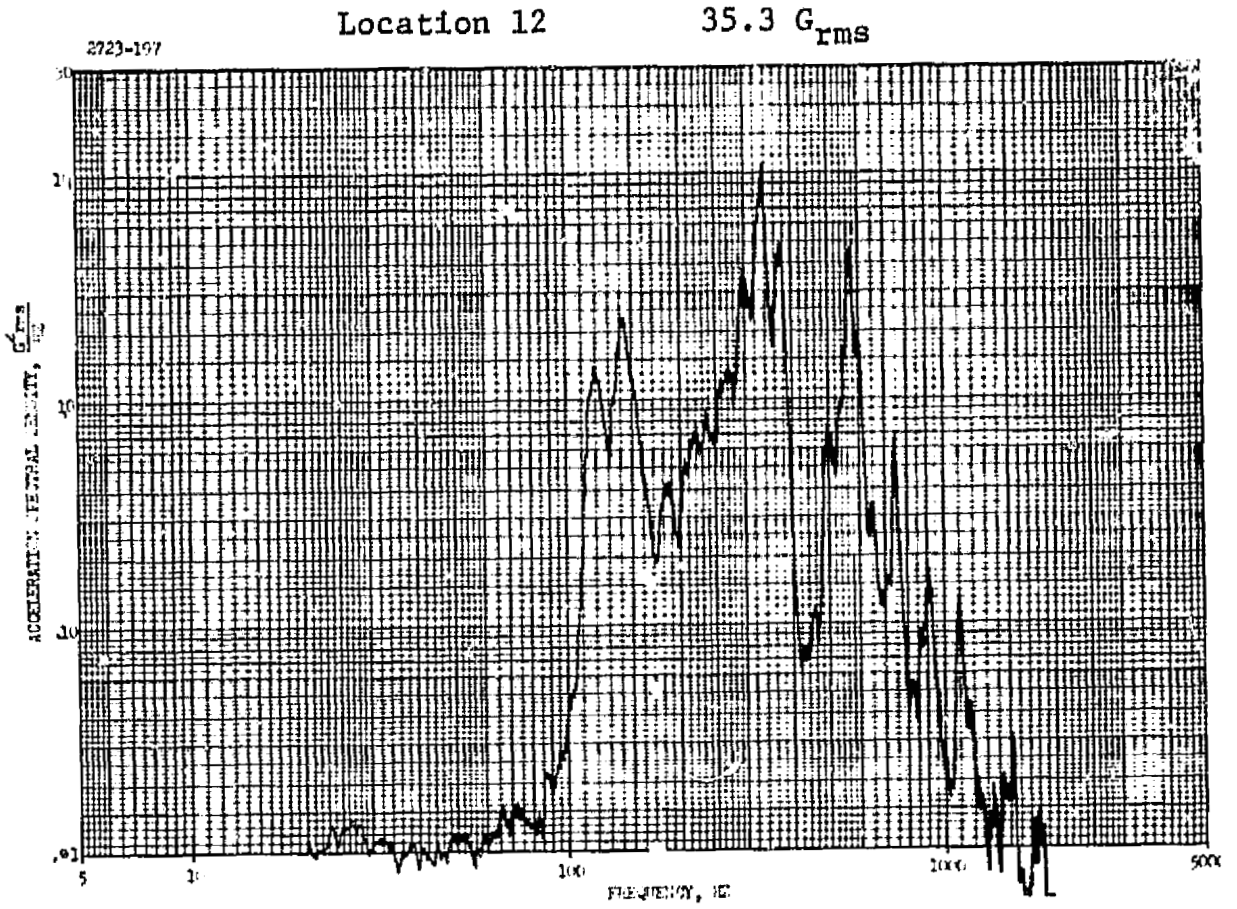

FIGURE 102. TEST #15 DATA (Continued)

Location 13 10.0 G_{rms}

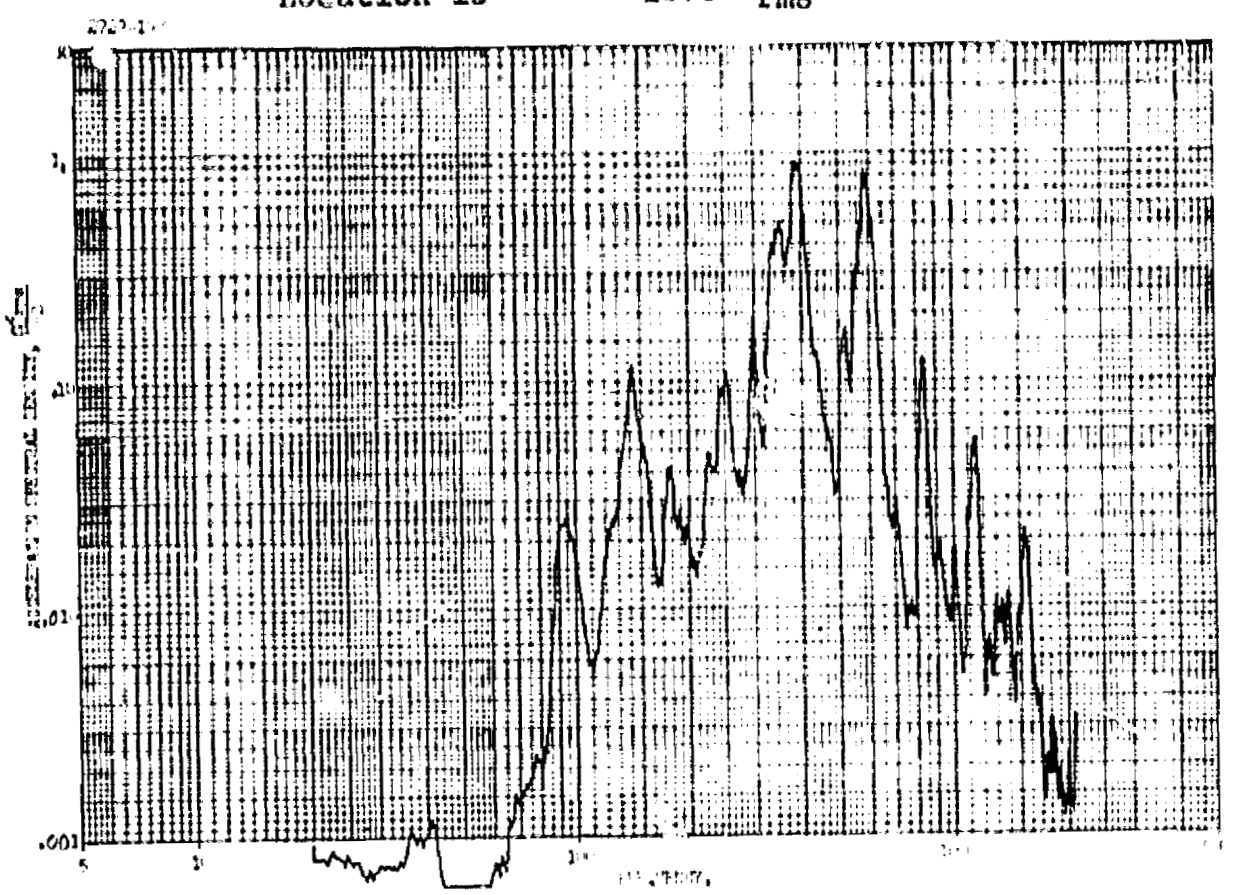

Location 14 8.84 G_{rms}

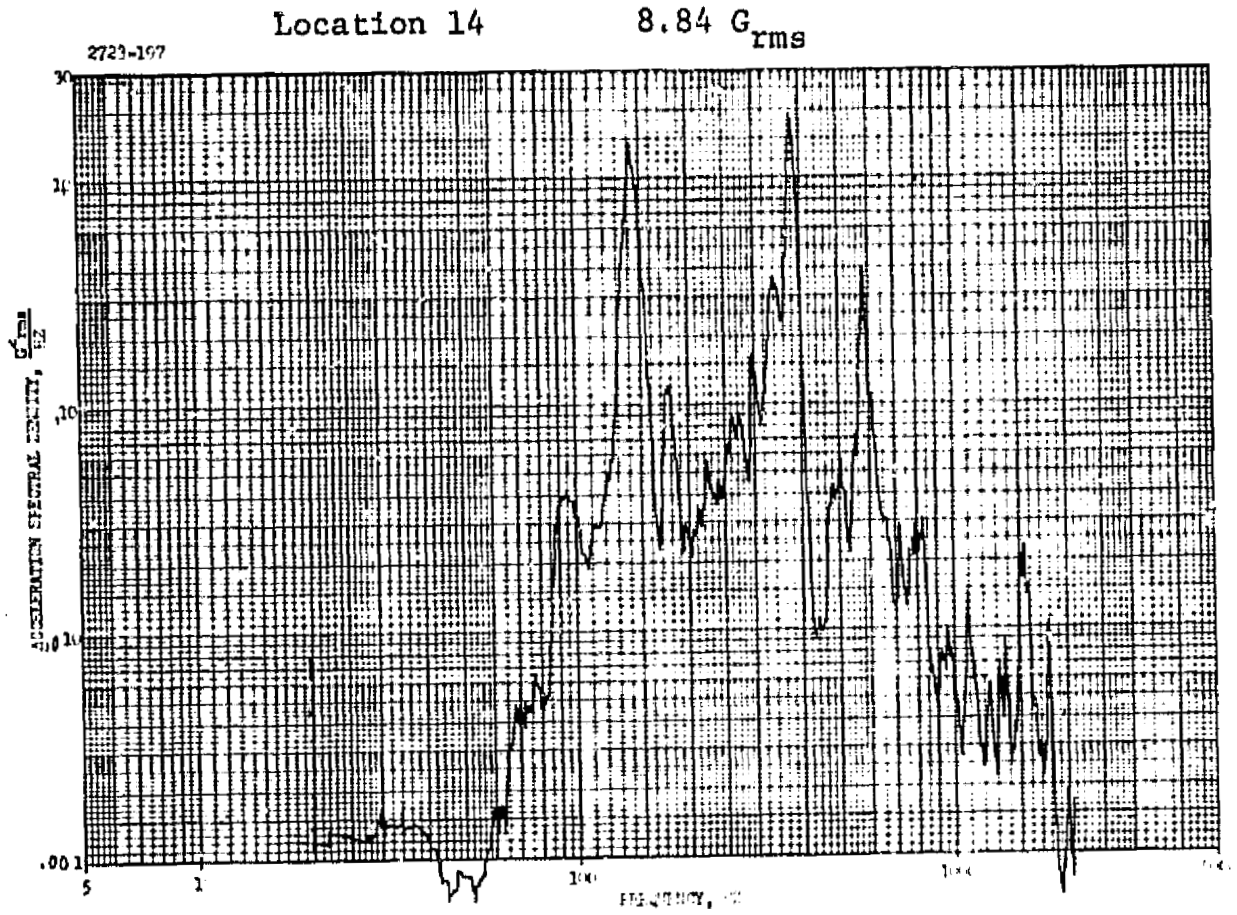

FIGURE 102. TEST #15 DATA (Continued)

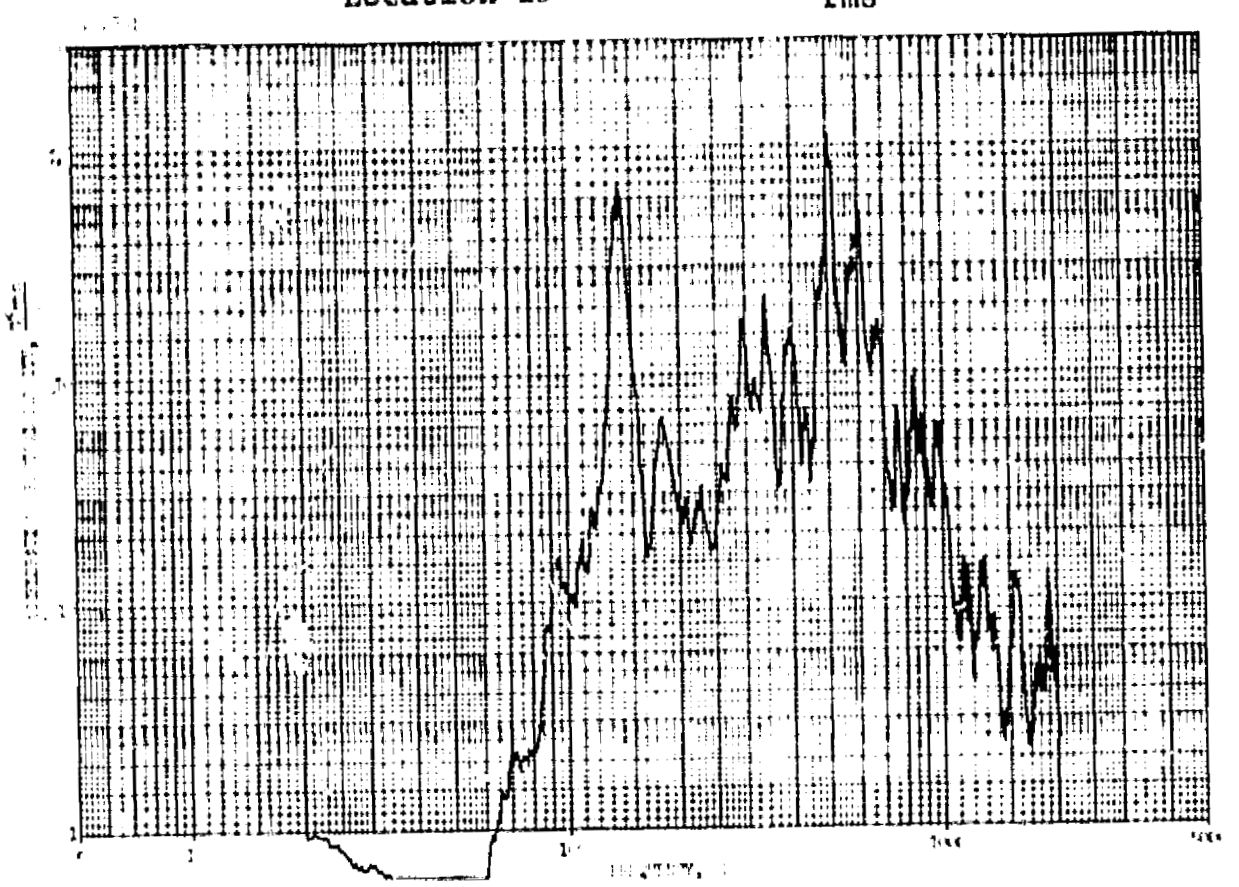

FIGURE 102. TEST #15 DATA (Concluded)

Location 1 7.07 G_{rms}

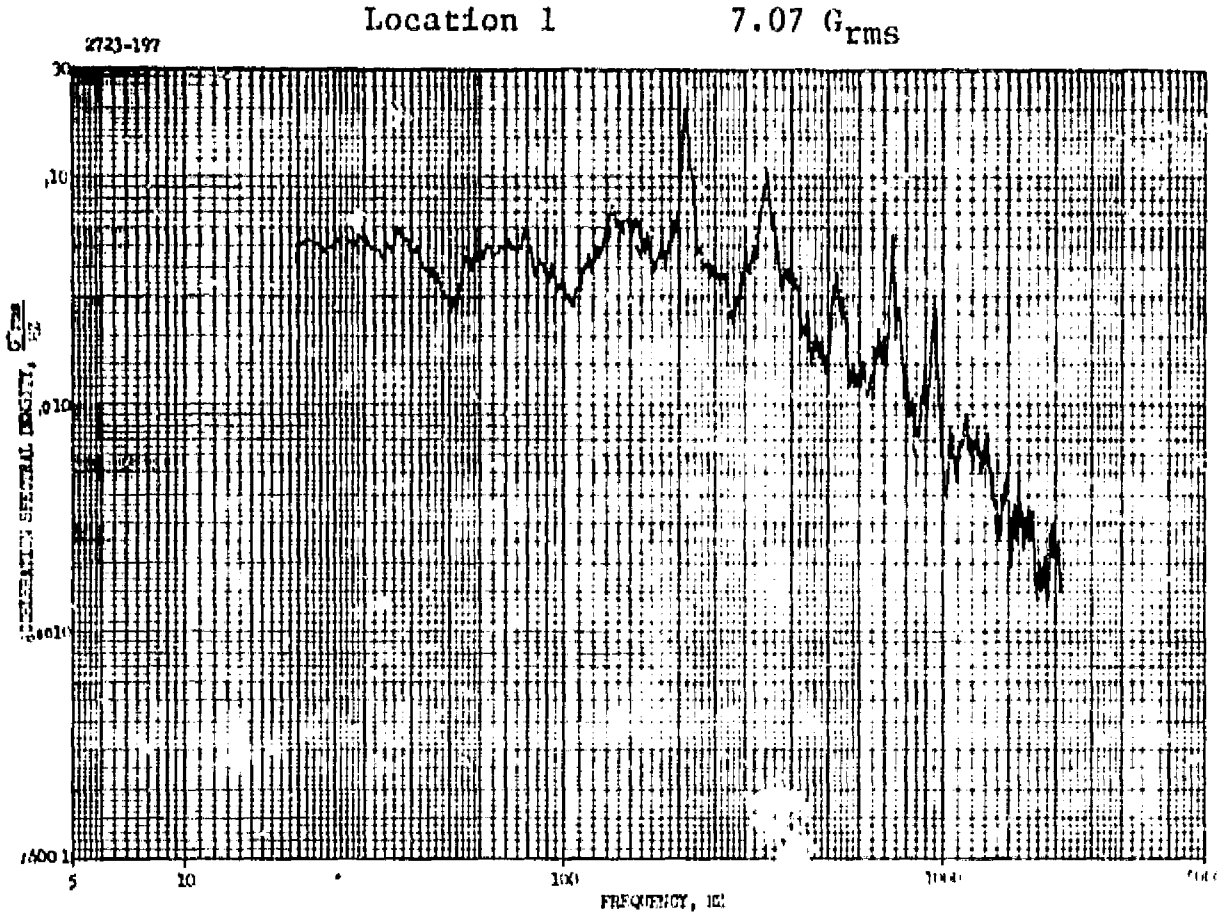

Location 2 29.4 G_{rms}

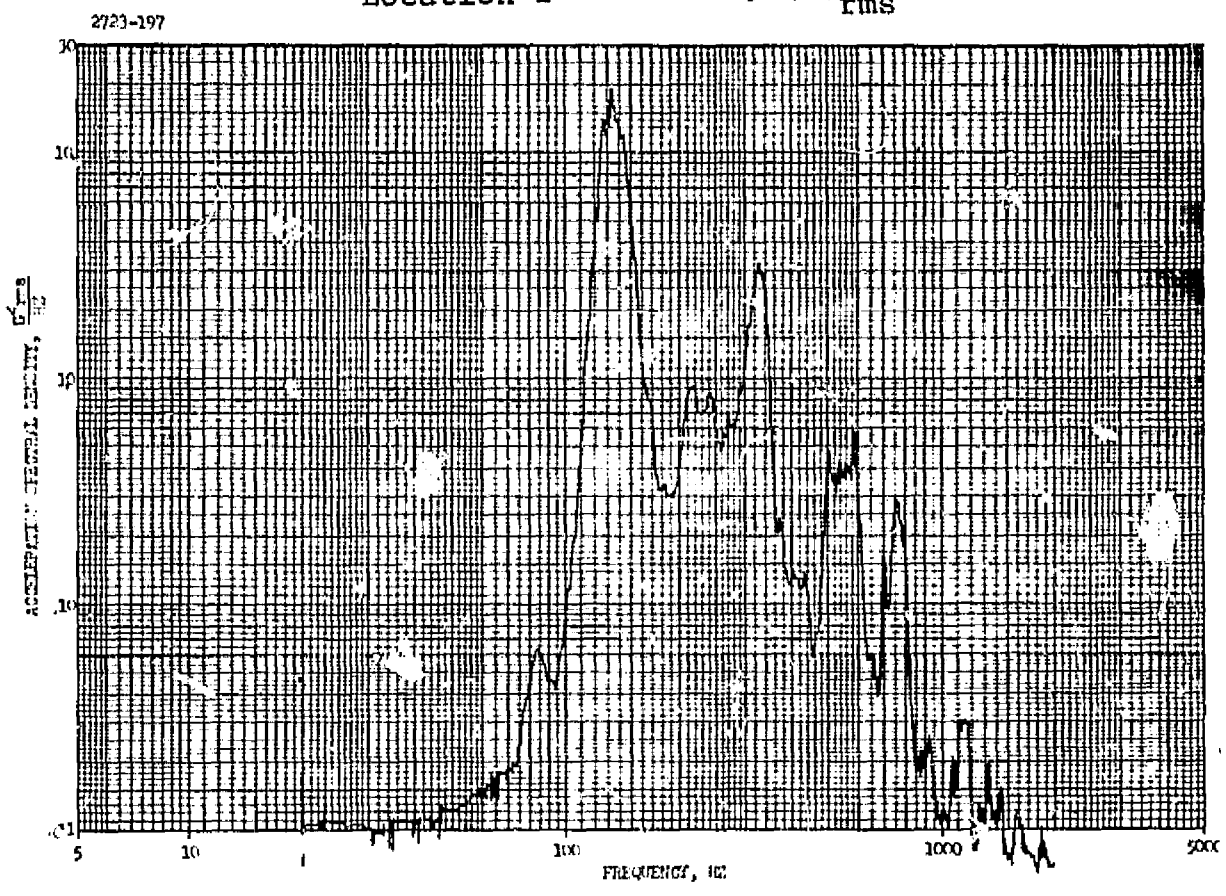

FIGURE 103. TEST # 16 - 16B DATA

Location 3 16.0 G_{rms}

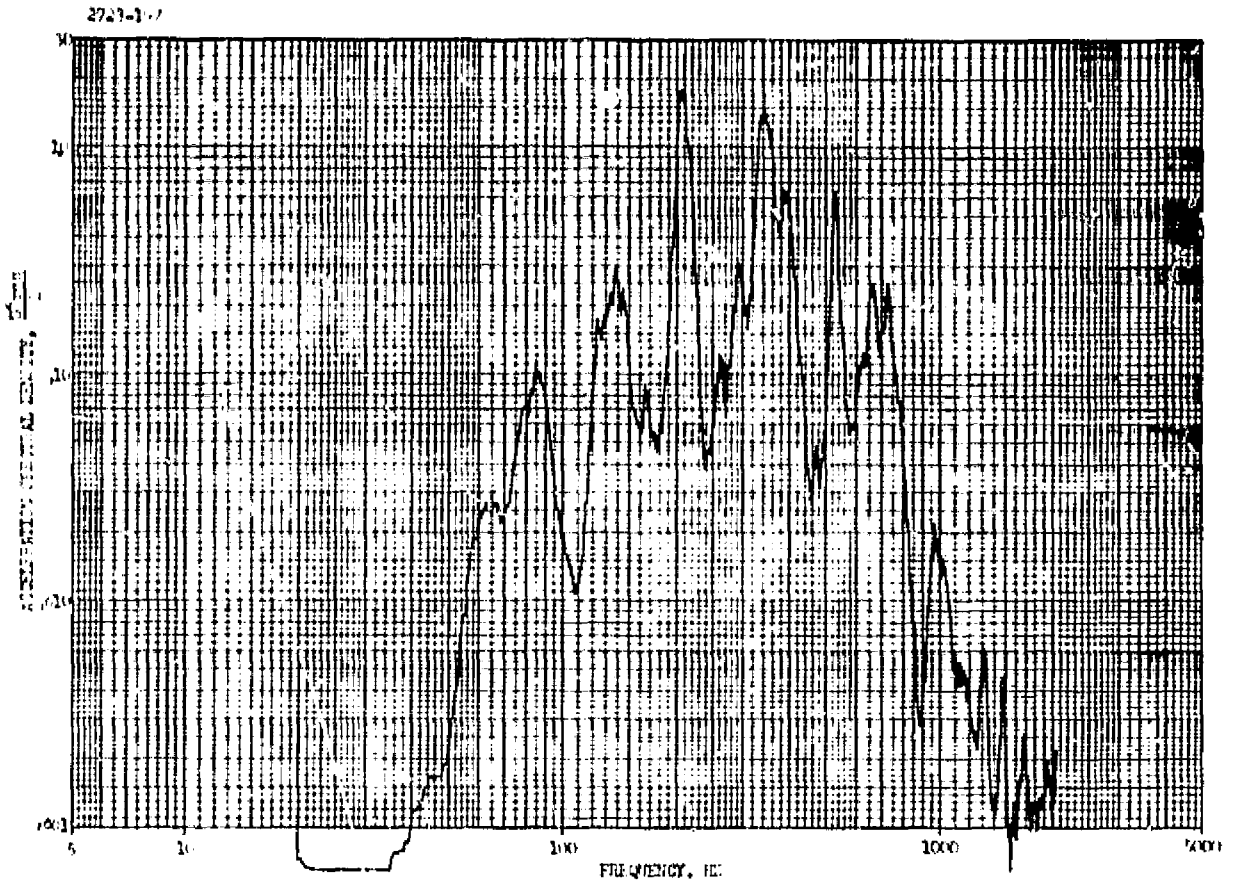

Location 4 5.3 G_{rms}

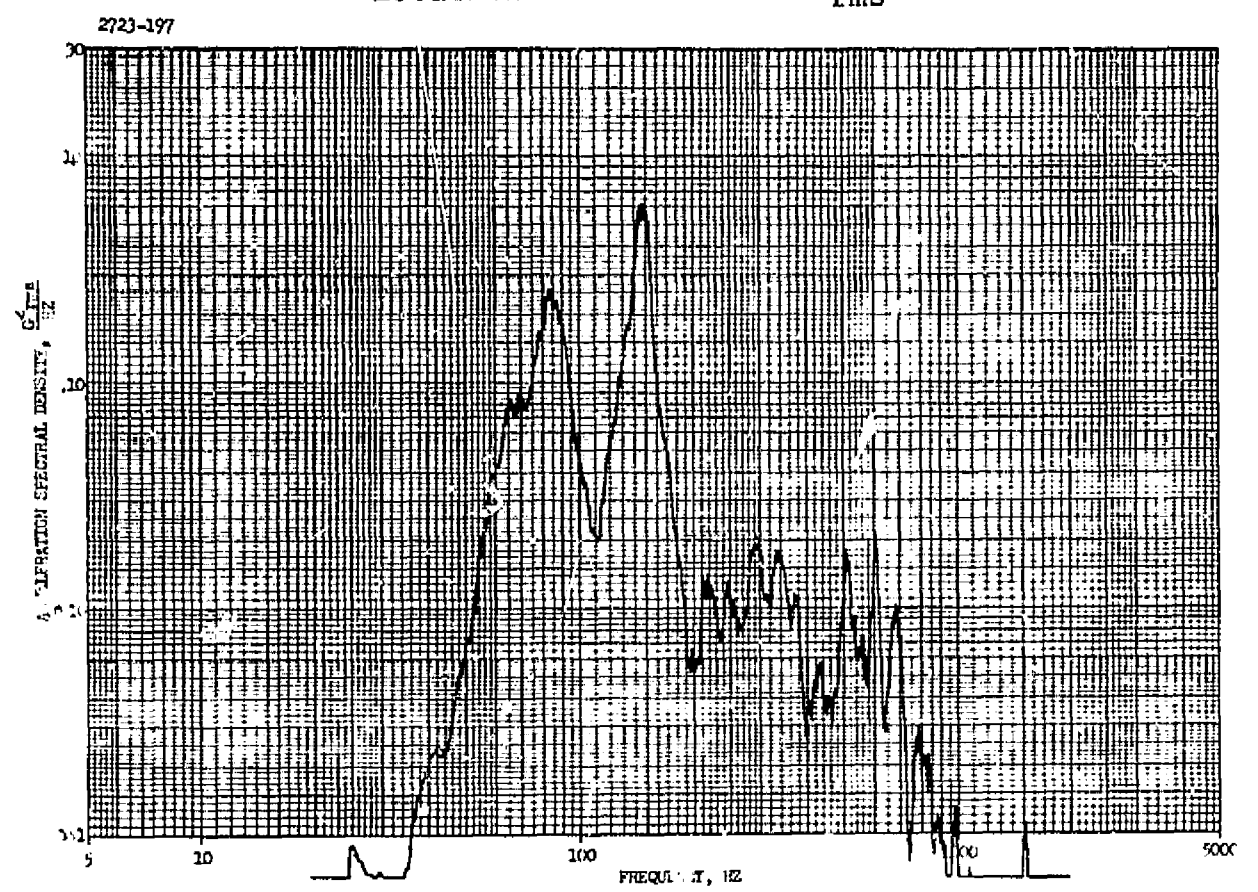

FIGURE 103. TEST #16-16B DATA (Continued)

Location 5 6.4 G_{rms}

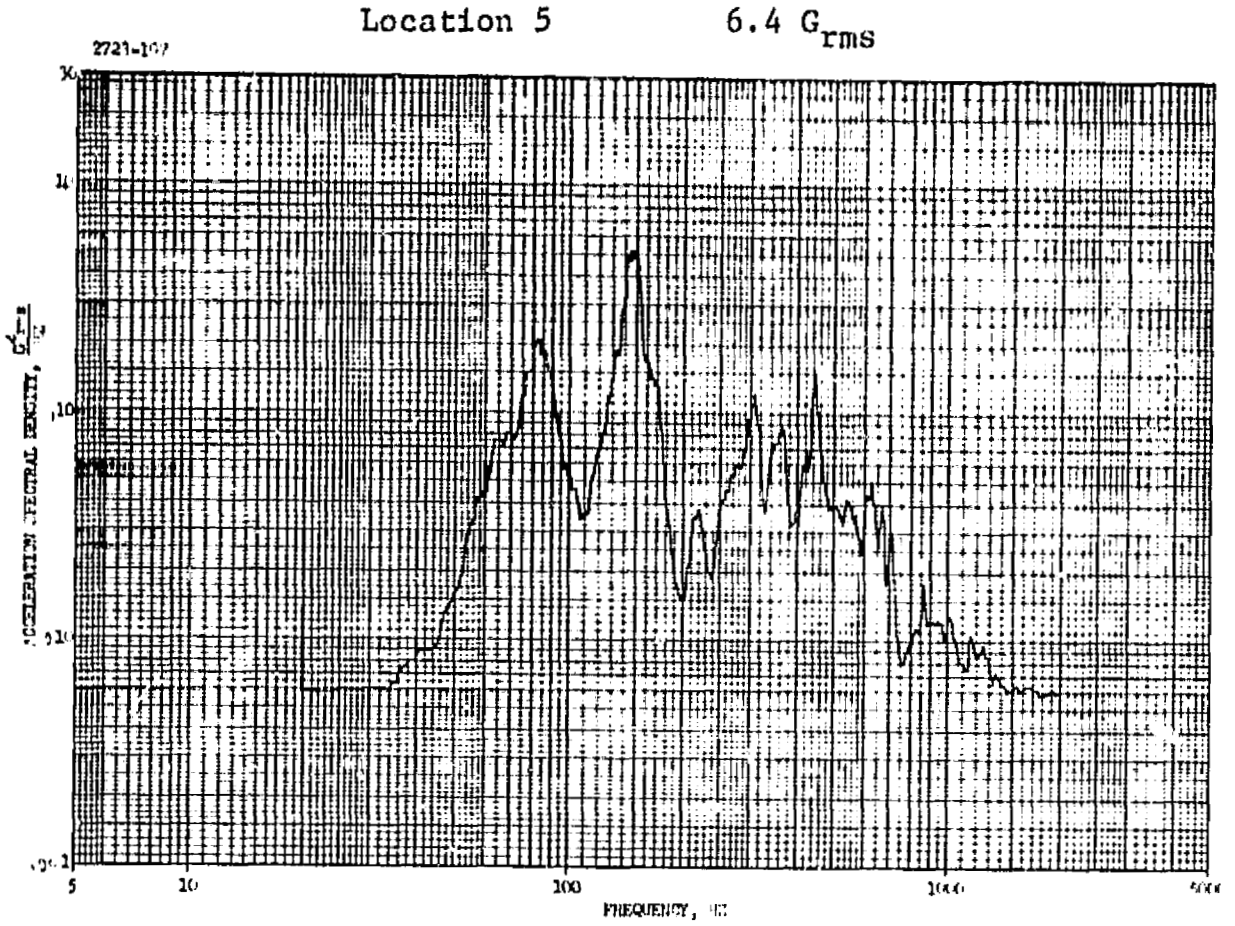

Location 6 6.4 G_{rms}

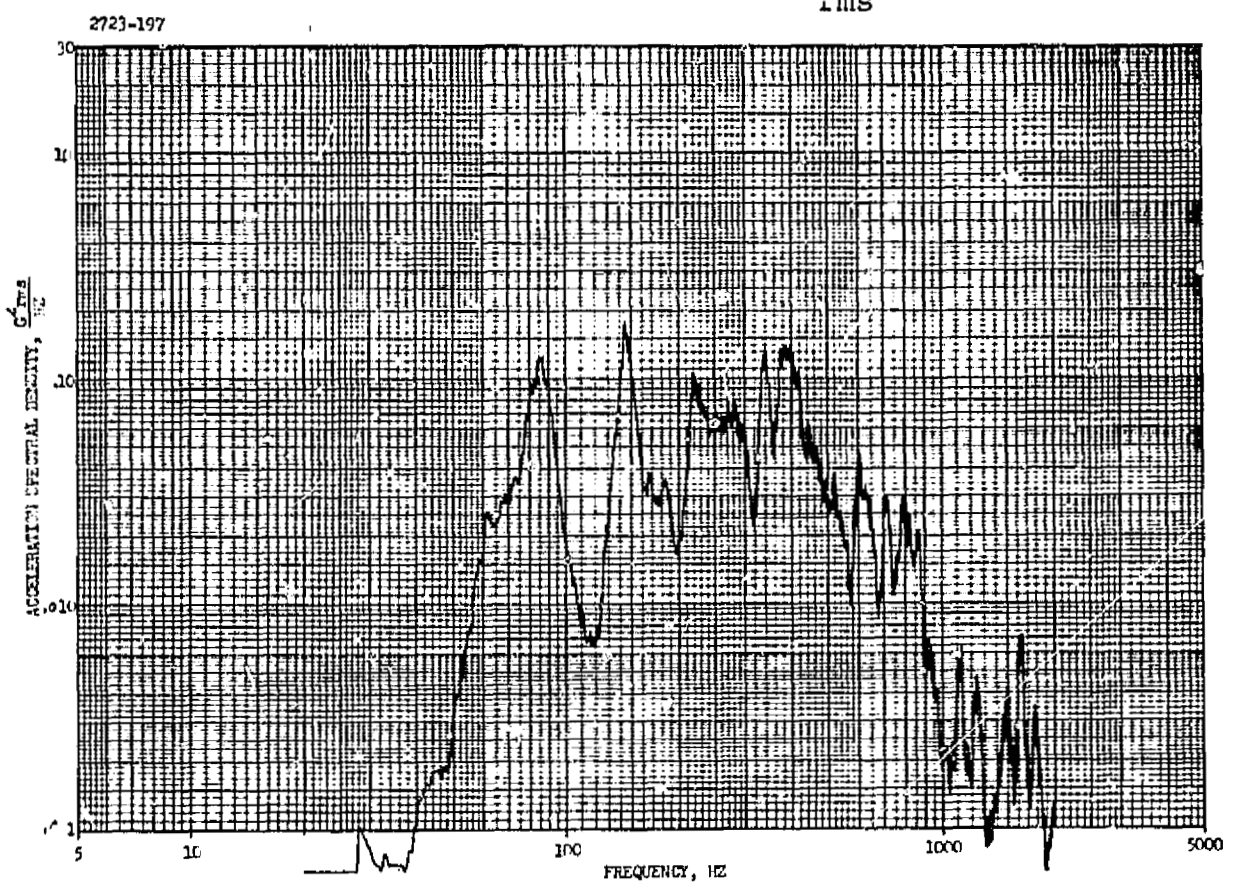

FIGURE 103. TEST #16-16B DATA (Continued)

Location 7 7.07 G_{rms}

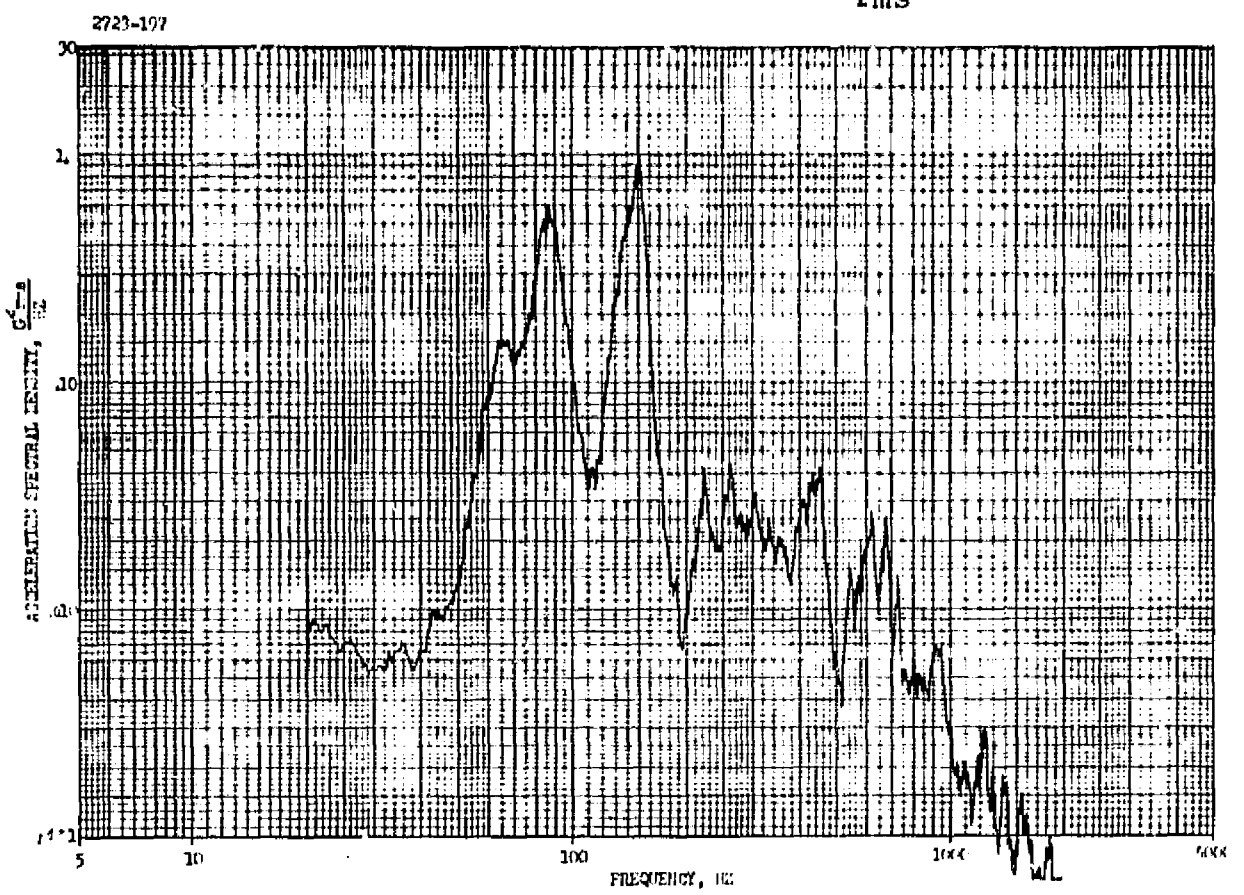

Location 8 14.1 G_{rms}

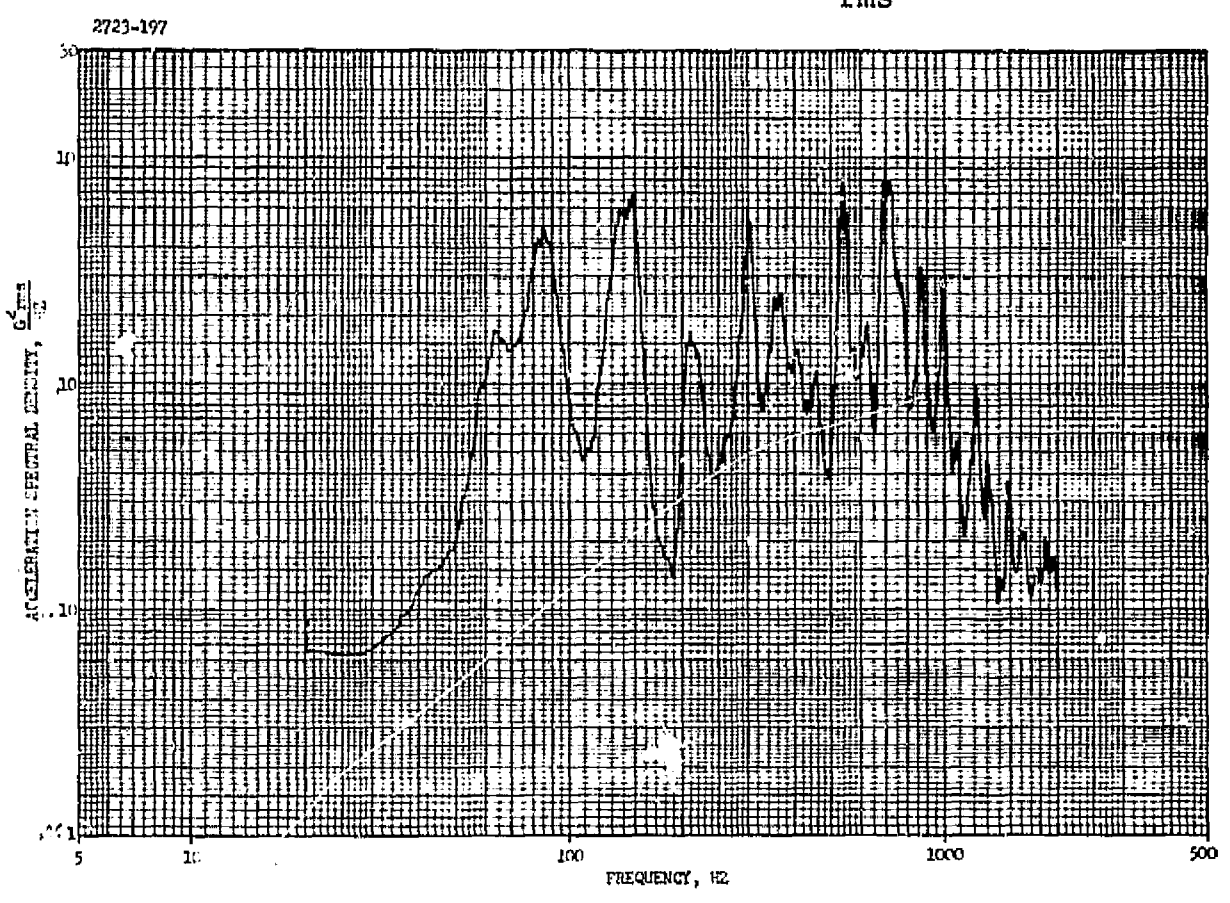

FIGURE 103. TEST #16-16B DATA (Continued)

Location 9 23.5 G_{rms}

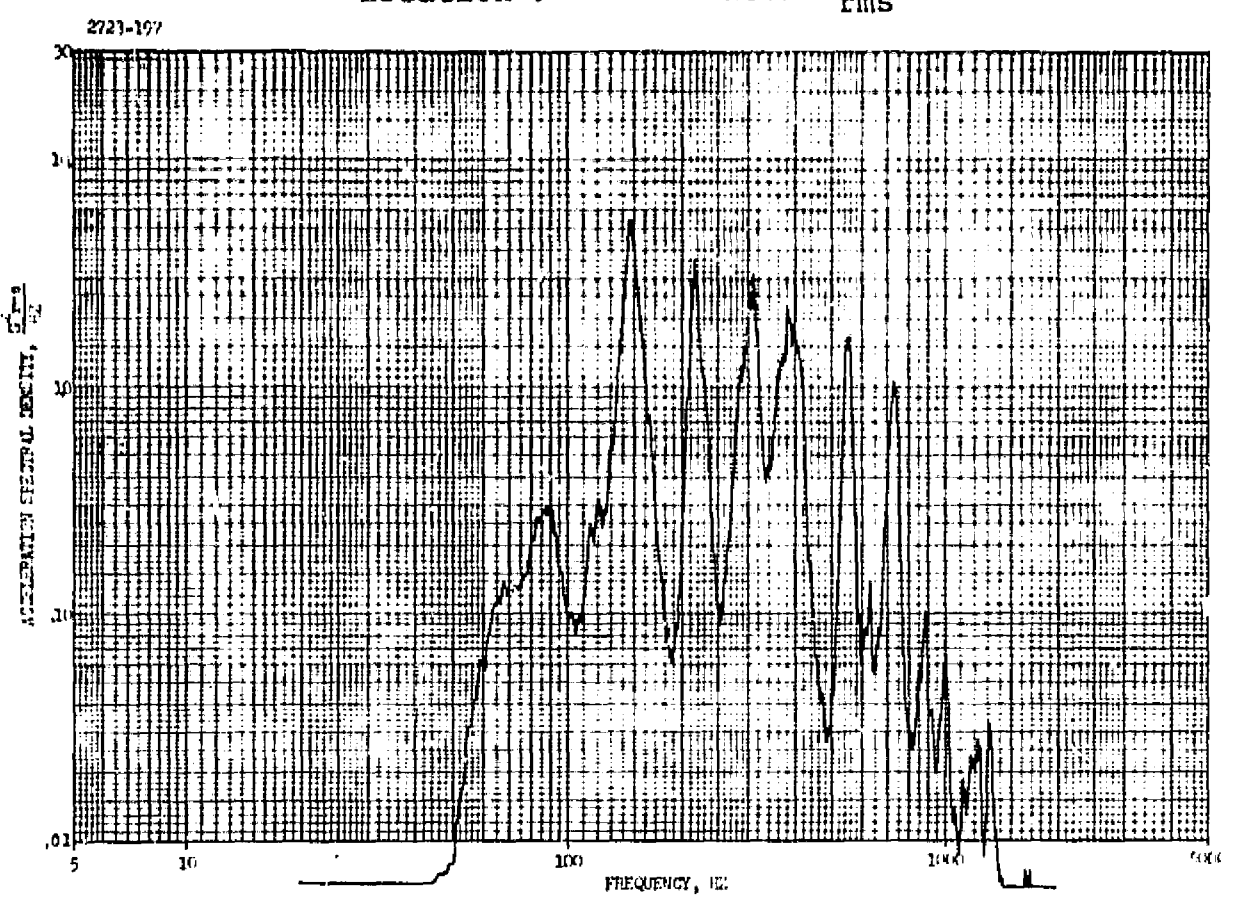

Location 10 29.4 G_{rms}

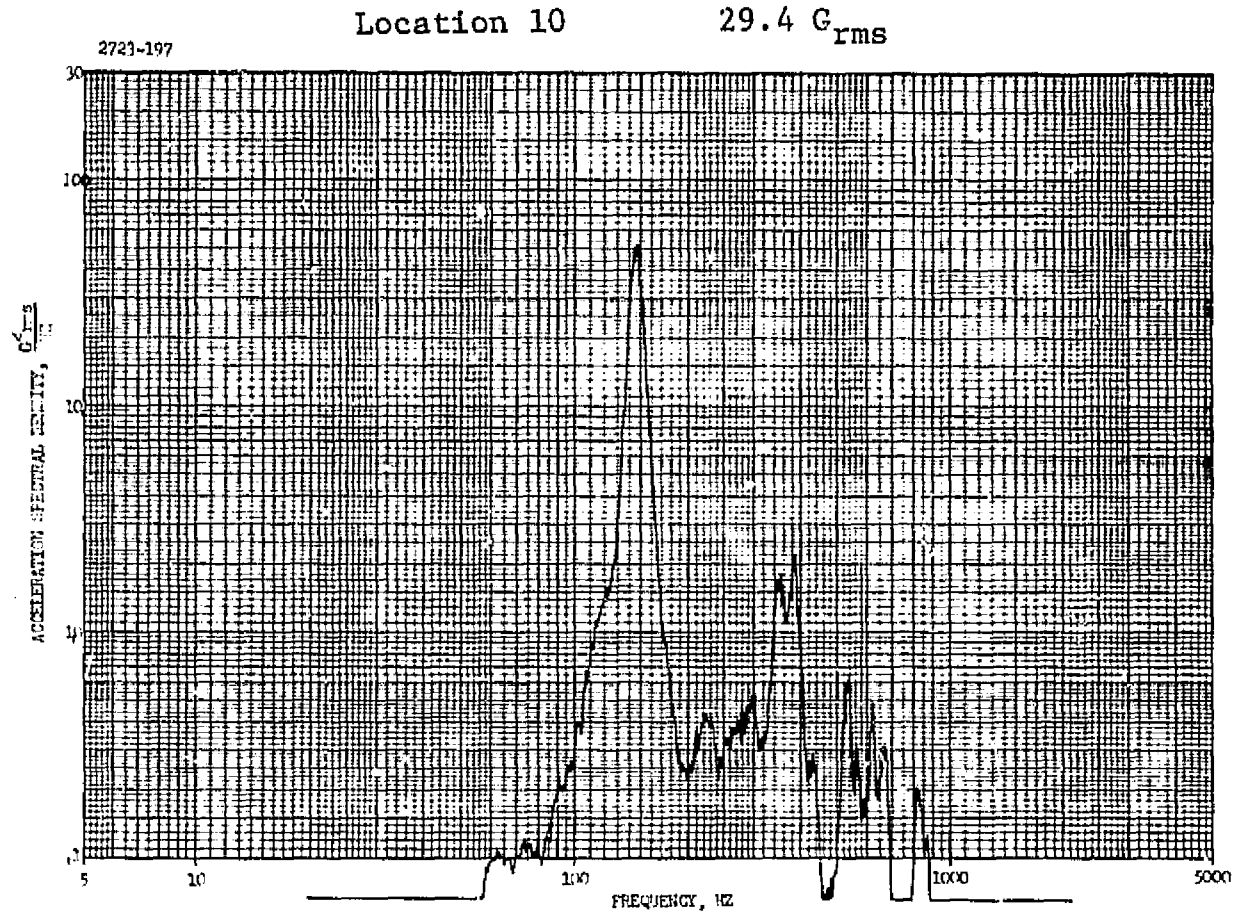

FIGURE 103. TEST #16-16B DATA (Continued)

Location 11 7.7 G_{rms}

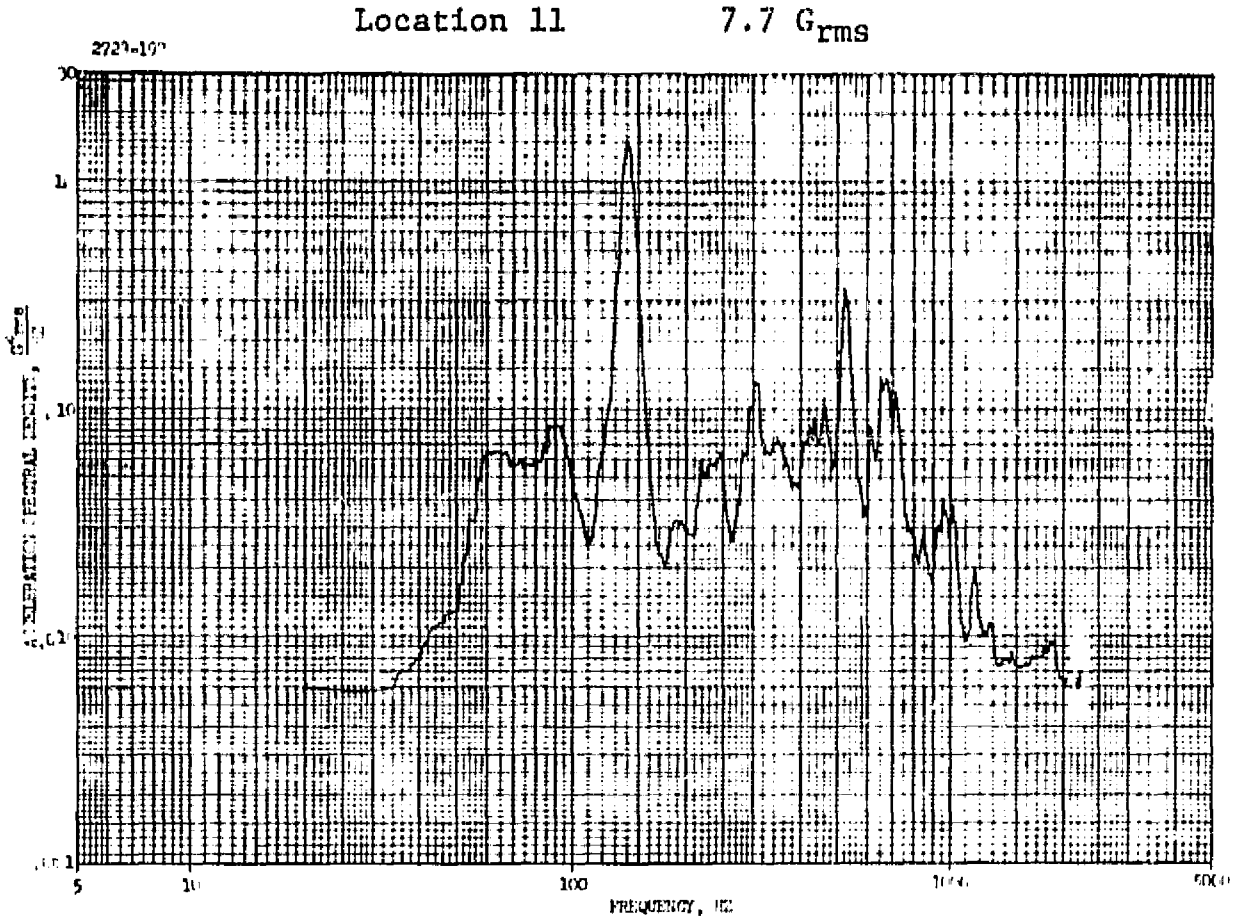

Location 12 24.7 G_{rms}

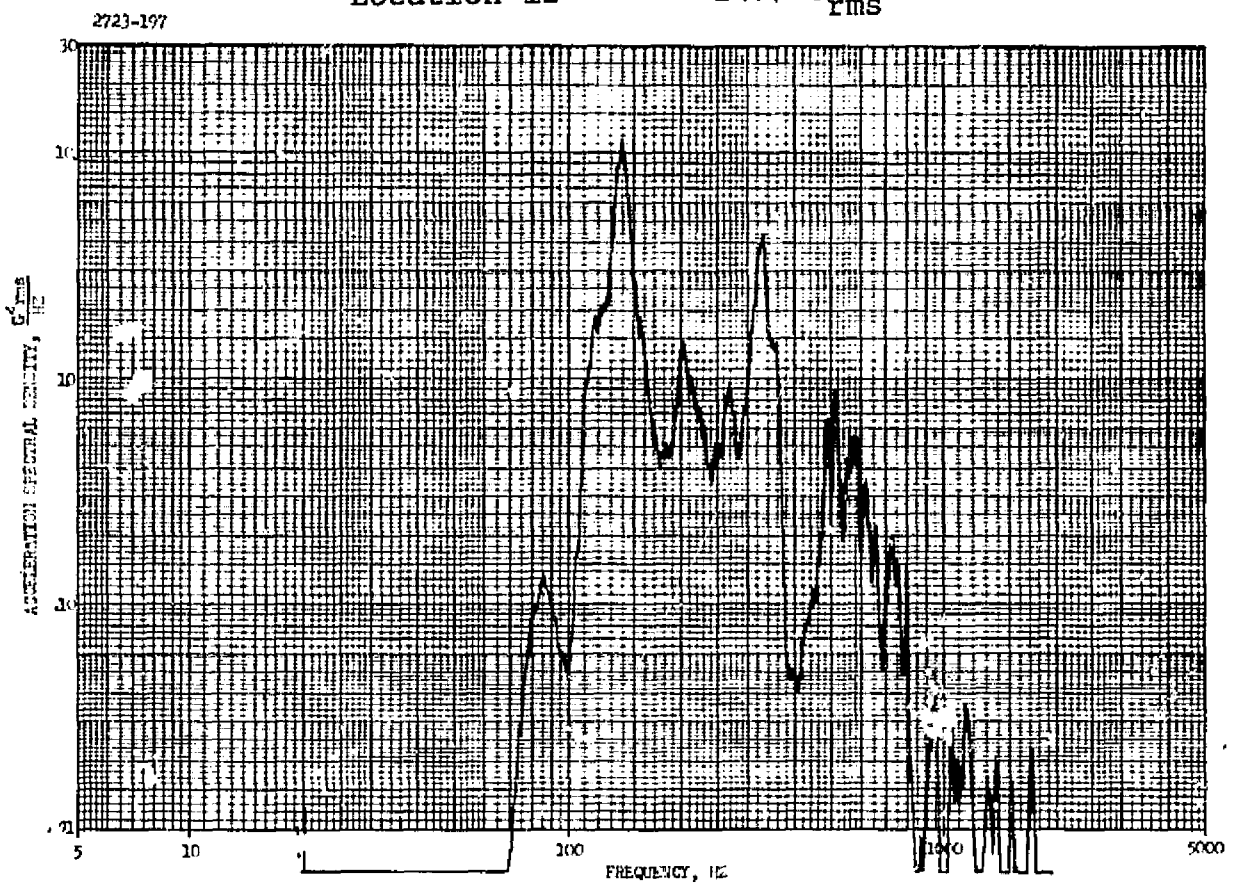

FIGURE 103. TEST #16-16B DATA (Continued)

Location 13 7.07 G_{rms}

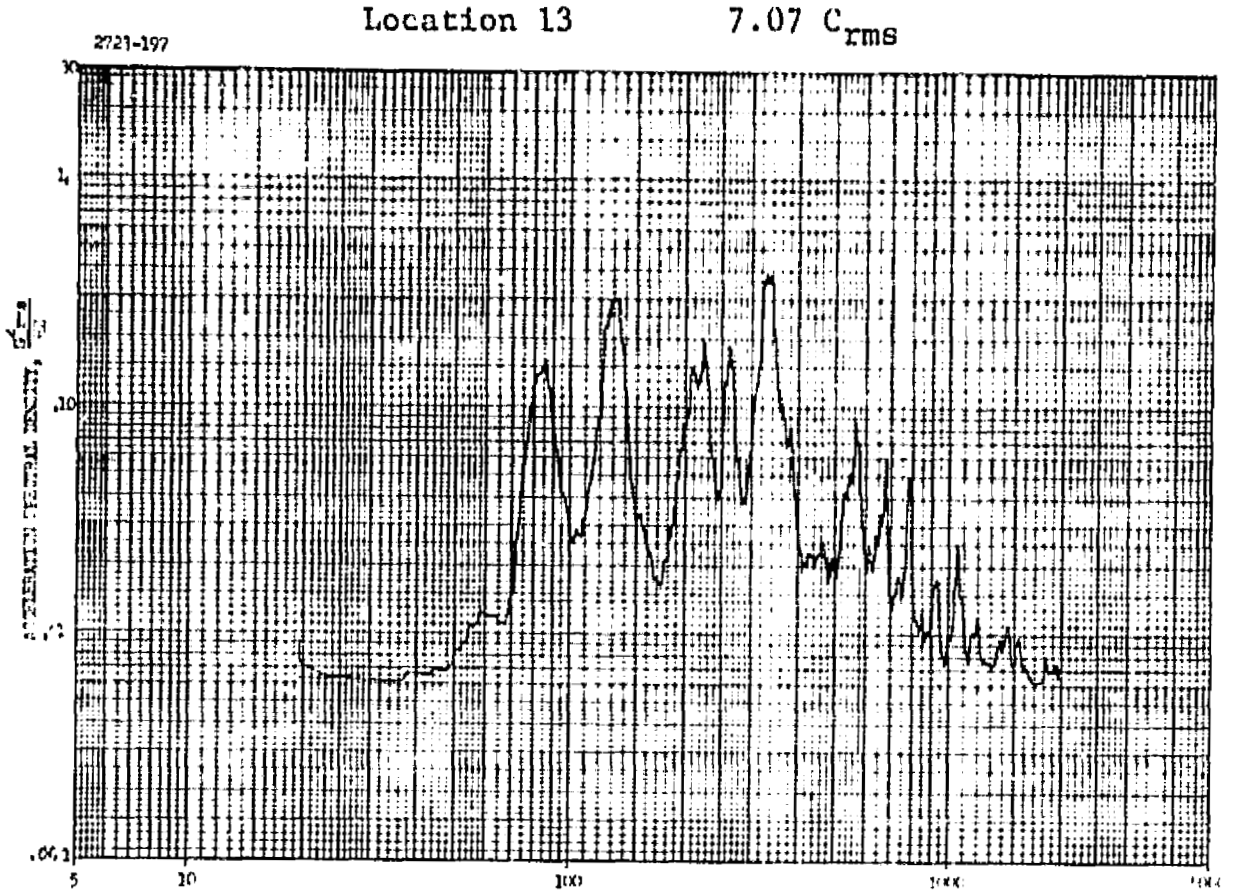

Location 14 9.9 G_{rms}

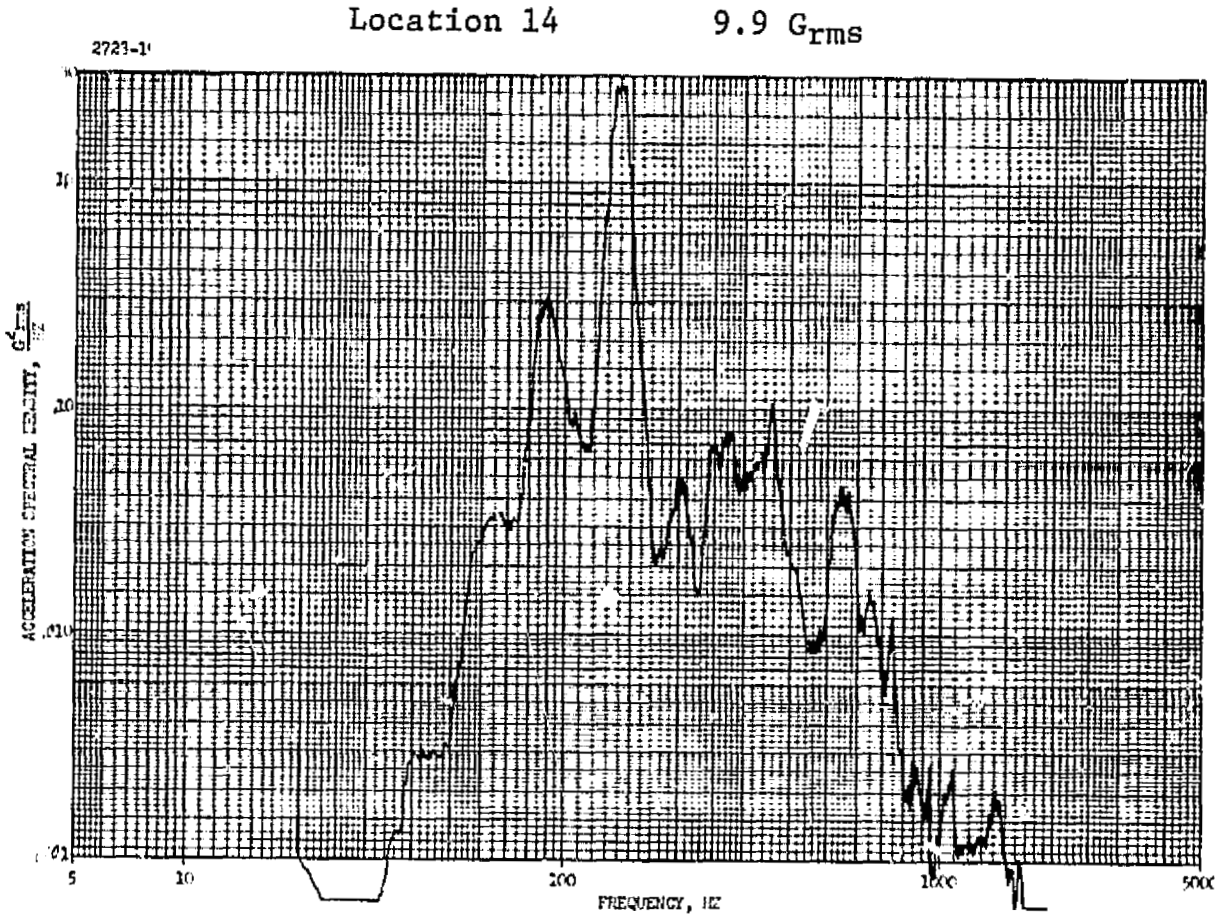

FIGURE 103. TEST #16-16B DATA (Continued)

Location 15

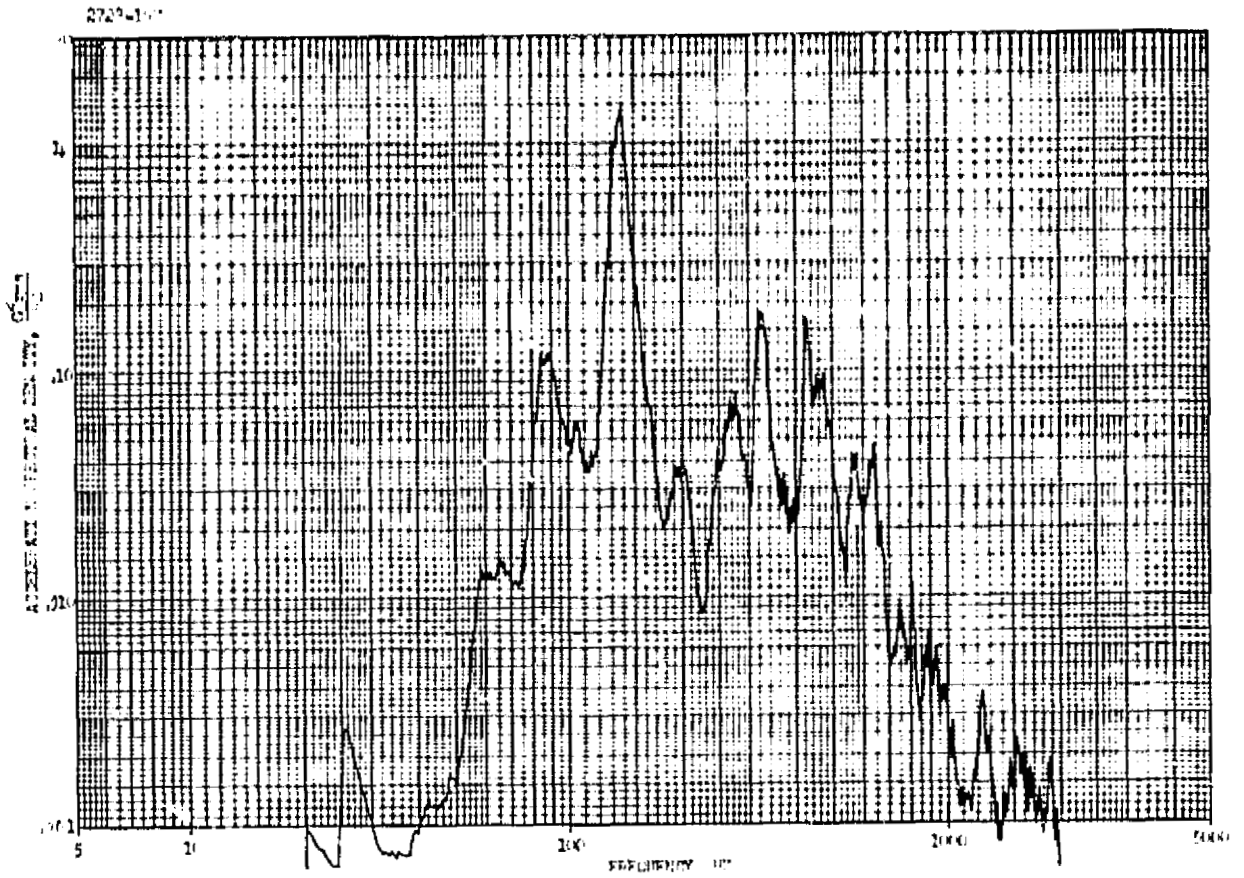

FIGURE 103. TEST #16-16B DATA (Concluded)

Location 1 29.4 Grms

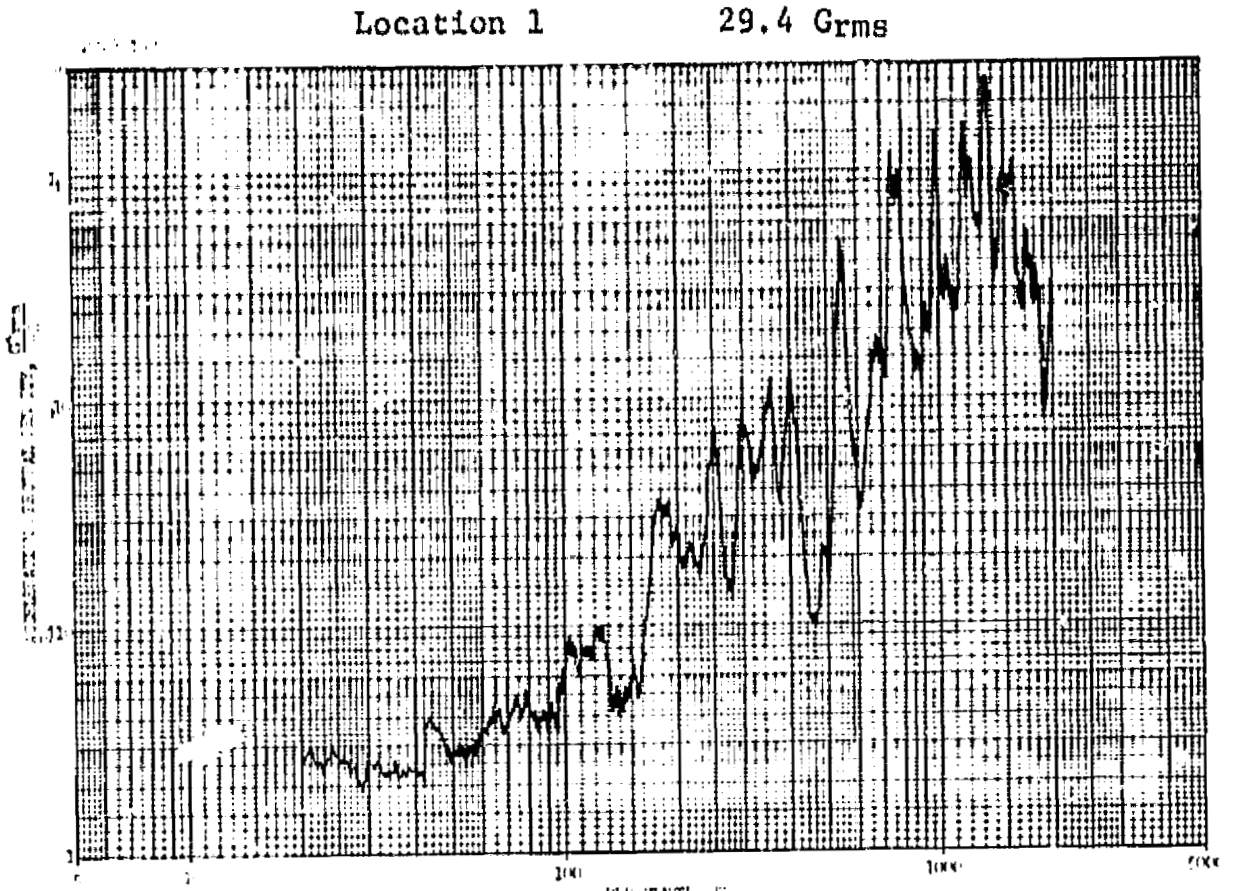

Location 2 56.0 G_{rms}

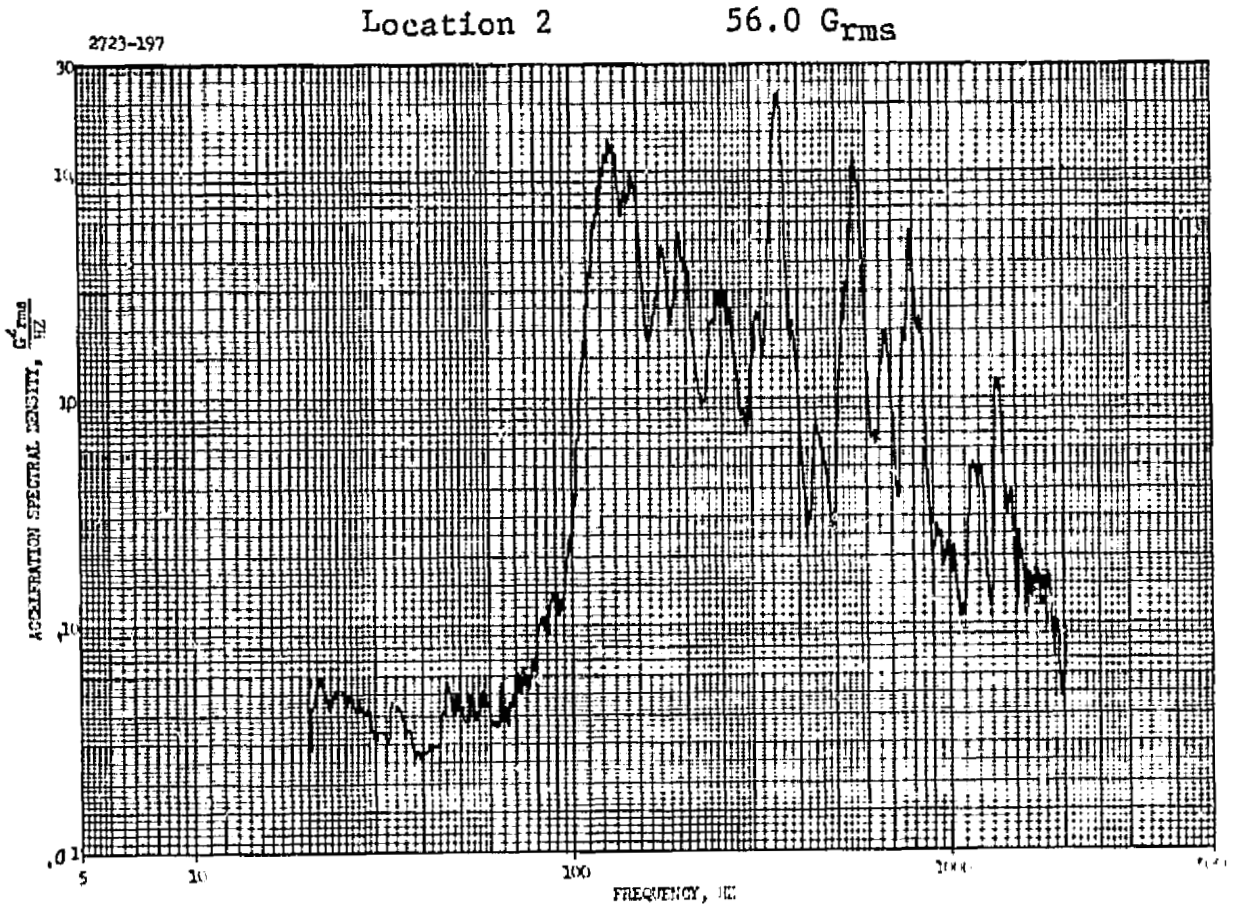

FIGURE 104. TEST # 17 DATA

Location 3 58.8 G_{rms}

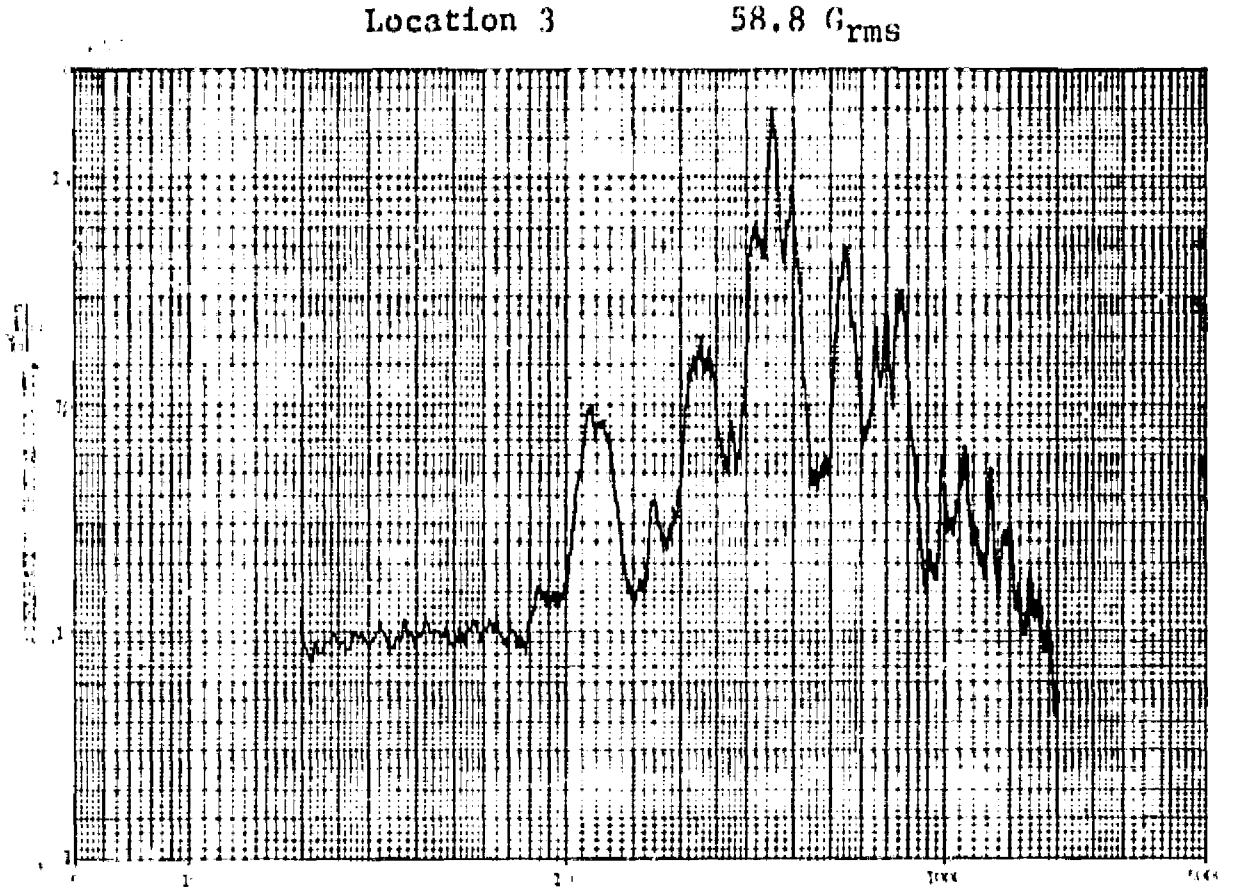

Location 4 11.3 G_{rms}

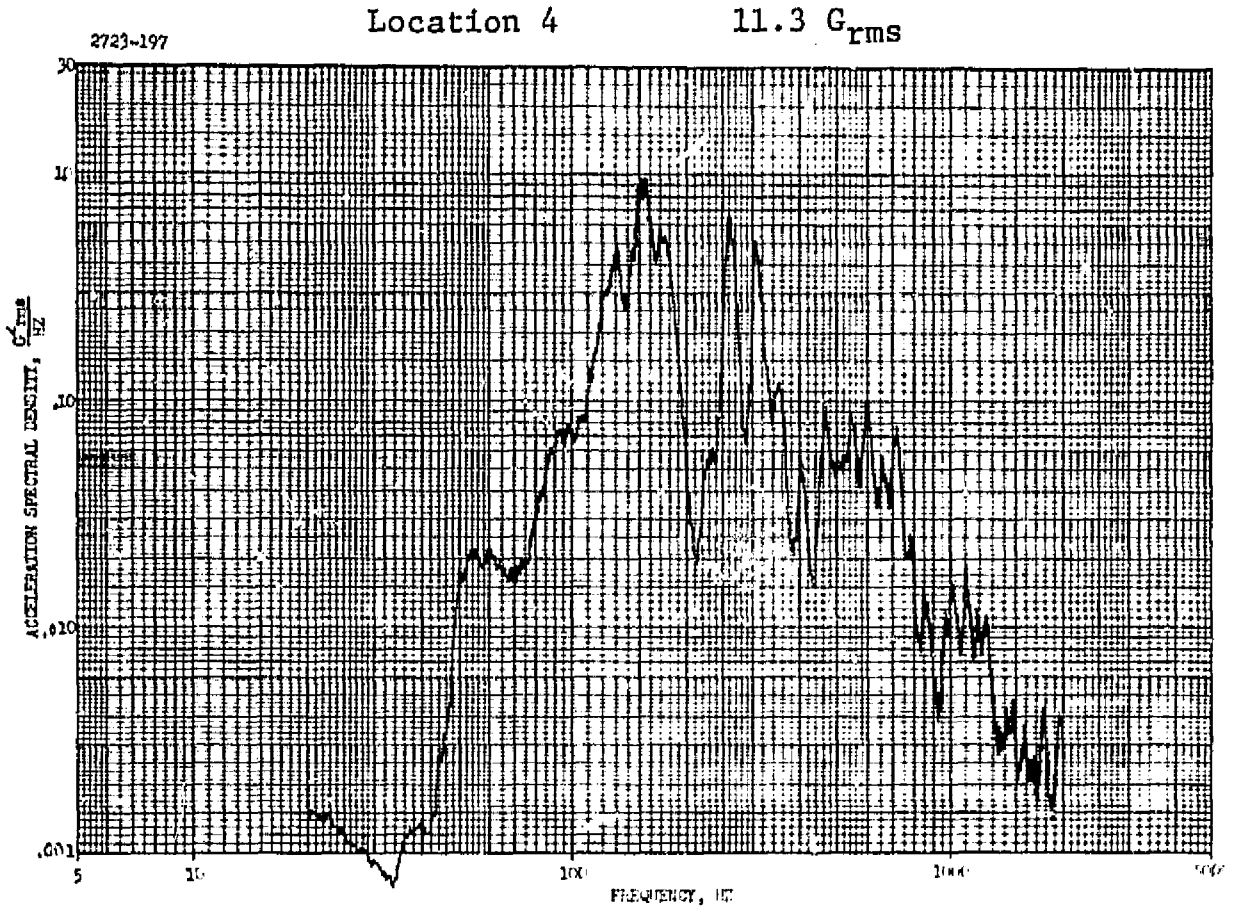

FIGURE 104. TEST #17 DATA (Continued)

Location 5 17.2 G_{rms}

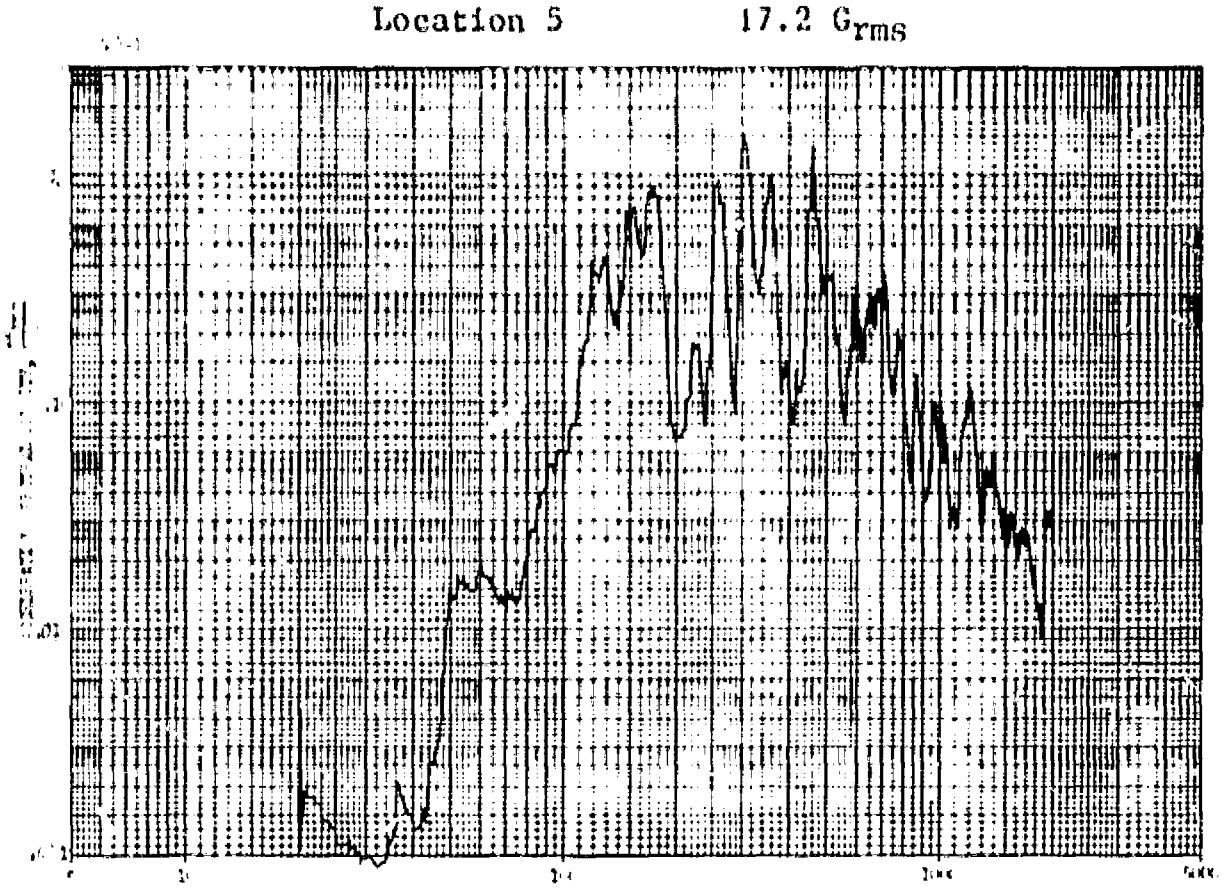

Location 6 22.1 G_{rms}

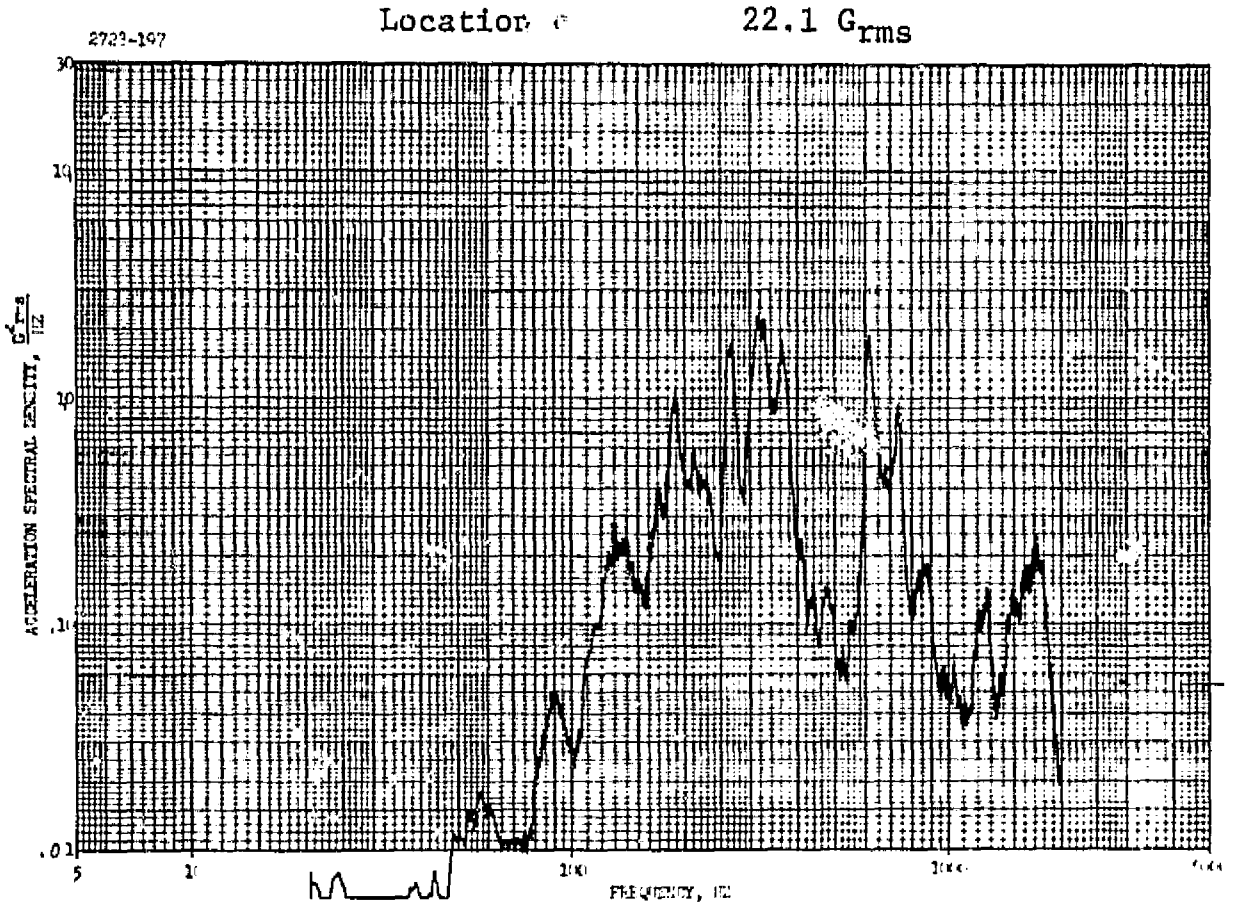

FIGURE 104. TEST #17 DATA (Continued)

Location 7 14.7 G_{rms}

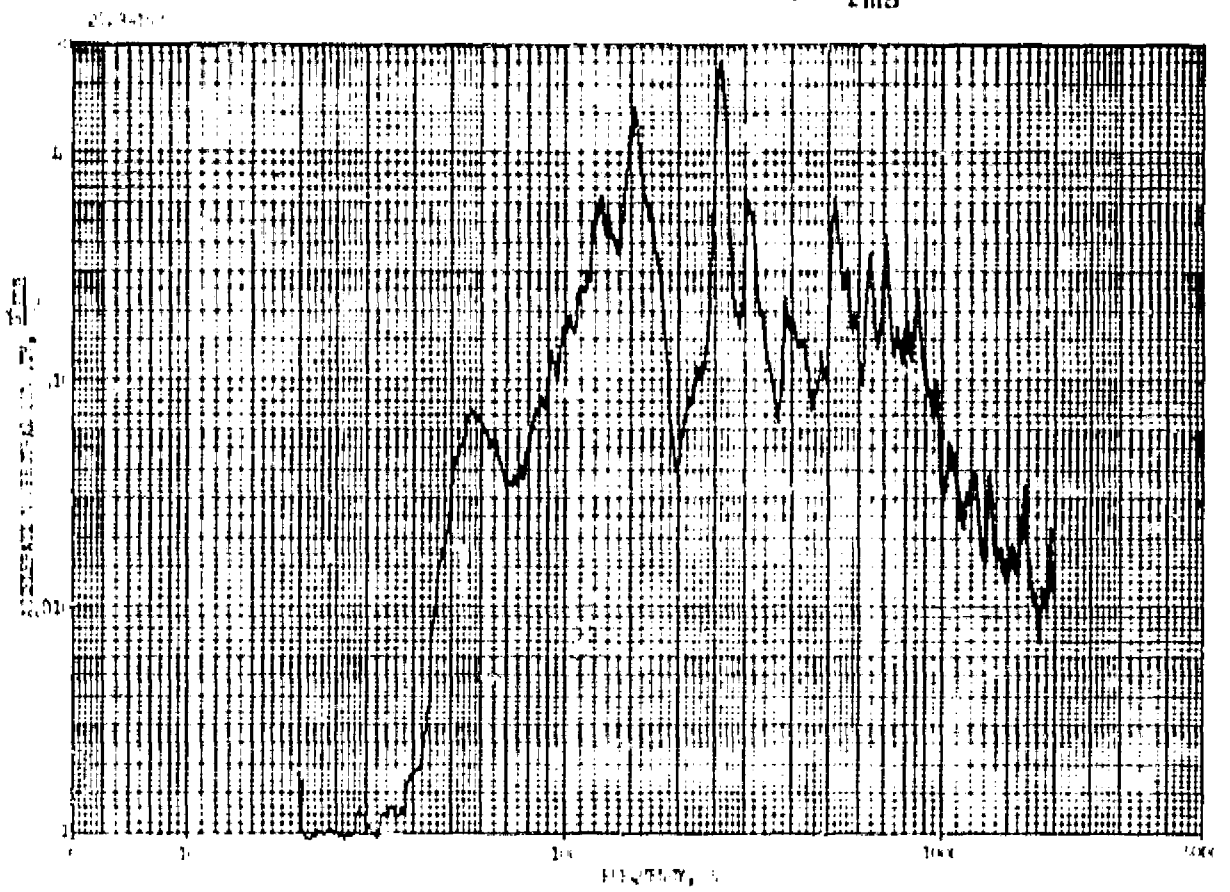

Location 8 53.0 G_{rms}

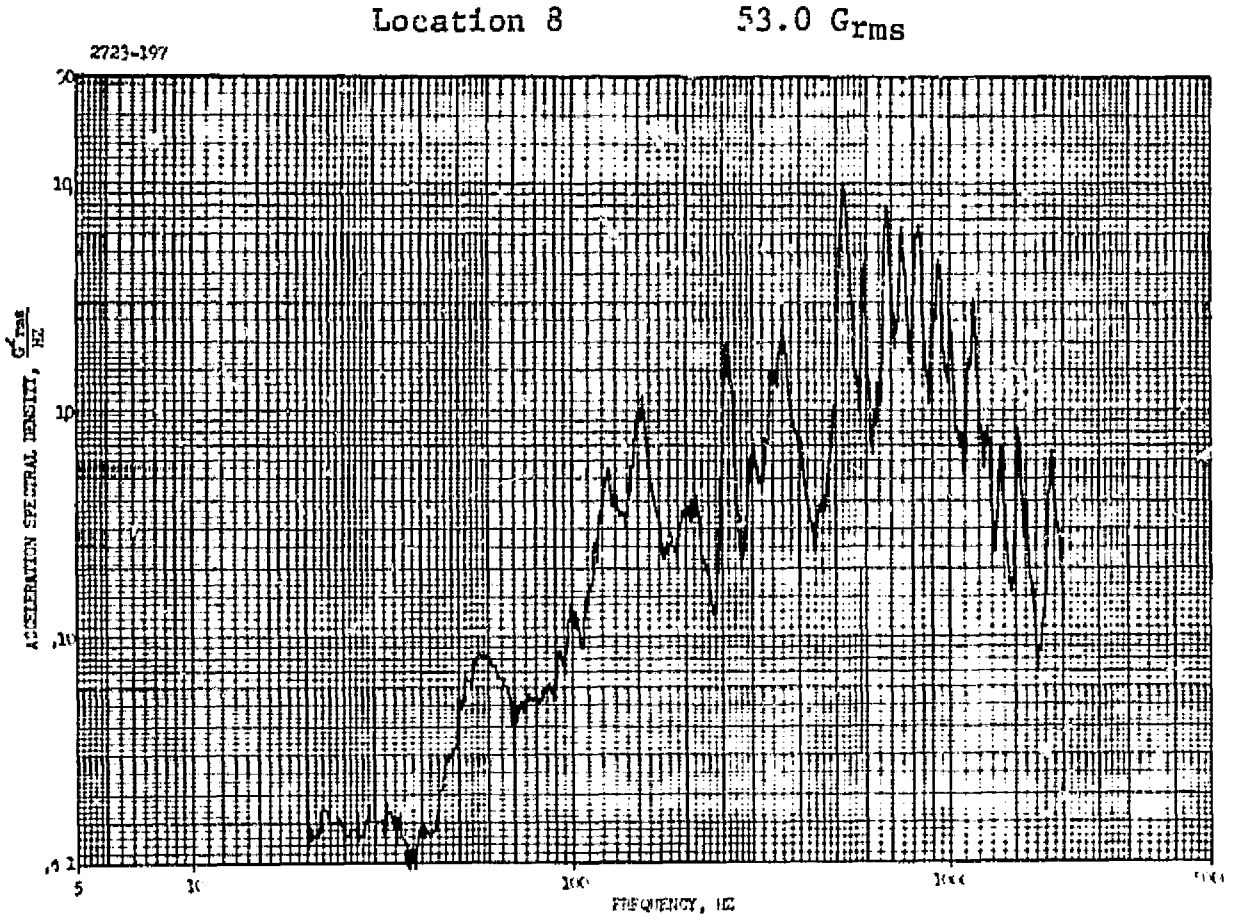

FIGURE 104. TEST #17 DATA (Continued)

Location 9 50.0 G_{rms}

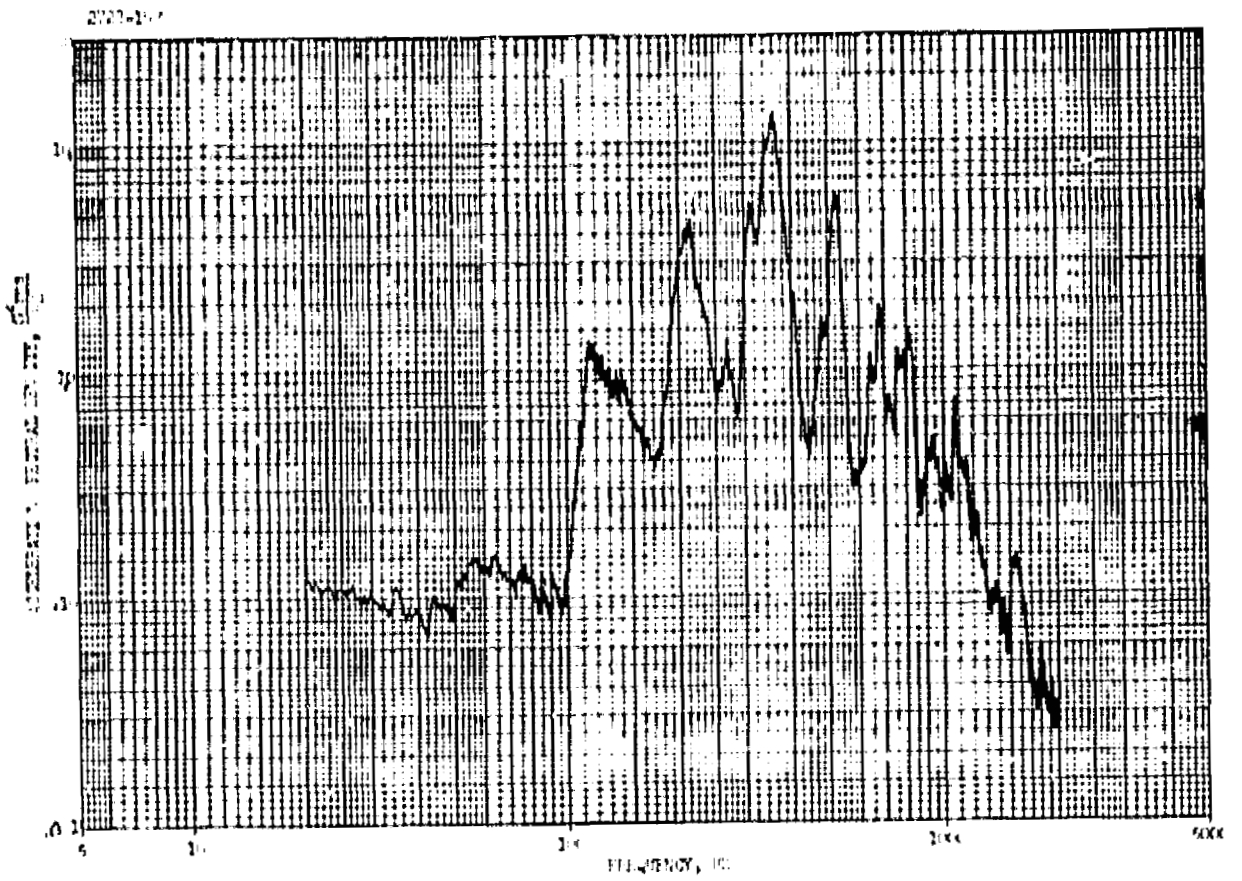

Location 10 73.5 G_{rms}

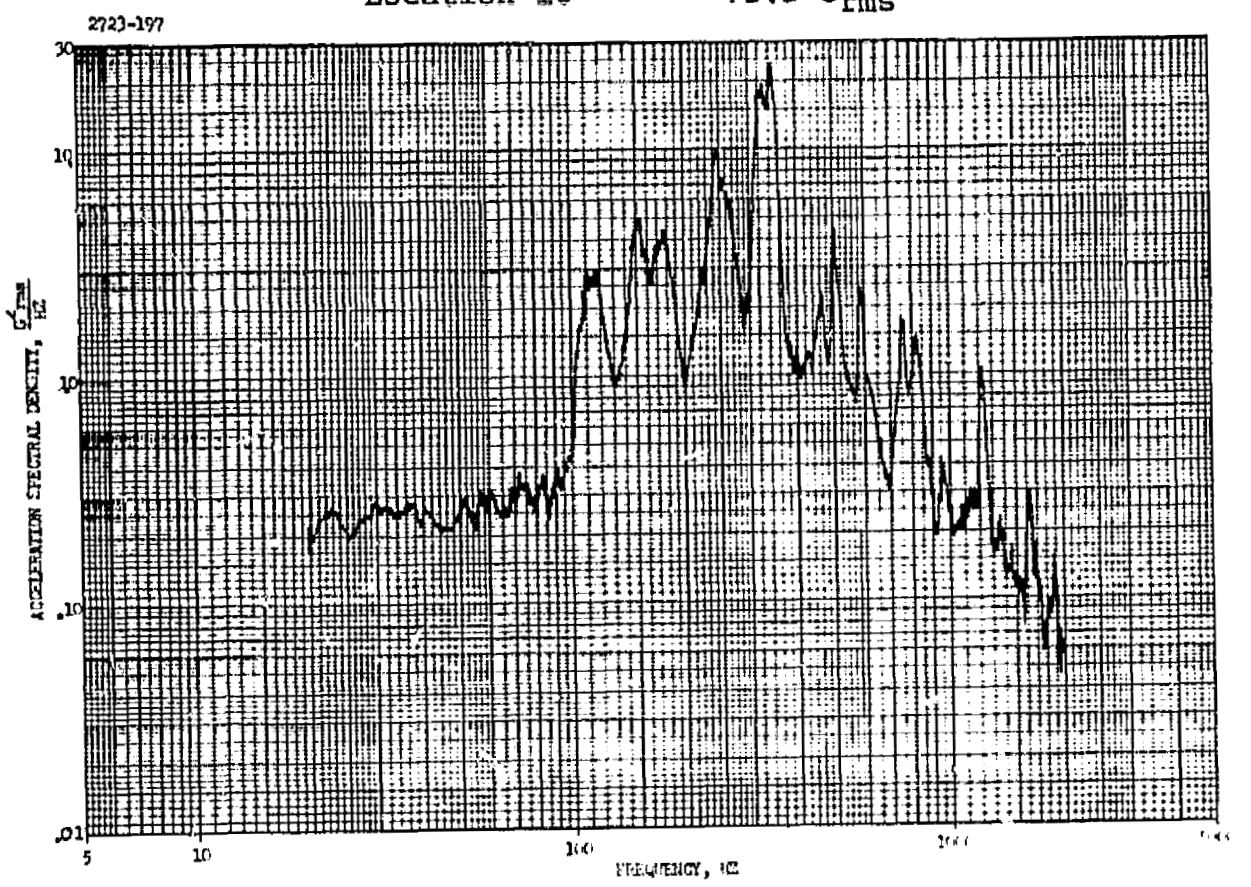

FIGURE 104. TEST #17 DATA (Continued)

Location 11 28.0 G_{rms}

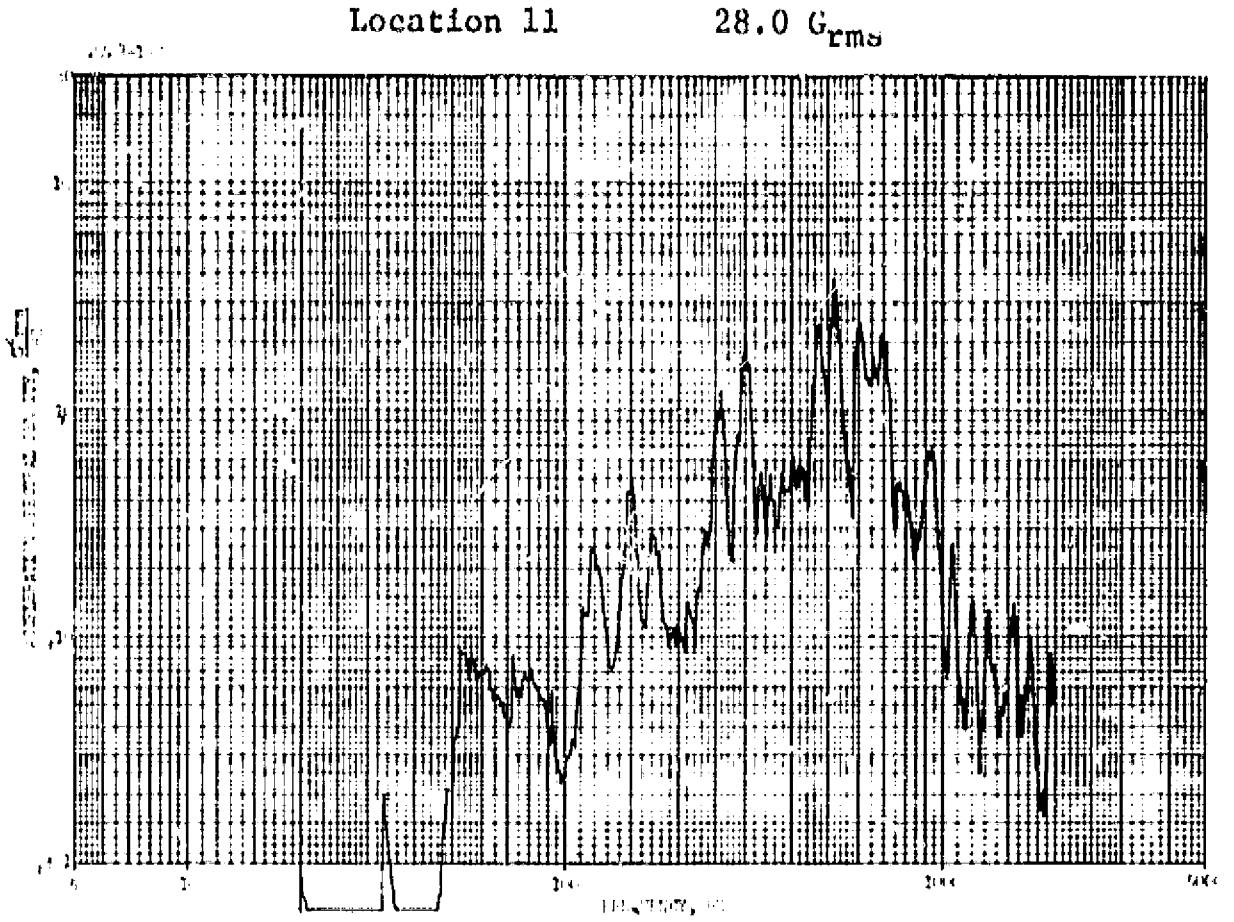

Location 12 44.2 G_{rms}

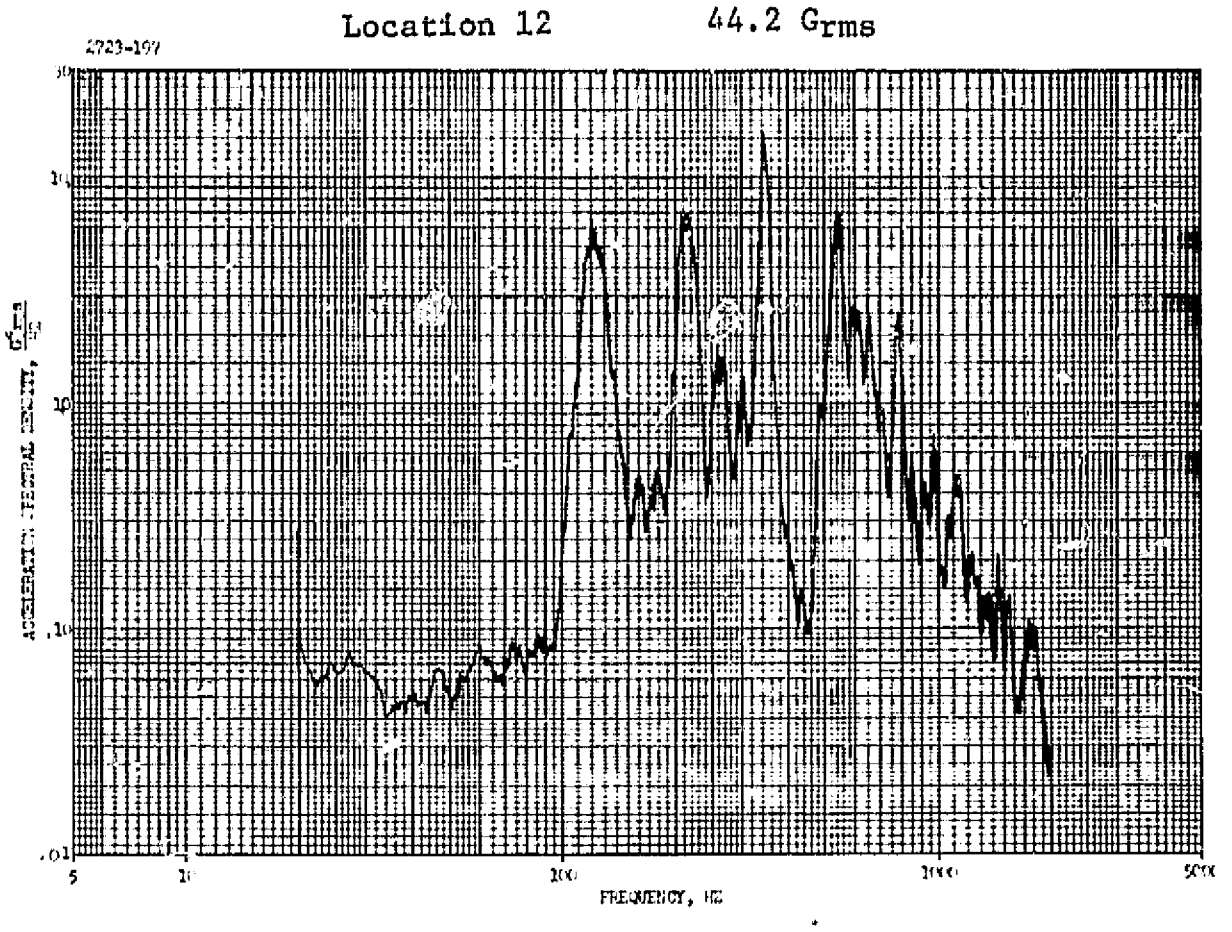

FIGURE 104. TEST #17 DATA (Continued)

Location 13 23.5 G_{rms}

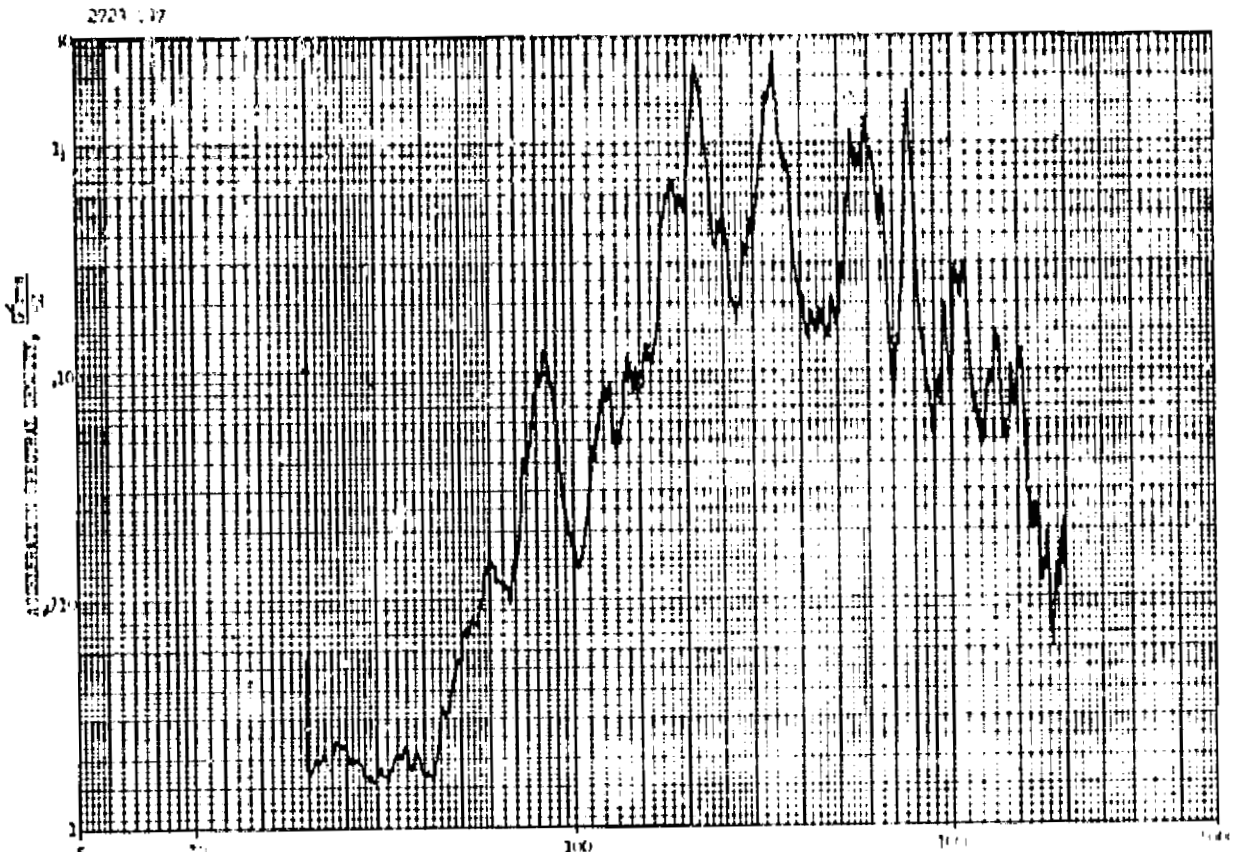

Location 14 16.5 G_{rms}

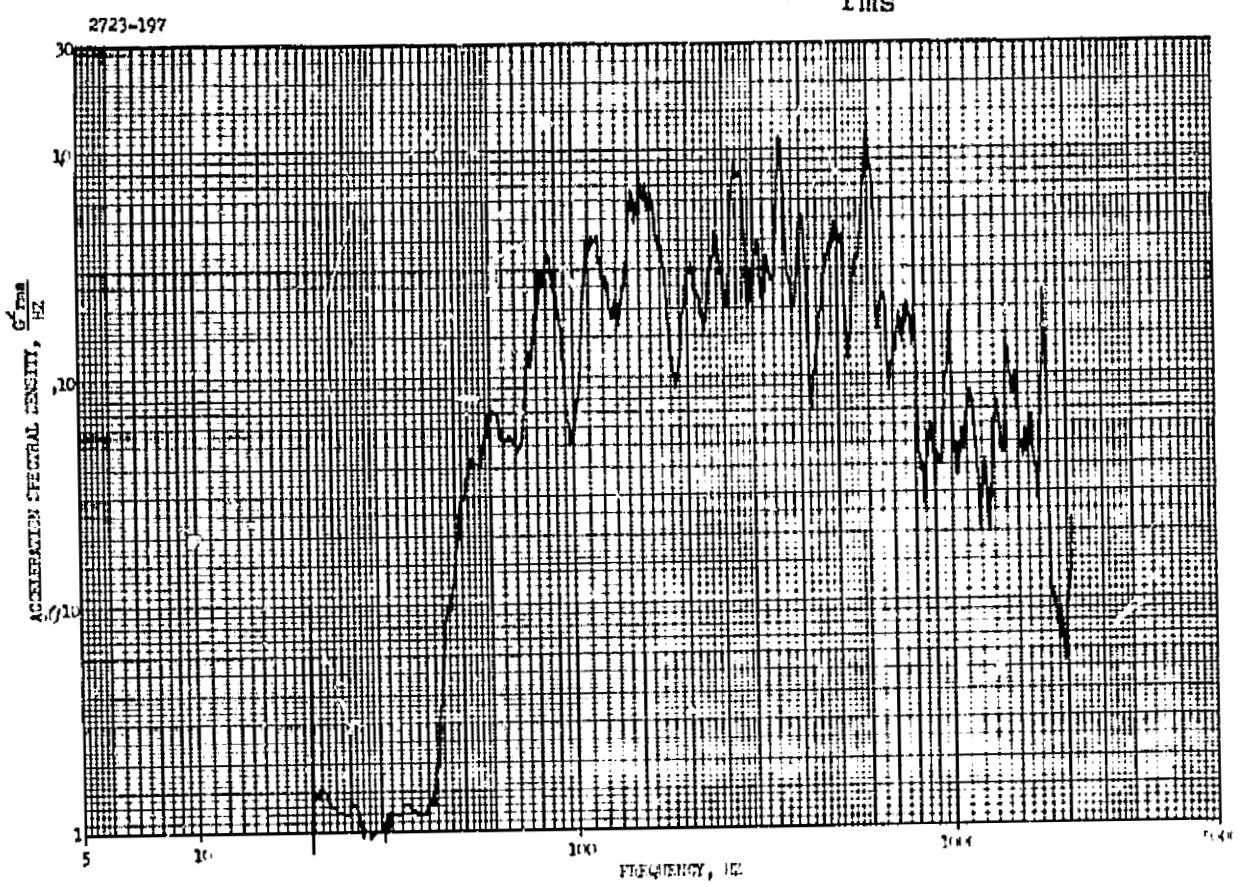

FIGURE 104. TEST #17 DATA (Continued)

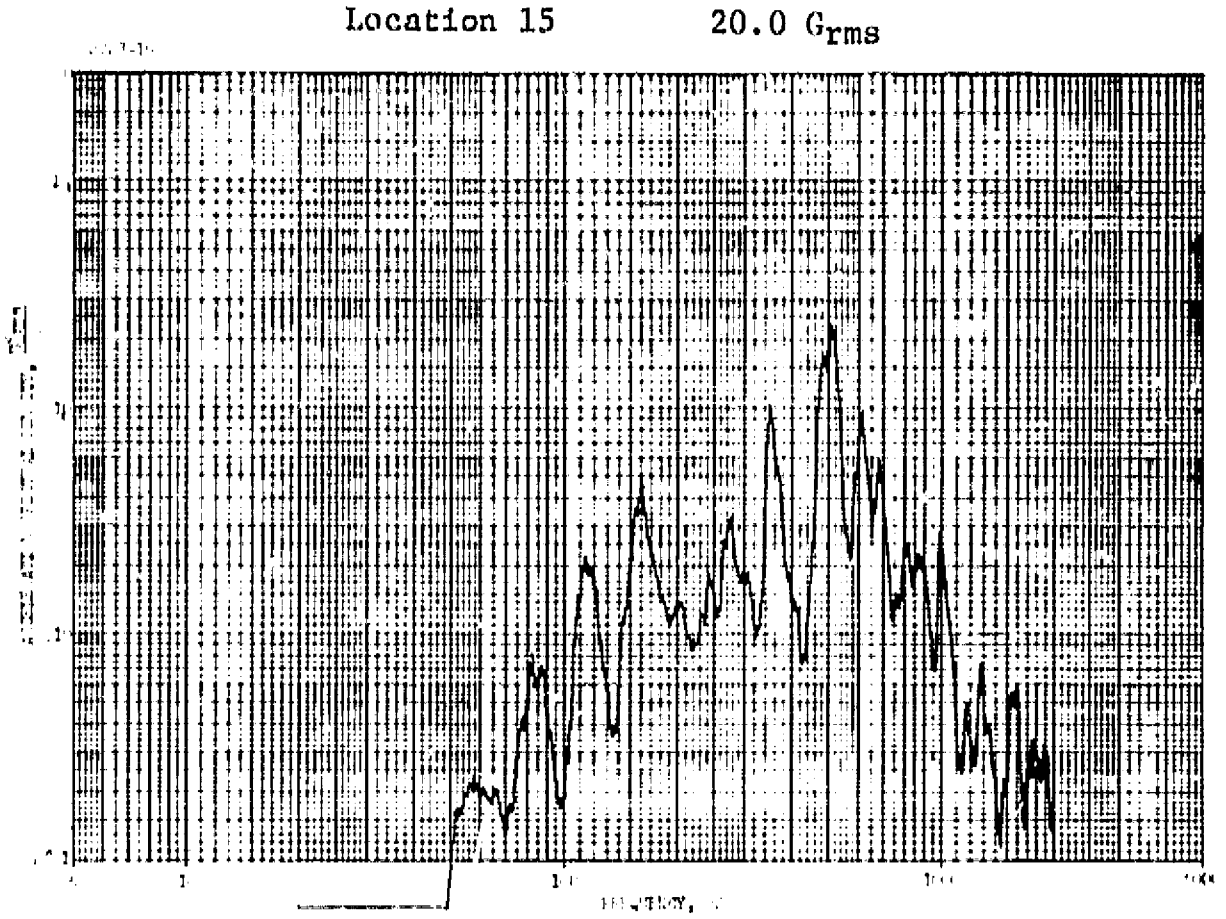

FIGURE 104. TEST #17 DATA (Concluded)

SECTION V. COMPARISONS

Comparison of experimental results with the anticipated analytical results is effected in this section. Empirical vibro-acoustic transfer function levels for test specimens I, II and III are compared to the prediction from a modal analysis computer program and the statistical treatment provided beforehand (Section III). The vibration responses of specimens I and II for various radiation damping coefficients are compared. The responses of test specimens III and IV are compared to evaluate mass loading and the results of localized progressive excitation are compared to full panel progressive wave excitation (both at parallel incidence).

A. Vibro-Acoustic Transfer Functions

Empirical vibro-acoustic transfer function levels were derived by subtracting the acoustic level (dB re 20 $\mu N/M^2$) from the acceleration level (dB re 1 g). This operation was performed manually for three locatons on test specimens I, II and III for three types of excitation - progressive wave normal incidence, progressive wave parallel incidence and reverberant field. The result are shown in figures 105-113. The results of analytic calculation are also presented on these figures and the results of statistical energy calculation are given for the reverberant acoustic excitation. The empirical transfer function levels are observed to be quite variant at frequencies within a decade of the fundamental frequency. Above this frequency data from the three measurement locations tend to coincide and gradually the response becomes smooth as frequency is further increased. The predicted response from the statistical energy treatment (for reverberant acoustic excitation) intersects the low frequency response and is gradually approached by the smoothed response in the higher frequency region. At 1000 Hz the average deviation for test specimens I, II, and III is 4 dB, the analytical method predicting a higher vibration response than actually measured. The classic modal analysis shows good agreement for test specimen III normal incidence progressive wave response, however, a combination of circumstances precludes valid comparisons for other cases.

The computer program currently operates only on modes up to 9 x 9. No mode with an index greater than 9 is considered. Thus the program utilizes all modes for test specimen I only between 6.6 and 196 Hz, for test specimen II only between 32.9 and 982 Hz and for test specimen III only between 100.5 and 4435 Hz. Also the correlation model utilized in the analysis could not be perfectly simulated for parallel incidence progressive wave and reverberant field acoustic excitation. The complication of an oscillating field could not be treated in the funded effort. Thus, for the above fields the model utilized is adequate only for low frequencies or low separation distance where oscillations do not occur. For a separation of 20 inches such as would be considered using the panel center as an origin, the frequency must be less than 150 Hz to prevent an oscillatory correlation field for sinusoidal correlation functions.

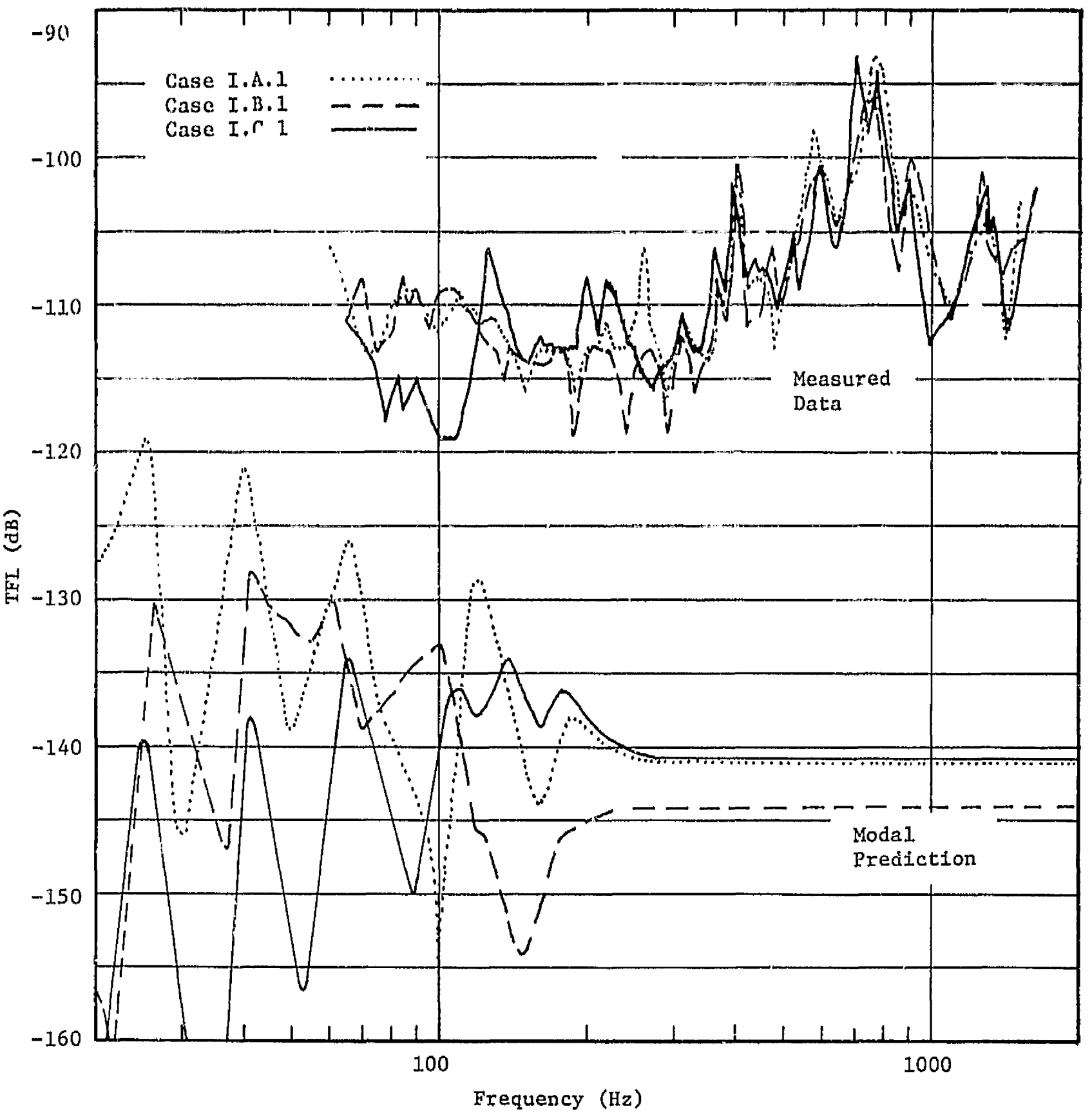

FIGURE 105. COMPARISON OF TFL, SPECIMEN I, NORMAL INCIDENCE PROGRESSIVE WAVE

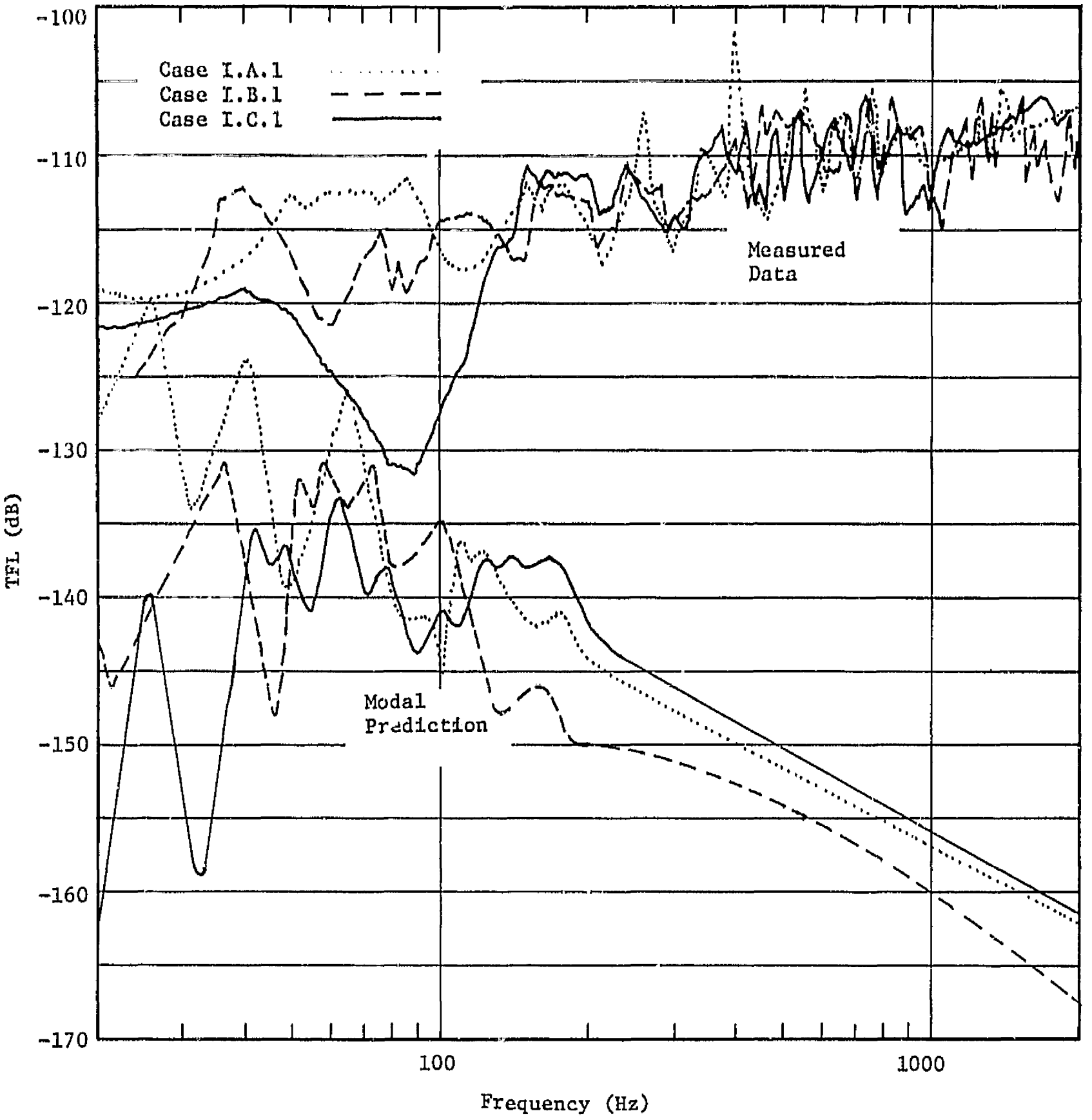

FIGURE 106. COMPARISON OF TFL [illegible]ECIMEN I, PARALLEL INCIDENCE PROGRESSIVE WAVE

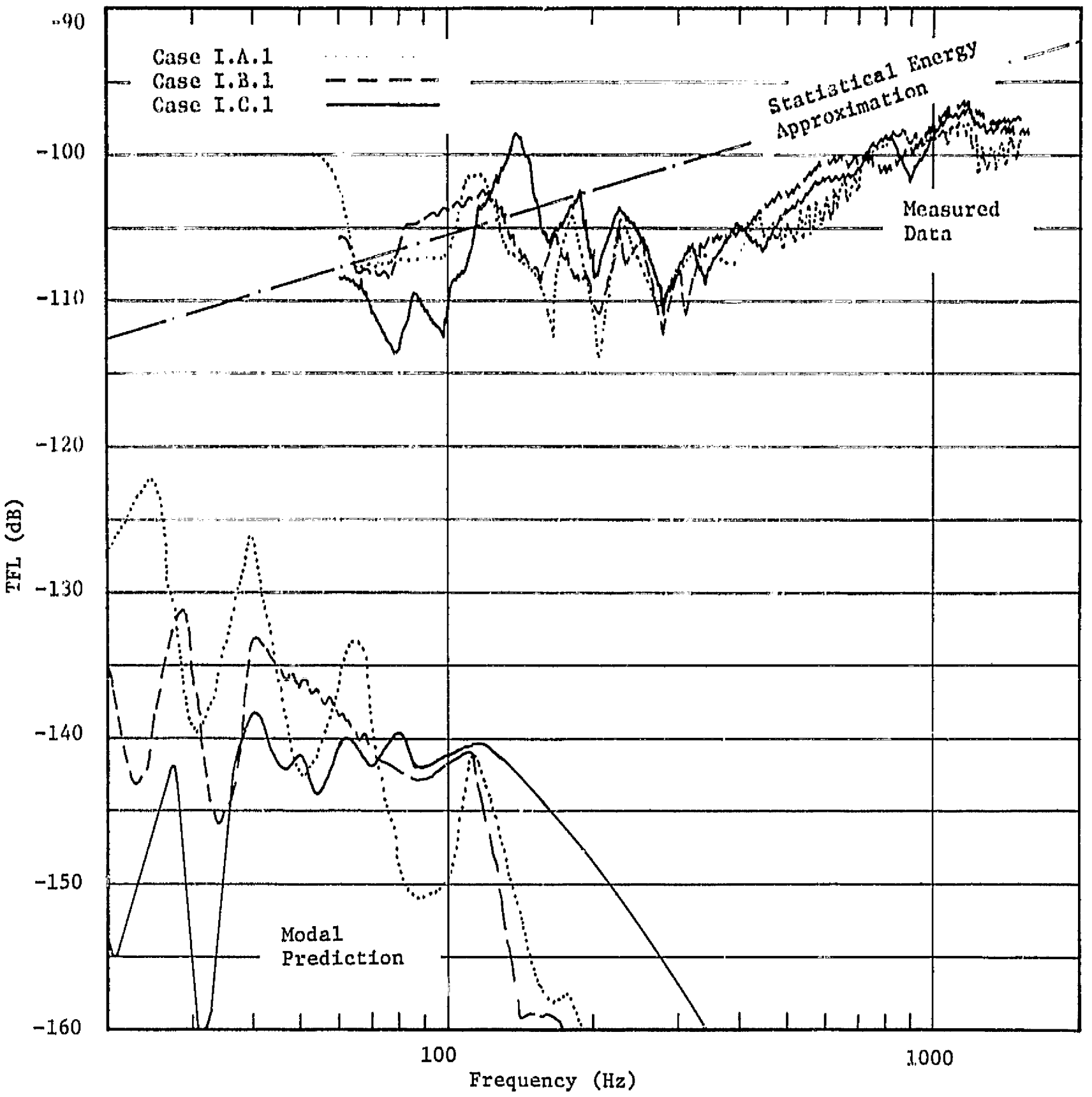

FIGURE 107. COMPARISON OF TFL, SPECIMEN I, REVERBERANT FIELD

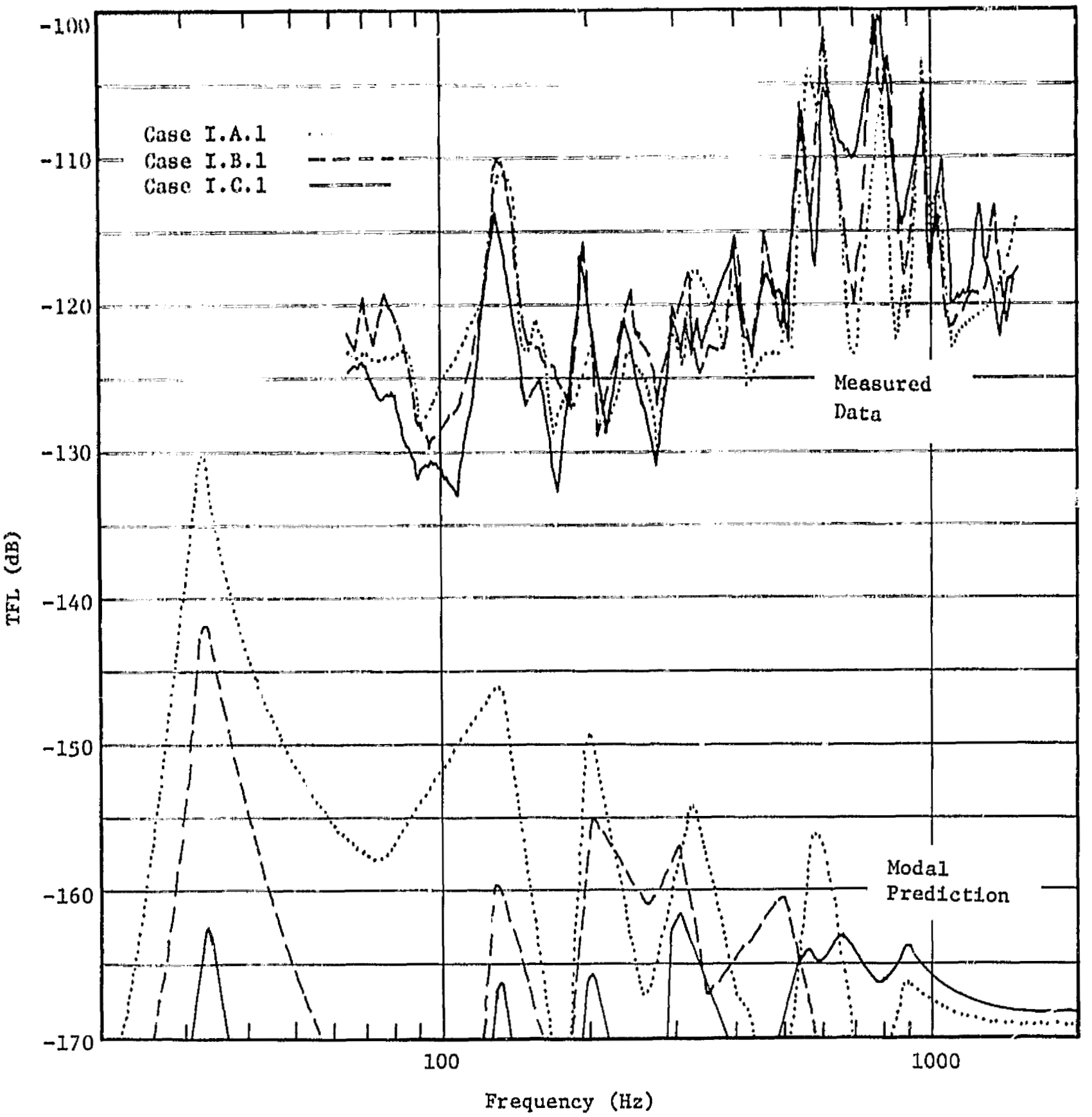

FIGURE 108. COMPARISON OF TFL, SPECIMEN II, NORMAL INCIDENCE PROGRESSIVE WAVE

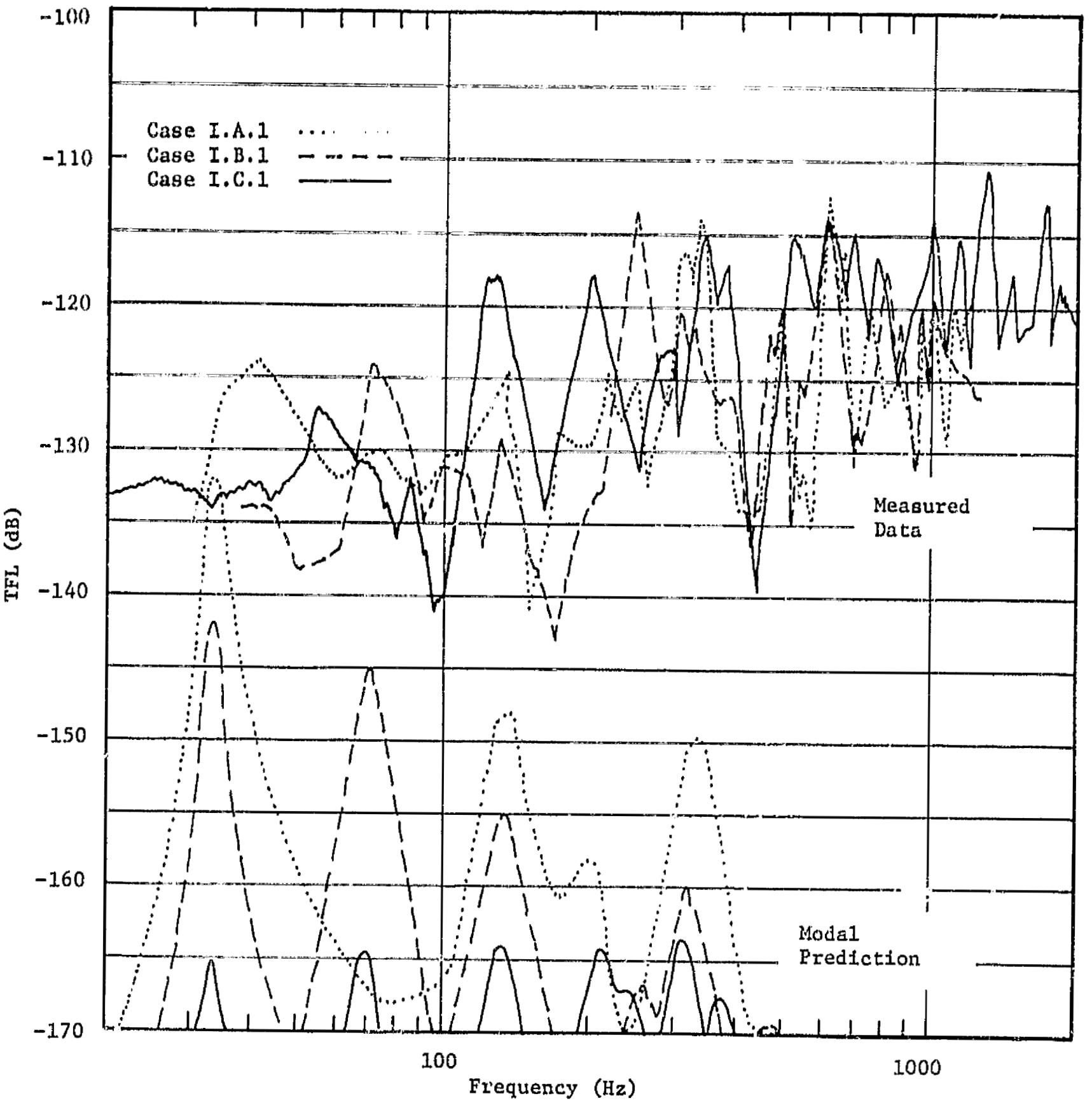

FIGURE 109. COMPARISON OF TFL, SPECIMEN II, PARALLEL INCIDENCE PROGRESSIVE WAVE

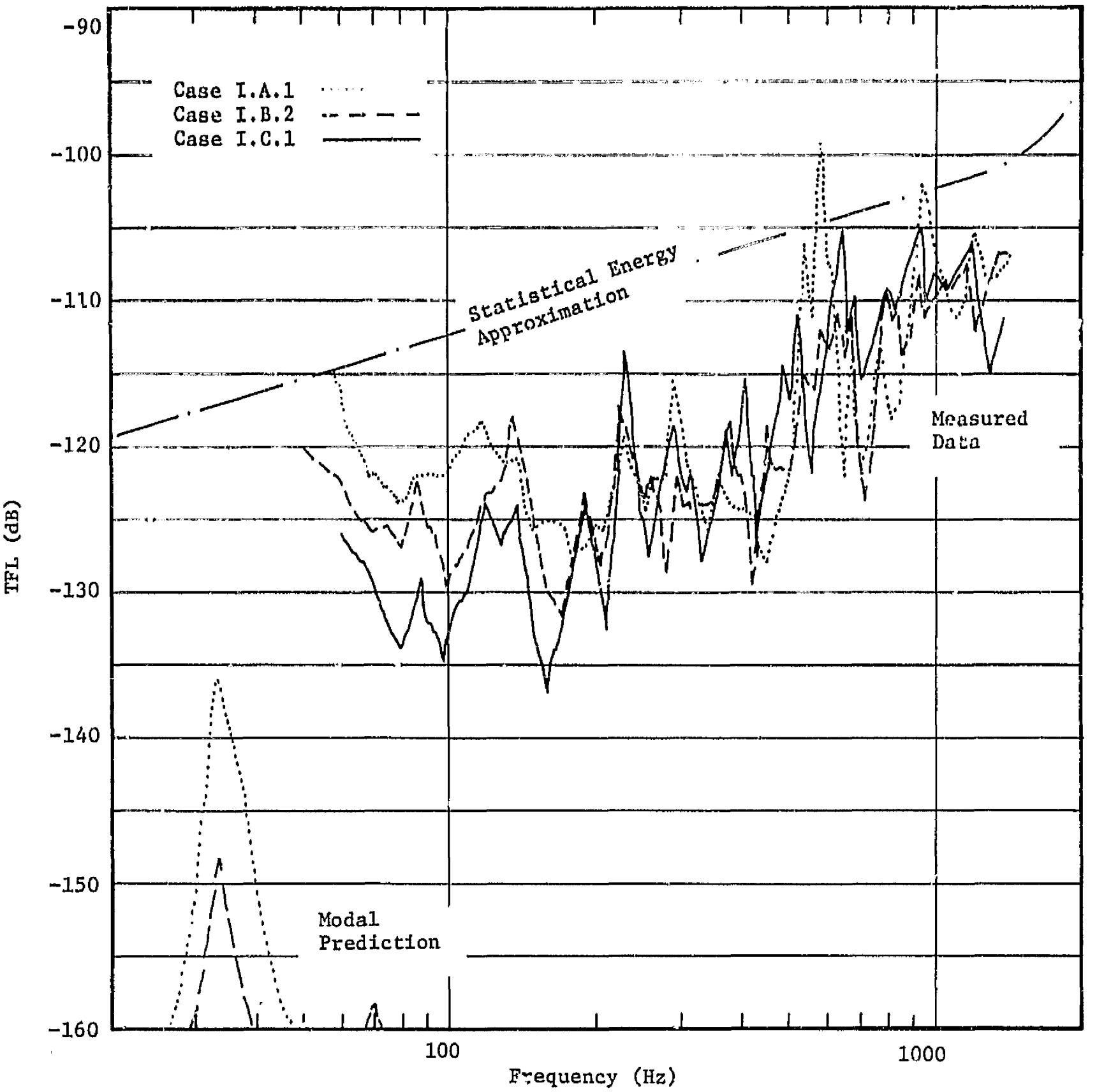

FIGURE 110. COMPARISON OF TFL, SPECIMEN II, REVERBERANT FIELD

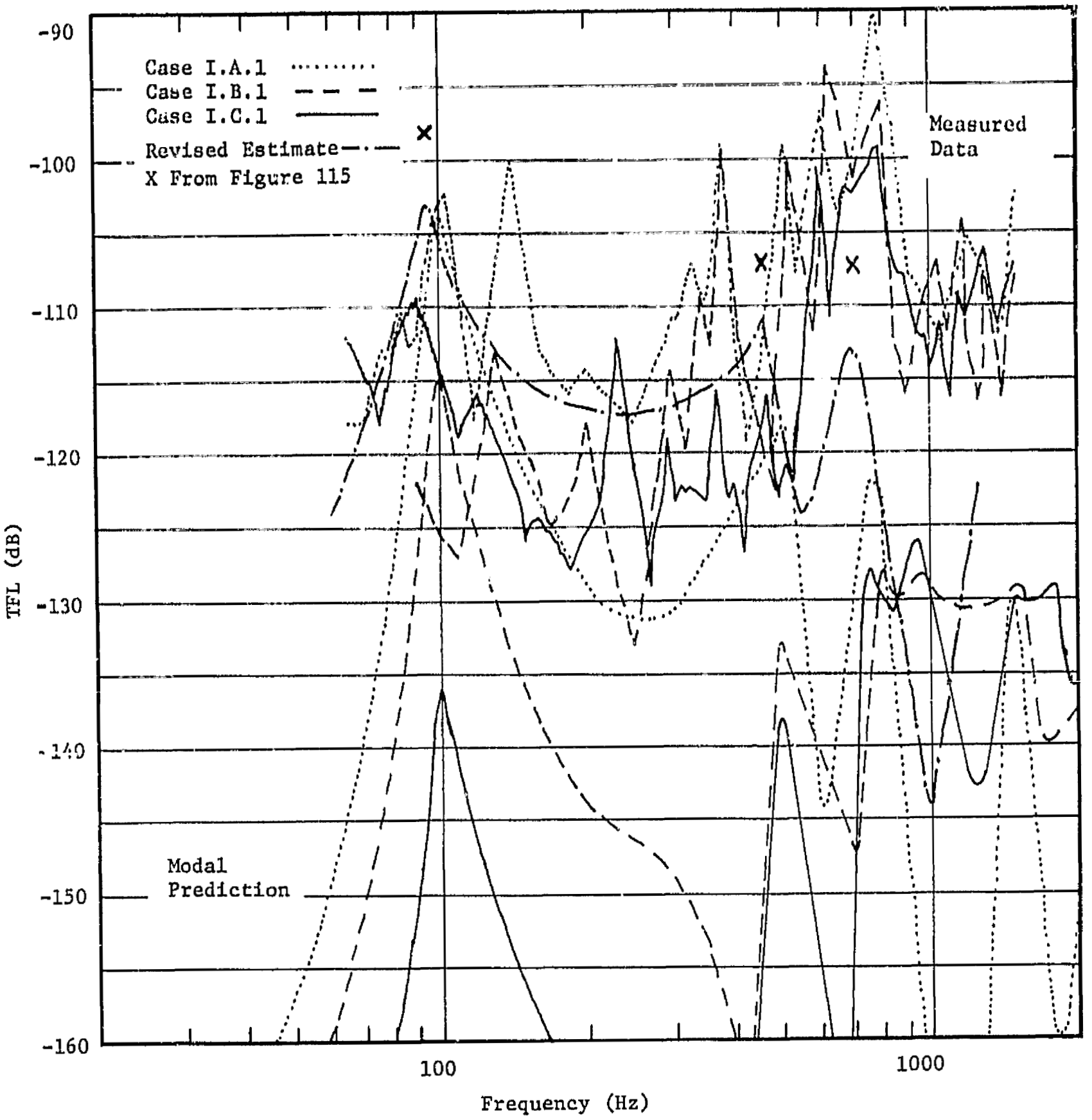

FIGURE 111. COMPARISON OF TFL, SPECIMEN III, NORMAL INCIDENCE PROGRESSIVE WAVE

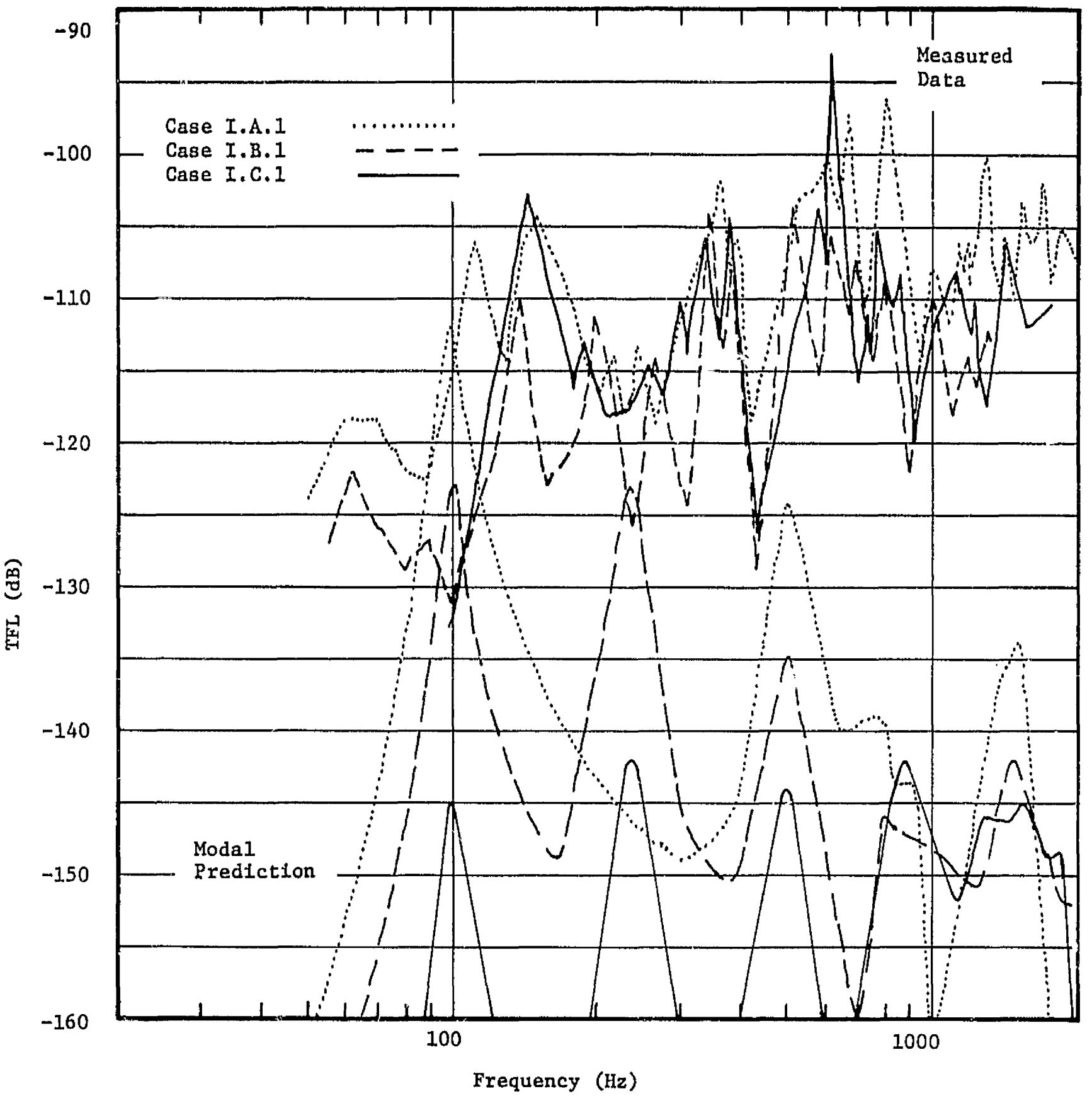

FIGURE 112. COMPARISON OF TFL, SPECIMEN III, PARALLEL INCIDENCE PROGRESSIVE WAVE

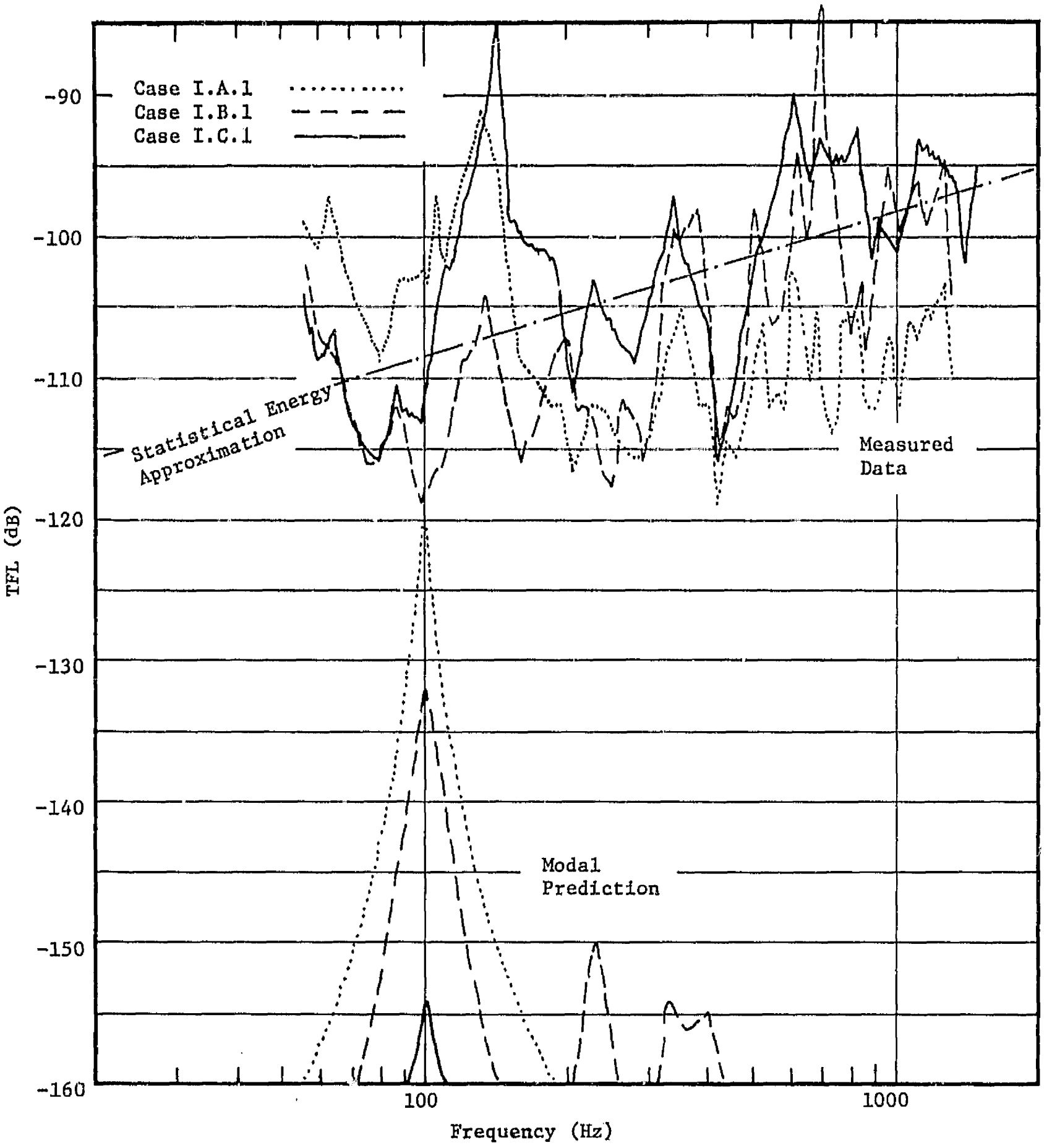

FIGURE 113. COMPARISON OF TFL, SPECIMEN III, REVERBERANT FIELD

Empirical data was obtained utilizing a ten Hz bandwidth filter and thus high Q modes can not be clearly ascertained below 100 Hz. Also in many cases data is not extant below 60 Hz or above 2000 Hz. Coincidence effects were not noticed in the measured frequency range. The critical frequency for Specimen II was 2300 Hz, slightly above measured frequencies. Thus the most meaningful comparison of predicted and measured transfer function level is given by figure 111. The comparison for the panel center (III.A.1) is very good at the fundamental mode but gradually decreases relative to the measured data as frequency increases. A second prediction for the location utilizing Program RSRPC2 (not available earlier for use) shows direct input of the measured excitation field (figure 114, see also figure 79) computing and plotting displacement, velocity and acceleration spectral densities. The program also computes and plots the transfer function level on a linear scale (figure 115). The revised estimate of the TFL shown on figure 111 shows that the shape of the TFL is a function of the excitation spectrum, i.e., the transfer function level is generally not a simple linear operator since the response at a single frequency is due to a summation of 625 modal components. Figure 115 is another predicted transfer function level for the center of specimen III utilizing a damping ratio of .04 and more increments per octave to improve the frequency resolution. The amplitude of the peaks of this TFL is shown on figure 111 by X's. It is expected that similar improvements could be obtained for other panel locations if further effort were expended.

A coarse comparison is shown in figures 116-118 of the mean transfer function level for each excitation on test specimens I, II and III. There is good separation on test specimen I (figure 116) throughout the test frequency range showing maximum energy transfer for reverberant excitation and minimum transfer for parallel incidence progressive wave excitation. The vibratory response to the reverberant field is 3 to 6 dB higher than the normal incidence progressive wave, the difference increasing with frequency. The response at normal incidence exceeds the response to parallel incidence progressive wave testing by approximately three dB. As the frequency tends toward modal frequencies, the transfer functions become more irregular and numerical differences are more difficult to obtain and less reliable. However, the reverberant excitation is generally the most severe and the parallel incidence progressive wave the least severe excitation.

The function $\langle D(\Omega) \rangle$ was not evaluated for progressive wave fields, however, preliminary empirical equations may be derived from the data of test specimen I in the same format as equation (97). For the progressive wave at normal incidence,

$$\begin{aligned} TFL &= -125.2 + 6.5 \log (f) \qquad f < 5795 \\ &= -75.70 - 3.5 \log (f_p) \qquad f > 11590 \end{aligned} \tag{112}$$

For the parallel incidence progressive wave,

$$\begin{aligned} TFL &= -128.2 - 6.5 \log (f) \qquad f < 5795 \\ &= -78.70 - 3.5 \log (f_p) \qquad f > 11590 \end{aligned} \tag{113}$$

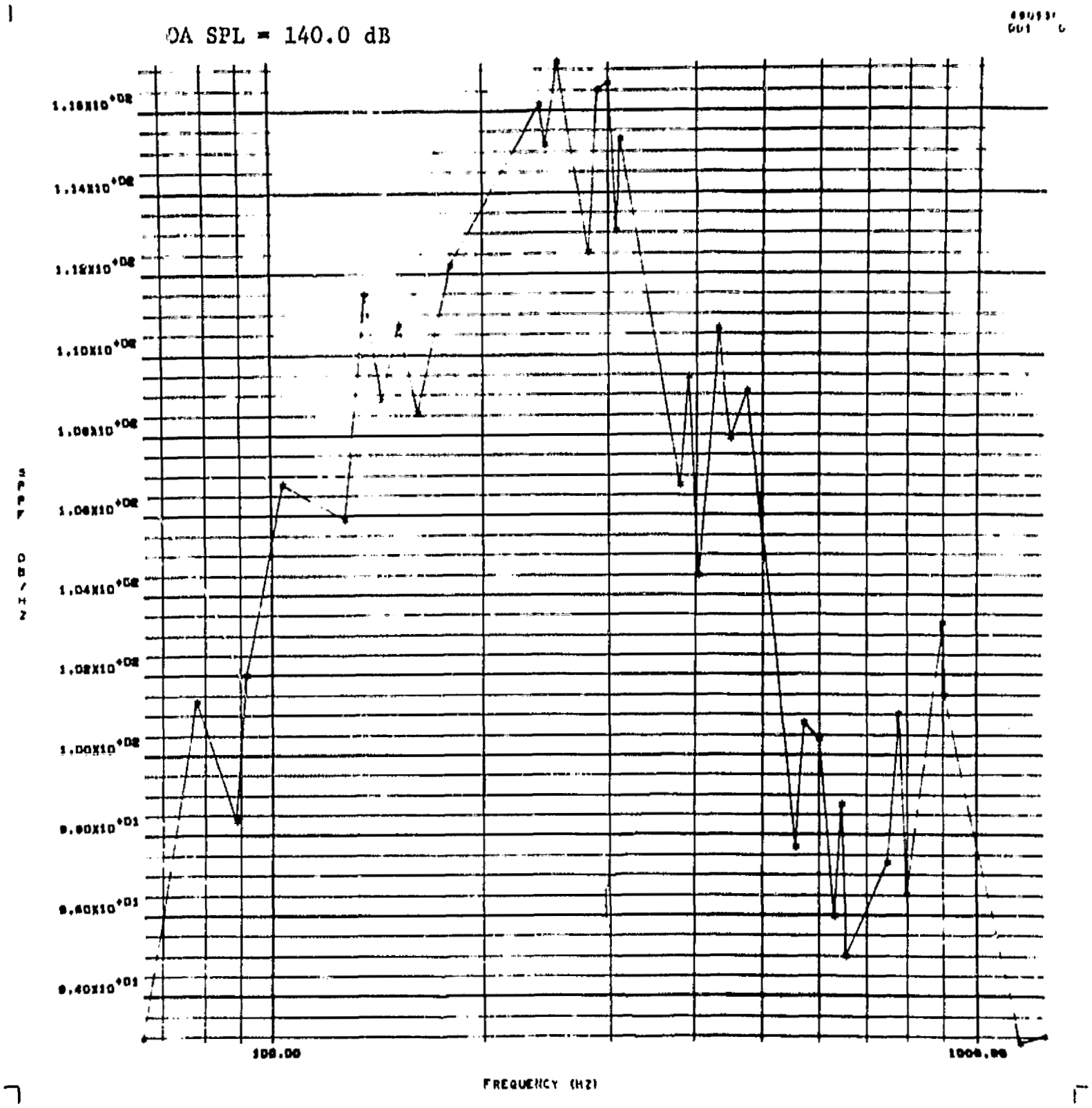

FIGURE 114. REVISED ACOUSTIC EXCITATION SPECTRAL DENSITY, PROGRAM RSRPC2

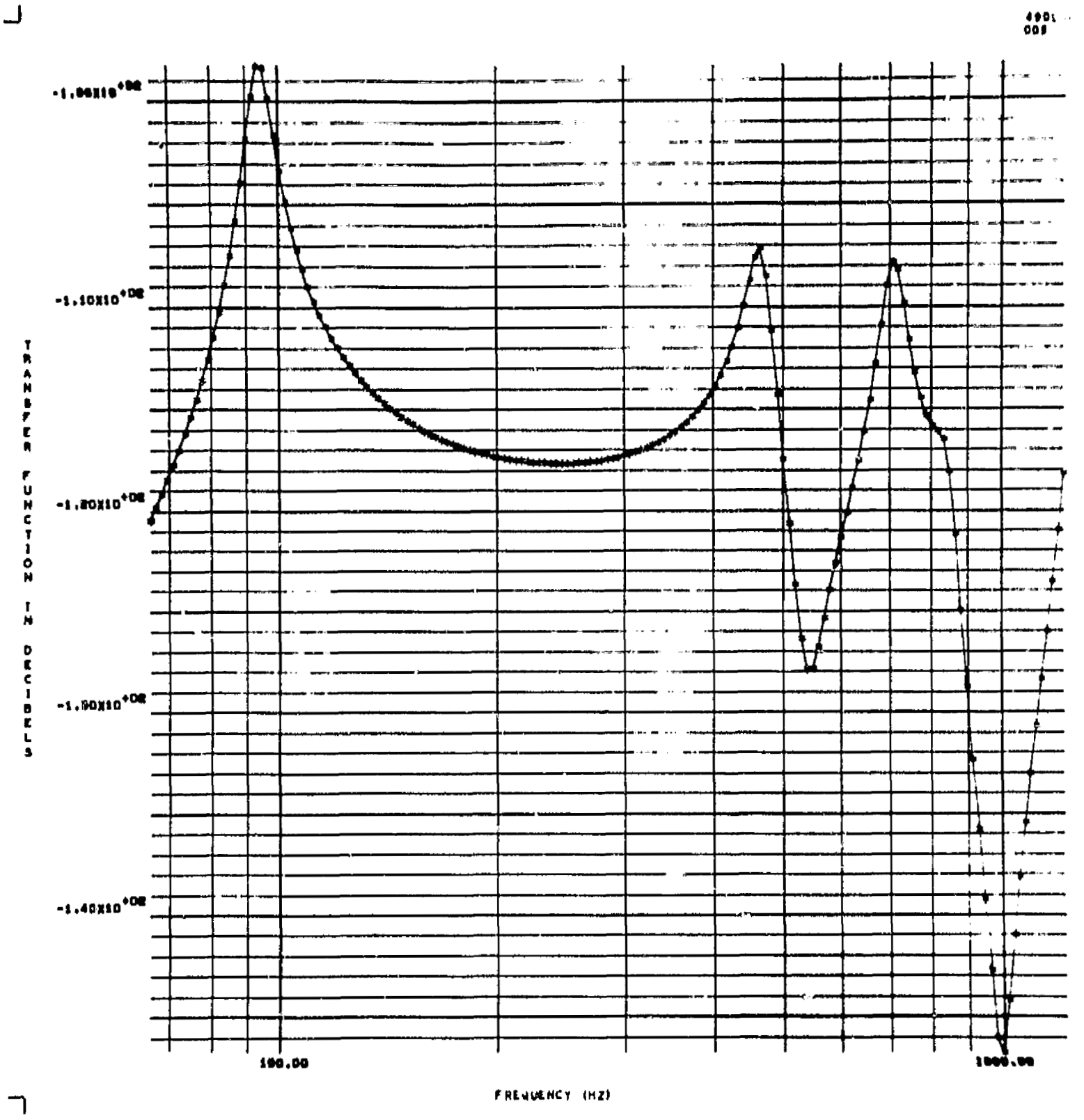

FIGURE 115. TRANSFER FUNCTION LEVEL, CASE III.A.1., PROGRAM RSRPC2

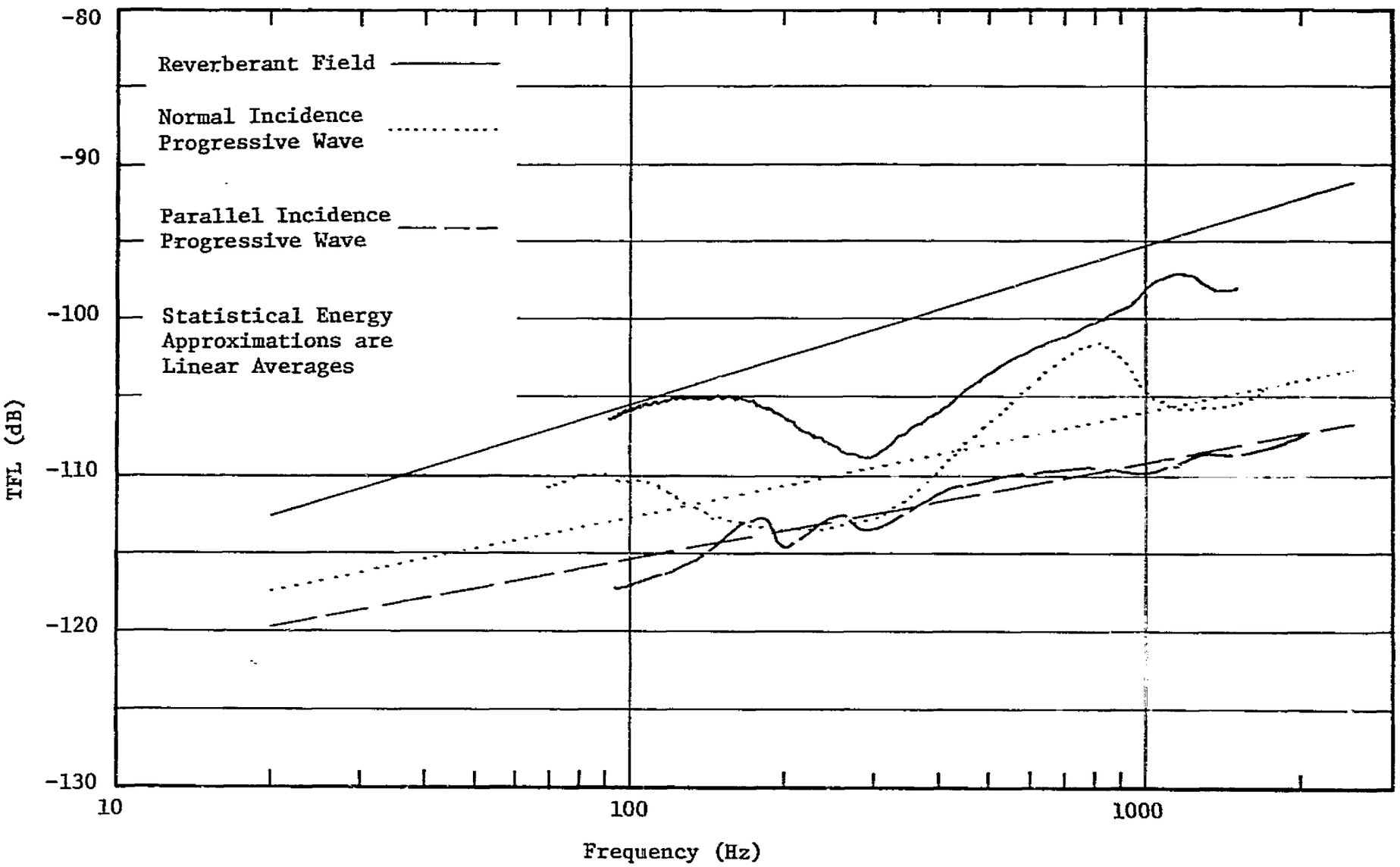

FIGURE 116. MEAN TFL'S FOR TEST SPECIMEN I

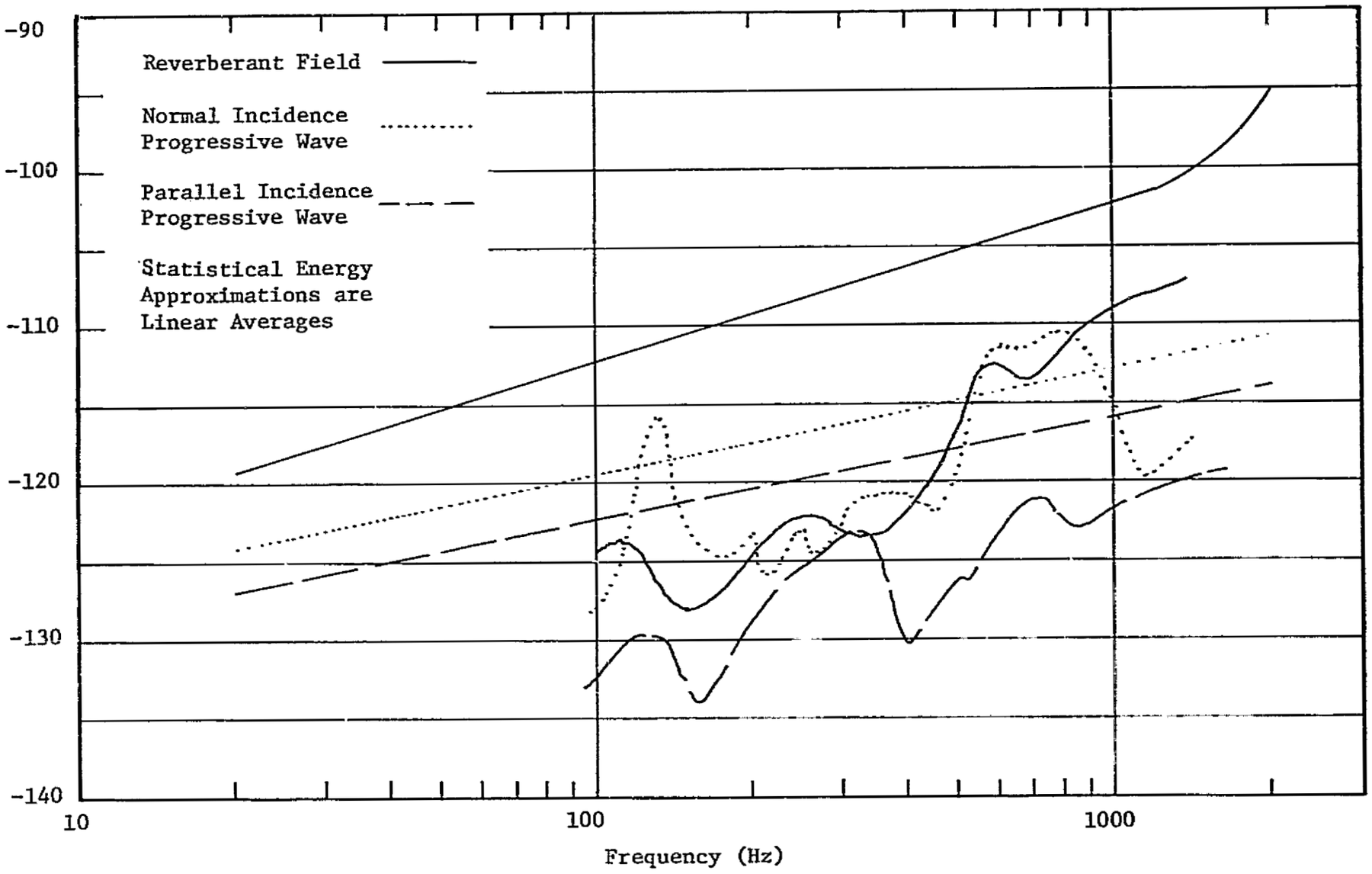

FIGURE 117. MEAN TFL'S FOR TEST SPECIMEN II

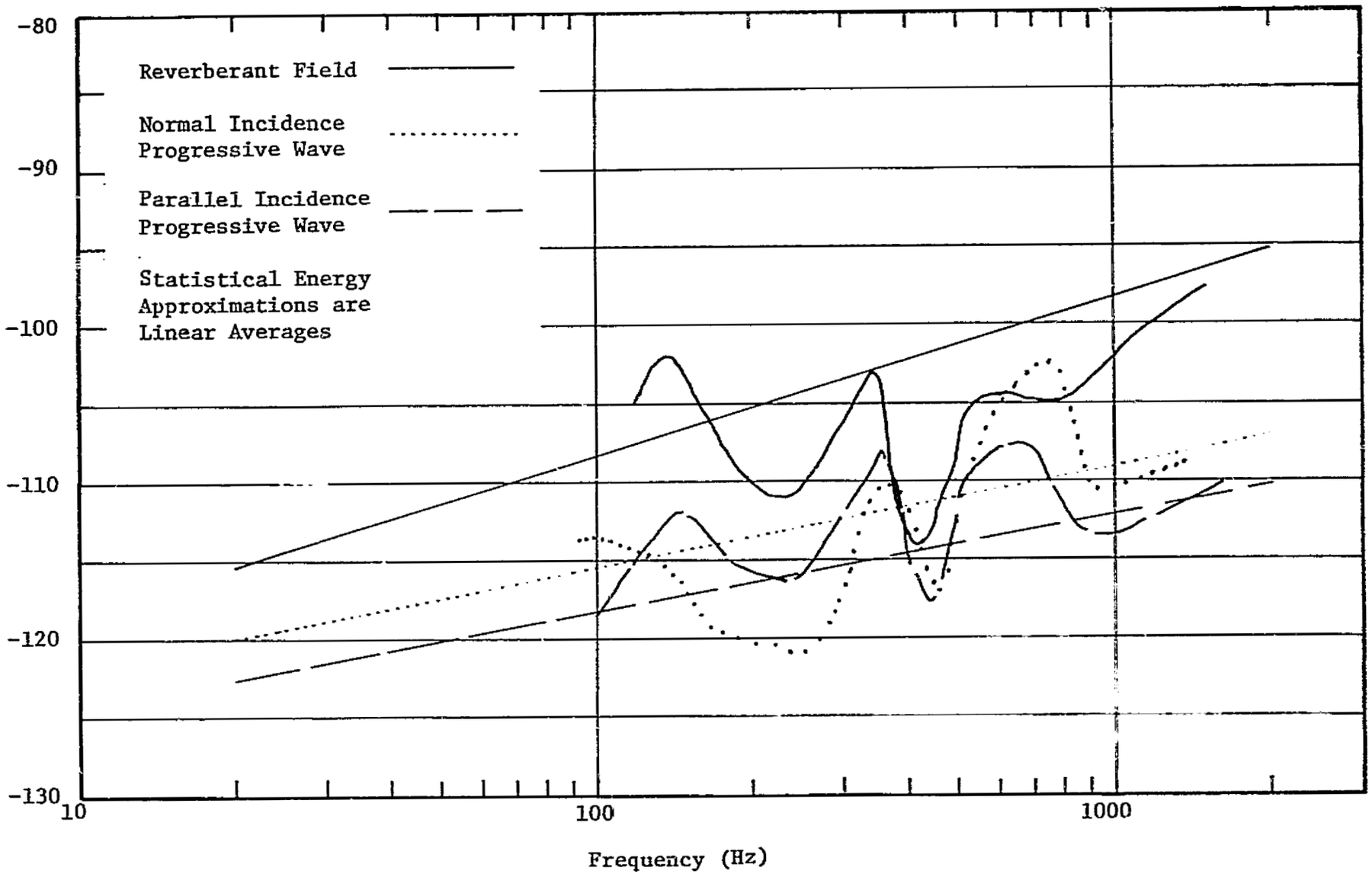

FIGURE 118. MEAN TFL'S FOR TEST SPECIMEN III

the above equations utilize the following values of

$$< D(\omega) > = (f)^{-.35},\ f < f_p/2,\ \text{normal incidence progressive wave} \qquad (114)$$

$$= (f_p)^{-.35},\ f > f_p$$

$$< D(\omega) > = 0.5(f)^{-.35},\ f < f_p/2,\ \text{parallel incidence progressive wave} \qquad (115)$$

$$= 0.5(f_p)^{-.35},\ f > f_p$$

Using the above empirical values of $< D(\omega) >$, transfer function level expectations were derived for test specimens II and III. These functions are shown on figures 117 and 118 and agree tolerably well with the measured data.

B. Radiation Damping Effects

Evaluation of the effects of a radiation damping on vibratory response of a specimen located in the wall of a progressive wave test facility was effected by obtaining comprative response measurements on a given test specimen (II) utilizing the variable cross-section feature of the progressive wave facility. Following are the pertinent parameters of the facility for utilization of equation 98.

Depth (in.)	Height (in.)	S_r(in.^{2})	ab(in.^{2})	ab/S_r
3.5	44.25	154.9	1200	7.75
6.375	44.25	282.1	1200	4.25
12.5	44.25	553.1	1200	2.17
18.5	44.25	818.6	1200	1.47
23.75	44.25	1050.9	1200	1.14

Figure 119 shows the radiation damping ratio, c_r/c_c for a range of K values and for the various area ratio encountered during the current testing program. Table 8 shows the predicted radiation damping ratio for test specimens I and II. The radiation damping should be negligible for all spacings at frequencies above those shown in the table. Figure 120 shows values of calculated radiation damping ratio as a function of frequency for various ratios of panel area to effective facility cross-sectional area. The mean-square vibratory response is inversely proportional to the damping ratio; therefore only the maximum estimated radiation damping is shown in figure 120.

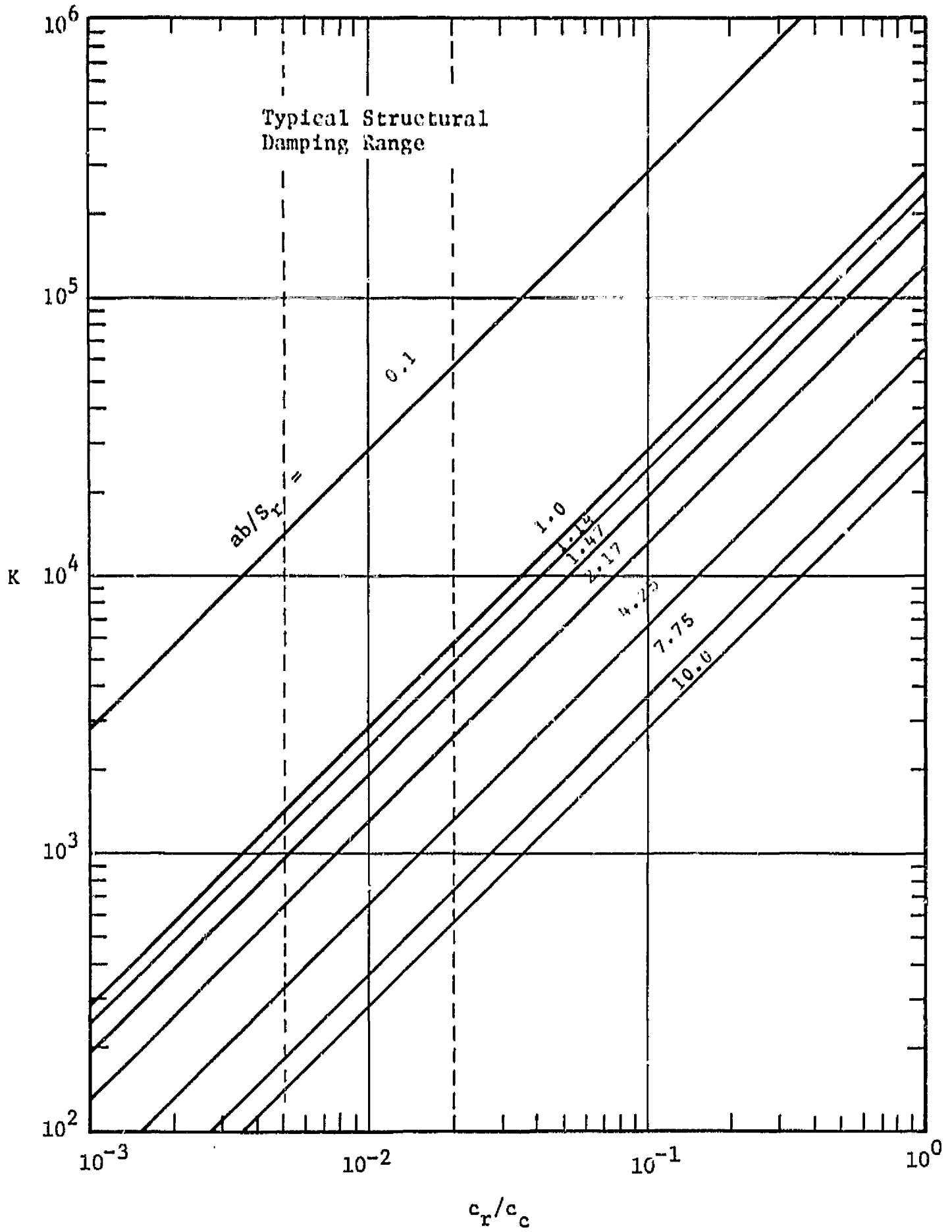

FIGURE 119. RADIATION DAMPING FOR A SIMPLY SUPPORTED PANEL a x b IN A PROGRESSIVE WAVE FACILITY WITH CROSS-SECTION S_r

TABLE 8. CALCULATED DAMPING RATIO FOR TEST SPECIMENS I AND II

TEST SPECIMEN I

Frequency / Spacing	6.6	13.7	19.2	26.4	25.6	40.3
	$K_{11} = 3.60 \times 10^5$	$K_{21} = 4.33 \times 10^4$	$K_{12} = 3.07 \times 10^4$	$K_{22} = 5.63 \times 10^3$	$K_{31} = 1.03 \times 10^4$	$K_{13} = 6.54 \times 10^3$
24	1.48	.160	.130	.023	.042	.027
18	1.90	.230	.160	.030	.053	.035
12	2.81	.340	.240	.043	.077	.050
6	5.51	.680	.460	.086	.155	.100
3	10.00	1.20	.830	.152	.280	.180

Frequency / Spacing	38.2	47.4	59.3	42.2	69.8	63.5
	$K_{32} = 1.72 \times 10^3$	$K_{23} = 1.39 \times 10^3$	$K_{33} = 4.94 \times 10^2$	$K_{41} = 3.52 \times 10^3$	$K_{14} = 2.12 \times 10^3$	$K_{51} = 1.49 \times 10^3$
24	.0071	.0059	.0020	.015	.0078	0.0063
18	.0091	.0075	.0026	.018	.011	0.0080
12	.013	.011	.0038	.027	.016	0.012
6	.026	.021	.0075	.054	.031	0.023
3	.048	.039	.0135	.098	.056	0.042

Frequency / Spacing	107.8	89.6	154.2	54.8	77.0
	$K_{15} = 8.80 \times 10^2$	$K_{61} = 7.35 \times 10^2$	$K_{16} = 4.27 \times 10^2$	$K_{42} = 6.75 \times 10^2$	$K_{24} = 4.82 \times 10^2$
24	0.0036	.0031	0.0017	0.0028	0.0020
11	0.0048	0.0040	0.0022	0.0036	.0026
12	0.0070	0.011	0.0033	0.0053	.0037
6	0.0140	0.021	0.0066	0.015	.0075
3	0.0250	0.026	0.012	0.019	.013

TABLE 8. CALCULATED DAMPING RATIO FOR TEST SPECIMENS I AND II (Concluded)

TEST SPECIMEN I

Frequency / Spacing	76.1 $K_{52} = 3.01 \times 10^2$	114.9 $K_{25} = 2.06 \times 10^2$	75.9 $K_{43} = 1.85 \times 10^2$	88.8 $K_{14} = 2.170 \times 10^2$
24	.0012	.0008	.0007	.0090
18	.0016	.0011	.0010	.0011
12	.0023	.0015	.0014	.0016
6	.0046	.0031	.0029	.0032
3	.0083	.0056	.0051	.0058

TEST SPECIMEN II

Frequency / Spacing	32.9 $K_{11} = 1.60 \times 10^4$	68.5 $K_{21} = 1.92 \times 10^3$	96.2 $K_{12} = 1.36 \times 10^3$	131.8 $K_{22} = 2.49 \times 10^2$	127.8 $K_{31} = 4.57 \times 10^2$	201.6 $K_{13} = 2.90 \times 10^2$
24	.066	.0079	.0055	.0010	.0019	.0012
18	.085	.010	.0071	.0013	.0025	.0015
12	.125	.015	.010	.0019	.0036	.0022
6	.245	.029	.020	.0039	.0071	.0045
3	.466	.053	.037	.0070	.013	.0080

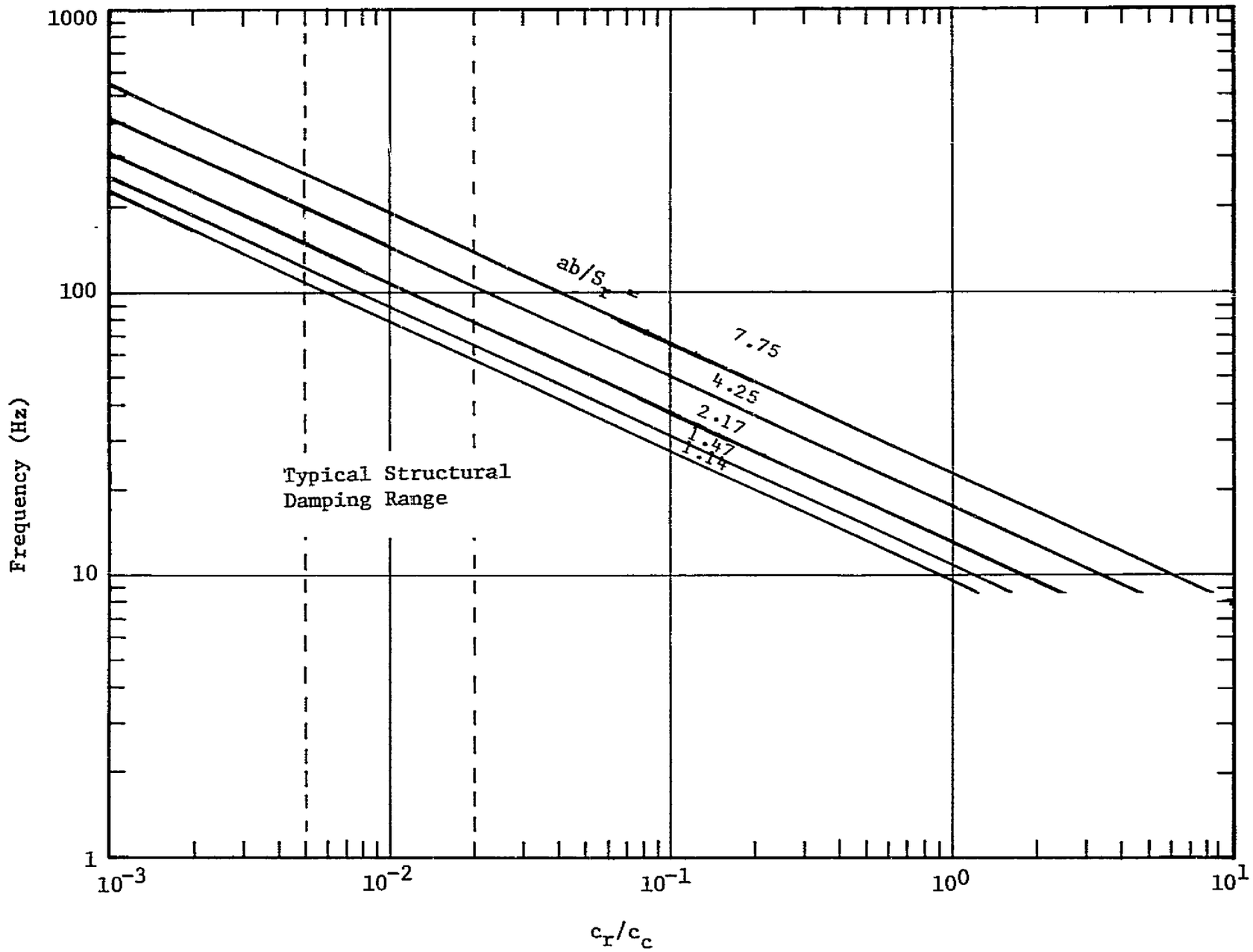

FIGURE 120. MAXIMUM CALCULATED RADIATION DAMPING FOR TEST SPECIMENS I, II AND III.

Typical measured results are shown in figure 121 for the center of test specimens I and II. Data is not presented for the 12 1/2 and 18 inch spacings since it is nearly identical to the 24 inch spacing. Empirical results are compared to predicted relative responses for three modal frequencies of test specimen II in table 9. The data complicated by the analysis bandwidth shows the expected trends however the agreement between analytical and empirical results is not sufficient to establish the theory.

C. Mass Loading

Effects of mass loading may be obtained from comparison of the results of test specimens III and IV. Figures 122 and 123 show the mass attenuation produced by addition of a 0.945 lb weight at measurement location 4. The frequency shift appears negligible but the attenuation is proportional to the square of the frequency. This indicates that the loading mass should be compared with the modal mass rather than the whole panel mass. Table 10 shows comparative levels at various measurement locations during parallel incidence and reverberant testing. It is observed that the mean square acceleration of the stiffeners is decreased by loading the stiffeners, while the amplitude of skin segments increases somewhat.

D. Exposed Area

The effects of varying test specimen area subjected to parallel incidence progressive wave acoustic excitation was examined in Tests 3, 4, 7, 8, 12, 13, 16 and 17. The series of tests involving whole panel (1200 $in.^2$) excitation were performed at 140 dB OA SPL. The center 12.5 inches of the test specimens (500 $in.^2$ area) was subsequently subjected to 150 dB OA SPL. Derived transfer functions levels for the center of test specimens I, II and III are shown in figure 124. These levels are very near those previously presented for parallel incidence progressive wave excitation. Table 11 allows comparison of actual and normalized levels within and outside of the exposed area. The relative rms levels at the center of the panels exposed to 150 dB OA SPL excitation would be 3.162 times the levels at 140 dB excitation, yielding 85.8, 23.5 and 66.4 g_{rms} for specimens I, II and III.

The relative vibration levels of test specimen I seem relatively unaffected by excitation area. The relative vibration levels of test specimen III likewise seem unaffected by excitation area. The thicker test specimen II however, shows a pronounced decrease outside of the excited area. The decrease is throughout the whole panel response frequency region. Utilization of a smaller area of excitation may have produced more observable effects.

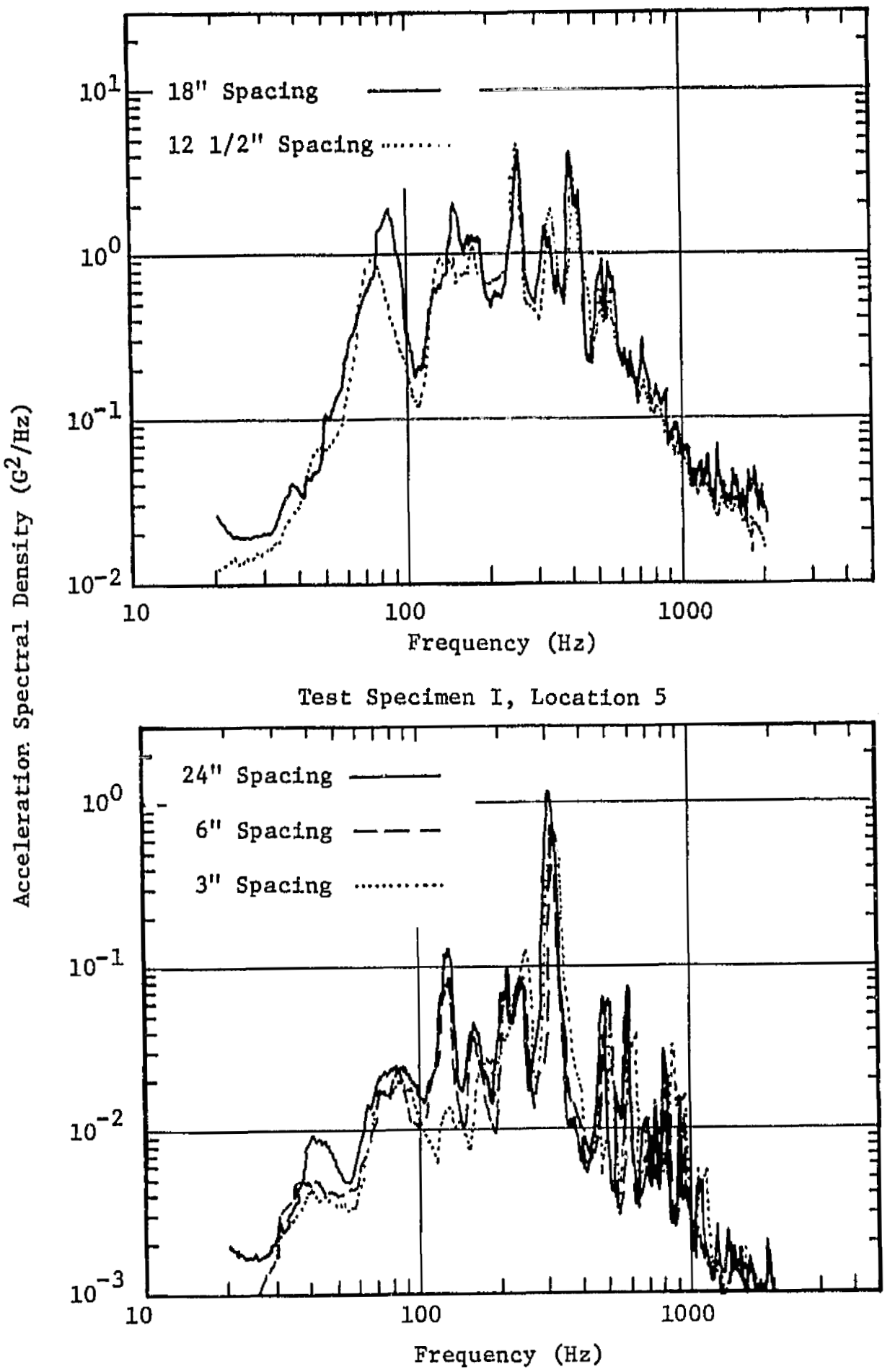

FIGURE 121. TYPICAL MEASURED RADIATION DAMPING EFFECTS FOR TEST SPECIMENS I AND II

TABLE 9. COMPARISON OF MEASURED AND PREDICTED RADIATION DAMPING EFFECT

TEST SPECIMEN II

Frequency - 32.9 (40 Hz Measured)

Spacing	Predicted Relative Response	Measured Relative Response
3.5	.16	.50
6.375	.31	.58
23.75	1.00	1.00

Frequency Range 68.5 -96.2 (80 Hz Measured)

Spacing	Predicted Relative Response	Measured Relative Response
3.5	.62	.76
6.375	.83	.88
23.75	1.00	1.00

Frequency - 127.8 (128 Hz Measured)

Spacing	Predicted Relative Response	Measured Relative Response
3.5	.95	.10
6.375	.98	.72
23.75	1.00	1.00

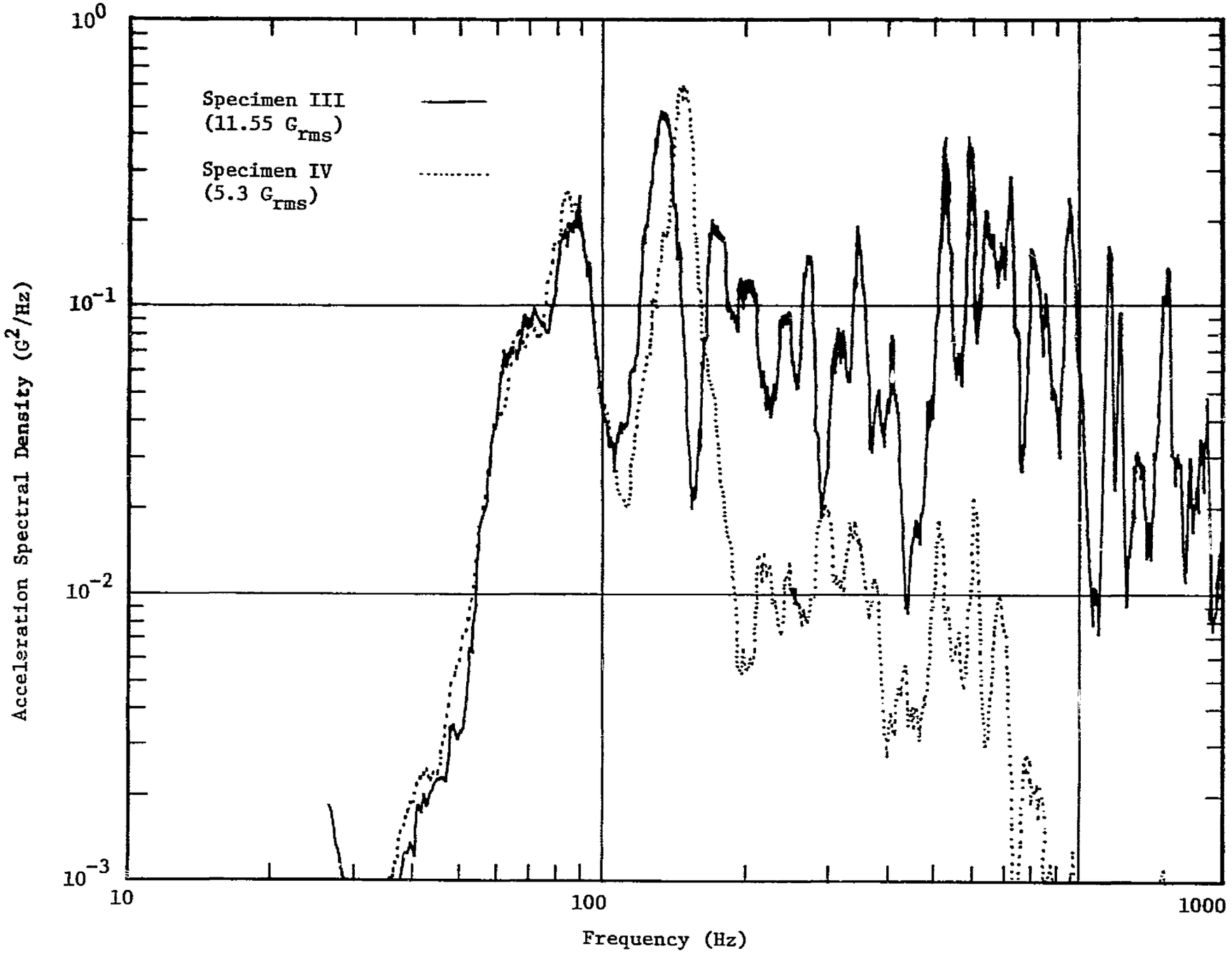

FIGURE 122. MASS LOADING EFFECTS, PARALLEL INCIDENCE PROGRESSIVE WAVE EXCITATION (LOCATION 4)

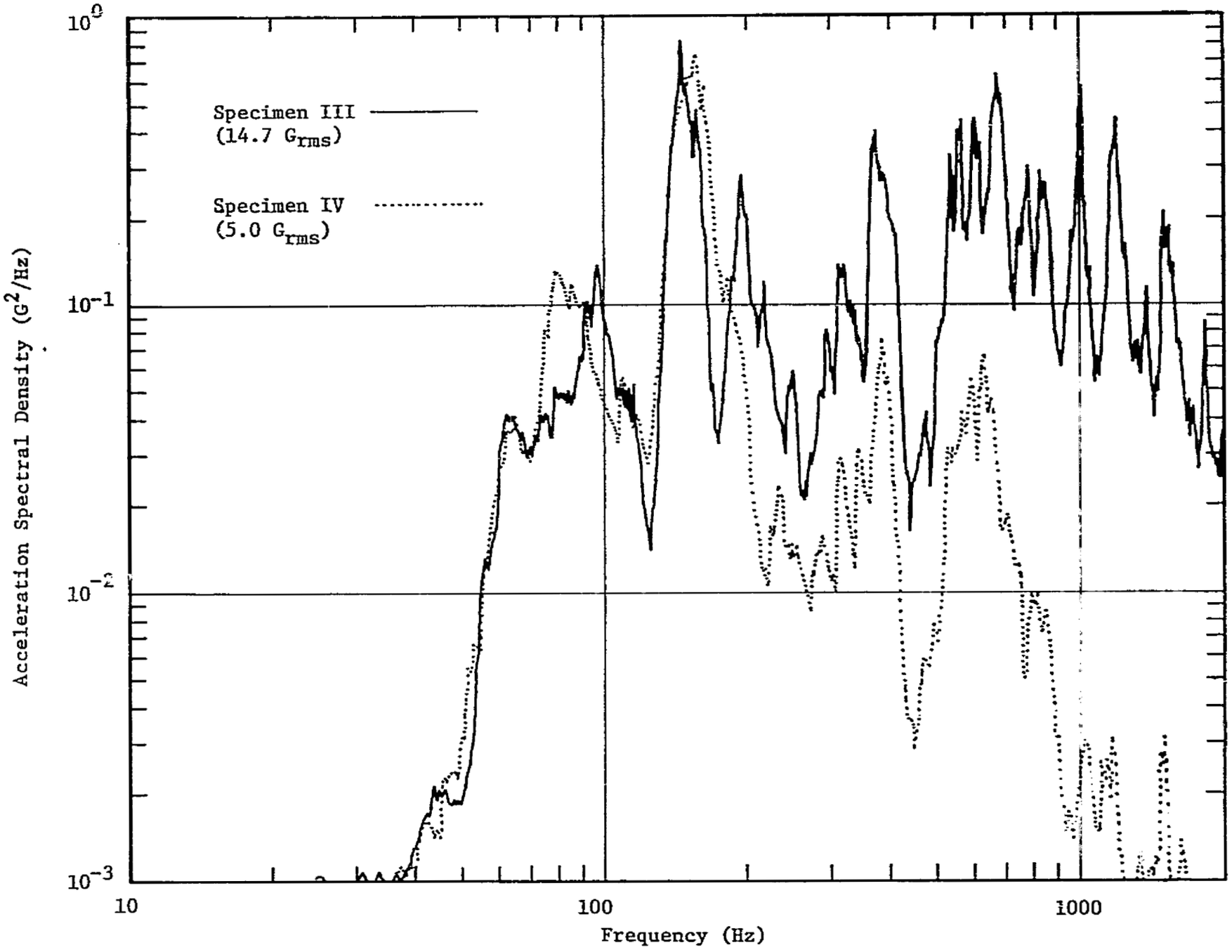

FIGURE 123. MASS LOADING EFFECTS, REVERBERANT FIELD EXCITATION (LOCATION 4)

TABLE 10. RMS ACCELERATION DURING MASS LOADING EXPERIMENTS

	Parallel Incidence			Reverberant		
Location \ Test	12	16	16/12	10	14	14/10
1	4.62	7.07	1.53	14.7	16.2	1.10
2	11.06	29.4	2.66	35.3	41.2	1.17
3	-	16.0	-	32.4	28.2	0.87
4	11.53	5.3	0.46	14.7	5.0	0.34
5	7.6	6.4	0.84	9.44	7.65	0.81
6	6.4	6.4	1.00	11.8	10.6	0.89
7	20.2	7.07	0.35	8.25	6.5	0.79
8	11.06	14.14	1.28	22.4	20.6	0.92
9	19.2	23.5	1.22	33.5	35.3	1.05
10	-	29.4	-	35.3	38.2	1.08
11	-	7.7	-	14.7	12.8	0.87
12	-	24.7	2.23	-	50.	1.42
13	-	7.07	1.10	-	11.2	0.95
14	-	9.9	0.49	-	8.54	1.04
15	-	-	-	-	8.24	0.87

Tests 10 and 16 were loaded with a 0.945 # weight aluminum block mounted at the junction of two stiffeners and separated from the panel skin by 0.1" at location 4. Measurement 4 was located on the loading mass for tests 14 and 16.

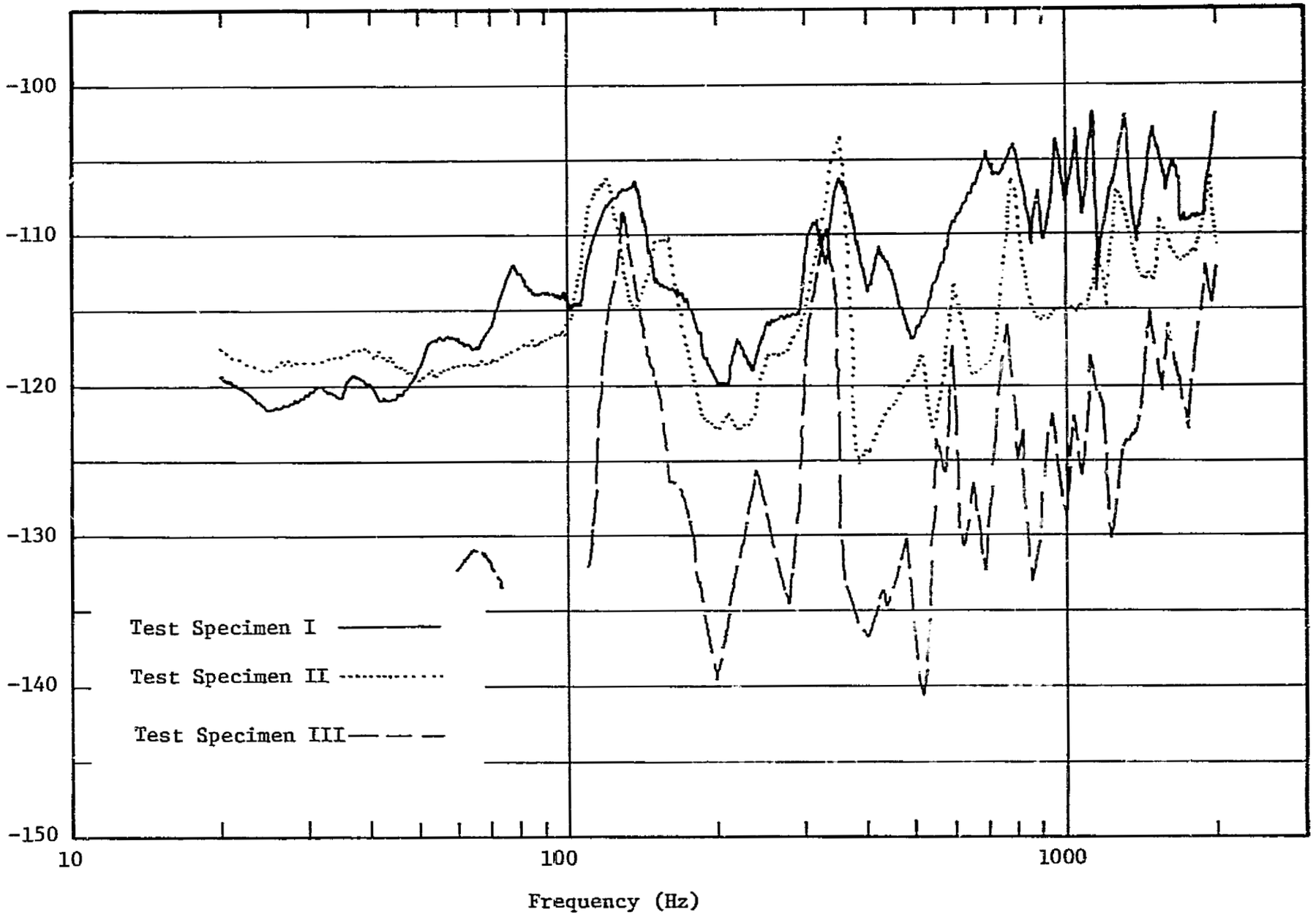

FIGURE 124. LOCALIZED EXCITATION TFL'S FOR TEST SPECIMENS I, II AND III.

TABLE 11. EFFECT OF EXCITATION AREA ON COMPOSITE ACCELERATION

TEST SPECIMEN I

	Test 3 (Whole Panel Exposed)		Test 4 (Center Section Exposed)	
Location	RMS	Normalized Compsite	RMS	Normalized Com osite
1	19.4	0.73	64.7	0.85
2	26.5	1.00	70.6	0.93
3	23.5	0.89	61.8	0.81
4	23.5	0.89	67.7	0.89
5	26.5	1.00	76.4	1.00

TEST SPECIMEN II

	Test 7 (Whole Panel Exposed)		Test 8 (Center Section Exposed)	
Location	RMS	Normalized Composite	RMS	Normalized Composite
1	3.15	0.42	3.81	0.17
2	8.8	1.18	7.96	0.36
3	9.31	1.25	7.52	0.34
4	6.18	0.83	15.65	0.71
5	7.42	1.00	22.1	1.00

TEST SPECIMEN III

	Test 12 (Whole Panel Exposed)		Test 13 (Center Section Exposed)	
Location	RMS	Normalized Composite	RMS	Normalized Composite
1	4.62	0.22	27	0.37
2	11.06	0.53	47	0.64
3	-	-	50	0.68
4	11.53	0.55	38.2	0.52
5	7.6	0.36	22.4	0.30
6	6.4	0.30	24.1	0.33
7	20.2**	-	17.0	0.23
8	11.06	0.53	47.0	0.64
9	19.2	0.91	47.0	0.64
10	21.0*	1.00	73.5	1.00
11	-	-	26.5	0.36

* Estimated from PSD
** Invalid data
Whole panel includes 1200 $in.^2$
Center section includes 500 $in.^2$ spaced equally above and below longitudinal axis of panel.
Tests 3, 7, 12 performed at 140 dB OA, 4, 8 13 performed at 150 dB OA.

SECTION VI. SIMULATION METHODS

The results of this program of research do not, in themselves, constitute a justification for concrete specification of acoustic testing methods and procedures. Certain conclusions may be drawn, however, and qualitative assessments may be presented concerning suitable acoustic fields, procedures, relative severity, and reasonable tolerances in the test conditions.

A. Sound Fields

Any available acoustic field should be satisfactory for exciting structural or component vibratory response provided that the characteristics of the field are known. This includes spatial variation in the excitation spectral density and correlation coefficient.

B. Procedures

The component should be isolated from any external vibratory source, actual or induced by the action of the acoustic field on an object external to the test specimen. Test specimens may be oriented in any manner with respect to the sound source (for example, at any angle of incidence to a progressive wave source) provided that the orientation effect on response severity is considered. Nominally the wall-mounted test specimen surface area should not exceed the cross-sectional area of a progressive wave tube and the component volume should not exceed ten percent of a reverberation chamber volume without adjusting the excitation for the effects of the facility on the specimen response. In a reverberation chamber, the facility should be large enough that the facility acoustic modes provide a continuous excitation throughout the test frequency range (at least the component response frequency range). Components in a reverberation chamber should not be located within a quarter wave length of the test facility wall for frequencies within the test frequency range. Measurement of the acoustic field characteristics should be obtained in the immediate proximity of the test specimen with a dummy specimen in place to account for perturbation of the acoustic field by the specimen.

C. Excitation Levels

The test excitation spectral density should be the actual anticipated spectral density adjusted by a safety margin and uncertainty factor. Further, the spectrum must be modified by the difference in acoustic fields in order to provide adequate testing without requiring severe overdesign of structure and components. For example, analysis of the current results show testing in a reverberant acoustic field may be 7 dB or more severe than testing in a progressive wave facility at parallel incidence at the identical input acoustic spectral density. Since the bulk of vehicle and payload structure is excited by a quasi-parallel incidence progressive acoustic wave, testing in a reverberant chamber could be performed by utilizing an acoustic spectral density up to 7 dB or more less than that of the service field. Actual numerical differences require further effort. Care must be maintained that no high level starting or termination transients occur.

D. Specification Tolerances

In order for any test specification to be reasonable, it must include tolerances in the amplitude and test duration. Acoustic test specifications are usually presented in one-third octave band levels. It is possible to maintain the amplitude within two dB of a desired level, provided the adjacent third octaves do not differ by more than 10 decibels from the third-octave band considered. Tolerances in the duration can be easily maintained within a few seconds.

SECTION VII. RECOMMENDATIONS

The results of this study show qualitatively that reverberant fields produce more severe response than progressive wave testing at normal incidence and normal incidence testing more severe than parallel incidence progressive wave in the frequency range of reverberant vibration. This result needs further study namely,

1. The response variability with test specimen size and shape.

2. The response variability with excitation amplitude and spectrum.

3. Numerical differences which may be utilized for different types of test facilities.

Further experimental effort would also yield an improved value of $\langle D(\Omega) \rangle$ as a semi-empirical estimator for utilization of statistical energy techniques. Also the useful frequency range for application of the statistical energy methods could be improved.

Improvements may be made in the analytical prediction of modal response to acoustic fields by,

1. Improved models of physical space correlations.

2. Expansion of analysis frequency range.

Further study may be performed to obtain the response of space vehicle structures to boundary layer noise. Such study may be performed advantageously in a wind tunnel facility where both the acoustic forcing field and the vibratory response may be thoroughly analyzed, provided a low ambient acoustic background is maintained.

Better definition of the correlation of the service excitation field is required in order to better simulate service acoustic fields in the laboratory.

REFERENCES

1. Serocki, J. E., and Gruner, W. J., "Uprated Saturn I/CSM/MM (0° Cant, 0 and 70 Second Ignition) Vibration and Acoustic Analysis." Chrysler Technical Note HSM-N81-67, 27 September 1967.

2. Swanson, W. L., and Gruner, W. J., "Voyager Spacecraft Flight Technology Acoustics," Chrysler Technical Memorandum HSM-M54-67, 23 June 1967.

3. Dyer, I., "Estimation of Sound Induced Missile Vibration," Random Vibration, Volume I, 1957 (Edited by S. H. Crandall).

4. Eldred, K. M., et al, "Suppression of Jet Noise with Emphasis on the Near Field," ASD - TDR-62-578, 1963.

5. Lighthill, M. J., "On Sound Generated Aerodynamically," Part I - Proceedings of Royal Society, A 211, page 564, 1952; Part II - Proceedings of Royal Society, A 222, page 1, 1954.

6. Lighthill, M. J., "Sound Generated Aerodynamically," The Bakerian Lecture, 1961.

7. Eldred, K., et al, "Structural Vibration in Space Vehicles," WADD TR 61-62, December 1961.

8. Serocki, J. E., and Sailors, C. W., "Internal Acoustic Characteristics of Saturn I/IB Vehicles," Chrysler Technical Report HSM-R75-68, 13 June 1968.

9. Willmarth, W. W., and Wooldridge, C. E., "Measurements of Fluctuating Pressure at the Wall Beneath a Thick Turbulent Boundary Layer," Journal of Fluid Mechanics, page 187, 1962.

10. Maestrello,L., "Measurement of Noise Radiated by Boundary Layer Excited Panels," Journal of Sound and Vibration, page 100, 1965.

11. Maestrello, L., "Measurement and Analysis of the Response Field of Turbulent Boundary Layer Excited Panels," Journal of Sound and Vibration, page 270, 1965.

12. Corcos, G.M., "The Structure of the Turbulent Pressure Field in Boundary Layer Flows," Journal of Fluid Mechanics, page 353, 1963.

13. Schlichting, Dr. Herman, "Boundary Layer Theory," McGraw-Hill Book Company, June 1962.

14. Wiley, D. R., and Seidel, M. G., "Aerodynamic Noise Tests on X-20 Scale Models," AFFDL-TR-65-192, Volumes I and II, 1965.

REFERENCES (Continued)

15. Four-Percent Saturn V Fluctuating Pressure Data from Schutzenhofer, L. A., "Four-Percent Saturn V Fluctuating Pressure Data Transmittal," MSFC Memorandum, R-AERO-AU-68-41, 12 August 1968.

16. Lehner, F. L., and Gruner, W. J., "A Scale Model Experimental Investigation of the Flow Induced Fluctuating Pressure Environment of the S-IB Stage of the Saturn IB Vehicle," Chrysler Corporation Technical Report HSM-R185, Volumes I and II, June 1966.

17. Gruner, W. J., "Apollo-Saturn IB Flight Technology Acoustics," Chrysler Corporation Technical Note HSM-N24-67, March 1967.

18. Chandiramani, K. L., et al, "Structural Response to Inflight Acoustic and Aerodynamic Environments," BBN Report No. 1417, July 1966.

19. Goldburg, A., et al, "Strouhal Numbers for the Hypersonic Wakes of Spheres and Cones," AIAA Journal, page 1332, 1965.

20. Goldburg, A., and Florsheim, B. H., "Transition and Strouhal Numbers for the Incompressible Wake of Various Bodies," Physics of Fluids, page 45, 1966.

21. Boone, J. R., and McCanless, G. F., "Evaluation of the Acoustic Sources of Background Noise in Wind Tunnels," Chrysler Technical Report HSM-R65-68, June 1968.

22. Lyon, R. H., "Random Noise and Vibration in Space Vehicles," U.S. Document of Defense Shock and Vibration Center, Monograph #1, 1967.

23. Mahaffey, P. T., and Smith, K. W., "A Method for Predicting Environmental Vibration Levels in Jet Powered Vehicles," Shock and Vibration Bulletin, No. 28, Part 4, p 1, August 1960.

24. Franken, P., "Sound Induced Vibration of Cylindrical Vehicles," JASA, V 34, p 453, April 1962.

25. White, R. W., Eldred, K. E., and Roberts, W. H., "Investigation of a Method for the Prediction of Vibratory Response and Stress in Typical Flight Vehicle Structure," ASD-TDR-62-801, August 1963.

26. White, R. W., Bozich, D. J., and Eldred, K. McK., "Empirical Correlation of Excitation Environment and Structural Parameters with Flight Vehicle Vibration Response," AFFDL-TR-64-160, December 1964.

27. Barrett, R. E., "Techniques for Predicting Localized Vibratory Environments of Rocket Vehicles," NASA TND-1836, October 1963.

REFERENCES (Continued)

28. Barrett, R. E., "Statistical Techniques for Describing Localized Vibratory Environments of Rocket Vehicles," NASA TND-2158, July 1964.

29. Lin, Y. K.,"Probablistic Theory of Structural Dynamics," McGraw-Hill Book Co., Inc., 1967.

30. Lee, T. N., "Computer Program for Prediction of Structural Vib a-tions to Fluctuating Pressure Environments, Progress Report No. 4," 8 November 1968.

31. Smith, P. W., and Lyon, R. H., "Sound and Structural Vibration," NASA CR-160, March 1965.

32. Chandiramani, K. L., et al, "Structural Response to Inflight Acoustic and Aerodynamic Environments," BBN Report 1417, 7 August 1966.

33. Ungar, E. E., "Fundamantals of Statistical Energy Analysis of Vibrating Systems," AFFDL-TR-66-52, May 1966.

34. Dyer, I., "Sound Radiation into a Closed Space from Boundary Layer Turbulence," BBN Report #602, December 1958.

35. Efowcs Williams, J. E., and Lyon, R. H., "The Sound Radiated from Turbulent Flows Near Flexible Boundaries," BBN Report #1054, August 1963.

36. Lyon, R. H., et al, "Aerodynamic Noise Simulation in Sonic Fatigue Facility," AFFDL-TR-66-112, November 1966.

37. Lyon, R. H., "Boundary Layer Noise Response Simulation with a Sound Field," Acoustical Fatigue in Aerospace Structures, p 213, 1965.

38. Lyon, R. H., et al, "Random Vibration Studies of Coupled Structures in Electronic Equipment," ASD-TDR-63-205, April 1963.

39. Eldred, K., "Problems in the Laboratory Qualification of Structures and Equipment Exposed to Intense Acoustic Environments," p 321, 1964 Proceedings of Institute of Environmental Sciences.

40. Beranek, L. L., and Sleeper, H. P., "The Design and Construction of Anechoic Sound Chambers," J. Acous. Soc. Am. 18, p 140, 1946.

41. Watters, B. G., "Design of Wedges for Anechoic Chambers," Noise Control, p 368, November 1958.

42. Harris, G. M., "Absorption of Sound in Air Below 1000 CPS," NASA CR-237, June 1965.

43. Nyborg, W. L., Mintzen, D., "Review of Sound Propagation in the Lower Atmosphere," WDAC TR-54-602, 1955.

DISTRIBUTION

PR-SC

MS-IL

MS-T

MS-I

*R-P&VE-RI (12) + reproducible master

*Attention: Mr. Charles E. Brewer